

Lecture Notes in Electrical Engineering 1097

Vivek Shrivastava  
Jagdish Chand Bansal  
B. K. Panigrahi *Editors*

# Power Engineering and Intelligent Systems

Proceedings of PEIS 2023, Volume 1

 Springer

# Lecture Notes in Electrical Engineering

## Volume 1097

### Series Editors

Leopoldo Angrisani, Department of Electrical and Information Technologies Engineering, University of Napoli Federico II, Napoli, Italy  
Marco Artega, Departament de Control y Robótica, Universidad Nacional Autónoma de México, Coyoacán, Mexico  
Samarjit Chakraborty, Fakultät für Elektrotechnik und Informationstechnik, TU München, München, Germany  
Jiming Chen, Zhejiang University, Hangzhou, Zhejiang, China  
Shanben Chen, School of Materials Science and Engineering, Shanghai Jiao Tong University, Shanghai, China  
Tan Kay Chen, Department of Electrical and Computer Engineering, National University of Singapore, Singapore, Singapore  
Rüdiger Dillmann, University of Karlsruhe (TH) IAIM, Karlsruhe, Baden-Württemberg, Germany  
Haibin Duan, Beijing University of Aeronautics and Astronautics, Beijing, China  
Gianluigi Ferrari, Dipartimento di Ingegneria dell'Informazione, Sede Scientifica Università degli Studi di Parma, Parma, Italy  
Manuel Ferre, Centre for Automation and Robotics CAR (UPM-CSIC), Universidad Politécnica de Madrid, Madrid, Spain  
Faryar Jabbari, Department of Mechanical and Aerospace Engineering, University of California, Irvine, CA, USA  
Limin Jia, State Key Laboratory of Rail Traffic Control and Safety, Beijing Jiaotong University, Beijing, China  
Janusz Kacprzyk, Intelligent Systems Laboratory, Systems Research Institute, Polish Academy of Sciences, Warsaw, Poland  
Alaa Khamis, Department of Mechatronics Engineering, German University in Egypt El Tagamoa El Khames, New Cairo City, Egypt  
Torsten Kroeger, Intrinsic Innovation, Mountain View, CA, USA  
Yong Li, College of Electrical and Information Engineering, Hunan University, Changsha, Hunan, China  
Qilian Liang, Department of Electrical Engineering, University of Texas at Arlington, Arlington, TX, USA  
Ferran Martín, Departament d'Enginyeria Electrònica, Universitat Autònoma de Barcelona, Bellaterra, Barcelona, Spain  
Tan Cher Ming, College of Engineering, Nanyang Technological University, Singapore, Singapore  
Wolfgang Minker, Institute of Information Technology, University of Ulm, Ulm, Germany  
Pradeep Misra, Department of Electrical Engineering, Wright State University, Dayton, OH, USA  
Subhas Mukhopadhyay, School of Engineering, Macquarie University, NSW, Australia  
Cun-Zheng Ning, Department of Electrical Engineering, Arizona State University, Tempe, AZ, USA  
Toyoaki Nishida, Department of Intelligence Science and Technology, Kyoto University, Kyoto, Japan  
Luca Oneto, Department of Informatics, Bioengineering, Robotics and Systems Engineering, University of Genova, Genova, Italy  
Bijaya Ketan Panigrahi, Department of Electrical Engineering, Indian Institute of Technology Delhi, New Delhi, Delhi, India  
Federica Pascucci, Department di Ingegneria, Università degli Studi Roma Tre, Roma, Italy  
Yong Qin, State Key Laboratory of Rail Traffic Control and Safety, Beijing Jiaotong University, Beijing, China  
Gan Woon Seng, School of Electrical and Electronic Engineering, Nanyang Technological University, Singapore, Singapore  
Joachim Speidel, Institute of Telecommunications, University of Stuttgart, Stuttgart, Germany  
Germano Veiga, FEUP Campus, INESC Porto, Porto, Portugal  
Haitao Wu, Academy of Opto-electronics, Chinese Academy of Sciences, Haidian District Beijing, China  
Walter Zamboni, Department of Computer Engineering, Electrical Engineering and Applied Mathematics, DIEM—Università degli studi di Salerno, Fisciano, Salerno, Italy  
Junjie James Zhang, Charlotte, NC, USA  
Kay Chen Tan, Department of Computing, Hong Kong Polytechnic University, Kowloon Tong, Hong Kong

The book series *Lecture Notes in Electrical Engineering* (LNEE) publishes the latest developments in Electrical Engineering—quickly, informally and in high quality. While original research reported in proceedings and monographs has traditionally formed the core of LNEE, we also encourage authors to submit books devoted to supporting student education and professional training in the various fields and applications areas of electrical engineering. The series cover classical and emerging topics concerning:

- Communication Engineering, Information Theory and Networks
- Electronics Engineering and Microelectronics
- Signal, Image and Speech Processing
- Wireless and Mobile Communication
- Circuits and Systems
- Energy Systems, Power Electronics and Electrical Machines
- Electro-optical Engineering
- Instrumentation Engineering
- Avionics Engineering
- Control Systems
- Internet-of-Things and Cybersecurity
- Biomedical Devices, MEMS and NEMS

For general information about this book series, comments or suggestions, please contact [leontina.dicecco@springer.com](mailto:leontina.dicecco@springer.com).

To submit a proposal or request further information, please contact the Publishing Editor in your country:

#### **China**

Jasmine Dou, Editor ([jasmine.dou@springer.com](mailto:jasmine.dou@springer.com))

#### **India, Japan, Rest of Asia**

Swati Meherishi, Editorial Director ([Swati.Meherishi@springer.com](mailto:Swati.Meherishi@springer.com))

#### **Southeast Asia, Australia, New Zealand**

Ramesh Nath Premnath, Editor ([ramesh.premnath@springernature.com](mailto:ramesh.premnath@springernature.com))

#### **USA, Canada**

Michael Luby, Senior Editor ([michael.luby@springer.com](mailto:michael.luby@springer.com))

#### **All other Countries**

Leontina Di Cecco, Senior Editor ([leontina.dicecco@springer.com](mailto:leontina.dicecco@springer.com))

**\*\* This series is indexed by EI Compendex and Scopus databases. \*\***

Vivek Shrivastava · Jagdish Chand Bansal ·  
B. K. Panigrahi  
Editors

# Power Engineering and Intelligent Systems

Proceedings of PEIS 2023, Volume 1

 Springer

*Editors*

Vivek Shrivastava  
National Institute of Technology Delhi  
New Delhi, Delhi, India

Jagdish Chand Bansal  
South Asian University New Delhi  
New Delhi, Delhi, India

B. K. Panigrahi  
Department of Electrical Engineering  
Indian Institute of Technology Delhi  
Delhi, India

ISSN 1876-1100

ISSN 1876-1119 (electronic)

Lecture Notes in Electrical Engineering

ISBN 978-981-99-7215-9

ISBN 978-981-99-7216-6 (eBook)

<https://doi.org/10.1007/978-981-99-7216-6>

© The Editor(s) (if applicable) and The Author(s), under exclusive license to Springer Nature Singapore Pte Ltd. 2024

This work is subject to copyright. All rights are solely and exclusively licensed by the Publisher, whether the whole or part of the material is concerned, specifically the rights of translation, reprinting, reuse of illustrations, recitation, broadcasting, reproduction on microfilms or in any other physical way, and transmission or information storage and retrieval, electronic adaptation, computer software, or by similar or dissimilar methodology now known or hereafter developed.

The use of general descriptive names, registered names, trademarks, service marks, etc. in this publication does not imply, even in the absence of a specific statement, that such names are exempt from the relevant protective laws and regulations and therefore free for general use.

The publisher, the authors, and the editors are safe to assume that the advice and information in this book are believed to be true and accurate at the date of publication. Neither the publisher nor the authors or the editors give a warranty, expressed or implied, with respect to the material contained herein or for any errors or omissions that may have been made. The publisher remains neutral with regard to jurisdictional claims in published maps and institutional affiliations.

This Springer imprint is published by the registered company Springer Nature Singapore Pte Ltd.

The registered company address is: 152 Beach Road, #21-01/04 Gateway East, Singapore 189721, Singapore

Paper in this product is recyclable.

# Preface

This book contains outstanding research papers as the proceedings of the International Conference on Power Engineering and Intelligent Systems (PEIS2023). PEIS 2023 has been organized by the National Institute of Technology Delhi, India, and technically sponsored by the Soft Computing Research Society, India. The conference is conceived as a platform for disseminating and exchanging ideas, concepts, and results of researchers from academia and industry to develop a comprehensive understanding of the challenges of the advancements of intelligence in computational viewpoints. This book will help in strengthening congenial networking between academia and industry. We have tried our best to enrich the quality of the PEIS 2023 through the stringent and careful peer-reviewed process. This book presents novel contributions to Power Engineering and Intelligent Systems and serves as reference material for advanced research. PEIS 2023 received many technical contributed articles from distinguished participants from home and abroad. After a very stringent peer-reviewing process, only 67 high-quality papers were finally accepted for presentation and the final proceedings.

New Delhi, India

Vivek Shrivastava  
Jagdish Chand Bansal  
B. K. Panigrahi

# Contents

<b>Control Strategies for Blood Pressure Regulation in the Diabetic Patients Post Surgery</b> .....	1
P. V. Gopi Krishna Rao, R. Hanuma Naik, N. Sreenivasa Rao, G. Sowmya, and M. V. Rajasekhar	
<b>Detecting Obfuscated Malware Using Graph Neural Networks</b> .....	15
Quang-Vinh Dang	
<b>Semi-Vector Controlled PM Synchronous Motor Drive</b> .....	27
Arabindo Chandra, Soumyajit Datta, Milan Basu, and Sumana Chowdhuri	
<b>A Comprehensive Review of Sensor-Based Smart Packaging Technology</b> .....	39
B. P. Aniruddha Prabhu, Rakesh Dani, Khairul Hafezad Abdullah, Tushar Sharma, Chandradeep Bhatt, and Rahul Chauhan	
<b>Comparative Analysis of RSA-RK and ECC-RK for Aadhaar Card</b> ....	53
R. Felista Sugirtha Lizy	
<b>Fundamental Security Risk Modeling in Smart Grid in the Modern Era of Artificial Intelligence</b> .....	67
Rakshit Kothari, Ayushi Gill, Vijendra Kumar Maurya, and Anurag Paliwal	
<b>Adaptive Multi-resolution Simulations of Cascaded Converters</b> .....	79
Asif Mushtaq Bhat and Mohammad Abid Bazaz	
<b>Efficient Solar Cell Using COMSOL Multiphysics</b> .....	89
Rama Devi, Yogendra Kumar Upadhyaya, S. Manasa, Abhinav, and Ashutosh Tripathi	

<b>Post Quantum Secure Blockchain Architecture for Data Dissemination</b> .....	105
Dushyant Kumar Yadav, Hemlal Sahu, Siva Gayatri Venkata Naga Datta Sai Ammanamanchi, Otturu Madhu Murali, Saurabh Rana, and Dharminder Chaudhary	
<b>An Open-Source Learning Management System</b> .....	117
Anshul J. Gaikwad, Pratik P. Shastrakar, Bhagyashri R. Sardey, and Nikhil S. Damle	
<b>Design and Implementation of Seven-Level Reduced Switch Count Multilevel Inverter for Electric Vehicle Applications</b> .....	133
Murugesan Manivel, Lakshmi Kaliappan, Lakshmanan Palani, and Sivaranjani Subramani	
<b>Ultrasound Image Classification and Follicle Segmentation for the Diagnosis of Polycystic Ovary Syndrome</b> .....	145
Jojo James, Sabeen Govind, and Jijo Francis	
<b>Twitter Data Analysis Using BERT and Graph-Based Convolution Neural Network</b> .....	155
Anusha Danday and T. Satyanarayana Murthy	
<b>A Topology for Reactive Power Compensation in Grid System Using a Low-Cost Thyristor Switched Capacitor Scheme</b> .....	167
Gaurav Shrivastava and Subhash Chandra	
<b>An Automated Two-Stage Brain Tumour Diagnosis System Using SVM and Geodesic Distance-Based Colour Segmentation</b> .....	179
S. Syedsafi, P. Sriramakrishnan, and T. Kalaiselvi	
<b>Assessment of Online Teaching Using Statistical and Unsupervised Learning Methods</b> .....	193
Raj Kishor Bisht, Sanjay Jasola, Ila Pant Bisht, and Yogesh Lohumi	
<b>An Image-Based Automated Model for Plant Disease Detection Using Wavelet</b> .....	205
Aditi Ghosh and Parthajit Roy	
<b>Computer Vision Assisted Bird–Eye Chilli Classification Framework Using YOLO V5 Object Detection Model</b> .....	217
Abhijit, S. Akhil, V. K. Akshat Kumar, Ben K. Jose, and K. M. Abubeker	
<b>An Effective Grid Connected Multi Level Inverter Based Hybrid Wind and Solar Energy</b> .....	227
G. Srinivas, K. Tejaswaroop, K. Saisamudra, K. Shiva Kumar, and G. Rakesh Kumar	



**A Comprehensive Analysis of Autism Spectrum Disorder Using Machine Learning Algorithms: Survey** ..... 241  
 D. Aarthi and S. Kannimuthu

**Energy-Efficient Cluster Head Election and Data Aggregation Ensemble Machine Learning Algorithm** ..... 255  
 Kavita Gupta, Shilpi Mittal, and Kirti Walia

**Multi-sensor Data Fusion for Early Fire Estimation Using ML Techniques** ..... 267  
 Priyanka Kushwaha, Muskan Sharma, Pragati Kumari, and Richa Yadav

**Design and Analysis of Solar Cell Coplanar Antenna for Wireless Applications** ..... 279  
 Kathika Jyothi Naga Nivas, Putha Sathish Kumar Reddy, Kappa Ravi Kiran Raju, Chintha Rithvik Kumar Reddy, T. Mary Neebha, and A. Diana Andrushia

**Open Permissioned Blockchain Solution for Private Equity Funding Using a Global, Cross-Cloud Network Blockchain Platform** ..... 289  
 S. Rajarajeswari, K. N. Karthik, K. Divyasri, Anvith, and Riddhi Singhal

**The Challenge of Recognizing Artificial Intelligence as Legal Inventor: Implications and Analysis of Patent Laws** ..... 299  
 Kanishka Vaish, Rajesh Bahuguna, Samta Kathuria, Kapil Joshi, Rishika Yadav, and Rajesh Singh

**Comparative Analysis of Imbalanced Malware Byteplot Image Classification Using Transfer Learning** ..... 313  
 M. Jayasudha, Ayesha Shaik, Gaurav Pendharkar, Soham Kumar, B. Muhesh Kumar, and Sudharshanan Balaji

**Recommender Systems for Personalized Business Marketing: Employing Artificial Intelligence and Business Intelligence in Machine Learning Techniques** ..... 325  
 N. Poornima, C. Sridharan, A. Pavithra, R. Narendiran, B. Vijay, and V. S. Neelesh

**Blockchain Technology for Secure Smart Grid Access Control** ..... 337  
 Vijendra Kumar Maurya, Rakshit Kothari, Payal Sachdev, and Narendra Singh Rathore

**Tie-Line Power Frequency Stability Control of an Interconnected Hybrid Power System Using a Virtual Inertia Controller by the GWO Algorithm** ..... 349  
 R. Aravinda Raj, P. Malathy, D. Manivasagan, N. Mayilvaganan, and S. Mohamed Basith

**Lithium-Ion Batteries: Prognosis Algorithms, Challenges and Future Scenario** ..... 369  
Gaurav Malik and Manish Kumar Saini

**Diseased Leaf Identification Using Bag-of-Features and Sigmoidal Spider Monkey Optimization** ..... 381  
Rajani Kuamri and Sandeep Kumar

**Detection of FDI Attacks on Power Grid Using Graph-Theoretical Methods** ..... 391  
Arpita Ghosh and Shubhi Purwar

**Author Index** ..... 403

## About the Editors

**Dr. Vivek Shrivastava** has approx. 20 years of diversified experience of scholarship of teaching and learning, accreditation, research, industrial, and academic leadership in India, China, and USA. Presently, he is holding the position of Dean Research & Consultancy at National Institute of Technology Delhi. Prior to his academic assignments, he has worked as System Reliability Engineer at SanDisk Semiconductors Shanghai China and USA. Dr. Shrivastava has significant industrial experience of collaborating with industry and government organizations at SanDisk Semiconductors; he has made significant contribution to the design development of memory products. He has contributed to the development and delivery of Five-Year Integrated B.Tech.–M.Tech. Program (Electrical Engineering) and master’s program (Power Systems) at Gautam Buddha University Greater Noida. He has extensive experience academic administration in various capacity of Dean (Research & Consultancy), Dean (Student Welfare), Faculty In-charge (Training & Placement), Faculty In-charge (Library), Nodal Officer (Academics, TEQIP-III), Nodal Officer RUSA, Experts in various committees in AICTE, UGC, etc. Dr. Shrivastava has carried out research and consultancy and attracted significant funding projects from Ministry of Human Resources & Development, Government of India, Board of Research in Nuclear Science (BRNS) subsidiary organization of Bhabha Atomic Research Organization. Dr. Shrivastava has published over 80 journal articles, presented papers at conferences, and has published several chapters in books. He has supervised 05 Ph.D. and 16 master’s students and currently supervising several Ph.D. students. His diversified research interests are in the areas of reliability engineering, renewable energy, and conventional power systems which include Wind, Photovoltaic (PV), Hybrid Power Systems, Distributed Generation, Grid Integration of Renewable Energy, Power Systems Analysis, and Smart Grid. Dr. Shrivastava is Editor/ Associate Editor of the Journals, International Journal of Swarm Intelligence, (IJSI) and International Journal of System Assurance Engineering and Management. He is Fellow of the Institution of Engineers (India) and Senior Member of the Institute of Electrical and Electronics Engineers (IEEE).

**Dr. Jagdish Chand Bansal** is Associate Professor (Senior Grade) at South Asian University New Delhi and Visiting Faculty at Maths and Computer Science, Liverpool Hope University UK. Dr. Bansal obtained his Ph.D. in Mathematics from IIT Roorkee. Before joining SAU New Delhi, he worked as Assistant Professor at ABV-Indian Institute of Information Technology and Management Gwalior and BITS Pilani. His primary area of interest is Swarm Intelligence and Nature-Inspired Optimization Techniques. Recently, he proposed a fission-fusion social structure-based optimization algorithm, Spider Monkey Optimization (SMO), which is being applied to various problems in the engineering domain. He has published more than 70 research papers in various international journals/conferences. He is Section Editor (Editor-in-Chief) of the journal *MethodsX* published by Elsevier. He is Series Editor of the book series *Algorithms for Intelligent Systems (AIS)*, *Studies in Autonomic, Data-driven and Industrial Computing (SADIC)*, and *Innovations in Sustainable Technologies and Computing (ISTC)* published by Springer. He is also Associate Editor of *Engineering Applications of Artificial Intelligence (EAAI)* and *ARRAY* published by Elsevier. He is General Secretary of the Soft Computing Research Society (SCRS). He has also received Gold Medal at UG and PG levels.

**B. K. Panigrahi** is Professor at the Electrical Engineering Department, IIT Delhi, India. Prior to joining IIT Delhi in 2005, he has served as Faculty in Electrical Engineering Department, UCE Burla, Odisha, India, from 1992 to 2005. He is Fellow of INAE, India. His research interest includes application of soft computing and evolutionary computing techniques to power system planning, operation, and control. He has also working in the field of bio-medical signal processing and image processing. He has served as Editorial Board Member, Associate Editor, and special issue Guest Editor of different international journals. He is also associated with various international conferences in various capacities. He has published more than 100 research papers in various international and national journals.

# Control Strategies for Blood Pressure Regulation in the Diabetic Patients Post Surgery



P. V. Gopi Krishna Rao, R. Hanuma Naik, N. Sreenivasa Rao, G. Sowmya,  
and M. V. Rajasekhar

**Abstract** In modern years, most patients have diabetic, mean blood pressure and glucose associated health conditions, which can be treated by infusion of an antidote, although the dosage amount depends on the severity of the individual. The monitoring and regulation of the degree of dose is therefore critical in improving the health status of patients. This paper suggests that the dose of the medication infusion be regulated and managed on the basis of its amount. This is done by developing an integrated monitoring device that increases safety in less time and reduces healthcare costs. A statistical model of patient reaction to drugs is obtained in this article. The model comprises five dimensions that range from patient to patient based on their drug response. The key purpose of the documentation is to enhance the efficiency and robustness of medication distribution activities. This Internal model control (IMC) based Proportional integral derivative (PI/PID) controller is introduced as a control system for patient distribution of drugs that will provide enhanced robustness and efficiency. The IMC driven PI/PID system has just one calibration parameter ( $\lambda$ ), which is calibrated depending on the highest sensitivity ( $M_S$ ). This method does not involve complex mathematical equations.

**Keywords** Internal model control · PID tuning; diabetic · Glucose level · Robust control · Performance · Antidote · MABP

## 1 Introduction

Mean arterial blood pressure (MABP) is one of the physiological factors to be controlled under appropriate limits during anesthesia, pre- and post-operative time. In general, postoperative problems, particularly adult cardiac patients have elevated

---

P. V. Gopi Krishna Rao (✉) · R. Hanuma Naik · M. V. Rajasekhar  
Rajeev Gandhi Memorial College of Engineering and Technology, Nandyal, Andra Pradesh, India  
e-mail: [p.vgopikrishnarao@rgmcet.edu.in](mailto:p.vgopikrishnarao@rgmcet.edu.in)

N. Sreenivasa Rao · G. Sowmya  
Santhiram Engineering College, Nandyal, Andra Pradesh, India

blood pressure, which escalate due to hypertension, notably after coronary artery bypass graft, valve replacement and pulmonary surgery [1–3]. It is important to monitor and regulate blood pressure (BP) to avoid bleeding from stitches in a patient’s cardiac surgery to enhance healing [2]. The correct MABP regulation medication is sodium nitroprusside (SNP), which has developed as an important vasodilator product [2–7]. Manual monitoring of MABP by hospital staff utilizing SNP is frequently stringent, meek and of low consistency due to differences in the reaction of patients to this substance regulation in blood pressure and regulated medication release over a prolonged period of time. Such factors also driven researchers to explore an automated management device that increases patient safety over a shorter amount of time and therefore decreases the incidence of disease [8–12]. P and PI controllers do not deliver the necessary output during induction due to their slow response. This promotes the option of a strategy where the configuration of the device includes the individual as an essential part of the system [13]. This solution is given by the Internal Model Control (IMC) framework, and the PID controller developed and calibrated using the IMC methodology should provide optimal efficiency, robustness and fast disturbance recovery [14–16]. The IMC-based PID controller would also increase the consistency of medical treatment and managed distribution of medications [14–16]. The key objective of the proposed research is the design of the controller to achieve efficiency, disturbance recovery and robustness.

The efficiency of the IMC calibrated PID controller meets output requirements such as optimum peak overshoot, steady-state offset, and durable stability. This approach records precise regulation of MABP as opposed to P and PI controls modified using traditional techniques.

## 2 Internal Model Control

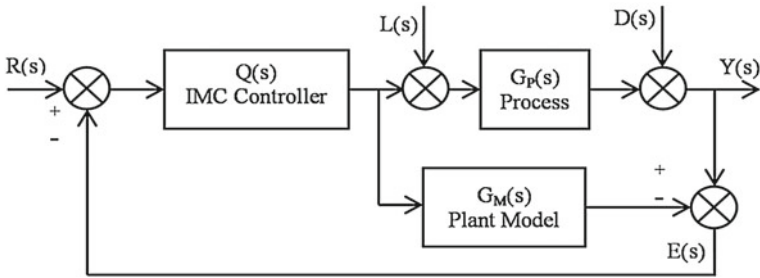
The efficiency of the IMC calibrated PID controller meets output requirements such as optimum peak overshoot, steady-state offset, and durable stability. This approach records precise regulation of MABP as opposed to P and PI controls modified using traditional techniques.

Garcia and Morari coined the concept of internal model control; the process model is clearly an integral part of the controller [14–18]. The IMC system is shown in Fig. 1. Where,  $Q(s)$  is the controller,  $G_M(s)$  is the plant model and  $G(s)$  is the actual plant/process [19–23].

The design of the IMC involves the following steps.

### 2.1 Factorization

It includes factorizing the transfer function into invertible  $G_{M-}(s)$  and non invertible parts  $G_{M+}(s)$ . The factor containing right hand poles zeros or time delays become the



**Fig. 1** Basic IMC structure

poles when the process model is inverted leading to internal stability. So this is a non-invertible part which has to be removed from the transfer function. Mathematically, it is given as Eq. (1) [20–24]

$$G_M() = G_{M-}()G_{M+}() \quad (1)$$

## 2.2 Design of IMC Control

The IMC is the inverse of the invertible part of the process model. It given as Eq. (2)

$$Q'(s) = [G_{M-}(s)]^{-1}, \quad (2)$$

$Q'(s)$  will be steady, yet may not be appropriate [30–34].

## 2.3 Adding Filter

Equation (3) is responsible for the generic transfer function of the system/controller. The value of the polynomial denominator will be almost equal to or greater than the numerator in order to render the system/controller semi-proper or worthy of physically understanding it [14, 17–25].

$$T(s) = Z(s)/P(s) \quad (3)$$

In order to make the controller proper mathematically a low pass filter  $F(s)$  is augmented to Eq. (2) and results in Eqs. (4) and (5) [14, 17–25]

$$Q(s) = Q'(s) * F(s) \quad (4)$$

$$Q(s) = [G_{M-}(s)]^{-1} * F(s) \quad (5)$$

## 2.4 Low Pass Filter

The filter  $F(s)$  described above is defined to have the form of Eq. (6) which represents a low pass filter [14, 17–25].

$$F(s) = 1/(\lambda s + 1)^n \quad (6)$$

where  $\lambda$  is the filter tuning parameter and  $n$  is the order of the process. The value of  $\lambda$  defines the performance and robustness of the controller. Maximum sensitivity  $M_s$  specification is an effective robustness measure and most recent inquisitive approach, which is defined by Eq. (7) [21]

$$M_s = \left| \frac{1}{C(j\omega)G(j\omega) + 1} \right| \quad (7)$$

The estimate of  $\lambda$  for IMC design of first order pulse dead time (FOPDT) system, is obtained by Eq. (8)

$$\lambda = \frac{1.508 - 0.451M_s}{1.45M_s - 1.508} T_i \quad (8)$$

A small value of  $M_s$  ensures high stability margin. So, the typical value of  $M_s$  is general adjusted to be in the range of 1.2–2.0 [14, 21, 26]

## 3 Design of the IMC Based PID Control

The purpose of this segment is to develop a basic feedback controller as an internal model system. The IMC rule for sundry modern cycle transfer functions is similar to the PID input system [14, 17, 21, 23, 25, 27], and The PID control algorithm is the basic input that has been developed for industrial processes due to its effortless and realistic applications. The regular IMC input equivalence is obtained by modifying Fig. 2. The standard feedback controller  $G_{PID}(s)$  or  $C(s)$  represented Fig. 2 and is the function of Plant model  $G_M(s)$  and IMC controller  $Q(s)$  shown in Eq. (9) is the IMC based PID relation, is approximated to the ideal PID controller of the form given by Eq. (10) [14, 20, 21].

$$C(s) = \frac{Q(s)}{[1 - G_M(s)Q(s)]}, e^{-\theta s} = \frac{(1 - 0.5\theta s)}{(1 + 0.5\theta s)} \quad (9)$$



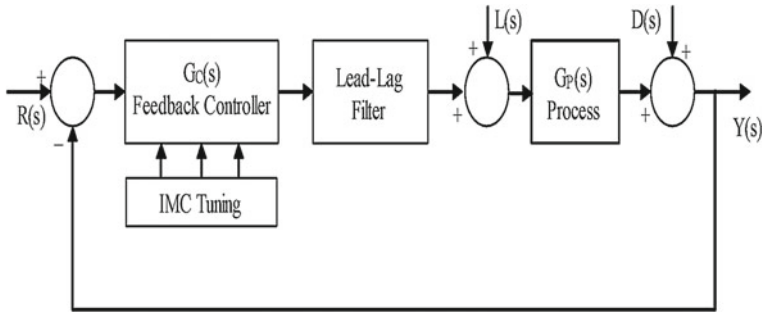


Fig. 2 Feedback control structure

$$G_{PID}(s) = C(s) = K_P[T_i T_d s^2 + T_i s + 1/T_i s] \quad (10)$$

In order to create a PID controller based on the IMC concept,  $Q(s)$  is not made appropriate. The  $Q(s)$  a polynomial numerator of one order is rendered higher than the polynomial denominator with a derivative alternative and this is important for receiving the PID controller [8, 14, 18, 27–29]. First order Padè approximation is used for the delay element  $\theta$  of the plant model  $G_M(s)$  to eliminate the behavior of predictive elements in the design of the PID controller. The first order Padè approximation is represented in Eq. (9) [14, 25, 30, 31]. The PID controller tuned using IMC principle has only one adjusting term  $\lambda$  which provides both performance and robustness in spite of model uncertainties.

The following steps are used in the IMC-Based PID control system design:

- Find the IMC controller transfer function, which includes a filter to make it semi-proper.
- Find the equivalent standard feedback controller using the transformation [21].

$$C(s) = \frac{Q(s)}{[1 - G_M(s)Q(s)]} \quad (11)$$

- Compare the above equation with this PID controller from and find  $K_P$ ,  $T_i$  and  $T_d$  [19].

$$G_{PID}(s) = C(s) = K_P[T_i T_d s^2 + T_i s + 1/T_i s] \quad (12)$$

- Perform closed-loop simulation for both the perfect model case and case with model mismatch. Choose the desired value for  $\lambda$  as a trade-off between performance and robustness.

## 4 Simulation Results

The MATLAB simulations are carried out on different patients based on their drug sensitivity (Nominal, Sensitive and Insensitive). The performance of the IMC based PI/PID, IMC and P controller to regulate the blood pressure by -30 mmHg to SNP drug infusion rate and error of different cases is carried out.

### *Case 1: Sensitive Patient*

IMC-Based PID design for a First order plus dead time process of sensitive patient of Eq. (13) is [24, 32–34]

$$G_M(s) = \frac{-9e^{-20s}}{(30s + 1)} \quad (13)$$

*Step 1:* First order Pade' approximation

$$e^{-\theta s} = \frac{(1 - 0.5\theta s)}{(1 + 0.5\theta s)} \quad (14)$$

$$G_M(s) = \frac{-9(1 - 10s)}{[(1 + 10s)(1 + 30s)]} \quad (15)$$

*Step 2:* Factorising the sensitive patient model with Pade' approximation into invertible Eq. (16) and non-invertible portions Eq. (17)

$$G_{M-}(s) = \frac{-9}{[(1 + 10s)(1 + 30s)]} \quad (16)$$

$$G_{M+}(s) = (1 - 10s) \quad (17)$$

*Step 3:* IMC controller is

$$Q(s) = \frac{[(30s + 1)(1 + 10s)]}{[-9(97.727s + 1)]} \quad (18)$$

*Step 4:* Closed Loop Controller (PID) is

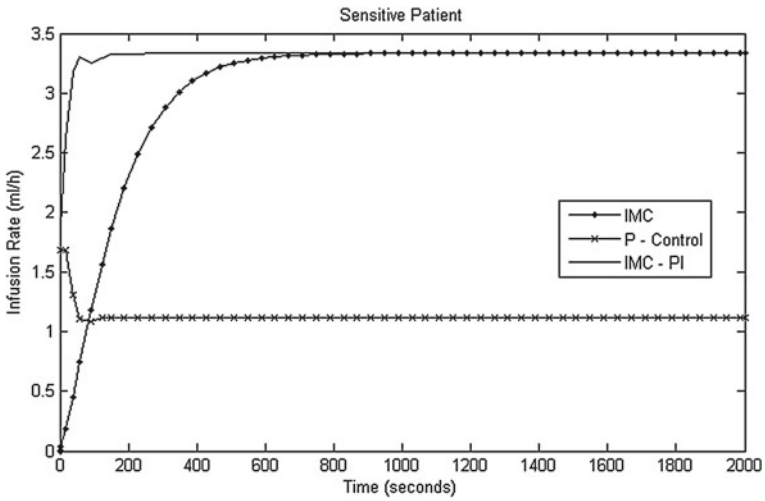
$$C(s) = \frac{\frac{(30s+1)(1+10s)}{[-9(97.727s+1)]}}{1 - (1 - 10s)(97.727s + 1)} \quad (19)$$

The  $K_P$ ,  $T_i$  and  $T_d$  values are obtained by comparing Eq. (19) with the standard PID equation Eq. (10).

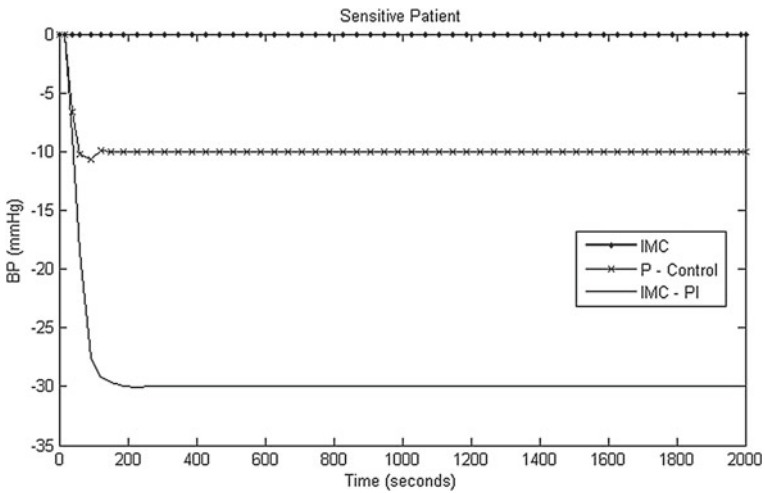
The simulation of the results of drug infusion rate, Blood pressure recovery and error of sensitive patient are represented in Figs. 3, 4 and 5 respectively.

*Case 2: Nominal Patient*

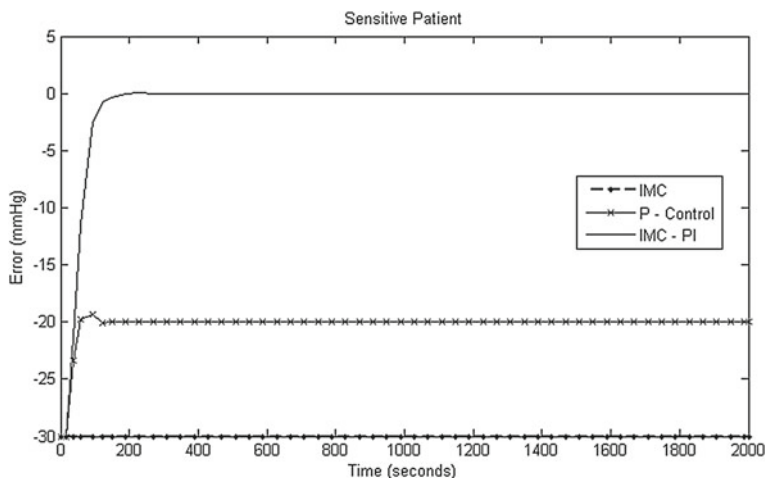
The mathematical model of nominal patient is given by Eq. (20) [24, 32–34]



**Fig. 3** SNP drug infusion rate in sensitive patient



**Fig. 4** Blood pressure recovery with drug infusion in sensitive patient



**Fig. 5** Error in BP regulation in sensitive patient

$$G_M(s) = -0.7143e^{-30s} \frac{(1 + 0.4e^{-45s})}{(1 + 40s)} \quad (20)$$

*Step 1:* First order Pade' approximation of time delay element is Eq. (21)

$$e^{-30s} = \frac{(1 - 15s)}{(1 + 15s)}, e^{-45s} = \frac{(1 - 22.5s)}{(1 + 22.5s)} \quad (21)$$

*Step 2:* Factorising the nominal patient model with Pade' approximation into invertible Eq. (22) and non-invertible portions Eq. (23)

$$G_{M-}(s) = \frac{-0.7143}{(1 + 15s)(1 + 40s)(1 + 22.5s)} \quad (22)$$

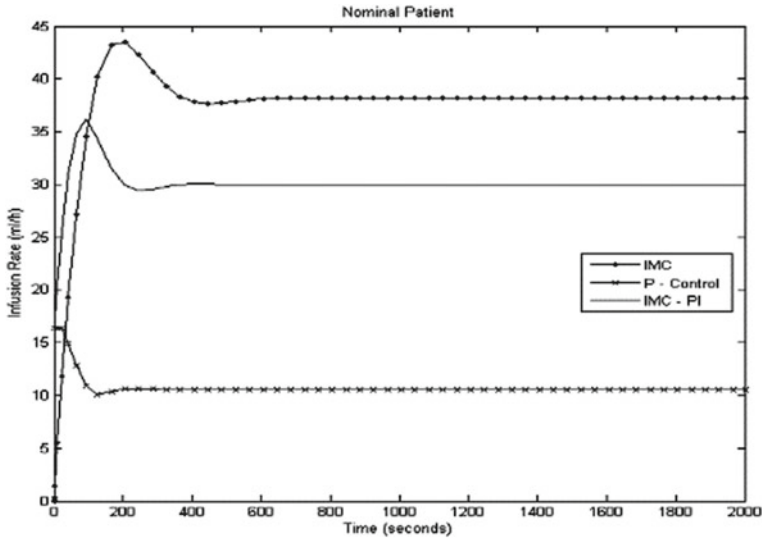
$$G_{M+}(s) = \frac{(1 - 15s)}{[(1 + 22.5s) + 0.4(1 - 22.5s)]} \quad (23)$$

*Step 3:* The IMC controller is

$$Q(s) = \frac{(1 + 40s)(1 + 22.5s)(1 + 15s)}{-0.7143} * \frac{1}{(1 + \lambda s)} \quad (24)$$

where value of  $\lambda$  as 97.273, which is having range  $\lambda > 0.2 \tau$ .

*Step 4:* The closed loop controller (PID) is Eq. (25)



**Fig. 6** SNP drug infusion rate in nominal patient

The simulation of the results of drug infusion rate, Blood pressure recovery and error of nominal patient are represented in Figs. 6, 7 and 8 respectively.

$$C(s) = \frac{\frac{(1+40s)(1+22.5s)(1+15s)}{-0.7143} * \frac{1}{(1+\lambda s)}}{1 - \left[ \frac{(1+40s)(1+22.5s)(1+15s)}{-0.7143} * \frac{1}{(1+\lambda s)} * [-0.7143e^{-30s}] \frac{(1+0.4e^{-45s})}{(1+40s)} \right]} \quad (25)$$

### Case 3: Insensitive Patient

The mathematical representation of the dynamics of insensitive patient are depicted in Eq. (26) [24, 32–34]

$$G_M(s) = -0.1786e^{-60s} \frac{(1 + 0.4e^{-75s})}{(1 + 60s)} \quad (26)$$

*Step 1:* First order Pade' approximation of time delay element is Eq. (27)

$$e^{-60s} = \frac{-30s + 1}{30s + 1}, \quad e^{-75s} = \frac{-37.5s + 1}{37.5s + 1} \quad (27)$$

*Step 2:* Factorising the nominal patient model with Pade' approximation into invertible Eq. (28) and non-invertible portions Eq. (29)

$$G_{M-}(s) = \frac{-0.1786}{(60s + 1)(30s + 1)(37.5s + 1)} \quad (28)$$

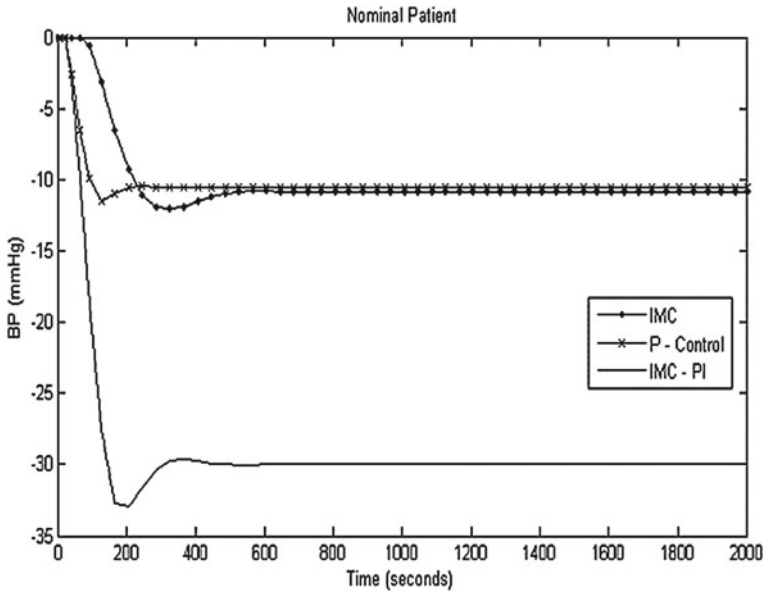


Fig. 7 Blood pressure recovery with drug infusion in nominal patient

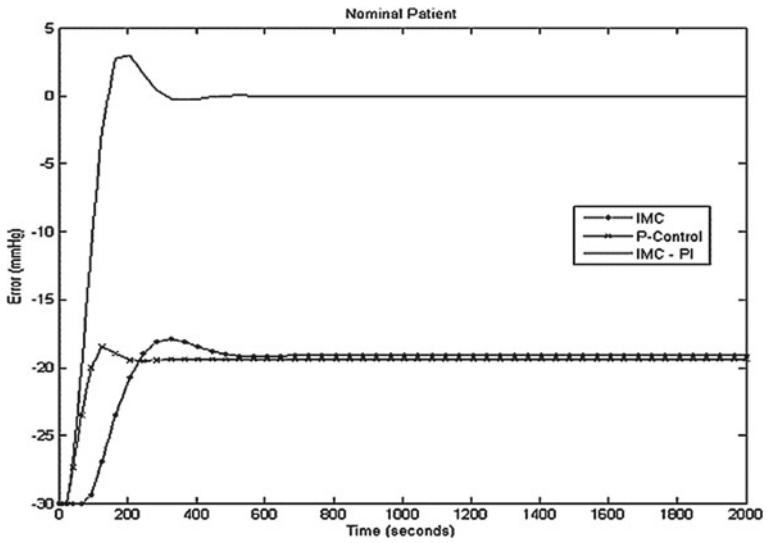


Fig. 8 Error in BP regulation in nominal patient

$$G_{M+}(s) = (30s + 1)(22.5s + 1.4) \tag{29}$$

Step 3: The IMC controller is

$$Q(s) = \frac{(60s + 1)(30s + 1)(37.5s + 1)}{-0.1786} \times \frac{1}{97.727s + 1} \tag{30}$$

Step 4: The closed loop controller (PID) is

$$C(s) = \frac{(60(30s + 1)(s + 1)(37.5s + 1))}{[-0.1786(97.727s + 1) * [1 - (-30s + 1)(22.5s + 1)]]} \tag{31}$$

The simulation of the results of drug infusion rate, Blood pressure recovery and error of insensitive patient are represented in Figs. 9, 10 and 11 respectively.

Table 1 depicts the PI tuning values obtained using IMC technique for three cases patients and also the IMC controller. The results described indicate that the PI/PID controller tuned using IMC principle provides best possible performance for all nature of patients for faster recovery and regulation of Mean Arterial Blood Pressure in comparison to other controller methodologies considered. This helps the patient to recover faster post surgery and regulates MABP in elderly persons with hypertension. This technique can be extended to other applications relating to biomedical, medical electronics and assistive devices.

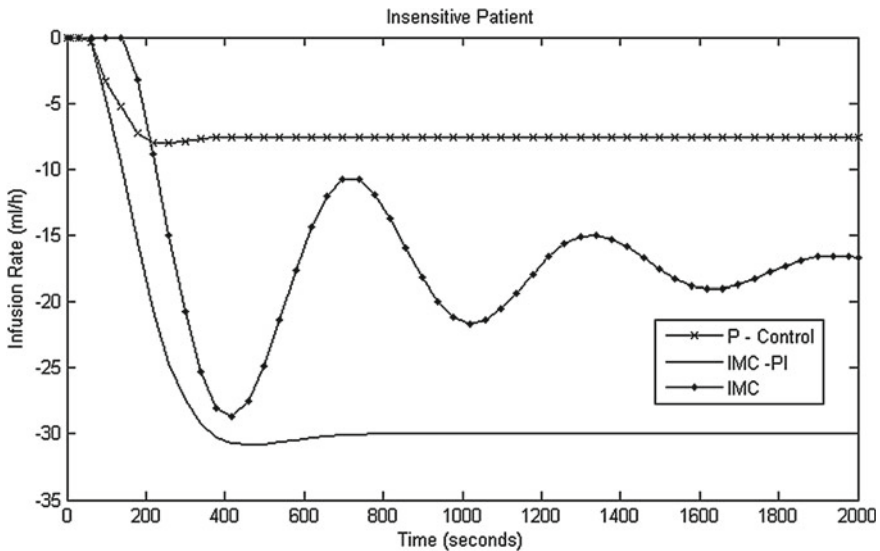


Fig. 9 SNP drug infusion rate in insensitive patient

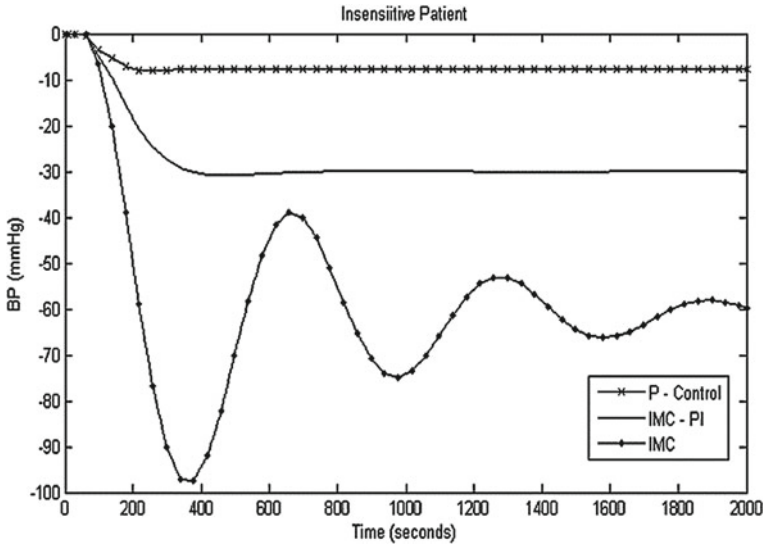


Fig. 10 Blood pressure recovery with drug infusion in Insensitive patient

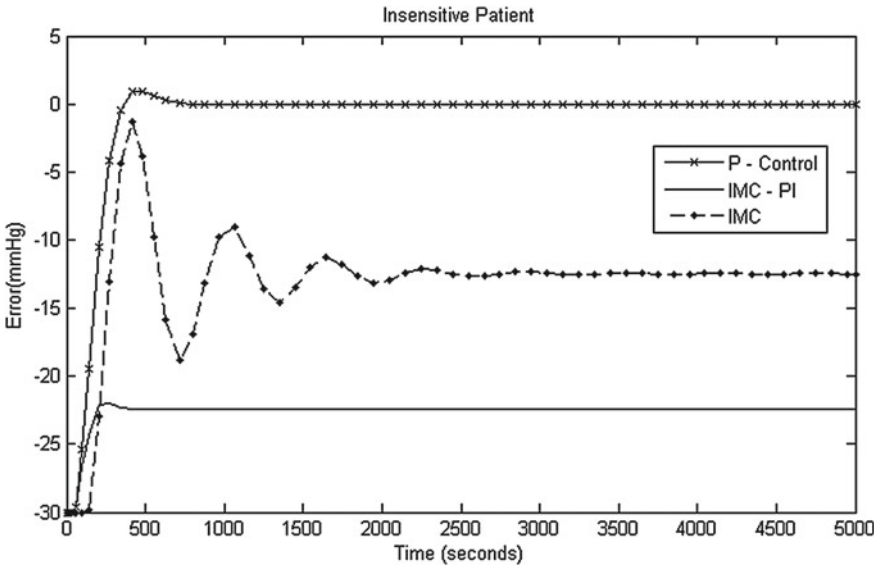


Fig. 11 Error in BP regulation in insensitive patient



**Table 1** PID tuning values and IMC controller

Patient	$K_p$	$K_i$	$Q(s)$
Sensitive	-0.0561	-0.0019	$\frac{(30s+1)}{(-879.543s-9)(1+97.7273s)}$
Insensitive	-1.3625	-0.0227	$\frac{(-60s+1)}{(17.4540s+0.1786)(1+97.7273s)}$
Nominal	-0.5450	-0.0136	$\frac{(-40s+1)}{(69.80s+1)(1+97.7273s)}$

## 5 Conclusion

Blood Pressure is a chronic disease, which causes serious health problems like kidney failure and heart stroke and recovery post-surgery is crucial in such patients. To control the mean arterial blood pressure a precise and accurate amount of external antidote SNP is needed to be injected into the human body. In this study, an IMC based PI/PID Controller is constructed for regulating the MABP and infusion of SNP in various nature of patients. The proposed methodology has provided faster recovery of MABP and precise control of SNP infusion, helping in faster recovery of patients.

## References

- Behbehani K, Cross RR (1991) A controller for regulation of mean arterial blood pressure using optimum nitroprusside infusion rate. *IEEE Trans Bio-med Eng* 38:513–521
- Frei C, Derighetti M, Morari M, Glattfelder A, Zbinden A (2000) Improved regulation of mean arterial blood pressure during anesthesia through estimates of surgery effects. *IEEE Trans Biomed Eng* 47:1456–1464
- Bajzer Ž, Maruši M, Vuk-Pavlovi S. 919960. Conceptual frameworks for mathematical modelling of tumor growth dynamics, *Math Comput Model* 23:31–46
- Bergman R, Phillips L, Cobelli C. 919810, Physiologic evaluation of factors controlling glucose tolerance in man, *J Clin Invest* 68:1456–1467
- Jeffrey AM, Xiaohua X, Craig IK (2003) When to initiate HIV therapy: a control theoretic approach. *IEEE Trans Bio-med Eng* 50:1213–1220
- Hernandez L, Shankar R, Pajunen G (1989) A microprocessor based drug infusion control system employing a model reference adaptive control algorithm to regulate blood pressure in I.C.U. patients. In: *Proc IEEE southeastcon*, pp 1261–1266
- Reves JG, Sheppard LC, Wallach R, Lell WA (1978) Therapeutic uses of sodium nitroprusside and an automated method of administration. *Int Anesthesiol Clin* 16:51–88
- Kovio AJ, Smollen VF, Barile RV (2012) An automated drug có có Fig. 9. Comparison of various techniques using IMC design. *Biomed Eng Lett* 2:240–248
- Sheppard LC, Shotts JF, Robertson NF, Wallace FD, Kouchoukos NT (1979) Computer controlled infusion of vasoactive drugs in post cardiac surgical patients. *Conf Proc IEEE Eng Med Biol Soc.* 280–284
- Slate JB, Sheppard LC, Rideout VC, Blackstone EH (1979) A model for design of a blood pressure controller for hypertensive patients. In: *Proceedings of IEEE EMBS Conference*, pp 867–872
- Slate JB, Sheppard LC (1982) A model-based adaptive blood pressure controller. In: *Proceedings of IFAC symposium on identification and system parameter estimation*, Washington DC, pp 1437–1442

12. Martin JF, Schneider AM, Smith NT (1987) Multiple-model adaptive control of blood pressure using sodium nitroprusside. *IEEE Tran Bio-med Eng BME-34*, 603–611
13. Kaufman H, Roy R, Xu X (1984) Model reference adaptive control of drug infusion rate. *Automatica* 20:205–209
14. Arnsparger JM (1983) Adaptive control of blood pressure, *IEEE T Bio-med Eng BME-30*:168–176
15. Hahn J, Edison T, Edgar TF (2002) Adaptive IMC control for drug infusion for biological systems. *Control Eng Pract* 10:45–56
16. Enbiya E, Hossain E, Mahieddine F (2009) Performance of optimal IMC and PID Controllers for blood pressure control. *IFMBE Proc* 24:89–94
17. Morari M, Zafriou E (1989) Robust process control. Prentice-Hall, Englewood Cliffs, NJ
18. Bequette BW (2003) Process control: modeling, design, and simulation. Prentice-Hall Inc., Upper Saddle River, New Jersey, USA
19. Saxena S, Hote YV (2012) Advances in internal model control technique: a review and future prospects. *IETE Tech Rev* 29(6):461–472
20. Wayne Bequette B (2002) Process control, modeling, design and simulation. Prentice Hall International Series in the Physical Chemical Engineering Science
21. Panyam Vuppu GKR, Makam Venkata S, Kodati S (2015) Robust design of PID controller using IMC technique for integrating process based on maximum sensitivity. *J Control Autom Electr Syst* 26:466–475
22. Gopi Krishna Rao PV, Subramanyam MV, Satyaprasad K (2014) Design of internal model control-proportional integral derivative controller with improved filter for disturbance rejection. *Syst Sci Contr Eng* 2(1):583–592
23. Hanuma Naik R, Ashok Kumar DV, Gopikrishna Rao PV (2020) Improved centralised control system for rejection of loop interaction in coupled tank system. *Indian Chem Eng* 62(2):118–137
24. Saxena S, Hote YV (2012) A simulation study on optimal IMC based PI/PID controller for mean arterial blood pressure. *Biomed Eng Lett* 2:240–248
25. Brosilow C, Joseph B (2002) Techniques of model-based control. Prentice-Hall, Englewood Cliffs, NJ
26. Zhao Z, Liu Z, Zhang J (2011) IMC-PID tuning method based on sensitivity specification for process with time-delay. *J Cent South Univ Technol* 18:1153–1160
27. Mäkilä P, Partington JR, Gustafsson TK (1995) Worst-case control relevant identification. *Automatica* 31:1799–1819
28. Shook DS, Mohtadi C, Shah SL (1992) A control-relevant identification strategy for GPC. *IEEE Trans Automat Contr* 37:975–980
29. Slate JB (1980) Model-based design of a controller for infusion sodium nitroprusside during postsurgical hypertension, Ph.D. Thesis, Univ. Wisconsin-Madison
30. Hu W, Xiao G, Cai W (2011) PID controller design based on two degrees-of-freedom direct synthesis. In: Chinese control decision conference, pp 629–634
31. Parker RS, Doyle FJ (2001) Control-relevant modelling in drug delivery. *Adv Drug Deliv Rev* 48:211–228
32. Slate JB, Sheppard LC, Rideout VC, Blackstone EH (1980) Closed loop nitroprusside infusion: modelling and control theory for clinical application. In: Proceedings of IEEE international symposium circul system, pp 482–488
33. Jones RW, Tham MT (2005) An undergraduate CACSD project: the control of mean arterial blood pressure during surgery. *Int J Eng Sci* 21:1043–1049
34. Auer LM, Rodler H (1981) Microprocessor control of drug infusion for automatic blood-pressure control. *Med Biol Eng Comput* 19:171–174

# Detecting Obfuscated Malware Using Graph Neural Networks



Quang-Vinh Dang 

**Abstract** In this paper, we propose a method for detecting obfuscated malware on Android using graph neural networks (GNNs). Obfuscation is a well-known technique used by malware creators to hide themselves from being detected by anti-virus softwares. Our approach uses GNNs to represent the code of an Android app as a graph and applies graph convolutional networks to classify the app as benign or malicious. We evaluated our method on a real-world dataset of Android apps and compared it to other state-of-the-art algorithms. Our results show that our method outperformed the other algorithms in many different metrics. The proposed method has potential for application in real-world scenarios, as it can detect obfuscated malware with high accuracy.

**Keywords** Obfuscated malware · Malware detection · Graph theory · Graph algorithms · Graph neural networks

## 1 Introduction

The increasing interconnectedness of the world has led to a dramatic rise in the risk of cyber attacks. Malware, or malicious software, has been a persistent threat to internet security for decades, and its impact on individuals and businesses alike can be devastating. The Global Threat Landscape Report by FortiGuard released in 2023 [10] highlighted that malware continues to pose a significant threat to internet security, with attackers becoming increasingly sophisticated in their techniques. To further exacerbate the issue, modern malware authors employ obfuscation techniques to evade detection. Obfuscation is a method of making programs difficult to comprehend, which can hinder traditional static analysis techniques from detecting the presence of such malware [20].

The use of machine learning and artificial intelligence (AI) is becoming increasingly prevalent in the field of cybersecurity. While a static analysis tool is difficult

---

Q.-V. Dang (✉)

Industrial University of Ho Chi Minh City, Ho Chi Minh City, Vietnam

e-mail: [dangquangvinh@iuh.edu.vn](mailto:dangquangvinh@iuh.edu.vn)

to update to keep pace with the updating velocity of new malware, other learning systems are designed to adjust themselves and process new types of malware in an automatic fashion [6, 14]. The most important difference between different machine learning models is the features fed to them, which determine the characteristics of the model. For example, a model might prioritize running time over classification metric. As machine learning research and optimization grow very fast from implementation details, many complex models can be executed with less running time than before.

There are multiple ways to analyze and assess software to detect malware [18]. In Sect. 2, we review some of these methods. In this paper, we apply the memory analysis technique [3], which uses dynamic analysis to analyze software based on its behavior. Our proposed method aims to improve the accuracy of malware detection using a novel algorithm and extending state-of-the-art research studies to the problem of multiclass case.

The use of AI and machine learning in cybersecurity has the potential to revolutionize the field. AI algorithms can analyze vast amounts of data and identify patterns, which can be used to predict and prevent cyber attacks. However, the effectiveness of these systems relies heavily on the quality and quantity of data available to them. As more data becomes available and the algorithms continue to improve, it is likely that AI will become an even more essential tool in the fight against cybercrime.

Moreover, AI can also assist in identifying and responding to cyber attacks in real time [17]. AI systems can monitor network traffic and detect anomalies, such as unusual activity or traffic patterns, which may indicate a cyber attack in progress. Once an attack has been identified, the AI system can automatically respond and mitigate the threat, potentially preventing significant damage. This real-time response is critical as cyber-attacks can occur quickly, and the longer it takes to identify and respond to an attack, the more damage it can cause.

Another area where AI can play a significant role in cybersecurity is in the area of access control. Access control is the practice of limiting access to sensitive information or resources to authorized individuals only. AI can help in identifying and authenticating users and devices, detecting and preventing unauthorized access attempts, and monitoring access logs to identify potential security threats. This can be particularly useful in large organizations where access control can be a complex and challenging task.

Despite the potential benefits of AI in cybersecurity, there are also potential risks and challenges. One of the main concerns is the potential for AI systems to be hacked or manipulated by attackers. If an attacker gains access to an AI system, they can potentially use it to launch attacks or manipulate the system to their advantage. Another concern is the potential for bias in AI systems, particularly in decision-making processes, which can have significant implications for cybersecurity.

In conclusion, the use of AI and machine learning in cybersecurity has the potential to transform the field and improve our ability to prevent, detect, and respond to cyber-attacks. However, it is essential to address the potential risks and challenges associated with these systems and ensure that they are designed and implemented in a secure and responsible manner. As the field of cybersecurity continues to evolve,

AI and machine learning will undoubtedly play an increasingly significant role in protecting our digital infrastructure and assets.

In this paper, we focus on fighting malware on Android systems by applying graph neural networks (GNN) [8, 21] to detect Android malware more efficiently. The GNN can learn the connections between malware and devices to provide a better understanding of the attacks. We evaluate our proposal using real-world dataset and it outperformed state-of-the-art algorithms.

## 2 Related Works

### 2.1 Malware Obfuscation Techniques

Malware is a growing concern in the world of cybersecurity, and with each passing day, malware authors are becoming more sophisticated in their attempts to evade detection [1]. There are several methods that these authors use to hide their malware from detection tools, and researchers have identified a range of techniques employed by these authors to obfuscate the behavior of malware.

One common technique is the use of encryption, where a malware is encrypted into a coded content that is difficult for manual analyzers to understand [16]. This technique makes it hard for a human analyst to identify the nature of the malware, but the encrypted content is often constant, which makes it detectable by signature matching techniques [9]. Signature matching involves comparing a pattern of code in the malware to a database of known malware signatures, and if there is a match, it is flagged as malware.

Another technique used by malware authors is dead code insertion [11]. In this technique, a malware is inserted with some unused code that does not affect its behavior but makes it appear different from its original version. This technique works by changing the visual appearance of the malware, making it harder for detection tools to recognize it.

Register reassignment and subroutine reordering are other techniques employed by malware authors to evade detection [20]. In these techniques, registers or subroutines are swapped in a random order, thereby changing the behavior of the malware completely. This technique makes it difficult for detection tools to recognize the malware and protect against it.

The use of these techniques by malware authors has made the job of cybersecurity experts much more challenging, and it highlights the need for the development of advanced detection and prevention tools.

We can also rewrite the code so no one can understand it, but it still functions. One example is presented in Fig. 1.

**Fig. 1** An example of code obfuscation

Original Source Code Before Control Flow Obfuscation	Reverse-Engineered Source Code After Control Flow Obfuscation
<pre>public int CompareTo(Object o) {     int n = occurrences -         ((WordOccurrence)o).occurrences;     if (n == 0) {         n = String.Compare             (word, ((WordOccurrence)o).word);     }     return (n); }</pre>	<pre>private virtual int _a(Object A_0) {     int local0;     int local1;     local 10 = this.a - (c) A_0.a;     if (local10 != 0) goto #0;     while (true) {         return local1;     }     if: local10 =         System.String.Compare(this.b, (c)         A_0.b);         goto #0; }</pre>

## 2.2 Malware Detection Techniques

Malware detection is a crucial aspect of cybersecurity. There are several methods and techniques for detecting malware, and researchers are constantly developing new approaches to improve the accuracy and efficiency of malware detection systems.

A popular detecting algorithm is called signature-based detection, which involves the extraction of signatures from malware and the storage of these signatures in a signature database. Rules are then designed to determine whether a software is malware. This technique belongs to the static analysis approach, as it does not require observation of the behavior of the applications. However, this method can be easily bypassed by malware that is modified to evade detection by changing its signature.

Another approach is to dynamically analyze the behavior of the malware. In this approach, the malware detector monitors the behavior of the applications. This technique belongs to the dynamic analysis approach, which involves the observation of the behavior of the applications at runtime. Malware detectors monitor different aspects of the behavior of the malware, such as file changes, network transmission, API calls, memory changes, and behavior in a sandbox. Sandboxing is a technique that isolates applications in a controlled environment, allowing the behavior of the malware to be observed without affecting the host system.

Machine learning has become an increasingly popular approach to malware detection in recent years, as it has shown promise in improving detection rates and reducing false positives. The authors of [3, 6] studied and assessed several well-known machine learning algorithms, such as Decision Tree, Random Forest, and Support Vector Machine (SVM) to classify malware. Other machine learning techniques used in malware detection include deep learning, reinforcement learning, and ensemble learning.

Intrusion detection is a related area of research to malware detection, which focuses on detecting unauthorized access to a network or system. The authors of [2, 4, 7, 13] evaluated various machine learning models for the problem of intrusion detection and found that gradient boosting algorithms achieved the highest performance. Other machine learning algorithms used in intrusion detection include K-Nearest Neighbor (KNN), Naive Bayes, and logistic regression.

One approach is to employ the trust score [12] to evaluate the trust of source files, or to apply techniques from computer vision [15, 19]. Graph theory is another possibility to deal with detection [5].

While there are several techniques for malware and intrusion detection, there are also techniques for obfuscating malware to avoid detection. These techniques include code obfuscation, encryption, and polymorphism. In code obfuscation, the code of the malware is modified to make it difficult to understand and reverse engineer. Encryption is used to encrypt the malware code, making it unreadable to anyone who does not have the decryption key. Polymorphism is a technique that changes the code of the malware every time it is executed, making it difficult to detect using signature-based detection techniques.

In conclusion, malware detection is an ongoing challenge for cybersecurity professionals, and the development of new techniques and approaches is critical to stay ahead of cyber threats. While signature-based detection and dynamic analysis are common techniques, machine learning algorithms have shown promise in improving detection rates. Additionally, the techniques for obfuscating malware highlight the importance of constantly evolving malware detection techniques to stay ahead of evolving cyber threats.

### 3 Methods

GNNs work by repeatedly passing messages between nodes in a graph. Each node in the graph maintains a representation of data of the neighborhood of itself, and these representations are updated by sending messages between nodes.

The messages contain information about the nodes and their neighbors, and the message-passing scheme updates the node representations based on the received messages.

This process is repeated for several iterations, allowing the nodes to exchange information and update their representations based on the global graph structure.

#### 3.1 *Types of GNNs*

Several types of GNN are available, each with its own strengths and limitations.

Some of the most common types of GNNs are:

Graph convolutional networks, or GCNs, use convolutional operations within the graph, collecting data from adjacent nodes. Their design is particularly effective for projects that require an understanding of the graph's local structure.

Similarly, graph attention networks, or GATs, use attention mechanisms to assess the significance of various nodes and connections within the graph. This functionality enables the model to skip the information that is most important by setting the corresponding weight to zero.

Lastly, GraphSAGE uses a method based on sampling to calculate node representations in an efficient manner, gathering data from the graph's nodes. This approach is effective for processing big graphs.

## 3.2 Applications of GNNs

GNNs have been shown to be effective for a variety of tasks, including:

**Social network analysis:** GNNs can be used to analyze social networks by learning representations of nodes that capture the relationships between them. This can be used for tasks such as predicting links between users or classifying nodes based on their properties.

**Knowledge graph completion:** GNNs can be used to complete knowledge graphs by inferring missing relations between entities. This can be used to improve the accuracy of knowledge graphs and make them more useful for applications such as question answering and natural language inference.

**Recommender systems:** GNNs can be used to learn user preferences for items by modeling the interactions between users and items. This can be used to provide personalized recommendations to users.

**Bioinformatics:** GNNs can be used to predict protein–ligand interactions and drug–target interactions. This can be used to discover new drugs and treatments for diseases.

## 4 Results

### 4.1 Dataset

In our research, we have employed the CIC-MalMem-2022 dataset, which is a publicly available dataset provided by the Canadian Institute for Cybersecurity (CIC) and can be accessed through their website at <https://www.unb.ca/cic/datasets/malmem-2022.html>. This dataset is specifically designed for the purpose of malware detection and analysis and has been widely used in the research community.

The dataset consists of a total of 58,596 memory dumps, with 29,298 belonging to benign software and the other 29,298 belonging to malware. These memory dumps are obtained from a diverse range of software applications and operating systems, providing a comprehensive and realistic representation of the memory usage patterns in real-world scenarios.

It is important to note that the CIC-MalMem-2022 dataset has been carefully validated and verified to ensure its quality and reliability. Additionally, the dataset has been thoroughly modified to eliminate any potential biases or inaccuracies, making it a great choice for conducting research in the field of malware detection and analysis.

The CIC-MalMem-2022 dataset has been introduced in a recent research paper by [3]. The paper provides detailed information about the dataset, including its construction, contents, and potential applications. Overall, the CIC-MalMem-2022 dataset serves as a valuable resource for researchers and practitioners in the field of cybersecurity, providing them with a reliable and comprehensive dataset for conducting research and developing new detection and analysis techniques.



The dataset under consideration is comprised of a total of 55 features that offer significant insight into various aspects of the problem at hand. These features have been carefully selected to include a wide range of parameters, such as the number of commit charges, number of protection, number of mutant handles, and several others. Each of these features contributes to a comprehensive understanding of the data, enabling more precise analysis and decision-making.

In order to conduct a thorough evaluation of the dataset, we have split it into three subsets: the training set, the validation set, and the test set. The ratio of this split is 60:20:20, respectively. This division is aimed at ensuring that the model is trained on a sufficient amount of data to achieve optimal performance, while still having enough data reserved for validation and testing purposes.

It is important to note that all experimental results are reported based on the evaluation of the test set. This is done to ensure that the results are unbiased and representative of the model’s ability to generalize to new, unseen data. By evaluating the model’s performance on the test set, we can gain a clear understanding of its strengths and weaknesses, and make informed decisions about its potential applications.

## 4.2 Results

### 4.2.1 Binary Classification

In this experiment, we evaluate the case of binary classification, similar to the work of [3]. It means that we evaluate the capability of being able to classify if a software is malware or not.

The result of the prediction is presented in Fig. 2.

We confirm that the performance of our proposed method is better than published algorithms [3]. we show the comparison in Table 1.

It takes 12 ms to perform the prediction for about 12,000 samples.

**Table 1** Comparison of performance. We used only the best models from published papers to present here

Model	Precision	Recall	F1	Accuracy
GNN (this paper)	0.9999	0.9999	0.9997	0.9997
Random Forest [3]	0.98	0.97	0.97	0.97
Naive Bayes + Random Forest + Decision Tree [3]	0.99	0.99	0.99	0.99



Fig. 2 Confusion matrix in binary prediction setting

### 4.2.2 Multi Classification

We extend the work of [3] by classifying in the case of the multi-class classification. The confusion matrix is presented in Fig. 3.

We observe that the model performs well in classifying malware and benign software. However, it is not as good at classifying the exact type of malware. To verify this assumption, we build another model to classify malware only and present the confusion matrix in Fig. 4. The phenomenon can be explained by the overlapping nature of malware.

Specifically, some malware may share common features, which can make it difficult for the model to distinguish between them. For example, a Trojan horse and a ransomware may both contain code that steals data from the victim’s computer. As a result, the model may classify wrongly a Trojan horse as ransomware, or vice versa.

This phenomenon can be mitigated by using a more sophisticated model that is able to learn the subtle differences between different types of malware. However, this can be a challenging task, as malware is constantly evolving and new variants are being created all the time.

Despite this challenge, the use of machine learning for malware detection is a promising area of research. As machine learning algorithms continue to improve, they will become increasingly effective at detecting and classifying malware. This will help to protect users from the ever-growing threat of malware attacks.

Furthermore, as we can see in Fig. 5, classifying subclasses of malware in fact does not yield a worse performance compared to the three-class classification case. Hence, the ambiguity lies on the difference of classes but not subclasses.

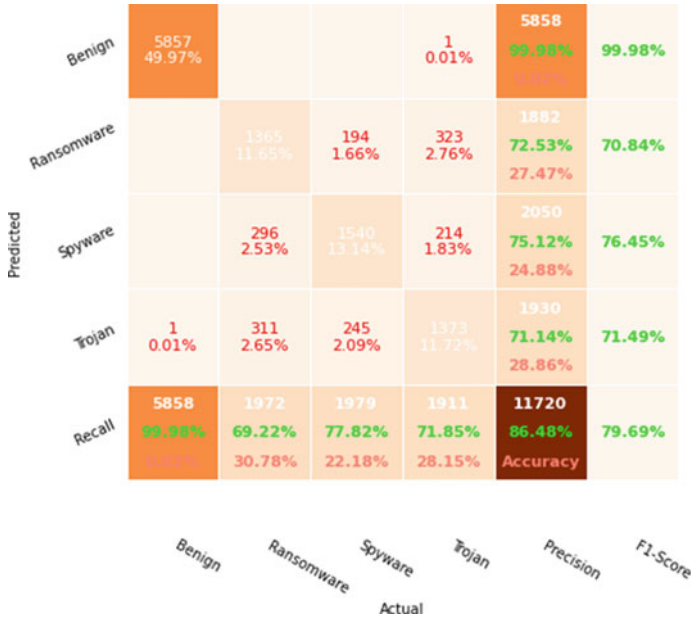


Fig. 3 Confusion matrix of multi-classification

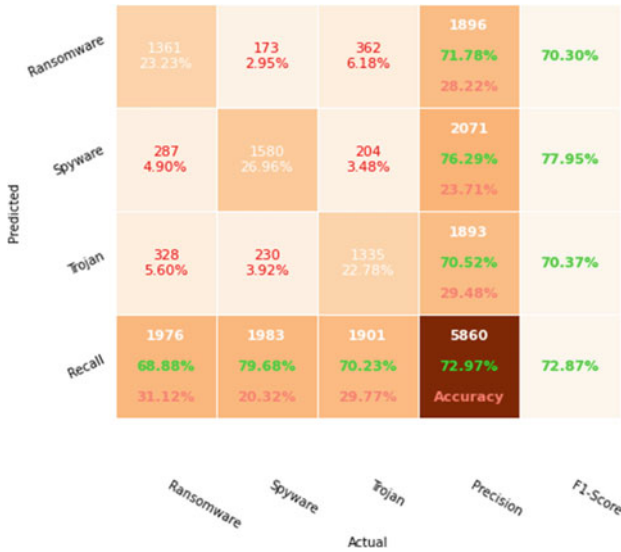


Fig. 4 Confusion matrix in classifying malware versus no-malware

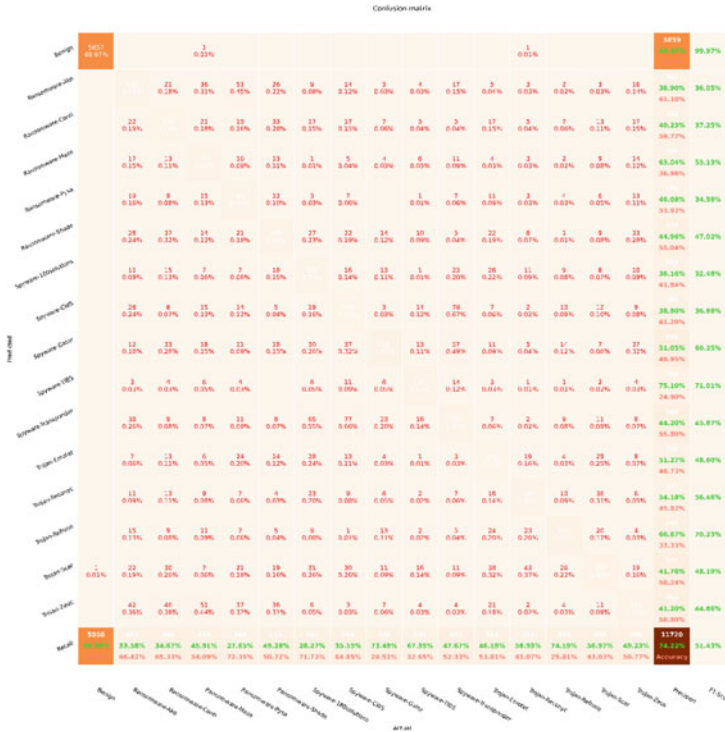


Fig. 5 Confusion matrix in classifying subclass of malware

### 5 Conclusions

In this paper, we investigate the problem of detecting obfuscated malware. We propose new models that are able to effectively detect malware, even when it has been obfuscated to make it more difficult to detect. Our experimental results show that our models outperform state-of-the-art methods. In a binary classification setting, our models achieve near-perfect accuracy. In future work, we plan to improve the performance of our models for multi-class classification.

### References

1. Aboaoja FA, Zainal A, Ghaleb FA, Al-rimy BAS, Eisa TAE, Elnour AAH (2022) Malware detection issues, challenges, and future directions: a survey. Appl Sci 12(17):8482
2. Aurangzeb S, Aleem M (2023) Evaluation and classification of obfuscated android malware through deep learning using ensemble voting mechanism. Sci Rep 13(1):3093
3. Carrier T, Victor P, Tekeoglu A, Lashkari A (2022) Detecting obfuscated malware using memory feature engineering. In: ICISSP, pp 177–188. INSTICC, SciTePress.

- 10.5220/0010908200003120
4. Dang QV (2019) Studying machine learning techniques for intrusion detection systems. In: *FDSE*, pp 411–426. Springer
  5. Dang QV (2021) Citation recommendation with random walking. In: *Comprehensible science: ICCS 2020*, pp 33–39. Springer
  6. Dang QV (2022) Enhancing obfuscated malware detection with machine learning techniques. In: *Future data and security engineering. Big data, security and privacy, Smart City and Industry 4.0 applications: 9th international conference, FDSE 2022, Ho Chi Minh City, Vietnam, November 23–25, 2022, proceedings*, pp 731–738. Springer (2022)
  7. Dang QV (2023) Multi-layer intrusion detection on the USB-IDS-1 dataset. In: *Hybrid intelligent systems: 22nd international conference on Hybrid Intelligent Systems (HIS 2022)*, December 13–15, 2022, pp 1114–1121. Springer (2023)
  8. Dang QV, Nguyen TL (2023) Detecting intrusion in wifi network using graph neural networks. In: Bindhu V, Tavares JMRS, Vuppapapati C (eds) *Proceedings of fourth international conference on communication, computing and electronics systems*, pp 637–645. Springer Nature Singapore, Singapore (2023)
  9. Elhadi AA, Maarof MA, Osman AH (2012) Malware detection based on hybrid signature behaviour application programming interface call graph. *Am J Appl Sci* 9(3):283
  10. FortiGuard Labs: global threat landscape report (2023). [https://www.fortinet.com/content/dam/maindam/PUBLIC/02\\_MARKETING/08\\_Report/report-2023-threat-landscape.pdf](https://www.fortinet.com/content/dam/maindam/PUBLIC/02_MARKETING/08_Report/report-2023-threat-landscape.pdf)
  11. Huidobro CB, Cordero D, Cubillos C, Cid HA, Barragán CC (2018) Obfuscation procedure based on the insertion of the dead code in the crypter by binary search. In: *ICCCC*, pp 183–192. IEEE (2018)
  12. Ignat CL, Dang QV (2021) Users trust assessment based on their past behavior in large scale collaboration. In: *2021 IEEE 17th international conference on intelligent computer communication and processing (ICCP)*, pp 267–274. IEEE (2021)
  13. Kingler S, Reddy BV, Jadhao S, Hambarde K, Hullur A (2022) Malware analysis using machine learning techniques. In: *2022 2nd international conference on intelligent technologies (CONIT)*, pp 1–9. IEEE (2022)
  14. Nath HV, Mehtre BM (2014) Static malware analysis using machine learning methods. In: *International conference on security in computer networks and distributed systems*, pp440–450. Springer (2014)
  15. O’Shaughnessy S, Sheridan S (2022) Image-based malware classification hybrid framework based on space-filling curves. *Comput Secur* 116:102660
  16. Sahay SK, Sharma A, Rathore H (2020) Evolution of malware and its detection techniques. In: *Information and communication technology for sustainable development*, pp 139–150. Springer (2020)
  17. Siddiqui MZ, Yadav S, Husain MS (2018) Application of artificial intelligence in fighting against cyber crimes: a review. *Int J Adv Res Comput Sci* 9(2):118–122
  18. Sihwail R, Omar K, Ariffin KZ (2018) A survey on malware analysis techniques: Static, dynamic, hybrid and memory analysis. *Int J Adv Sci Eng Inf Technol* 8(4–2):1662–1671
  19. Tran K, Di Troia F, Stamp M (2023) Robustness of image-based malware analysis. In: *Silicon valley cybersecurity conference: third conference, SVCC 2022, Virtual Event, August 17–19, 2022, revised selected papers*, pp 3–21. Springer (2023)
  20. You I, Yim K (2010) Malware obfuscation techniques: a brief survey. In: *International conference on broadband, wireless computing, communication and applications*, pp 297–300. IEEE (2010)
  21. Zhou J, Cui G, Hu S, Zhang Z, Yang C, Liu Z, Wang L, Li C, Sun M (2020) Graph neural networks: a review of methods and applications. *AI Open* 1:57–81

# Semi-Vector Controlled PM Synchronous Motor Drive



Arabindo Chandra, Soumyajit Datta, Milan Basu, and Sumana Chowdhuri

**Abstract** Vector control and self-control are the most widely used control techniques of the PM synchronous motor. Self-control technique is comparatively simple and cost-effective compared to vector control. However, this technique is unable to provide satisfactory performance for sinusoidal back E.M.F. machines. Self-control is suitable for trapezoidal back EMF motors. The vector control technique is the best high-performance control technique of sinusoidal back E.M.F. machines. In this paper, a semi-vector control scheme is discussed for sinusoidal back E.M.F. machines. The major advantage of this scheme over vector control is that reference frame transformations of motor variables and close current control are not required which makes the drive simple and less costly than vector control drive. The performance of the semi-vector control drive is in between vector control and self-control drives. The developed drive can be used for many industrial and domestic applications in place of a self-control drive. Performance of the drive is being validated by experimental study and satisfactory results are found.

**Keywords** PM synchronous motor · BLDC · Semi-vector control · Vector control drive · SVM · V/f control

## 1 Introduction

A wide interest is created in PM Synchronous Motor (PMSM) due to its unique advantage over DC or induction motor, such as high-power density, better efficiency, improved power factor, low rotor inertia, and reduction in size and weight [1–3]. PM synchronous motor can be classified as trapezoidal back E.M.F. machines and sinusoidal back E.M.F. [3–5]. Self-control is the simplest kind of control technique

---

A. Chandra (✉) · S. Datta · S. Chowdhuri  
Department of Applied Physics, University of Calcutta, Kolkata, India  
e-mail: [arabindo.chandra@gmail.com](mailto:arabindo.chandra@gmail.com)

M. Basu  
Department of Electrical Engineering, Techno International Newtown, Kolkata, India

of PMSM [6–8]. In the self-control technique, the motor phases are excited with a current wave synchronized with rotor instantaneous position and speed [9]. Optical encoder or Hall sensor is generally used to detect the rotor position and speed. Self-control techniques can be used to control both types of motors. However, the trapezoidal back E.M.F. motor will give better performance compared to sinusoidal motor. For satisfactory performance of the sinusoidal motor, the phase current must be sinusoidal and synchronized with rotor position and speed [10–13]. Vector control is used for this said purpose [14–16]. However, vector control technique is complex compared to self-control, and costly resources are necessary to implement this technique [3, 4, 10]. In the present work, a semi-vector control technique is developed. In this technique, a stator voltage vector is positioned  $90^\circ$  apart from rotor flux position and stator voltage vector magnitude is varied proportional to the frequency of the rotor for providing current regulation without using closed loop current control. The position and magnitude of the stator voltage is controlled by using rotor position synchronized Space Vector PWM control of the inverter. Therefore, optimal performance of the drive is achieved. The semi-vector control drive is relatively simple and less costly compared to vector control drive, as current feedback, reference frame transformation, and stator flux calculations are not involved in this technique. The performance of the drive is somewhere between vector control and self-control technique. Experimental study is carried out to establish the drive performance.

## 2 Modeling of PM Synchronous Motor

The most convenient way to model PMSM is to express the instantaneous current, voltage, and flux linkage phasors in a synchronously rotating reference frame (d-q frame) attached with the rotor. The stator voltages given in the d-q reference are

$$V_q = RI_q + \frac{d\lambda_q}{dt} + \omega_s \lambda_d \quad (1)$$

$$V_d = RI_d + \frac{d\lambda_d}{dt} - \omega_s \lambda_q \quad (2)$$

where

$$\lambda_q = L_q I_q \text{ and } \lambda_d = L_d I_d + \lambda_f$$

$V_q$ ,  $V_d$ ,  $I_q$ , and  $I_d$  are the d-q axis stator voltages and currents,  $L_q$ ,  $L_d$ ,  $\lambda_q$ , and  $\lambda_d$  are the d-q axis inductances and stator flux linkages, while  $\omega_s$  and  $R$  are the inverter frequency and stator resistance, respectively.  $\lambda_f$  is the rotor flux linkage.

The electromagnetic torque is

$$T_e = 3P/2[\lambda_f I_q + (L_d - L_q)I_d I_q] \quad (3)$$

And, the equation for the dynamics of the motor is

$$T_e = T_L + B\omega_r + J \frac{d\omega_r}{dt} \quad (4)$$

$T_L$  is load torque and  $P$  is pole pairs,  $B$  is damping coefficient,  $\omega_r$  is speed, and  $J$  is moment of inertia. The relationship of inverter frequency and speed is given by the following equation:

$$\omega_s = P\omega_r$$

### 3 Review of Vector Control Scheme

In vector control, the stator current vector is aligned quadrature to the rotor flux vector position. To achieve this, d-axis current of the stator is made zero. This will modify the torque equation as follows:

$$T_e = 3P/2[\lambda_f I_q] \quad (5)$$

It is evident from Eq. (5) that the electromagnetic torque is directly proportional to the q-axis current as the rotor flux linkage is constant. The phasor diagram of the vector control scheme is presented in Fig. 1. The vector control scheme block diagram is shown in Fig. 2. First, the speed error is converted to q-axis current ( $i_q^*$ ) through the PI controller. The rotor position is acquired from the absolute rotor position sensor. Position vectors ( $\sin\theta_e$  and  $\cos\theta_e$ ) are calculated from rotor position information using a predefined lookup table. The vector rotator (VR) and 2-phase to 3-phase conversion block converts the d-q current references to 3-phase instantaneous current references using the position vectors. The inverter is operated in a hysteresis current control scheme to produce reference currents.

For implementation of vector control schemes, the measurement of phase currents and reference frame transformation of these currents are necessary. In this work, a semi-vector control scheme is developed in which measurement of phase currents and reference frame transformation are not required. In the next section, the new scheme is discussed in detail.

### 4 Semi-Vector Control Scheme

The phasor diagram of the semi-vector control system is shown in Fig. 3. In this scheme, the position of the rotor flux vector is determined by the absolute rotor position sensor. The stator voltage vector is positioned  $90^\circ$  ahead of the rotor flux



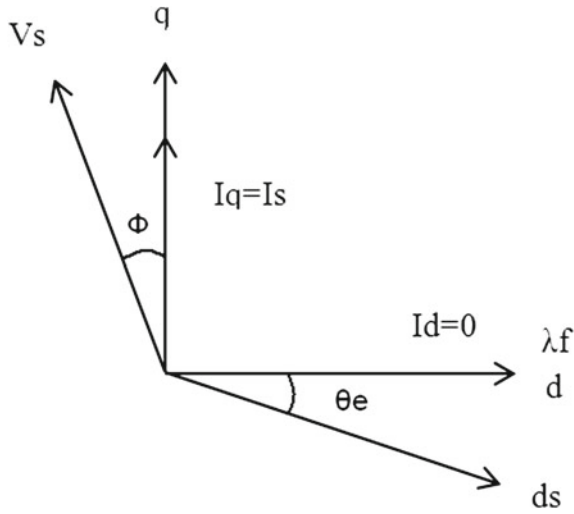


Fig. 1 Vector diagram of vector control PMSM

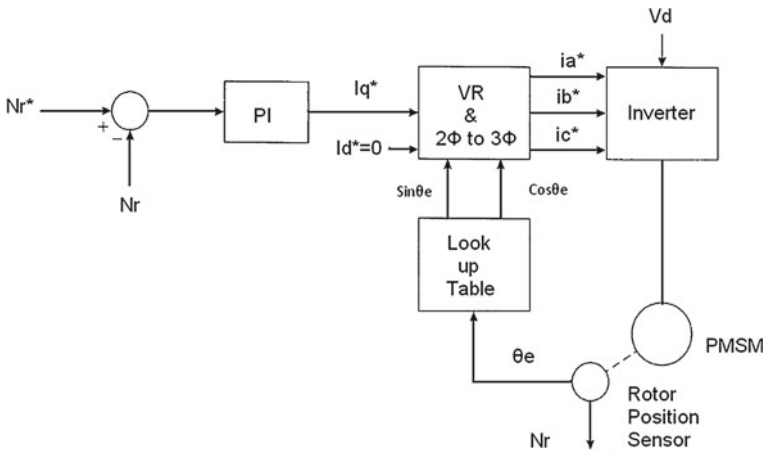
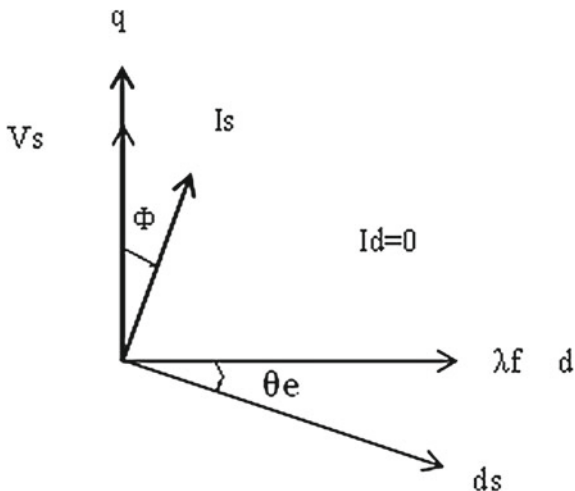


Fig. 2 Vector control scheme of PMSM

position. The SVM technique is used to orient the stator voltage vector. However, the magnitude of the stator voltage vector is to be determined. In conventional vector control voltage vector amplitude is determined by comparing the stator d-q current with current commands. In a semi-vector control scheme, stator d-q currents are not available. This problem is solved by using the concept of volt/Hz control. The core concept of voltage/Hz control of PMSM is that the stator voltage varies proportional to rotor frequency [17–19].

**Fig. 3** Vector diagram for semi-vector control scheme



Here, the same concept is used to determine the magnitude of the voltage vector. The frequency of the rotor is obtained by the differentiating rotor position obtained from the position sensor. The main difference between this control scheme compared to vector control is that here the stator voltage vector is placed  $90^\circ$  apart from the rotor flux vector instead of the stator current vector. This will degrade the motor torque to current ratio and dynamic response compared to vector control. However, dynamic response of this scheme is better than the self-control scheme. So, this scheme can be considered as a semi-vector control scheme.

## 5 Implementation

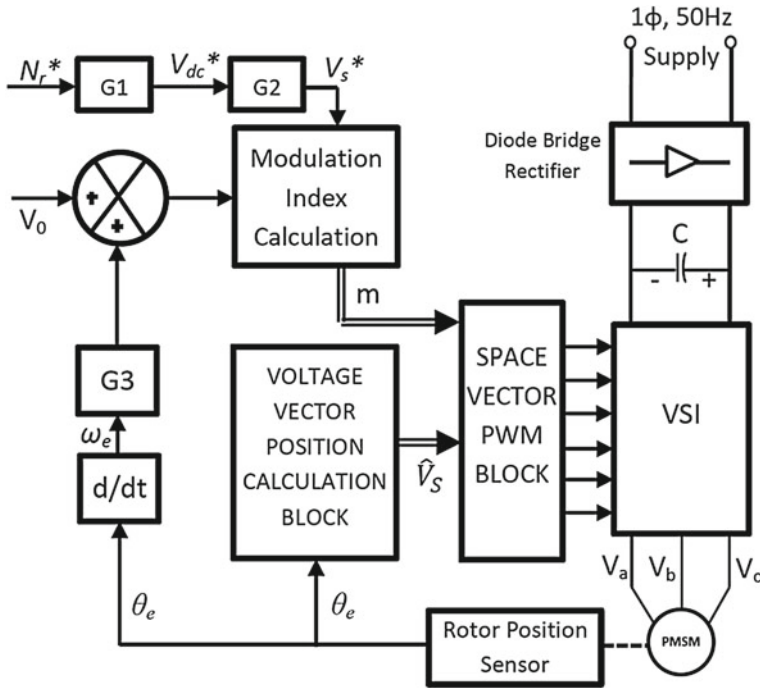
The drive schematic is shown in Fig. 4. Here, the drive is operated in open loop control mode. The controller reads the reference speed command ( $N_r^*$ ) and converts it to DC bus voltage ( $V_{dc}^*$ ). However, in this drive option of automatic DC bus control is not available. The problem is solved using the following technique. Inverter DC bus voltage is related to the AC line voltage by the following equation for a SVPWM voltage source inverter (VSI).

$$\hat{V}_s = 0.57m\sqrt{3}V_{dc} \quad (6)$$

where 'm' is the modulation index.

The maximum value of  $\hat{V}_s$  is obtained when  $m = 1$

$$\hat{V}_{sm} = 0.57\sqrt{3}V_{dc} \quad (7)$$



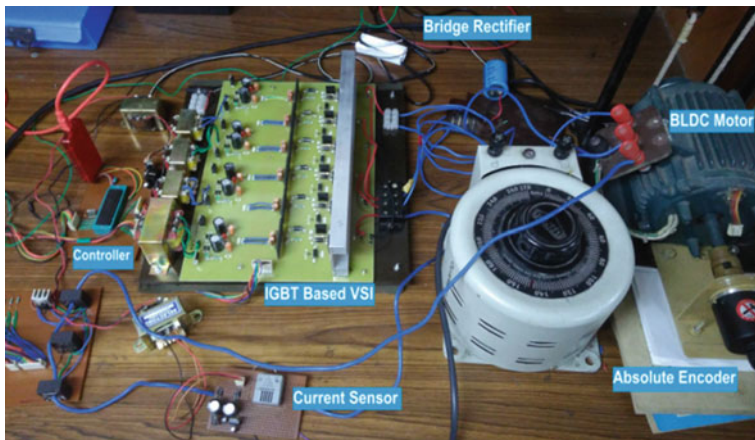
**Fig. 4** Block diagram of the semi-vector control scheme

Now by using Eq. (7), the peak value of fundamental line voltage can be calculated for a particular value of DC bus voltage  $V_{dc}$  by the following equation:

$$\hat{V}_s^* = 0.57m\sqrt{3}V_{dc}^* \quad (8)$$

Now as  $V_{dc}$  is constant in this system, inverter modulation index is to be varied to produce the line voltage corresponding to the DC bus voltage. The modulation index can be calculated by Eqs. (7) and (8). However, if the modulation index is set to the value given by the above equations, the starting current will be very high. So, to keep the motor torque at maximum value and to maintain the starting current within the permissible maximum limit, the line voltage magnitude is to be increased gradually, proportional to rotor frequency. This is achieved by the following technique. The frequency of the rotor ( $\omega_r$ ) is determined by differentiating the position of the rotor ( $\theta_r$ ), acquired from encoder. Now the amplitude of the line voltage ( $\hat{V}_s$ ) is determined by multiplying  $\omega_r$  with G4 and adding a boost voltage  $V_0$ , where G4 is expressed by a ratio of rated line voltage and angular frequency. The PWM duty cycle calculation block compares  $\hat{V}_s$  with  $\hat{V}_s^*$  and calculates modulation index as follows:

$$\text{If } \hat{V}_s < \hat{V}_s^* \text{ then } m = \frac{\hat{V}_s}{\hat{V}_{sm}}$$



**Fig. 5** Experimental prototype

$$\text{Else, } m = \frac{\widehat{V}_s^*}{\widehat{V}_{Sm}}$$

The stator voltage vector position calculation block determines the position of stator voltage vector depending on the rotor position ( $\theta_r$ ). The SVPWM block takes voltage vector position and modulation index ( $m$ ) as inputs and generates the gate pulses signal for VSI to create the voltage vector at an angle ( $\theta_r + 90^\circ$ ).

The experimental prototype is shown in Fig. 5. The prototype consists of a diode rectifier, IGBT-based 3-phase inverter, gate drive and protection circuit, 10-bit absolute optical encoder, Atmel SAM3X8E microcontroller-based control circuit, and encoder signal processing circuit. The motor is a sinusoidal back E.M.F., 230 V, 0.5 Hp, 4 pole, PMSM.

## 6 Result and Discussion

An extensive experimental study is carried out to support the efficacy of the drive. The current waveform for the semi-vector control drive is indicated in Fig. 6. The currents for conventional vector control and self-control drives are also shown in Figs. 7 and 8 for comparison.

As the motor is a sinusoidal machine, it is obvious that it will provide superior performance when the stator current is sinusoidal with minimum amount of harmonic distortion. From the result, it is evident that the current waveform for semi-vector control technique is better compared to self-control technique but inferior to conventional vector control.

The drive torque response is shown in Fig. 9. The torque response of the vector control drive is also shown. The speed response of the drive for a reference speed of

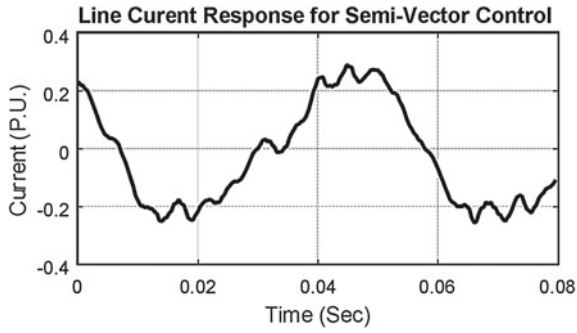


Fig. 6 Current waveform of semi-vector control drive

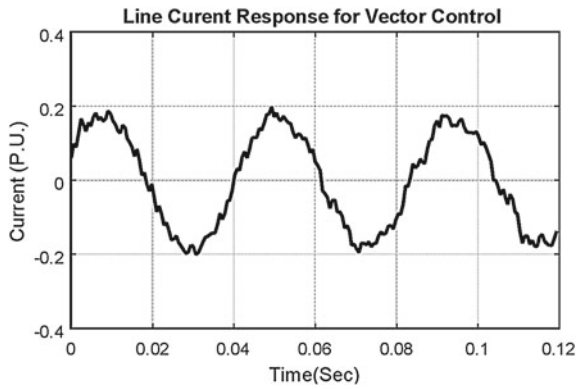


Fig. 7 Current waveform of vector control drive

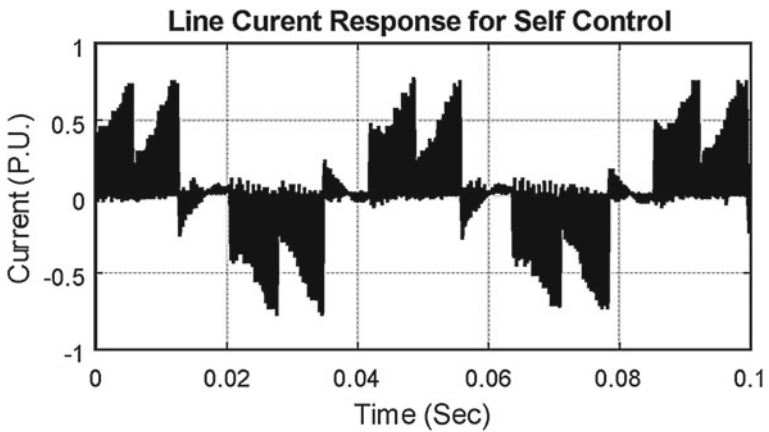


Fig. 8 Current waveform of self-control drive

750 rpm is shown in Fig. 10. The speed response for vector and self-control are also shown in that figure for the same reference speed.

A quantitative comparison of the semi-vector control drive with vector control and self-control drive is presented in Table 1.

By comparing the experimental result of the present scheme with existing vector control and self-control schemes, it can be decided that the overall performance of the semi-vector control drive is in between vector control and self-control drives.

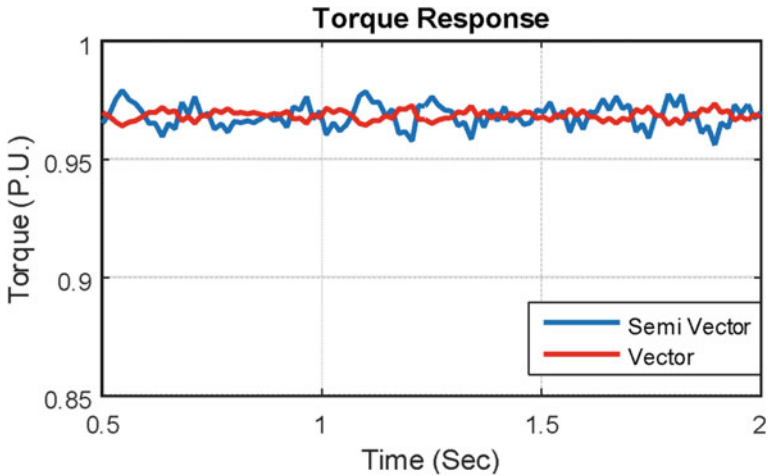


Fig. 9 Torque response

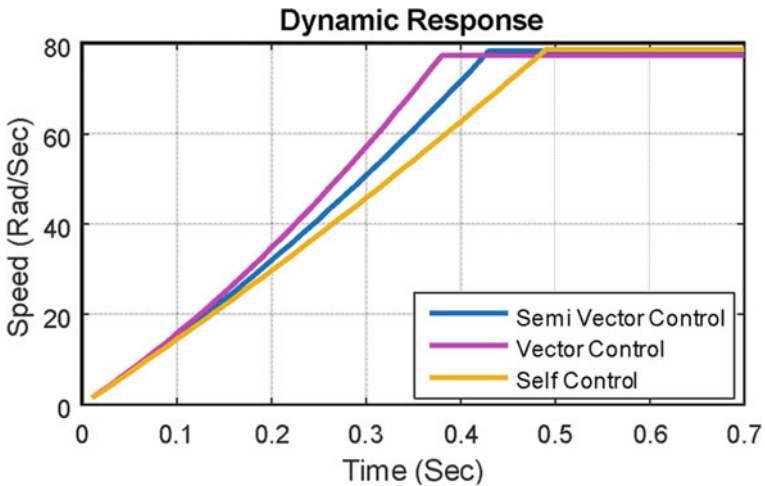


Fig. 10 Dynamic response for a reference speed of 1500 rpm

**Table 1** Result comparison

Type of control	Speed reference (RPM)	Torque (Nm)	Acceleration time (s)	Current	Torque ripple (Avg.)
Self-control	1500	0.9	0.5	0.7	0.5
Semi-vector control	1500	0.9	0.43	0.3	0.025
Vector control	1500	0.9	0.38	0.2	0.015

## 7 Conclusion

SVPMW-based semi-vector control technique for the PMSM is discussed in this paper. Experimental results are included to justify the efficacy of the technique. The experimental finding exhibits that the performance of the semi-vector control drive is somewhat superior to the self-control technique. In this drive, reference frame transformations of motor variables and closed loop control of motor phase currents are not required. These features reduce the cost and complexity of the semi-vector control drive compared to conventional vector control. However, it has inherent limitations, such as relatively inferior dynamic performance, and absence of over current protection. The semi-vector control technique is relatively simple and cost-effective compared to the vector control technique. Performance of the drive lies somewhere between the performances of conventional self-control and vector control. The semi-vector control drive can fulfill the needs of different industrial and domestic applications, except for some applications which require excellent dynamic performance like industrial robots, machine tools, etc. The necessity of absolute rotor position sensing for the operation of the semi-vector control drive is a disadvantage over self-control drive, as for self-control drive rotor position sensing is required for each 60° intermission, which can be found using comparatively less expensive Hall sensor.

## References

1. Richter E, Miller TJE, Neumann TW, Hudson TL (1985) The ferrite permanent magnet Ac motor a technical and economical assessment. *IEEE Trans Ind Appl Ia-21(4):644–650*
2. Gieras JF, Wing M (2022) Permanent magnet motor technology. Marcel Dckker. Inc.
3. Bose BK (2002) Modern power electronics and AC drive. PHE
4. Jahns TM (1994) Motion control with permanent-magnet AC machines. *Proc IEEE 82(8)*
5. Venkataraman K (2008) Special electrical machines. Published by CRC Press, November
6. Le-Huy H, Jakubowicz A, Perret R (1982) A self-controlled synchronous motor drive using terminal voltage system. *IEEE Trans Ind Appl IA-I 8(11)*
7. Nishikata S, Muto S, Kataoka T (1982) Dynamic performance analysis of self-controlled synchronous motor speed control systems. *IEEE Trans Ind Appl IA-18(3)*
8. Tian-Hua L, Chung-Ming Y, Chang-Huan L (1988) Microprocessor-based controller design and simulation for a permanent magnet synchronous motor drive. *IEEE Trans Ind Electron 35(4):516–523*

9. Pillay P, Krishnan R (1989) Modeling, simulation, and analysis of permanent-magnet motor drives, part II: the brushless DC motor drive. *IEEE Trans Ind Appl* 25(2)
10. Chandra A, Datta S, Chowdhuri S (2015) Open loop speed control of a space vector PWM inverter fed PM synchronous motor. In: *Proceedings of Michael Faraday IET International Summit (MFIIS)*, September, vol 1, pp 136–144
11. Bose BK, Poul M (1988) A microcomputer-based control and simulation of an advanced IPM synchronous machine drive system for electric vehicle propulsion. *IEEE Trans Ind Electron* 35(4)
12. Finch JW, Giaouris D (2008) Controlled AC electrical drives. *IEEE Trans Ind Electron* 55(2)
13. Abdes Khan M, Nasir Uddin M, Azizur Rahman M (2013) A novel wavelet-neural-network-based robust controller for IPM motor drives. *IEEE Trans Ind Appl* 49(5)
14. Nerg J, Rilla M, Ruuskanen V, Pyrhönen J, Ruotsalainen S (2014) Direct-driven interior magnet permanent-magnet synchronous motors for a full electric sports car. *IEEE Trans Ind Electron* 61(8)
15. Han Ho C, Hong Min Y, Yong K (2015) Implementation of evolutionary fuzzy PID speed controller for PM synchronous motor. *IEEE Trans Ind Inf* 11(2)
16. Pellegrino G, Armando E, Guglielmi P (2010) Field oriented control of IPM drives for flux weakening applications. *EPE J* 20(1):50–57
17. Sala-Perez P, Heaxts-Aragones M, Galceran-Arellano S, Montesinos-Miracle D (2014) Reduced saliency PMSM V/f sensorless control with initial rotor position estimation. *EPE J* 24(1):30–36
18. Chandra A, Datta S, Chowdhuri S (2017) Design and implementation of low cost sensor-less PM synchronous motor drive for pump and compressor applications. *Eur J Adv Eng Technol* 4(4):302–310
19. Datta S, Chandra A, Chowdhuri S (2016) Design and development of an 8 bit microcontroller based space vector PWM inverter fed volt/Hz induction motor drive. In: *Control, instrumentation, energy and communication (CIEC)*, 2016 2nd international conference on, pp 353–357. IEEE



# A Comprehensive Review of Sensor-Based Smart Packaging Technology



**B. P. Aniruddha Prabhu, Rakesh Dani, Khairul Hafezad Abdullah,  
Tushar Sharma, Chandradeep Bhatt, and Rahul Chauhan**

**Abstract** Economic growth for good quality food contributed to packaging advancements. The topic of discussion in this research paper is intelligent packaging technologies, their applications in food packaging, as well as research and breakthroughs in the packaging industry. Food products with more intelligent and active packaging are both healthier and of higher quality. Active packaging makes use of additives to maintain or extend the quality and freshness of the food inside. During the entire process of storage and transportation, intelligent systems check packed foods for correct information. These advances satisfy the demand for foods that are healthier and can be stored for longer. It is anticipated that the market would expand as a result of the incorporation of active and intelligent packaging technologies.

**Keywords** Active packaging · Intelligent packaging · Food

## 1 Introduction

The primary goals of conventional food packaging are security, information dissemination, portability, and confinement [1]. To prevent the food material from being harmed by factors such as temperature, sunlight, humidity, pressure, bacteria, exhaust fumes, and so on, it is packaged and stored in a suitable container. It comes in a

---

*Present Address:*

B. P. Aniruddha Prabhu (✉)

Alliance College of Engineering and Design, Alliance University, Bangalore, India

e-mail: [aniprabhubp@gmail.com](mailto:aniprabhubp@gmail.com)

R. Dani

Department of Hospitality Management, Graphic Era (Deemed to be) University, Dehradun, India

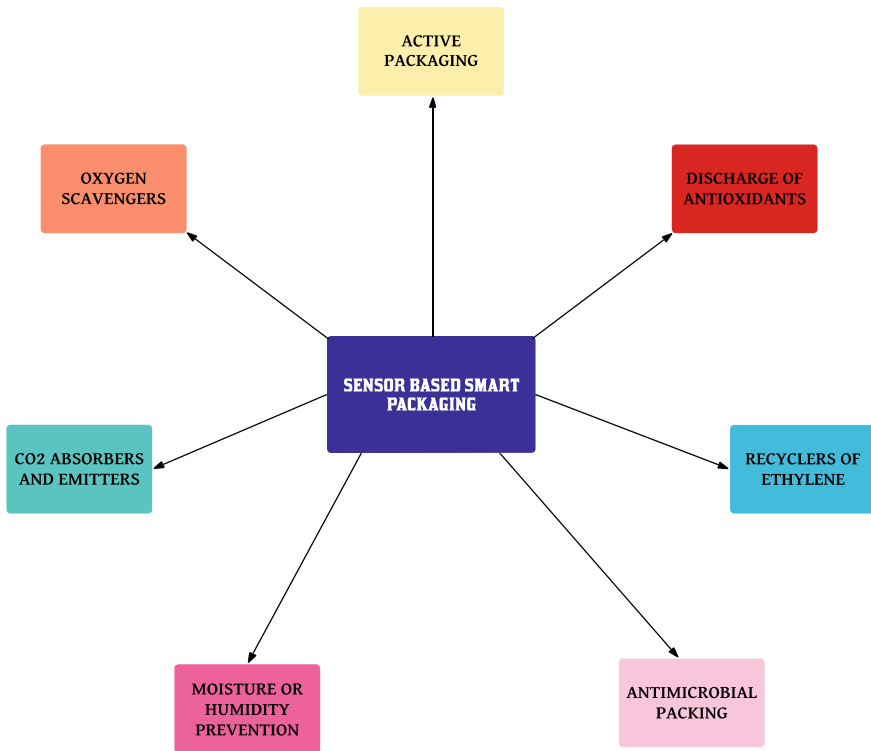
K. H. Abdullah

Department of Academic Affair, UniversitiTeknologi MARA, Perlis Branch, Arau Campus, Shah Alam, Malaysia

T. Sharma · C. Bhatt · R. Chauhan

Department of computer Science and Engineering, Graphic Era Hill University, Dehradun, India

number of different forms, which makes it more convenient to use and cuts down on the amount of time it takes the user [2]. In conventional packaging, the absence of reactivity in the materials used for packaging is the key issue for ensuring the safety of the item. To ensure the highest level of food safety, intelligent packaging technologies are designed to respond to the dynamic relationship that exists between the product being packaged and its surrounding environment [3]. Active and smart packaging ideas, on the other hand, are based on the perceived relationship between the eco-system of the packaging and the food in order to just provide effective security to the food [4]. In-depth descriptions of the most significant novel packaging technologies (Fig. 1) now employed in the food sector are provided in this research paper.



**Fig. 1** Sensor-based smart packaging technologies

## 2 Active Packaging

Active packaging is defined as packaging that serves a purpose other than merely protecting its contents from the elements [5]. To attain certain qualities or to increase the food product's life span, active packaging involves a beneficial interaction between the item, the package, and the ecosystem [6]. It has also been referred to as a method for preserving food for an extended time frame, making it safer or more appetizing, or enhancing its sensory properties while maintaining its initial shape [7]. To keep or enhance the quality of packaged food products, active materials and articles are required to comply with regulations 1935/2004/EC and 450/2009/EC [8]. The packaging and its surroundings are planned to be a source of discharge or absorption of chemicals. The goal of active packaging is to extend the shelf life of packaged food through the application of one or more of a variety of methods, such as the control of internal temperature and/or humidity, the elimination of oxygen, the addition of ingredients such as salt, sweetener, carbon dioxide, and natural acids, or a combination of these [9]. Recent innovations in active packaging have facilitated progress in a wide range of fields, such as the delaying of oxidizing in food products, the adjustment of breathing rate in farm commodities, the suppression of microbiological growth, and the prevention of moisture transfer in dried goods [10]. Coating, tiny holes, laminating, joint extrusion, and polymer blends are all examples of active packaging techniques that can be used to adjust selectivity and hence change the air concentrations of gaseous chemicals inside the container [11].

## 3 Oxygen Scavengers

Food packaging oxidizes faster. Oxygen promotes aerobic microorganism proliferation, off-flavor and foul smell growth, discoloration, nutritional declines, and muscle food shelf-life stability. Controlling oxygen levels in food packaging helps reduce spoiling [12]. MAP or vacuum packaging cannot totally remove air from oxygen-sensitive goods. The device can't remove air from the packaging film. By using oxygen predators, the value of oxygen-sensitive meals can be lowered. Oxygen absorbers lower package head space oxygen to below 100 ppm [13]. Commercial oxygen scavengers oxidize iron powder, ascorbic acid, photosensitive dye, enzymes, saturated fatty acids, immobilized yeast, etc. [14]. Most oxygen scavengers are based on iron powder oxidation and come in little sachets with a variety of catalysts [15]. The chemicals combine with the food's water to form a hydrated metallic reducing agent that scavenges oxygen. Oxygen scavengers can remove oxygen from packets with moderate barrier qualities. MAP or oxygen scavengers can be utilized [16]. Oxygen scavengers eliminate leftover oxygen from MAP. Alternatives to sachets comprise card, sheet, or layer packaging inserts. The oxygen scavenger in the package prevents unwanted sachet breakage and unintended intake [17]. Oxygen-scavenging chemicals can be mixed with polyethylene, which permits oxygen and water to

quickly diffuse from headspace or food to reactive components [18]. Oxygen-scavenging plastic films and laminates are less effective than steel sachets or tags [19].

## 4 CO<sub>2</sub> Absorbers and Emitters

Adding carbon dioxide to a package slows the rate of oxygen and stops the development of microorganisms in foods including meat, chicken, fish, dairy, and baked products. As a result, foods that benefit from high CO<sub>2</sub> levels (10–80%) have a significantly longer shelf life. Fragility in flexible packaging has been linked to the relative vacuum formed by oxygen scavenger packets [20]. And while carbon dioxide is soluble at low temperatures, a temporary vacuum is created when it is passed through a container together with oxygen [21]. A method called soluble gas stabilization (SGS) can incorporate enough carbon dioxide (CO<sub>2</sub>) into the item in pure CO<sub>2</sub> in as short as a short time before it becomes available for purchase [22]. Muscle meals can be stored in a regular MAP tray, which features a false bottom with perforations and a sachet. The food's juices work in tandem with the sachet to release carbon dioxide into the package, keeping it from collapsing [23]. Absorbers of carbon dioxide are added to packages to get rid of the buildup of carbon dioxide. Because fresh roasted coffees release a large amount of carbon dioxide (CO<sub>2</sub>) into the air immediately after roasting, the package will rupture without the use of a CO<sub>2</sub> scavenger [24]. Sachets designed for CO<sub>2</sub> removal are available from Mitsubishi Gas Chemical Company. As an alternative to the traditional "aging" period following coffee roasting, CO<sub>2</sub> scavengers can be used to keep the coffee's flavorful volatile compounds from escaping during storage [25].

## 5 Antimicrobial Packing

Antimicrobial packaging reduces, inhibits, or retards the development of microorganisms in packaged food products or packaging material. Antimicrobial chemicals can be added to food packaging to control germs [26]. Onion, cardamom, ginger, mint, basil, thyme, garlic, mustard, and radish are organic antimicrobials. Other natural antimicrobials include polypeptide nisin, natamycin, pediocin, and bacteriocins [27]. There are two different types of antimicrobial packages: those that allow the antimicrobial chemicals to travel to the surface, and those that are efficient against surface germs without allowing the chemicals to travel to the foodstuff [28]. Direct surface application of antibacterial chemicals to food has limited applicability since the active material is neutralized on contact or diffuses quickly to the food. Antimicrobials added to meat formulations may be partially inactivated by flesh ingredients, limiting their impact on the surface microflora [29].

Antimicrobial packaged goods should have a longer lag phase and a smaller developmental level of microorganisms to increase storage life and maintain safety. Meat, chicken, bread, cheese, fruits, and legumes are all infused with antimicrobial chemicals [30]. Polymers are modified with bio-active compounds such as antimicrobials for use in the delivery of medicines and insecticides, as well as in the production of textiles, surgical implants, and other biomedical equipment [31]. The most popular antibacterial agent is zeolite that has been treated with silver. There is a wide range of bacteria that can be killed by silver ions, and they are also able to inhibit a number of metabolic enzymes [32]. The surface in touch with food is coated with silver zeolite. A silver ion release occurs when food solubility penetrates the open spaces of the porous laminate. Zeomic, Apacider, AgIon, Bactekiller, and Novaron are just a few of the zeolites that have had silver added to them [33]. The polymers contain antibiotics, metals like copper, antimicrobial enzymes like lactoperoxidase and lactoferrin, and antimicrobial peptides such as megainins, cecropines, and defensins. Chlorine dioxide, sulfur dioxide, carbon dioxide, and ethanol are all gases that are released by antimicrobial packaging techniques [34]. With this setup, plastic is kept well away from edible items. Here, packaging materials have antimicrobial chemical extrusion or are coated immediately into polymers or carriers. The packaging of a volatile antimicrobial solution must have high barrier properties to reduce the loss of active ingredients. Apply ethanol directly to food with a spray bottle or make your own with ethanol sachets. Both Ethicap and Antimold work by drawing out dampness and then releasing ethanol vapors. Moist baked goods, cheese, and shellfish all benefit from the use of ethanol vapor producers. Ethanol can be removed from the products by heating it before use. Chlorine dioxide is another antibacterial chemical that is effective against bacteria, yeasts, and viruses. Hydrophobic and hydrophilic copolymerization of sodium chlorite with acid precursors yields chlorine dioxide. Hydrochloric acid is formed when food humidity comes into touch with the hydrophobic phase, and it reacts with sodium chlorite to generate chlorine dioxide [35].

Covalently immobilized antibiotics or fungicides are used in certain antimicrobial packing. Peptides, enzymes, polyamines, and organic acids have structural features. Films and coatings utilize antibacterial polymers like chitosan [36]. Chitosan is used to preserve fresh produce against mold. It protects micronutrients from microorganisms. Antimicrobial edible coatings and films made from polysaccharides, proteins, and lipids are biodegradable, edible, biocompatible, and aesthetically pleasing [37]. Whey protein coverings and films can include consumable antimicrobial compounds as lysozyme, nisin, potassium sorbate, etc. Use pediocin or nisin on cellulose shell to suppress *Listeria monocytogenes* on chicken, lamb, pork, and beef. Nisin and lysozyme in soya protein and corn zein films inhibit *Lactobacillus plantarum* and *Escherichia* bacteria on labmedia [38].

## 6 Moisture or Humidity Prevention

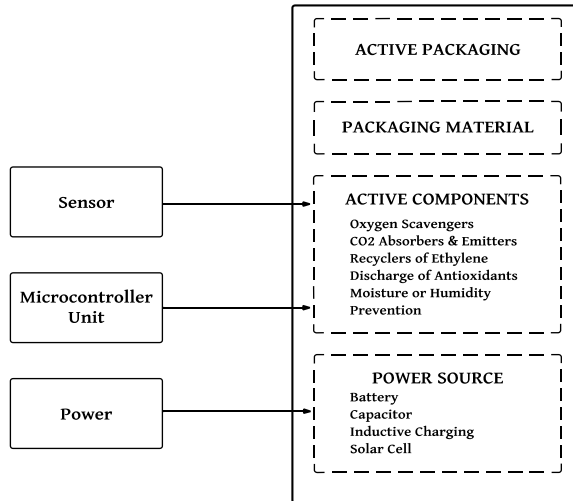
The presence of moisture is a crucial factor in food spoiling; hence moisture regulators are used to reduce the item's moisture content and so stop microorganisms from growing. When fresh fruits and veggies are packaged in a section that is colder than the rest of the container, they undergo a process of respiration that results in condensation. Microbial deterioration and diminished aesthetic appeal are both caused by soluble nutrients leaching into the water. Dry, crunchy items get soggy, while hygroscopic items like milk powder, instant coffee powder, chocolates, etc. become cake, when there is too much humidity in the packaging [39].

To prevent fish, meat, poultry, fruits, and vegetables from becoming soggy, wet pads, sheets, and blankets are utilized. Melted ice is absorbed by large sheets and blankets during air freight carriage of chilled fish. To make drip absorbent sheets, a super absorbent polymer is sandwiched between two layers of a micro-porous polymer like polyethylene or polypropylene. Cheese, chips, nuts, sweets, spices, and other food items all employ desiccants [40]. Dry meals are packaged with desiccants like silica gel, molecular sieves, or calcium oxide, while wet foods are buffered with micro-porous bags or pads of inorganic salts and a layer of solid polymeric humectants [41].

## 7 Discharge of Antioxidants

Antioxidants are commonly used in food to increase its oxidation resistance and hence its storage life. Certain foods get their antioxidants from the containers they come in, in response to rising buyer's desire for natural, minimally processed meals. Incorporating antioxidants into the polymers can also stabilize it, protecting the sheets from deterioration. Han et al. looked at how adding ButylatedHydroxy Toluene (BHT) to HDPE packaging affected oat flakes (1987). Seventy percent of the BHT left the cereal and only twenty-five percent stayed [42]. Adding a layer of low-permeability polymer can stop the loss from going out. However, the accumulation of BHT in human adipose tissue has raised concerns about the influence of BHT on people's health [43]. The oxidative reactions that cause rancid odor, and color changes in fatty fishes can be mitigated by using natural antioxidants on packing films, such as Vitamins C and E. Vitamin E has been shown to be stable under processing circumstances and to dissolve very well in polyolefins, making it an ideal preservative for low- to moderate cereals and junk foods [44].

**Fig. 2** Sensor integration in smart packaging



## 8 Recyclers of Ethylene

Aroma or flavor absorbers and emitter volatile compounds including aldehydes, amines, and sulfides are created during food spoiling, and they can be selectively scavenged from the packaging [8]. Smell absorbents prevent shipments from taking on each other’s overbearing aromas on the road. An adequate thickness of polyethylene terephthalate (PET) or polyethylene, a port for the flow of breathing gases and an odor-absorbing sachet comprising charcoal and nickel make up the components of the package [45]. Polymers that incorporate acidic compounds, such as citric acid, can reduce or eliminate volatile amines, which are byproducts of protein degradation in fish flesh. The film used to create ANICO bags (Japan) comprises ferrous salt and an organic acid such as citric acid or ascorbic acid, both of which are capable of oxidizing the amines. High barrier packaging materials can also prevent the transmission of scents that are not associated with food, such as taints [46]. Sensor incorporation into different types of packaging to enable smart functionalities is represented in Fig. 2.

## 9 Other Forms of Activated Packaging

Active packaging will find widespread use in the future, and one potential use is the self-heating packaging of ready-to-eat meals. When the internal pressure or steam level in the pack reaches a certain threshold, the package automatically releases the steam. Using techniques including shielding, field modulation, and the incorporation of susceptors, microwaveable active packaging aims to improve the heating behavior of food heated in the microwave [47]. Microwave susceptors, made of aluminum or

stainless steel that has been placed on a substrate such as polyester film or paper-board, facilitate uniform heating, surface browning, and crisping [48]. Along with the functional microwave packs are steam valves that let steam out easily while cooking in the microwave. For steaming or microwaving convenience foods, the Flexis™ Steam Valve is a commercial pressure-sensitive steam valve that may be attached to most of the flexible food packaging lidding films or molded containers. It creates a tight seal that keeps the product's contents safe at first and then opens up during cooking. The quality of the meal is preserved by maintaining a steady temperature throughout cooking [47].

## 9.1 *Intelligent Packaging*

Intelligent packing is connected to the idea of contaminants migrating within food-stuff and the packaging's ability to communicate to assist consumers in making choices. By "intelligent materials and products," we mean those that keep tabs on the temperature and humidity of the space in which the product is stored or the packaging it came in [49]. The state of the food or its environment can be communicated to the consumer using intelligent packaging solutions (temperature, pH). It can monitor, sense, and document changes in the goods environment and presents this information to the consumer in a way that standard packaging cannot. Intelligent components, in contrast to active ingredients, are not designed to leach their nutrients into the meal [50]. HACCP and QACCP are systems designed to detect unsafe food at the source, determine the nature of any potential health risks, and implement measures to prevent them. Intelligent packaging can help improve these systems. It also aids in determining which steps can most effectively enhance the end product's quality by focusing on the procedures that have the most significant impact on the quality attributes. Sensors, indicators, and radio-frequency identification (RFID) devices are the three primary forms of intelligence in modern technological infrastructures [51].

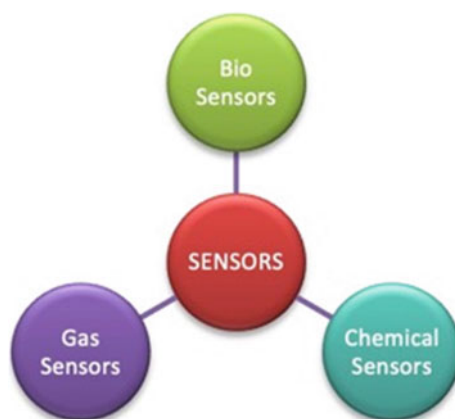
## 9.2 *Sensors*

One definition of a sensor is "an instrument for detecting, localizing, or quantifying energy or matter by generating a signal indicative of some measurable physical or chemical attribute." Whenever a sensor is activated, it will send out a signal. For most sensors, the receiver and the transmitter are the two most important components [52]. Different types of sensors (Fig. 3) are given below.

**Biosensor:** With the help of biosensors, researchers may observe, monitor, and share data on biological and chemical processes. Biosensors have bio-receptors and bio-transducers [53]. The target analyte is recognized by the bio-receptors, and the biochemical signals are transformed into a measurable electronic response by the



**Fig. 3** Different types of sensors



transducer. Enzymes, hormones, nucleic acid, antigens, microorganisms, and so on are all examples of bio-receptors. The optic, acoustic, or electro chemical transducers are all acceptable [54].

**Gas Sensor:** Gas sensor measures package gaseous analytes. Sensors based on piezoelectric crystals, organic conducting polymers, and metal oxide semiconductor field effect transistors are all part of the package [55]. Direct contact with the analyte causes either a quenching of luminescence or a change in absorbance, which optical oxygen sensors rely on. Optochemical sensors can determine the quality of products by analyzing gas analytes such hydrogen sulfide, carbon dioxide, and volatile amines [56].

**Chemical Sensor:** Surface adsorption can be used to assess the presence, activity, composition, and concentration of a target chemical or gas, and this is where chemical sensors and receptors come in. Transducers sense the presence of specific substances and turn those observations into signals. Whether a transducer is active or passive is determined by how much external power is necessary for the measurement [57]. Nanoparticles, graphene, graphite, nanofibers, and nanotubes are all examples of carbon nanomaterials that are used in chemical sensors because of the significant particular surface size that these materials possess in addition to their remarkable electrical and mechanical properties [58].

## 10 Indicators

Indicators are chemicals that can be used to identify the presence or absence of a component, the capacity to concentrate on a specific component, or the strength of a reaction between two or more substances. The term “indicator” refers to any material that can reveal information about the existence, absence, concentration, or intensity

**Fig. 4** Different types of indicators



of a response between one or more components [59]. Different types of indicators (Fig. 4) are given below.

### ***10.1 Freshness Indicators***

Indicators of freshness reveal the extent to which a food item has degraded due to microbial growth or chemical changes. Indicators on the packaging react with the metabolites produced during microbial development, allowing for a visible inspection of the product's microbiological quality [60].

### ***10.2 Time Temperature Indicators***

When it comes to the rate at which food spoils physically, chemically, and microbiologically, temperature is considered to be among the most influential environmental factors. The purpose of these indicators is to provide feedback on whether or not a predetermined temperature has indeed been consistently exceeded, and/or to provide a rough estimate of how long a product has been at an unsafe temperature (time temperature history) [61]. With the help of these labels, you can easily see how the temperature of your shipment or storage space changed over time. As a result, they are able to report instances of mistreatment of refrigerated or frozen goods [62].

### 10.3 Integrity Indicators

Adding a leak detector to a shipment guarantees that nothing is ever lost in transit. Redox dyes are used in visual oxygen indicators because they alter color depending on the oxygen content [63]. The system's disadvantages include the need for a very delicate instrument and the susceptibility of the product's residual oxygen to indications [64].

## 11 Conclusion

There has been significant development in smart packaging technology over the past few years, and these advancements are now being incorporated into packaging systems to improve upon the requirements of the food distributed generation. This action is being taken to better accommodate the needs of the food distribution network. The food business can benefit from the use of advanced packaging technologies since these advancements can increase the longevity of products, boost their quality and safety, and inform consumers about what they're buying. An investigation of such "smart packaging" methods might result in improvements to the process that is already in place. There is a lot of unrealized potential in smart packaging that has not yet been explored, but there is a lot of promise that can be achieved to make people's lives more convenient in the future.

**Acknowledgements** We would like to express our deep and sincere gratitude to all who helped or contributed to this research paper.

**Conflict of Interest** The authors confirm that they have no financial or personal ties with anybody or anything that might be seen as influencing the results described in this research.

## References

1. Rossi M, Passeri D, Sinibaldi A, Angjellari M, Tamburri E, Sorbo A, Carata E, Dini L (2017) Nanotechnology for food packaging and food quality assessment. *Adv Food Nutr Res* 82:149–204
2. Vaclavik VA, Christian EW, Campbell T, Vaclavik VA, Christian EW, Campbell T (2021) Food preservation. In: *Essentials of food science*, pp 327–346
3. Firouz MS, Mohi-Alden K, Omid M (2021) A critical review on intelligent and active packaging in the food industry: research and development. *Food Res Int* 141:110113
4. Langley S, Phan-Le NT, Brennan L, Parker L, Jackson M, Francis C, Lockrey S, Verghese K, Alessi N (2021) The good, the bad, and the ugly: food packaging and consumers. *Sustainability* 13(22):12409
5. Vermeiren L, Devlieghere F, van Beest M, de Kruijf N, Debevere J (1999) Developments in the active packaging of foods. *Trends Food Sci Technol* 10(3):77–86


6. Yildirim S, Röcker B, Pettersen MK, Nilsen-Nygaard J, Ayhan Z, Rutkaite R, Radusin T, Suminska P, Marcos B, Coma V (2018) Active packaging applications for food. *Compr Rev Food Sci Food Saf* 17(1):165–199
7. Ariyamuthu R, Albert VR, Je S (2022) An Overview of food preservation using conventional and modern methods. *J Food Nutr Sci* 10(3):70–79
8. Biji KB, Ravishankar CN, Mohan CO, SrinivasaGopal TK (2015) Smart packaging systems for food applications: a review. *J Food Sci Technol* 52:6125–6135
9. Martillanes S, Rocha-Pimienta J, Cabrera-Bañegil M, Martín-Vertedor D, Delgado-Adámez J (2017) Application of phenolic compounds for food preservation: food additive and active packaging. *Phenolic Compd-Biol Activity* 3(8):39–58
10. Brockgreitens J, Abbas A (2016) Responsive food packaging: recent progress and technological prospects. *Compr Rev Food Sci Food Saf* 15(1):3–15
11. Wang S, Zhang P, Li Y, Li J, Li X, Yang J, Ji M, Li F, Zhang C (2023) Recent advances and future challenges of the starch-based bio-composites for engineering applications. *Carbohydr Polym* 120627
12. Haq IU, Sarwar MK, Mohyuddin Z (2021) Microbial determinants in silage rotting: a challenge in winter fodders. In: *Sustainable winter fodder*, pp 301–329. CRC Press
13. Ringpirom P, Rattanarat P, Kulchan R (2022) Absorption efficiency of oxygen scavenger and shelf-life prolongation of bakery product. *J Food Sci Agric Technol (JFAT)* 6(1):85–92
14. Awulachew MT (2022) A review of food packaging materials and active packaging system. *Int J Health Policy Plann* 1(1):28, 35
15. Siddiqui A, Chand K (2022) Enhancement of shelf life of food using active packaging technologies. *Innovative approaches for sustainable development: theories and practices in agriculture*. Springer International Publishing, Cham, pp 133–143
16. Cruz-Romero M, Kerry JP (2017) Packaging systems and materials used for meat products with particular emphasis on the use of oxygen scavenging systems. In: *Emerging technologies in meat processing: production, processing and technology*, pp 231–263
17. Rooney ML (1995) Overview of active food packaging. In: *Active food packaging*, pp 1–37
18. Busolo MA, Lagaron JM (2012) Oxygen scavenging polyolefin nanocomposite films containing an iron modified kaolinite of interest in active food packaging applications. *Innov Food Sci Emerg Technol* 16:211–217
19. Gaikwad KK, Singh S, Lee YS (2018) Oxygen scavenging films in food packaging. *Environ Chem Lett* 16:523–538
20. Arvanitoyannis IS, Stratakos AC (2012) Application of modified atmosphere packaging and active/smart technologies to red meat and poultry: a review. *Food Bioprocess Technol* 5:1423–1446
21. Mohan CO, Ravishankar CN (2019) Active and intelligent packaging systems-application in seafood
22. Morales-Castro J, Ochoa-Martínez LA (2010) 10 safety and quality effects in foods stored under modified atmosphere conditions. In: *Processing effects on safety and quality of foods*, p 253
23. Kerry JP, O’grady MN, Hogan SA (2006) Past, current and potential utilisation of active and intelligent packaging systems for meat and muscle-based products: a review. *Meat Sci* 74(1):113–130
24. Gaikwad KK, Lee YS (2017) Current scenario of gas scavenging systems used in active packaging—A review. *Korean J Packag Sci Technol* 23(2):109–117
25. Nicoli MC, Manzocco L, Calligaris S (2009) 11 packaging and the food packaging and shelf life: a practical guide, p 199
26. Rawdkuen S (2019) Edible films incorporated with active compounds: their properties and application. In: *Isil V, Uzunlu S (eds) Active antimicrobial food packaging*, pp 71–85
27. Amiri S, Moghanjoughi ZM, Bari MR, Khaneghah AM (2021) Natural protective agents and their applications as bio-preservatives in the food industry: An overview of current and future applications. *Ital J Food Sci* 33(SP1):55–68

28. Irkin R, Esmer OK (2015) Novel food packaging systems with natural antimicrobial agents. *J Food Sci Technol* 52:6095–6111
29. Yemencioğlu A (2017) Handbook of antimicrobial coatings. Izmir Institute of Technology, Izmir, Turkey, p 63
30. Sung SY, Sin LT, Tee TT, Bee ST, Rahmat AR, Rahman WAWA, Tan AC, Vikhraman M (2013) Antimicrobial agents for food packaging applications. *Trends Food Sci Technol* 33(2):110–123
31. Aggarwal V (2020) Utility of nanotechnology in various disciplines. In: *Nanotechnology*. CRC Press, pp 61–70
32. Xu Z, Zhang C, Wang X, Liu D (2021) Release strategies of silver ions from materials for bacterial killing. *ACS Appl Bio Mater* 4(5):3985–3999
33. Hemavathi AB, Siddaramaiah H (2018) Food packaging: polymers as packaging materials in food supply chains. In: *Encyclopedia of polymer applications*. CRC Press, Boca Raton, pp 1374–1397
34. Cristina N, Paula V, Elena C (2017) Active and intelligent food packaging. In: *Food safety and protection*. CRC Press, pp 459–491
35. Singh S, Maji PK, Lee YS, Gaikwad KK (2021) Applications of gaseous chlorine dioxide for antimicrobial food packaging: a review. *Environ Chem Lett* 19:253–270
36. Sakala GP, Reches M (2018) Peptide-based approaches to fight biofouling. *Adv Mater Interf* 5(18):1800073
37. Kouhi M, Prabhakaran MP, Ramakrishna S (2020) Edible polymers: an insight into its application in food, biomedicine and cosmetics. *Trends Food Sci Technol* 103:248–263
38. Sason G, Nussinovitch A (2021) Hydrocolloids for edible films, coatings, and food packaging. In: *Handbook of hydrocolloids*. Woodhead Publishing, pp 195–235
39. Siddiq M, Ahmed J, Lobo MG, Ozadali F (eds) (2012) *Tropical and subtropical fruits: postharvest physiology, processing and packaging*. John Wiley & Sons
40. Majid I, Thakur M, Nanda V (2018) Innovative and safe packaging technologies for food and beverages: updated review. In: *Innovations in technologies for fermented food and beverage industries*, pp 257–287
41. Matche SR, Oswal M (2021) Smart packaging in food sector. In: *Advances in processing technology*. CRC Press, pp 261–308
42. Lin JF (1996) Mass transfer of alpha-tocopherol (vitamin E) from a multi-layer laminate structure and its influence on product stability. Michigan State University
43. Race S (2009) *Antioxidants. The truth about BHA, BHT, TBHQ and other antioxidants used as food additives*. Tigmor Books, Saltburn by the Sea, UK
44. Brody AL, Strupinsky EP, Kline LR (2001) *Active packaging for food applications*. CRC Press
45. Wrona M, Silva F, Salafranca J, Nerín C, Alfonso MJ, Caballero MÁ (2021) Design of new natural antioxidant active packaging: screening flowsheet from pure essential oils and vegetable oils to ex vivo testing in meat samples. *Food Contr* 120:107536
46. Vermeiren L, Devlieghere F, De Kruijf N, Debevere J (2000) Development in the active packaging of foods. *J Food Technol Africa* 5(1):6–13
47. Perry MR, Lentz RR (2020) Susceptors in microwave packaging. In: *Development of packaging and products for use in microwave ovens*. Woodhead Publishing, pp 261–291
48. Thanakkasaranee S, Sadeghi K, Seo J (2022) Packaging materials and technologies for microwave applications: a review. *Critical Rev Food Sci Nutr* 1–20
49. Barska A, Wyrwa J (2016) Consumer perception of active intelligent food packaging. *Probl Agric Econ* (4\_2016)
50. Ahmed I, Lin H, Zou L, Li Z, Brody AL, Qazi IM, Lv L, Pavase TR, Khan MU, Khan S, Sun L (2018) An overview of smart packaging technologies for monitoring safety and quality of meat and meat products. *Packag Technol Sci* 31(7):449–471
51. Ghoshal G (2018) Recent trends in active, smart, and intelligent packaging for food products. In: *Food packaging and preservation*. Academic Press, pp 343–374
52. Wu D, Zhang M, Chen H, Bhandari B (2021) Freshness monitoring technology of fish products in intelligent packaging. *Crit Rev Food Sci Nutr* 61(8):1279–1292

53. Haleem A, Javaid M, Singh RP, Suman R, Rab S (2021) Biosensors applications in medical field: a brief review. *Sens Int* 2:100100
54. Chadha U, Bhardwaj P, Agarwal R, Rawat P, Agarwal R, Gupta I, Panjwani M, Singh S, Ahuja C, Selvaraj SK, Banavoth M (2022) Recent progress and growth in biosensors technology: a critical review. *J Ind Eng Chem*
55. Steinhauer S (2014) Gas sensing properties of metal oxide nanowires and their CMOS integration (Doctoral dissertation)
56. Hogan SA, Kerry JP (2008) Smart packaging of meat and poultry products. In: *Smart packaging technologies for fast moving consumer goods*, pp 33–54
57. Javaid M, Haleem A, Rab S, Singh RP, Suman R (2021) Sensors for daily life: a review. *Sensors Int* 2:100121
58. Raya I, Kzar HH, Mahmoud ZH, Al Ayub Ahmed A, Ibatova AZ, Kianfar E (2021) A review of gas sensors based on carbon nanomaterial. *Carbon Lett* 1–26
59. Kennedy AD, Jacoby CA (1999) Biological indicators of marine environmental health: meiofauna—a neglected benthic component? *Environ Monit Assess* 54:47–68
60. Kanatt SR (2020) Development of active/intelligent food packaging film containing Amaranthus leaf extract for shelf life extension of chicken/fish during chilled storage. *Food Packag Shelf Life* 24:100506
61. Sahin E, ZiedBabaï M, Dallery Y, Vaillant R (2007) Ensuring supply chain safety through time temperature integrators. *Int J Logist Manag* 18(1):102–124
62. Cheng H, Xu H, McClements DJ, Chen L, Jiao A, Tian Y, Miao M, Jin Z (2022) Recent advances in intelligent food packaging materials: principles, preparation and applications. *Food Chem* 375:131738
63. Akhila K, Ramakanth D, Gaikwad KK (2022) Development of novel gallic acid-and cellulose acetate-coated paper as pH-responsive oxygen indicator for intelligent food packaging. *J Coat Technol Res* 19(5):1493–1506
64. Abraham J (2022) Future of food packaging: intelligent packaging. In: *Nanotechnology in intelligent food packaging*, pp 383–417

# Comparative Analysis of RSA-RK and ECC-RK for Aadhaar Card



R. Felista Sugirtha Lizy 

**Abstract** Hackers are inventing novel strategies to breach the encrypted information of practically all existing cryptographic algorithms, and therefore network security has always been an emerging study in communication technology. “Elliptic Curve Cryptography” (ECC) is a new cryptographic approach that has been demonstrated to work in public-key cryptosystems. ECC’s benefits ensure secure data transmission across an insecure medium. The standard ECC key pact procedure is based on El-Gamal encryption. ECC is the handiest procedure for network security because it offers good security with smaller key sizes, quicker computations, lower computing power, and less storage space. By merging ECC and Runge–Kutta (RK) methods, the performance of the ECC cryptanalysis technique is enhanced in relation to speed and security in this paper. The key advantages of RK techniques are that they are simple to use and have a low error rate. The Runge–Kutta-ECC procedure is designed to improve the avalanche effect, speed, throughput, and power consumption of the method. The enhanced performance of the RKECC method is discussed, in addition to the experimental results. There is also a detailed mathematical justification for the RKECC algorithm.

**Keywords** Elliptic curve cryptography · Speed · Throughput · Power consumption · Runge–Kutta

## 1 Introduction

Various essential services in India, such as driving authorizations, school studentships, cooking gas subventions, pensions, passports, and prudent fund accounts, are now linked to the Aadhaar card. The Aadhaar card is also being considered for integration with Indian Railway System services, particularly for online reservations. In June 2016, the Developmental Supportive Bank was introduced an

---

R. Felista Sugirtha Lizy (✉)

Department of Computer Science, A.P.C. Mahalaxmi College for Women, Thoothukudi, Tamil Nadu, India

e-mail: [21felistaa@gmail.com](mailto:21felistaa@gmail.com)

Aadhaar-based ATM using biometric fingerprints for added consumer security. The significance of Aadhaar cannot be overstated, as it contains data of billions of people, making its security a major political concern. However, Aadhaar has faced core and authorized challenges, together with significant leaks and defects in its inclusive safety, further complicating the situation.

Authentication, confidentiality, non-repudiation, integrity, access control, and other functions are all conceivable with cryptography. Various cryptography algorithms are used to encrypt data (methods of encryption). Together, key and cryptography algorithms are employed for data encoding and decoding (unscrambling) in information and system security.

Cryptography involves secure handover evidence through encryption and decryption procedures, playing a crucial role in data security. Here are two categories of cryptography: “Symmetric Key Cryptography (SKC)” using one key for both operations, and “Asymmetric Key Cryptography (AKC)” using two keys, one public and one private.

PKC classifies public key generation into three families based on mathematical difficulty: (1) Rivest, Shamir, and Adleman (RSA) family, (2) Diffie–Hellman (DH) family, and (3) Elliptic Curve Cryptography (ECC) family.

ECC offers unbreakable security, requiring more arithmetic but easy implementation on hardware or software.

The rest of the document is structured as follows: Section 2 provides an overview of DES, Sect. 3 explains the ECC algorithm, Sect. 4 outlines the proposed system, Sect. 5 analyzes the results, and the Sect. 6 presents the conclusions.

## 2 Literature Survey

Siddharth Raju et al. published a brief study on the Aadhaar card in 2017, discussing the scope and benefits of integrating the card into other systems. We also offer a number of scenarios in which the Aadhaar card may constitute a security risk [1].

In 2010, Paar [2] stated that Cryptography has become ubiquitous, finding its way into various aspects of our lives, including web browsers, email applications, cell phones, credit cards, cars, and even medical implants.

In 2015, Urvasi [3] suggested a new technique for steganography. To conceal visual information, a variety of steganographic and encryption techniques are employed. Some strategies are superior to others, while others have advantages and disadvantages.

In 2019, Aldabagh [4] reported a variety of security scenarios, cryptography being the most widely used strategy. The main problem is implementing security without interfering with personal information. In this scenario, steganography is the most appropriate alternate technique.

In 2020, Hoobi [5] conducted a study aiming to enhance the security of the Data Encryption Standard (DES) algorithm by improving the encryption key. The research utilized a combination of two efficient encryption algorithms, incorporating



the elliptic curve cryptography (ECC) algorithm to achieve a higher level of security for the Data Encryption Standard method.

In [6], the authors explained a technique for encrypting and decrypting text messages and image files in the spatial domain using a comparative linear congruential generator to improve random number generation and security.

Singh et al. [7] presented an implementation for ECC encryption and decryption of audio files in 2014.

Luma et al. [8] reported an ECC-based encryption and decryption method for audio files transmitted over the network in 2015. The study found ECC to be suitable for handling large data volumes and recommended it over RSA due to its ability to provide the same security with a smaller key size.

In 2016, Kumar et al. [9] proposed a novel solution for picture security by encoding RGB images with DNA and applying Elliptic Curve Diffie–Hellman encryption (ECDHE), adding an extra layer of protection.

In 2017, Fang et al. [10] explored the details of elliptic curve cryptography, covering its basics, message partitioning, encoding/decoding, and usage for encryption, key exchange, and digital signatures. The study concluded that ECC is preferred for these tasks due to its speed and memory efficiency.

### 3 Elliptic Curve Cryptography Algorithm

ECC is an element of PKI for generating keys; it is not an independent method that just takes care of the end-to-end safety of user data. Asymmetric PKI cryptography requires a user or system to have public and private keys that are a set of keys.

The private key is a secret key that only the user knows about, whereas the public key is shared with one or more users who have agreed to communicate. Key agreement protocols are used to manipulate such keys for data encryption and decryption. This proposed work is concerned with the encryption of data.

The proposed algorithm's province constraint is the prime  $p$ , which defines the scope of the field, together with values  $a$  and  $b$ , which fix the coefficients of the elliptic curve equation.

ECC implements all important asymmetric cryptosystem capabilities, including encryption, signatures, and key exchange. ECC is regarded as an ordinary contemporary replacement for the RSA cryptosystem since it uses lesser keys and signs for the identical level of security as RSA and allows for extremely rapid key generation, key agreement, and signatures.

“Elliptic Curve Cryptography” is one of several dissimilar types of public-key cryptography. RSA, Diffie–Hellman, and added algorithms are examples. As a starting point, let's go over the basics of public-key cryptography; when you have the time, you go into public-key cryptography in greater depth.

Figure 1 shows how public-key cryptanalysis enables the following:

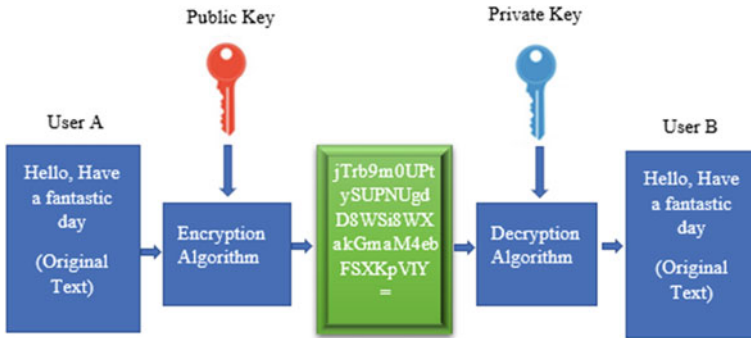


Fig. 1 The ECC algorithm's structure

A private key and a public key are generated. Then, the public key is publicly distributed, and anyone can use it to encrypt data. The private key, on the other hand, is kept secret, and only those who possess it will be able to decrypt data with it.

### 3.1 Runge–Kutta Methods

Consider the subsequent example of a differential equation:

$$\frac{db}{da} = f(a, b) \text{ with } y(a = a_0) = b_0 \text{ as the initial condition.}$$

Our aim is to fix  $y(x)$  in a described space.

The solution is as follows, using Euler's approach:

$$b_{i+1} = b_i + hf(a_i, b_i) \text{ (Here, the notations are } a(i) = a_i, b(i) = b_i \text{) where } h = a_{i+1} - a_i.$$

$$b_{i+1} = b_i + hb_i \text{ and } b_i = f(a_i, b_i)$$

We can derive the above formula from Taylor's series expansion:

$$b_{i+1} = b(a_{i+1} + h) = b_i + hb_i = b_i + hf(a_i, b_i)$$

Because we ignore the higher order component of Taylor's series, which leads to the truncation error  $O(h^2)$ , Euler's method is first-order accurate. As a result, the Euler technique is also referred to as the first-order Runge–Kutta method.

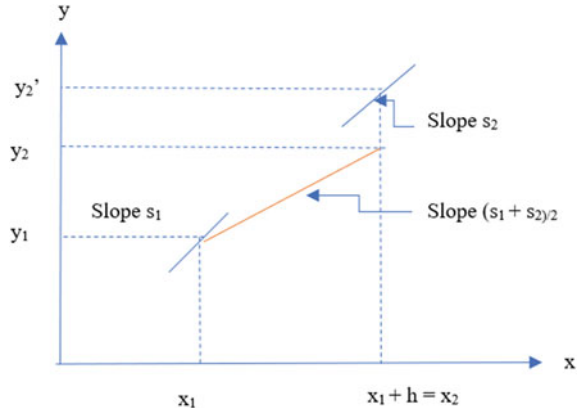
Consider the standard first-order differential equation once more to understand the second-order Runge–Kutta method:

$$\frac{db}{da} = f(a, b) \text{ with } b(a = a_1) = b_1 \text{ as the initial condition.}$$

Assume that 'h' is the equidistance value of x, that is,

$$a_2 = a_1 + h; a_3 = a_2 + h; \dots; a_{i+1} = a_i + h$$

**Fig. 2** The RK method's structure



To understand the second-order Runge–Kutta method, refer to Fig. 2. First of all, we compute the slope  $s_1 = f(a_i, b_i)$  of the result curve is  $b(a)$  at point  $(a_i, b_i)$ . Then, let us draw a straight line from the primary point  $(a_i, b_i)$  with the slope  $s_1$ . Let's assume that the conventional line cuts the vertical line through  $a_1 + h$  at  $(a_1 + h, b'_2)$ . Note that by definition,  $s_1 = (b'_2 - b_1)/(a_2 - a_1) = (b'_2 - b_1)/h$ . This implies that  $b'_2 = b_1 + s_1h$ .

Determine the slope of the resolution curve  $b(a)$  at the point  $s_2 = f(a_1 + h, b'_2) = f(a_2, b_1 + s_1h)$ . Return to the point  $(a_1, b_1)$  position and draw a straight line with a slope  $s = (s_1 + s_2)/2$ . The approximate explanation of the considered differential equation at the point  $a_1 + h$  in the second-order Runge–Kutta method is the point  $b_2$ , where this straight line cuts the vertical line  $a_1 + h$ . The slope is defined as follows:

$$s = (b_2 - b_1)/(a_2 - a_1) = (b_2 - b_1)/h$$

$$b_2 = b_1 + hs$$

$$b_2 = b_1 + h(s_1 + s_2)/2$$

where  $s_1 = f(a_1, b_1)$  and  $s_2 = f(a_2, b_1 + s_1h)$ .

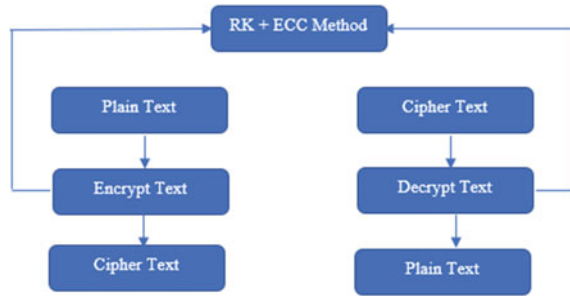
In general, the  $i + 1$ th is calculated using the formula from the  $i$ th point:

$$b_{i+1} = b_i + h(s_i + s_{i+1})/2$$

where  $s_i = f(a_i, b_i)$  and  $s_2 = f(a_{i+1}, b_i + s_ih)$ .

Heun's method is another name for this method. The Runge–Kutta second-order approach is second-order accurate, i.e., we demonstrate that the truncation error is  $O(h^3)$  using Taylor's series expansion.

**Fig. 3** Structure of RKECC algorithm



## 4 Proposed RKECC Algorithm

The Aadhaar card security is the most important in this country. So that, we need to improve the “Aadhaar card” security is very emerge. The proposed Runge–Kutta-ECC method, which is founded the RSA and Runge–Kutta (RK) approaches, is depicted in Fig. 3 for improving the Aadhaar card security and speed also. The RKECC algorithm is discussed in further detail below.

### 4.1 RKECC

Using the new function, RKECC now outperforms the ECC algorithm in terms of speed and security. The modified function allows for the encryption and decryption of a file’s whole contents. To shorten the time needed for each decryption, the procedures are carried out in three steps. The previous research paper reported an implementation for RKRSA encryption and decryption text file [11]. So this paper is compared with the RKECC algorithm and RKRSA algorithm.

## 5 Experimental Results

The text files used in this study are 226–289 bytes in size. By averaging the ten values (ten times), the file size is premeditated [12]. The execution speed, avalanche effect encryption throughput, and decryption throughput make up the overall performance parameters. In MATLAB, the RKECC algorithm is implemented.

The trial results for different performance indicators for the RKECC and RKRSA algorithms are listed below. The implications are numerous, as seen in the tables.

### 5.1 Time for Encryption

Figure 4’s representation of encryption time shows how long it takes to convert a message from plaintext to ciphertext during encryption [13]. For different input sizes, the average encryption time is computed. And finally, compared to the RKRSA algorithm, the RKECC algorithm requires the least amount of time for encryption. Table 1 details the comparative analysis of encryption time.

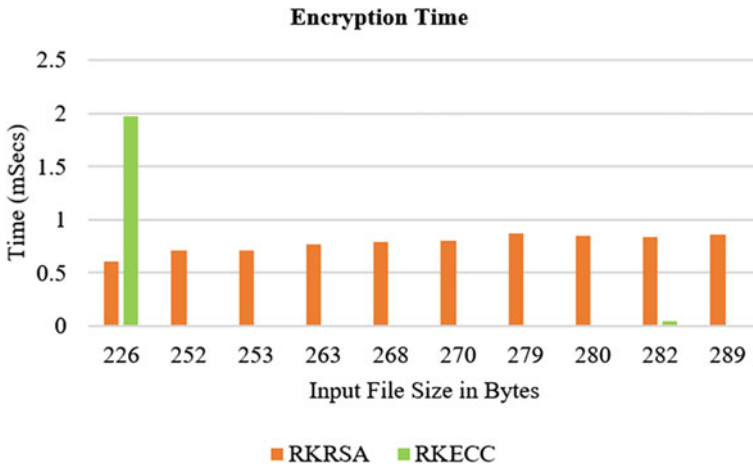


Fig. 4 Analysis of encryption times in comparison

Table 1 Analysis of encryption times in comparison

Size of the input (Bytes)	RKRSA	RKECC
226	0.6135	1.9734
252	0.7126	0.0111
253	0.7125	0.0109
263	0.7734	0.0112
268	0.7903	0.0120
270	0.7995	0.0122
279	0.8714	0.0118
280	0.8471	0.0120
282	0.8378	0.0450
289	0.8589	0.0144
Average time (s)	0.7817	0.2114
Throughput (KB/s)	0.3405	1.2592

### 5.2 Time for Decryption

Decryption time is one of the metrics used to measure overall performance. This metric measures how long it takes to translate a message from ciphertext to plaintext at the time of decryption (see Fig. 5). And finally, when compared to the RKRSA method, the RKECC technique requires the least amount of time to decode data. Table 2 provides a comparison analysis of decryption time.

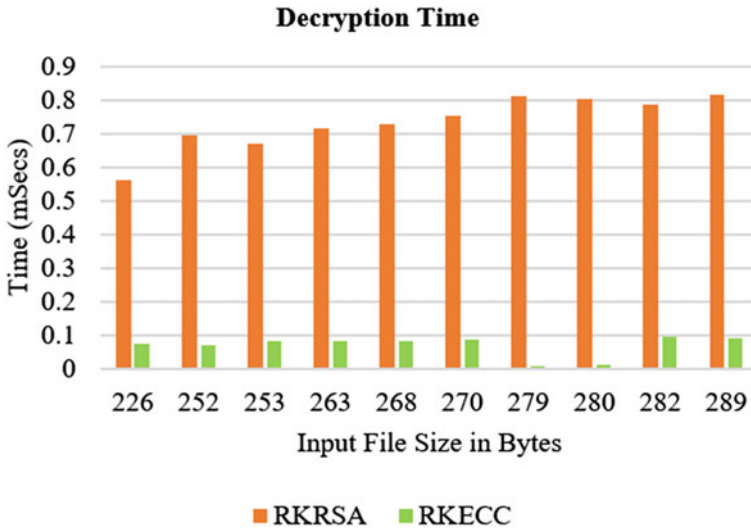


Fig. 5 Analysis of decryption times in comparison

Table 2 Analysis of decryption times in comparison

Size of the input (Bytes)	RKRSA	RKECC
226	0.5643	0.0752
252	0.6947	0.0712
253	0.6724	0.0834
263	0.7173	0.0843
268	0.7311	0.0818
270	0.7525	0.0896
279	0.8119	0.0096
280	0.8031	0.0122
282	0.7857	0.0945
289	0.8158	0.0936
Average time (s)	0.73488	0.06954
Throughput (KB/s)	0.3622	3.8281

### 5.3 Time for Execution

The time it takes to create a ciphertext from plaintext and create plaintext from the ciphertext, as seen in Fig. 6, is referred to as the execution time. And finally, compared to the RKRSA algorithm, the RKECC algorithm requires the least amount of time to execute. Table 3 provides a description of the comparative analysis of execution time.

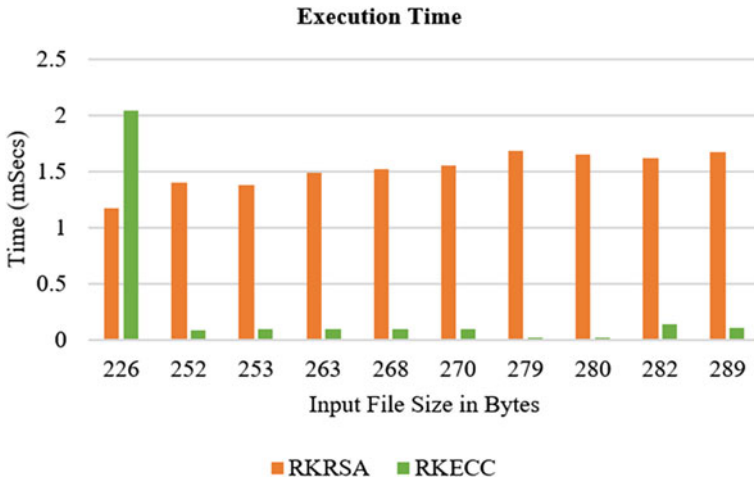


Fig. 6 Analysis of execution times in comparison

Table 3 Analysis of execution times in comparison

Size of the input (Bytes)	RKRSA	RKECC
226	1.1778	2.0486
252	1.4073	0.0823
253	1.3849	0.0943
263	1.4907	0.0955
268	1.5214	0.0938
270	1.551	0.1018
279	1.6833	0.0214
280	1.6502	0.0242
282	1.6235	0.1395
289	1.6747	0.1081
Average time (s)	1.51648	0.28095
Throughput (KB/s)	0.1726	0.9475

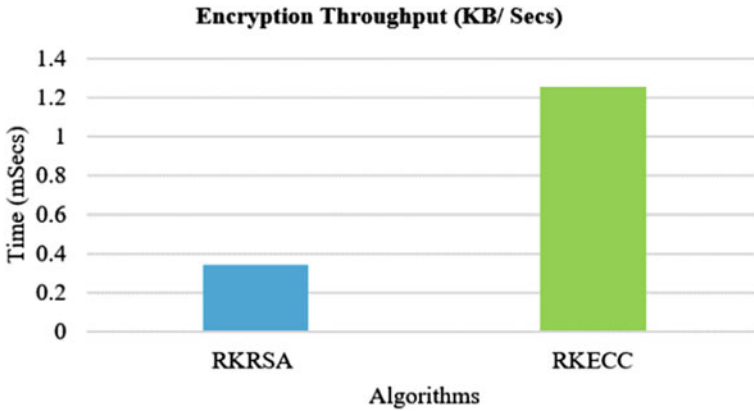


Fig. 7 Analysis of encryption throughput in comparison

Table 4 Analysis of throughputs in comparison (KB/s)

Total plaintext in MB	Algorithms	Encryption throughput	Decryption throughput	Execution throughput
2662	RKRSA	0.3405	0.3498	0.1726
	RKECC	1.2592	3.8280	0.9475

### 5.4 Encryption Throughput

The encryption throughput of the RKECC algorithm with various input files is displayed in Fig. 7.

The encryption throughput is calculated by dividing the full plaintext in Megabytes by the encryption time in Seconds.

Total Plaintext in Megabytes/Encryption Time is the throughput.

Table 4 presents the findings.

### 5.5 Decryption Throughput

The RKECC algorithm’s decryption throughput with various input files is shown in Fig. 8.

The Decryption Throughput is calculated by dividing the total plaintext in Megabytes by the Decryption time in seconds.

Total Plaintext in Megabytes/Decryption Time is the throughput.

Table 4 provides a summary of the findings.



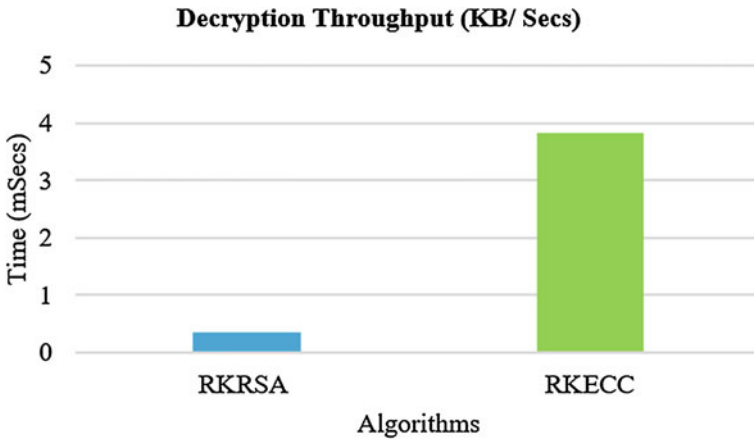


Fig. 8 Analysis of decryption throughput in comparison

### 5.6 Execution Throughput

Figure 9 shows the execution throughput of the RKECC method with various input files.

The Execution Throughput is calculated by dividing the total plaintext in Megabytes by the execution time in Seconds.

Total plaintext in megabytes divided by execution time is the measure of throughput.

The results are summarized in Table 4.

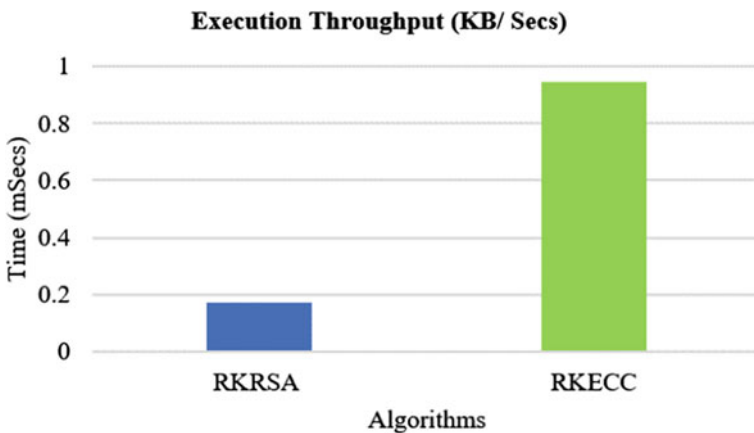
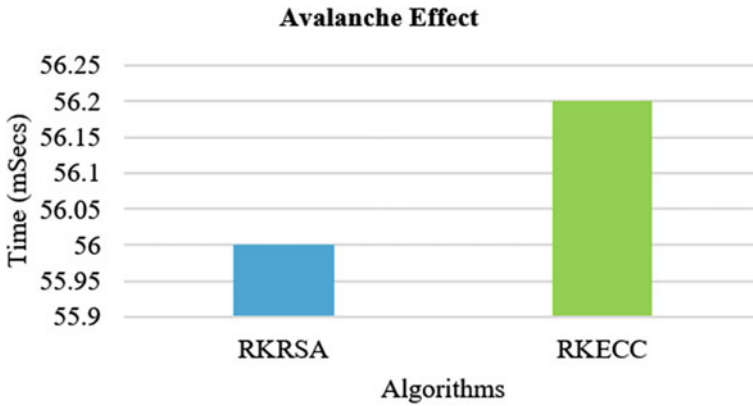


Fig. 9 Analysis of execution throughput in comparison



**Fig. 10** Analysis of avalanche effect in comparison

**Table 5** Analysis of avalanche effect in comparison

Encryption technique	Avalanche effect
RKRSA	56
RKECC	56.2

### 5.7 Avalanche Effect

The avalanche effect takes place when a single bit of the original text or a single bit of the key scheduling scheme is modified, causing changes in numerous bits of the ciphertext (see Fig. 10). As a result, the avalanche effect increases with security strength [14, 15]. Table 5 provides a summary of the results. When compared to the RKECC algorithm, the RKRSA algorithm has the least amount of avalanche impact.

### 5.8 Power Consumption

According to the aforementioned data, the RKECC algorithm uses the least amount of electricity and has the highest Execution Throughput [16]. Compared to the RKRSA algorithm, the RKECC algorithm offers the highest execution throughput.

## 6 Conclusion

For planning messages to an elliptic curve point, this study provides two algorithms: Runge–Kutta and Elliptic Curve Cryptography. In both techniques, groups are created by combining a list of ASCII values for the input text and creating enormous integers. Formerly, at the transmitter end, we use elliptic curve encryption, followed by decryption at the receiver end. The new techniques outperform the current approach and are appropriate for huge input information. The procedures offer the same level of protection as existing ECC-based encryption methods. The procedures are scalable, meaning they can handle any form of input message language. This new hybrid algorithm is used to secure the Aadhaar card and Smart card.

## References

1. Siddharth Raju R, Singh S, Khatter K (2017) Aadhaar card: challenges and impact on digital transformation
2. Paar C, Pelzl J (2010) Understanding cryptography. Springer-Verlag, Berlin Heidelberg, Germany, pp 239–255
3. Urvashi, Kaur A (2015) A review on various approaches for image steganography. *Int J Sci Res* 4(8):2024–2028
4. Aldabagh GMTK (2019) Proposed hybrid algorithm for image steganography in text security using fish algorithm 54(6). <http://jsju.org/index.php/journal/article/view/441>
5. Hoobi MM (2020) Efficient hybrid cryptography algorithm. *J Southw Jiaotong Univ* 55(3):1–9
6. Celestin Vigila M, Muneeswaran K (2012) Nonce based elliptic curve cryptosystem for text and image applications. *Int J Netw Secur* 14(4):236–242
7. Singh R, Chauhan R, Ritu G, Vinit K, Singh P (2014) Implementation of elliptic curve cryptography for audio-based application. *Int J Eng* 3(1)
8. Luma A, Selimi B, Ameti L (2015) Using elliptic curve encryption and decryption for securing audio messages. In: Yang GC, Ao SI, Gelman L (eds) *Transactions on engineering technologies*. Springer, Dordrecht
9. Kumar M, Iqbal A, Kumar P (2016) A new RGB image encryption algorithm based on DNA encoding and elliptic curve Diffie-Hellman cryptography. *Signal Process* 125:187–202
10. Fang X, Wu Y (2017) Investigation into the elliptic curve cryptography. In: *Information Management (ICIM)*. International conference on IEEE, pp 412–415
11. Felista Sugirtha Lizy R (2020) Performance enhancement of RSA Using Runge-Kutta technique. *Test Eng Manag* 11850–11857
12. Felista Sugirtha Lizy R (2021) Image encryption using RK-RSA algorithm in Aadhaar Card. *Turkish J Comput Math Educ* 4683–4693
13. Felista Sugirtha Lizy R (2021) Improvement of RSA algorithm using Euclidean technique. *Turkish J Comput Math Educ* 4694–4700
14. Shamina Ross B (2016) Security evaluation of blowfish and its modified version using GT's one-shot category of nash equilibrium. *Int J Contr Theory Appl* 4771–4777
15. Shamina RB (2015) Enhancing the performance of blowfish encryption algorithm in terms of speed and security by modifying its function. *Int J Appl Eng Res* 10(79):621–624
16. Shamina RB (2017) Performance enhancement of blowfish encryption using RK-blowfish technique. *Int J Appl Eng Res* 12:9236–9244

# Fundamental Security Risk Modeling in Smart Grid in the Modern Era of Artificial Intelligence



Rakshit Kothari, Ayushi Gill, Vijendra Kumar Maurya, and Anurag Paliwal

**Abstract** The world is moving toward viable as well as reliable energy sources. The implementation of smart grids is one such drive that aims to coordinate the generation, distribution, and consumption of energy more efficiently. However, managing the smart grid is not an easy task as it involves dealing with a large amount of data and making real-time decisions. Artificial Intelligence has emerged as a promising solution to address these challenges. Smart grids enable utilities to optimize their current infrastructure while reducing the need to build more power plants since they are autonomous and increase the effectiveness and efficacy of electrical power management. In this paper, we have analyzed the management of smart grids using AI with various algorithms used in Smart Grid and focusing on power generation and distribution systems. The paper also highlights the benefits of using AI such as improved efficiency, reduced costs, and enhanced reliability with applications for fault detections and provides the comparison of traditional and modern technology in smart grids.

**Keywords** Artificial intelligence · Energy consumption · Smart grid · Conventional grid

## 1 Introduction of Artificial Intelligence in Smart Grid

As the world moves toward a sustainable energy future, the use of AI in the management of smart grids will become increasingly important way. AI is playing an increasingly important role in managing power distribution in smart grid systems.

---

R. Kothari (✉) · A. Gill · V. K. Maurya  
Department of Computer Science and Engineering, Geetanjali Institute of Technical Studies,  
Dabok, Udaipur, India  
e-mail: [rakshit007kothari@gmail.com](mailto:rakshit007kothari@gmail.com)

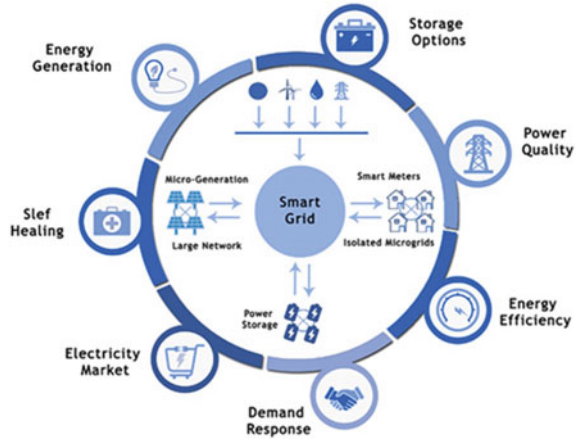
A. Paliwal  
Department of Electronics and Communication, Geetanjali Institute of Technical Studies, Dabok,  
Udaipur, India  
e-mail: [anurag.paliwal@gits.ac.in](mailto:anurag.paliwal@gits.ac.in)

By analyzing large volumes of data in real time and making predictions about energy demand and supply power, AI algorithms are enabling utilities to operate more and more efficiently, reliably, and sustainably than ever before.

Electricity has become an essential part of our regular lives. From powering our homes to driving our economy, it has become an indispensable commodity. The demand for electricity of human beings has increased symbolic over the decade. The primary requirement of electricity for human beings is to power our homes along with our workplaces. Without electricity, we would have to resort to alternative and often less efficient sources of energy such as candles together with firewood. In addition, electricity enables us to have access to modern conveniences such as refrigeration, heating, cooling, and entertainment. Electricity is also essential for businesses as well as industries [7]. Without electricity, the businesses would not be able to operate their full potential as well as our economy would suffer. For instance, hospitals rely on electricity to achieve life-saving equipment such as respirators as well as heart monitors. The demand for electricity has been growing due to the growing populations and urbanizations. By 2050, it is projected that there will be 9.7 billion people on the globe this will lead to an increased demand for electricity power [13]. The urbanization trend also means that more people will be living in cities [20], which will require more electricity to power buildings, infrastructure, and transportation. Another factor driving the requirement for electricity is the need to transition toward renewable energy sources. Fossil fuels, which have been the key source of electricity power generation for decades are finite along with, contribute to climate change. Humans must switch to energy power produced from renewable sources like solar, wind as well as hydroelectric power in order to reduce the effects of warming temperatures. This transition requires a significant increase in the amount of electricity generated from renewable sources.

The journey from the conventional grid to the smart grid has been a significant development in the field of power system. The conventional grid is a traditional electrical grid that is designed to generate and distribute power supply from centralized power plant to homes as well as workplaces. While it has served us well for over a century the conventional grid has several limitations that have become increasingly evident over and over time. The conventional grid is inefficient, inflexible, and prone to outages. It relies heavily on fossil fuels and is a significant contributor to greenhouse gas release. Additionally, the conventional grid is unable to handle the increasing demand for energy as well as particularly during peak hours. These limitations have led to a search for a more efficient, reliable including sustainable solution to power generation and distribution [4, 16, 19]. The smart grid is an electrical grid that uses new technologies such as sensors and communication networks to enable efficient and reliable power generation, distribution, and consumption. The smart grid is made adjustable and responsive to changes in demand and supply which enables optimizing power delivery and reducing energy waste. The journey from the conventional grid to the smart grid has not been without its challenges. The journey from the conventional grid to the smart grid has not been without its challenges. It requires significant investments in infrastructure, technology, and human resources. The implementation of the smart grid requires the cooperation of different stakehold-

**Fig. 1** Smart grid in artificial intelligence



ers that includes utilities, regulators, policymakers, and consumers [14]. Even after the challenges, the benefits of the smart grid contain too much costs [8]. The smart grid gives improved efficiency, reliability, and sustainability that’s the result of value saving, decreased emissions, and a better pleasant existence for consumers. As an end result, the transition to the smart grid instead of from the conventional grid is a vital step into a destiny powered by way of renewable resources. The smart grid is a progressed electrical device that carries cutting aspect technology to promote the most desirable and trustworthy energy era, distribution, and its applications. Smart grids are a critical step toward accomplishing sustainable strength future. Figure 1 represents the application of smart grid in artificial intelligence. The implementation of smart grids involves the use of advanced sensors, communication technologies, and data analytic to manage the generation and distribution of energy systems. However, managing the smart grid is a tedious task because it involves dealing with large volumes of data with real-time decisions [5, 22].

## 2 Need of Smart Grid

Earlier we were only consumer of electricity, so a traditional or conventional grid was sufficient for this purpose. Nowadays, we are both consumer as well as producer, so two-way communication is needed. Due to the lack of smart transformers, two-way communications are not possible in traditional grids. It is only possible by smart grid. It not only provides two-way communication of electricity but also provides communication of data. Due to some geographical imbalance in nature, some areas are rich in thermal plants due to the easy availability of coals, some are rich in solar and some are rich in hydro energy due to their own reason. To fulfill the requirement of uniform energy distribution across the country, energy transmission

is required. The results of these transmission losses are generated. This is called electricity evaporation. Also wind, solar, and some hydro plants do not generate constant power, so there is always a possibility of load imbalance [11]. So to avoid load imbalance as well as to avoid transmission losses, smart grids are needed for loss-free and uniform distribution of energy.

### 3 Comparison Between Traditional Grid and Smart Grid

The conventional grid is a centralized system that relies on large-scale power plants to generate electricity, which is then transmitted over long distances to distribution centers and finally delivered to customers. Table 1 shows the comparison between the traditional grid and smart grid system. The transmission and distribution infrastructure is typically based on copper wires and transformers and the system is designed to operate at a constant frequency and voltage level [18, 21, 25]. Decentralized systems that include decentralized energy sources, such as solar panels and wind turbines, into the grid are known as smart grids. To monitor and control the flow of power in real time, modern sensors, communication networks, and control systems are also utilized. As a result, energy may be distributed in a more effective and flexible way, and there is a chance that the system's supply and demand for electricity can be balanced.

### 4 AI-Based Power Generation and Distribution Through Smart Grid

Power generation and distribution must be optimized for smart grid management. By offering predictive analytics to enhance the power-generating process, AI may play a significant part in this. This can assist utilities in managing their capacity for elec-

**Table 1** Comparing traditional grid and smart grid

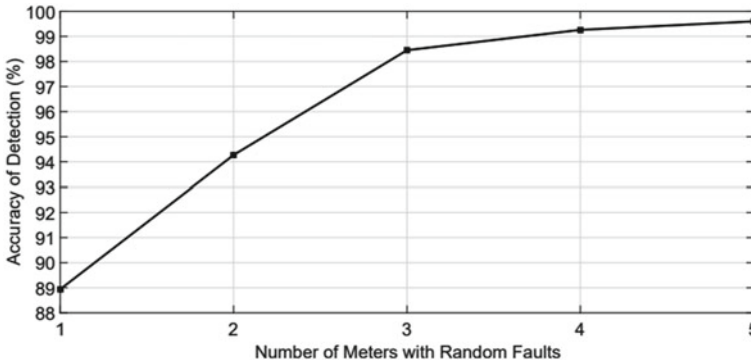
S. no.	Features	Traditional grid	Smart grid
1	Technology	Electrometrical technology	Digital technology
2	Requirement	Simple metering	Net metering
3	Communication	Less	More
4	Power generation	Centralized	Distributed
5	Monitoring	Manual	Self
6	Restoration	Manual	Self
7	Failures	More chances	Less chances

tricity generation, cutting costs, and increasing efficiency. AI can assist in managing power distribution by analyzing sensor data to find flaws and foresee outages. This can enable utilities to take preventive measures to minimize downtime and improve reliability. Power distribution in a smart grid is a complex and sophisticated process that involves the integration of advanced technologies such as sensors, communication networks, and data analytic. The smart grid is intended to improve electricity the delivery process, reduce utility recyclables, and encourage the grid's incorporation of energy produced from renewable sources [1]. A smart grid generates power from various renewable sources. The generated power is then sent through high-voltage transmission lines to substations, where its is voltage decreased before being supplied to end customers. One of the primary benefits of a smart grid is the inclusion of cutting-edge sensors and communication networks, which allows for real-time grid performance monitoring [19]. These sensors and networks offer important information on the grid's state, such as power demand, power supply status, and the presence of any defects or disturbances in the system. The smart grid can optimize electricity distribution by dynamically altering power supply and demand thanks to this real-time monitoring. For example, at times of heavy demand, the smart grid can redistribute electricity from less crucial systems to more vital systems to maintain continuous power delivery. It can also utilize demand response systems to encourage users to lower their energy consumption during peak hours, minimizing grid pressure. A smart grid also makes use of data analytic to make educated decisions about electricity generation and delivery. This entails evaluating massive volumes of data collected from sensors, weather predictions, and other sources in order to estimate energy demand and alter power supply accordingly. This allows the smart grid to run more effectively, waste less energy, and save money [9, 15]. In addition, the smart grid promotes the integration of renewable energy sources such as solar and wind power. These sources are intermittent and variable in nature, which can create challenges for power grid stability. However, the smart grid can use advanced technologies to predict renewable energy production and adjust power generation and distribution to accommodate fluctuations in energy supply. The power distribution in a smart grid involves the integration of advanced sensors, communication networks, and data analytic to optimize power delivery, reduce energy waste, and promote the integration of renewable energy sources. It is designed to operate more efficiently, reliably, and sustainably than the conventional grid and it represents a necessary step toward a more sustainable energy future.

## 5 Role of AI in the Management of Smart Grid

AI can help in managing the smart grid in different ways. One of the important interests of using AI is that it can analyze very big amounts of data as well as provide insights that can be used to optimize the grid's performance system. AI can also help in predicting demand and required power supply accordingly, which can also help to prevent blackouts with brownouts during demands [17]. Additionally, AI can enable



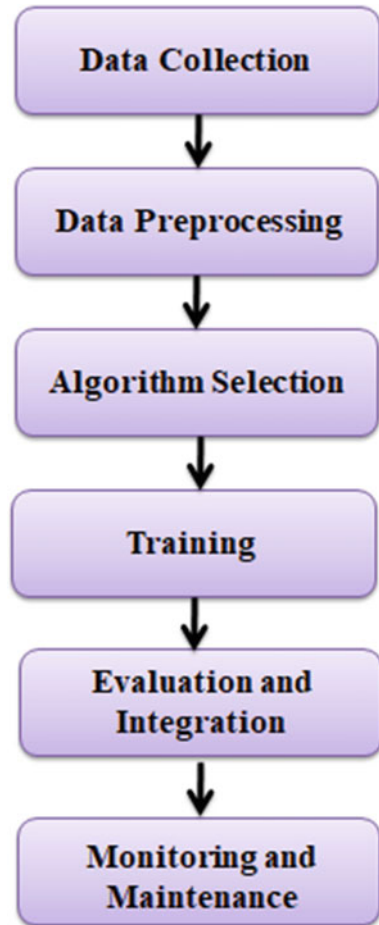


**Fig. 2** Accuracy of detection with the random faulty meters in smart grid

the integration of renewable energy sources into the grid by optimizing the distribution of power from these sources. AI is revolutionizing the way power distribution is managed in smart grids. AI algorithms and machine learning techniques can analyze large volumes of data in real time and make predictions about energy demand and supply, allowing for more efficient and optimized power distribution. Figure 2 shows the accuracy of Detection in percentage with faulty meters in smart grid. Demand response algorithms are one method AI is employed in power distribution. These initiatives employ artificial intelligence algorithms to incentivize consumers to lower their energy consumption during peak hours. By providing incentives such as discounts or rebates, consumers may alter their energy use, lowering strain on the system during peak demand periods. AI is a vital technology in smart grid power distribution management. By evaluating vast volumes of data, forecasting power demand, and changing power generation and distribution appropriately, AI integration enables the smart grid to run more effectively, reliably, and sustainably.

Machine learning algorithms are used in AI-based systems to assess real-time data from multiple sources such as smart meters, weather predictions, and other sensors in order to estimate power demand and modify power generation and distribution appropriately. This enables the smart grid to run more efficiently by decreasing energy waste and assuring continuous power supply [2]. In Fig. 3 shows the procedure of Smart Grid in AI. Load forecasting involves predicting future power demand based on historical data and other factors such as weather patterns, time of day, and seasonal changes. AI-based load forecasting models can analyze vast amounts of data to accurately predict power demand, allowing utilities to adjust power generation and distribution accordingly. AI-powered load forecasting systems can analyze large amounts of data to accurately anticipate power demand, allowing utilities to adjust power generation and distribution appropriately. AI may be used to enhance power distribution by controlling the flow of electricity via the grid. This requires altering the voltage and frequency of power transmission in real time to ensure that electricity is effectively and reliably transferred. AI-based systems can identify areas of the grid that are experiencing high levels of demand and adjust power flow to meet this demand while minimizing energy waste [6, 23]. AI-based systems can identify high-

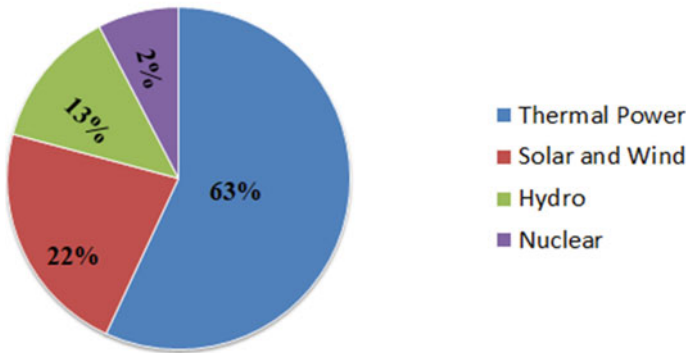
**Fig. 3** Steps in smart grid using AI



demand parts of the grid and alter power flow to fulfill this demand while minimizing energy loss. Fault identification and diagnosis is another major use of AI in the smart grid. Power outages and other interruptions can be caused by grid faults, resulting in severe economic and social consequences. Data from sensors and other sources may be analyzed by AI-based fault detection systems to swiftly identify errors and diagnose the underlying causes. This enables utilities to take corrective action swiftly and effectively, reducing customer damage.

AI can also help with the grid integration of renewable energy resources. The reliability of electrical systems may be compromised since renewable energy sources such as solar and wind power are irregular and inconsistent [26]. Renewable energy output may be forecasted using data from weather predictions and other sources and electricity generation and distribution can be changed accordingly [3, 12]. AI algorithms can also predict energy demand and supply with greater accuracy than

### Energy Sources in India categorized by Operational Capacity



**Fig. 4** Energy sources by operational capacity—India

traditional forecasting methods. By analyzing weather patterns, historical usage data, and other factors. AI can predict future energy demand and adjust power generation and distribution accordingly. This enables utilities to avoid power outages and reduce the need for expensive and inefficient peak power plants. Figure 4 represents a pie chart of Energy Sources by Operational Capacity in India. Diagnose and repair of faults is a further field where AI is having a big influence. Smart grids have thousands of sensors monitoring the grid's performance in real time. By analyzing this data, AI algorithms can detect faults and diagnose the source of the problem more quickly and accurately than traditional methods. This enables utilities to respond to outages faster and minimize the impact on consumers. Furthermore, the usage of renewable energy sources like wind and solar electricity may be optimized using AI. These sources are intermittent and variable in nature, making it challenging to integrate the min to the grid. On the other hand, utility may increase the usage of renewable energy sources and lessen dependency on fossil fuels by using AI algorithms to estimate renewable energy production and modify electricity generation and distribution appropriately. Figure 5 illustrates the energy consumption in Mega tonnes (Mtoe) with year.

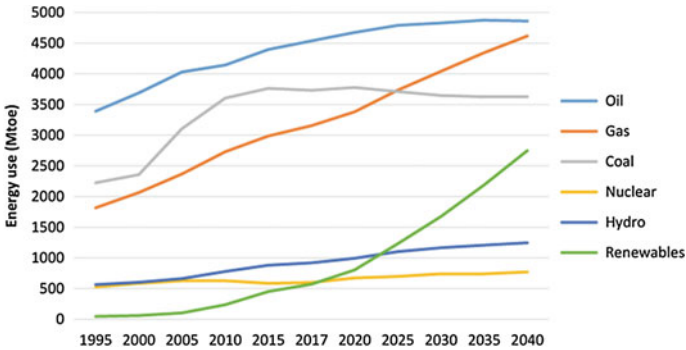


Fig. 5 Energy versus year traditional and modern technology

## 6 Algorithms Used in Smart Grid

### 6.1 Neural Networks

Neural networks are Machine learning algorithms that are designed after the human brain [10]. They are mostly used in the smart grid to forecast energy demand as well as optimize energy generation and distribution networks. Neural networks are used to analyze historical data along with weather patterns to predict energy demand accurately.

### 6.2 Fuzzy Logic

Fuzzy logic is an AI algorithm that is used in the smart grids to control energy flows, optimize energy usage as well as manage energy storage systems. Fuzzy logic-based system can adjust energy flows based on real-time data and ensure stable and reliable energy supply networks. These systems are the best for controlling energy flows, optimizing energy usage along with managing energy storage systems. Support vector machines are effective for classifying data and identifying patterns while decision trees are good for optimizing energy distribution network systems.

### 6.3 Reinforcement Learning

Reinforcement learning is an AI algorithm that is likely used in the smart grids to optimize energy consumption as well as reduce energy wastage. It requires training an AI model to make decisions based on rewards along with the punishments in form of cost which leads to most efficient way to use energy.

## **6.4 Support Vector Machines (SVMs)**

Support Vector Machines (SVMs) are machine learning algorithms which are mostly used in the smart grid systems to classify the data as well as identify the patterns too. SVMs can be used to analyze energy usage patterns with predict energy demand.

## **6.5 Decision Trees**

Decision Trees are also a type of machine learning algorithm which is used in the smart grid systems to optimize energy distribution networks to reduce energy wastage. DT analyzes data from sensors embedded with electrical network and also from other sources to make real-time decisions about the energy distribution system that ensures the efficient and reliable energy supply-demand [24].

## **6.6 Particle Swarm Optimization**

Particle Swarm Optimization (PSO) is a part of AI algorithm which is used in the smart grids systems to optimize energy generation along with distribution network. PSO-based systems can analyze the real-time data for adjustment of energy generations and distributions to ensuring an efficient and reliable energy supply network.

## **7 Conclusion**

The management of smart grid networks is a very tedious task in the energy sector and AI has emerged as a promising solution to address the challenges associated with it. The integration of AI in smart grid management represents a significant step toward a more sustainable and efficient energy in future. AI is a critical technology in managing the power system distribution in the smart grids. The integration of AI enables the smart grids to operate more efficiently, reliably, and sustainably by analyzing large amounts of data, predicting power demand with adjusting power generations and distributions accordingly. AI-based systems can support services to optimize power distribution, detect, and diagnose faults quickly also support the integration of renewable energy sources into the grid, making the smart grids, a much-needed step toward a more sustainable energy power. As per desire for green energy and advanced technologies, it continues to grow the AI-based smart grid is likely to play an important role in the world of electricity.

## References

1. Ahmad T, Zhang D, Huang C, Zhang H, Dai N, Song Y, Chen H (2021) Artificial intelligence in sustainable energy industry: status Quo, challenges and opportunities. *J Clean Prod* 289:125834
2. Ahmed M, Zheng Y, Amine A, Fathiannasab H, Chen Z (2021) The role of artificial intelligence in the mass adoption of electric vehicles. *Joule* 5(9):2296–2322
3. Boneh D, Boyen X (2004) Efficient selective-id secure identity-based encryption without random oracles. In: 34th annual international conference on the theory and applications of cryptographic techniques (EUROCRYPT), pp 223–38, Switzerland Springer
4. Bose BK (2017) Artificial intelligence techniques in smart grid and renewable energy systems—some example applications. *Proc IEEE* 105(11):2262–2273
5. Chen C, Chen J, Lim HW, Zhang Z, Feng D, Ling S, Wang H (2013) Fully secure attribute-based systems with short ciphertexts/signatures and threshold access structures. In: CT-RSA, lecture notes in computer science, vol 7779, pp 50–67 (2013)
6. Cheung L, Newport CC (2007) Provably secure ciphertext policy abe. In: ACM conference on computer and communications security, pp 456–465
7. Delerablée C (2007) Identity-based broadcast encryption with constant size ciphertexts and private keys. In: ASIACRYPT, vol 4833, pp 200–215
8. Foster I, Kesselman C, Tuecke, S (2001) The anatomy of the grid: enabling scalable virtual organizations. *Int J Supercomput Appl* 15(3):200–222
9. Goyal V, Pandey O, Sahai A, Waters B (2006) Attribute-based encryption for fine-grained access control of encrypted data. In: Juels A, Wright RN, di Vimercati SDC (eds) ACM conference on computer and communication security, pp 89–98. ACM
10. Guo F, Mu Y, Susilo W, Wong DS, Varadharajan V (2014) CP-ABE with constant-size keys for lightweight devices. *IEEE Trans Inf Forensics Secur* 9(5):763–771
11. Guo F, Mu Y, Chen, Z (2007) Identity-based encryption: how to decrypt multiple ciphertexts using a single decryption key. In: Proceedings pairing, vol 4575, pp 392–406
12. Guo F, Mu Y, Chen Z, Xu, L (2007) Multi-identity single-key decryption without random oracles. In: Proceedings inscrypt, vol 4990, pp 384–398
13. Guo F, Mu Y, Susilo, W (2012) Identity-based traitor tracing with short private key and short ciphertext. In: Proceedings ESORICS, vol 7459, pp 609–626
14. Guo H, Xu C, Li Z, Yao Y, Mu Y (2013) Efficient and dynamic key management for multiple identities in identity-based systems. *Inf Sci* 221:579–590
15. Khaleel M, Abulifa SA, Abulifa AA (2023) Artificial intelligent techniques for identifying the cause of disturbances in the power grid. *Brill: Res Artif Intell* 3(1):19–31
16. Khan F, Kothari R, Patel M (2022) Advancements in blockchain technology with the use of quantum blockchain and non-fungible tokens. In: Advancements in quantum blockchain with real-time applications, pp 199–225. IGI Global
17. Khan F, Kothari R, Patel M, Banoth N (2022) Enhancing non-fungible tokens for the evolution of blockchain technology. In: 2022 International conference on sustainable computing and data communication systems (ICSCDS), pp 1148–1153. IEEE
18. Kim SK, Huh JH (2018) A study on the improvement of smart grid security performance and blockchain smart grid perspective. *Energies* 11(8):1973
19. Kothari R, Choudhary N, Jain K (2021) CP-ABE scheme with decryption keys of constant size using ECC with expressive threshold access structure. In: Emerging trends in data driven computing and communications: proceedings of DDCT 2021, pp 15–36. Springer, Singapore
20. Lewko AB, Okamoto T, Sahai A, Takashima K, Waters B (2010) Fully secure functional encryption: attribute-based encryption and (hierarchical) inner product encryption. In: Gilbert H (ed) EUROCRYPT. Lecture notes in computer science, vol 6110, pp 62–91
21. Lo KL, Zakaria Z (2004) Electricity consumer classification using artificial intelligence. In: 39th international universities power engineering conference, 2004. UPEC 2004, vol 1, pp 443–447. IEEE
22. Musleh AS, Yao G, Muyeem SM (2019) Blockchain applications in smart grid—review and frameworks. *IEEE Access* 7:86746–86757

23. Ostrovsky R, Sahai A, Waters B (2007) Attribute-based encryption with non-monotonic access structures. In: Proceedings ACM conference on computer and communication security, pp 195–203
24. Pilkington M (2016) Blockchain technology: principles and applications. In: Research handbook on digital transformations, pp 225–253. Edward Elgar Publishing
25. Richter L, Lehna M, Marchand S, Scholz C, Dreher A, Klaiber S, Lenk S (2022) Artificial intelligence for electricity supply chain automation. *Renew Sustain Energy Rev* 163:112459
26. Vyas K, Jain G, Maurya VK, Mehra A (2016) Comparative analysis of MCML compressor with and without concept of sleep transistor. In: Proceedings of international conference on ICT for sustainable development: ICT4SD 2015, vol 1, pp 251–260. Springer, Singapore

# Adaptive Multi-resolution Simulations of Cascaded Converters



Asif Mushtaq Bhat and Mohammad Abid Bazaz

**Abstract** This paper presents an efficient modeling strategy for fast and accurate simulation of cascaded power electronic converters. The computational cost of simulations is drastically reduced by using Adaptive Multi-resolution Simulation (AMRS) algorithm. The numerical experiments on a benchmark model validate the efficacy of the proposed strategy.

**Keywords** High fidelity · Stiff · Switched state space

## 1 Introduction

Accurate simulation of power electronic converters (PECs) is crucial to minimize the need for design alterations and physical prototyping [1]. This helps to get the hardware prototype ready in the first attempt and prevents needless cost overruns. It helps in characterizing their dynamic nature as well. These circuits pose distinctive simulation challenges that are not usually encountered in simulating their digital circuit counterparts. While a power electronic circuit's schematic is substantially more straightforward than a digital circuit for a given size, its analysis and layout complexity is noticeably higher [2].

The highly nonlinear behavior of the components employed in these circuits sets them apart from others. The nonlinearities are mathematically stiff because the circuit's time constants span several orders of magnitude [3, 4]. The time constants of snubbers and other transient-shaping components are substantially smaller than those of power stage inductors and capacitors, whose time constants are larger than the conversion period. To ensure numerical stability, the fastest transients necessitate an exceedingly small time step. Additionally, to accurately capture slowly changing dynamics, the simulation must be run for an extended period. So, the simulation

---

A. M. Bhat (✉) · M. A. Bazaz

Department of Electrical Engineering, National Institute of Technology Srinagar, Srinagar, India  
e-mail: [aasifmushtaq111@gmail.com](mailto:aasifmushtaq111@gmail.com)

M. A. Bazaz

e-mail: [abid@nitsri.ac.in](mailto:abid@nitsri.ac.in)



routine must take tiny steps and run for a longer period of time. This makes the simulation of PECs challenging, and the computational resources needed for simulation also grow significantly. Fixed-time step solvers like Runge–Kutta (RK), Euler, etc., are not an option because of the inherent stiffness. The simulation is still sluggish even when using techniques based on numerical and backward differentiation formulae (NDFs and BDFs) [5].

The amplitude of the system transients places a limit on the step size. Moreover, if the transition from *on* to *off* and vice versa is not calculated with an accuracy of  $10^{(-4)}$  or higher, the solution could potentially become unstable. For accurate simulation, high-fidelity models that include impacts of stray parasites, electromagnetic interference, etc., must be incorporated. Although numerous efforts have been made to address the power electronic simulation challenge, it largely remains unresolved [3, 4, 6–16].

## 2 High-Fidelity Modeling of PECs

State-space modeling is an important tool used to represent dynamical systems and efficiently capture both their transient and steady-state behaviors. Modeling switch mode power converters is a simple extension of this method. Here switches are considered ideal, which can either be *on* or *off*. Now, if there are  $n$  number of switches present in the circuit, then there will be  $2^n$  switch modes. Using basic circuit analysis each switch mode of PEC can be represented by the form:

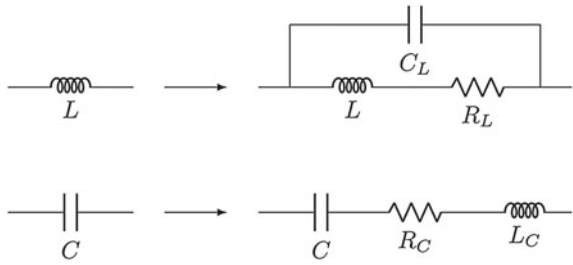
$$\begin{aligned}\dot{\mathbf{x}}^i(\mathbf{t}) &= \mathbf{A}^i\mathbf{x}^i(\mathbf{t}) + \mathbf{B}^i\mathbf{u}(\mathbf{t}) \\ \mathbf{y}(\mathbf{t}) &= \mathbf{C}^i\mathbf{x}^i(\mathbf{t})\end{aligned}\quad (1)$$

where “i” denotes the  $i_{th}$  switch mode. A switching rule [17] controls the change from one switching mode to another. The representation shown in (1) is known as the switched state-space representation, which precisely illustrates the dynamic characteristics of the circuit. It also aids in the estimation of peak current and voltage values, and switching losses during switching transitions.

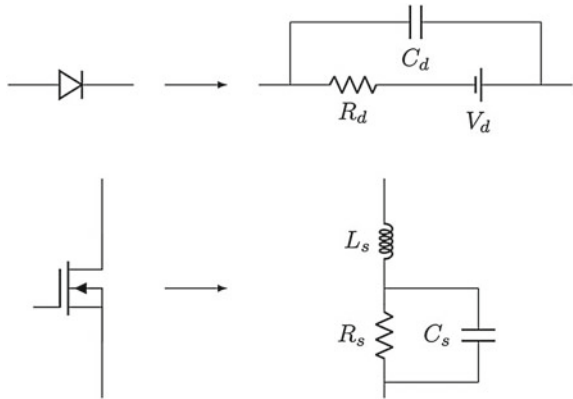
Passive elements, such as inductors, capacitors, and other similar components, are considered to be linear and time-invariant elements. Modeling these components allows for the inclusion of parasitics like stray capacitance of an inductor [18] and series resistance as depicted in Fig. 1. The equivalent series resistance (ESR) and leakage inductance of a capacitor can also be included in the analysis.

Diode and MOSFETs are modeled as switch-mode dependent elements. The components  $R_d$ ,  $C_d$ , and  $V_d$  are assembled to form a diode in the manner as depicted in Fig. 2. The state of a diode is determined by its current and voltage. Elements  $R_s$ ,  $L_s$ , and  $C_s$  can be used to simulate the MOSFET drain-to-source properties. The MOSFET’s parasitic effects are represented by the elements  $L_s$  and  $C_s$ .

**Fig. 1** High-fidelity model of inductor and capacitor



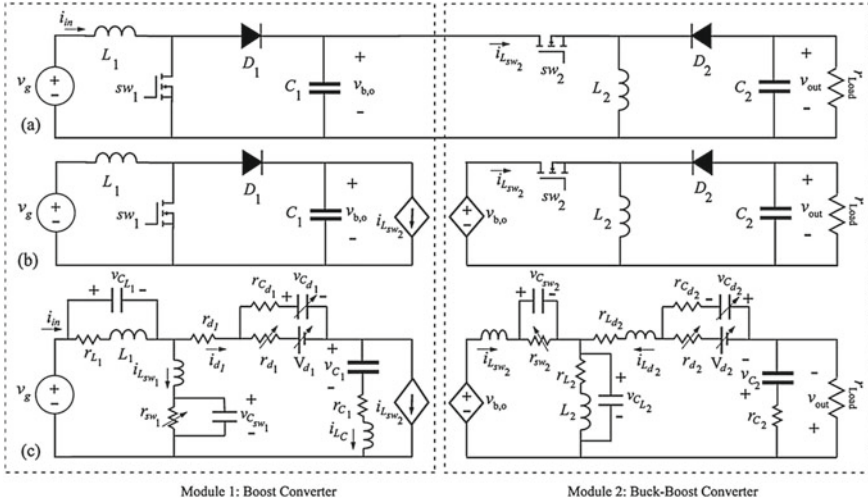
**Fig. 2** High-fidelity model of diode and MOSFET



## 2.1 Cascaded Converters

Power electronics applications often involve the presence of multi-converter systems, such as cascaded converters. The most common example is found in solar PV systems. In this section, we will discuss the high-fidelity modeling of cascaded converters which tend to have a greater number of switches than the conventional switch mode power converters.

The cascaded converter topology that we have considered here is a cascaded boost/buck–boost converter system where a boost converter is on the input side and buck–boost converter is on the output side. Figure 3a shows an equivalent circuit of the cascaded converter where the boost converter’s output voltage  $v_{b_o}$  of is fed as an input to the buck–boost converter. In this converter topology, we have four switches, and the piece-wise linear state space modeling will result in  $2^4$  i.e., 16 state-space models. Instead of dealing with 16 state-space models if we model the converters in cascade, individually, we need to deal with  $(2^2 + 2^2)$  i.e., only 8 state-space models. Dealing with 8 state-space models is much easier than dealing with 16 state-space models. For that, we need to model the output and input of boost and buck–boost converters respectively as dependent sources. The output of the boost converter is represented by a dependent current source  $i_{L_{sw2}}$ , which is actually a state variable of the buck–boost converter, and the input of the buck–boost converter is represented



**Fig. 3** Cascaded boost/buck-boost converter. **a** Equivalent circuit representation. **b** Representation in a modular form using coupling exchange variables. **c** Representation with high-fidelity model

by a dependent voltage source  $v_{b,o}$ , which is actually a linear combination of state variables of boost converter. Figure 3b shows a modular representation of the above-mentioned cascaded converter. For high-fidelity modeling, every circuit element of the cascaded converter is replaced by its high-fidelity model, where parasitic effects and other nonlinearities present in the circuit are modeled. With this, additional capacitances and inductances are added to the circuit, and the order of each modular converter becomes equal to seven. Figure 3c shows high-fidelity models of each converter circuit. During the course of the simulation, we need to pass on these variables simultaneously for every time step.

### 3 AMRS Framework for Cascaded Converters

The stiffness and switched state space representation of cascaded converters make their simulation computationally very expensive, in terms of time and resources. So, in order to reduce the computational burden of simulation Adaptive Multi-resolution Simulation (AMRS) [19–21] is used. In AMRS, various resolutions of different orders are extracted without any extra computational effort, that switch during the course of the simulation. The order of minimum resolution for a particular converter unit is decided based on the switching frequency of that converter. The simulation starts with the full-order or maximum resolution and adaptively shifts to the next maximum resolution based on the predefined tolerance until it reaches the minimum resolution. For cascaded converters, the AMRS algorithm is applied to the individual

converter circuits and the coupling variables are passed on simultaneously during the course of the simulation. The state-space modeling approach for cascaded converters discussed in the previous section allows us to do so. Otherwise, it becomes very difficult to apply the AMRS algorithm to cascaded converters.

### Problem Formulation

High-fidelity modeling of PECs [19, 22] leads to a switched state space

$$\begin{aligned}\dot{x}^i(t) &= A^i x^i(t) + B^i u(t) \\ y(t) &= C^i x^i(t)\end{aligned}\quad (2)$$

where the system matrices  $A^i$ ,  $B^i$  and  $C^i$  are defined and  $i$  signifies the switch mode. The state, output, and input vectors are represented by  $x$ ,  $y$  and  $u$ , respectively. Similarity transformation is used to decouple the dynamics

$$x^i(t) = P^i z^i(t) \text{ where, } P^i \in \mathbb{R}^{n \times n} \quad (3)$$

which gives a system

$$\begin{aligned}\dot{z}^i(t) &= \Lambda^i z^i(t) + \beta^i u(t) \\ y(t) &= \Gamma^i z^i(t)\end{aligned}\quad (4)$$

representing every PEC switching mode. where  $\Lambda^i$ ,  $\beta^i$  and  $\Gamma^i$  are the decoupled-system matrices. The large range of eigenvalues allows the system to be divided into non-dominant and dominant components. Matrix  $\Lambda^i$  is partitioned as

$$\Lambda^i = \begin{bmatrix} \Lambda_k^i & 0 \\ 0 & \Lambda_{n-k}^i \end{bmatrix} \quad (5)$$

where  $n$  represents order of the system and eigenvalues ( $\Lambda$ ) are listed in order of decreasing dominance. The index of the retained eigenvalues is given by the subscript  $k \leq n$  in (5). Then the system in (4) can be written as

$$\begin{aligned}\begin{bmatrix} \dot{z}_k^i \\ \dot{z}_{n-k}^i \end{bmatrix} &= \begin{bmatrix} \Lambda_k^i & 0 \\ 0 & \Lambda_{n-k}^i \end{bmatrix} \begin{bmatrix} z_k^i \\ z_{n-k}^i \end{bmatrix} + \begin{bmatrix} \beta_k^i \\ \beta_{n-k}^i \end{bmatrix} u \\ y &= [\Lambda_k^i \ \Lambda_{n-k}^i] \begin{bmatrix} z_k^i \\ z_{n-k}^i \end{bmatrix}\end{aligned}\quad (6)$$

In the beginning maximum resolution model, i.e., full order is simulated where  $k = n$ . In this scenario, the behavior of every eigenvalue is taken into account. To achieve lower resolutions, the transient part of the states associated with the non-dominant eigenvalues are left. Substituting  $\dot{z}_{n-k}^i = 0$  in (6), we get a system represented by (7) and (8).

$$\begin{bmatrix} \dot{z}_k^i \\ \mathbf{0} \end{bmatrix} = \begin{bmatrix} \Lambda_k^i & 0 \\ 0 & I \end{bmatrix} \begin{bmatrix} z_k^i \\ z_{n-k}^i \end{bmatrix} + \begin{bmatrix} \beta_k^i \\ (\Lambda_{n-k}^i)^{-1} \beta_{n-k}^i \end{bmatrix} u \quad (7)$$

$$y = \begin{bmatrix} \Lambda_k^i & \Lambda_{k-n}^i \end{bmatrix} \begin{bmatrix} z_k^i \\ z_{n-k}^i \end{bmatrix} \quad (8)$$

This can be denoted in a standard descriptor model as

$$E_k^i \dot{z}_k^i = A_k^i z_k^i + B_k^i u y = \Lambda^i z^i \quad (9)$$

where the matrices,

$$E_k^i = \begin{bmatrix} I_{k \times k} & 0 \\ 0 & 0 \end{bmatrix}, \quad A_k^i = \begin{bmatrix} \Lambda_k^i & 0 \\ 0 & I_{(n-k) \times (n-k)} \end{bmatrix} \quad (10)$$

$$B_k^i = \begin{bmatrix} \beta_k^i \\ (\Lambda_{n-k}^i)^{-1} \beta_{n-k}^i \end{bmatrix}$$

represents the  $i$ th mode of the simulation where the behavior of eigenvalues, having magnitudes greater than  $\Lambda_k^i$ , is excluded.

As the simulation progresses, the index  $k$  varies. The model with maximum-resolution is represented by  $k = n$ , whereas the model with minimum-resolution model is represented by  $k = 1$  (or  $k = 2$ , for a complex conjugate pair of eigenvalues). Instead of simulating the entire model throughout the entire simulation interval, the system is solved in an adaptive manner, where the order of the system adapts over time.

## 4 Simulations

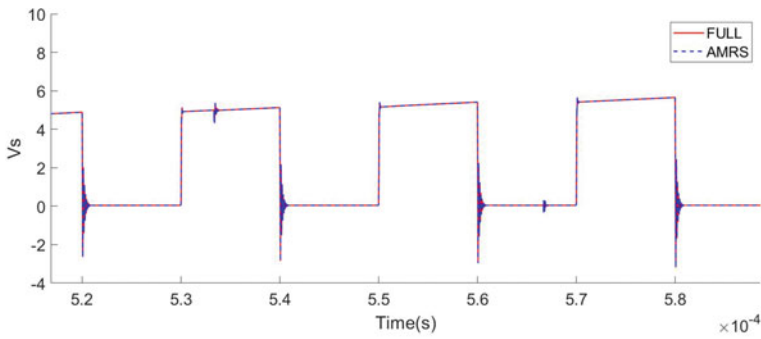
We have simulated the above-mentioned cascaded converter with the parameters given in Table 1 using MATLAB 2021a on an Intel Core i7-7600U Workstation with a clock frequency of 2.80 GHz. MATLAB's inbuilt stiff solver "ode23s" is used for the simulations. The simulations are carried out for an input voltage of 10 V and switching frequencies of 50 kHz and 30 kHz for boost and buck–boost converters respectively, with a duty ratio of 50% in each case. Two sets of simulations are performed: full-order model simulations and an adaptive multi-resolution simulation (AMRS). The tolerance setting for AMRS is set to  $10^{-4}$ . The comparison of simulation time and the number of integration steps are given in Table 2, when the model was simulated up to 1 milli-second. While the original model took 543 s, the AMRS took only 89 s. Figure 4 shows the waveforms of boost converter switch voltage  $V_s$  for full-order simulations and AMRS.

**Table 1** Circuit parameters: cascaded converter

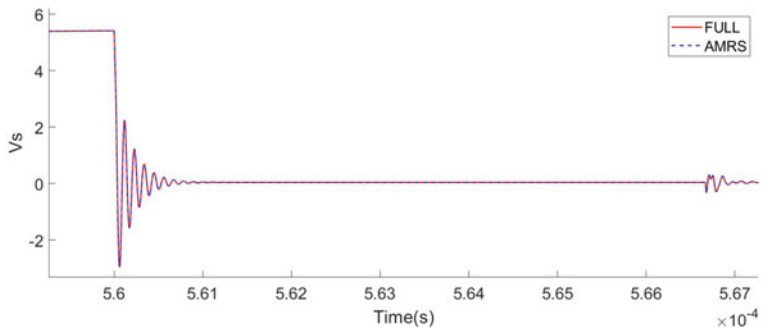
$v_g$	10 V	$r_{sw1}, r_{sw2}$ (on)	20 mΩ	$C_{d1}, C_{d2}$ (off)	10 nF	$R_{load}$	64.5 Ω
$L_1$	2.16 mH	$r_{sw1}, r_{sw2}$ (off)	20 MΩ	$r_{Ld}$	1mΩ	$f_{sw1}$	50 KHz
$L_2$	4.54 mH	$r_{d1}, r_{d2}$ (on)	220 mΩ	$L_d$	50 nH	$f_{sw1}$	30 KHz
$r_{L1}, r_{L2}$	20 mΩ	$r_{d1}, r_{d2}$ (off)	10 MΩ	$C_1, C_2$	96 μF	$d_1, d_2$	0.49
$C_{L1}, C_{L2}$	5 nF	$V_{d1}, V_{d2}$ (on)	0.58 V	$L_{C1}, L_{C2}$	1nF	$L_{sw1}, L_{sw2}$	20 nH
$C_{sw1}, C_{sw2}$	10 nF	$C_{d1}, C_{d2}$ (on)	1.5 nF	$r_{C1}, r_{C2}$	345 mΩ		

**Table 2** Simulation statistics: cascaded converter

	CPU time (s)	Integration steps
Original model	543.7	1,000,000
AMRS	89.2	163,455



Multiple Cycles



Zoomed in Version

**Fig. 4** Cascaded converter: A comparison of waveforms of the voltage across the MOSFET of the boost converter

## 5 Conclusion

In this paper, a new modeling strategy for fast simulation of cascaded converters is proposed. The time of simulation as well as the computational resources required are significantly reduced. The proposed modeling strategy simplifies the use of an adaptive multi-resolution simulation (AMRS) algorithm for fast simulation of cascaded converters. The number of state-space models to be solved for the simulation is significantly reduced which translates into the reduction of computational resources as well as the time of the simulation. The results are numerically validated on a cascaded converter with a boost converter in cascade with a buck–boost converter.

## References

1. Mohan N, Robbins WP, Undeland TM, Nilssen R, Mo O (1994) Simulation of power electronic and motion control systems-an overview. *Proc IEEE* 82(8):1287–1302
2. Wilson TG (1988) Life after the schematic: the impact of circuit operation on the physical realization of electronic power supplies. *Proc IEEE* 76(4):325–334
3. Christoph D, Peter T (1999) Fast simulation technique for power electronic circuits with widely different time constants. *IEEE Trans Ind Appl* 35(3):657–662
4. Toshiji K, Kaoru I, Takayuki F, Yoshinori K (2009) Multirate analysis method for a power electronic system by circuit partitioning. *IEEE Trans Power Electron* 24(12):2791–2802
5. Shampine LF, Reichelt MW (1997) The matlab ode suite. *SIAM J Sci Comput* 18(1):1–22
6. Hovland S, Gravdahl JT (2006) Order reduction and output feedback stabilization of an unstable cfd model. In: 2006 American control conference, pp 436–441. IEEE
7. Telescu M, Tanguy N, Bréhonnet P, Vilbé P, Calvez L-C, Huret F (2005) Model-order reduction of VLSI circuit interconnects via a Laguerre representation. In: Proceedings 9th IEEE workshop on signal propagation on interconnects, 2005, pp 107–110. IEEE
8. Karen W, Jaime P, Jacob W (2002) An Arnoldi approach for generation of reduced-order models for turbomachinery. *Comput Fluids* 31(3):369–389
9. Phillips JR (2003) Projection-based approaches for model reduction of weakly nonlinear, time-varying systems. *IEEE Trans Comput-Aided Des Integr Circuits Syst* 22(2):171–187
10. Remis RF, van den Berg PM (1997) A modified Lanczos algorithm for the computation of transient electromagnetic wavefields. *IEEE Trans Microw Theory Tech* 45(12):2139–2149
11. Nicola F, Giovanni S, Vincenzo T (1995) State-space models and order reduction for Dc-Dc switching converters in discontinuous modes. *IEEE Trans Power Electron* 10(6):640–650
12. Pekarek SD, Wasynczuk O, Walters EA, Jatskevich JV, Lucas CE, Wu N, Lamm PT (2004) An efficient multirate simulation technique for power-electronic-based systems. *IEEE Trans Power Syst* 19(1):399–409
13. Nahvi SA, Bazaz MA, Khan H (2017) Model order reduction in power electronics: issues and perspectives. In: 2017 international conference on computing, communication and automation (ICCCA), pp 1417–1421. IEEE
14. Khan H, Bazaz MA, Nahvi SA (2017) Model order reduction of power electronic circuits. In: 2017 6th international conference on computer applications in electrical engineering-recent advances (CERA), pp 450–455. IEEE
15. Sanders SR, Noworolski JM, Liu XZ, Verghese GC (1991) Generalized averaging method for power conversion circuits. *IEEE Trans Power Electron* 6(2):251–259
16. Fung KK, Hui SYR (1996) Fast simulation of multistage power electronic systems with widely separated operating frequencies. *IEEE Trans Power Electron* 11(3):405–412
17. Liberzon D (2003) Switching in systems and control, vol 190. Springer

18. Massarini A, Kazimierczuk MK (1997) Self-capacitance of inductors. *IEEE Trans Power Electron* 12(4):671–676
19. Khan H, Bazaz MA, Nahvi SA (2020) Adaptive multi-resolution framework for fast simulation of power electronic circuits. *IET Circuits Devices Syst* 14(4):537–546
20. Khan H, Bazaz MA, Nahvi SA (2018) Simulation acceleration of high-fidelity nonlinear power electronic circuits using model order reduction. *IFAC-PapersOnLine* 51(1):273–278
21. Khan H, Bazaz MA, Nahvi SA (2019) Accelerated simulation across multiple resolutions for power electronic circuits. In: 2019 fifth Indian control conference (ICC), pp 195–200. *IEEE*
22. Maksimovic D, Stankovic AM, Thottuvelil VJ, Verghese GC (2001) Modeling and simulation of power electronic converters. *Proc IEEE* 89(6):898–912



# Efficient Solar Cell Using COMSOL Multiphysics



Rama Devi, Yogendra Kumar Upadhyaya, S. Manasa, Abhinav,  
and Ashutosh Tripathi

**Abstract** This research is concentrated on building solar cells with greater efficiency than standard solar cells. The main aim of this work is to extend solar cells in such a way that their efficiency can be increased in comparison to regular solar cells. Our project's model is a one-dimensional silicon p–n junction with carrier generation and Shockley–Read–Hall recombination. This model represents how solar cells behave under forward bias at various voltages. For the front surface doping, a geometric doping model is employed, whereas an analytical doping model is used for the uniform bulk doping (the surface is specified in the Boundary Selection for Doping Profile sub-node). The Shockley–Read–Hall recombination model is implemented in a Trap-Assisted Recombination feature, while the photogeneration is carried out in a User-Defined Generation feature. Two Metal Contact features are used to make the electrical connections to the front and back surfaces. The generation rate is expressed simply as a user-defined spatially dependent variable using an integral equation involving the silicon absorption spectrum and solar irradiation. Additionally, the primary recombination impact is captured using the Shockley–Read–Hall model. Photo-generated carriers are swept to either side of the p–n junction's depletion zone during normal operation. A moderate forward bias voltage is used to generate the electrical power, which is produced by the photo-current and the applied voltage. After reviewing numerous studies, we have been led to the realization that adjusting the dimensions of the solar cell under ID configuration in the COMSOL Multiphysics software has improved the efficiency. We prefer COMSOL Multiphysics because it is simple to use, gives us a lot of exposure, and provides accurate data for whatever material we utilize.

**Keywords** Solar cells · Shockley–Read–Hall model · COMSOL Multiphysics

---

R. Devi · Y. K. Upadhyaya · S. Manasa (✉) · Abhinav · A. Tripathi  
Chandigarh University, Mohali, Punjab 140413, India  
e-mail: [manasa.sreerama1999@gmail.com](mailto:manasa.sreerama1999@gmail.com)

# 1 Introduction

A solar cell is a type of electric appliance that converts light energy into electrical energy using the photovoltaic effect. A photovoltaic cell, or PV cell, is another name for this kind of cell [1]. A solar cell is essentially a p–n junction diode. A photoelectric cell, which includes solar cells, is a device whose electrical characteristics, such as current, voltage, and resistance, change when exposed to light. Many solar cells are combined to form solar panels, also known as modules or solar panels [2]. A common silicon single junction solar cell is capable of producing an open-circuit voltage of up to 0.6 V. Considering how little these solar cells are, this isn't much on its own. Quite a bit of renewable energy may be produced when solar cells are merged into a big solar panel [3]. The use of alternative energy sources is being encouraged by growing energy demand, global environmental concerns, and technological advancements in renewable energy. Solar energy is the most affordable and widely available type of long-term natural resource [4]. Solar PV technology, which turns sunlight into direct current in solar cells or PV cells, is one of the best ways to use solar energy to generate electricity.

Gallium arsenide (GaAs), amorphous silicon (a-Si), and copper indium gallium selenide (CIGS) are examples of additional semiconductor materials that are frequently used in the structure of thin-film technology. A traditional (c-Si) solar cell is substantially thicker than a thin-film solar cell [5].

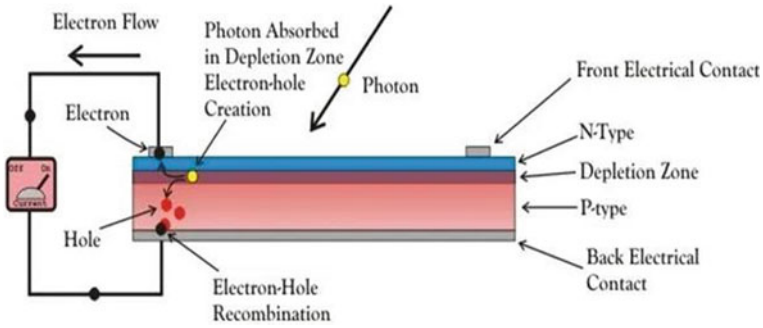
Thin-film modules can be light and flexible due to the thickness of the film, which ranges from a few nanometers (nm) to tens of micro meter's (um). Additionally, thin-film technology is typically more affordable than (c-Si) wafer-based technology [6].

The (a-Si) solar cell is one of the most common thin-film technologies, which has a cell efficiency of (5–7%). Efficiency rises to 8–10% with double and triple junction designs. The efficiency of a-Si thin film is lower than that of (c-Si) modules. Furthermore, a-Si thin film is vulnerable to deterioration as a result of a-Si reaction's when exposed to the environment, such as with water vapor or air. Additionally, in terms of price per watt, CdTe thin film is almost on par with (c-Si) cells. Nevertheless, cadmium is extremely hazardous, and tellurium supplies are scarce. The CIGS PV cell is another film technique with a decent cell efficiency of (20%) [7].

## 1.1 Construction of the Solar Cell

The fundamental structure of a solar cell resembles a p–n junction diode, despite some differences in manufacture. The top side of an n-type semiconductor, which is considerably thicker, p-type semiconductor is created. A few finer electrodes are then added on top of the p-type semiconductor layer [8].

Figure 1 depicts the basic structure of a Solar Cell. These electrodes do not obstruct the thin layer of p-type. In the immediate vicinity of the p-type layer are p–n junctions.



**Fig. 1** Operation of photovoltaic cell

The n-type layer also features a current-collecting electrode on its underside. To protect the solar cell from any mechanical impact, we encapsulate the complete device in a thin glass casing [7].

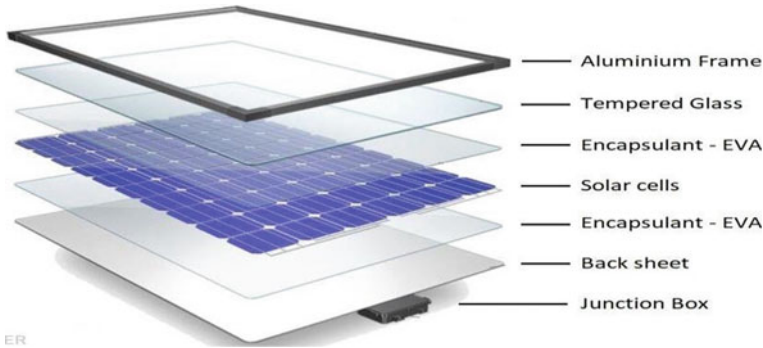
### 1.2 Working of Solar Cell

When light interacts with the extremely thin p-type layer at the p–n junction, light photons travel through it with ease. The connection receives enough energy from the photons from the light source to create several electron–hole pairs. The incoming light disturbs the thermal equilibrium state of the connection [9]. Free electrons in the depletion zone have a high mobility to the n-type side of the junction. The p-type side of the junction may be easily accessed by the holes, just as the depletion. As they reach the n-type side of the junction, newly created free electrons cannot continue to cross it due to their barrier potential [6].

As one portion of the junction (“On Certain Integrals of Lipschitz-Hankel Type Involving Products of Bessel Functions,” 1955) ion, the n-type side, encounters high ionization concentrations, the other part, the p-type edge, receives larger hole concentrations, the p–n junction will behave like a small battery cell. The photovoltage is raised as a voltage [10]. If we connect a little load across the junction, a weak current will flow across it.

### 1.3 Solar Cell Panels

Figure 2 consists of different layers in a solar panel. A solar panel consists of several solar cells connected in parallel and series to produce a certain quantity of power. Since one PV cell can only provide about 0.5 V, most applications are not viable with just one [11]. The cell contains the exact current as a single cell and ideal 3 V



**Fig. 2** Solar panel (ref: <https://shrturl.app/3BqCqH>)

(6 0.5 V), for instance, when six cells are connected in series. For greater capacity of current, series cells are also connected in parallel. If the six cells can produce 2 A, the twelve-cell series–parallel configuration is expected to produce 4 A and 3 V [12].

Thin-film, polycrystalline, and monocrystalline solar cells are three different varieties. Understanding the distinctions between the three is the first step in selecting the best panel for your residence, place of business, or neighborhood. Solar panels are enormous frames that are organized and electrically connected into a tidy array of photovoltaic cells. Silicon semiconductors are used in solar cells to absorb sunlight and convert it to power [13].

#### ***1.4 Solar Power System Components***

Figure 3 represents all the components involved in a solar power plant. Solar panel is a supercapacitor, and an inverter makes up a PV system. Through the PV process, the photon energy is converted into electrical energy by the solar cell. Only on sunny days does the supercapacitor backup provide additional energy. To make the generated DC power suitable for home usage, it is converted into AC loads [14].

#### ***1.5 Depletion Region Formation***

Figure 4 shows the depletion region in the p–n junction. Knowing the distinctions between the three is the first step in deciding which panel is best for your house, place of business, or neighborhood. Diodes are made of only one crystal semiconductor material, mostly silicon, that is doped on a single side with pentavalent impurities to create an n-type and on the other with trivalent impurities to create a p-type [4].

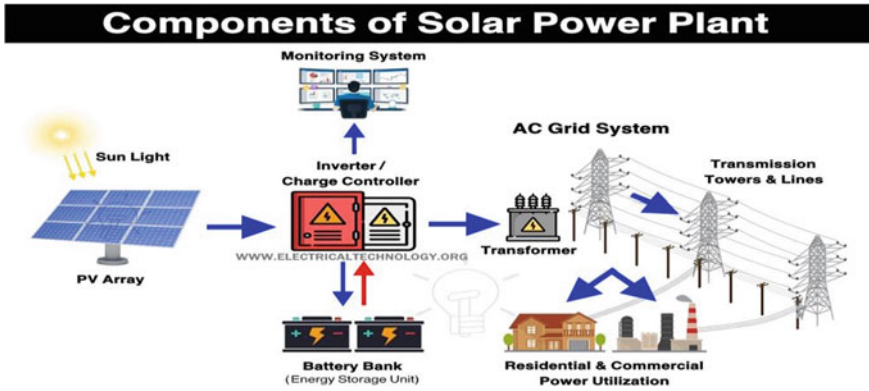


Fig. 3 Components of a solar power plant

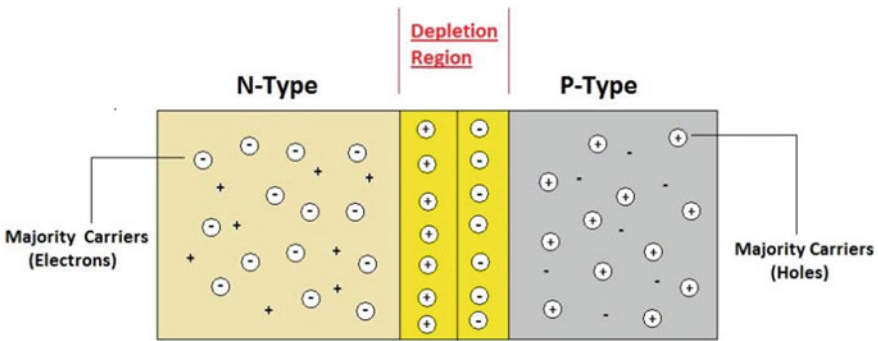


Fig. 4 P-N junction diode

The majority of carriers are produced in each individual location by the doping process. When n- and p-region semiconductors are brought together, an area of positively charged donor atoms will persist at the p–n interface near the n-zone as a result of the diffusion of n-section electrons into the p-section [15]. Similar to this, a net of negatively charged acceptor atoms is left behind in the p–n junction near the p-zone as holes diffuse from the p-region to the n-region. The motion of the holes can be observed as a result of the valence electron jumps. The depletion region, also known as the space charge region, and diffusion current, abbreviated Idiff, are produced by the diffusion of electrons and holes, respectively [4].

## 2 Literature Review

In 2011, Brenadel et al. [3] after their study concluded that understanding and enhancing the performance of the solar cell can be accomplished by modeling the movement and recombination of charge carriers. They combined the fully coupled transport equations for electrons and holes using the finite element partial differential equation system COMSOL [16]. For semiconductor equations, the back surface field layers, floating junctions, and other dopant-diffused surface regions are regarded as conductive volume boundaries. The so-called conductive boundary (CoBo) model uses the sheet resistances and diode saturation current densities of diffused layers to characterize them. Both are easily accessible for testing purposes. The CoBo model allows for two-dimensional simulations on a laptop and demonstrates high numerical stability. When comparing simulations created with the CoBo model for one-dimensional devices and the two-dimensional COMSOL implementation, we discover agreement.

In 2012, Fontenault et al. [5] present their observation that when the photovoltaic (PV) cell's temperature rises, its electrical efficiency falls. Because PV cells are supposed to be positioned in direct sunlight in order to generate power, heating is unavoidable. A heat exchanger can be added to a PV cell to remove heat, increasing conversion efficiency; while using the heat, the cells absorb for further uses. The thermal system is created by water flowing through a rectangular aluminum reservoir that is positioned behind the PV panels. Utilizing the COMSOL Multiphysics program, the suggested photovoltaic–thermal (PV/T) solar panel design was examined. Several combinations of water flow rates and reservoir thicknesses were looked at to see which offered the optimum PV/T overall efficiency. A greater total panel efficiency (additive efficiency of thermal and electrical efficiencies) was reached in designs using the highest flow rates and maximum reservoir thickness. Yet, high flow rates led to hardly detectable net temperature differences between the input and output of the PV/T panel.

In 2018, Shah et al. [6] gave their observation that the photovoltaic panel's temperature rises from constant solar exposure, which lowers its efficiency. The current research focuses on using a hybrid photovoltaic–thermal (PVT) system to increase the solar panel's efficiency. Water is used as the coolant in the cooling channel, flowing through the provided copper tubing, under the photovoltaic panel, where the temperature is the maximum. The system's total efficiency can be increased by using the thermal energy that is extracted during the operation in a variety of ways. In order to create a theoretical model, COMSOL Multiphysics was used. The results of the experimental setup are measured. The photovoltaic panel's efficiency was increased by cooling, which allowed for an average temperature of 303.38 K under Standard Test Conditions (STC), as opposed to the temperature of the panel without cooling rising to 333.15 K under ambient conditions. Later in the paper, the idea is used to improve the overall efficacy of a whole solar power plant by cooling the photovoltaic panel and creating hot water as a byproduct.

In 2019, Zandi et al. [13] proposed that three dimensions are optical photogeneration, electrical characteristics, and thermal/heat dispersion throughout the structure of a perovskite solar cell with a reduced graphene oxide (RGO) surface (three-dimensionally, or 3D). The associated optical–electrical–thermal modules for this hybrid cell were solved using the COMSOL Multiphysics software. To increase heat dissipation and device stability, the RGO was used as the bottom electrode instead of a conventional metallic contact. The Wave Optic, Semiconductor, and Heat Transport in Solid modules were connected in order to solve for the correct input parameter values obtained from relevant literature. Displayed information on the cell includes its optical photogeneration, current–voltage characteristics, electric-field map, and thermal maps. The optical and electrical output of the cell is barely impacted by the RGO contact, although heat dissipation is accelerated. Light absorption, Shockley–Read–Hall nonradiative recombination, and Joule heating are the three basic processes that cause heat to be produced throughout the cell. The RGO contacted cell, as compared to the cell with the Au electrode, exhibits a reduced heat accumulation and gradient at the bottom junction of the RGO/Spiro interface, which indicates that the cell will remain thermally stable. The RGO-contacted cell’s moderated density in the non-radiative and Joule heat distribution is attributed to the RGO layer’s higher heat conductivity than that of conventional metallic electrodes. Our simulation results demonstrate the advantages of these devices by using thermal simulations that are rarely provided.

Again in 2019, Hussain et al. [4] concluded that stretchable solar cells are gaining popularity because they are essential to the development of numerous applications, including wearables and medicinal devices. These energy harvesting devices must have biocompatibility, ultra-stretchability, and mechanical robustness. The fabrication of wafer-scale monocrystalline silicon solar cells with world-record ultra-stretchability (95%) and efficiency (19%) is demonstrated here using a corrugation technique based on laser-patterning [17]. With almost any loss in electric performance in terms of current density, open-circuit voltage, and fill factor, the proposed technology transforms rigid solar cells with interdigitated back contacts (IBC) into ultra-stretchable, mechanically reliable cells. The corrugation technique uses alternating grooves to produce silicon islands with various forms. The stretchability of a biocompatible elastomer (Ecoflex) is achieved by orthogonally matching the active silicon islands to the applied tensile stress. The ensuing mechanics guarantee that upon asymmetrical stretching, the brittle silicon regions won’t be subjected to severe mechanical stresses. Distinct patterns, such as linear, diamond, and triangular ones, are investigated. Different levels of stretchability and loss of active silicon area are produced by each of these layouts. Finally, a finite element simulation is performed in order to assess the resulting deformation in the variously built solar cells.

In the year 2020, Al-Najideen et al. [18] concluded that a financial, thermal, and environmental analysis of a useful solar-powered mobile vaccination refrigeration is provided. The main goals of the current study are to combine a finned heat sink with a suitable Peltier module, select advanced software for thermal analysis, assess the combination’s environmental effects, and compare it to other refrigerators. Professional designers created the Peltier module and the finned heat sink to

improve the thermal efficiency of the solar-powered portable vaccine refrigerator. It is suggested that a capable solar panel be used to power the Peltier module for clean thermal energy. The entire surface efficiency and the total heat dissipation from the refrigerator are determined using a set of formulae [19]. COMSOL Multiphysics is used to calculate the temperature gradient and heat flow of the Peltier module with the finned heat sink during the steady-state process. The thermal measurements show that the highest overall surface efficiency is 78% with one Peltier module and ten fins. According to the sustainability evaluation approach, the environmental results demonstrate that the solar portable vaccine refrigerator's carbon footprint and overall energy usage are reasonable. The findings also demonstrate that the solar portable vaccine refrigerator's manufacturing costs are competitive with those of similar products [20].

In 2020, Allam et al. [21] concluded that Excellent core-shell refractory plasmonic nanoparticle-based nano antennas are used to boost the efficiency of lead-free perovskite solar cells (PSCs).  $\text{SiO}_2$  is used as the shell coating because of its high refractive index and low extinction coefficient, which provide control over sunlight directivity. A three-dimensional optoelectronic model was developed using the finite element method (FEM) and used in COMSOL Multiphysics to calculate the optical and electrical properties of unmodified and  $\text{ZrN/SiO}_2$ -modified PSCs. For fair comparison,  $\text{ZrN}$ -decorated PSCs are also simulated. When  $\text{ZrN/SiO}_2$  core/shell nanoparticles are used, the PCE significantly improves to reach 20%, and when  $\text{ZrN}$  nanoparticles are used to decorate the PSC, the PSC's PCE rises from 12.9% to 17%. The PCE enhancement is examined in detail [22].

### 3 Methodology

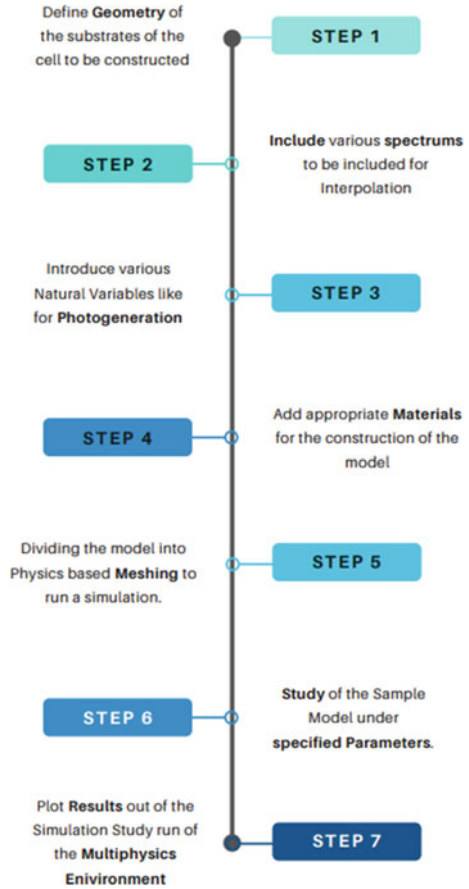
The steps involved in making the efficient solar cell are clearly shown in Fig. 5.

#### 3.1 Geometry

Geometry plays a vital role in the construction of not only ours but also any model throughout the Design-Build-Simulation Workflow. As we would be going with different sets of simulation models for our proposed solution, dimensions must be specified very particularly.



**Fig. 5** Methodology of the suggested work



### 3.2 Interpolation Spectrums

Interpolation is a mathematical way of finding or constructing new data points based of an available set of discrete data of known behavior. In our proposed model, we would be requiring 2 Interpolations:

- a. Solar Spectrum
- b. Silicon Absorption Spectrum.

### 3.3 Variables

As our proposed model works under the virtue of some natural elements, we also have to introduce them as variables for the ease of the Multiphysics Environment

to run more précised simulations. Here, we are going to use photogeneration as our Natural Variable.

### ***3.4 Materials***

Every Model Construction would require a specific material according to the requirement of the project and other mathematical factors on which the construction and simulations are dependent upon. Material selection in Multiphysics would have other instances such as

- a. Analytical Doping Models
- b. Boundary Selection for Doping Profiles
- c. Trap-Assisted Recombinations
- d. User-Defined Generations
- e. Metal Contacts.

### ***3.5 Meshing***

Meshing or dividing the whole space of the model into coordinated triangular spaces is a very important step before the simulation process to be done because meshing helps the software to consider every precise element of the nodes in performing in an accurate simulation. In our case we would choose Physics Controlled Meshing.

### ***3.6 Study***

The study contains various other parameters and their ranges like Applied Voltage and mentioning of start point and end points of the model for a more organized simulation. It may also include sweep type which here would be Auxiliary Sweep.

### ***3.7 Results***

It is the end part of the sequence where simulations are complete and the possible behavior of the model under the set conditions is determined. It would be the part where we would plot graphs of the parameters we mentioned in Pre-simulation Phase.

### 4 Results and Analysis

The solar cell model consists of a one-dimensional silicon p–n junction with carrier generation and Shockley–Read–Hall recombination. The primary recombination effect is captured using the Shockley–Read–Hall model. After properly implementing the dimensions and experimentally verifying many times, we arrived at the conclusion that this shown solar cell is the most effective at this dimension. All the outputs are according to the best efficient dimensions. Figure 6 showcases the Solar Cell in COMSOL Multiphysics.

Figure 7 demonstrates the concentrations of the donors and acceptors for the first 10 m below the surface. Checking the doping profile for inadvertent setup problems is always a good idea.

Figure 8 displays the user-specified photogeneration rate and the Shockley-Read-Hall recombination rate over the cell's thickness.

By comparing Figs. 9 and 10 for P–V and I–V curves respectively, these graphs allow us to read off crucial functioning information, such as the open-circuit voltage (0.61 V), the short-circuit current (33 mA), and the maximum power (16.7 mW).

Figure 11 indicates the energy diagram for Donor Concentration and Acceptor Concentration which are extracted from the COMSOL Multiphysics environment.

The electron and hole concentration plotted in Figs. 12 and 13 is extricated from the COMSOL Multiphysics environment.

We may simulate chemical phenomena, heat transfer, fluid flow, electromagnetic phenomena, structural mechanics, acoustics, and structural mechanics using COMSOL Multiphysics in a single environment and process. Regardless of the kind of physics involved, all simulation apps are constructed using the same tool, the



Fig. 6 Solar cell in COMSOL Multiphysics

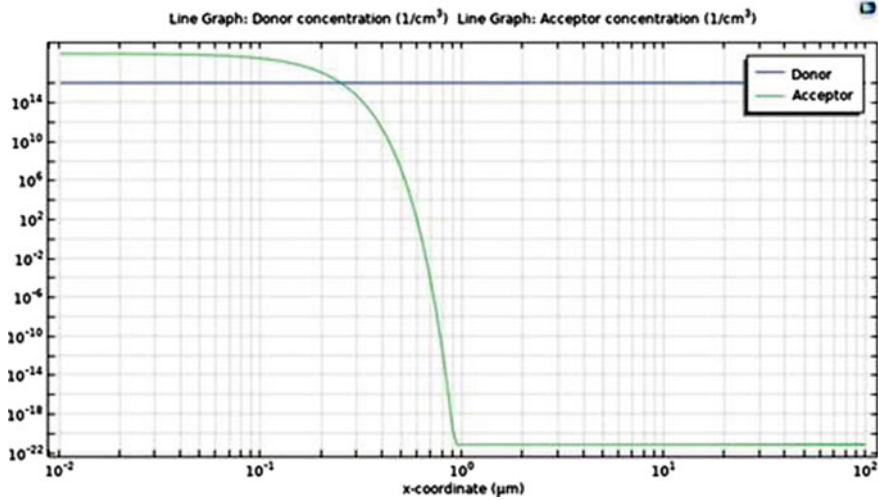


Fig. 7 Concentrations of donors and acceptors in COMSOL

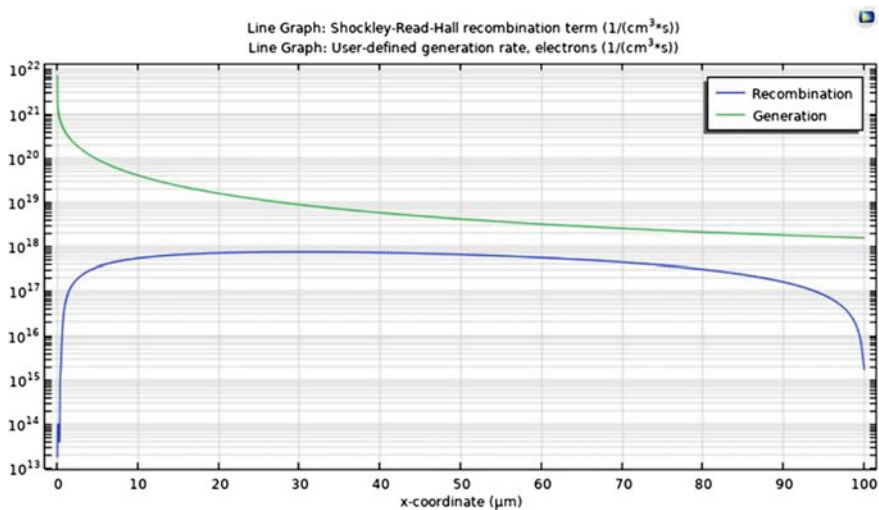


Fig. 8 Recombination and photogeneration rate

Application Builder. A typical industrial silicon cell delivers greater efficiency than any other single-junction device that is produced in large quantities. Because fewer solar cells must be produced and installed for a given output, higher efficiencies lower the ultimate installation cost. The building blocks of crystalline silicon cells are silicon atoms inter-connected to create a crystal lattice. This lattice offers a well-organized structure that improves the efficiency of turning light into electricity.

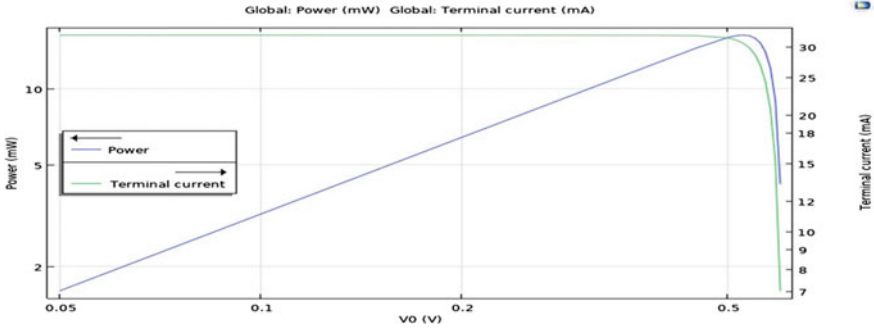


Fig. 9 P-V curves

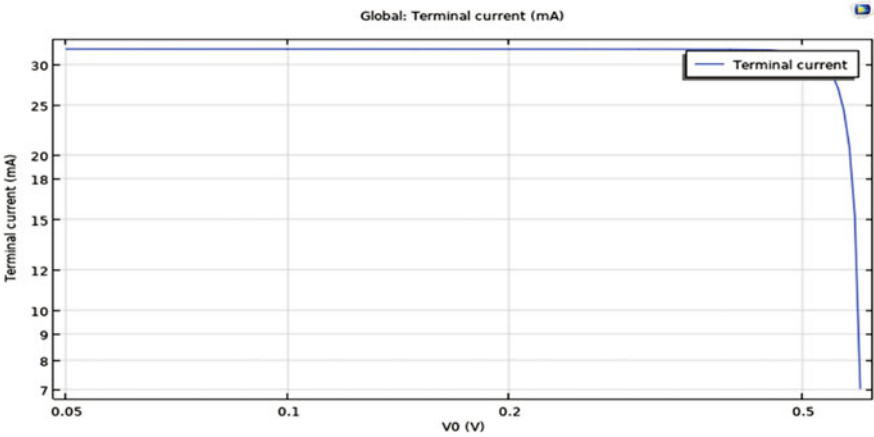


Fig. 10 I-V curves

## 5 Conclusion and Future Work

In the end, we conclude that by altering the dimensions and comparing the current model to the past, solar cell efficiency can be increased. The photovoltaics convert the solar energy into electrical energy. Solar cell arrays are necessary for every PV system to produce enough electricity. The theory underlying the operation of solar cells, as well as design elements and technological details, was covered in this paper. Issues with PV cells, materials employed, the importance of thin films in solar technology, hopes for the future, and some numerical modeling of p-n junction solar cells are only a few of the topics covered. The capacity of COMSOL Multiphysics is to create mathematical and numerical models of solar cells.

This project's future goals are to increase efficiency. In India, there is a vast potential for the production of solar energy. The country's geographic location makes it beneficial for producing solar energy. The reason behind this is that India is a

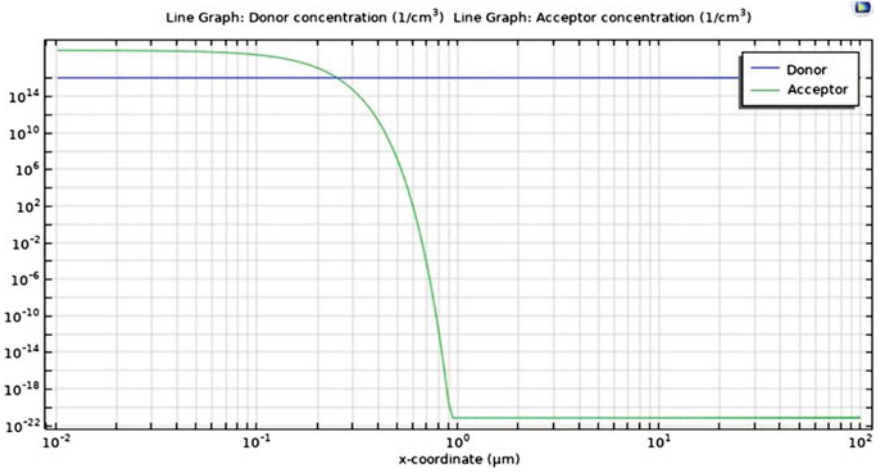


Fig. 11 Energy diagram

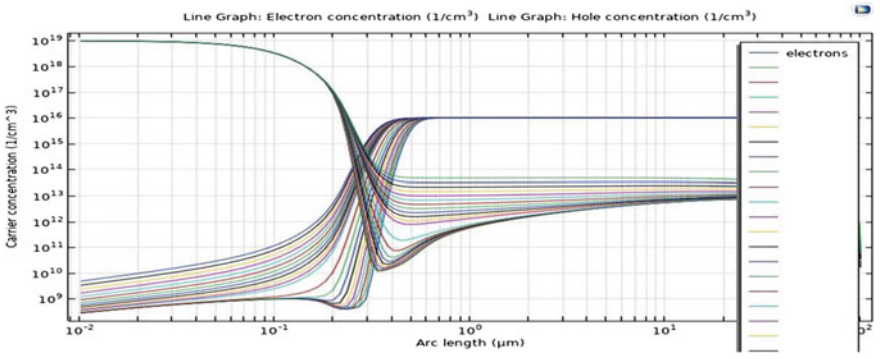


Fig. 12 Electron and hole concentrations

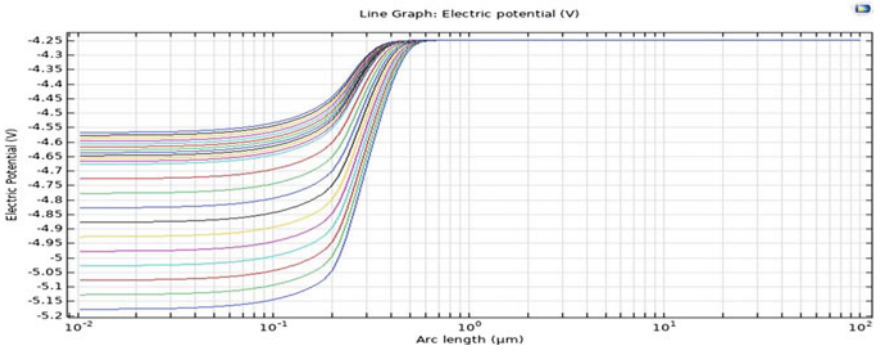


Fig. 13 Electric potential graph

tropical nation with about 3,000 h of sunshine each year and solar radiation. This is close to 5,000 trillion kWh. Nearly everywhere in India, there are 4–7 kWh of sun radiation per square meters. This is 2,300–3,200 h of sunlight each year. States like Madhya Pradesh, Andhra Pradesh, Haryana, Bihar, Maharashtra, Orissa, Gujarat, Punjab, Rajasthan, and West Bengal have a lot of potential to harness solar energy because of their geographic location.

## References

1. Makableh YF, Alzubi H, Tashtoush G (2021) Design and optimization of the antireflective coating properties of silicon solar cells by using response surface methodology. *Coatings* 11(6). <https://doi.org/10.3390/coatings11060721>
2. Jahantigh F, Bagher Ghorashi SM (2019) Optical simulation and investigation of the effect of hysteresis on the perovskite solar cells. *Nano*. <https://doi.org/10.1142/S1793292019501273>
3. On certain integrals of Lipschitz-Hankel type involving products of Bessel functions. *Philos Trans Royal Soc London. Series A, Math Phys Sci* 247(935):529–551 (1955). <https://doi.org/10.1098/rsta.1955.0005>
4. Zandi S, Saxena P, Razaghi M, Gorji NE (2020) Simulation of CZTSSe thin-film solar cells in COMSOL: three-dimensional optical, electrical, and thermal models. *IEEE J Photovolt* 10(5):1503–1507. <https://doi.org/10.1109/JPHOTOV.2020.2999881>
5. Fontenault BJ, Gutierrez-Miravete E. Modeling a combined photovoltaic-thermal solar panel
6. Zandi S, Saxena P, Gorji NE (2020) Numerical simulation of heat distribution in RGO-contacted perovskite solar cells using COMSOL. *Sol Energy* 197:105–110. <https://doi.org/10.1016/j.solener.2019.12.050>
7. Shah R, Srinivasan P (2018) Hybrid photovoltaic and solar thermal systems (PVT): performance simulation and experimental validation. [www.sciencedirect.com/www.materialstoday.com/proceedings2214-7853](http://www.sciencedirect.com/www.materialstoday.com/proceedings2214-7853)
8. Elangovan NK, Sivaprakasam A (2020) Investigation of parameters affecting the performance of Perovskite solar cells. *Mol Cryst Liq Cryst* 710(1):66–73. <https://doi.org/10.1080/15421406.2020.1829425>
9. Aly AH, Sayed H, Elsayed HA (2019) Development of the monolayer silicon solar cell based on photonic crystals. *SILICON* 11(3):1377–1382. <https://doi.org/10.1007/s12633-018-9936-7>
10. Saxena P, Gorji NE (2019) COMSOL simulation of heat distribution in perovskite solar cells: coupled optical-electrical-thermal 3-D analysis. *IEEE J Photovolt* 9(6):1693–1698. <https://doi.org/10.1109/JPHOTOV.2019.2940886>
11. Iqbal T et al (2019) An optimal Au grating structure for light absorption in amorphous silicon thin film solar cell. *Plasmonics* 14(1):147–154. <https://doi.org/10.1007/s11468-018-0787-2>
12. El-Atab N, Hussain MM (2020) Flexible and stretchable inorganic solar cells: Progress, challenges, and opportunities. *MRS Energy Sustain* 7(1). Springer Nature. <https://doi.org/10.1557/mre.2020.22>
13. Al-Madhhachi H, Al-Najideen M (2021) Thermal, environmental, and cost analysis of effective solar portable vaccine refrigerator by COMSOL. *Multiphys Heat Transf* 50(1):179–195. <https://doi.org/10.1002/htj.21870>
14. Mohsen AA, Zahran M, Habib SED, Allam NK (2020) Refractory plasmonics enabling 20% efficient lead-free perovskite solar cells. *Sci Rep* 10(1). <https://doi.org/10.1038/s41598-020-63745-7>
15. Institute of electrical and electronics engineers, communications for sustainable development IEEE MENACOMM' 19 : 2nd IEEE Middle East and North Africa communications conference: 2019, 19–21 November, the Diplomat Radisson Blu Hotel, Kingdom of Bahrain

16. Makableh YF, Aljauoosi G, Al-Abed R (2019) Comprehensive design analysis of electron transmission nanostructured layers of heterojunction perovskite solar cells. *Superlattices Microstruct* 130:390–395. <https://doi.org/10.1016/j.spmi.2019.05.017>
17. Khalate SA, Kate RS, Deokate RJ (2018) A review on energy economics and the recent research and development in energy and the  $\text{Cu}_2\text{ZnSnS}_4$  (CZTS) solar cells: a focus towards efficiency. *Solar Energy* 169:616–633. Elsevier Ltd. <https://doi.org/10.1016/j.solener.2018.05.036>
18. Dhar A, Pradhan D, Roy JN (2017) Nanostructures for highly efficient ultra-thin silicon solar cells. In: International conference on 21st century energy needs—Materials, systems and applications, ICTFCEN 2016, Institute of Electrical and Electronics Engineers Inc. <https://doi.org/10.1109/ICTFCEN.2016.8052741>
19. Liu L, Diao Y, Lv Z, Sun Y (2021) Enhanced optical absorption of  $\text{Al}_x\text{Ga}_{1-x}\text{As}$  nanoarrays with variable Al composition structure for solar cell applications. *Mater Res Bull* 141. <https://doi.org/10.1016/j.materresbull.2021.111364>
20. Roy AB, Dhar A, Choudhuri M, Das S, Hossain SM, Kundu A (2016) Black silicon solar cell: analysis optimization and evolution towards a thinner and flexible future. *Nanotechnology* 27(30). <https://doi.org/10.1088/0957-4484/27/30/305302>
21. IEEE Staff, 2019 2nd IEEE middle east and North Africa communications conference (MENACOMM). IEEE (2019)
22. Wang W et al (2014) Device characteristics of CZTSSe thin-film solar cells with 12.6% efficiency. *Adv Energy Mater* 4(7). <https://doi.org/10.1002/aenm.201301465>



# Post Quantum Secure Blockchain Architecture for Data Dissemination



Dushyant Kumar Yadav, Hemlal Sahu,  
Siva Gayatri Venkata Naga Datta Sai Ammanamanchi,  
Otturu Madhu Murali, Saurabh Rana, and Dharminder Chaudhary

**Abstract** Post quantum cryptography is the key idea to resist quantum attacks. The Fiat-Shamir were the first who introduce efficient lattice-based signatures. A lattice-based signature ensures the security of blockchain architecture against quantum computers. However, a blockchain is always consisting of multiple communicating nodes, so there is a need to develop a verification method for multiple nodes. We have proposed a blockchain using module lattices. Blockchain security relies upon two assumptions, (1) Module Learning With Errors and (2) Module Short Integer Solution. The system can provide security against quantum attacks.

**Keywords** Cyber system · Security · Privacy · Blockchain technology

## 1 Introduction

Blockchain is a sort of distributed ledger system that preserves all committed online transfers that have been validated by various independent centers by coming to an agreement on an item added to the ledger, doing away with the requirement of needing a central authoritative factor [1, 2]. A “chain” is described as the connection between one “block,” which describes a collection of confirmed transfers inside a blockchain system, and another block. Figure 4 depicts an example blockchain made up of several temporally related blocks. Once all four of the following conditions are met (shown in Fig. 5), the particular chain is been added with a block.

---

D. K. Yadav · H. Sahu  
Department of Mathematics, J.Y. Govt. College, Raipur, India

S. Rana  
Department of Mathematics (SCSET), Bennett University, Noida, India

S. G. V. N. D. S. Ammanamanchi · O. M. Murali · D. Chaudhary (✉)  
Department of Computer Science and Engineering, Amrita School of Computing Amrita Vishwa Vidyapeetham, Chennai, India  
e-mail: [manndharminder999@gmail.com](mailto:manndharminder999@gmail.com)

- When a client uses a digital signature to sign a transfer and sends it to a computer network known as a peer-to-peer (P2P), known to be nodes for transfer validation, the transfer is said to have been launched. The digital signature of the sender, the recipient, the transfer data, and the sender are all recorded in the transfer.
- The node checks the sender's digital signature after acquiring the signed transfer to ensure its legitimacy. A block is created by aggregating all transfers that are validated in the same time frame. The blockheader of this block contains additional data such as the date (the time at which the block was created), nonce (a value used to create a valid block hash), and prior hash (to relate to the block before).
- By randomly choosing a nonce and utilizing the cryptographic hashing technique to carry out the hashing operation, the node creates a secure hash for the block. Since no two blocks have the same hash, the hash serves as the block's unique identifier. By adding the hash of the previous block to the new block, the new block is chained to the prior block. This chaining configuration guarantees the integrity of transfers because any alteration to the transfers will result in a change to the hash value of the block, which will then affect the hash values of all succeeding blocks in the given chain.
- After successfully generating a legitimate hash, the node broadcasts its block to the P2P network to undergo validation. Other nodes verify the block's integrity by confirming the presence of legitimate transfers and ensuring that its hash matches that of the preceding block. Each node uploads this to its blockchains if all checks pass. It is at this point that network nodes come to a consensus.

A person going by the alias Satoshi Nakamoto first proposed the idea of blockchain in 2008 to act as a transaction log for the widely recognized digital currency, Bitcoin. Other blockchain applications have been developed as a result of the Bitcoin concept. Today's blockchain technology offers a broader range of applications, along with private and public administration. Ethereum and Hyperledger Fabric are two notable platforms that have garnered significant interest for providing decentralized blockchain smart applications. By eliminating the need for middlemen (like central authority), the implementation of these two platforms may assist both the private and public sectors in increasing their efficiency. It also improves data security and lowers operating costs. However, the research community is divided on whether Hyperledger Fabric can be considered a generic blockchain platform due to its consensus mechanism that does not depend on individual coin mining. Instead, Fabric establishes consensus with the help of supporting peers. The literature widely supports the notion that Fabric is a permissioned blockchain system. So, we will make the assumption in our work that it is a blockchain. The use of smart contracts to enable more intricate programmable transactions represents a development for blockchain decentralized applications [3]. Nick Szabo first presented the idea of a smart contract in the 90s [4, 5] as a computerized protocol that could carry out a contract's terms and conditions. Blockchain has smart contracts built in to let parties conduct transactions in accordance with the terms of the contract. Once the contract's conditions are fulfilled, the transaction is executed automatically according to the specified contract statement and verified by network nodes. The most widely used

blockchain for smart contracts is Ethereum [2, 6]. Its construction involved the use of a Turing-complete programming language, which allows it to facilitate and carry out a diverse range of computational instructions [7]. This Turing completeness attribute of Ethereum allows programmers to create custom rules for transactions to implement decentralized blockchain applications. Public blockchains, private blockchains, and consortium blockchains are the three subcategories of the existing blockchain system [7, 8]. The term “permissionless blockchain” is used to describe the public blockchain, whereas “permissioned blockchain” is used to describe the private blockchain. Contrarily, consortium blockchain is often referred to as semi-private or semi-public blockchain. Table 2 contains a comparison of the three different forms of blockchain. We specifically compare consortium blockchain to public, private, and other blockchains in the below-mentioned areas:

- **Autonomy:** The term “autonomy” describes the capacity to possess or manage the blockchain system. Inside an open blockchain, all the peers have autonomy over the system because anybody can join the network and become a node. Private blockchain, on the other hand, is solely under the control of one organization, which has the power to choose a small number of specified nodes from this particular company to participate in the network. While consortium blockchain is controlled by chosen groups rather than a single organization, it is managed similarly to closed blockchain, i.e., by choosing peers from inside their own company.
- **Participants:** The public can see and access the public blockchain. Each and every peer joining the system is able to look at and participate in the transaction validation. Private and consortium blockchains, in comparison to the public blockchain, both include entry restrictions; only chosen and approved peers are permitted to take part in the system. These preset peers have a varied amount of permission to view and confirm the transactions. Depending on the preferences of the organization, some nodes might only be able to look at the transfers, while other peers might be capable of both reading and writing the transactions.
- **Time Efficiency:** Comparing public blockchain to restricted and collaborative/consortium blockchains, the efficiency of the former is lower. This is because a sizable number of users on the open blockchain network must come to an agreement to validate the transactions. The efficiency of blockchain systems decreases as the amount of nodes within the network increases. In contrast, the constrained network in private and consortium blockchains enables higher efficiency because there are fewer nodes required to carry out the confirmation process. As we can see in Table 5, more study has been done on restricted blockchains than on open ones for this reason.
- **Immutability:** A blockchain network’s immutability is its capacity to survive changes. Because every node synchronizes and gets a blockchain copy once consensus is obtained and because blockchain hashing holds the complete chain, it is immutable. A rogue node must seize control of a minimum of 52% of the blockchain system in order to overthrow the agreement in order to alter transactions. It can disrupt the system and replace the required block by obtaining the 52% majority, making the blockchain changeable. Due to the enormous number of

nodes that are responsible for preserving the shared transaction data on the public blockchain, alteration is practically impossible. However, because there are fewer nodes in private and consortium blockchains, there is a slight chance that the dominant organization or the consortium as a whole may act improperly and alter the ledger. The probability of change in a blockchain network tends to decrease as the number of entities managing the network and network nodes increases, suggesting that more decentralization leads to less likelihood of significant changes.

- **Exemplary Platforms:** Two examples of the open blockchain platforms, most commonly used for cryptocurrencies, are Bitcoin and Ethereum. MultiChain [9] and GemOS [10] are two examples of blockchain platforms. These open source platforms assist businesses in establishing their own restricted blockchain systems. Alternatively, the most commonly used blockchain platforms that facilitate consortium systems involving both private and public enterprises are Hyperledger Fabric and Ethereum.

## 2 Blockchain Characteristics

To give a general summary of blockchain traits, we adopted several categorizations derived in [11–15]. The fundamental principles in each classification and group the essential qualities of this technology into functional and developing traits. Emergent traits appear to be a result of functional traits, whereas functional characteristics are necessary for the existence of the blockchain system. We quickly go over these two traits as follows.

### 2.1 *Functional Characteristics*

Decentralization, distributed ledgers, and consensus protocols are examples of functional characteristics. These three components make up the blockchain.

- **Decentralization:** Decentralized blockchain architectures are those that are not reliant on a single main authority to validate and keep their transaction information. Alternatively, the information is checked, duplicated, and disseminated throughout a P2P network of end-points that communicate the most recent transaction information with one another to have each end-point current. Every node authenticates the transactions and keeps a duplicate of the whole chain in a private or consortium blockchain, similarly. The sole distinction between these two kinds of blockchains is whether one or more organizations oversee deciding which users are qualified to validate transactions and obtain copies of the data, increasing privacy. Private and consortium blockchains are seen as somewhat decentralized due to the network autonomy. As each end-point in the connected network participates

in handling the blockchain information, no point of failure risk exists as there is with centralized systems [16]. The other nodes are able to maintain the network functioning normally even if one node is unable to authenticate transactions because of a malfunction or issues on the technical side.

- **Distributed Ledger:** A shared and synchronized database that is used by several users or places is known as a distributed ledger. Due to the fact that every node in the network stores and maintains the transaction data, blockchain is a type of distributed ledger. Blockchain has a distinctive feature that sets it apart from other distributed ledger technologies: The database is kept in blocks that are linked to each other in order to form a chain in a secure data structure. In addition to the security benefits that the blockchain architecture already provides, the distributed ledger added useful features to blockchain, preventing the systems from loss of data because the information is stored on several nodes.
- **Consensus Protocol:** Blockchain transactions are coordinated by consensus protocol, which is carried out by all network nodes to guarantee that each transaction is legitimate and consistent before it is appended into the blockchain [17, 18]. Each end-point interacts with the others to produce a block of transactions that is legitimate, and it is rewarded with Bitcoin for doing so. A block of transactions will be chosen to be appended to the chain and rewarded by the node that creates it first. With the use of incentives, nodes are encouraged to join the system and take part in the agreement attempts. Proof-of-Work (PoW), the original blockchain consensus technology, is principally utilized for cryptocurrency applications by Bitcoin and Ethereum. Each round of consensus in a PoW system requires competing nodes to use their computing resources to produce a valid block hash value. A node must locate a random nonce that generates a hash that meets the network's requirements in order to provide a legitimate hash. By changing the nonce, this can only be accomplished through a trial-and-error process. A significant amount of computing power is required to carry out several trial-and-error processes that ultimately result in the creation of the proper nonce that complies with the hash standard. Other consensus protocols, such as Proof-of-Stake (PoS), have been suggested as alternatives to Proof-of-Work (PoW) for various blockchain applications. PoS uses stake competitiveness to decide which node should start a new block. The likelihood that a node will be chosen as the block maker by doing the hashing block computation increases with the size of the stake it owns. Another type of node choosing is provided, such as the coin age-based choosing method, to stop the network's wealthiest node from being the only one selected for the consensus. With this strategy, nodes with a greater collection of coins are given preference when attempting to form a block. Delegated-Proof-of-Stake (DPoS), a PoS variant, offers greater efficiency than PoS [19]. Stakeholder nodes in a DPoS vote for other nodes to become block creators. The ability to verify a block is granted to the elected nodes with the highest number of votes. Another type of consensus system utilized for blockchain applications is called a PBFT (Practical Byzantine Fault Tolerance) [20]. While the backup nodes give their opinion on the blocks generated by the main, the main node builds the block. For each round of agreement, a new primary node is chosen. To agree on transactions, each round of Practical

Byzantine Fault Tolerance goes through four different phases: (i) pre-prepare, (ii) prepare, (iii) commit, and (iv) respond. When the system of nodes receives at least  $3p + 1$  identical responses from all the end-points, where the value of  $p$  is the maximum no. of flawed end-point systems that the network may allow, the block is admitted into the chain. In essence, PoS selects the end-point with the largest points as a block maker, whereas PoW selects the node with the most computing power.

## 2.2 Security Issues

During incorporation of computer technology into intelligent cities makes life easier for residents, but it also poses security and privacy problems. If the security architecture is inadequate, using a lot of devices to distribute a huge amount of data might result in serious data breaches for the smart city. A single server is responsible for carrying the weight of carrying out all activities and managing all devices in the network in the conventional smart city architecture, which is based on centralized systems and is affected by architectural restrictions [21]. A single broken part might bring the entire system to an end. A centralized model's reliance on a third party may also be unreliable since it creates room for fraud and abuse. Without any consent, a third party can change and manipulate data. A centralized model's reliance on a third party may also be unreliable since it creates room for fraud and abuse. Without any consent, a third party can change and manipulate data. Data distribution in intelligent cities requires a variety of data types—from very sensitive to the public—and varied privacy limitations for various users. In Smart structures, for example, authority over a building has access to all systems to oversee building works, during which visitors are given authority to building areas and systems for a certain period of time, which is subsequently revoked when the time period is up [22]. A nurse in the healthcare industry could have more entry to a patient's file than a doctor actually treating the patient [23]. For the purpose of facilitating educational planning, various government entities in the field of education have access to school data across the city. Consumers can manage their own, timely smart meter data to control their electricity use in the context of smart energy [24]. In other words, not all data may be made available to the public. Various access controls are needed for different types of data to ensure privacy.

## 3 Proposed Post Quantum Secure Blockchain Architecture

This section illustrates the proposed scheme for node/user communication based on module learning with errors, and module short integer solution assumptions respectively. The scheme consists of four phases: (1) setup phase, (2) subkeys generation

phase, (3) signature phase, and at last (4) verification phase. This construction uses *Trap – Gen* to generate public key  $B_0 \leftarrow \mathbb{Z}_q^{n \times m}$  with basis  $T_{B_0} \leftarrow \mathbb{Z}_q^{m \times m}$  satisfying the condition  $\|\tilde{T}_{B_0}\| \leq O(\sqrt{n \log(q)})$ ,  $m = O(n \log(n))$ . The wallet contains the seed value  $(B_0, T_{B_0})$  that is lattice basis to generate subkeys using Bonsai tree algorithm.

### 3.1 Parameters Selection/Setup Phase

This phase takes input  $n$ , and  $q$ , then it uses algorithm *Trap – Gen*( $q, n$ ) to generate random  $B_0 \leftarrow \mathbb{Z}_q^{n \times m}$ , with basis  $T_{B_0}$  satisfying  $\|\tilde{T}_{B_0}\| \leq O(\sqrt{n \log(q)})$ . It uses  $H_2 : \{0, 1\}^* \rightarrow \mathcal{C} = \{c \in \mathit{mathbb{R}} : \|c\|_1 = d, \|c\|_\infty = 1\}$  be random oracle with  $d$  such that  $|\mathcal{C}| > 2^{2\kappa}$ , where  $\kappa$  is the security parameter.

1. The Setup takes input  $n$ , and  $q$ , then it uses algorithm *Trap – Gen*( $q, n$ ) to generate random  $B_0 \leftarrow \mathbb{Z}_q^{n \times m}$ .
2. It generates basis  $T_{B_0}$  satisfying  $\|\tilde{T}_{B_0}\| \leq O(\sqrt{n \log(q)})$ .

### 3.2 Public/Private Key

#### *Generation*( $B_0, T_{B_0}, B_1, B_2, B_3, \dots, B_n$ )

The algorithm *Subkey-Generation*( $B_0, T_{B_0}, B_1, B_2, B_3, \dots, B_n$ ) chooses matrices  $B_1, B_2, B_3, \dots, B_n$  for the nodes/users  $(U_1, U_2, U_3, \dots, U_n)$ , and uses the algorithm *Ext – Basis*, and it outputs  $T_{B'_1} \leftarrow \mathit{Ext – Basis}(T_{B_0}, B'_1 = B_0|B_1), T_{B'_2} \leftarrow \mathit{Ext – Basis}(T_{B_0}, B'_2 = B_0|B_2), \dots, T_{B'_n} \leftarrow \mathit{Ext – Basis}(T_{B_0}, B'_n = B_0|B_n)$ , and it generates private/public key pairs  $(SK_1 = s_1 \leftarrow T_{B'_1}, PK_1 = B'_1.s_1), (SK_2 = s_2 \leftarrow T_{B'_2}, PK_2 = B'_2.s_2), \dots, (SK_n = s_n \leftarrow T_{B'_n}, PK_n = B'_n.s_n)$  for each of nodes/users in the blockchain. These subkeys are published in the blockchain network,

and used to perform the signature and verification of corresponding nodes/users (see Algorithm 1).

### 3.3 Address Generation

Different addresses are generated from different public keys of nodes/users. Suppose, the nodes/users  $U_{B_1}$  has public key  $B'_1 = (b_1, b_2, \dots, b_{2m}) \in \mathbb{Z}_q^{n \times 2m}$ , then it applies a hashing like SHA-256 to generate a hashed public key. First, the node/user  $U_{B_1}$  sends a request to another node/user  $U_{B_2}$ , then the node/user  $U_{B_2}$  chooses pair of subkeys from its wallet, and it generates the address, and sends to  $U_{B_1}$ . Finally, the node/user

---

**Algorithm 1:** Algorithm for Private/Public Key Generation
 

---

Inputs :  $B_0, T_{B_0}, B_1, B_2, B_3, \dots, B_n$

Output:  $(SK_1, PK_1), (SK_2, PK_2), \dots, (SK_n, PK_n)$

1. Uses Extraction Phase:  $T_{B'_1} \leftarrow Ext - Basis(T_{B_0}, B'_1 = B_0|B_1),$   
 $T_{B'_2} \leftarrow Ext - Basis(T_{B_0}, B'_2 = B_0|B_2), \dots, T_{B'_n} \leftarrow Ext - Basis(T_{B_0}, B'_n = B_0|B_n)$
  2. Generates:  $(SK_1 = s_1 \leftarrow T_{B'_1}, PK_1 = B'_1.s_1), (SK_2 = s_2 \leftarrow T_{B'_2}, PK_2 =$   
 $B'_2.s_2), \dots, (SK_n = s_n \leftarrow T_{B'_n}, PK_n = B'_n.s_n)$
- 

$U_{B_1}$  generates a transaction for this particular address, and this is broadcasted in the whole network.

### 3.4 Transaction Block Generation

Any of the nodes can initiate a transaction in the blockchain, and its private key is used to generate the signature. A node with mining capacity can add a new block to the proposed blockchain framework. The node is responsible for collecting all the transactions and creating of random oracle to generate a new transaction block. A node/user broadcasts a transaction to other nodes/users, and it uses algorithm  $Sign(SK, M)$  is used to generate a signature on the transaction with one private from the wallet. It transaction bearing signature is different because of different time stamps, and the private key used to sign. A node/user samples  $y \leftarrow D$ , and computes  $u = [B'_1] \cdot y \in Q_q^k$ ,  $c = H(u, PK_1, M)$ , and  $z = s_1 \cdot c + y$  with probability  $(1 - P_{rej})$ , where  $P_{rej} = \min\{1, \frac{D_c^{\ell+k}(z)}{M} \cdot D_{c,s,s}^{\ell+k}(z)\}$ . The final signature is  $\sigma = (u, z)$  (see Algorithm 2).

---

**Algorithm 2:** Transaction Block Generation
 

---

Inputs :  $SK, M$

Output:  $\sigma = (u, z)$

1. Samples:  $y \leftarrow D$
  2. Computes:  $u = [B'_1] \cdot y \in Q_q^k, c = H(u, PK_1, M), z = s_1 \cdot c + y$
  3. If  $1 - P_{rej} = 1 - \min\{1, \frac{D_c^{\ell+k}(z)}{M} \cdot D_{c,s,s}^{\ell+k}(z)\}$   
 Then return  $\sigma = (u, z)$   
 Else recompute  $\sigma$
  4. Broadcast Block  $(B_i, \sigma_i)$  to Blockchain Network
-



### 3.5 Consensus Participation with Aggregate Signature

A node/user broadcasts a transaction to other nodes/users, and it uses aggregate signature algorithm  $Agg - Sign(PK = PK_j, M = M_j)$  is used to generate a signature for more than one node/user. To find an aggregate signature, the node/user computes  $c_j = H(u_j, PK_j, M_j)$ , and queries  $e_j \leftarrow H_2(c_1, c_2, \dots, c_N, j)$  for  $j \in [N]$ . Further, he computes  $z = \sum_j e_j \cdot z_j$  satisfying the norm condition  $\|z\| \leq \beta = O(\sqrt{N}B)$ . Finally, the node/user broadcasts the aggregate signature  $\sigma_{agg} = ((u_j)_j, z)$  (see Algorithm 3).

---

#### Algorithm 3: Consensus Aggregate Signature

---

Inputs :  $PK = PK_j, M = M_j$  for  $j \in \{1, 2, \dots, N\}$

Output:  $\sigma_{agg} = ((u_j)_j, z)$

1. Computes:  $c_j = H(u_j, PK_j, M_j)$
  2. Queries:  $e_j = H_2(c_1, c_2, \dots, c_N, j)$  for  $j \in [N]$
  3. Computes:  $z = \sum_j e_j \cdot z_j$  where  $\|z\| \leq \beta = O(\sqrt{N}B)$
  4. Output:  $\sigma_{agg} = ((u_j)_j, z)$
- 

### 3.6 Verification of Block

The algorithm  $Verification(u, z)$  run by a node/user takes the input public key matrix  $PK_1$ , message  $M$ , and signature  $\sigma$  respectively. The receiver node computes  $c = H(u, PK_1, M)$ , and if  $\|z\| < \beta$ , and  $B'_1 z = PK_{1 \cdot c+u}$ , then only accepts the signature.

### 3.7 Consensus with Aggregate Signature Verification

All the nodes in the blockchain network are the member of the consensus algorithm. In a blockchain networking system of  $N$  nodes, particular nodes receives  $(N - 1)$  transaction blocks from other nodes. Therefore, A blockchain networking system contains  $N$  blocks at a time. All the nodes verify each block before adding it to the consensus. A node can verify other  $(N - 1)$  nodes using the concept of aggregate signature concept. In this way, it provides scalability to the system in the form of aggregate signature in a single step for multiple blocks, and nodes. The public keys are available in the blockchain network to complete the process. The aggregate signature technique considers a tuple of finite length as a single piece of information. Although a methodology of the aggregate signature has

been introduced in [25], post-quantum security and efficiency in the key generation is the key idea of the proposed framework. A node/user broadcasts a transaction to other users, then the node/user verifies the aggregate signature using algorithm  $VAgg - Sign(PK = PK_j, \sigma_{agg})$ . It computes  $c_j = H(u_j, PK_j, M_j)$  for  $j \in [N]$ , and queries  $e_j \leftarrow H_2(c_1, c_2, \dots, c_N, j)$  for  $j \in [N]$ . Further, it computes  $PK.z = \sum_j e_j.(PK_j.c_j + u_j)$ , and if  $\|z\| \leq \beta = O(\sqrt{N}B)$ , then only accepts aggregate signature (see Algorithm 4).

---

**Algorithm 4:** Consensus with Aggregate Signature Verification

---

Inputs :  $PK = PK_j, \sigma_{agg}$

Output: Accept/Reject

1. Computes:  $c_j = H(u_j, PK_j, M_j)$  for  $j \in [N]$
  2. Queries:  $e_j = H_2(c_1, c_2, \dots, c_N, j)$  for  $j \in [N]$
  3. Computes  $PK.z = \sum_j e_j.(PK_j.c_j + u_j)$
  4. If  $\|z\| \leq \beta = O(\sqrt{N}B)$  Accepts  
Else Rejects
  5. Returns Null
- 

## 4 Performance

Both “time” and “latency” are the first parameters that have been considered for the evaluation. Note that, the inclusion of both key generation time and signature time is the main reason for this linear growth of latency. The key generation time increases with the number of blocks in the order  $O(N)$ , where  $N$  is the number of nodes. Additionally, the complexity is  $O(1)$  and the aggregate signature time is static because the production and verification of the signatures are performed in a single operation. The process of generating aggregate signatures is unaffected even as the number of nodes or blocks increases. Since the key generation time needs to be further optimized for better effect, our proposed approach is scalable under this condition. When compared to current methods, our proposed solution performs better for transaction latency, which exhibits the same behavior as read latency. The proposed technique has a 60% higher overall transactional throughput. It is effective in this way because the aggregated approach is used. The cost of various operations involved is polynomial selection  $t_p \approx 0.014$  s, lattice creation  $t_l \approx 0.128$  s, multiplication in ring  $t_* \approx 0.118$  s, addition in ring  $t_a \approx 0.008$  s, and hashing algorithm  $t_h \approx 0.012$  s. The framework proposed by Kiktenko et al. [1] takes  $2t_p + 2t_* + 2nt_l$  operations in key generation,  $2t_p + 2nt_* + 4t_h + 2nt_a$  in a signature generation, and  $nt_p + 4nt_* + 2nt_h + nt_a$  in verification. The framework proposed by Chao-yang et al. [26] takes  $4t_p + 4t_* + 2nt_l$  operations in key generation,  $4t_p + 2nt_* + 2t_h + 4t_a$  in signature generation, and

**Table 1** Comparison between computation costs of proposed with related frameworks

Frameworks	Key generation	Signature	Verification
[A] Kiktenko et al. [1]	$2t_p + 2t_* + 2nt_l$	$2t_p + 2nt_* + 4t_h + 2nt_a$	$nt_p + 4nt_* + 2nt_h + nt_a$
[B] Chao-Yang Li et al. [26]	$4t_p + 4t_* + 2nt_l$	$4t_p + 2nt_* + 2t_h + 4t_a$	$nt_p + 4nt_* + 2nt_h + nt_a$
[C] Chao-Yang Li et al. [27]	$4t_p + 4t_* + nt_l$	$2t_p + 2nt_* + 4t_h + 2nt_a$	$nt_p + 4nt_* + nt_h + 2nt_a$
[D] Saha et al. [28]	$2t_p + 3t_* + t_l$	$2t_p + 4t_* + 2t_h + t_a + nt_l$	$t_p + 2t_h + (n - 1)t_l$
[E] Proposed Framework	$t_p + 3t_*$	$2t_p + 4t_* + 2t_h + t_a + nt_l$	$t_p + 2t_h + (n - 1)t_l$

$nt_p + 4nt_* + 2nt_h + nt_a$  in verification. The framework proposed by Chao-Yang et al. [27] takes  $4t_p + 4t_* + nt_l$  in key generation,  $2t_p + 2nt_* + 4t_h + 2nt_a$  in signature, and  $nt_p + 4nt_* + nt_h + 2nt_a$  in verification. The framework proposed by Rahul et al. [28] takes  $2t_p + 3t_* + t_l$  operations in key generation,  $2t_p + 4t_* + 2t_h + t_a + nt_l$  in signature, and  $t_p + 2t_h + (n - 1)t_l$  in verification. The proposed Framework takes  $t_p + 3t_*$  operations in key generation,  $2t_p + 4t_* + 2t_h + t_a + nt_l$  in signature, and  $t_p + 2t_h + (n - 1)t_l$  in verification (see Table 1).

## 5 Conclusion

Because of its appealing decentralization feature, blockchain technology is being used for information sharing among intelligent devices which is a new area of research that has gained substantial interest from both business and academia. We have provided a thorough analysis of blockchain integration. We have covered the definition, elements, enabling technologies, and problems of smart devices. Then, we discussed the history and features of blockchain in detail. We evaluated the benefits and drawbacks of blockchain integration for data information sharing. We have proposed a solution to the security of blockchain.

## References

1. Kiktenko EO, Pozhar NO, Anufriev MN, Trushechkin AS, Yunusov RR, Kurochkin YV, Lvovsky AI, Fedorov AK (2018) Quantum-secured blockchain. *Quantum Sci Technol* 3(3):035004
2. Charles S, Feniosky P-M (2018) Blockchain for cities-a systematic literature review. *IEEE Access* 6:76787–76819
3. Ream J, Chu Y, Schatsky D (2016) Upgrading blockchains: smart contract use cases in industry, vol 12
4. Szabo N (1996) Smart contracts: building blocks for digital markets. *EXTROPY: J Transhumanist Thought* (16) 18(2):28
5. Szabo N et al (1994) Smart contracts
6. Xiaoqi L, Peng J, Ting C, Xiapu L, Qiaoyan W (2020) A survey on the security of blockchain systems. *Futur Gener Comput Syst* 107:841–853
7. Xie J, Tang H, Huang T, Yu FR, Xie R, Liu J, Liu Y (2019) A survey of blockchain technology applied to smart cities: research issues and challenges. *IEEE Commun Surv Tutor* 21(3):2794–2830

8. Zheng Z, Xie S, Dai H, Chen X, Wang H (2017) An overview of blockchain technology: architecture, consensus, and future trends. In: 2017 IEEE international congress on big data (BigData congress), pp 557–564. IEEE
9. Ismailisufi A, Popović T, Gligorić N, Radonjic S, Šandi S (2020) A private blockchain implementation using multichain open source platform. In: 2020 24th international conference on information technology (IT), pp 1–4. IEEE
10. Haibo T, Jiejie H, Yong D (2019) Medical data management on blockchain with privacy. *J Med Syst* 43:1–6
11. Emanuele B, Youssef I, Ernesto D (2020) Blockchain-based distributed trust and reputation management systems: a survey. *IEEE Access* 8:21127–21151
12. Hunhevicz JJ, Hall DM (2020) Do you need a blockchain in construction? Use case categories and decision framework for DLT design options. *Adv Eng Inf* 45:101094
13. Labazova O, Dehling T, Sunyaev A (2019) From hype to reality: a taxonomy of blockchain applications. In: Proceedings of the 52nd Hawaii international conference on system sciences (HICSS 2019)
14. Xu X, Weber I, Staples M, Zhu L, Bosch J, Bass L, Pautasso C, Rimba P (2017) A taxonomy of blockchain-based systems for architecture design. In: 2017 IEEE international conference on software architecture (ICSA), pp 243–252. IEEE
15. Zibin Z, Shaoan X, Hong-Ning D, Xiangping C, Huaimin W (2018) Blockchain challenges and opportunities: a survey. *Int J Web Grid Serv* 14(4):352–375
16. Ali S, Wang G, White B, Cottrell RL (2018) A blockchain-based decentralized data storage and access framework for ping. In: 2018 17th IEEE international conference on trust, security and privacy in computing and communications/12th IEEE international conference on big data science and engineering (TrustCom/BigDataSE), pp 1303–1308. IEEE
17. Laphou L, Zecheng L, Songlin H, Bin X, Songtao G, Yuanyuan Y (2020) A survey of IoT applications in blockchain systems: architecture, consensus, and traffic modeling. *ACM Comput Surv (CSUR)* 53(1):1–32
18. Aiya L, Xianhua W, Zhou H (2020) Robust proof of stake: a new consensus protocol for sustainable blockchain systems. *Sustainability* 12(7):2824
19. Aggarwal S, Chaudhary R, Aujla GS, Kumar N, Choo K-KR, Zomaya AY (2019) Blockchain for smart communities: applications, challenges and opportunities. *J Netw Comput Appl* 144:13–48
20. Miguel C, Barbara L et al (1999) Practical byzantine fault tolerance. In: *OsDI*, vol 99, pp 173–186
21. Sharma PK, Park JH (2018) Blockchain based hybrid network architecture for the smart city. *Futur Gener Comput Syst* 86:650–655
22. Bindra L, Lin C, Stroulia E, Ardakanian O (2019) Decentralized access control for smart buildings using metadata and smart contracts. In: 2019 IEEE/ACM 5th international workshop on software engineering for smart cyber-physical systems (SEsCPS), pp 32–38. IEEE
23. Junqin H, Linghe K, Guihai C, Min-You W, Xue L, Peng Z (2019) Towards secure industrial IoT: blockchain system with credit-based consensus mechanism. *IEEE Trans Ind Inform* 15(6):3680–3689
24. Brendan C, Jerome G, Zeynep G, Lucas H, Sakshi M, Aynur T, Samra V (2012) The smart meter and a smarter consumer: quantifying the benefits of smart meter implementation in the united states. *Chem Central J* 6(1):1–16
25. Zhao Y (2018) Aggregation of gamma-signatures and applications to bitcoin. *Cryptology ePrint Archive*
26. Chao-Yang L, Xiu-Bo C, Yu-Ling C, Yan-Yan H, Jian L (2018) A new lattice-based signature scheme in post-quantum blockchain network. *IEEE Access* 7:2026–2033
27. Chaoyang L, Yuan T, Xiubo C, Jian L (2021) An efficient anti-quantum lattice-based blind signature for blockchain-enabled systems. *Inf Sci* 546:253–264
28. Saha R, Kumar G, Devgun T, Buchanan W, Thomas R, Alazab M, Kim T-H, Rodrigues J (2021) A blockchain framework in post-quantum decentralization. *IEEE Trans Serv Comput*

# An Open-Source Learning Management System



Anshul J. Gaikwad , Pratik P. Shastrakar , Bhagyashri R. Sardey ,  
and Nikhil S. Damle 

**Abstract** In recent years, the need to integrate new technologies into the educational process has been increasing. The use of the Internet in education has increased steadily over the last decade as new technologies make it easier for students to learn. Using distance learning tools, students' learning can be flexible across location and time constraints. Therefore, students can access information anytime, anywhere, whether in the library or in the classroom. Distance education is notoriously expensive, and as schools become major providers of distance education, budgeting becomes even more important. Cost relative to the learning environment is a disadvantage of distance education, and the work of education management can eliminate it. Using comprehensive learning management will help improve learning tools and improve learning quality. A web-based learning management system called the Learning Management System (LMS) assists teachers in meeting objectives, planning lessons, and inspiring students. In the twenty-first century, learning management systems (LMS) have emerged as a crucial instrument for delivering education. This white paper provides an overview of LMSs, including their features, capabilities, and future directions. This article discusses the main features and roles, advantages and limitations of LMS, and current trends in LMS development. The essay also analyses difficulties with LMS adoption and makes suggestions for further study. It also discusses the LMS that has been developed and can be integrated directly into the organization if needed. The comparison of several LMSs is also included in the article.

**Keywords** Virtual classrooms · Content management system · AWS · WordPress · Domain · Hosting · Payment

---

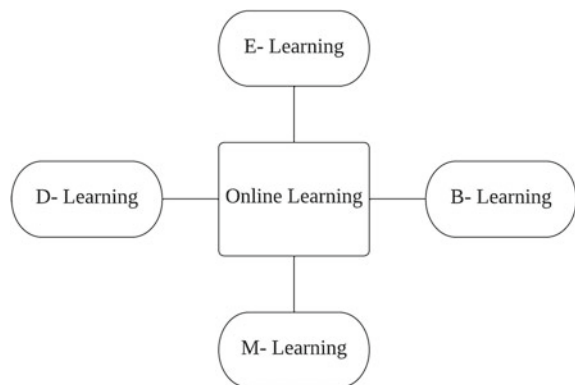
A. J. Gaikwad (✉) · P. P. Shastrakar · B. R. Sardey · N. S. Damle  
Shri Ramdeobaba College of Engineering and Management, Nagpur, Maharashtra, India  
e-mail: [gaikwadaj@rknc.edu](mailto:gaikwadaj@rknc.edu); [jogendranath86@gmail.com](mailto:jogendranath86@gmail.com)

Department of Electronics Engineering, Shri Ramdeobaba College of Engineering and Management, Nagpur, Maharashtra, India

## 1 Introduction

The Internet's quick development has altered people's behavior. People utilize the internet for research as well as job and shopping. E-learning is a term that is frequently used to describe using the Internet for educational purposes. Learning management systems (LMS) and content management systems (CMS) are the two categories of technology used in e-learning. A learning management system (LMS) is a web-based tool that connects instructors and learners during the learning process and can take the place of face-to-face instruction in the classroom. Numerous opportunities in education and other fields have been made possible by the enormous advancements in information and communication technology and Internet connectivity. Students may have a wide range of learning opportunities in the new technology-based learning environment. When students and professors are occasionally in separate locations, distance education is a recommended alternative [1]. In distance learning, learning management systems (LMSs), often referred to as virtual learning environments (VLEs) or learning platforms, are crucial. At several stages of the remote learning process, open-source software can be employed. For example, application software that completes the learning content's preparation and LMS software that provides the learning content shown on the website environment are two examples. These new courses are being welcomed by both industry and schools. The learning options are depicted in Fig. 1 by the letters E-learning, D-learning, M-learning, and B-learning, which stand for electronic learning, distance learning, mobile learning, and blended learning, respectively.

**Fig. 1** Typical block diagram of online learnings



## 1.1 *Different Types of Learning*

**Distance Learning.** “Distance learning,” sometimes known as “d-learning,” refers to all forms of distance education, including e-learning and mobile learning. Surprisingly, the definition of distance education also covers correspondence courses, which date back to the eighteenth century [2].

**Electronic Learning.** Electronic learning (e-learning, sometimes referred to as web-based training) is anytime, anywhere education delivered via the Internet or a corporate intranet to learners equipped with a browser. Online learning allows students, trainees, and casual learners to participate in organized learning experiences wherever they are [3].

**Mobile Learning.** Mobile learning is a novel approach of accessing learning content via mobile devices. As long as we have a modern mobile device connected to the internet, we can study whenever and wherever we want [4].

**B Learning.** B-learning stands for blended learning, which refers to the combination of face-to-face training (in the classroom with a teacher) and online training (courses via the Internet or other digital formats). Thus, B-learning is a hybrid learning system that mixes these two systems [5].

## 1.2 *LMS*

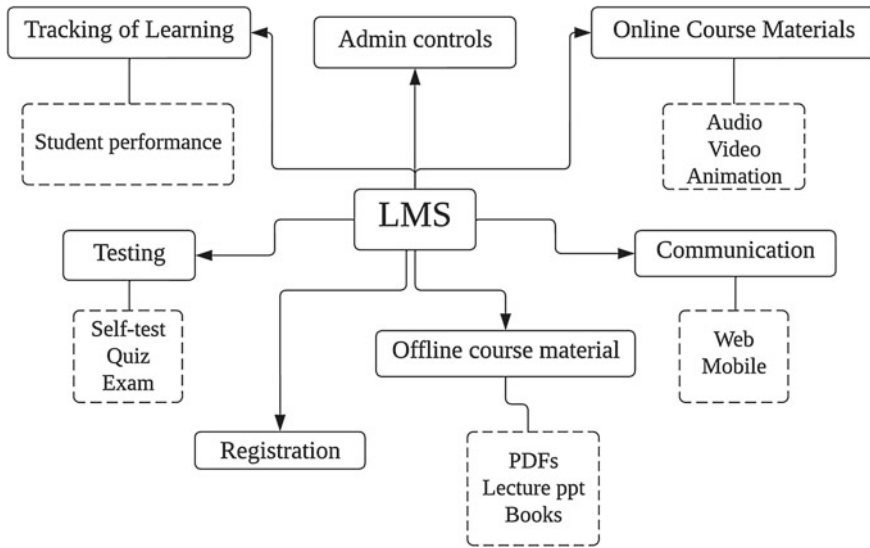
A software platform known as a learning management system (LMS) is created to make it easier to create, administer, and distribute educational content and activities. Online learning platforms frequently use this technology to provide courses and programs to students all around the world. A learning management system (LMS) often offers facilities for developing and uploading course materials like videos, tests, and assignments. Students can access the material remotely, frequently at their own convenience. The platform also provides tools like discussion forums, gamification components, and peer reviews to boost student motivation and engagement. Additionally, LMS platforms often offer analytics tools for course designers to monitor learner progress and spot areas that require more assistance.

Overall, an LMS is a powerful tool for delivering online education, providing learners with access to high-quality content and a range of features to support their learning experience [6]. There are several factors to consider while picking an online learning platform. Some reasons to choose a platform over other alternatives include:

**Course Selection.** The platform should offer a diverse selection of courses covering a wide range of topics and skill levels.

**Quality of Content.** The courses should be created by experts in the industry or leading educators to ensure high-quality content.

**Flexibility.** The platform should allow for flexible learning options, enabling learners to complete coursework at their own pace and on their own schedule.



**Fig. 2** Illustration of LMS

**Certification.** The platform should offer certifications of completion to demonstrate skills and knowledge to employers or for personal development.

**Community and Support.** The platform should provide access to a community of learners and resources for support to help learners stay motivated and on track.

Overall, a platform that offers a combination of diverse course selections, high-quality content, flexibility, certification, and community support can be an attractive option for online learning [6].

Figure 2 shows the components LMS can have and gives a brief idea about LMS. Also, different stages of LMS like frontend, backend, and database.

There are several factors to consider while picking an online learning platform. Some reasons to choose a platform over other alternatives include:

**Course Selection.** The platform should offer a diverse selection of courses covering a wide range of topics and skill levels.

**Quality of Content.** The courses should be created by experts in the industry or leading educators to ensure high-quality content.

**Flexibility.** The platform should allow for flexible learning options, enabling learners to complete coursework at their own pace and on their own schedule.

**Certification.** The platform should offer certifications of completion to demonstrate skills and knowledge to employers or for personal development.

**Community and Support:** The platform should provide access to a community of learners and resources for support to help learners stay motivated and on track.

Overall, a platform that offers a combination of diverse course selections, high-quality content, flexibility, certification, and community support can be an attractive option for online learning [6].



## 2 Related Work

Salomão Bento Nilo Pena and others have analyzed that e-learning has been widely implemented in educational institutions to improve the learning process and meet the new challenges posed by technology, but it is not enough that online learning becomes the dominant teaching standard is essential [7].

In this study, Ruben Manhiça et al. attempt to provide an overview of research on the application of artificial intelligence in higher education management systems (ELMS). From 2010 to 2022, 306 articles were identified from the Scopus and EBSCOhost databases, and 33 articles were ultimately selected for analysis. Moodle is the most commonly used LMS for implementing AI solutions in education, and AI is most commonly used for student performance assessment based on student data. Some of the AI algorithms used include Random Forests, Neural Networks, K-means, Naive Bayes, Support Vector Machines, and Decision Trees [8].

S. V. Phulari illustrates how we can enhance manual processes with e-learning management systems for safer, more secure, and effective learning, improving user experience and resource utilization [9].

With the help of various sources, Ignatius Adrian Mastan et al., in this study analyzed e-learning models and trends and identified seven criteria for further study in the area [10].

Ahmet Dogukan Sariyalcinkaya et al. concluded that distance learning has been hastened by the COVID-19 pandemic, necessitating more educational content and management in electronic settings. The study looks into virtual classroom software, learning management systems, and content management systems before, during, and after the epidemic [11].

Institutions of higher learning employ data science to assess the effectiveness of student learning. In order to enhance teaching and learning procedures, Muhammad Abu Arqoub et al. proposed a framework for extending the free and open-source Moodle learning management system [12].

The study by Binar Kurnia Prahani et al. examined the trends in LMS research from 1991 to 2021 with a particular emphasis on conference papers, English, and the United States. It reveals that English is the most widely spoken language worldwide, while the United States is the most well-liked nation. The National Natural Science Foundation of China, Bina Nusantara University, and Lecture Notes in Computer Science are the primary funding sponsors, respectively [13].

The study by Abednego Kofi Bansah and Douglas Darko Agyei looks at how students' adoption of learning management systems (LMS) is impacted by perceptions of ease, efficacy, and usefulness [14].

Soyeong Kwon et al. explained that the pandemic has caused a movement toward blended and flipped learning as well as other technology-integrated teaching strategies. Many institutions, though, find it difficult to adjust to this new setting. An LMS should be created as a learning community, with instructors and students repositioned as co-participants, in order to integrate identity shifts [15].

In a blended learning context, Tiong-Thye Goh and Bing Yang investigated the connection between e-learning engagement, flow experience, and continued use of the learning management system. It reveals that flow has a direct favorable effect on system continuation and influences e-engagement and perceived ease of use [16].

Nhu-Ty Nguyen investigated the variables affecting student satisfaction with learning management systems at the International University—Vietnam National University HCMC, specifically Blackboard and Edusoft. Significant effects on learners' satisfaction, including direct and indirect relationships, are revealed by a quantitative survey. In order to increase system efficacy, the study also investigates the connection between learning management technologies and student happiness [17].

Nigar M. Shafiq Surameery and Mohammed Y. Shakor introduce the Cloud-Based Educational System (CBES), a theoretical framework for a cloud-based learning management system that offers administrators, staff, and teachers a comfortable setting in which to manage e-learning duties [18].

Rushna Khalil Awan and others have analyzed implementing e-learning in higher education institutions a difficult, thorough analysis of the literature from 2005 to 2020 has revealed compatibility, preparedness, factors, advantages, and implementation methodologies [19].

Meyliana et al. studied the use of UTAUT 2 and trusted methodologies to identify factors influencing the acceptance and use of learning management systems (LMS) by university professors. The results show that performance expectations, habits, and trust have the greatest impact on adoption, while habits and behavioral intentions are the main factors influencing user behavior [5].

Dr. Lester Reid, in his qualitative case study, investigated how learning management systems affect traditional teaching methods, transformative learning, and the acquisition of knowledge by adult learners. It reveals favorable reactions from both teachers and pupils [20].

Learning management systems (LMS) have revolutionized education, causing e-learning in higher education institutions to rise tremendously. For e-learning to become the preeminent teaching method, a systematic evaluation by Salomão Bento Nilo Pena and Arnaldo Manuel Pinto Santos identifies research themes and emphasizes the significance of stakeholders' digital literacy [7].

Seyed Mohammadbagher Jafari et al. investigated the relationship between student achievement and information quality, system quality, and online learning readiness through system usage and user satisfaction. The results show that the most influential path is the impact of information quality on user satisfaction and perceived usefulness, while the least influential path is preparation [6].

In Zheng Ninghan et al.' article, an online learning management system, THUOJ, is proposed, which focuses on grading programming assignments and customizing curriculum assessments for various programming courses. According to the design of potential users, the author proposes a system structure design using Linux+Apache+MySQL+PHP (LAMP). A simple website demo has been implemented to demonstrate the use of the system and the online assessment module [2].

L. Abazi-Bexheti et al. conclude that learning management systems (LMS) are designed for learning, but some educators believe that students may be better served by LMS alternatives, such as social bookmarking tools, document sharing apps, social networking apps, timeline tools, and media options. This article examines both sides of the debate and its implications for teaching [1].

Cansu Cigdem Aydin et al. found that using open-source software can make distance learning more flexible and cost-effective. Moodle is an excellent LMS designed to improve the quality of education and includes the tools that an online learning system should have [3].

Matjaz Kljun et al. examined what the authors think is relevant to the LMS. We also compared articles from different years to see if there are functional patterns associated with specific time periods, how the need for new features has changed over time, and how LMS developers have responded to this question. They also try to find out what the current needs are and what new features will be included in future versions of the LMS [4].

## 3 Software Used

### 3.1 *WordPress*

In this paper, the software used to create the LMS is WordPress. All the implementation of the LMS is done by using WordPress. WordPress is a free and open content management system (CMS). It's a popular tool for people with no coding experience but who want to build websites and blogs. The software costs nothing. Anyone can install, use, and modify it for free, and originally WordPress was mainly used for creating blogs. UI/UX designers are using it to create websites. You can create a hobby or lifestyle blog, professional portfolio, business website, mobile app, membership site, and most importantly, e-commerce website. Security is a major concern for businesses. With the number of data breaches increasing every year, you want peace of mind knowing that your data (and that of your customers) will be protected. As long as you keep your plugins up to date and your passwords safe, WordPress is one of the most secure and reliable CMS platforms out there. The platform offers several features to secure your website, such as logging out inactive users and adding two-factor authentication making it simple for use to beginners. Also, WordPress supports all media types and it is free to use. WordPress consists of lots of resources and plugins which can be very useful for the creation of a website. This paper will discuss the plugins which were used in the creation of LMS [21]. WooCommerce is one of the plugins of WordPress which has made online business easier with the platform having unrestricted customization and built-in blogging to help your business grow. It includes all the transactions and payment gateways.

Elementor is used by more than 3 million websites for using its WordPress page builder feature. With no technical skills, you can design stunning web pages from templates.

## 4 Implementation

WordPress is a well-liked content management system (CMS) for creating websites and blogs that is renowned for its adaptability and user-friendliness, making it a perfect option for people and organizations of all sizes. A helpful WordPress plugin for website building is Elementor. It enables users to develop their own pieces or utilize pre-made themes and widgets to create bespoke pages and layouts. Elementor has a user-friendly interface that allows users with no coding experience to easily create complex page designs. With Elementor, you can create custom designs for your LMS (Learning Management System) website without hiring a professional web developer. Elementor gives you full control over the design of your pages, so you can create a unique look that matches your brand. Overall, using WordPress with Elementor is a great option for building custom websites, especially for those who aren't good at coding. This LMS site allows for the creation of paid and free courses, including various types of lectures such as audio, video, and podcasts. Moreover, it provides options to create different types of quizzes including True or False, Fill in the Blank, Multiple Choice, and Multiple Choice. Additionally, the site includes a teaching feature that allows individuals to teach on the platform and create their own courses. For each sale of their courses, the platform receives a commission. The website will also integrate various payment gateways to accept payments for paid courses. By using a page builder, website designs are not only easy to create but also beautiful. Moreover, the website will be optimized for mobile devices, fast, safe, and secure. To handle secure and efficient online transactions, the WooCommerce payment plugin was integrated into the LMS. This plugin supports multiple payment gateways, and for this particular system, the Paytm payment gateway was selected to ensure secure payment processing. A significant aspect of the LMS implementation was the storage of video lectures. To ensure reliability and scalability, the lectures were stored in an Amazon Web Services (AWS) S3 bucket. AWS S3 offers numerous advantages, including high durability, availability, and scalability, which are crucial for hosting and delivering large amounts of video content. For hosting the LMS website, an AWS EC2 instance was utilized. This cloud-based hosting solution provided the necessary distribution and scalability required for handling the anticipated user traffic and resource demands of the LMS. With AWS EC2, the LMS can efficiently accommodate growing user bases and adapt to varying workloads. An essential consideration during the implementation process was the user interface (UI) design. The LMS was designed to have an intuitive and user-friendly UI, ensuring that learners, instructors, and administrators could easily navigate through the system. By prioritizing user-centered design principles, the LMS aimed to optimize the user experience and facilitate efficient interactions with the platform. In

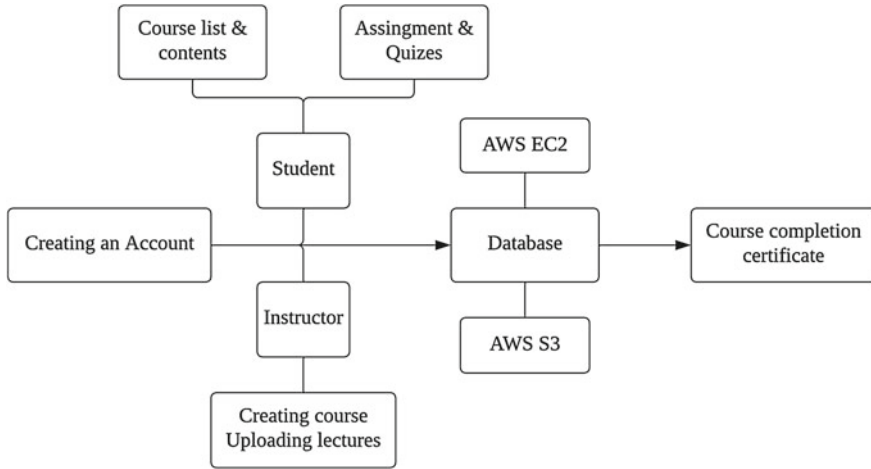


Fig. 3 Implementation of LMS

summary, the implementation of the LMS involved leveraging the capabilities of WordPress, with the aid of the Elementor page builder plugin for visually appealing page creation. The WooCommerce payment plugin, specifically integrated with the Paytm payment gateway, ensured secure and seamless online transactions. AWS S3 was utilized to store video lectures, providing advantages such as reliability and scalability. Hosting the LMS on an AWS EC2 instance allowed for distributed and scalable deployment. Finally, the user interface was carefully designed to be user-friendly, ensuring ease of navigation and enhancing the overall learning experience within the LMS. Figure 3 shows the pathway of student creating an account and completing the course and getting the certificate. Also, it shows creating account as an instructor to create course.

### 4.1 Selection of Domain

For our website, we have chosen GoDaddy as the domain registrar; the domain name is virtualclassroomlms.co, and the validity period is 1 year. We made our pick after researching numerous providers, including Name.com and Namecheap, and determined that GoDaddy was the best fit for our needs. GoDaddy is a well-known and reputable domain registrar that provides a variety of domain registration, hosting, and website-building services. Their prices and plans are competitive and they offer reliable and efficient customer service. Furthermore, we found GoDaddy’s user interface to be simple to use and to offer a unified experience for domain registration and management. Their domain transfer process is also simple, which could be useful if we decide to switch to another provider in future. Overall, we believe GoDaddy is

the greatest alternative for our domain name needs, and that their services will assist us in reaching our online objectives.

## ***4.2 Selection of Domain***

SSL certificates are issued by LMS to ensure secure communication between clients and servers. Amazon Web Services (AWS) hosts the website, and AWS S3 hosts the database. This ensures that all courses and resources are kept and protected securely. Furthermore, the website provides payment choices for purchasing courses, with Paytm serving as a payment channel. Paytm is a trusted and secure payment gateway that ensures the safety and security of all online transactions. In general, this website was developed with security in mind and takes all essential precautions to protect user data and transactions. Course materials, such as videos, are securely stored in S3 buckets by the instructor. Videos are only accessible within the LMS and cannot be viewed outside of the platform, keeping course content private and confidential. In addition, the link to the video is not visible to the public, which increases the level of confidentiality. Additionally, course administrators can revoke access to courses as needed. This feature provides an additional layer of security and control over course content. Together, these features ensure that course content remains private and accessible only to authorized users.

## ***4.3 Creation of Page***

The LMS website offers users the option to log in or create an account. There are two accounts with different access levels: Student Login and Teacher Login. Student IDs allow users to access all courses offered on the platform. Users can enroll in any course and access all course materials and assessments. Teacher connections, on the other hand, allow you to create courses from scratch and subscribe to courses created by other teachers. Instructors can also create new courses, add course content, and manage course evaluations. Additionally, instructors can access a dashboard showing their courses, student enrollments, and course progress. By providing different levels of access for different types of accounts, LMS sites can ensure users have a personalized experience based on their role. This functionality allows the site to respond effectively to the needs of students and teachers.

## 4.4 *Creation of Course*

LMS has a comprehensive course page that includes multiple fields and options to provide students with a detailed course overview and help them make an informed decision about enrollment. These fields include:

**Course Name.** The name of the course.

**Course Subtitle.** Brief description of the course.

**Course Image.** Image representing a course.

**Course Description.** A detailed outline of the course, including what the student will learn and what the course covers.

**Instructor Information.** Information about the course instructor, including name, biography, and credentials.

**Courses.** List of course modules, sections, and courses including video lectures, text lectures, quizzes, and assignments.

**Course Requirements.** Any prerequisites or requirements to take a course, including required knowledge or skills.

**Course Outcomes.** Expected learning outcomes or benefits associated with course attendance.

**Course Ratings.** Ratings and grades from other students who have taken the course.

**Course Price.** Price of the course, including any discounts or promotions.

**Course Duration.** The duration of the course, in hours or weeks.

**Course Language.** The language in which the course is offered.

**Course Level.** Course levels, such as Beginner, Intermediate, or Advanced.

**Course Category.** The category or subject of the course, such as business, technology, or art.

**Course Certification.** If the course provides a certificate upon completion.

**Lesson Previews.** Previews of course content, such as video previews or sample lessons.

LMS tries to provide a thorough and extensive overview of each course by integrating these aspects, making it easier for students to evaluate a course and decide if it suits their needs and interests. As an instructor, you can construct a course from start, with various choices for customizing course content. Course image, course duration, and course type are all mandatory fields. A course photo is an essential element that represents a course and makes a first impression on potential students. Visually appealing high-quality images can attract more students to your courses. The duration of the course is another important factor that should be included in the course details. This information informs students of the time required to complete the program and helps them plan accordingly. Course categories are also necessary since they assist students in locating and exploring courses of interest to them. It provides an overview of course topics and assists students in identifying courses that meet their learning objectives. Course data also contains a course description, instructor information, course requirements, course results, course grades, course cost, course level, and course material. a summary of the course. These areas help students make informed

decisions about whether they match their interests, learning goals, and expectations. The course description should be a detailed outline of the course content, including what students will learn and what the course covers. Instructor information should provide the instructor's name, resume, and credentials, which helps establish the instructor's authority and credibility. The course requirements should include any prerequisites or requirements needed to take the course, including required knowledge or skills. The course outcomes should list the expected learning outcomes or benefits associated with course participation. Course grades should include the grades and grades of other students who have taken the course. Course prices should be transparent and clearly communicated to prospective students, including any discounts or promotions available. A course level should be specified to help students determine which course is appropriate for their skill levels, such as Beginner, Intermediate, or Advanced. Course previews should be included to give students an overview of course content, such as video previews or sample lessons. In conclusion, as a course instructor, it is important to provide detailed and accurate information about a course in order to attract potential students and help them decide on enrollment in the course. By including all required and optional fields in the course details, instructors can ensure that their courses are clear.

#### ***4.5 Payment Method***

In WordPress, payments are made using WooCommerce plugins, which include various payment gateways. In WordPress, there are multiple payment gateways available for secure payment and transactions. These are PayPal, Stripe, Authorize.net, Amazon Pay, Google Pay, Apple Pay, Square, 2Checkout. But in LMS, the payment system is implemented through the Paytm payment gateway as it is easy to use, user-friendly, and secure. All of the courses in our LMS use the Paytm Payment Gateway to ensure secure payment transactions. Users can enter their UPI ID to make a payment, or an automatic QR code is generated for them to scan and finish the transaction instead. The user must input the correct transaction ID in order to proceed after making the payment. The course will not be assigned to the user if the transaction ID is submitted incorrectly, and the transaction will be paused until the proper transaction ID is entered. This guarantees a simple and secure payment process while ensuring that only authorized users may access the courses they have paid for. In this paper, we set up a merchant account and use the Paytm payment gateway. To accept payments from customers using credit cards, debit cards, net banking, and UPI, we set up a customer account with Paytm as part of this process. As a merchant account holder, we adhere to all applicable taxes and laws and only use morally and legally acceptable payment methods. Scalability is one of the main benefits of using the Paytm payment gateway. Payment gateways can be integrated into our website or mobile application to simplify payments for our clients. For companies aiming to grow and give their clients a free payment alternative, this tool



is ideal. Millions of people in India rely on Paytm as their preferred payment method because of its user-friendly interface and versatility with various payment methods.

## **4.6 Data Storage**

The Learning Management System (LMS) uses an Amazon Web Services (AWS) S3 bucket to securely store all course videos. These videos are uploaded by teachers and are automatically linked to the modules they create. This ensures learners have easy access to the necessary materials and can view them seamlessly in the LBS. By using AWS S3, we can take advantage of their free offer for up to 5 GB of storage. We can quickly and cheaply increase our storage capacity to meet our expanding needs as our website gets bigger. Additionally, AWS S3 offers top-notch security features to deter unauthorized access and safeguard the data of our consumers. AWS S3 offers a dependable and scalable solution for storing and delivering course materials in addition to guaranteeing the security of our users' data. Our students can relax knowing they have access to the most recent course material and can quickly navigate the LBS to find what they need.

## **5 Applications**

A Learning Management System (LMS) is an application used to plan, implement, and evaluate the learning process. It is used in online education and most commonly has two elements: a server that performs basic functions, and a user interface run by teachers, students, and leaders. In general, learning management systems allow teachers to create and deliver content, monitor student engagement, and measure student performance. Learning management can also provide students with the ability to use interactive methods such as chat, video conferencing, and meetings.

LMSs are used as a medium of learning irrespective of number of learners. The system can improve traditional teaching methods while saving organizations time and money. An effective system allows teachers and administrators to manage things like user registration, content, programs, user access, communication, confirmation, and notification. Supported by the US Department of Defense, the Advanced Learning Team developed a special system called SCORM (Shareable Content Object Reference Model) to support training management design.

## 6 Future Scope

Multi-Channel Learning Style, in future, many young tech-savvy learners will continue their learning process and prefer small modules that they can complete and learn easily. The number of people learning through video and audio available online will increase. Administrators will find that the content library will be used more to meet acute learning needs that are more akin to on-the-job training than traditional instructor-led training. This year, good reporting will ultimately help shape the culture within the organization to characterize lifelong learning. AI in Learning: AI plays an important role in all aspects of our lives. Whether it's a virtual assistant giving you weather information or any news, artificial intelligence will be more integrated into our lives than we think. AI will personalize and correlate learning with insights based on user behavior, data, and other preferences [8]. AI will transform enterprise learning with its incredible ability to automate and personalize learning to revolutionize the way students learn. An AI-powered LMS will not only provide a personalized learning environment with content but also improve the quality of courses [22]. How Moodle Analytics helps promote student engagement Adaptive learning will help adult learners: Adult learners often have their own specific needs and are more skilled and experienced. Adaptive learning will have a major impact on how learners enroll in courses and how they use them at appropriate times, learning paths, and interests [3]. Since adult education courses have specific goals, adaptive learning in the LMS can help them achieve the main goals easily. Higher education and corporate training programs can now view them as individuals from diverse backgrounds, with expertise and real-world experience, and must respond to their real needs. LMSs will focus more on user engagement and experience new LMSs will focus more on learner engagement and experience rather than just messaging. Traditional LMSs need to improve their functionality in order to stay competitive in the market. The future of the LMS will also see more engaging features such as personalized learning, social learning, gamification, and personalized coaching and support [23].

## 7 Conclusion

We created a learning management system with the necessary functionality, similar to other LMSs. The platform is intended to provide users with a seamless learning experience by offering a wide range of courses taught by instructors from various backgrounds. Our learning management system offers a straightforward and user-friendly interface that allows users to navigate and locate relevant courses. In order to improve the learning experience and motivate students to keep studying, we have also incorporated elements like course evaluations, quizzes, and certifications. Additionally, we have protected our consumers' privacy and safety by making sure that both their personal data and financial transactions are secure. With features like voice

support and permissions, we've made sure that individuals of different backgrounds may use our platform. Overall, our learning management system offers a reasonably priced environment for workers to learn and develop. We think that our system will advance education and aid in the objectives of pupils.

## References

1. Abazi-Bexheti L, Apostolova-Trpkovska M, Kadriu A (2014) Learning management systems: trends and alternatives. In: 2014 37th international convention on information and communication technology, electronics and microelectronics (MIPRO), Opatija, Croatia, 2014
2. Zheng N, Tian S, Chen Y (2015) Online learning management system. In: 2015 international conference on computational science and computational intelligence (CSCI), Las Vegas, NV, USA, 2015
3. Aydin CC, Tirkes G (2010) Open-source learning management systems in e-learning and Moodle. In: IEEE EDUCON 2010 conference, Madrid, Spain, 2010
4. Kljun M, Vicić J, Kavsek B, Kavcic A (2007) Evaluating comparisons and evaluations of learning management systems. In: 2007 29th international conference on information technology interfaces, Cavtat, Croatia, 2007
5. Meyliana, Widjaja HAE, Santoso SW, Petrus S, Jovian J (2019) The enhancement of learning management system in teaching learning process with the UTAUT2 and trust model. In: 2019 International conference on information management and technology (ICIMTech), Jakarta/Bali, Indonesia, 2019
6. Jafari SM, Salem SF, Moaddab MS, Salem SO (2015) Learning Management System (LMS) success: an investigation among the university students. In: 2015 IEEE conference on e-Learning, e-Management and e-Services (IC3e), Melaka, Malaysia
7. Pena SBN, Santos AMP (2022) Implementation of a Learning Management System (LMS) in an Angolan higher education institution: a systematic literature review. In: 2022 17th Iberian conference on information systems and technologies (CISTI), Madrid, Spain, 2022
8. Manhiça R, Santos A, Cravino J (2022) The use of artificial intelligence in learning management systems in the context of higher education: systematic literature review. In: 2022 17th Iberian conference on information systems and technologies (CISTI), Madrid, Spain, 2022
9. Phulari SV (2022) Web platform for E-learning. *Int J Res Appl Sci Eng Technol*
10. Mastan IA, Sensuse DI, Suryono RR, Kautsarina K (2022) Evaluation of distance learning system (e-learning): a systematic literature review
11. Sariyalcinkaya AD, Altun E, Erümit AK (2022) Managing distance learning systematically
12. Arqoub MA, El-Khalili N, Hasan MA-S, Banna AA (2022) Extending learning management system for learning analytics. In: 2022 international conference on business analytics for technology and security (ICBATS), Dubai, United Arab Emirates, 2022
13. Prahani BK, Alfin J, Fuad AZ, Saphira HV, Hariyono E, Suprpto N (2022) Learning management system (LMS) research during 1991–2021: how technology affects education. *Int J Emerg Technol Learn (iJET)* 17(17):2022
14. Bansah A, Agyei D (2022) Perceived convenience, usefulness, effectiveness and user acceptance of information technology: evaluating students' experiences of a learning management system. *Technol, Pedagog Educ*
15. Kwon S, Kim W, Bae C et al (2021) The identity changes in online learning and teaching: instructors, learners, and learning management systems. *Int J Educ Technol High Educ* 18:67
16. Goh TT, Yang B (2021) The role of e-engagement and flow on the continuance with a learning management system in a blended learning environment. *Int J Educ Technol High Educ* 18:49
17. Nguyen N-T (2021) A study on satisfaction of users towards learning management system at International University – Vietnam National University HCMC. *Asia Pac Manag Rev* 26(4)

18. Surameery NMS, Shakor MY (2021) CBES: cloud based learning management system for educational institutions. In: 2021 3rd East Indonesia conference on computer and information technology (EIconCIT), Surabaya, Indonesia, 2021
19. Awan RK, Afshan G, Memon AB (2021) Adoption of E-learning at higher education institutions: a systematic literature review. *Multidiscip J Educ Soc Technol Sci*
20. Reid L (2019) Learning management systems: the game changer for traditional teaching and learning at adult and higher education institutions
21. Maragatham G, Balaji SNA, SaiKarthikeyan K, Gokulakrishnan V, Siddharth M (2018) A study on performance analysis for different wordpress and hand code webpages. In: 2018 international conference on smart systems and inventive technology (ICSSIT), Tirunelveli, India
22. Pardamean B, Suparyanto T, Cenggoro TW, Sudigyo D, Anugrahana A, Anugraheni I (2021) Model of learning management system based on artificial intelligence in team-based learning framework. In: 2021 International conference on information management and technology (ICIMTech), Jakarta, Indonesia, 2021
23. Llamas M, Caeiro M, Castro M, Plaza I, Tovar E (2011) Use of LMS functionalities in engineering education. In: 2011 frontiers in education conference (FIE), Rapid City, SD, USA

# Design and Implementation of Seven-Level Reduced Switch Count Multilevel Inverter for Electric Vehicle Applications



Murugesan Manivel, Lakshmi Kaliappan, Lakshmanan Palani,  
and Sivaranjani Subramani

**Abstract** This article introduces a novel workup of a multilevel inverter which can be used for electric vehicles. This multilevel inverter is implemented with seven number of power switches and two asymmetrical sources. The most common modulation technique used in multilevel inverters is pulse width modulation and sinusoidal pulse width modulation is used in this multilevel inverter to eliminate harmful low-order harmonics. In this multilevel inverter, seven switches are used to get the desired output voltage and current waveforms at seven levels. In conventional multilevel inverters, more number of power components are used to obtain seven-level output waveform, which increases harmonic distortion as well as switching losses and cost. This usage of seven switches in the proposed inverter significantly minimizes switching costs, low-order harmonics, and switching losses, thereby reducing total harmonic distortions.

**Keywords** Total Harmonic Distortion (THD) · Pulse Width Modulation (PWM) · Direct Current (DC) · Multilevel Inverter (MLI)

---

M. Manivel (✉)

Department of EEE, Karpagam Institute of Technology, Coimbatore, Tamil Nadu, India  
e-mail: [murugesan.kec@gmail.com](mailto:murugesan.kec@gmail.com)

L. Kaliappan

Department of EEE, K.S.R. College of Engineering, Tiruchengode, Tamil Nadu, India

L. Palani

Department of EEE, Narasaraopeta Engineering College, Andhra Pradesh, India

S. Subramani

Department of EEE, Sri Krishna College of Engineering and Technology, Coimbatore, Tamil Nadu, India

## 1 Introduction

Rodriguez et al. [1], presented that Multilevel Inverters (MLI) are now widely used in a variety of power applications including electric vehicles, photovoltaic systems, small power loads, and grid-integrated systems as given by Ravanan et al. [2] and Manjrekar et al. [3]. It is more appealing due to its extremely low harmonic distortion, small installation footprint, lack of filters, low number of drivers, decreased voltage stress, and switching losses as given by Rodriguez et al. [4] and Poorfakhraei [5]. Peng et al. [6], Tolbert et al. [7], Tolbert et al. [8], and Corzine et al. [9] proposed low-power applications, a brand-new multilayer inverter with single DC source is offered. MLI is broadly categorized into flying capacitor, neutral point clamped (NPC), and cascaded H Bridge topologies. Recently, cascaded multilayer inverters have been used in hybrid systems. The output voltage produced by the suggested inverter is eight times greater than the input voltage, examining different MLI configurations in terms of switching device count and modulation methods as given by Fracchia et al. [10]. There are numerous topologies available to build stepped voltages with higher levels and fewer power elements. It has been noted that as the voltage levels increase, the harmonic content exists in the load voltage and current waveforms decreases as mentioned in Corzine et al. [11] and Peng [12]. The overall harmonic distortion for resistive and resist-inductive loads is examined for the proposed inverter. Majumdar et al. [13], Barzegarkhoo et al. [14] and Zhao [15] proposed several equal and unequal DC sources hybrid MLI topologies were created using different counts of power elements, used in the inverter circuits are diodes and capacitors. Moreover, an analysis of the total standing voltages and THD generation of all setups is done. All topologies have a few flaws, including switch count, voltage imbalance, and number of DC sources as given by Patel and Hoft [16]. Dhanamjayulu et al. [17] proposed a reduced switch count structure and it was analyzed for several PWM techniques. Two new MLI structures have been designed by Meraj et al. [18] and it was connected to the PV system. Hamidi et al. [19] proposed a MLI structure with less number of power switches and produced nine levels of output. Das et al. [20] proposed a 3-level active NPC-MLI for electric traction drive applications. A symmetrical and asymmetrical reduced switch count multilevel inverter is proposed by Sivamani and Mohan [21].

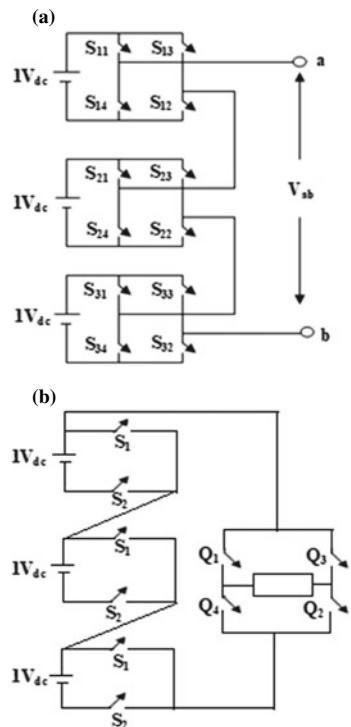
The proposed configuration involves only seven numbers of power components to produce seven levels in the output voltage or current. Moreover, a method is proposed to calculate the required DC voltage source with magnitude to generate all levels of output voltages. This structure uses sinusoidal PWM technique where total harmonic distortion is significantly reduced by seven levels. It reduces price, weight, and complexity while delivering exceptional output voltage with low THD, suitable for EVs.

## 2 Cascaded H-bridge Multilevel Inverter

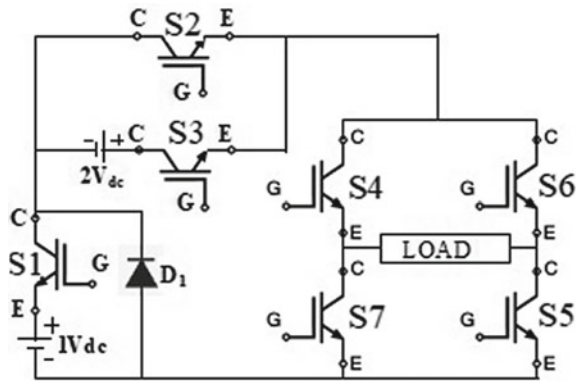
Figure 1 depicts the configuration of existing MLIs. Each cell requires a separate symmetrical voltage source (A1, A2, A3) connected in series to create more levels. The first configuration contains 12 number of power components that generate seven levels of output voltage or current. There are three H-bridges involved in this structure, it was proposed by Rodriguez et al.. Peng presented a configuration that requires ten components to produce the same seven-stage output. In this configuration, there are three cells, each cell has one DC source and two power switches, giving a multi-stage unidirectional output. To produce positive and negative half-cycle waveforms in the output H-bridge circuit is used before connecting to the load [12]. The major problem of these cascaded MLIs are usage of more power switches. The “S” DC sources and the related output levels can be obtained by using this equation:

$$N_{\text{level}} = 2S + 1 \tag{1}$$

**Fig. 1** Topology of  
**a** Cascaded H-bridge MLI.  
**b** New Cascaded MLI



**Fig. 2** Proposed multilevel inverter



### 3 Cascaded H-bridge Multilevel Inverter

The assembly of the proposed MLI is shown in Fig. 2. There are two single-ended voltage sources which are connected to seven number of switches. Three power switches are in the circuit producing a DC seven-level output and the other four are for producing an AC output waveform. From this diagram, when  $S_1$  and  $S_2$  are turned on, the load voltage is  $+1V_{dc}$ , and when  $S_3$  alone is turned on, it produces  $+2V_{dc}$ . To acquire  $+3V_{dc}$ , switches  $S_1$  and  $S_3$  are turned on. Figure 3 shows the mode of operation proposed, multi-level inverter to produce a positive half-cycle and Fig. 4 shows the operation of a multi-level inverter producing a negative half-cycle. Table 1 shows the suggested multi-level inverter operation. The major merit of this structure is to obtain seven levels with seven power switches and two DC sources. The “S” DC sources and the associated output levels can be obtained by equation

$$N_{level} = 2^{S+1} - 1 \tag{2}$$

For example, if  $S = 2$ , the output waveform has seven levels ( $\pm 3, \pm 2, \pm 1$ , and 0).

### 4 PWM for Harmonics Reduction

The PWM method is most widely utilized to eliminate destructive low-order harmonics in MLIs [15]. In PWM control, devices are put on and off continuously for positive and negative half-cycles, the output is varied by varying the pulse widths [14]. Sinusoidal PWM is a widely used control technique in inverter circuits. It has merits such as lower switching losses, fewer harmonics in the output voltage, and it is a simple method of contrivance. The sinusoidal PWM is calculated by constant magnitude pulses with various values of duty cycle for each cycle. The harmonics content is reduced by this PWM method and also output voltages are varied by this



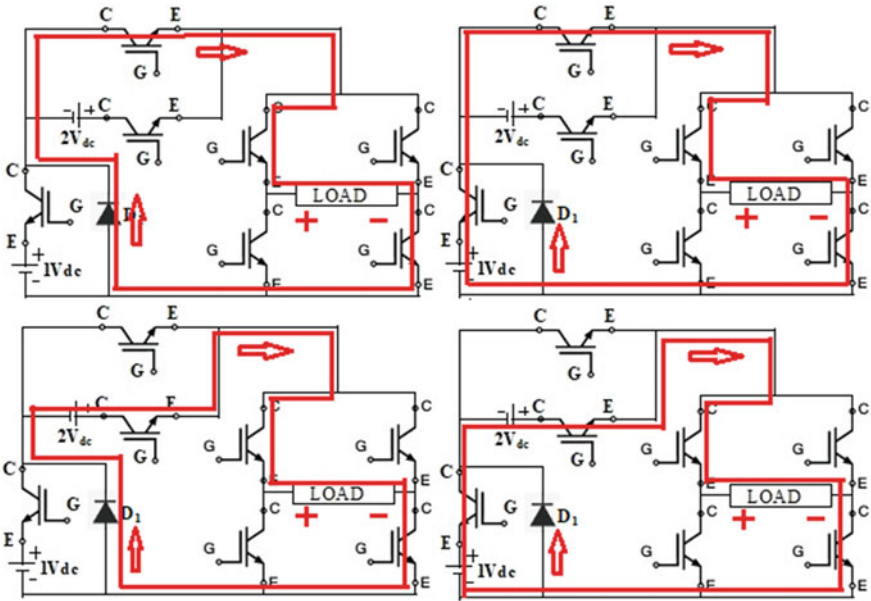


Fig. 3 Operation of proposed seven-level MLI for producing positive half-cycle

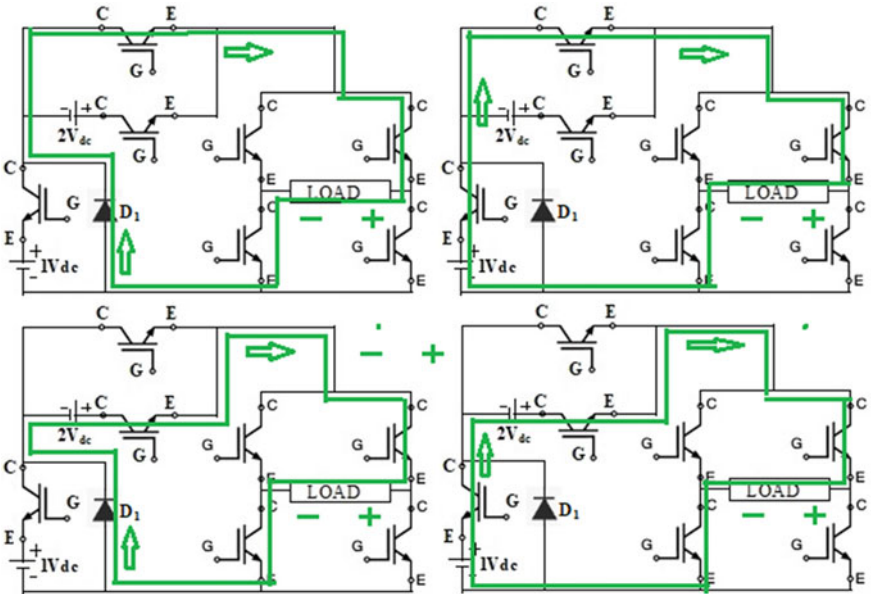


Fig. 4 Operation of proposed seven-level MLI for producing negative half-cycle

**Table 1** Switching pattern of proposed multilevel inverter

S. no.	Mode	S <sub>1</sub>	S <sub>2</sub>	S <sub>3</sub>	S <sub>4</sub>	S <sub>6</sub>	S <sub>5</sub>	S <sub>7</sub>	Output Voltage (V)	
1	Positive half cycle	I	0	1	0	1	0	1	0 V	
2		II	1	1	0	1	0	1	1V <sub>dc</sub>	
3		III	0	0	1	1	0	1	2V <sub>dc</sub>	
4		IV	1	0	1	1	0	1	1V <sub>dc</sub> +2V <sub>dc</sub>	
5		V	1	0	1	1	0	1	1V <sub>dc</sub> +2V <sub>dc</sub>	
6		VI	0	0	1	1	0	1	2V <sub>dc</sub>	
7		VII	1	1	0	1	0	1	1V <sub>dc</sub>	
8		VIII	0	1	0	1	0	1	0 V	
9	Negative half cycle	XIV	0	1	0	0	1	0	1	0 V
10		XV	1	1	0	0	1	0	1	1V <sub>dc</sub>
11		XVI	0	0	1	0	1	0	1	2V <sub>dc</sub>
12		XVII	1	0	1	0	1	0	1	1V <sub>dc</sub> +2V <sub>dc</sub>
13		XVIII	1	0	1	0	1	0	1	1V <sub>dc</sub> +2V <sub>dc</sub>
14		XIX	0	0	1	0	1	0	1	2V <sub>dc</sub>
15		XX	1	1	0	0	1	0	1	1V <sub>dc</sub>
16		XXI	0	1	0	0	1	0	1	0 V

method. Sinusoidal PWM is the most widely utilized method in inverter-fed electric drive-controlled applications [14, 15]. The performance of the proposed multistage inverter at the required output with amplitude and reduced harmonic content, an SPWM is programmed and used to obtain the required switching angles. It has been shown that to control the output voltage and remove “n” harmonics, the “n + 1” equation is meticulous. The techniques of removing lower order harmonics are presented for the seven-level inverter. Solutions for three different angles were obtained. Extend the Fourier series of the output voltage using a frequency conversion scheme as follows:

$$V_o(\omega t) = \sum_{n=1,3,5}^{\infty} \frac{4V_{dc}}{n\pi} (\cos(n\theta_1)) + \cos(n\theta_2) + \dots + \cos(n\theta_M)) \sin(n\omega t) \quad (3)$$

where “M” is the switching angles required for the seven-level. Ideally, for a given voltage V<sub>1</sub>, it is necessary to get the switching angles θ<sub>1</sub>, θ<sub>2</sub>, ..., θ<sub>K</sub> so that output V<sub>o</sub>(ω t) = V<sub>1</sub>sin(ω t) and a specific higher harmonics of V<sub>n</sub>(n ω t) are zero. The switching angles can be solved using the following equations:

$$\cos(\theta_1) + \cos(\theta_2) + \cos(\theta_3) + \cos(\theta_4) + \cos(\theta_5) + \cos(\theta_6) = m$$

$$\cos(5\theta_1) + \cos(5\theta_2) + \cos(5\theta_3) + \cos(5\theta_4) + \cos(5\theta_5) + \cos(5\theta_6) = 0$$

$$\cos(7\theta_1) + \cos(7\theta_2) + \cos(7\theta_3) + \cos(7\theta_4) + \cos(7\theta_5) + \cos(7\theta_6) = 0 \quad (4)$$

where modulation index,  $m = \frac{V_1}{(\frac{4V_{dc}}{\pi})}$

$\theta_1 = 6.57^\circ$ ,  $\theta_2 = 18.94^\circ$ ,  $\theta_3 = 27.18^\circ$  this indicates that power switches are put to use in the positive half-cycle for  $+1V_{dc}$  at  $6.57^\circ$ ,  $+2V_{dc}$  at  $18.94^\circ$ ,  $+3V_{dc}$  at  $27.18^\circ$ , similarly in the negative half-cycle to  $-V_{dc}$  at  $186.57^\circ$ ,  $-2V_{dc}$  at  $198.94^\circ$ , and  $-3V_{dc}$  at  $207.18$ . The output of the seven-level inverter will not contain the 5th, 7th-, and 11th-order harmonics. Newton–Raphson method with iteration is used to solve the set of nonlinear equations[11]. Unlike the iterative method, the approach at present is created on solving polynomial equations using resultant theory yielding all possible solutions[12]. The transcendental equation that characterizes the harmonic components can be changed into a polynomial equation. The resulting technique is then used to compute solutions as they exist. These solution sets need to be checked for their respective THD to select the solution set that produces the lowest order harmonics (mainly due to the 5th, 7th, and 11th harmonics). THD is calculated as a percentage determined by

$$THD\% = \frac{\sqrt{V_3^2 + V_5^2 + V_7^2 + \dots + V_{19}^2}}{V_1^2} \times 100 \quad (5)$$

## 5 Results and Discussions

The performance of the proposed seven-level inverter is verified through MAT Lab simulation for resistive load. The total single-phase peak voltage is 210 V for seven levels. Figure 5 shows the switching schemes for switches  $S_1$ ,  $S_2$ , and  $S_3$ , and similarly, Fig. 6 shows the switches pulses of switches  $S_4$ ,  $S_5$ ,  $S_6$ , and  $S_7$ .

Figure 7 shows the output voltage waveform for seven levels. This figure clearly shows that the output is a stepped seven-level waveform that looks almost sinusoidal. From the output voltage waveform, any filter arrangement is not needed to smoothen the waveform further.

According to Fig. 8, the THD value of a seven-level inverter is 10.30%. When compared to the other two conventional inverters listed in Table 2, the total harmonics distortion is reduced.

Simulation results are validated by hardware setup. MOSFETs are used as switching devices in a prototype of 210 V, single-phase, seven-level suggested architecture. The inverter is made up of seven MOSFET switches. IRF840 MOSFETs are employed in the hardware setup. The gate signal for inverter switches is generated

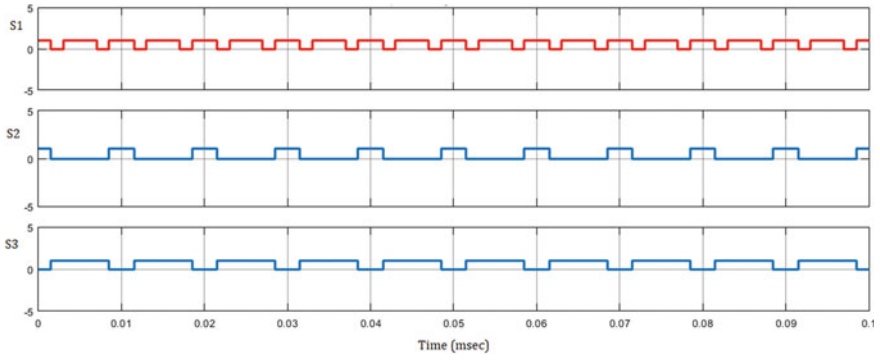


Fig. 5 Switching pulses of  $S_1$ ,  $S_2$ , and  $S_3$

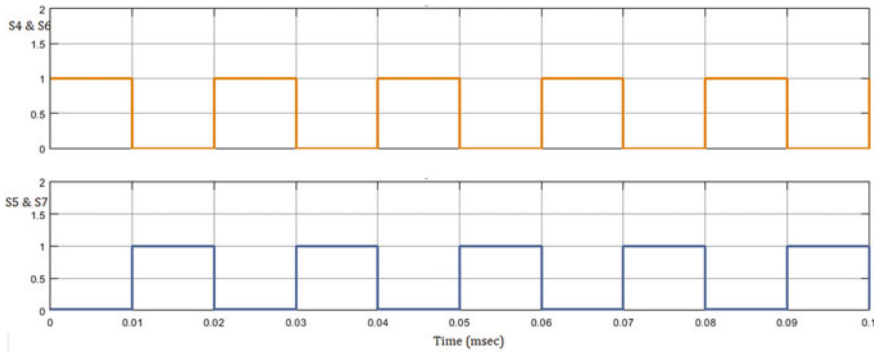


Fig. 6 Switching pulses of  $S_4$ ,  $S_5$ ,  $S_6$ , and  $S_7$

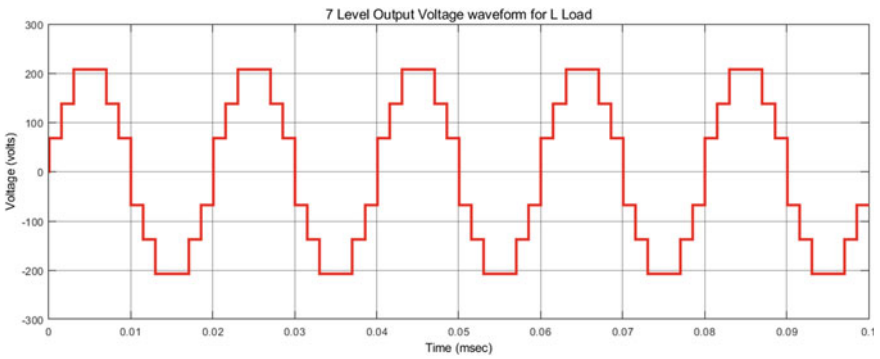


Fig. 7 Single-phase output voltage waveform for seven levels

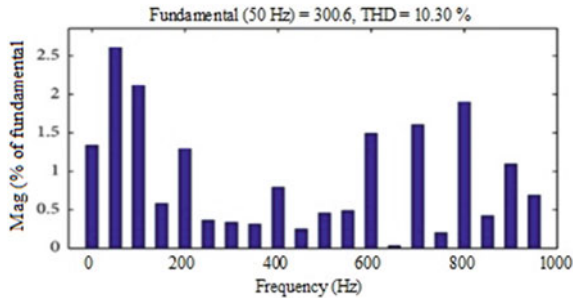


Fig. 8 FFT analysis of proposed MLI

Table 2 Performance comparison of conventional and proposed MLI

S. no.	Structure	THD (%)	Switches needed
1	Cascaded H-Bridge MLI	12.39	12
2	New Cascaded MLI	11.34	10
3	Proposed MLI	10.30	7

by Arduino micro controller. In the input side of the proposed seven-level inverter, two asymmetric DC sources, 140 V and 70 V, are deployed. The suggested inverter outputs are verified by a resistive load (3 K-50w) and Resistive-Inductive (RL) load. Figure 9 shows the hardware output voltage for RL load. From the above figure, it clearly depicts that the output voltage waveform is almost sinusoidal in nature. So, it can be easily utilized to drive a motor of electric vehicle. From this analysis, we find as the number of levels increases, the harmonics and THD will decrease. Table 2 a comparison of THD and number of switches used for seven levels of existing and recommended multistage inverters is shown. Figure 10 shows a comparison of the THDs of different multi-level inverters. From the analysis, cascaded MLI needs 12 switches to produce 7 levels with THD of 12.39%. New cascaded MLI requires 10 switches to produce same seven levels with THD of 11.34%. The proposed topology needs only seven switches and also produces less THD of 10.30% for producing seven levels.

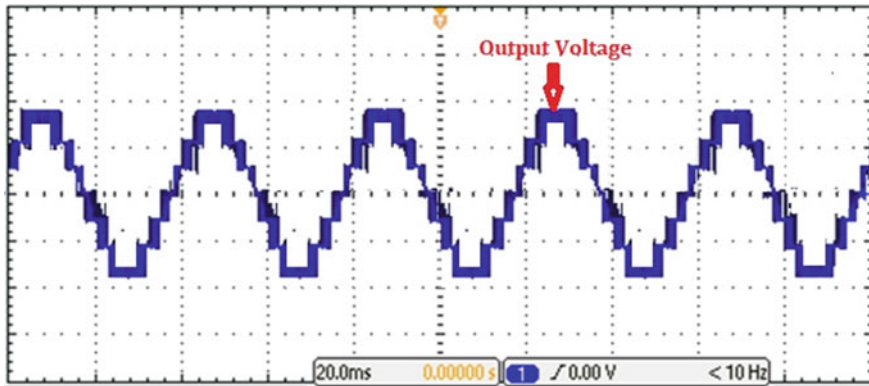
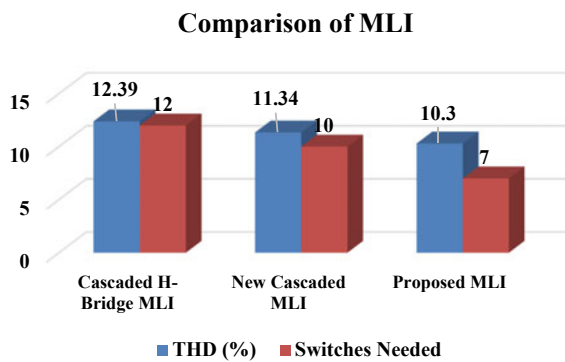


Fig. 9 Experimental output voltage and current waveform for R load

Fig. 10 Comparison of THD of different MLIs



## 6 Conclusion

This article presented a novel multi-level inverter with decreased power components. This multi-level inverter’s circuit and its operations have been conversed. The method for calculation of the needed level of output with respect to the power switches required is also discussed. In the classical structure, when the number of output levels increase, the number of power components also increases. Due to the use of more power switches, harmonics, switch losses, costs, and THD increase. The proposed structure considerably reduces the power semiconductor switches to seven for seven-level output and total harmonics distortion is also less than 10.30% for seven levels. Due to the reduced number of devices, the overall complexity and cost of multi-level inverters are also reduced. Hence, this proposed structure produces a sinusoidal current waveform for RL load which is the most suitable for electric vehicle applications.

## References

1. Rodriguez J, Lai JS, Peng FZ (2002) Multilevel inverters: a survey of topologies, controls and applications. *IEEE Trans Ind Electron* 49(4):724–738
2. Ravanan SD, Arivukannu S, Tankappan P, Muthiah R (2022) Harmonic performance analysis of a wind driven micro grid inverter. *Int J Ambient Energy* 43(1):3497–3506
3. Manjrekar MD, Steimer PK, Lipo T A (2020) Hybrid multilevel power conversion system: a competitive solution for high-power applications. *IEEE Trans Ind Appl* 36(3):834–841
4. Rodriguez J, Bernet SP, Steimer K, Lizama IE (2010) A survey on neutral-point-clamped inverters. *IEEE Trans Ind Electron* 57(7):2219–2230
5. Poorfakhraei A, Narimani M, Emadi A (2021) A review of multilevel inverter topologies in electric vehicles: current status and future trends. *IEEE Open J Power Electron* 2:155–171
6. Peng FZ, McKeever JW, Adams DJ (1998) A power line conditioner using cascade multilevel inverters for distribution systems. *IEEE Trans Ind Appl* 34(6):1293–1298
7. Tolbert LM, Peng FZ, Habetler TG (1998) Multilevel inverters for electric vehicle applications. *Proc Power Electron Trans* 79–84
8. Tolbert LM, Peng FZ (1999) Multilevel converters for large electric drives. *IEEE Trans Ind Appl* 35(1):36–34
9. Corzine KA, Wielebski MW, Peng FZ, Wang J (2004) Control of cascaded multilevel inverters. *IEEE Trans Power Electron* 19(3):732–738
10. Fracchia M, Ghiara T, Marchesoni M, Mazzucchelli M (1992) Optimized modulation techniques for the generalized N-level converter. In: *Proceedings of. IEEE power electronics specialist conference*, pp 1205–1213
11. Corzine KA, Baker JR (2002) Reduced parts-count multilevel rectifiers. *IEEE Trans Ind Electron* 49(3):766–774
12. Peng FZ (2004) A generalized multilevel inverter topology with self voltage balancing. *IEEE Trans Ind Appl* 37:611–618
13. Majumdar S, Jana KC, Pal PK, Sangwongwanich A, Blaabjerg F (2022) Design and implementation of a single source 17-level inverter for a single-phase transformer-less grid-connected photovoltaic systems. *IEEE J Emerg Sel Top Power Electron* 10(4):4469–4485
14. Barzegarkhoo, Forouzesh M, Lee SS, Blaabjerg F, Siwakoti YP (2022) Switched-capacitor multilevel inverters: a comprehensive review. *IEEE Trans Power Electron* 37(9):11209–11243
15. Zhao J (2010) A novel PWM control method for hybrid-clamped multilevel inverters. *IEEE Trans Ind Electron* 57(7)
16. Patel HS, Hoft RG (1973) Generalized techniques of harmonic elimination and voltage control in thyristor inverters: part I - harmonic elimination. *IEEE Trans Ind Appl* 3:310–317
17. Dhanamjayulu C, Arunkumar G, Jaganatha Pandian B, Padmanaban S (2020) Design and implementation of a novel asymmetrical multilevel inverter optimal hardware components. *Int Trans Electron Energy Syst* 30(2):e12201
18. Meraj ST, Hasan K, Masaoud A (2019) A novel configuration of cross-switched T-type (CT-type) multilevel inverter. *IEEE Trans Power Electron* 35(4):3688–3696
19. Hamidi MN, Ishak D, Zainuri MAAM, Ooi CA (2020) Multilevel inverter with improved basic unit structure for symmetric and asymmetric source configuration. *IET Power Electron* 13(7):1445–1455
20. Das PP, Satpathy S, Bhattacharya S, Veliadis V (2022) Design considerations of multi-phase multilevel inverters for high-power density traction drive applications. In: *IEEE transportation electrification conference and Expo (ITEC)*
21. Sivamani S, Mohan V (2022) A three-phase reduced switch count multilevel inverter topology. *Int Trans Electr Energy Syst* 1–16

# Ultrasound Image Classification and Follicle Segmentation for the Diagnosis of Polycystic Ovary Syndrome



Jojo James , Sabeen Govind , and Jijo Francis 

**Abstract** PCOS is a prevalent hormonal disorder that impacts women in the reproductive age bracket. Timely and accurate diagnosis of PCOS is crucial for the proper treatment. To diagnose the presence of PCOS, ultrasound images of the ovaries are widely used by the physicians. Automated detection of PCOS shall reduce the risk of making errors. This study seeks to propose a machine learning classification technique for PCOS detection and to mark the cysts on the ovary using image segmentation. Convolution Neural Network (CNN) architectures such as Inception V3, VGG16, and ResNet are used for classifying images. The model is trained over 781 ovary ultrasound images to distinguish between PCOS and non-PCOS cases. Among the three models used VGG16 model comes with better accuracy. The results of this study show that this approach is effective in detecting PCOS with high accuracy.

**Keywords** Polycystic ovary syndrome · Follicle · Classification · Segmentation · Annotation · Ultrasound images

## 1 Introduction

Polycystic Ovary Syndrome (PCOS) is a disorder that affects many women in their reproductive age; i.e., this can occur at any stage between menarche and menopause [1]. PCOS can lead to the formation of multiple cysts in the ovaries [2]. Eventually, PCOS can possibly lead to many other health issues: cardiovascular diseases [3], pregnancy complications [4], infertility [5], hormonal imbalance, etc. Obesity, lifestyle, genetics, and neuroendocrine are instrumental in the existence of PCOD

---

J. James (✉) · S. Govind  
Rajagiri College of Social Sciences (Autonomous), Kalamassery, Kerala, India  
e-mail: [jojojames17@gmail.com](mailto:jojojames17@gmail.com)

J. Francis  
Jubilee Centre for Medical Research, Jubilee Mission Medical College and Research Institute,  
Thrissur, Kerala, India



[6]. Early and accurate diagnosis of PCOS is essential for proper management and treatment. However, traditional diagnostic methods such as clinical examination and blood tests can be time-consuming and often inconclusive.

The diagnosis of PCOS is usually made through clinical examination and the measurement of hormone levels. However, the physicians also commonly use ultrasound images of the ovaries of the patients to find out the presence of follicular cysts to diagnose the existence of PCOS [7]. Ultrasound images provide direct visual evidence of the presence of cysts in the ovaries and can help in the early detection of PCOS.

In recent years, there has been growing interest in using computer-aided methods for the analysis of ultrasound images for the diagnosis of PCOS. These methods can automate the process of image analysis, reduce the need for human intervention, and increase the accuracy of diagnosis.

## 2 Literature Review

There have been several studies and works related to PCOS detection using ultrasound images:

Rachana et al. [8] described how we can detect the PCOS using follicle recognition. The intention was to diagnose PCOS at beginning stage by decreasing the time taken to find the follicles and the size of the same. The established model could give the accuracy which is greater than 97%. KNN classifier gave this accuracy. They found that the time taken to diagnose PCOS and the accuracy of the model could be improved.

In 2021, Gopikrishnan et al. [9], has done a study to detect PCOS using ultrasound images. They used the classification system using supervised machine learning algorithms to classify the images into affected and unaffected ones. They made use of a Gaussian filter to do the pre-processing, proceeding to image segmentation and PCOS classification. As a result of the study, they have put forward a computer-aided automated system to diagnose PCOS. They claim an accuracy of 93.82% using a support vector machine.

Kiruthika et al. [10] have also done a study to detect the ovaries with PCOS by ultrasound images. They used the artificial neural network to develop this automated ovarian classification system. This was a system to help the physician to measure the follicle. This system claimed an accuracy of 96%.

So, there is evidence to support the use of ultrasound images in the prediction of PCOS. Studies have shown that ultrasound imaging can accurately detect the presence of multiple cysts in the ovaries. Machine learning techniques have shown promising results in improving the accuracy of PCOS prediction, and further research in this area may lead to more efficient and effective diagnostic tools.

However, it should be noted that ultrasound imaging is not a definitive diagnostic tool for PCOS and should be combined with other clinical and laboratory findings to

confirm the diagnosis [11]. Other factors such as age, body mass index (BMI), and hormonal imbalances can also affect the interpretation of ultrasound images [12].

### 3 Methodology

In this study the PCOS and non—PCOS ovaries are classified using Convolution Neural Network (CNN) architecture. Ultrasound images of the ovaries are given as input to check whether the images indicate PCOS. The stages involved in this study are depicted in Fig. 1 and briefly discussed below:

In the data acquisition and pre-processing step, the images are obtained and prepared for the process by normalizing and transforming to be suitable for training the model. Data augmentation increases the size of the training set by creating new images from the existing ones, for example by rotating, flipping, or zooming in on the images.

In the model definition and training step, the architecture of the model is defined and trained it on the augmented data. The objective of training is to find the best set of weights for the model so that it accurately classifies the images into infected or non-infected categories.

In the classification step, the trained model is used to make predictions on new, unseen images. The output of this step is the class prediction for each image, indicating whether it's infected or non-infected. Then the model evaluation is done to assess the performance of the models and identify any potential issues or areas for improvement.

The annotation step is performed after the classification step. If the image is classified as infected, the follicles are then annotated to provide additional information

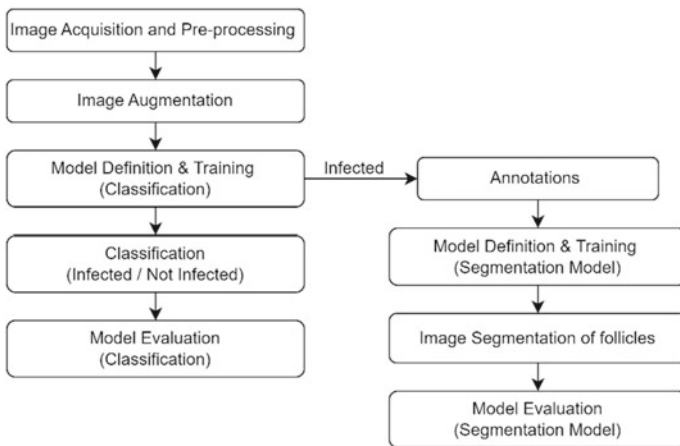


Fig. 1 Block diagram

for the image segmentation step. This step could be useful for medical analysis and understanding the progression of the infection.

Here are the steps involved in analyzing ultrasound images of ovaries for the purpose of diagnosing polycystic ovary syndrome in this study:

1. Load dataset of ultrasound images of ovaries
2. Split dataset into train, validation, and test sets
3. Pre-process data
  - a. Rescale pixel values to be between 0 and 1
  - b. Apply data augmentation techniques (e.g., rotation, shear, zoom)
4. Define a CNN model for classifying images into infected or non-infected of PCOS
5. Train CNN model on train set
  - a. Set number of epochs
  - b. Define optimizer (e.g., Adam)
  - c. Define loss function (e.g., categorical cross-entropy)
  - d. Monitor validation loss and accuracy
6. Evaluate trained CNN model on test set
  - a. Report test loss and accuracy
7. For infected images, define a segmentation model to highlight follicles on the image
8. Apply segmentation model to infected images in the test set
  - a. Visualize highlighted follicles
9. Save trained models for future use

### ***3.1 Image Acquisition and Pre-Processing***

The ultrasound images of the ovaries are used as the input here. The dataset, which is entitled “PCOS Detection using Ultrasound Images”, is taken from *Kaggle* [13]. This dataset contains 781 ultrasonic images of ovaries that are infected and 1143 images that are non-infected with PCOS.

Neural networks are designed to work with numerical data, and having a consistent range of values for the input data is important for good performance. So rescaling is implemented here to bring the pixel values in the range [0, 1].

### 3.2 Deep Learning Technique

After having done the above stages, a deep learning technique with CNN is performed. Three pre-trained models in the CNN are used in this study: InceptionV3, VGG16, and ResNet. A convolutional neural network (CNN) is composed of multiple layers that perform different tasks in processing the input image data. The following are the steps involved in the process of each layer in a CNN: [14, 15].

1. Convolution Layer: The convolution layer performs a dot product between the filters and small regions of the input image. The filters are trained to detect specific features of the input image. This step produces a set of feature maps that capture different aspects of the input image.
2. Pooling Layer: The pooling layer reduces the spatial size of the feature maps produced by the convolution layer, by taking the maximum or average of the values in a given region. This step helps to reduce the computational cost and helps to handle overfitting.
3. Fully Connected Layer: The fully connected layer takes the output of the previous layer and performs a dot product with a set of weights. The output of this layer is a set of values representing the predicted class of the input image.

In this study, a binary classification task was tackled using a Convolutional Neural Network (CNN) model. The model was trained using the “binary cross-entropy” loss function and “Adam” optimizer [16], with the accuracy of each classifier per epoch being the primary evaluation metric. The deep learning approach was trained for 30 epochs using the input images and was capable of providing a categorization output. The internal neural network within the model was designed to automatically extract relevant features from the input images for effective classification.

### 3.3 Performance Analysis

The effectiveness of the predictive models was determined using various performance metrics, such as accuracy, precision, and recall on the test data [17].

$$\text{Accuracy} = \frac{TP + TN}{TP + FN + TN + FP} \quad (1)$$

$$\text{Precision} = \frac{TP}{FP + TP} \quad (2)$$

$$\text{Recall} = \frac{TP}{FP + TP} \quad (3)$$

where

TP (True Positive): A true positive is an instance where the model correctly classifies an image as infected and the ground truth label for that image is also infected.

TN (True Negative): A true negative is an instance where the model correctly classifies an image as non-infected and the ground truth label for that image is also non-infected.

FP (False Positive): A false positive is an instance where the model classifies an image as infected, but the ground truth label for that image is actually non-infected.

FN (False Negative): A false negative is an instance where the model classifies an image as non-infected, but the ground truth label for that image is actually infected.

### 3.3.1 Annotating

Annotating follicles on the ultrasound images of the ovaries is the process of manually marking the location and size of each follicle in each image. The process of annotating [18] follicles can be time-consuming and requires a high degree of expertise, but it is critical for training machine learning models to accurately detect follicles [19].

Here, VGG Image Annotator is used to annotate the follicle on the image. The annotations will be saved in a CSV file, which will then be used to generate masks for the infected images. These masks will highlight the regions of the image corresponding to the follicles, which can then be visualized and used for further analysis.

Here's a detailed process for annotating ultrasound images using the VGG Image Annotator (VIA) and generating masks to highlight the follicles:

1. Install the VGG Image Annotator (VIA) software and launch it.
2. Import the ultrasound images into VIA.
3. Annotate each image by drawing a polygon around each follicle in the image.
4. Export the annotations as a CSV file.
5. Write a Python script to convert the CSV annotations into binary masks for each follicle as in Fig. 2.
6. Load the ultrasound images and their corresponding masks into the segmentation model.
7. Use the segmentation model to generate highlighted masks that emphasize the follicles.
8. Overlay the highlighted masks on the original ultrasound images to visualize the highlighted follicles.
9. Save the highlighted images for future use.

This study involves the development of a user-friendly front-end interface for the detection of PCOS in ultrasound images. The interface allows users to upload ultrasound images and get a prediction on whether the image is infected or not. If the image is infected, the front-end also incorporates a segmentation model to highlight the follicles on the ovarian ultrasound image.

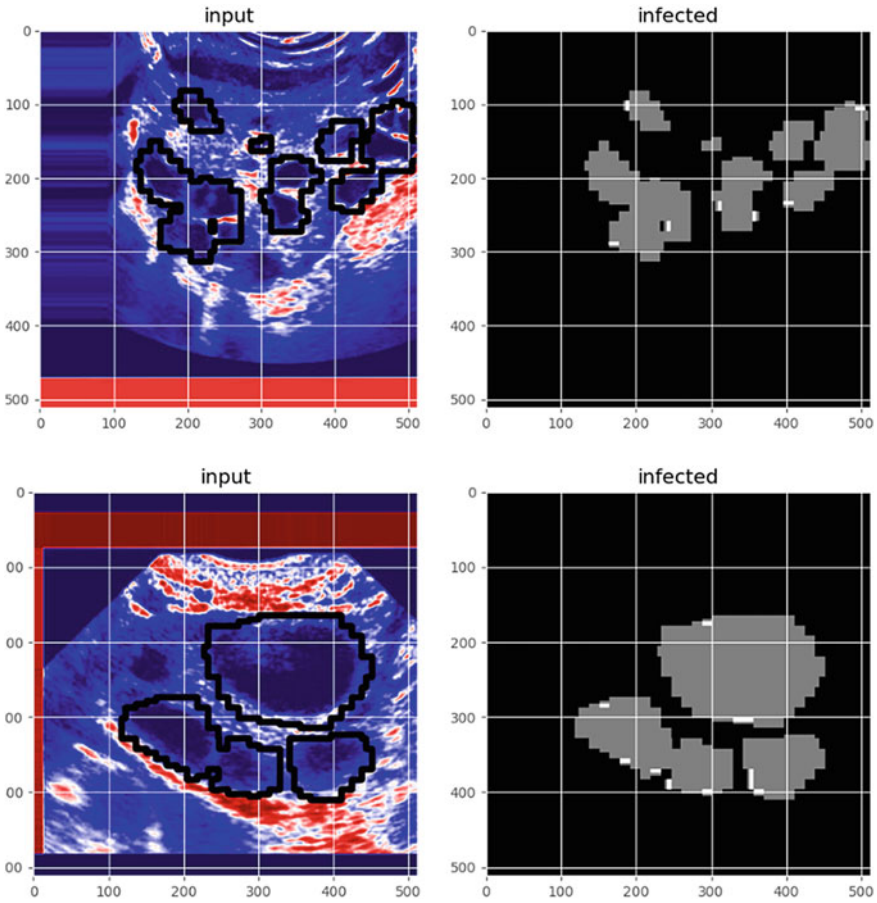


Fig. 2 Masking of the ovary images

## 4 Results and Discussions

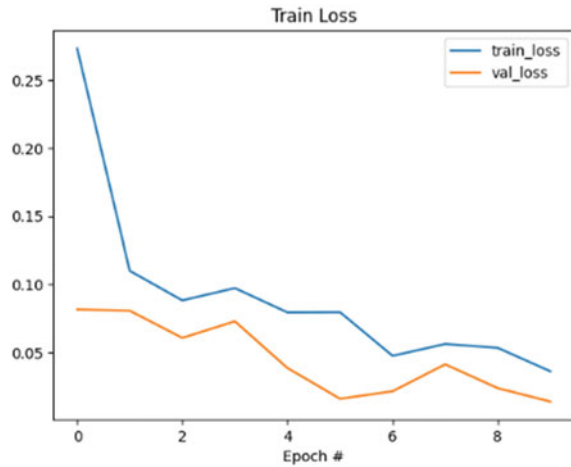
### 4.1 Classification

The classification of the ultrasound images of the ovaries has been performed on the dataset with great accuracy. Table 1 and the training and validation loss curves in Fig. 3 show the result.

The blue line represents the training loss, which measures how well the model is fitting the training data. As the model learns and adjusts its parameters, the training loss should decrease over time. The orange line represents the validation loss, which measures how well the model is generalizing to new, unseen data. During training, a small portion of the data is held back as a validation set, and the model’s performance

**Table 1** Accuracy of the models

Models	Accuracy
InceptionV3	0.9870
VGG16	0.9967
ResNet	0.9792

**Fig. 3** Training and validation loss

on this set is evaluated periodically. The validation loss should ideally decrease during the initial epochs. The loss values on the y-axis represent the error or cost of the model's predictions. Lower values indicate better performance. By monitoring the loss curves during training, you can get an idea of how well the model is learning and whether it is overfitting or underfitting the data.

## 4.2 Segmentation

The infected ovary images are further undergone image segmentation to identify the follicles on the ovaries as given in Fig. 4. The loss curve is also given in Fig. 5.

## 5 Conclusions and Future Perspectives

Recent advances in computer vision and machine learning have made it possible to use ultrasound images for automated PCOS detection [20]. In this study, a classification on the ultrasound image is done to differentiate images whether they are infected of PCOS or not. If the ovary is found infected, then image segmentation is done on

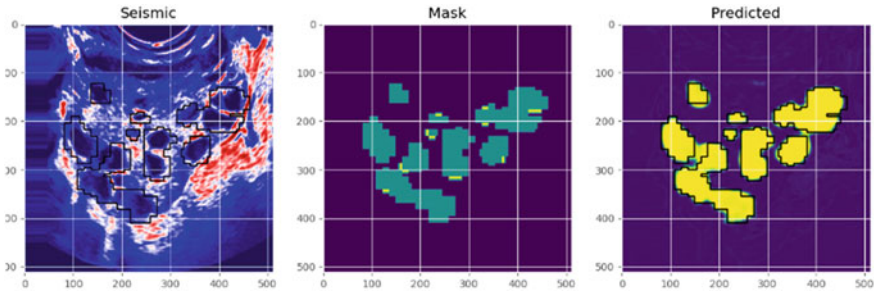
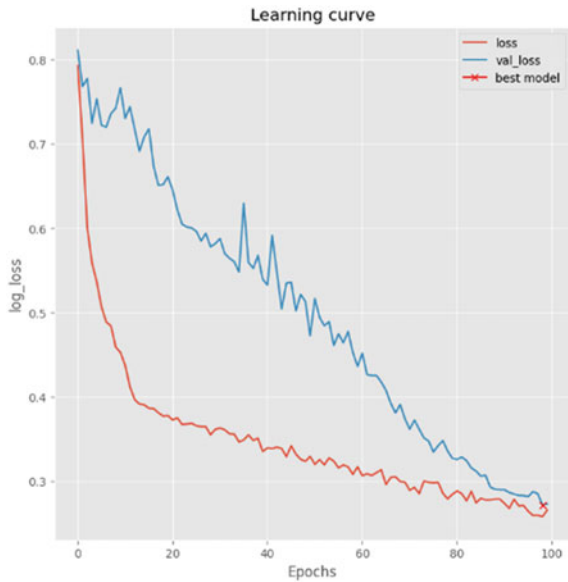


Fig. 4 Follicles on the ovaries—predicted

Fig. 5 Training and validation loss curves



the image to highlight the follicles. Highlighting follicles is important for further clinical evaluations. The result shows high accuracy on the test data. In the future, an extension of the study could be made to find the size of the follicles to diagnose the PCOS more effectively and accurately. To implement it in the real-time scenario, the machine needs to study more diverse images of the ovary to put forward more accurate result.



## References

1. Witchel S (2006) Puberty and polycystic ovary syndrome. *Mol Cell Endocrinol* 254–255:146–153
2. Suha SA, Islam MN (2022) An extended machine learning technique for polycystic ovary syndrome detection using ovary ultrasound image. *Sci Rep*
3. Dokras A (2013) Cardiovascular disease risk in women with PCOS. *Steroids* 78(8):773–776
4. Homburg R (2006) Pregnancy complications in PCOS. *Best Pract Res Clin Endocrinol Metab* 20(2):281–292
5. Brassard M, Ainmelk Y, Baillargeon J-P (2008) Basic infertility including polycystic ovary syndrome. *Med Clin North Am* 92(5):1163–1192
6. Bulsara J, Patel P, Soni A, Acharya S (2021) A review: brief insight into polycystic ovarian syndrome. In: *Endocrine and metabolic science*, vol 3
7. pulluparambil S, Bhat S (2021) Medical Image processing: detection and prediction of PCOS—a systematic literature review. *IJHSP* 80–98
8. Rachana B, Priyanka T, Sahana KN, Supritha TR, Parameshachari BD, Sunitha R (2021) Detection of polycystic ovarian syndrome using follicle recognition technique. *Glob Transit Proc* 304–308
9. Gopikrishnan C, Iyapparaja M (2021) Multilevel thresholding based follicle detection and classification. In: *SREQOM*
10. Kiruthika V, Sathiya S, Ramya M (2020) Machine learning based ovarian detection in ultrasound images. *Int J Adv Mechatron Syst* 8
11. Dumesic DA, Laven JS, Stanczyk FZ (2009) Hormonal and metabolic aspects of polycystic ovary syndrome. *Endocr Rev* 14–34
12. Franks S, Stark J, Hardy K, Willis D (2007) Polycystic ovary syndrome. *The Lancet* 685–697
13. Choudhari A (2021) PCOS detection using ultrasound images. *Kaggle*
14. Yamashita R, Nishio M, Gian Do RK (2018) Convolutional neural networks: an overview and application in radiology. *Insights Imaging* 9:611–629
15. Saha S (2018) A comprehensive guide to convolutional neural networks. *Towards Data Sci* 15 December 2018
16. Kitchell LM (2023) Loss functions and optimizers, Github, 2018. <https://kitchell.github.io/DeepLearningTutorial/7lossfunctionsoptimizers.html>. Accessed 21 Feb 2023
17. Kumar A (2023) Accuracy, precision, recall & F1-score—python examples, 14 January 2023. <https://vitalflux.com/accuracy-precision-recall-f1-score-python-example/>. Accessed 14 Feb 2023
18. Smistad E, Ostvik A, Lasse L (2021) Annotation web—an open-source web-based annotation tool for ultrasound images. In: *2021 IEEE international ultrasonics symposium (IUS)*, Xi'an, 2021
19. Krivanek A, Sonka M (1998) Ovarian ultrasound image analysis: follicle segmentation. *IEEE Trans Med Imaging*
20. Alzubaidi L (2021) Review of deep learning: concepts, CNN architectures, challenges, applications, future directions. *J Big Data*

# Twitter Data Analysis Using BERT and Graph-Based Convolution Neural Network



Anusha Danday and T. Satyanarayana Murthy 

**Abstract** Twitter Data Analysis in Social media plays an essential role in spreading information during disasters and needy situations. May it be for seeking help or sharing and updating the seriousness of the situation or communicating the status or response to the public in need, social media plays a major role in case of emergencies. This research focuses on generating word embedding vectors using DistillBERT and generating a similarity matrix to construct the Graph-based Convolution Network model to classify text sequences and to analyse the performance of the DistillBERT with GCN model in Text classification. To implement this, contextual word embeddings are introduced for generating word vectors. The contextual word embeddings and the concept of graph neural networks has gained importance in capturing contextual relationship among the text to improve the performance of classification. This semi supervised model is used to detect and classify the need and availability of resource tweets with an accuracy of 96% as compared with state-of-the-art approaches.

**Keywords** Tweets · Neural network · Disaster · Classification · Graph convolution network

## 1 Introduction

Social media plays an essential role in exchanging information during calamities, as it allows users to share and contribute to the monitoring of conditions by reporting incidents related to disaster events. On the other hand, the voluminous and noisy data generated in social media creates hardships in crisis management by limiting the availability of information from social media. Different organizations need to

---

A. Danday  
Liverpool John Moores University, upGrad, Liverpool, India  
e-mail: [anushadanday@gmail.com](mailto:anushadanday@gmail.com)

T. S. Murthy (✉)  
Chaitanya Bharathi Institute of Technology, Hyderabad, India  
e-mail: [murthyteki@gmail.com](mailto:murthyteki@gmail.com); [tsmurthy\\_it@cbit.ac.in](mailto:tsmurthy_it@cbit.ac.in)

extract diverse information from tweets to enhance disaster management operations. However, the challenges lie in loc tweets from other information like damages [1, 2, 4, 5] incurred, opinions, and sympathetic responses, designing suitable features for discerning and identifying specific classes is a tough task to perform, differentiating the disaster-related tweets from non-disaster tweets, and also with scarce labels. The classification of disaster-related tweets has a huge importance in terms of research. In-depth investigations have been carried out in this domain and the efficiency of established algorithms is analysed; the introduction of graph concepts has proved a major change in the performance of algorithms. With the advent of robust approaches like attention mechanism and the availability of pre-trained models, text classification has become one of the interesting and challenging domains of research in NLP. The use of contextual embedding techniques has its own potential advantages of predicting the text based on context. Hence, they have proven improved performance in text classification applications. Similarly, Graph-based learning has achieved remarkable success in different domains. This attention and progress are owing to advances in computational power, model design flexibility, and newly researched training methods. Social media plays a crucial role as a medium for disseminating news and information during crises. It is critical to obtain as much information as possible regarding the damage, impact, and requirements. Knowing what people need and what is going on in the impacted area allows the government, disaster management authorities, and humanitarian actors to act and respond more effectively [6]. As the crisis unfolds, affected people share vital information on Twitter on real-time basis, this if handled quickly and properly can be used for monitoring and other quick salvage operations [11]. Every activity in crisis management, such as monitoring evacuation plans and conducting rescue missions, necessitates precise and up-to-date information in order to provide an early, prompt, and economical response that minimizes the potential for loss of life and property. Obtaining data from many regions of a crisis-stricken area at the right moment is a difficult and time-consuming operation. People can now communicate information in real time; thanks to the wider spectrum and global reach of social media. Natural catastrophes frequently impede routine communication due to damaged infrastructure, resulting in data loss. Individuals use social networks to seek immediate help for shelter, food, and transportation and to get in touch with others both inside and beyond the catastrophe zone. As a result, the massive flow of information across social media can help in more efficiently addressing relief, contributions, and rehabilitation during a natural disaster. Though the use of social media appears enticing, the majority of the programme still lacks capabilities and are unusable [7].

## 2 Related Work

This section explores prior investigations in the context of classification of disaster tweets, and the performance of fundamental Machine Learning algorithms to advanced Deep Learning algorithms is discussed. A collection of traditional

methods [9] is presented based on the information to detect the medical resource tweets during an emergency. Majority Voting is considered for the ensemble methods. The performance has been far better than the traditional algorithms on various parameters. It also combines this method's performance over Bag of Words. The performance of accuracy (82.4%)—this analysis is restricted only to the Nepal and Italy earthquake datasets owing to the lack of labelled data. A model to identify NAR tweets [10, 11] at the time of crisis. They suggest that the layering of a CNN with conventional classifiers (based on features) is effective for identifying informative tweets. The authors recommend that the combination of Convolutional Neural Networks, KNN and SVM with specific features of domain exceeded the performance of diverse assemblages. This suggested model performs better than earlier methods on Nepal and Italy earthquake datasets. Le et al. proposed a comparison analysis of basic ML models with pretrained model, BERT. They underlined that any DL algorithm, LSTM or CNN with LSTM or a Convolutional Neural Networks (CNN), learns from onehot encoding vectors of text. If onehot embedded its vector length equals to the word size, then this technique has dimensionality issues. A solution to this is to represent input as a lowdimensional space vector. This is implemented using many types of embedding techniques TF\_IDF and Count Vector are considered for word representation and BERT architecture is used for implementing customized classification task. Disaster Tweets dataset from the Kaggle repository is considered for this analysis. This paper substantiates that BERT (by tuning its parameters) is very constructive in classifying text [12–15]. This paper investigates the performance of a text classification algorithm that uses TFIDF Vectorizer, and a linear classification algorithm for a vector machine. The model predicts if a tweet is for a real emergency or not using a binary classifier. The BERT layer is followed by a dropout layer and then by a dense layer. This study highlights the performance of BERT as a Text Classifier. In this paper, the authors through their work, emphasize on the significance of data processing. This paper throws light on the importance of the information split affecting the efficiency of the classifier. They have used crisis\_NLP and crisis\_LexT26 datasets to make imbalanced and balanced datasets. Applied various information pre-processing methods to enhance the efficiency of the classifier and further equate the performance of models (BERT, Default BERT, BERT with NonLinear Layer, BERT with Long-Short Term Memory, and BERT with Convolutional Neural Network) on imbalanced and balanced datasets. They concluded that the elimination of unessential data can lead to enhanced classifications. The models give better performance with balanced dataset. (Ma, n.d.) In this study, the authors have presented a comparison analysis on performance of the default BERT architecture and other custom-based BERT architectures with the default BiLSTM for classification [16–29]. Glove is used for embedding text into numerical vectors. The dataset used for the analysis is m CrisisLexT6 Hurricane Sandy dataset and n Crisis\_NLP. The bidirectional LSTM with Twitter embeddings is set as the baseline and several BERT-based models (baseline BERT, BERT with Nonlinearity, BERT with LSTM, and BERT with CNN) are developed and they outperform the baseline performance [16]. This paper highlights the comparison of word embeddings using CNN and BiLSTM as encoders for text classification. This article explains the implementation of the proposed methodology

used for this study. This article is structured as follows. It starts with the introduction, which explains the overview of the execution, which is followed by the dataset and training specifications. Next to that, the implementation is detailed and finally the evaluation metrics used are presented. The datasets used, and the challenges are elucidated. The performance evaluation metrics used are F1-Score, Accuracy, Precision, Recall, and AUCROC curve. It focuses on contextual embeddings and BERT. Word frequency, Tf-Idf, N-grams, and other high-dimensional, sparse representations ignores sequence along with contextual relationship of the words. Embedding, on the other hand, converts varied length text into dense vector representations, overcoming problems such as the curse of dimensionality and failure to capture semantic and syntactic information in representations. Furthermore, embeddings are learned unsupervised, capturing knowledge in vast unlabeled corpora and transferring that knowledge to subsequent tasks with labelled datasets. As a result, embedding maps have become an inevitable text representation option. ELMo and BERT are frequent models that build contextual vector representations of a token. These representations aim to train these models over enormous amounts of text data. In downstream tasks, ELMo representations are employed as input features, but BERT can be used in two approaches, namely feature-based and finetuning. The final hidden state vectors of BERT are utilized as input features in the featurebased method, whereas in the finetuning method, task specific layers are placed on top of BERT and the entire model is trained using task specific labelled data [8]. BERT employs Encoder, which was introduced in the Transformer design, because it is an attention-based architecture (contains Encoder and Decoder). The Encoder output in BERT is generated by stacking N encoders together. Distinct encoding blocks look for different correlations between tokens and encode them in their output [3]. BERT employs a novel strategy to use bidirectionality by pretraining on “masked language model” and “next sentence prediction”. (Masked Language Model) is a model that forces the model to anticipate masked tokens. Based on the context provided by words that aren't masked in the sequence, the model attempts to estimate the right value of masked words. To forecast output words, three steps are necessary. First, a classification layer must be built on top of an encoder layer. Second, multiply the embedding matrices by the output vectors to convert them to the vocabulary's dimension. Finally, using SoftMax, calculate the likelihood of each word in the dictionary.

### 3 Proposed System

The DistilBERT analyzes the sentence and transfers some of the information it gleans to the next model. It's a faster variant of BERT with performance that's enhanced as compared to BERT's. This was pretrained on raw texts solely, with no human labelling (which is why it can use a lot of publically available data), and then used the BERT base model to produce inputs and labels from those texts. It was specifically pre-trained with three goals in mind. The model was trained to yield the same probabilities as the BERT basic model, resulting in distillation loss. This variant is considered for

the implementation of this proposed methodology. The number of embedding and pooling layers is 6 and outputs a vector of dimension 768. A similarity graph can be generated in three ways from the embedding vectors as mentioned below and the appropriate method would be chosen. The  $s$ -neighbourhood graph is created to connect texts whose pairwise distances are less than  $s$ . The  $k$ -nearest neighbour graph is an undirected graph if any two texts are in the  $k$ -neighbourhood of each other and they are connected by an edge and the fully connected graph in which all texts are connected. Adjacency Matrix(A): Adjacency Matrix is a two-dimensional array of size  $(n \times n)$  where 'n' is the no. of vertices in a graph. If an element  $a[i][j]$  in the adjacency matrix is 1, it indicates that there is an edge from vertex  $i$  to vertex  $j$ .  $A_{ij}=1$ , if text  $I$  is connected to text  $J$ , else 0.

Graph Convolutional Model [17] has employed deep learning algorithms such as CNNs and RNNs in text classification. A direct approach is to employ BOW and ngrams to capture the frequency of words, but these ignore the order and placement of tokens in the text; one advanced approach which extracts the relationship among the tokens along with frequencies. Due to this ability in modelling non-Euclidean, graphs can capture more complex relations on par with traditional approaches. This makes graph-based networks as the best possible approach to improve the performance of varied applications of NLP. Graph neural networks are becoming an increasingly popular range of predictive analytics jobs. Graph neural networks surpass the performance of other machine learning or deep learning methods [18–31] when it comes to modelling data with graphical representations. Because of their ability to simulate complicated text representations, graph neural networks are also being used extensively in the NLP. Out of the research that used GCN for Text classification, focused on creating a single graph for the corpus that captured the document's word relations. For word embeddings, a one-hot representation is employed. Despite the use of external word embeddings, this model beats all other traditional approaches on standard datasets. Its potency is increased when the percentage of training data is reduced. In graph embeddings, graph neural networks have proved to be effective at tasks with complicated relationship structures and can preserve a graph's global structure information. A GCN is a simple but strong graph-based neural network that collects data about high-order neighbourhoods. Word co-occurrence data is utilized to create an edge between two word nodes, whereas frequency of words and in documents are used to create an edge between two word nodes. The challenge of text classification is therefore turned into a problem of node classification. The technique can produce better classification [32–47] results with a minimal number of marked documents. Consider the graph with  $V$  and  $E$ , where  $V$  and  $E$ , respectively, are sets of nodes and edges. Every node is assumed to be connected to itself, i.e.,  $(v, v) \in E$  for any  $v$ . Let  $X \in \mathbb{R}^{(n \times m)}$  be a matrix holding all  $n$  nodes and their vectors, with  $m$  being the feature vectors' dimension and each row  $x_{(v)} \in \mathbb{R}^m$  being the feature vector for  $v$ .  $G$ 's adjacency matrix  $A$  and its degree matrix  $D$  are introduced, with

$$D = \sum_j A_{ij} \tag{1}$$

Because of self-loops, the diagonal elements of  $A$  are set to 1. With only one layer of convolution, GCN can gather information of its neighbourhood. Information knowledge about larger neighbourhoods is merged when numerous GCN layers are overlaid. The new  $k$ -dimensional node matrix  $L^1$  ( $m \times k$ ) is calculated for a one-layer GCN as

$$L^1 = \rho(AXW_0) \quad (2)$$

where

$$\text{Normalized Features} = D^{-1/2}AD^{-1/2} \quad (3)$$

is the normalized symmetric adjacency matrix and

$$W_0 = R^{m \times k} \quad (4)$$

is a weight matrix.  $\rho$  is an activation function, e.g. a ReLU ( $x$ ) = max(0,  $x$ ). As mentioned before, one can incorporate higher order neighbourhoods information by stacking multiple GCN layers:

$$L^{j+1} = \rho((A)L^j W_j) \quad (5)$$

where  $j$  denotes the layer number and

$$L^0 = X \quad (6)$$

Edges between nodes are based on documentword edges (documentword edges) and corpuswide word cooccurrence (wordword edges). The term frequency-inverse document frequency (TFIDF) of the word in the document is the weight of the edge between a document node and a word node, where term frequency is the number of times the word appears in the document and IDF is the logarithmically scaled inverse fraction of the number of documents that contain the word. We discovered that TFIDF weight is superior to term frequency alone. We employ a fixed size sliding window on all documents in the corpus to collect cooccurrence data in order to use global word cooccurrence information.

$$A_{i,j} = \begin{cases} PMI(i, j) & i, j \text{ are words, } PMI(i, j) \text{ greater than } 0 \\ TF - IDF_{i,j} & i \text{ is the document } j \text{ is the word} \\ 1 & i = j \\ 0 & \text{otherwise} \end{cases} \quad (7)$$

The PMI value of a word pair  $i, j$  is computed as

$$PMI(i, j) = \log((p(i, j))/(p(i)p(j))) \quad (8)$$

$$p(i, j) = (W(i, j))/(W) \quad (9)$$

$$p(i) = (W(i))/W \quad (10)$$

where  $w(i)$  is the number of sliding windows in a corpus that contain word  $i$ ,  $w(i, j)$  is the number of sliding  $w$  is the total number of sliding windows in the corpus, and windows that contain both words  $i$  and  $j$ . A positive PMI number shows that words in a corpus have a high semantic correlation, whereas a negative PMI value suggests that the corpus has little or no semantic association. As a result, only edges among paired words with positive PMI values are added. We feed the text graph into a simple two-layer GCN as described in (Kipf and Welling 2017), with the second layer node (word/document) embeddings having the same size as the labels set and being fed into a softmax classifier:

$$Z = \text{softmax}(\tilde{A}ReLU(AXW_0)W_1) \quad (11)$$

$$\tilde{A} = D^{-1/2}AD^{-1/2} \quad (12)$$

is the same as in Eq. (1), and

$$\text{Softmax}(x_i) = 1/Z(\exp(x_i)) \quad (13)$$

With

$$Z = \sum_i \exp(x_i) \quad (14)$$

The loss function is defined as the cross-entropy error over all labelled sentences

$$L = \sum_{d \in Y_D} \sum_{f=1}^F Y_{df} \ln Z_{df} \quad (15)$$

$F$  is the dimension of the output features, which is equal to the number of classes, and  $Y\_D$  is the set of document indices that have labels. The label indicator matrix is denoted by the letter  $Y$ . Gradient descent can be used to train the weight parameters  $W_0$  and  $W_1$ , and  $E_1$  and  $E_2$  are computed using Eqs. (1)–(16).

$$E_1 = (\tilde{A}XW_0) \quad (16)$$

contains the first layer document and word embeddings, while

$$E_2 = (\tilde{A}ReLU(AXW_0)W_1) \quad (17)$$

contains the second layer sentence and word embeddings. The second layer document and word embeddings are found in  $W_1$ . Accuracy is the measure used to assess the model's performance. Because of the unbalanced structure of our dataset (with the



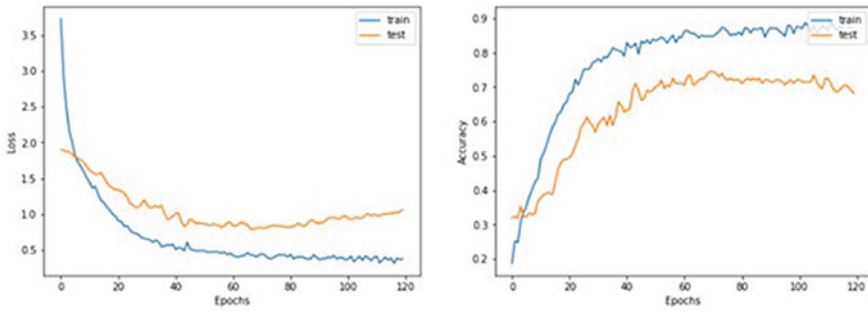
great majority of tweets being “not disaster related”), a model with high accuracy is not always desirable because it could obtain high accuracy simply by classifying every tweet as non-disaster related. As a result, we need to know how many of the few “non-disaster related” samples the classifier properly finds, as well as how many tweets categorized as “disaster related” are actually disaster related. The ratio between the number of right guesses and the total number of forecasts is used to compute it. Accuracy is formulated as shown in Eq. (18).

$$Accuracy = ((TP + TN))/((TP + TN + FP + FN)) \quad (18)$$

## 4 Results and Discussion

All module implementation is done in the python3 language in Jupyter notebook format as part of the programming environment setup. Tensorflow 2, Keras, and NetworkX are the deep learning frameworks used. The dataset used for this study is “nlp-getting-started” from Kaggle, which has training and testing data provided. The training data has “id”, “keyword”, “location”, “text”, and “target” as columns. From these, text represents the tweets and target represents the classes[0/1], while “1” represents if the text is related to disaster and “0” represents if the tweet is not related to disaster. Firstly, the data is analysed to know about the influence of data elements on the target. In checking the basic info about the dataset, the “keyword” and “location” column are found to have missing values. To measure statistical measures about the “text” column, characteristics like average word length, length of the tweets, count of words, links, hashtags, digits, and punctuation’s are analysed for a better understanding of the tweets. Baseline models must be included for a variety of reasons. They give a wealth of data that can be used to guide the next steps in a machine learning project. Baseline models helps to comprehend the data better. These models can guide if data is insufficient for the machine learning task being worked on. The baseline neural network model for classification purposes uses five blocks of feed forward network created with predefined hyper parameters. As there is no over fitting observed in the curve, this is a good fit baseline model where the Loss and Accuracy Curves for Baseline Classifier Model and Accuracy for Baseline Classifier Model are shown in Fig. 1.

Experimental Results of GCN Classifier as the normalized data is transformed to right shape to be fed as input to GCN model. The GCN layer performs product of inputs, weights and the normalized adjacency matrix. A 2layer GCN is implemented with predefined hyper parameters. This supports that the model is able to predict with good accuracy after being trained. The accuracy calculated as shown in Fig. 2. evidences better performance over the baseline classifier model. A Majority Voting-based Ensemble technique based on informative features is suggested in this paper to categorize medical resource tweets during a crisis. The proposed strategy beat state-of-the-art methods on a number of factors, according to the findings. The proposed informative characteristics also outperform the BOW model, which is demonstrated.



**Fig. 1** Loss and accuracy curves for Baseline classifier model as shown in left and accuracy for baseline classifier model

The results show that in the Majority Voting-based Ensemble, standard ML algorithms are particularly useful for spotting medical resource tweets during a crisis. The accuracy at 100 epoch for this proposed reaches around 96% and clearly the proposed work outperforms the traditional approaches to classify tweets as related to disaster.

## 5 Conclusion

In this article, the emphasis is given to improve the performance of Text classification algorithms by incorporating the potential advantages of context-based word embedding and graph structures. The GNNs are targeted to analyse graphical data, but the application domain is not only limited to problems in graphs as GNN models can be generalized to any study that can be modelled as graphs. Unlike the traditional “black box” machine learning algorithms that are trained only on features of training data and lack meaningful logic to perform, models based on the graph neural networks can also process the inherent logic and analyse a problem with more natural thinking. One of the areas to progress with this research ideas is to employ lexical semantic vector models to transform vector space models to graph models. Existing graph libraries could support more complex datasets, or the GNN model construction process might be made more flexible so that it could be easily adjusted for a wider range of applications. The chosen model could be examined and analysed on a variety of complicated and larger datasets, which can aid in determining algorithm adaptability and if it can be applied to real-world applications. Because the implemented models are shallow, developing a deep graph neural network can be a substantial challenge and will aid in a better understanding of GNNs.

## References

1. Ameen YA, Bahnasy K, Elmahdy A (2020) Classification of Arabic tweets for damage event detection. 114:160–166
2. Chanda AK (2021) Efficacy of BERT embeddings on predicting disaster from Twitter data. In: Association for computing machinery 1–14
3. Devlin J, Chang MW, Lee K, Toutanova K (2019) BERT: pre-training of deep bidirectional transformers for language understanding. In: NAACL HLT 2019 - 2019 conference of the North American chapter of the association for computational linguistics: human language technologies - proceedings of the conference, vol 1, pp 4171–4186
4. Gao H, Barbier G (2011) Harnessing the crowdsourcing power of social media for disaster relief. IEEE Intell Syst 11–14
5. Goswami S, Raychaudhuri D (2020) Identification of disaster-related Tweets using natural language processing
6. Irawan R, Isa SM (2020) Social media disaster relevance classification for situation awareness during emergency response in Indonesia 87:3216–3222
7. Kabir Y (2019) A deep learning approach for Tweet classification and rescue scheduling for effective disaster management, pp 1–14
8. Kalyan KS, Sangeetha S (2020) SECNLP: a survey of embeddings in clinical natural language processing. J Biomed Inform 103323
9. Madichetty S, Sridevi M (2020) Improved classification of crisis-related data on Twitter using contextual representations. Procedia Comput Sci 1672019:962–968
10. Madichetty S, Sridevi M (2021) A stacked convolutional neural network for detecting the resource tweets during a disaster. Multimed Tools Appl 803:3927–3949
11. Malekzadeh M, Hajibabae P, Heidari M, Zad S, Uzuner O, Jones JH (2022) Review of graph neural network in text classification, pp 0084–0091
12. Messages C, Imran M, Mitra P, Castillo C (n.d.) Twitter as a lifeline: humanannotated Twitter corpora for NLP of crisis-related messages, ppp 1638–1643
13. Naaz S, Abedin ZU, Rizvi DR (2021) Sequence classification of Tweets with transfer learning via BERT in the field of disaster management. EAI Endorsed Trans Scalable Inf Syst 831:1–8
14. Peters ME, Neumann M, Iyyer M, Gardner M, Clark C, Lee K, Zettlemoyer L (2018) Deep contextualized word representations. NAACL HLT 2018—2018 conference of the North American chapter of the association for computational linguistics: human language technologies—proceedings of the conference, vol 1, pp 2227–2237
15. Weimar B, Wiegmann M, Kersten J, Potthast M (2020) Analysis of detection models for disaster-related Tweets, pp 872–880
16. Wang C, Nulty P, Lillis D (2020) A comparative study on word embeddings in deep learning for text classification, pp 37–46
17. Wee TS (2019) Text-based graph convolutional network—bible book classification—a semi-supervised graph-based approach for text classification and inference
18. Murthy TS, Varma MK, Sumender R (2020) Improving the performance of association rules hiding using hybrid optimization algorithm. J Appl Secur Res Taylor & Francis 15(3):423–437. <https://doi.org/10.1080/19361610.2020.1756155>
19. Murthy TS, Gopalan NP, Yakubu D (2019) An efficient un-realization algorithm for privacy preserving decision tree learning using McDiarmid's Bound. Int J Innov Technol Explor Eng (IJITEE) 1–8(4S2):499–502
20. Murthy TS, Gopalan NP, Sasidhar G (2018) A novel optimization based algorithm to hide sensitive item-sets through sanitization approach. Int J Mod Educ Comput Sci (IJMECS) 10(10):48–55. <https://doi.org/10.5815/ijmeecs.2018.10.06>
21. Murthy TS, Gopalan NP, Alla DSK (2018) The power of anonymization and sensitive knowledge hiding using sanitization approach. Int J Mod Educ Comput Sci (IJMECS) 10(9):26–32. <https://doi.org/10.5815/ijmeecs.2018.09.04>
22. Murthy TS, Gopalan NP (2018) A novel algorithm for association rule hiding. Int J Inf Eng Electron Bus (IJIEEB) 10(3):45–50. <https://doi.org/10.5815/ijieeb.2018.03.06>

23. SaiBabu A, Murthy TSN (2012) Security provision in publicly auditable secure cloud data storage services using SHA-1 algorithm. (IJCSIT) Int J Comput Sci Inform Technol 3(3):4084-4088
24. Sathyanarayana Murthy T, Mohan Krishna Varma N, Ravuri D, Kishore Babu D, Nazeer S (2022) Classification of precious and non-precious tweets using deep learning. In: Rout RR, Ghosh SK, Jana PK, Tripathy AK, Sahoo JP, Li KC (eds) Advances in distributed computing and machine learning. Lecture notes in networks and systems, vol 427. Springer, Singapore. [https://doi.org/10.1007/978-981-19-1018-0\\_33](https://doi.org/10.1007/978-981-19-1018-0_33)
25. Murthy TS, Mohan Krishna Varma N, Roy S, Nazeer S (2022) Effective classification of Tweets using machine learning. In: Kumar R, Ahn CW, Sharma TK, Verma OP, Agarwal A (eds) Soft computing: theories and applications. Lecture notes in networks and systems, vol 425. Springer, Singapore. [https://doi.org/10.1007/978-981-19-0707-4\\_40](https://doi.org/10.1007/978-981-19-0707-4_40)
26. Murthy TS, Gopalan NP, Ramachandran V (2019) A Naive Bayes classifier for detecting unusual customer consumption profiles in power distribution systems—APSPDCL. In: 2019 third international conference on inventive systems and control (ICISC) at JCT college. Coimbatore, India 2019:673–678
27. Murthy TS, Preethi G, Gopalan NP (2018) An efficient way of anonymization without subjecting to attacks using secure matrix method. In: Proceedings of the IEEE international conference on intelligent computing and control systems at VAIGAI COLLEGE OF ENGG, MADURAI, June-2018, pp 1462–1465
28. Murthy TS, Gopalan NP (2018) An efficient meta-heuristic chemical reaction based algorithm for association rule hiding using an advanced perturbation approach. In: Proceedings of the IEEE international conference on intelligent computing and control systems, at VAIGAI COLLEGE OF ENGG, MADURAI, June-2018. Indexed in IEEE
29. Gopalan NP, Murthy TS (2017) Association rule hiding using chemical reaction optimization. Presented a paper at 7th international conference on soft computing for problem solving—SocProS 2017, December 23–24, 2017, IIT Bhubaneswar, ORISSA
30. Devarajan D, Alex DS, Mahesh TR, Kumar VV, Aluvalu R, Maheswari VU, Shitharth S (2022) Cervical cancer diagnosis using intelligent living behavior of artificial jellyfish optimized with artificial neural network. IEEE Access 10:126957–126968
31. Maheswari VU, Aluvalu R, Kantipudi MP, Chennam KK, Kotecha K, Saini JR (2022) Driver drowsiness prediction based on multiple aspects using image processing techniques. IEEE Access 10:54980–54990
32. Murthy TS, Gopalan NP, Banothu B (2023) A modified un-realization approach for effective data perturbation. Int J Intell Enterprise Inder Sci 408–421. <https://doi.org/10.1504/IJIE.2023.10054103>
33. Murthy TS, Udayakumar P, Alenezi F, Laxmi Lydia E, Ishak MK (2023) Coot optimization with deep learning-based false data injection attack recognition. Comput Syst Sci Eng 46(1):255–271
34. Yonbawi S, Alahmari S, Sathyanarayana Murthy T, Maddala P, Laxmi Lydia E et al (2023) Harris hawks optimizer with graph convolutional network-based weed detection in precision agriculture. Comput Syst Sci Eng 46(2):1533–1547
35. Yonbawi S, Alahmari S, Murthy TS, Daniel R, Lydia EL et al (2023) Modified metaheuristics with transfer learning based insect pest classification for agricultural crops. Comput Syst Sci Eng 46(3):3847–3864
36. Ahmed MA, Murthy TS, Alenezi F, Lydia EL, Kadry S et al (2023) Design of evolutionary algorithm based unequal clustering for energy aware wireless sensor networks. Comput Syst Sci Eng 47(1):1283–1297
37. Devaraj FS, Murthy TS, Alenezi F, Laxmi Lydia E, Md Zawawi MA et al (2023) Enhanced metaheuristics with trust aware route selection for wireless sensor networks. Comput Syst Sci Eng 46(2):1431–1445
38. Kalyani K, Parvathy VS, Abdeljaber HAM, Murthy TS, Acharya S et al (2023) Effective return rate prediction of blockchain financial products using machine learning. Comput Mater Continua 74(1):2303–2316

39. Murthy TS (2022) An efficient diabetic prediction system for better diagnosis. *Int J Intell Enterprise Inder Sci* 408–421. <https://doi.org/10.1504/IJIE.2022.126397>
40. Murthy TS, Gopalan NP, Athira TR (2022) Hiding critical transactions using modified un-realization approach. *Int J Bus Intell Inder science Publishers* 15(3):223–234
41. Navaneetha Krishnan S, Sundara Vadivel P, Yuvaraj D, Murthy TS, Malla SJ et al (2022) Enhanced route optimization for wireless networks using meta-heuristic engineering. *Comput Syst Sci Eng* 43(1):17–26
42. Shanmuga Priya S, Yuvaraj D, Murthy TS, Chooralil VS, Navaneetha Krishnan S et al (2022) Secure key management based mobile authentication in cloud. *Comput Syst Sci Eng* 43(3):887–896
43. Murthy TS, Varma MK, Yadav AK (2021) A diaetic prediction system based on mean shift clustering. *ISI IETA Publisher* 36(2):231–235. <https://doi.org/10.18280/isi.260210>
44. Murthy TS, Varma MK, Harsha (2021) Brain tumour segmentation using U-net based adversarial networks. *Traitement du Signal, IETA Publisher* 36(4):353–359. <https://doi.org/10.18280/ts.360408>
45. Murthy TS, Banothu B, Varma MK (2019) An un-realization algorithm for effective privacy preservation using classification and regression trees. *Rev d'Intelligence Artif IETA Publ* 33(4):313–319. <https://doi.org/10.18280/ria.330408>
46. Murthy TS, Varma MK, Sumender R (2020) Improving the performance of association rules hiding using hybrid optimization algorithm. *J Appl Secur Res Taylor & Francis* 15(3):423–437. <https://doi.org/10.1080/19361610.2020.1756155>
47. Danday A, Murthy TS (2022) Twitter data analysis using distill BERT and graph based convolution neural network during disaster, 13 September 2022, PREPRINT (Version 1) available at research square. <https://doi.org/10.21203/rs.3.rs-2041154/v1>

# A Topology for Reactive Power Compensation in Grid System Using a Low-Cost Thyristor Switched Capacitor Scheme



Gaurav Shrivastava and Subhash Chandra

**Abstract** The device described in this publication is a thyristor-switched capacitor (TSC) device used in a 200 kV/11 kV, 200 MW grid system. In addition to the capacitor bank's transient-free switching, a technique for compensating VAR is described. This study's goal is to offer a topology at the lowest possible price. Flexible AC transmission systems (FACTS) have been developed as an alternative to conventional methods for enhancing the efficiency, reliability, and power quality of electrical energy networks. These systems are currently in use in many countries across the world. FACTS are generally referred to as systems that control voltage, impedance, and phase angle in AC systems. Furthermore, due to advancements in semiconductor technology, static VAR compensation devices have begun to be used on the medium and high-voltage sides. The ability of these systems to make adjustments without relying on VAR from the grid is their key strength. In this study, a static VAR compensator made up of three TSCs and one TCR structure is used to supply the system with the necessary VAR. In the simulation studies, the static compensator is used to supply the VAR instead of a voltage source. This prevented the system from using its capacity inefficiently. The use of static VAR compensators is advised, especially when an unbalanced load and instant VAR are needed.

**Keywords** VAR (Reactive Volt-Amp) · Static VAR Compensator (SVC) · Transient-free switching · Reactive power compensation · Thyristor Switched Capacitor (TSC) · FACTS · Potential Transformer (PT) · Current Transformer (CT)

## 1 Introduction

Increased reactive power demand results in a poor power factor, which further increases losses. This study suggests a low-cost configuration that uses static VAR compensation (SVC) technology to reduce losses and improve the voltage profile

---

G. Shrivastava (✉) · S. Chandra  
Department of Electrical Engineering, GLA University, Mathura, U.P, India  
e-mail: [gauravsri005@gmail.com](mailto:gauravsri005@gmail.com)

through VAR compensation. The two components of SVC are TCR and TSC. The TSC scheme is employed in this case because it doesn't emit any harmonics and doesn't need to be filtered, making it a cost-effective solution. The circuit is designed using resistive-inductive loads, fast-acting thyristors, and an SVC controller. Reactive power and work energize the magnetic component, which aids in carrying out physical work. Perceived power is the end result of combined power. Reactive power makes up the majority of the active power in the electrical network, despite being the primary contributor to a poor power factor [6].

A transmission line's power factor can be improved using a variety of methods, such as synchronous condensers, fixed capacitors, and static VAR compensators. Synchronous condensers have rotating components, so their maintenance is expensive. In the fixed capacitor bank method, one capacitor is used across each load, which is more expensive [8]. Again, it is very challenging to compensate for reactive power as the load changes. It may either under or overcompensate for the load. To solve these problems, rapid-acting power semiconductor switches (FACTS) were created. High-frequency switching is made possible by these compact, non-rotating devices.

The suggested architecture offers periodic compensation for changes in reactive power that occur quickly. It significantly raises the power factor, increases feeder effectiveness, and enhances the voltage profile at the load end [20].

- Rapid deviance in the dynamic correction of reactive power.
- It is possible to lessen voltage sag when an induction motor is starting.
- The TSC can also be employed to avoid the harmonic resonance condition.
- It can also be utilized for long transmissions and to charge high-rated transformers.

The following are some of the different features of this control strategy:

- It may adjust reactive power in a practically continuous manner.
- It doesn't produce harmonics.
- Inrush issues during connection and/or disconnection while attempting to leave the system.

The compensator's major component is the controller. The observed voltage and current quantities are delivered to the controller at PCC using the PT and CT, respectively. The controller decides to get the desired VAR compensation.

## 2 Background

Hingorani and Gyugyi [1] described strategies for compensating reactive power, the operating principles, design features, and examples of applications for Var compensators that use thyristors and self-commutated converters. Huang et al. [2] suggested the GSES algorithm as a means of quickly dampening interarea oscillations in the SVC. For minimizing power quality concerns, Chakraborty et al. [3] proposed a hybrid compensator with a new coordinated control. Ikram et al. [4] suggested a

unique, straightforward method for measuring reactive current and reactive power based on binary (on/off) control of an analog switch. Shojaei et al. [5] developed a novel strategy to address the problems with the filter-based reactive power calculation methods used in the control system of static VAR compensators.

Satyamsetti et al. [6] proposed that reactive power for high-voltage transmission networks is provided by using a new configuration of a VAR compensator. Using the passivation approach, Keskes et al. [7] developed a nonlinear coordinated control of the generator excitation and the static VAR compensator (SVC). Terriche et al. [8] proposed a method for solving power quality problems in ship-board micro-grids (SMs), which are mostly caused by the rising installation of power converters. For enhancing the transient performances of frequency and voltage in multi-machine power systems, Wan [9] suggested an extended SVC model with a thyristor firing angle law. For static synchronous compensators (STATCOMs), Camacho et al. [10] presented a control scheme that regulates the positive-sequence voltage to the nominal value, cancels the negative-sequence voltage, and limits the peak of the injected currents. After creating an SVC model for dispatch purposes, Liu et al. [11] offered the formulation of the decision-making process as a mixed-integer non-convex programming (MINCP) issue.

In order to improve the frequency control of high-voltage transmission lines, Wan et al. [12] suggested a decentralized control based on static var compensator (SVC) devices. A technique to enhance the power quality of the electric arc furnace in a distribution power system was proposed by Liu et al. [13]. An active filter and the static var compensator (SVC) may both adjust the power factor and balance three phase currents at the same time. A modified reactive power compensation technique described by Das et al. [14] makes use of a single-equivalent delta-connected thyristor-controlled reactor (TCR) and a mix of Y and  $\Delta$  connected thyristor-switched capacitors.

A model structure option for modeling and parameter identification in power systems was put up by Bogodorova and Vanfretti [15].

The sequence of events throughout the installation, commissioning, and use of the SVC was described by Morello et al. [16].

In place of the traditional design that uses a  $\Delta$  connected reactor bank with a harmonic current filter, Mukhopadhyay et al. [17] presented a new thyristor-controlled reactor scheme in which the total bank is divided into one Y and one  $\Delta$  connected reactor bank with the addition of a low-rating zig-zag autotransformer.

In order to successfully limit the harmonic generation of the TCR, Mukhopadhyay et al. [18] suggested a concept consisting of two identical "Delta" connected reactor banks, one with phase switching via thyristors and the other with a line switching thyristor arrangement. It is particularly efficient to use VAR compensators (SVCs), such as fixed capacitor-thyristor-controlled reactors (FC-TCRs) and thyristor switching capacitors (TSCs).

Panda et al. [19] suggested a Shunt capacitive compensation method to improve the power factor using TSC. Goyal et al. [20] proposed a thyristor-switched capacitor that is programmable microcontroller-controlled and shows how the power factor can



be increased to unity with low system loading and maintained at 0.98 pu with higher system loading.

### 3 Thyristor Switched Capacitor

The TSC is made up of a tiny fixed inductor, a thyristor valve that is bidirectional and a fixed capacitor, as depicted in Fig. 1. The TSC cannot be switched at any angle other than the TCR [14]. A discontinuity in the capacitor voltage will result in a large current through the thyristors that could damage the device since the current through the device is  $i_s(t) = C (dv_c)/dt$ . As a result, the thyristors can only be activated when  $V_s(t) = V_c(t)$ .

Thyristors are also vulnerable to significant changes in the current. Therefore, the best time for switching is at the voltage peak,  $V_s(t)$  [1]. There is no transient current when thyristors are fired at a peak supply voltage if the capacitor voltage stays constant. The intended compensating power determines the capacitor's capacitance. The reactor's inductance is chosen so that it has a tuned frequency that is less than the system's lowest harmonic frequency when the capacitor and reactor are used to create a series resonant circuit. A reactor must be linked in series with power capacitors to prevent resonance problems in harmonic settings and restrict the inrush current of the capacitor [19]. As a result, the design may adjust for reactive power at a fundamental frequency without amplifying harmonics. Volt-ampere(VI) curves are used to characterize the SVC's general steady-state properties. It is common to use an automated voltage regulator with a transfer function of  $[K * 1/(1 + sTp)]$  [1].

The TSCs of an SVC can only be changed in one of two ways: in or out. The only way to change the quantity of reactive power that the TSCs deliver in stages is to change the number of TSCs that are turned on at once.

The TCR, on the other hand, allows switching between a full-conducting state ( $\alpha = 90^\circ$ ) and a non-conducting state ( $\alpha = 180^\circ$ ) as necessary, allowing flexible

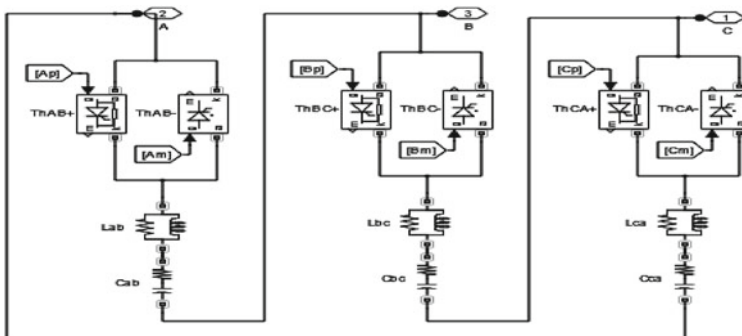
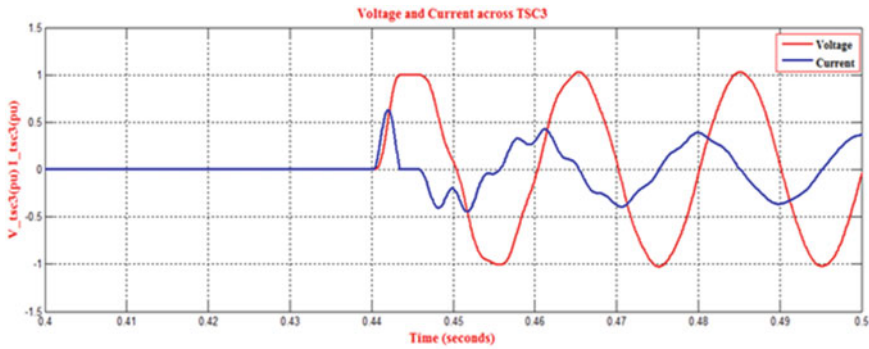


Fig. 1 Simulink diagram of TSC



**Fig. 2** Voltage and current across TSC

and continuous modification of the amount of VAR that the SVC exchanges with the linked AC power supply. When no VAR is needed to rectify the voltage in the AC power system linked to the TCR-TSC type SVC, all the TSCs are turned off, and the TCR is set to the non-conducting condition ( $\alpha = 180^\circ$ ) [1]. When the SVC needs to provide VAR to balance the voltage in the AC supply system, a number of TSCs are turned on so that the quantity of VAR they create is greater than what the SVC must deliver. Figure 2 shows that the capacitor voltage across TSC remains constant until the thyristors are switched on again. The  $\alpha$  of the TCR is then altered to exactly balance the additional VAR supplied by the TSCs. The  $\alpha$  is changed such that the TCR absorbs precisely the exact amount of VAR supplied by the TSCs when the SVC has to deliver more or less VAR to correctly adjust the AC supply system voltage [1].

Figure 3 shows the firing unit which consists of three subsystems, one for each phase, and is synchronized.

#### 4 Simulink Model of Test System

The settings of the system voltage in pu [1.0,1.025,0.93,1.0] at instants [0,0.1,0.4,0.7] seconds are established for the test system’s voltage regulation mode in Fig. 4. The analysis is as follows:

The findings are zoomed out independently for the analysis.

For each phase (AB, BC, and CA), three distinct subsystems are used by the firing unit. For the TCR and TSC branches, each subsystem has a PLL synchronized on line-to-line secondary voltage and a pulse generator. The Distribution Unit’s TSC status and firing angle are used by the pulse generator to create pulses. TSC branches can fire continuously or synchronously (one pulse is supplied to each positive and negative thyristor every cycle).

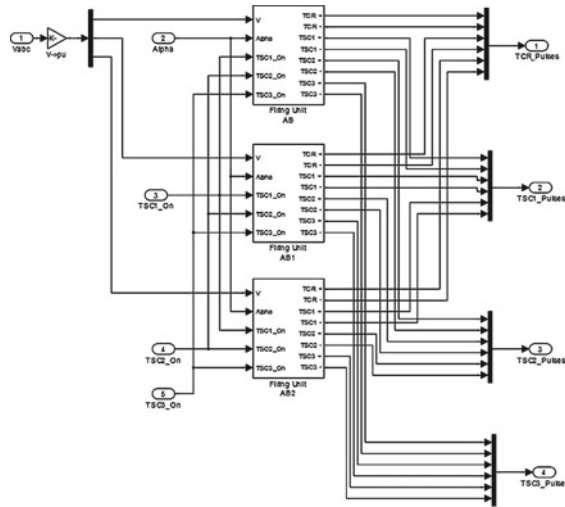


Fig. 3 Firing unit for TSC

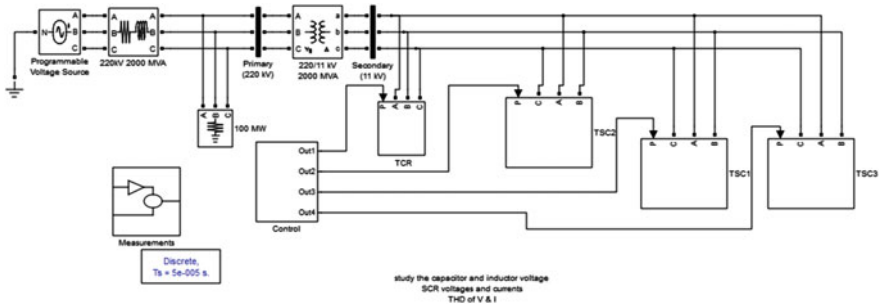
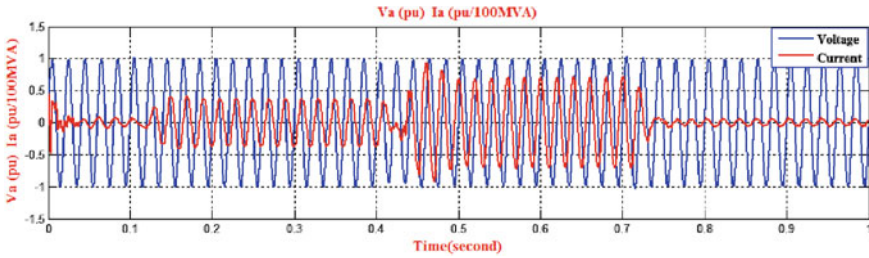


Fig. 4 Test system

### 5 Results and Discussion

The voltage and current waveforms for the grid are displayed in Fig. 5. The current’s nature may be seen in its waveform when the grid voltage is set at 1.0 p.u. In under 0.1 s, the system voltage surges to 1.025 p.u., forcing the TCR to either send reactive power or absorb it. As a result, the grid current may be delayed by up to 0.4 s. The grid current is leading until 0.7 s because the system absorbs the reactive power from the TSCs when the voltage drops to 0.93 p.u. at 0.4 s. The grid current and the AC supply system voltage are almost in phase at 0.7 s, or when the system voltage approaches 1.0 p.u., which is the voltage in the required range.

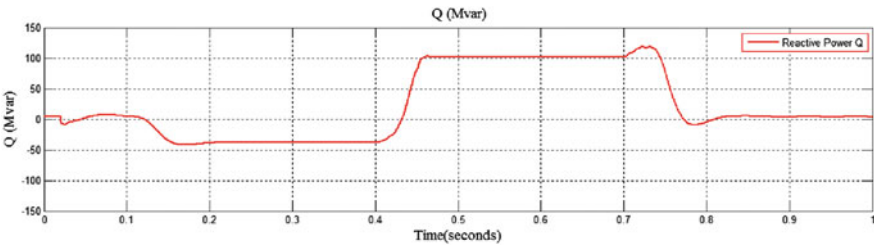
At  $t = 0.1$  s, the voltage in Fig. 6 abruptly rises to 1.025 pu. Reactive power ( $Q = 47$  Mvar) is absorbed by the SVC in response, bringing the voltage back to 1.01



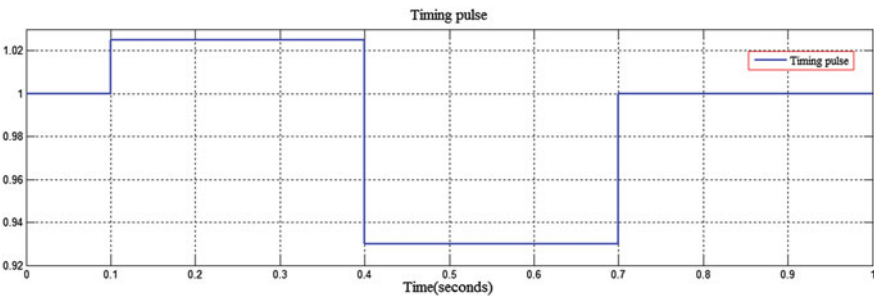
**Fig. 5** Grid voltage and current

pu. The 95% settling time takes about 135 ms. The TCR is currently almost at full conduction ( $\alpha = 94^\circ$ ), and all TSCs are out of service. The source voltage abruptly drops to 0.93 pu at time  $t = 0.4$  s. The voltage rises to 0.972 pu as a result of the SVC's reaction, which involves producing 100 Mvar of reactive power. The TCR currently absorbs about 40% of its nominal reactive power ( $\alpha = 120^\circ$ ), and the three TSCs are operational. The timing pulses delivered by the SVC controller at various times are shown in Figs. 7, and 8 shows the number of TSCs required.

Figure 9 shows the graph of the observed voltage in relation to the reference voltage. The reference voltage ( $V_{ref}$ ) is 1.0 p.u. The recorded system voltage increases from 1.025 p.u. to 0.93 p.u. to 1.025 p.u. again in 0.7 s after reaching 1.025 p.u. in



**Fig. 6** Reactive power



**Fig. 7** Timing pulse

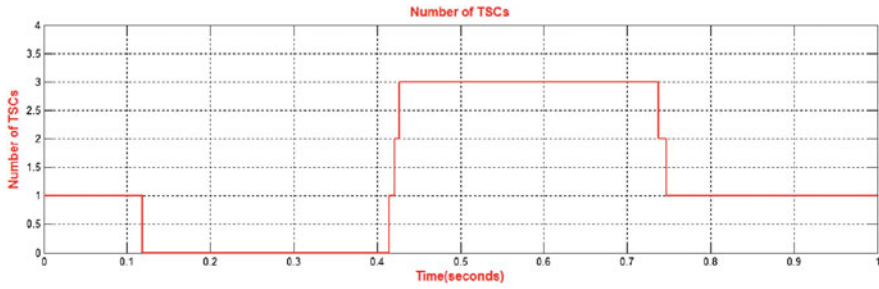


Fig. 8 No. of TSC's required

0.1 s. The voltage then remains at 1.0 p.u. Before the SVC controller moves the system voltage closer to unity, the voltage regulator unit continuously compares the observed voltage to the reference value. Figure 10 shows the firing angle alpha required for TCR. Figure 11 shows the graph of secondary voltage. The secondary voltage is sinusoidal in nature and almost is equal to the reference voltage. Figure 12 shows the current across the load. The current across the load is sinusoidal in nature and at the desired limit. Figure 13 shows the voltage across the load. The voltage waveform is almost sinusoidal in nature. The waveform in Fig. 14 shows that the active power flow from the source to the load is almost constant.

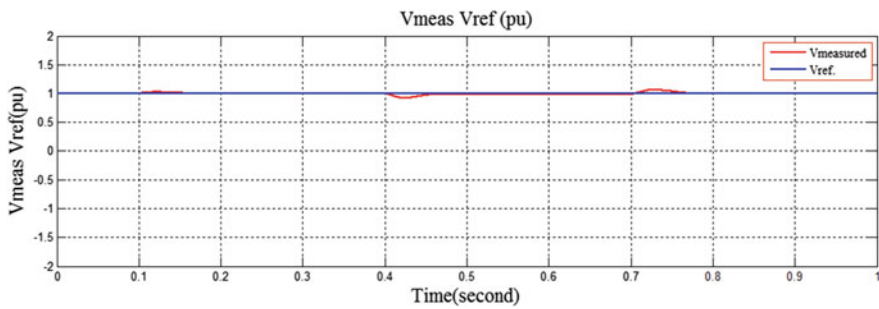


Fig. 9  $V_{measured}$  and  $V_{reference}$

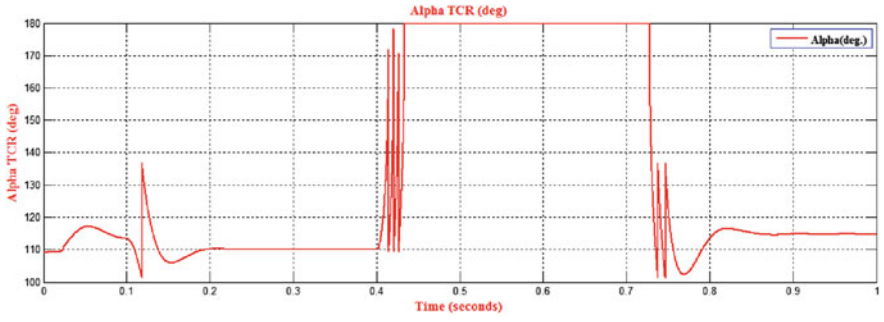


Fig. 10 Firing angle alpha of TCR

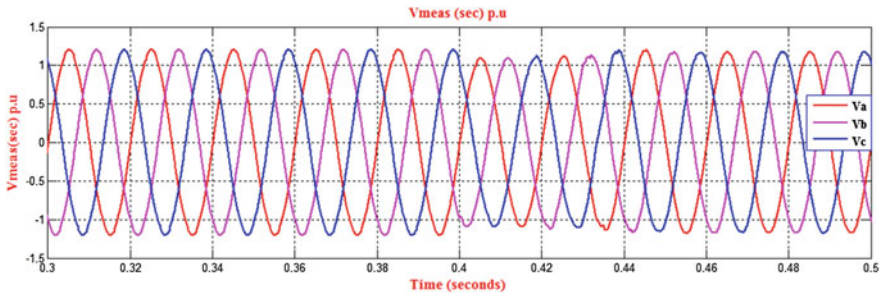


Fig. 11 Secondary voltage

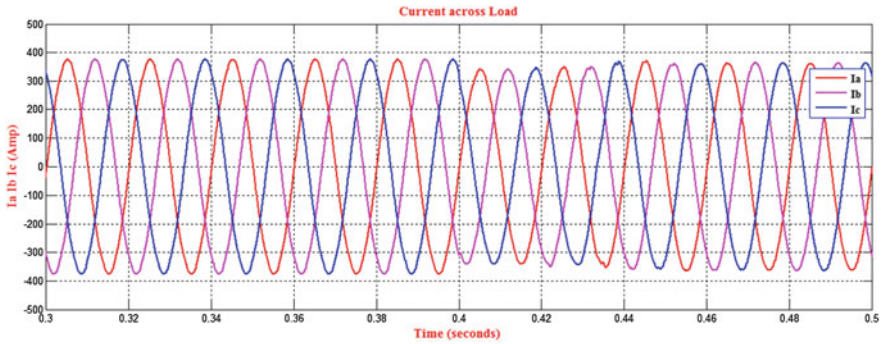


Fig. 12 Current across load

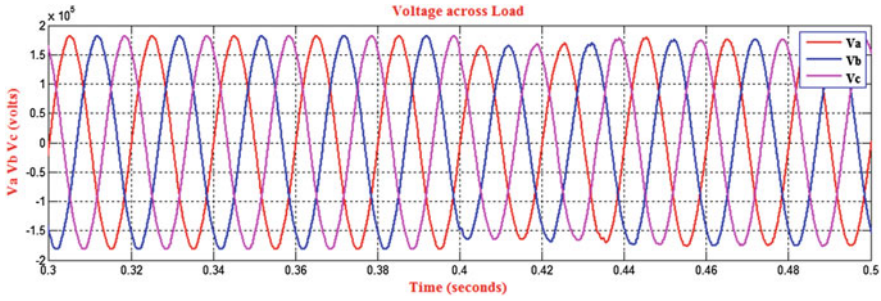


Fig. 13 Voltage across load

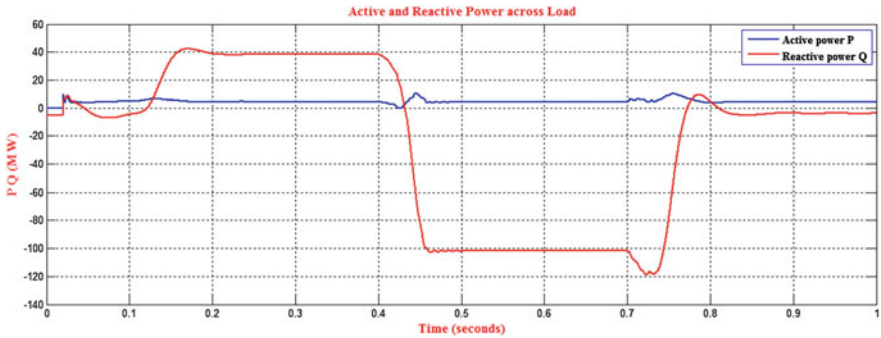


Fig. 14 Active and reactive power

## 6 Conclusion

In order to balance reactive power and enhance the voltage profile, this research presents a TSC architecture that is both efficient and affordable, based on fast-acting thyristors. The voltage on the secondary side is nearly identical to the reference voltage and has a sinusoidal shape. According to the findings in the previous figure, the SVC keeps the receiver voltage  $E_R$  at a level that is nearly comparable to the AC supply system voltage. So, based on the voltage across the alternating current supply system where it is attached, an SVC appropriately corrects for it. To maximize the flow of active power, SVC automatically regulates VAR. From the source to the load, the active power is essentially constant. For sudden variations in reactive power, the proposed architecture provides periodic reactive power adjustments. It significantly increases feeder efficiency and enhances the voltage at the load end. TSCs can function well for such loads because of the thyristor’s rapid switching capabilities.

## References

1. Hingorani NG, Gyugyi L (1989) Understanding FACTS: concepts and technology of flexible AC transmission system', Wiley IEEE press (December 1999). Young, the technical writer's handbook. University Science
2. Huang R, Gao W, Fan R, Huang Q (2023) A guided evolutionary strategy based static Var compensator control approach for interarea oscillation damping. *IEEE Trans Ind Inform* 19(3):2596–2607
3. Chakraborty S, Mukhopadhyay S, Biswas SK (2023) A hybrid compensator for unbalanced AC distribution system with renewable power. *IEEE Trans Ind Appl* 59(1):544–553
4. Ikram MK, Amrr SM, Asghar MSJ, Islam T, Iqbal A (2023) Voltage independent reactive current based sensor for static VAR control applications. *IEEE Sensors J* 23(9):10023–10031
5. Shojaei F, Samet H, Ghanbari T (2022) Electric arc furnaces reactive power optimized calculation used in SVC. *IEEE Trans Ind Electron* 69(6):6361–6370
6. Satyamsetti V, Michaelides A, Hadjianonis A, Nicolaou T (2022) A novel simple inductor-controlled VAR compensator. *IEEE Trans Circuits Syst II* 69(2):524–528
7. Keskes S, Salleem S, Chrifi Alaoui L, Ben Ali Kammoun MBA (2021) Nonlinear coordinated passivation control of single machine infinite bus power system with static VAR compensator. *J Mod Power Syst Clean Energy* 9(6):1557–1565
8. Terriche Y, Su C, Lashab A, Mutarraf MU, Mehrzadi M, Guerrero JM, Vasquez JC (2021) Effective controls of fixed capacitor-thyristor controlled reactors for power quality improvement in shipboard microgrids. *IEEE Trans Ind Appl* 57(3):2838–2849
9. Wan Y (2021) Extended SVC modeling for frequency regulation. *IEEE Trans Power Deliv* 36(1):484–487
10. Camacho A, Castilla M, Miret J, Velasco M, Guzman R (2021) Positive-sequence voltage control, full negative-sequence cancellation, and current limitation for static compensators. *IEEE J Emerg Sel Top Power Electron* 9(6):6613–6623
11. Liu B, Meng K, Dong ZY, Wong PKC, Ting T (2020) Unbalance mitigation via phase-switching device and static Var compensator in low-voltage distribution network. *IEEE Trans Power Syst* 35(6):4856–4869. <https://doi.org/10.1109/TPWRS.2020.2998144>
12. Wan Y, Murad MAA, Liu M, Milano F (2019) Voltage frequency control using SVC devices coupled with voltage dependent loads. *IEEE Trans Power Syst* 34(2):1589–1597. <https://doi.org/10.1109/TPWRS.2018.2878963>
13. Liu Y-W, Rau S-H, Wu C-J, Lee W-J (2018) Improvement of power quality by using advanced reactive power compensation. *IEEE Trans Ind Appl* 54(1):18–24. <https://doi.org/10.1109/TIA.2017.2740840>
14. Das S, Chatterjee D, Goswami SK (2018) A reactive power compensation scheme for unbalanced four-wire system using virtual Y-TCR model. *IEEE Trans Ind Electron* 65(4):3210–3219. <https://doi.org/10.1109/TIE.2017.2758720>
15. Bogodorova T, Vanfretti L (2017) Model structure choice for a static VAR compensator under modeling uncertainty and incomplete information. *IEEE Access* 5:22657–22666. <https://doi.org/10.1109/ACCESS.2017.2758845>
16. Morello S, Dionise TJ, Mank TL (2017) Installation, startup, and performance of a static VAR compensator for an electric arc furnace upgrade. *IEEE Trans Ind Appl* 53(6):6024–6032. <https://doi.org/10.1109/TIA.2017.2731964>
17. Mukhopadhyay S, Maiti D, Banerji A, Biswas SK, Deb NK (2017) A new harmonic reduced three-phase thyristor-controlled reactor for static VAR compensators. *IEEE Trans Ind Electron* 64(9):6898–6907. <https://doi.org/10.1109/TIE.2017.2694409>
18. Mukhopadhyay S, Maiti D, Banerji A, Biswas SK, Deb NK (2017) Dual Delta Bank TCR for harmonic reduction in three-phase static VAR controllers. *IEEE Trans Ind Appl* 53(6):5164–5172. <https://doi.org/10.1109/TIA.2017.2720142>
19. Panda KP, Samantaray S, Rout S (2017) Prototype design of power factor correction circuit for transmission lines using Thyristor switched capacitor scheme. *World J Model Simul* 13(4):314–321



20. Goyal A, Kapil N, Mahapatra S (2014) 'Implementation of thyristor switched capacitors for power factor improvement', *adv. Electron Electron Eng* 4(3):225–230

# An Automated Two-Stage Brain Tumour Diagnosis System Using SVM and Geodesic Distance-Based Colour Segmentation



S. Syedsafi , P. Sriramakrishnan , and T. Kalaiselvi 

**Abstract** In the medical profession, brain tumour is a very crucial illness. A brain tumour is an unwanted mass growing in the brain cells; if it's not prevented, it will eventually cause death. Therefore, tumour diagnosis is essential. Magnetic resonance imaging (MRI) is used to identify the brain tumour quickly. The approach of detecting a brain tumour from human eyesight is quite difficult. The proposed work automatically diagnoses the brain tumour. This proposed technique has two stages: classification and segmentation. The classification stage is used to classify the T2W-MRI images into a tumour and normal using  $8 \times 8$  blocks with gray-level co-occurrence matrix (GLCM) features using a support vector machine (SVM). The second stage segments the FAIR and T1C type MRI images using colour-based segmentation technique. This proposed method uses the BraTS2013 dataset. Classification and segmentation result is calculated by sensitivity, specificity and accuracy. In the segmentation, it additionally uses the dice similarity coefficient (DSC) to find the accuracy. The outcomes denote the proposed method's accuracy of classification as 96.66% and the DSC of segmentation accuracy as 80%.

**Keywords** Brain tumour · Feature extraction · Feature selection · Binary classifier · RGB image · Segmentation

---

S. Syedsafi (✉)

Department of Computer Applications, Kalasalingam Academy of Research and Education, Krishnankoil, Tamil Nadu 626126, India  
e-mail: [syedsafi.safi@gmail.com](mailto:syedsafi.safi@gmail.com)

P. Sriramakrishnan

Department of Mathematics, Amrita School of Physical Sciences, Amrita Vishwa Vidyapeetham (Deemed to be University), Coimbatore, Tamil Nadu 641112, India

T. Kalaiselvi

Department of Computer Science and Applications, The Gandhigram Rural Institute (Deemed to be University, Dindigul, Tamil Nadu 624302, India

## 1 Introduction

In the human life brain tumour is a highly dangerous disease. All human people need long life, but sometimes they are affected by some deadly diseases. The second-most lethal disease recorded by the World Health Organization (WHO) worldwide is a brain tumour [1]. As reported by the National Brain Tumour Society (NBTS), seven lakh Americans are expected to have a brain tumour by 2022 [2]. Tumour refers to the abnormal development of brain cells. A primary type tumour is one that begins in the brain and does not spread; a secondary type tumour spreads to the other body parts.

A brain tumour is classified into two types: benign and malignant. Benign is a non-cancerous type and malignant is a cancerous type. Glioma is one of the most severe forms of malignant brain tumours since it attacks both adults and children commonly. It has two types: low-grade glioma (LGG) and high-grade glioma (HGG). The WHO has classified the glioma into four grades (Grades I–IV) [3]. Generally, imaging techniques are used to find the tumour. When compared with all imaging techniques, magnetic resonance imaging (MRI) is very safe and gives detailed information; it produces 2D and 3D MR images. It has different MRI modalities like T1W, T2W, T1C and FLAIR [4]. The various MRI imaging types are displayed in Fig. 1.

Need an early detection of brain tumour and proper diagnosis are used to extending patient life days. It is difficult to locate the tumorous slices in the MR volume. Next, separating the tumour component from the tumorous MRI is a difficult process. To categorise the tumorous MR image, a classification procedure is required. Moreover, tumour regions must be segmented into tumorous slices using a segmentation technique.

Manual classification and segmentation take more time and provide false results, they are difficult to handle. Machine learning methods are now often applied in medical imaging [5]. In machine learning, many automated algorithms for classification and segmentation are available [6]. It provides quick, precise findings for the right, effective therapy for doctors [7]. To do the classification, MRI discovers characteristics that are used. These characteristics were used by the SVM binary classifier during the validation, training and testing phases of the classification procedure for MR images [8]. A lot of brain tumour techniques are developed but still accuracy is a major issue in finding the tumour clearly because the normal and tumour cell regions are very close.

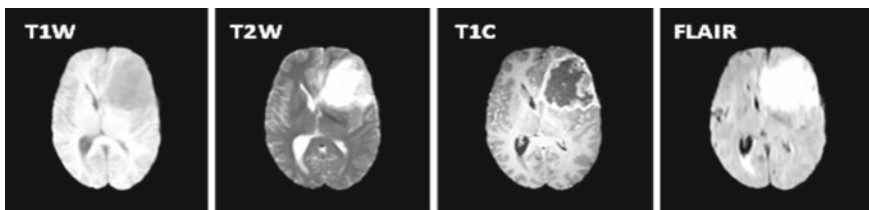


Fig. 1 MRI images

The proposed method uses the BraTS2013 dataset. This proposed technique has two stages: classification and segmentation. Under the given classification stage, the MR image is divided into  $8 \times 8$  blocks. Every  $8 \times 8$  block in MRI is used to extract one of the nineteen GLCM features. The chi-square test technique is used to pick the most significant features from the nineteen features. SVM gets this best feature as input from the training and does the testing process. In the segmentation stage, it used the automatic colour-based region technique. The initial region is selected the tumour area is a segment from the normal brain areas in the MR image.

The main contributions of these works are as follows:

- The suggested classification method automatically divides an MR image into normal and tumour images.
- The classification uses SVM, which produces reliable results.
- The suggested automatic segmentation technique divides the tumour area in the MR image precisely.

The structure of this manuscript is arranged in the following parts: Related work reports the work related to classification and segmentation in MRI. The materials and metrics part reports the dataset and measurements used in this manuscript. The methodology part reports the method used in this manuscript. The results and discussion part report and discuss the outcome of this manuscript. The conclusion part concludes this manuscript.

## 2 Related Works

Early brain tumour identification is highly valued and necessary. There are several methods that have been developed for detecting brain tumours. Zhao et al. [9] developed a fully automatic tumour segmentation technique using deep learning techniques. This method used the combination of a high-speed neural network and conditional random fields (CRF). It has three steps: pre-processing, segmentation and post-processing. It also used recurrent neural networks (RNN) in the CRF part. A CNN-based automated segmentation approach was put out by Pereira et al. [10], it employed a tiny kernel size ( $3 \times 3$  kernels) so that a deep architecture could be designed. It has the following steps: classification, pre-processing and post-processing. In the pre-processing step, it used the patch normalisation technique. This method used a data augmentation technique to overcome the variation of different tumours.

Havaei et al. [11] developed a brain tumour segmentation technique using a deep neural network. This method used a two-path infrastructure with local and global contextual features. The training process also has a two-phase procedure. Finally, it used the cascade architecture to get the results. Zhuge et al. [12] proposed a holistically nested neural technique. It also used the inhomogeneity method, so one group of pixels is merged with other pixels, so the result is low. This method gives the DSC result of 78% for segmentation.

Hussain et al. [13] developed a brain tumour segmentation technique using Deep CNN. It used max-out and drop-out layers. The pre-processing stage uses the image normalisation method, and the post-processing stage uses the morphological technique. During the training time, it uses a patch-based method. A brain tumour segmentation approach is an automated method, and was created by Rajinikanth et al. [14]. Image fusion, thresholding and segmentation make up the three main stages of this methodology. It used MR images with a size of  $216 \times 160$ . This method also uses watershed segmentation and the social group optimization methodology using Shannon's entropy. It utilised  $216 \times 160$  sized Flair + T1C + T2W MR images.

Using extremely random trees, Pinto et al. [15] created a fully automated hierarchical brain tumour segmentation approach. For HGG and LGG, this approach uses a two-step categorization process. It used the intensity normalisation method. In the LGG-type tumours the local and contextual features are used to improve the segmentation, it also used the data augmentation technique to increase the accuracy. A technique of automated 3D super voxel-based learning was put out by Soltaninejad et al. [16]. Pre-process, super voxel partitioning, feature extraction, classification and segmentation are the four processes that make up this approach. The information fusion from MRI images is used to discover the super voxels. Random Forest (RF) was employed in this technique to classify data.

Using hybrid CNN, Sajid et al. [17] created a deep learning-based automated brain tumour segmentation system. This method has three parts: pre-processing, CNN and post-processing. It used two and three-path CNN and also used a patch-based approach. It also used a two-phase training procedure. Amin et al. [18] suggested a transfer learning-based automated segmentation approach based on score-level fusion. Normalisation, segmentation, classification and fusion score are the four processes in this methodology. Segmentation techniques include morphological and thresholding techniques. Alex Net and Google Net are used to classify the data.

A probabilistic local ternary pattern (PLTP) automated brain tumour segmentation approach was put out by Sriramakrishan et al. [19]. SVM was utilised in this approach for classification, while FCM was employed to gather the elements. To shorten the time, it employed a Graphics processing unit with compute unified device architecture. Ejaz et al. [20] proposed a feature approach-based brain tumour segmentation method. This method used HGG-type Flair and T2W images only. The thresholding method is used to find the tumour region. It also used texture features and Gabor filters. Di-phase midway convolution and deconvolution network was the basis for the automated brain tumour segmentation system presented by Chithra and Deepa [21]. In the layers of up sampling and down sampling, it employed the  $3 \times 3$  and  $7 \times 7$  kernels. Softmax classification handles the classification task. With a tissue-type mapping approach, segmentation is performed. Rehman et al. [22] proposed an encoder decoder modified architecture of 2D type U-Net and added the residual extended skip (RES) and wide context (WC) for loss function. It was evaluated on BraTS 2017 and 2018. The drawback of this work is that it loses the local details.

### 3 Materials and Metrics

#### 3.1 Materials

In this research paper, the BraTS2013 MRI image multimodal dataset is used [23]. There are four different MRI multimodal T1W, T2W, FLAIR and T1C types in this dataset. The gold standard (Ground truth) images are also included in this dataset. Every image has a  $240 \times 240$ -pixel size. The dataset has only glioma-type brain tumours combined with 20 HGG volumes and 10 LGG volumes images.

#### 3.2 Metrics

The four metrics sensitivity, specificity, accuracy and dice similarity coefficient (DSC) were employed in this study. The effectiveness of the suggested task is determined using these indicators. The classification and segmentation steps described in Eqs. (1)–(3) both employ the first three metrics. DSC compares the output segmentation image with the ground truth image provided in Eq. (4) to determine how comparable, the two images are. It is only utilised during the segmentation step. The above metrics are computed from true positive (TP), true negative (TN), false positive (FP) and false negative (FN).

$$\text{Sensitivity}\% = \frac{TP}{TP + FN} \quad (1)$$

$$\text{Specificity}\% = \frac{TN}{TN + FP} \quad (2)$$

$$\text{Accuracy}\% = \frac{TP + TN}{TP + TN + FP + FN} \quad (3)$$

$$\text{DSC}\% = \frac{2TP}{2TP + FP + FN} \quad (4)$$

### 4 Proposed Methodology

This study suggests a method for utilising MRI to classify and segment well-organised brain tumours. Segmentation and classification are the first two steps of this approach. The first step only focuses on whether a certain MR image has a tumour. Segmentation occurs in the second stage. The BraTS2013 dataset, which includes four different MRI multi-modals like T1W, T2W, T1C and FLAIR, was employed

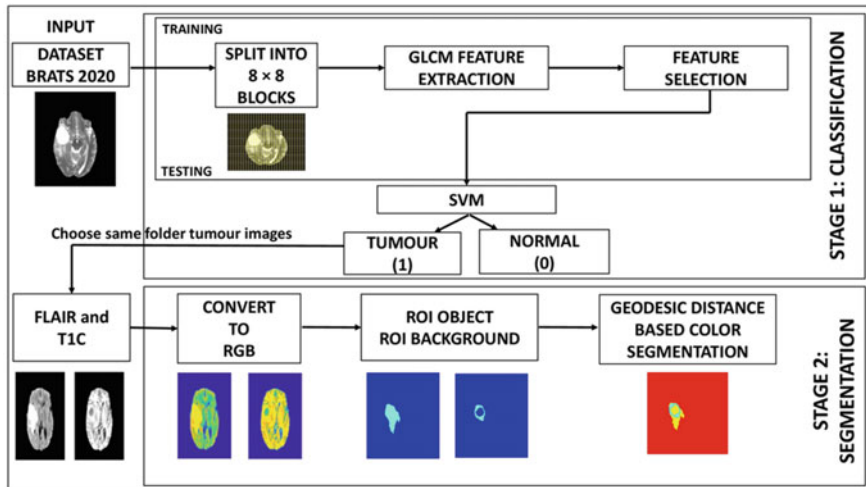


Fig. 2 Proposed method workflow architecture

in this technique. The only images utilised in the proposed study were T2W, TIC and FLAIR. Figure 2 displays the workflow architecture of this effective proposed approach.

### Stage 1: Classification

In this stage the proposed method used T2W-BraTS2013 MR images, it did not need any pre-processing work like noise removal and head stripping. A single T2W image's overall size is  $240 \times 240$  pixels it is split into  $8 \times 8$ -pixel sizes finally, it has 900 blocks for every single image. Compared with other splitting sizes, the  $8 \times 8$  gives the most relevant results [24].

Every feature has a unique identity, making feature extraction crucial for classification since it makes categorization simple. To extract features, this approach utilised GLCM features. The co-occurrence matrix is used by the GLCM feature to express texture and spatial characteristics [25, 26]. The GLCM technique uses a variety of projection angles; the  $45^\circ$  projection angle was employed in this suggested approach. It extracts nineteen different types of features, and compares all the GLCM features. This method assigns labels manually to differentiate the tumour and normal blocks. These labels are called response variables. All feature values are different. It has positive and negative feature values for every block. Table 1 displays the nineteen GLCM features for normal and tumour block.

Next, this approach chooses features using the Chi-square test technique [27]. The output of the nineteen GLCM features' related response variables is based on the input values of the nineteen GLCM features. Table-formatted GLCM feature data are provided for both normal and tumour blocks. To determine which GLCM feature is most appropriate for the response variable, this approach compares the GLCM

**Table 1** GLCM features of normal and tumour block

S.no	GLCM feature names	Normal block	Tumour block
1	Correlation	0.9362	NaN
2	Energy	0.3369	1
3	Contrast	0.3673	0
4	Autocorrelation	52.6122	64
5	Entropy	1.5492	-2.22E-16
6	SOS: variance	50.5774	63.7502
7	Sum variance	170.2387	256
8	Sum average	14.3265	16
9	Homogeneity	0.8163	1
10	Maximum probability	0.5510	1
11	Cluster prominence	112.4442	0
12	Sum entropy	1.4940	-2.22E-16
13	Cluster shade	-16.7942	0
14	Difference entropy	0.6575	-2.22E-16
15	Dissimilarity	0.3673	0
16	Information measure of correlation	-0.6342	0
17	Difference variance	0.3673	0
18	Inverse difference moment normalized (IDM)	0.9943	1
19	Inverse difference normalized (INN)	0.9561	1

features with their corresponding response variables. Every feature is ranked and a bar chart is created.

In the bar chart, the first four high bar values indicate which are the best values. The remaining fifteen feature has low bar values This method chooses only the first four rank features: SOS: Variance, Autocorrelation, Sum average and Sum variance. SOS: Variance is used in the MRI to find the separation of gray pixels. Autocorrelation is used in the MRI to find the links between the pixels. In the MRI, each gray pixel’s mean is determined using the sum average, and the sum variance is utilised to calculate the mean of several gray pixels.

**Support Vector Machine (SVM)**

Using two class labels of 0 and 1, the suggested approach employed the SVM for binary classification to distinguish between normal and tumour images. SVM has two major steps: training and testing. The proposed technique used all HGG and LGG—T2W images, it has 4650 T2W images, 20% of images are used for validation, 60% for training, and the remaining 20% for testing.

**Training:** In the training process, the SVM used the T2W image 8 × 8 block best GLCM features selected by the chi-square test method. It has only the above features given in the Table 1 formulas (4), (6), (7) and (8) with manual class labels. The



training process quickly understands why the feature has that particular class label. This process used 2790 (40% of data) T2W images, it is a combination of normal and tumour images for training. It creates a separate pattern for every label, when the label gets the new feature value the pattern will update automatically.

**Validation:** In the validation process, this method used 20% of images, it gets the knowledge from the training data. This method used 930 (20% of data) T2W images for validation.

**Testing:** The testing process used 930 (20% of data) T2W images for testing. The selected best features were given as input, but they did not have any labels. The testing process features are not the same as the training process features. These features are loaded into SVM which provides labels by comparing them with the training pattern. It gives 96.66% testing accuracy.

## Stage 2: Segmentation

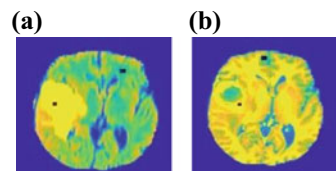
The tumour images selected from the classification stage are done in this step. FLAIR and T1C tumour pictures were used in this stage. FLAIR and T1C-MR type images provide more information about tumours than other MRI kinds do. T1C has the tumour core region, while FLAIR has the whole tumour region.

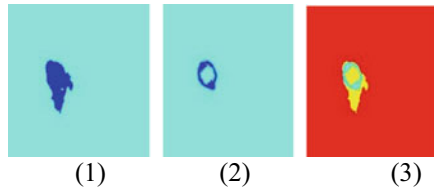
**Convert Gray image to RGB image:** Grayscale FLAIR and T1C images are transformed to RGB images. The RGB image provides more precise information about tumour locations when compared to the gray image and makes it simple to distinguish between tumour and healthy brain areas. The grayscale image was converted using the `ind2rgb` function [28].

**Region of Interest (ROI):** In this process, two regions are selected automatically: The Region of background (background) and the region of object (foreground). The ROI object denotes the tumour part, and the ROI background denotes the normal part. In the RGB-type image, the tumour is yellow and other brain parts are green colour. A red colour rectangle box denotes the ROI object, and the ROI background is denoted by a blue colour rectangle box. These both are separately selected in FLAIR and T1C images. The selected ROI—FLAIR and T1C are exposed in the following Fig. 3.

**Imseggeodesic:** A geodesic distance-based colour segmentation uses two or three regions for segmentation [29]. The proposed method used two-region segmentation. The ROI selected foreground and background are called initial regions (scribbles). The FLAIR image is employed to segment the whole tumour, whereas the T1C

**Fig. 3** ROI selection for foreground and background.  
**a** FLAIR image, **b** T1C image





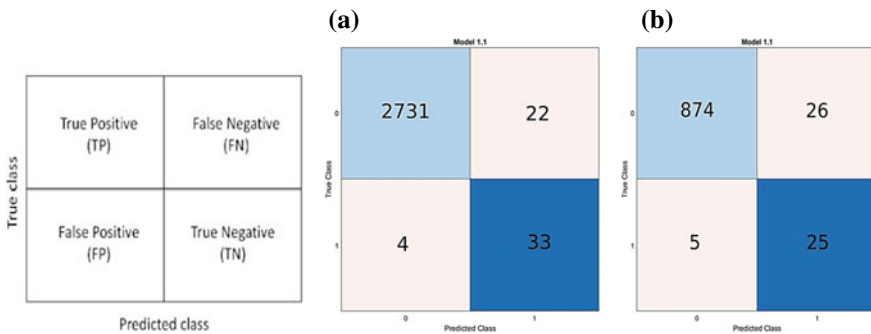
**Fig. 4** Imseggeodesic-based segmentation. (1) L1 image, (2) L2 image, (3) imadd image

image is employed to segment the tumour core. The FLAIR-based segmentation part is denoted by label 1 (L1) and the T1C-based segmentation part is denoted by label 2 (L2). These two label areas are separated from the whole brain image. The imadd function is used it adds the L1 and L2 segmented areas and merges them into a single image. The merged image is in RGB format this is shown in Fig. 4.

### 5 Results and Discussion

This paper utilises the BraTS2013 dataset to automatically classify and segment brain tumours. This method uses Laptop Intel® Core™ i3-1115G4@3.00GHZ, which has a 6 GB RAM specification and MATLAB R2021a student version. This part represents the outcomes of the classification and segmentation of a proposed method.

The multimodal dataset proposed method used T2W images for classification and FLAIR, T1C images for segmentation. The proposed method uses SVM for the classification process and imseggeodesic for the segmentation process. In the classification phase, this method used a combination of HGG and LGG of T2W-BraTS2013 images. A total of 930 images were utilised for testing, 930 images for validation and 2790 images for training in this approach. The SVM classified the images into two labels 0 and 1. It has two steps: training and testing. The confusion matrix for testing and training is displayed in Fig. 5.



**Fig. 5** Confusion matrix. **a** Training data, **b** Testing data

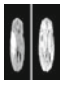
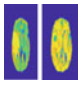

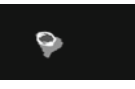
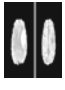
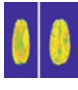

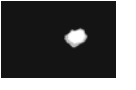
The above picture denotes the confusion matrix of SVM classification. The confusion matrix has two class labels: Predicted class and True class. The true class is the actual class, and the predicted class is the proposed method result class. These classes have two class labels tumour (1) and normal (0). 2790 T2W MRI is selected for training, 930 images for validation and the remaining 930 images for the testing process. In the training process, 2731 images are correctly classified as normal (0) and 33 images are classified as tumour (1). 22 normal images are misclassified as tumours and 4 tumour images are misclassified as normal. It gives 99.06% training accuracy. It takes 8 min and 45 seconds to validate the data. This method used sensitivity, specificity and accuracy metrics for classification. From the above confusion matrix table this method got sensitivity of 97.11%, specificity of 83.33% and accuracy of 96.66%.

In the BraTS2013 dataset, each volume has MRI multimodal images. The unique number denotes the four different types of images. SVM classifier classifies the tumour images from the T2W images. In the dataset the particular sequence no of T2W image has a tumour than the same sequence no of another multimodal images like T1W, T1C and FLAIR type images also have a tumour. The classification is completed by T2W images, and the segmentation uses the same unique number of FLAIR and T1C images. It automatically segments the tumour parts from the MRI images using the Geodesic distance-based colour segmentation method. The tumour's initial region is identified from the RGB image. Table 2 displays the segmentation image findings for the suggested method.

Table 2 gives the proposed method segmentation results. In Table 2, the fifth column represents the original FLAIR and T1C images. The sixth column represents the RGB image of the original image, the seventh column represents the segmented result of the proposed method, and the last column represents the ground truth image. The following metrics measure the proposed method segmentation results: DSC, Sensitivity, Specificity and Accuracy. This method segments both HGG and LGG-type brain tumours. The overall average of the HGG and LGG results are shown in Table 3.

Table 3 gives the details about the overall segmentation results of the proposed method. This method got DSC 80%, Sensitivity 80%, Specificity 99% and Accuracy

**Table 2** Proposed method segmentation results

Data Set	Volume number	Type	Multimodal type	Original image	RGB image	Segmented image	Ground Truth (GT) image
BRATS 2013	HG001	HIGH GRADE	FLAIR and T1C				
	LG009	LOW GRADE					

**Table 3** The overall result of the proposed method of BraTS2013

Dataset	DSC	Sensitivity	Specificity	Accuracy
HGG	0.8110	0.8059	0.9963	0.9851
LGG	0.7986	0.7972	0.9971	0.9891
AVERAGE	0.8048	0.8015	0.9967	0.9871

**Table 4** Comparison result of the proposed method with state-of-the-art methods using DSC

Methods	DSC (%)
Festa et al. [9] (2013)	66
Meier et al. [10] (2013)	76
Cordier et al. [11] (2013)	77
Demirhan et al. [14] (2015)	61
Zhuge et al. [18] (2017)	78
Proposed method	80

98% for the whole tumour. The DSC metric is very important, and it is acknowledged and approved by the medical field. The proposed technique result is compared with other well-efficient techniques. Our proposed method got better results than the results displayed in Table 4.

The segmentation result of the suggested method is measured by three metrics sensitivity, specificity and accuracy. These metrics are used only for measurement and not for comparison. The proposed technique is compared with many state-of-the-art methods with one metric DSC. Observed from our proposed method is efficiently segmenting all glioma-type tumours from MRI. It works very effectively in the same size and shape and different sizes and shapes. Our method got a DSC of 80% from the comparison, but it will also segment the glioma-type tumour perfectly. It happens because the tumour pixels are not in a single group. When converting the gray image into an RGB image, it clearly shows that tumour pixels are very near the normal pixels. This affects our proposed method’s segmentation accuracy.

## 6 Conclusion

In this manuscript, a two-stage brain tumour diagnosis method is developed. This method used the BraTS2013 dataset. In the first stage, T2W MR images are used for classification, it is done by using the GLCM features by the SVM classification technique. In the second stage, automatic segmentation process is done using the FLAIR and T1C images. It used the Geodesic distance-based colour segmentation method. The tumour initial region is automatically selected. Finally, the proposed

method achieves **96.66%** classification accuracy and **80%** DSC segmentation accuracy for the whole tumour. In the future, we hope to enhance the effectiveness of the suggested model and test it on more benchmark datasets.

## References

1. Zehong C, Chin-Teng L (2017) Inherent fuzzy entropy for the improvement of EEG complexity evaluation. *IEEE Trans Fuzzy Syst* 26(2):1032–1035
2. National brain tumour society. <https://braintumor.org/brain-tumor-information/brain-tumor-facts/>. Accessed 02 Dec 2023
3. Syedsafi S, Sriramakrishnan P, Kalaiselvi T (2023) MR image block-based brain tumour detection using GLCM texture features and SVM. In: *Lecture notes in networks and systems*, vol 612. Springer, Singapore
4. Mohsen H et al (2018) Classification using deep learning neural networks for brain tumors. *Future Comput Inform J* 3(1):68–71
5. Zhang D, Shen D (2012) Alzheimer’s disease neuroimaging initiative: predicting future clinical changes of MCI patients using longitudinal and multimodal biomarkers. *PLoS ONE* 7(3):e33182
6. Shree NV, Kumar TNR (2018) TNR: Identification and classification of brain tumor MRI images with feature extraction using DWT and probabilistic neural network. *Brain Inform* 5(1):23–30
7. Wang G et al (2017) Automatic brain tumor segmentation using cascaded anisotropic convolutional neural networks. In: *International MICCAI Brainlesion workshop*. Springer, Cham, pp 178–190
8. Khalil M et al (2018) Performance evaluation of feature extraction techniques in MR-brain image classification system. *Procedia Comput Sci* 127:218–225
9. Zhao X, Wu Y, Song G, Li Z, Fan Y, Zhang Y (2016) Brain tumor segmentation using a fully convolutional neural network with conditional random fields. In: Crimi A, Menze B, Maier O, Reyes M, Winzeck S, Handels H (eds) *Brainlesion: Glioma, multiple sclerosis, stroke and traumatic brain injuries*. *BrainLes 2016*. *Lecture notes in computer science*, vol 10154. Springer, Cham. [https://doi.org/10.1007/978-3-319-55524-9\\_8](https://doi.org/10.1007/978-3-319-55524-9_8)
10. Pereira S, Pinto A, Alves V, Silva CA (2016) Brain tumor segmentation using convolutional neural networks in MRI images. *IEEE Trans Med Imaging* 35(5):1240–1251. <https://doi.org/10.1109/TMI.2016.2538465>
11. Havaei M, Davy A, Warde-Farley D, Biard A, Courville A, Bengio Y, Larochelle H (2016) Brain tumor segmentation with deep neural networks. *Cornell university library*. [arXiv:1505.03540](https://arxiv.org/abs/1505.03540)
12. Zhuge Y, Krauze AV, Ning H, Cheng JY, Arora BC, Camphausen K, Miller RW (2017) Brain tumor segmentation using holistically nested neural networks in MRI images. *Med Phys* 44(10):5234–5243
13. Hussain S, Anwar SM, Majid M (2017) Brain tumor segmentation using cascaded deep convolutional neural network. In: *2017 39th annual international conference of the IEEE engineering in medicine and biology Society (EMBC)*. IEEE, pp 1998–2001
14. Rajinikanth V, Satapathy SC, Dey N, Vijayarajan R (2018) DWT-PCA image fusion technique to improve segmentation accuracy in brain tumor analysis. In: *Microelectronics, electromagnetics and telecommunications: proceedings of ICMEET 2017*. Springer Singapore, pp 453–462
15. Pinto A, Pereira S, Rasteiro D, Silva CA (2018) Hierarchical brain tumour segmentation using extremely randomized trees. *Pattern Recogn* 82:105–117
16. Soltaninejad M, Yang G, Lambrou T, Allinson N, Jones TL, Barrick TR, Howe FA, Ye X (2018) Supervised learning based multimodal MRI brain tumour segmentation using texture features

- from supervoxels. *Comput Methods Programs Biomed* 157:69–84. <https://doi.org/10.1016/j.cmpb.2018.01.003>. Epub 2018 Jan 11. PMID: 29477436
17. Sajid S, Hussain S, Sarwar A (2019) Brain tumor detection and segmentation in MR images using deep learning. *Arab J Sci Eng* 44:9249–9261
  18. Amin J, Sharif M, Yasmin M, Saba T, Anjum MA, Fernandes SL (2019) A new approach for brain tumor segmentation and classification based on score level fusion using transfer learning. *J Med Syst* 43:1–16
  19. Sriramakrishnan P, Kalaiselvi T, Rajeswaran R (2019) Modified local ternary patterns technique for brain tumour segmentation and volume estimation from MRI multi-sequence scans with GPU CUDA machine. *Biocybern Biomed Eng* 39(2):470–487
  20. Ejaz K, Rahim MSM, Bajwa UI, Rana N, Rehman A (2019) An unsupervised learning with feature approach for brain tumor segmentation using magnetic resonance imaging. In: *Proceedings of the 2019 9th international conference on bioscience, biochemistry and bioinformatics*, pp 1–7
  21. Chithra PL, Dheepa G (2020) Di-phase midway convolution and deconvolution network for brain tumor segmentation in MRI images. *Int J Imaging Syst Technol* 30(3):674–686
  22. Rehman MU, Cho S, Kim JH, Chong KT (2020) Bu-net: brain tumor segmentation using modified u-net architecture. *Electronics* 9(12):2203
  23. Menze BH, Jakab A, Bauer S, Kalpathy-Cramer J, Farahani K, Kirby J, Van Leemput K (2014) The multimodal brain tumor image segmentation benchmark (BRATS). *IEEE Trans Med Imaging* 34(10):1993–2024
  24. Kalaiselvi T, Kumarashankar P, Sriramakrishnan P (2020) Three-phase automatic brain tumor diagnosis system using patches based updated run length region growing technique. *J Digit Imaging* 33:465–479
  25. Mohanaiah P, Sathyanarayana P, GuruKumar L (2013) Image texture feature extraction using GLCM approach. *Int J Sci Res Publ* 3(5):1–5
  26. RM V, Elsoud MA, Alkhambashi M (2018) Optimal feature level fusion based ANFIS classifier for brain MRI image classification
  27. Mathworks. [https://in.mathworks.com/help/stats/fscchi2.html#mw\\_3a4e15f8-e55d-4b64-b8d0-1253e2734904\\_head](https://in.mathworks.com/help/stats/fscchi2.html#mw_3a4e15f8-e55d-4b64-b8d0-1253e2734904_head). Accessed 20 Feb 2023
  28. MathWorks. <https://in.mathworks.com/help/matlab/ref/ind2rgb.html>. Accessed 22 Feb 2023
  29. MathWorks. <https://in.mathworks.com/help/images/ref/imseggeodesic.html>. Accessed 22 Feb 2023

# Assessment of Online Teaching Using Statistical and Unsupervised Learning Methods



Raj Kishor Bisht, Sanjay Jasola, Ila Pant Bisht, and Yogesh Lohumi

**Abstract** The objective of the present study is to assess different aspects of online teaching from faculties' perspective. We investigate the level of the difficulties faced by faculty members in handling Moodle, the satisfaction level of online teaching, and online evaluation, and the role of previous awareness/training programs in facing difficulties handling Moodle. Finally, we find the grey areas in online teaching. We collected data from 104 faculty members of Graphic Era Hill University (GEHU) for the present study. Analysis of variance approach and t-test are used for different purposes. K-Means Clustering method is used for analyzing the role of training programs in facing difficulties in handling Moodle. We found that different aspects of Moodle handling were considered equally difficult; satisfaction level in content delivery only is considered high. Satisfaction levels in two components of evaluation, multiple choice questions (MCQ) and descriptive questions (DQ) were neither considered the same nor high; however, satisfaction in MCQ is considered a little more than in DQ. Through clustering patterns, we found a significant effect of previous awareness/training in facing difficulty in handling Moodle. These findings may be useful for making strategies for online teaching in the future.

**Keywords** Online teaching · Statistical methods · Unsupervised learning

---

R. K. Bisht (✉)

School of Computing, Graphic Era Hill University, Dehradun, Uttarakhand, India  
e-mail: [bishtrk@gmail.com](mailto:bishtrk@gmail.com)

S. Jasola

Department of Computer Science and Engineering, Graphic Era Hill University, Dehradun, Uttarakhand, India

I. P. Bisht

Department of Economics and Statistics, Government of Uttarakhand, Dehradun, India

Y. Lohumi

Department of Computer Science and Engineering, Graphic Era Deemed to be University, Dehradun, India

## 1 Introduction

The COVID-19 crisis affected human life in too many ways, and education is one of the most affected areas. The lockdown forced the education system to shift from face-to-face teaching and learning mode into an online mode [1–3]. This unprecedented situation increased the dependency of the education system on digital resources. Though online education was taking place together with face-to-face education at a medium pace, the current pandemic accelerated its speed.

The growth in digital technology has changed our conventional education system. With the continuous growth of digital technology, face-to-face teaching in classrooms has been shifting towards online education for the last two decades [4]. Changes are inevitable in society; thus, there is a need to accept the challenges and work accordingly. The authors of [5] presented an overview of shifting towards online education. In [6], the authors discussed the conceptualization of online learning regarding the existing methodology at the beginning of online learning. Online learning is quite different from classroom face-to-face learning, here a virtual environment exists where you need to feel the presence of students, thus, there are too many challenges in online learning and there is a need to make strategies and plans to cope with its challenges [7]. Due to the sudden rise of the pandemic and successive lockdowns, online education overlapped with face-to-face education. Thus, the institutions/universities used Learning Management Systems (LMSs) for the conduction of online classes [8]. Though online teaching is still going on in some places and somehow online education has taken place in parallel to face-to-face classroom education, it is debatable whether online teaching will successfully overlap face-to-face teaching in the future. Thus, assessing online teaching in different aspects like difficulty in handling LMS, satisfaction level in delivering lectures, satisfaction level in online evaluation, and getting information about grey areas in online learning may be pretty helpful for making strategies and planning for implementing future online education.

GEHU adopted Moodle as LMS, keeping in view the various inbuilt facilities of Moodle for the teaching–learning–evaluation process. Since different universities may have different models; thus, to assess a particular teaching and evaluation model, we have focused our study on GEHU. Faculty members were provided an online training in Moodle LMS. Course content including assignments, tutorials, and quizzes were developed in Moodle. Online classes were conducted in Microsoft Team (MS Team). Examinations were conducted in two parts; the first part included multiple choice questions (MCQ), and the second part included descriptive questions (DQ) using Moodle. For true evaluation of students, the ratio of MCQ and DQ components was kept at 40:60. A fixed time limit of three and half hours (half-hour for uploading answer sheets) was given to the students for submission of answers. It was a quite changed scenario for the education system. Thus, assessing the online teaching and evaluation process from faculties' point of view is quite useful for further strategies.

The emergence of the Internet and digital technology compelled the face-to-face education system to adopt new methodologies [5]. It has provided new dimensions



to distance education. The change from distance education to online education, key turning points, and successes have been studied in [9]. Changing from traditional to online mode has its own impact [10]. It is important to understand the needs of students, particularly in online education [11]. Different variables based on students' experience with online tutoring have been identified in [12]. Interaction has an important role in learning outcomes in online education [13]. Online examination is also another important aspect as there are many issues like submission of answers, network connectivity, and vigilance during examination, etc. A discussion of the factors of the adoption of online examinations by students has been made in [14].

The adoption of a new system in place of a face-to-face education system to online education is a task full of challenges for faculty members [15]. For online teaching, faculty needs a different pedagogical approach in comparison to face-to-face teaching [16]. Students' satisfaction and proper evaluation under the various constraints are the main points of focus. Students' satisfaction in online learning depends on the involvement and instructions of faculty [17]. Moodle provides various facilities for conducting online classes and is quite useful for the teaching process. The experiences of faculties on the first use of Moodle for classroom teaching and learning are discussed in [18]. The attitude of faculties of Jordanian universities in terms of various factors towards adopting an e-learning system is discussed in [19]. The influence of culture and language background on online teaching from a faculty point of view is studied in [20]. Some new concepts in online teaching are proposed in [21] provided. The online teaching, learning and examination model adopted by Mizoram University is presented in [22].

Assessment in online learning is also a matter of concern. Lack of invigilation and opportunity of cheating are some main issues in the online evaluation. Thus, making a robust design of online evaluation is a challenging task. In the research works [23, 24], the authors suggested a computer-based model for assessment and found ease and playfulness are the effecting factors. Grey correlation method is used by [25] for online teaching resources. A model for timeliness evaluation in online learning is proposed in [26]. Self-evaluation of online teaching of faculty members is analyzed in [27]. Online assessment has its own challenges and hence it needs a lot of further research to find a proper method of true evaluation. Data science methods may play a significant role in suggesting the appropriateness of different processes in teaching and learning.

The present study mainly focuses on the following research questions (RQs) from faculties' point of view: RQ1: Is the difficulty level in handling Moodle was same in terms of creating courses, contents, assignments, Quizzes, MCQ and DQ? In which aspects difficulty level is considered high? RQ2: To know the role of previous awareness/training programs in facing difficulties handling Moodle. RQ3: Is the satisfaction level the same for online teaching in terms of content delivery, interaction with students, dealing with Students' queries and regularity of students? In which aspects satisfaction level is high? RQ4: Is the satisfaction level is same in the two components of evaluation MCQ and DQ? In which component satisfaction level is high.

RQ5: Finding the grey areas in online teaching like interaction and communication gap, network connectivity, students' evaluation, students' regular participation, face-to-face interaction, competition among students, need for infrastructure etc.

## 2 Methodology

Here we describe the methodology used for conducting the research, i.e., the population and sample considered for the study, and tools used for data analysis.

### 2.1 Population and Sample

The data is collected from GEHU considering the faculty members of GEHU as the population which is around 400. Faculty members randomly and willingly participated in the survey; thus, it is a random sampling. A total of 104 faculty members from 20 different departments participated in the survey. Among these faculty members, 66 male, and 38 female; 74 Assistant Professor, 23 Associate Professor, and 7 Professors participated. The age group of participants was 25–55 years. An online survey was conducted among the faculty members of three campuses (Dehradun, Bhimtal and Haldwani) of GEHU using Google Forms from 5th July 2021 to 10th July 2021.

The questionnaire contained five parts having questions on basic information, use of various software and hardware for conducting online classes, difficulty level in handling Moodle, satisfaction level of online classes, satisfaction level in two components of evaluation MCQ and DQ and finally, regarding the grey areas of online teaching. In the last four parts, the opinion of faculty members is asked on a 0–10 point scale regarding their level of difficulty in handling Moodle and satisfaction level in online teaching/satisfaction in evaluation/agreement with the grey areas considering 0 as minimum and 10 as the maximum level of agreement. The questionnaire contained 26 questions. The internal consistency of 20 questions (questions related to opinion on a 0–10 scale, other than basic information) is examined and found consistent (Cronbach's Coefficient Alpha = 0.789).

### 2.2 Tests and Methods

We use basic descriptive statistics to display the outcomes of the study regarding the first part of the survey. To check whether the average difficulty level/satisfaction level in different aspects is equal or not, we use one-way analysis of variance approach (ANOVA). Further, to check which aspect is considered as the most significant, we use t-test and to check whether the average characteristic levels of two populations are same or not, we use paired t-test. Since the sample size is large enough, and for each

of the variables, the population is the same; thus, the basic assumptions of normality and same population variance are satisfied. Further, to know the effectiveness of previous awareness (self or through training program), we find clustering patterns based on previous awareness and difficulty in handling LMS Moodle using K-Means clustering algorithm in Python.

For different characteristics (difficulty level, satisfaction level, agreement level), the null and alternative hypotheses are as follows:  $H_0$  : Average characteristic levels in all aspects under study are equal,  $H_1$  : Average characteristic levels in all aspects under study are not equal. For checking whether a characteristic is highly considered or not, we use  $t$  test. Since the characteristic level is measured on an 11-point scale (0–10), where 0 indicates the minimum level of characteristic and 10 indicates the maximum level of characteristic; thus, a score more than seven is considered as a high level. Let  $\mu_i$  denotes the population mean of  $i$ th characteristic, then the null and alternative hypotheses are as follows:

$$H_0 : \mu_i \leq 7 \text{ and } H_1 : \mu_i > 7$$

we use these hypotheses for different research questions consistently. Similarly, for paired  $t$ -test, the hypotheses are as follows:  $H_0$  : The two population means are equal  $H_1$  : The two populations’ means are significantly different. We choose 5% level of significance for our analysis.

### 3 Analysis

Figure 1 shows the usage of different software/hardware for online teaching. From Fig. 1, we observe that PowerPoint is highly used for online classes. Further MS Word and Screen recorder are also used by majority of the faculty members.

RQ1: Descriptive summary of different aspects is given in Table 1 and the results of ANOVA are given in Table 2. From Table 2, we observe that the  $p$ -value is greater

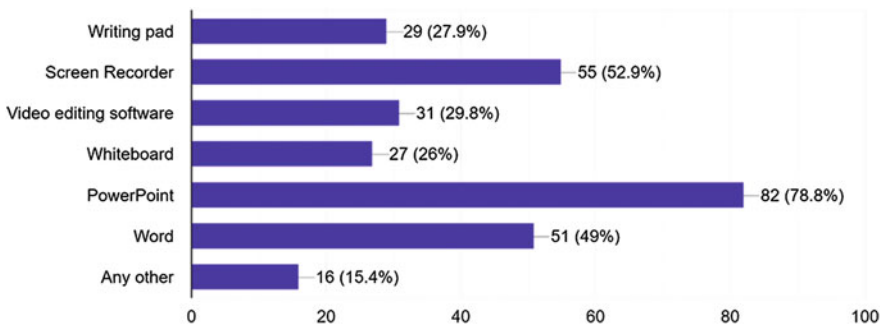
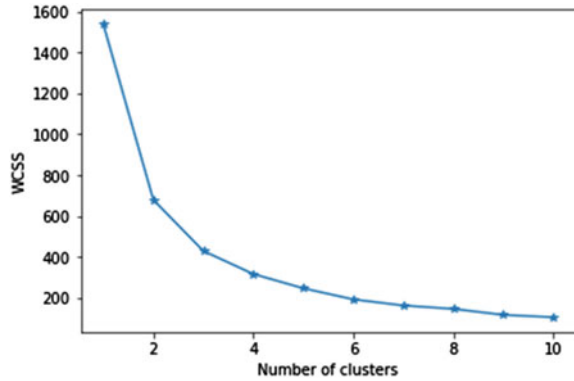


Fig. 1 Usage of different software/hardware for online teaching



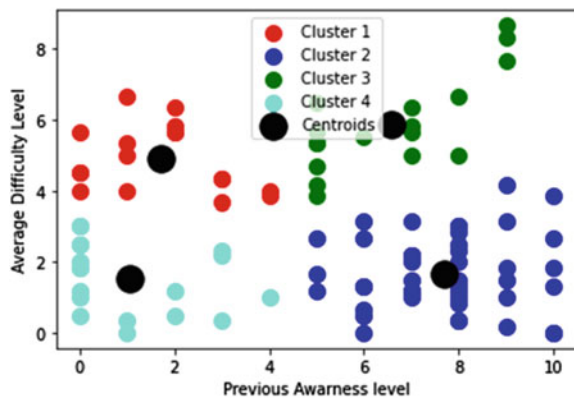
**Fig. 2** The Elbow method for optimal number of clusters



of the faculty members from 30–40 age group, comprises the faculty members with less previous awareness of Moodle and faced above-average difficulty in handling Moodle. The second cluster, which includes 47% of the faculty members from each age group, comprises the faculty members who have a good level of awareness with Moodle and experience less difficulty in handling Moodle. The third cluster, which includes 17% of faculty members, comprises faculty members who have a good level of awareness of Moodle and experienced above-average difficulty in handling Moodle. Most of the faculty members in this group are middle aged with an average age of 36. The fourth cluster, which includes 18% of the faculty members from almost all age groups, comprises the faculty members having less than average awareness and less than average difficulty in handling Moodle.

RQ3: We check whether the average satisfaction level of online teaching is the same in different aspects or not. A summary of different aspects is given in Table 4 and results of ANOVA are given in Table 5. From Table 5, we observe that the  $p$ -value is less than 0.05, thus we reject the null hypothesis and conclude that the average satisfaction levels in different aspects are not the same.

**Fig. 3** Clustering pattern based on awareness and average difficulty level



**Table 4** Summary of various aspects of satisfaction level in online teaching

Groups	Count	Sum	Average	Variance
Content delivery	104	770	7.40	3.00
Interaction with students	104	665	6.39	4.82
Students' query	104	743	7.14	3.85
Regular attendance	104	650	6.25	5.41

**Table 5** ANOVA for satisfaction level in various aspects of online teaching

Source of variation	SS	Df	MS	F	<i>p</i> -value
Between groups	98.83	3	32.94	7.71	0.00
Within groups	1760.21	412	4.27		
Total	1859.04	415			

In order to find the aspect with a high satisfaction level, we use *t*-test. Basic statistics and *p*-value for the upper tail test are given in Table 6. From Table 6, we see that *p*-value is less than 0.05 only for the satisfaction level in content delivery; thus, we reject the null hypothesis, and we conclude that in online teaching, the satisfaction level is high only in content delivery. In all other aspects, the satisfaction level is not high.

RQ4: For equality of satisfaction level in two aspects MCQ and DQ, we use paired *t*-test. The null and alternative hypotheses are as follows:  $H_0$  : There is no significant difference between the two population means and  $H_1$  : There is a significant difference between the two population means. Table 7 shows the results of paired *t*-test. From Table 7, we see that *p*-value is less than 0.05; hence, we reject the null hypothesis and conclude that the satisfaction level in the two components is not the same.

Further, to know the component of examination in which the satisfaction level of evaluation is high, Table 8 shows the basic statistics and *p*-values for the *t*-test. From Table 8, we observe that the *p*-value is more than 0.05 in each case; thus, we fail to reject the null hypothesis and conclude that the satisfaction level is not high in both evaluation patterns.

**Table 6** Basic statistics and *p*-value for satisfaction level in different aspects of online teaching

	Content delivery	Interaction with students	Addressing students' query	Students' regular attendance
Sample mean	7.40	6.39	7.14	6.25
Sample variance	3.00	4.82	3.85	5.41
<i>T</i>	2.38	-2.81	0.75	-3.29
<i>p</i> -upper tail	0.01	1.00	0.23	1.00

**Table 7** Basic statistics and  $p$ -values for paired  $t$ -test

	S_MCQ	S_DQ
Sample mean	7.04	6.38
Sample variance	5.32	6.35
Df	103.00	
$t$	4.11	
$p(T < = t)$ two-tail	0.00	

**Table 8** Summary of  $t$ -test for satisfaction in evaluation

	Satisfaction level in MCQ exam pattern	Satisfaction level in DQ exam pattern
$t$	0.17	-2.53
$p$ -upper tail	0.43	0.99

**Table 9** Summary of  $t$ -test for acknowledging grey area of online education

Grey areas	Sample mean	Sample variance	$t$	$p$ -upper tail
Interaction and communication	6.34	4.21	-3.30	1.00
Network connectivity	6.29	5.08	-3.22	1.00
Students' evaluation	5.93	4.22	-5.30	1.00
Students' regular participation	6.17	4.47	-3.99	1.00
Face-to face interaction	6.62	5.37	-1.69	0.95
Competition among students	6.04	5.28	-4.27	1.00
Infrastructure	5.43	5.72	-6.68	1.00

RQ5: To find the areas considered high grey areas in online teaching, we provided a list of grey areas like lack of interaction and communication, poor network connectivity, improper students' evaluation, lack of students' regular participation, competition among students, lack of face-to-face interaction during teaching and lack of infrastructure for the opinion of faculty members. Table 9 shows the summary of  $t$ -test. From Table 9, we observe that no area is considered a high grey area but from the sample mean, we observe that the most considered grey areas were face-to-face interaction, followed by interaction and communication, network connectivity, and students' regular participation.

## 4 Discussion

The present study was conducted to know faculties' perspectives on online teaching regarding the difficulty in handling Moodle, satisfaction level in online teaching, satisfaction level in two components of the examination, and knowing the grey areas

of online teaching. We found that faculties experienced equal difficulty in different aspects of Moodle handling and none of the aspects is considered highly difficult; it is a good sign for the future of online teaching that new technology can be adopted easily. This also indicates that any further improvements in Moodle for the betterment of online teaching can be adopted quickly.

The clustering pattern based on previous awareness and difficulty levels shows that previous awareness/training program has an influential role in experiencing less difficulty handling Moodle, which is ultimately beneficial for students in online learning. The third cluster is quite crucial for further research to know the reasons behind experiencing above-average difficulty despite having a good awareness of Moodle. There is a need to sort out these deficiencies for achieving the goals of online education in a holistic manner. The fourth cluster is also essential for further research to know the additional skills of the faculty members who have experienced less difficulty despite having less awareness of Moodle.

For a faculty, satisfaction in his/her teaching in different aspects like content delivery, students' participation, interaction with students, query solving etc. are quite necessary. We found that satisfaction level is high in content delivery only and other important aspects are lacking which is a real concern in online teaching.

The satisfaction level in the two components of evaluation MCQ and DQ is not equal and further in both components, the satisfaction level is not high. Based on the average satisfaction level in the two components of evaluation, we found that satisfaction in MCQ is a little higher than DQ.

Finally, lack of face-to-face interaction, lack of interaction and communication, poor network connectivity, and students' irregular participation were found some grey areas in online teaching which need to be addressed.

## 5 Conclusion

The present study was an effort to assess various aspects of online teaching in higher education with respect to the faculties' point of view by considering the model adopted by GEHU. There are fewer studies considering the faculties' perspective, keeping this in mind, the present study is conducted to know faculties' point of view regarding online teaching. The study reveals that a new technology can be adopted easily but there are other aspects which need to be taken care of. The findings show that high satisfaction is missing from faculty's point of view in different aspects of online teaching and evaluation which is a matter of real concern; hence the findings suggest a major improvement in the methodology of online teaching and evaluation process. Since for other universities, the online teaching model may be different, thus the research is limited to one university only. This is the limitation of the present work. In the future, a generalized survey of online teaching may be conducted by including the faculties of various universities.



## References

1. Bisht RK, Jasola S, Bisht IP (2022) Acceptability and challenges of online higher education in the era of COVID-19: a study of students' perspective. *Asian Educ Dev Studies* 11. <https://doi.org/10.1108/AEDS-05-2020-0119>
2. Cohen E, Davidovitch N (2020) The development of online learning in Israeli higher education. *J Educ Learning* 9. <https://doi.org/10.5539/jel.v9n5p15>
3. Devkota KR (2021) Inequalities reinforced through online and distance education in the age of COVID-19: The case of higher education in Nepal. *Int Rev Education* 67. <https://doi.org/10.1007/s11159-021-09886-x>
4. Meyen EL, Aust R, Gauch JM, Hinton HS, Isaacson RE, Smith SJ, Tee MY (2002) e-Learning: A programmatic research construct for the future. *J Spec Educ Technol* 17. <https://doi.org/10.1177/016264340201700303>
5. Harasim L (2000) Shift happens: Online education as a new paradigm in learning. *Internet High Educ* 3. [https://doi.org/10.1016/S1096-7516\(00\)00032-4](https://doi.org/10.1016/S1096-7516(00)00032-4)
6. Wallace RM (2003) Online learning in higher education: a review of research on interactions among teachers and students. *Educ, Commun & Information* 3. <https://doi.org/10.1080/14636310303143>
7. Jones, N., O'Shea, J.: Challenging hierarchies: The impact of e-learning, (2004). <https://doi.org/10.1023/B:HIGH.0000035560.32573.d0>
8. Villegas CHW, Román-Cañizares M, Palacios-Pacheco X (2020) Improvement of an online education model with the integration of machine learning and data analysis in an LMS. *Appl Sci (Switz)* 10. <https://doi.org/10.3390/APP10155371>
9. Mason R (2000) From distance education to online education. *Internet High Education* 3. [https://doi.org/10.1016/S1096-7516\(00\)00033-6](https://doi.org/10.1016/S1096-7516(00)00033-6)
10. Bennett S, Lockyer L (2004) Becoming an online teacher: Adapting to a changed environment for teaching and learning in higher education. *EMI Educ Media Int* 41. <https://doi.org/10.1080/09523980410001680842>
11. Young S (2006) Student views of effective online teaching in higher education. *Am J Distance Education* 20:65–77
12. Hanham J, Lee CB, Teo T (2021) The influence of technology acceptance, academic self-efficacy, and gender on academic achievement through online tutoring. *Comput Educ* 172. <https://doi.org/10.1016/j.compedu.2021.104252>
13. Joksimović S, Gašević D, Loughin TM, Kovanović V, Hatala M (2015) Learning at distance: Effects of interaction traces on academic achievement. *Comput Educ* 87. <https://doi.org/10.1016/j.compedu.2015.07.002>
14. Sugilar S (2017) The online examinations at Universitas Terbuka: an innovation diffusion viewpoint. *Asian Assoc Open Univ J* 12. <https://doi.org/10.1108/AAOUJ-01-2017-0004>
15. Kebritchi M, Lipschuetz A, Santiago L (2017) Issues and challenges for teaching successful online courses in higher education. *J Educ Technol Systems* 46. <https://doi.org/10.1177/0047239516661713>
16. Rapanta C, Botturi L, Goodyear P, Guàrdia L, Koole M (2020) Online university teaching during and after the covid-19 crisis: Refocusing teacher presence and learning activity. *Postdigital Sci Education* 2. <https://doi.org/10.1007/s42438-020-00155-y>
17. Lee SJ, Lee H, Kim TT (2018) A study on the instructor role in dealing with mixed contents: How it affects learner satisfaction and retention in e-learning. *Sustainability (Switzerland)* 10. <https://doi.org/10.3390/su10030850>
18. Beatty B, Ulasewicz C (2006) Faculty perspectives on moving from blackboard to the moodle learning management system. *TechTrends* 50. <https://doi.org/10.1007/s11528-006-0036-y>
19. Al-Alak BA, Alnawas IAM (2011) Measuring the acceptance and adoption of e-learning by academic staff. *Knowl Manag E-Learning* 3. <https://doi.org/10.34105/j.kmel.2011.03.016>
20. Jayatilleke BG, Gunawardena C (2016) Cultural perceptions of online learning: transnational faculty perspectives. *Asian Assoc Open Univ J* 11. <https://doi.org/10.1108/AAOUJ-07-2016-0019>

21. Gonzalez C (2009) Conceptions of, and approaches to, teaching online: A study of lecturers teaching postgraduate distance courses. *High Educ (Dordr)* 57. <https://doi.org/10.1007/s10734-008-9145-1>
22. Mishra L, Gupta T, Shree A (2020) Online teaching-learning in higher education during lockdown period of COVID-19 pandemic. *Int J Educ Res Open* 1. <https://doi.org/10.1016/j.ijedro.2020.100012>
23. Terzis V, Economides AA (2011) The acceptance and use of computer based assessment. *Comput Educ* 56. <https://doi.org/10.1016/j.compedu.2010.11.017>
24. Maqableh M, Masa'deh RMT, Mohammed AB (2015) The acceptance and use of computer based assessment in higher education. *J Softw Eng Applications* 08. <https://doi.org/10.4236/jsea.2015.810053>
25. Zhang D, Zhao T (2022) Evaluation of English online teaching resources for college students based on grey correlation method. *Tehnicki Vjesnik* 29. <https://doi.org/10.17559/TV-20210809112442>
26. Lv W, Ding X, Salam ZA (2021) Research on timeliness evaluation model of online teaching based on intelligent learning. *Int J Contin Eng Educ Life Long Learn* 31. <https://doi.org/10.1504/ijceell.2021.114390>.
27. Wu W, Yao R, Xie Z (2022) The relationship between university teachers' self-evaluation of online teaching and their background: based on the survey of 334 Chinese universities. *Asian Educ Dev Stud* 11. <https://doi.org/10.1108/AEDS-08-2020-0185>.

# An Image-Based Automated Model for Plant Disease Detection Using Wavelet



Aditi Ghosh and Parthajit Roy

**Abstract** The popularity of using automated models in every sector is increasing day by day. Developing an automated model to recognize various diseases in plants from leaf images is the main focus of this research study. Various diseases can occur in plants during their entire lifetime. Automated identification saves time and eliminates human intervention. This study uses image segmentation to separate affected and unaffected regions from leaf images. The discrete wavelet transform has been used to take out significant patterns from images. Local binary pattern has also been used as a texture feature descriptor. The study shows a significant improvement in accuracy using these feature combinations. To train and test the model, a benchmark data set has been used. The efficiency of our model outperforms state-of-the-art models in comparison. The efficiency of our model is 95.08%.

**Keywords** Plant disease detection · Machine learning · Deep learning · Artificial neural network · Image processing · Discrete wavelet transform

## 1 Introduction

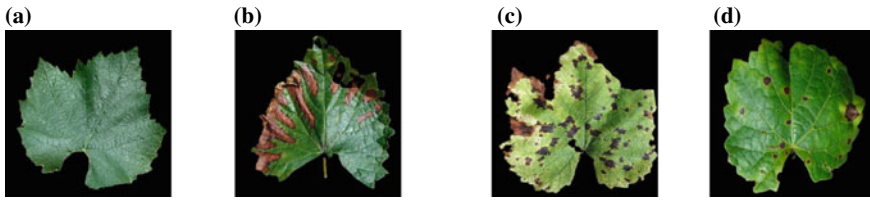
An impairment that prevents a plant to perform its normal function is called plant disease. Plant diseases develop due to specific conditions. These are host plants, the presence of pathogens, and favorable environmental conditions [1]. Pathogen is an organism that can cause disease. These can be fungi, viruses, bacteria, nematodes, etc. The most common fungal diseases are Leaf Blight, Leaf Spot, Rust, Downy Mildew, Powdery Mildew, etc. Some of the bacterial diseases are bacterial Leaf Blight, Leaf Streak, Leaf Spot, Rot, etc. Mosaic, Spotted Wilt, etc., are the diseases caused by viruses [1, 2]. Along with pathogens, some environmental factors such as temperature, humidity, soil moisture, soil pH, etc., are also responsible for the diseases to occur. This study deals with identifying different diseases of grapes.

---

A. Ghosh · P. Roy (✉)

The Department of Computer Science, The University of Burdwan, Purba Bardhaman 713104, West Bengal, India

e-mail: [roy.parthajit@gmail.com](mailto:roy.parthajit@gmail.com)



**Fig. 1** **a** Healthy grape leaf. **b** Black measles containing tiger strip pattern. **c** Red to brown spot in leaf blight. **d** Black rot containing dark brown spots

Isariopsis [3], Esca [4] and Black Rot [5] are the most common diseases that can be seen in grapes. Isariopsis is a kind of leaf spot that can be seen in the presence of the fungi *Pseudocercospora vitis*. Lesions found due to this disease are dull red to brown in color with irregular patches. Later these lesions turn black. The fungi *Phaeoacremonium aleophilum* and *Phaeomoniella chlamydospora* are the pathogen of Esca that is popularly known as Black Measles. This disease is also known as grapevine trunk disease. Interveinal striping that forms a tiger strip pattern is the main symptom of this disease. The color of the lesions is yellow-brown or red-brown. The fungi *Guignardia bidwellii* is the pathogen of Black Rot. The lesions are small brown circular spots surrounded by black margins. Figure 1 shows healthy grape leaf and leaf affected by Esca, Isariopsis, and Black Rot respectively.

Manual identification of these diseases is a tedious and time-consuming task. It is not always possible for farmers to correctly detect a particular disease without domain experts. Sometimes, for the domain specialist, it becomes too tough to distinguish the diseases because of various complications. More than one disease can have the same symptoms or a particular disease can have various symptoms. These things can be eliminated through the application of an automated model. From the discussion of the literature review, it has also been found that the accuracy of the models was not so high, and the feature vector's dimension is also high. So there is still a need for improvement in this area. Here, we have developed an automated model to recognize various diseases of plants from leaf images.

Machine Learning (ML) [2] is the central idea of any automated model. The present study is also based on ML technology. Discrete Wavelet Transform (DWT) has been applied to extract the most important pattern from the images. Local Binary Pattern (LBP) has also been used as a texture feature descriptor. The novelty of this study is the use of a minimum number of features from the spatial and frequency domain together. The main contribution of this study is to make a minimum set of features with high efficiency using the trial and error method.

In this domain, there are some research studies developed by the researchers have been discussed now. Hasan et al. [6] developed a model for grape leaf disease recognition using Convolutional Neural Network (CNN). They used the Plant Village data set of grape leaves. Three diseases of grapes were identified. The accuracy rate of their model was 91.37%. The same type of diseases of grapes were classified by Sonar et al. [7]. They achieved 93.03% accuracy from Support Vector Machine

(SVM). A lightweight CNN model was developed by Lin et al. [8]. In this model, the accuracy was 86.29%. Padol et al. [9] introduced a model for the same using SVM. Image segmentation was used in their study. They worked on classifying two types of diseases Downy Mildew and Powdery Mildew. The efficiency of the model was 88.89%. A model for identifying tomato leaf disease was introduced by Sabrol et al. [10]. They have also used image segmentation. Then after extracting features, a decision tree classifier was used and the accuracy rate was 78%. Ghosh et al. [11] proposed an automated model to recognize plant diseases using deep learning. They worked on the two species of potato and grape. Using CNN the overall efficiency was 87.47 and 91.96% for potato and grape, respectively. The same authors worked on automated disease detection on apple leaf [12] using ANN. Authors in [13] worked on Plant disease detection using drones in precision agriculture. The Phalaenopsis seedling disease detection model was proposed by Huang [14]. Three types of diseases were recognized by this model. Back Propagation Neural Network (BPNN) has been used with an average efficiency of 89.6%. Authors in [15] worked on automated plant disease classification using a vision transformer. This model used the concept of deep learning. A 15-layer CNN model was introduced by Ferdouse et al. [16] to recognize tomato leaf diseases. However, accuracy was not significant. It was only 76%. A model to detect Downy Mildew disease present in grapes has been proposed by Kole et al. [17] based on the fuzzy importance factor. The success rate of the model was 87.09%.

Various research studies on automated plant disease detection have been discussed above. But there are some drawbacks to each one due to which research is still going on in this domain. The aim of our study is to develop an automated model for recognizing grape diseases that overcome the limitations of existing models.

Till now, we have given an introduction and literature review on automated disease detection through leaf images. The remaining sections of the study have been organized as follows. Section 2 describes the proposed model and the experimental setup is given in part 3. The experimental findings of our study have been thoroughly analyzed in Sect. 4. In the end, the conclusion has been drawn.

## 2 Suggested Model

Our proposed model consists of some sequence of steps. Each step has been described below.

### 2.1 *Image Acquisition*

All the affected and healthy leaf images used in this study have been gathered from the most popular Plant Village data set [18]. This data set is one of the most popular data

sets, available in the public domain containing several disease-affected leaf images of different crops and fruits. It also contains healthy leaf images of each category.

## 2.2 Image Pre-processing

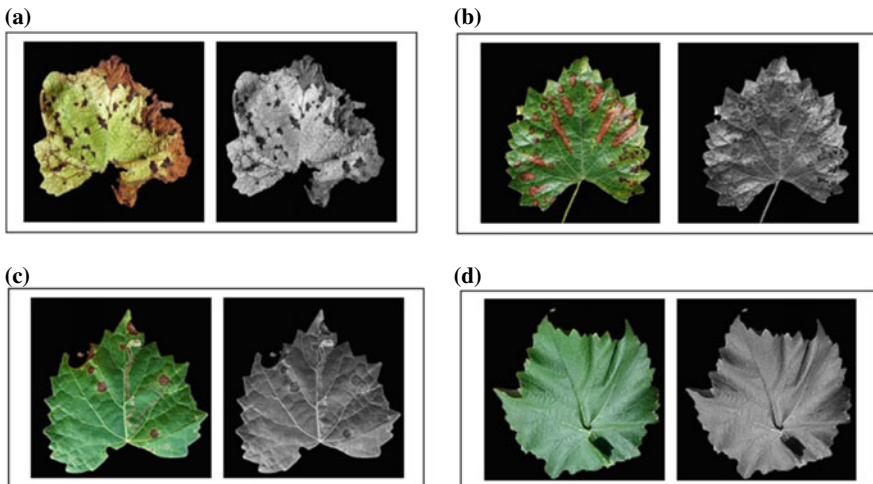
To obtain better performance, some pre-processing on the images is needed. This is the next phase in our research work. The data set contains RGB color images. All these images have been converted to grayscale images for the feature extraction step. The mathematical equation for conversion into a grayscale image has been shown in Eq. 1 [19]. The outcome of this step has been shown in Fig. 2.

$$G = \alpha + \beta + \gamma \quad (1)$$

where  $\alpha = 0.2989 * R$ ,  $\beta = 0.5870 * G$  and  $\gamma = 0.1140 * B$ .

## 2.3 Image Segmentation

Disease-affected regions of an image contain the most useful information in order to detect diseases from the image. To extract only the disease-affected region from the whole image, segmentation has been done in this study. Image segmentation is



**Fig. 2** Outcome of image pre-processing of each disease type and healthy leaf. **a**, **b**, **c**, and **d** represent Isariopsis, Esca, Black Rot, and Healthy Leaf, respectively, with their corresponding grayscale images

nothing but the grouping of pixels together with similar attributes. Here, K means clustering [2] has been used for image segmentation. The outcome of image segmentation for each type of disease has been shown in Fig. 3. These figures show only the disease-affected area which contains more useful information for further processing. The number of pixels in the affected regions has been computed and taken as a feature.

## 2.4 Feature Extraction

This study presents a combination of some spatial features and frequency domain features. LBP and color features have been used as spatial features. DWT has been used as a frequency domain feature. It is done on a grayscale image.

**Discrete Wavelet Transform** DWT [20] is one of the most important transformations that has been applied extensively in image processing. Information present in an image after DWT can be divided into approximation and details discrete components. Application of the high- and low-pass filters divides the image into high- and low-frequency components, respectively. The detail coefficients carry the high-frequency elements, while the low-frequency portion is known as approximation coefficients. The overall trend of pixel values can be obtained from approximation coefficients (LL sub-band), whereas the detail coefficients represent horizontal (HL sub-band), vertical (LH sub-band), and diagonal (HH sub-band) coefficients. All these four sub-bands can be obtained from the following equations:

$$LL = \psi(a, b) = \psi(a)\psi(b) \quad (2)$$

$$LH = \chi^H(a, b) = \chi(a)\psi(b) \quad (3)$$

$$HL = \chi^V(a, b) = \psi(a)\chi(b) \quad (4)$$

$$HH = \chi^D(a, b) = \chi(a)\chi(b) \quad (5)$$

where  $\chi^H, \chi^V$  and  $\chi^D$  measure intensity variations along horizontal, vertical, and diagonals.

The DWT of an image  $f(a, b)$  of size  $E \times F$  can be obtained from the following equations:

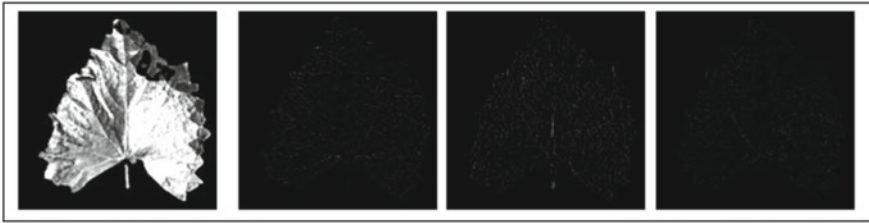
$$W_\psi(j_0, e, f) = \frac{1}{\sqrt{EF}} \sum_{a=0}^{E-1} \sum_{b=0}^{F-1} f(a, b) \psi_{j_0, e, f}(a, b) \quad (6)$$

$$W_{\chi^i}^i(j, e, f) = \frac{1}{\sqrt{EF}} \sum_{a=0}^{E-1} \sum_{b=0}^{F-1} f(a, b) \chi_{j, e, f}^i(a, b) \quad (7)$$



**Fig. 3** Outcome of the image segmentation of each disease type. **a–d** represent Esca with its corresponding disease-affected area, **e–h** represent Isariopsis with its corresponding disease-affected area, **i–l** represent Black Rot with its corresponding disease-affected area





**Fig. 4** Outcome of the first level approximation, horizontal, vertical, and diagonal coefficients, respectively, of a sample image of Esca

where  $i = H, V, D$ .

The approximation coefficient (LL sub-band) can be further decomposed into the next level of transformation and the same four respective sub-bands can be obtained. In this study, three level of decomposition of the images has been done to obtain the coefficients. The result of the first level decomposition has been shown in Fig. 4. Four figures that have been shown in Fig. 4 represent the first-level approximation, horizontal, vertical, and diagonal coefficients, respectively.

**Local Binary Pattern** Each image carries some patterns based on different characteristics like smoothness, roughness, etc. This is referred to as image texture which is based on spatially structured pixel intensity values. There are so many texture feature descriptors (like Histogram of oriented gradients, Pyramid histogram of oriented gradients, Local Binary Pattern (LBP) [21], Gray-Level Co-occurrence Matrix (GLCM) [20], etc.) that are used extensively in texture classification. In this study, the LBP texture feature has been taken for classification. LBP has been applied to segmented images. Figure 5 represents the LBP of different types of diseases and healthy leaves after segmentation.

An image can be represented locally through an LBP feature descriptor. In the present research work, a 5\*5 neighborhood with 16 sample points has been taken to extract the LBP code. Equation 8 has been used to represent the decimal value of the LBP code located at pixel position  $(p_c, q_c)$ .

$$LBP_{S,R}(p_c, q_c) = \sum_{s=0}^{S-1} f(i_s - i_c)2^s \tag{8}$$



(a) Isariopsis (b) Esca (c) Black Rot (d) Healthy Leaf

**Fig. 5** a LBP of Isariopsis. b LBP of Esca. c LBP of Black Rot. d LBP of Healthy Leaf

Here,  $(S, R)$  has been used to represent  $S$  sampling points within the neighborhood of radius  $R$ . The notation  $i_s$  has been used to represent gray values of those  $S$  sampling points and  $i_c$  has been used to represent gray values of the central pixel within each neighborhood. The energy and entropy have been computed from this feature descriptor.

## 2.5 Classification

After completion of all the above steps classification has been done using ANN. There are three hidden layers, one output layer, and one input layer that have been used in this study.

## 3 Experimental Setup

Now, the next phase is to analyze the efficiency of our model. This section presents a brief illustration of the data set, accuracy measurement indices, and a comparative study of the suggested model with others already in use.

**Data Set:** Plant Village data set [18] is one of the most popular benchmark data sets which is available in the public domain and contains a huge collection of disease-affected leaf images of several crops and fruits. For training and evaluating the model, images of disease-affected and unaffected grape leaves have been used in this study. In this data set, there are 4063 RGB grape leaf images of dimension  $256 \times 256$ , out of which the number of healthy leaves is 423. The presentation of this data set is given in the Table 1. The train–test ratio of the data set has been taken as 80:20.

**Standard Indexes:** In this study, the performance of the model has been measured through standard indices like Precision, Recall, and F1-score. These indices work well for the imbalanced data set. Mathematical equations of these three indices have been given in Eqs. 9, 10 and 11.





$$\text{Precision} = \frac{TP}{(TP + FP)} \quad (9)$$

$$\text{Recall} = \frac{TP}{(TP + FN)} \quad (10)$$

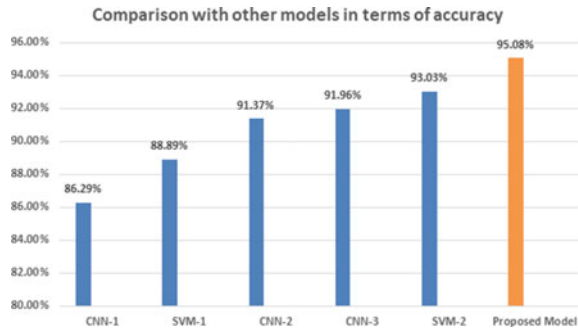
$$F1\_Score = \frac{2 * (\text{Precision} * \text{Recall})}{(\text{Precision} + \text{Recall})} \quad (11)$$

where  $TP$ ,  $FP$ , and  $FN$  are the acronyms for True Positive [22], False Positive [22], and False Negative [22], respectively.

**Table 1** Presentation of the data set. Total number of healthy and unhealthy grape leaf was 4063. Train–test ratio is 80:20

Disease name	Image samples for each class	Sample size	Sample size for training	Sample size for testing
Isariopsis		1076	856	220
Black rot		1180	934	246
Esca		1384	1120	264
Grape healthy		423	340	83

**Fig. 6** Accuracy comparison of our model with CNN-1 [8], SVM-1 [9], CNN-2 [6], CNN-3 [11] and SVM-2 [7]







**Comparison with other models:** This section compares our model with state-of-the-art models. A corresponding graphical representation has been shown in Fig.6. In all the models, grape leaf disease has been used. Figure 6 shows that our model outperforms all the existing models shown in the graph.

### 4 Experimental Findings

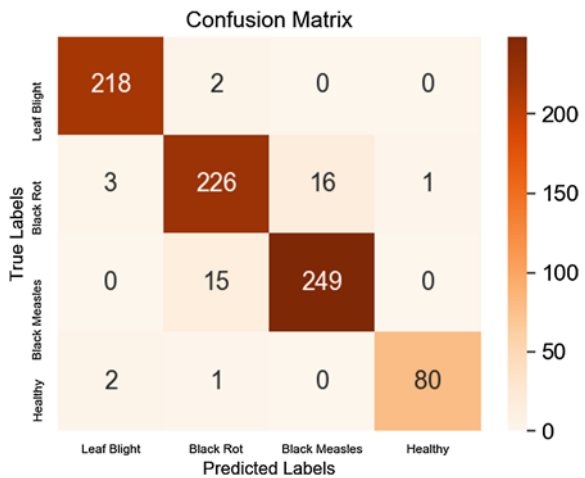
The experimental findings of our study have been analyzed in this section. The overall efficiency of our model is 95.08%. Precision, Recall, and F1-score have been used to measure the efficiency of the study. From Table 2 it is clear that the maximum Precision has been achieved in the case of a healthy leaf, showing low false positive

**Table 2** Details of three performance measurement metrics in each category

Disease name	Image sample for each class	Precision	Recall	F1 score
Isariopsis		0.98	0.99	0.98
Black rot		0.93	0.92	0.92
Esca		0.94	0.94	0.94
Healthy leaf		0.99	0.96	0.98

rates. On the other hand, the highest Recall has been achieved in the case of Leaf Blight, showing low false negative rates. In the case of Black Rot, the lowest Precision and Recall have been achieved. This indicates a high false positive and false negative rate. This is also clear from the confusion matrix shown in Fig. 7. Diagonal entries in the confusion matrix of Fig. 7 represent total true positive cases in each class. The sum of each row excluding the true positive value represents the total number of false negative values in each case. However, the sum of each column excluding the

**Fig. 7** Confusion matrix of our model with leaf blight, black rot, and black measles along with healthy leaf



true positive value represents the total number of false positive values in each case. For example, the total number of true positive cases that occurred in Leaf Blight is 218. False positive in this case is  $(3 + 2) = 5$  and false negative is only 2.

## 5 Conclusion and Future Scope

An automated model to recognize various diseases of plants from leaf images has been developed in this study. Healthy and disease-affected grape leaf images have been used for classification. Image segmentation has been applied to obtain disease-affected regions using K means clustering. DWT has been used to take out the most appropriate features along with LBP feature descriptors. These feature combinations in the spatial domain and frequency domain give better results in terms of accuracy. It has been seen that our model achieved 95.08% accuracy which outperforms all the existing models shown in Fig. 6. One of the main drawbacks of our model is that only plain background has been considered. An automated disease detection model with complex background can be interesting research work.

## References

1. Leonberger K, Jackson K, Smith R, Gauthier N (2016) Plant diseases
2. Kaur S, Pandey S, Goel S (2018) Plants disease identification and classification through leaf images: a survey. *Arch Comput Methods Eng* 26:01
3. Mehmet F (2017) Occurrence of isariopsis leaf spot or blight of vitis rupestris caused by pseudocercospora vitis in Turkey
4. Mugnai L, Graniti A, Surico G (1999) Esca (black measles) and brown wood-streaking: two old and elusive diseases of grapevines. *Plant Dis* 83:404–418
5. Jermini M, Gessler C (1996) Epidemiology and control of grape black rot in southern switzerland. *Plant Dis* 80:322–325
6. Arie Hasan M, Riana D, Swasono S, Priyatna A, Pudjiarti E, Prahartiwi LI (2020) Identification of grape leaf diseases using convolutional neural network. *J Phys: Conf Ser* 1641(1):012007
7. Sonar PS, Wankhade NR (2022) Grape leaf disease identification using machine learning techniques. *Int Res J Mod Eng Technol Sci*
8. Lin J, Chen X, Pan R, Cao T, Cai J, Chen Y, Peng X, Cernava T, Zhang X (2022) Grapenet: a lightweight convolutional neural network model for identification of grape leaf diseases. *Agriculture* 12(6)
9. Padol PB, Yadav AA (2016) Svm classifier based grape leaf disease detection. In: 2016 conference on advances in signal processing (CASP), pp 175–179
10. Sabrol H, Kumar S (2016) Intensity based feature extraction for tomato plant disease recognition by classification using decision tree. *Int J Comput Sci Inf Secur* 14:622–626
11. Ghosh A, Roy P (2021) AI based automated model for plant disease detection, a deep learning approach, pp 199–213
12. Ghosh A, Roy P (2022) A leaf image-based automated disease detection model. In: Saraswat M, Sharma H, Balachandran K, Kim JH, Bansal JC (eds) *Congress on Intelligent systems*. Springer Nature, Singapore, pp 863–875
13. Chin R, Catal C, Kassahun A (2023) Plant disease detection using drones in precision agriculture

14. Huang K-Y (2007) Application of artificial neural network for detecting phalaenopsis seedling diseases using color and texture features. *Comput Electron Agric* 57(1):3–11
15. Borhani Y, Khoramdel J, Najafi E (2022) A deep learning based approach for automated plant disease classification using vision transformer. *Sci Rep* 12
16. Ferdouse Ahmed Foysal M, Shakirul Islam M, Abujar S, Akhter Hossain S (2020) A novel approach for tomato diseases classification based on deep convolutional neural networks. In: Shorif Uddin M, Chand Bansal J (eds) *Proceedings of international joint conference on computational intelligence*. Springer, Singapore, pp 583–591
17. Kole DK, Ghosh A, Mitra S (2014) Detection of downy mildew disease present in the grape leaves based on fuzzy set theory. In: Kundu MK, Mohapatra DP, Konar A, Chakraborty A (eds) *Advanced computing, networking and informatics*, vol 1. Springer International Publishing, Cham, pp 377–384
18. Mohanty SP, Hughes DP, Salathé M (2016) Using deep learning for image-based plant disease detection. *Front Plant Sci* 7:1419
19. Wu SG, Bao FS, Xu EY, Wang YX, Chang YF, Xiang QL (2007) A leaf recognition algorithm for plant classification using probabilistic neural network
20. Siravenha AC, Carvalho SR (2016) Plant classification from leaf textures. In: *2016 international conference on digital image computing: techniques and applications (DICTA)*, pp 1–8
21. Huang D, Shan C, Ardabilian M, Wang Y, Chen L (2011) Local binary patterns and its application to facial image analysis: a survey. *IEEE Trans Syst Man Cybern Part C* 41:765–781
22. Fawcett T (2006) An introduction to roc analysis. *Pattern Recognit Lett* 27(8):861 – 874. *ROC Analysis in Pattern Recognition*

# Computer Vision Assisted Bird–Eye Chilli Classification Framework Using YOLO V5 Object Detection Model



Abhijit, S. Akhil, V. K. Akshat Kumar, Ben K. Jose, and K. M. Abubeker

**Abstract** A computer vision-based bird-eye chilli sorting system has become essential due to the rising demand for quality verification and effective sorting of chilli products. The quality of bird-eye chilli, or ‘kantari mulaku’, directly affects the flavour and is a highly sought-after ingredient in many different cuisines around the globe. Computer vision technology-based automated sorting systems can precisely recognize and categorize chillies based on various quality factors like size, shape, colour, and texture. Additionally, computer vision-based sorting systems are perfect for large-scale production facilities because they can constantly run for prolonged periods with little supervision. This paper describes a method for categorizing bird-eye chilli using a 3 DOF robotic manipulator and the You Only Look Once-V5 object recognition algorithm. Images of bird-eye chillies in various orientations and settings make up the dataset used in this research. This dataset was used to train the algorithm, and the model successfully identified and classified bird-eye chilli. The chillies were then grabbed by a robotic manipulator and sorted according to their degree of maturity. The proposed approach obtained an average precision of 0.90 and a mAP of 0.94. Chillies can be graded with high precision, consistency, and efficiency using a robotic manipulator, which boosts output and lowers human error rates. The developed YOLO V5 framework is deployed in Raspberry Pi 4B graphical processing unit, verifying the efficacy. The outcomes of this work show how successfully classifying bird-eye chilli using YOLO V5 can be applied in the food and agricultural industries.

**Keywords** Bird-eye chilli · Computer vision · Artificial intelligence · YOLO

---

Abhijit · S. Akhil · V. K. A. Kumar · B. K. Jose · K. M. Abubeker (✉)

Department of Electronics and Communication Engineering, Amal Jyothi College of Engineering, Kanjirapally, Kerala, India

e-mail: [kmabubeker82@gmail.com](mailto:kmabubeker82@gmail.com); [kmabubeker@amaljyothi.ac.in](mailto:kmabubeker@amaljyothi.ac.in)

## 1 Introduction

One of the most significant challenges is meeting the world's growing population with enough sustenance. The time and money producers spend getting their fresh fruits and veggies to market are primarily concentrated on harvesting, processing, and packaging. Products must be sorted and graded in the processing and manufacturing industries for business and production reasons. The demand for automatic screening and classification systems has increased recently to reduce waste during gathering, manufacturing, and distribution [1]. Among the many names for the bird-eye chilli known as *Capsicum annuum*, or kanthari mulaku is one of the most well-known. It is used as a flavouring and hunger stimulant in cooking and in traditional plant medicine, particularly in South Asia. Its medical advantages include: lowering blood pressure, and cholesterol levels, treating and preventing cardiac problems, assisting with weight reduction, clearing the airways, and stimulating the digestive system [2]. A quicker metabolism and lower cholesterol level help reduce the risk of heart failure, vessel blockage, and other cardiovascular problems [3]. Bird's-eye chilli, particularly, has been shown to kill cancer cells without affecting healthy ones. Bird's-eye stew has numerous health benefits, including protecting eyesight owing to its high vitamin B2 content. Because of these qualities make bird-eye chilli more desirable than regular green chillies. The worldwide price edge for high-quality goods has increased the value of picking, organizing, and classifying bird-eye chillies. Consumers are likelier to buy a product with a consistent look and feel. Manually picking and arranging chilli peppers is a laborious process. Using qualified examiners to select and sort chillies is one approach; however, this technique is prone to bias. Due to their curative qualities, bird's-eye chillies are in great demand internationally.

Smart farming, which uses various automated systems to boost output and quality while decreasing the need for human intervention, is one example of automation in the agricultural sector [4]. Since bird's-eye chillies are small, gathering them automatically presents a significant task. Chillies, both red and green bird's-eye, are still graded and sorted today, but the process is entirely physical and based on ocular inspection. The limitations of the human vision system, witness weariness, and differences in opinion regarding quality all work against the reliability of this approach [5]. The time it takes to sift through the chillies and determine their quality can impact the final product. Before the chillies can be correctly organized, this must be expected by employing a process and using instruments for early decision-makers. A quicker post-harvest processing system with a low mistake rate is required to help normalize and equalize opinions on the quality of classification and chillies rating among all stakeholders. Image analysis is one alternative technology that can be used to evaluate things like height, colour, substance, bodily power, scent, and handling. The primary benefits of image processing that have been stressed in workplaces and sectors are mechanization, quick filtering, and reduction of human mistakes. The suggested sorting system, which uses computer vision, is anticipated to provide a permanent and effective answer for separating and making early decisions regarding



the grade of red jalapenos. The following are efforts made by the suggested computer vision system running on a Raspberry Pi 4B computer:

- Development of a YOLO V5 framework for the real-time detection of red and green bird-eye chillies using a computer vision framework.
- Development of an automated sorting machine using Raspberry Pi 4B GPU hardware.

## 2 Related Work

Classifiers like the Support Vector Machine (SVM) and the k-Nearest Neighbour (k-NN) are just two examples of how machine learning is applied outside of agricultural tracking to handle categorization issues in picture processing and object recognition [6]. In addition, machine learning models have demonstrated remarkable success in a variety of contexts when it comes to accurate object classification. Even more so, they have enormous analytical promise in agribusiness. Automating technologies to improve productivity and reduce labour costs is a pressing need in today's factories, where organizing products is a tedious and time-consuming process. Automatic object classification based on hue and height was a topic of discussion by Abu Salman Shaikat et al. [7]. Computer Vision (CV) arranges objects by colour, while the Haar cascade technique organizes them by height. To accomplish this, an artificial limb with six degrees of freedom is used in conjunction with computer vision.

Technologies that could improve phenotyping and tracking total plant development are the focus of a new study by Chanchal Gupta et al. [8]. In this case, the height and breadth of jalapeno plants in the yard are measured using a real-time picture analysis method. The RMSE determines the quality of the Open CV modules and the PyCharm Editor. Md. Abdullah et al. [9] argue for using an automatic method to classify objects according to their hue, form, and size. This study uses a PixyCMU video sensor to identify objects based on their hue. The outline function determines the object's dimensions and form. To improve the efficiency of the pick-and-place sorting process, an autonomous arm equipped with a stepper motor and other necessary components has been created. Lennon Fernandes et al. [10] present a robotic arm-based mechanization for speedy and accurate colour and shape-based object categorization. The modified border fill method is used to determine the outlines, and the Douglas-Peucker algorithm is used to identify the forms within the boundaries.

Using convolutional neural network designs, Juan Daniel et al. [11] created a method to improve the effectiveness of quality assurance checks, particularly for identifying bruises. The system uses a combination of near-infrared and colour CMOS sensors, each lit by a different light. A computerized tomato sorting system was created to eliminate the human mistake that occurred when physically separating tomatoes by colour. Two TCS3200 RGB Colour Monitors are used in the suggested system to determine whether or not a tomato is ready for consumption. Colour, form, and HOG (History of Gradient) are just some image processing characteristics that can be used to categorize fruits and veggies [12].

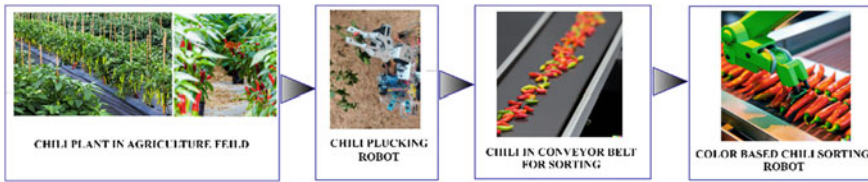
Since farming accounts for the primary source of income in India, improvements in agricultural technology are particularly pressing there. This could improve farm productivity while reducing expenses [13]. Sorting algorithms have a high rate of erroneous positive detections, AI functions are severely restricted, and there is no readily replaceable colour sensor, just a few restrictions. We built a YOLO V5 framework to overcome these obstacles and deployed it in Raspberry Pi 4B computer to organize bird's-eye chillies in real-time. The developed computer vision-assisted robotic system uses an autonomous tool to inspect and grade chillies as they move along a moving line for differences in hue.

### 3 Methodology

Research in computer vision and machine learning has lately focused on bird's-eye chillies because of their widespread appeal and distinctive qualities. Specifically, bird's-eye chillies have been categorized using the YOLO V5 object recognition model's size, form, and colour analysis. YOLO is a cutting-edge paradigm for object recognition that has found widespread application in research and commercial settings [14]. YOLO is built to be quick and precise, setting it apart from other object recognition algorithms and making it suitable for real-time uses like driverless cars and monitoring systems [15]. Counting bird's-eye chillies is recognizing and tallying such peppers through machine learning and computer vision. In this article, we'll look into using the YOLO object recognition algorithm to tally bird's-eye chillies.

The YOLO object recognition algorithm for counting bird's-eye chillies begins with generating a labelled image collection. This is done by taking images of bird's-eye chillies at various phases of development and annotating them with bounding frames that pinpoint the chillies within the image. Using this data, we train the YOLO algorithm to identify bird's-eye chillies in images. A labelled image collection is needed for YOLO to be useful for bird's view chillies classification. Ideally, the collection would include many different types of chillies images, each annotated to correctly identify the size, colour, and form of the pepper depicted. Both human labelling and current annotation tools that autonomously identify and name items in images can be used to make comments. The YOLO model can be taught in a deep learning system like TensorFlow once a labelled sample is made accessible.

During training, a deep neural network is fed the information and taught to identify the relevant Chillies' characteristics for categorization. A high degree of precision on the training and confirmation data is the goal of this procedure, which is done repeatedly until it is reached. The learned algorithm can then be used to label fresh pictures of chillies. The YOLO model accepts a picture as input and outputs a collection of bounding boxes that identify the locations of items in the image. The model supplies a likelihood value for each enclosing area that represents the certainty of the discovery. Despite the presence of other items in the frame, the YOLO model is still able to identify bird's-eye chillies accurately. Farmers who want to keep an eye on their chillies plants and know how much they'll produce will find this helpful aid.



**Fig. 1** YOLO powered bird-eye chillies classification and sorting system using computer vision and Raspberry Pi 4B computer

Counting bird's-eye chillies with the YOLO approach is more efficient for growers than traditional hand techniques.

### 3.1 Architecture of the Proposed System

The proposed mechanism is depicted in detail in Fig. 1. The system's computer vision technology includes colour recognition and the separation of green and red chillies via a YOLO-powered architecture. The device can conduct classification using a motorized tool and a mechanical actuator operated by a Raspberry Pi 4B. We suggest an autonomous tool for the farming sector that can automatically grade and arrange chillies by colour. The proposed system uses a YOLO architecture for quick red and green bird's-eye recognition using computer vision. Controlling the location of an autonomous tool is a frequent application for the Raspberry Pi 4B, one of a series of tiny single-board processors. Using a set of 5 reference photos, the system compares the real-time photographs to locate each chillie.

Figure 2 illustrates the labelling and training procedures required to generate data sets. To train a classification model, we must first gather many pictures of chillies and manually name each one by drawing a rectangle around each one with labelling software. Each picture with its respective class labelled in red and green chillies is turned into a text file. Then, the Google Colab tool is used to teach these data. Following the completion of training, a weight\_chilli weights file is produced.

We have used 739 pictures of red and green chillies to build a collection for this algorithm. Using the Labelling program, we changed each picture and assigned it a new category description. The labelled images will be stored in the specified place and transformed into a Word document without further intervention, as the labelling process will automatically generate both files. An archive containing both the Word document and its accompanying photographs is created. The compressed file is submitted to a Google Drive subdirectory, and the images are trained with the Google Colab GPU platform [16]. A collection by training these images and loading the required tools into Google Colab supports GPU processing. To make a comparison between the recorded image and the learned dataset, the former is used.

In conclusion, using the YOLO object identification method, bird's-eye chillies can be sorted by size, colour, and overall look. The YOLO model could be a valuable

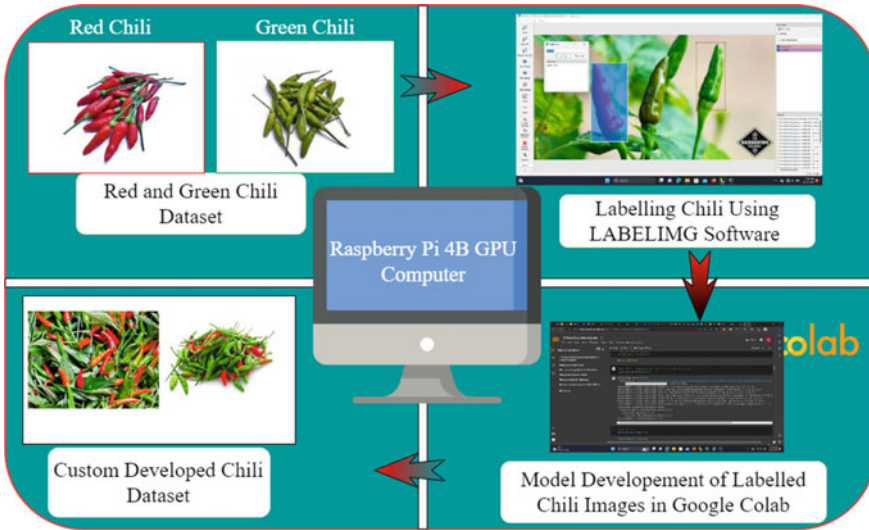


Fig. 2 Control flow of dataset labelling and dataset creation

tool for keeping track of food quality and figuring out how long fragile things can be kept by taking advantage of annotated datasets and deep learning frameworks. It has a lot of possible applications, including in veggie farming, food processing, and food preservation [17].

### 4 Experimental Setup

It is critical to develop a conveyor-based automated system for sorting. Hand sorting is more expensive because of the time and tools needed to complete the task. Therefore, overall expenditures will rise. Many local companies have begun adopting automation to increase efficiency and cut costs.

The sorting machine comprises a conveyor belt, a stepper motor to turn the belt, and a camera that captures photos of the chillies. The camera is stabilized by a stand and placed above the sorting engine. The precision suffers because of the shaking. Red and green peppers are separated using a camera and a Raspberry Pi to distinguish between the two. The Raspberry Pi is the central component of the sorting system and is responsible for managing all of the data used in the process. The CSI camera scans chillie peppers as they move along the conveyor line. The red chillies go to the left, the green chillies go to the right, and the defective chillies and other goods move straight, all thanks to the Raspberry Pi 4B that sends signals to the sorting motor. And with the same camera, we can do a split tally of both red and green chillies. Real-time images are compared to a dataset to determine the chillies' quality. Size, shape, colour, and physical deformations are just some of the measures of physical

characteristics considered when assessing chilli for quality. Previous images are used to identify and categorize the real-time captured images into red and green chillies. Bounding bars are used to locate the chilli peppers. The numbers of red and green chillies were determined by counting the contents of their corresponding bounding boxes.

A computer vision camera is used to identify the chillies as they move along the conveyor belt. A robotic manipulator classifies these chillies by colour. After a quality review of the detection is performed, the previously trained dataset can identify red and green chillies. Low-quality chillies are passed through a conveyor line and eliminated, while high-quality red and green chillies are sorted to separate piles.

In Fig. 3, red chillies are detected using bounding boxes, which can be seen around each identified chillie with their respective colour labelled on top. This is done by comparing the real-time image captured with the pre-trained models; about 739 images were trained. It also gives information about the total number of chillies present in each image and also gives the exact number of green and red chillies present in each image.

From Table 1, we can identify the red chillies and green chillies and their accuracy. The first column shows the number of chillies in an image, the second column gives the number of chillies identified in each image, and the last column shows the accuracy percentage. We can understand that the accuracy of chillies identified decreases with the total number of chillies present. If the number of chillies is less, the system could give an accuracy of about 100%. The decrease in accuracy may be due to the broken-off chillies or physically damaged chillies; the blurred images can also cause a decrease in accuracy.

At the first attempt, the total number of red chillies present in the images was 15, and the number of chillies identified was 13, which gives an accuracy of 86.66%. For the green chillies in its first attempt, the total number of green chillies present is about 14, out of which 13 are identified, and this detection gives an accuracy of 92.85%. At the fourth attempt of both red and green chillies, the total number of chillies is less, and therefore, the number of identified chillies is more or almost all chillies are identified, which gives a high accuracy percentage. For the red chillies, we get an average accuracy of 94.39%, and for green chillies, the average accuracy rate is about 94.365%.

## 5 Conclusion

This paper exhibits the design and development of a computer vision-based robotic manipulator for the agriculture industry. It uses computer vision technology that uses the YOLO V5 framework for real-time detection of red and green bird-eye chillies. The architecture of the proposed system uses a Raspberry Pi 4B to control the complete identification and sorting process. The real-time identified data is compared with the trained database by the YOLO framework. In comparison, red and green



**Fig. 3** Detected images with bounding box having information about the total number of chillies and number of chillies based on their colour respectively

**Table 1** Accuracy of bird-eye chillies detection

No. of attempts	No. of red chillies			No. of green chillies		
	Actual no. of chillies	No. of identified chillies	Accuracy (%)	Actual no. of chillies	No. of identified chillies	Accuracy (%)
1	15	13	86.66	14	13	92.85
2	11	10	90.90	13	11	84.61
3	9	9	100	8	8	100
4	6	6	100	5	5	100
Average accuracy	94.39%			94.365%		

chillies are identified; the robotic manipulator sorts them. The servo motor in the manipulator helps in the sorting process; the Raspberry Pi controls the servo motors in the manipulator it acts as the control unit and sorts the chillies based on the identified colour. The systems perform the sorting of red and green chillies to a predefined place and also do a quality check using the same chillies detection method. When implemented, this system could help farmers do the tedious task without human interference for hours. This technology without the Raspberry Pi architecture could also benefit the farmers as it aids in keeping an eye on the number of chillies grown. This system can be modified into a fully automated robotic manipulator that can detect chillies using computer vision technologies and identify them as red and green chillies using the YOLO V5 framework. The proposed system possesses a huge scope in further development into a controlled agricultural robot that could move around, sort and pluck chillies.

## References

1. Mahendran R, Vino SA, Anandakumar S (2016) Fundamentals of computer vision system for sorting and grading of food products. Reference Module in Food Science, Elsevier
2. Kenig S, Baruca-Arbeiter A, Mohorko N, Stubelj M, Černelič-Bizjak M, Bandelj D, Jenko-Pražnikar Z, Petelin A (2018) Moderate but not high daily intake of chillies pepper sauce improves serum glucose and cholesterol levels. *J Funct Foods*, 44:209–217
3. Yamani N, Musheer A, Gosain P, Sarfraz S, Qamar H, Waseem MM, Arshad MS, Almas T, Figueredo V (2021) Meta-analysis evaluating the impact of chillies-pepper intake on all-cause and cardiovascular mortality: A systematic review. *Ann Med Surg* 70
4. Shaikh TA, Rasool T, Lone FR (2022) Towards leveraging the role of machine learning and artificial intelligence in precision agriculture and smart farming. *Comput Electron Agric* 198
5. Brosnan T, Sun D-W (2004) Improving quality inspection of food products by computer vision—a review. *J Food Eng* 61(1):3–16
6. Tace Y, Tabaa M, Elfilali S, Leghris C, Bensag H, Renault E (2022) Smart irrigation system based on IoT and machine learning. *Energy Rep* 8(Supplement 9):1025–1036
7. Shaikat AS, Akter S, Salma U (2020) Computer vision based industrial robotic arm for sorting objects by color and height. *J Eng Adv* 1(04):116–122. <https://doi.org/10.38032/jea.2020.04.002>
8. Gupta C, Tewari VK, Machavaram R, Shrivastava P (2021) An image processing approach for measurement of chillies plant height and width under field conditions. *J Saudi Soc Agric Sci* 21. <https://doi.org/10.1016/j.jssas.2021.07.007>
9. Abdullah-Al-Noman M, Eva AN, Yeahyea TB, Khan R (2022) Computer vision-based robotic arm for object color, shape, and size detection. [journal.umy.ac.id/index.php/jrc](http://journal.umy.ac.id/index.php/jrc)
10. Fernandes L, Shivakumar BR (2020) Identification and sorting of objects based on shape and colour using robotic arm. <https://doi.org/10.1109/ICISC47916.2020.9171196>
11. Arango JD, Staar B, Baig AM, Freitag M Quality control of apples by means of convolutional neural networks— Comparison of bruise detection by color images and near-infrared images. <https://doi.org/10.1016/j.procir.2021.03.043>
12. Utai K, Nagle M, Hämmerle S, Spreer W, Mahayothee B, Müller J (2019) Mass estimation of mango fruits (*Mangifera indica* L., cv. ‘Nam Dokmai’) by linking image processing and artificial neural network. *Eng Agric, Environ Food* 12(1):103–110. ISSN 1881–8366. <https://doi.org/10.1016/j.eaef.2018.10.003>

13. Javaid M, Haleem A, Singh RP, Suman R (2022) Enhancing smart farming through the applications of Agriculture 4.0 technologies. *Int J Intell Netw* 3:150–164. ISSN 2666–6030. <https://doi.org/10.1016/j.ijin.2022.09.004>
14. Jiang C, Ren H, Ye X, Zhu J, Zeng H, Nan Y, Sun M, Ren X, Huo H (2022) Object detection from UAV thermal infrared images and videos using YOLO models. *Int J Appl Earth Obs Geoinformation* 112:102912. ISSN 1569–8432. <https://doi.org/10.1016/j.jag.2022.102912>
15. Yan J, Wang Z (2022) YOLO V3 + VGG16-based automatic operations monitoring and analysis in a manufacturing workshop under Industry 4.0. *J Manuf Syst* 63:134–142. ISSN 0278–6125. <https://doi.org/10.1016/j.jmsy.2022.02.009>
16. Carneiro T, Medeiros Da Nóbrega RV, Nepomuceno T, Bian G-B, De Albuquerque VHC, Filho PPR (2018) Performance analysis of google colaboratory as a tool for accelerating deep learning applications. *IEEE Access* 6:61677–61685. <https://doi.org/10.1109/ACCESS.2018.2874767>
17. Likith S, Reddy BR, Sripal Reddy K (2021) A smart system for detection and classification of pests using YOLO AND CNN techniques. In: 2021 International conference on computational performance evaluation (ComPE), Shillong, India. pp 049–052. <https://doi.org/10.1109/ComPE53109.2021.9752185>



# An Effective Grid Connected Multi Level Inverter Based Hybrid Wind and Solar Energy



G. Srinivas, K. Tejaswaroop, K. Saisamudra, K. Shiva Kumar,  
and G. Rakesh Kumar

**Abstract** A modified multi-level inverter with a cascaded H-bridge with a grid connected hybrid wind-solar energy system is given. Utilising their individual MPPT (maximum power point tracking) systems. In this paper, both solar and wind energy are used as input sources to the system. The total harmonic (THD) is reduced so that the appliances in the system are least affected or damaged. The dc/dc booster converters are used to step up the voltage and the maximum power is obtained by using maximum power point tracking (MPPT). Due to non-linear loads, the harmonics are produced in the system so in order to reduce the harmonics we use the MLI, as the level increases the harmonic distortion in the system decreases, so that we can reduce the disturbances and increase the appliances efficiency. So, the pulse width modulation (PWM) is used as an inverter in the system to produce the sinusoidal ac output. In this paper, we discuss mostly about, to obtain balanced voltage and current of two sources when connected by a dc-link, reducing the THD and Improve the Power quality. As the frequency is constant but the voltage is variable the voltage and frequency will be matchable as the frequency maintains constant. Hence, the output waveforms of multi-level inverter, and the simulation investigations were verified and completed in MATLAB/Simulink.

**Keywords** Total Harmonic Distortion (THD) · Multi-level Inverter (MLI) · Pulse Width Modulation (PWM) · Maximum Power Point Tracking (MPPT)

## 1 Introduction

The grid integration of renewable energy sources has a significant positive impact on energy consumption. To meet the rising energy demand, hybrid renewable energy sources have been developed gradually. Their abundance and lack of contamination have drawn a lot of attention in recent years. The most often and successfully

---

G. Srinivas · K. Tejaswaroop (✉) · K. Saisamudra · K. S. Kumar · G. R. Kumar  
Department of Electrical and Electronics Engineering, Vignan Institute of Technology and  
Science, Hyderabad, Telangana, India  
e-mail: [nani8186093149@gmail.com](mailto:nani8186093149@gmail.com)

combined renewable energy sources among these are wind and solar energy. Since it can be produced by wind turbines with considerable power outputs and is readily available, wind energy is one of the most widely used renewable energy sources. Another advantageous green energy source is solar energy. PV modules may easily and frequently capture it. Wind and solar energy actually work best together since strong winds are more frequent than weak ones, even if solar energy is less abundant at night and on cloudy days [1]. Therefore, a hybrid wind-solar energy system can deliver consistent output power supply regardless of changing weather conditions, in contrast to classic individual power generating systems. There has been a significant growth in the use of grid connected wind and solar energy as a result of the quick development of power electronics technology and control methods [2]. The operation of the hybrid wind and solar hybrid model causes a few power quality issues, such as voltage changes, harmonic production, flickering, and imbalanced dc-link capacitor voltages. These harmonics are produced by power converters [3]. MLIs are used in power systems because they have low levels of harmonic distortion and electromagnetic interference and can adhere to power quality and rating criteria. Because they can generate high-quality voltage waveforms while operating at low switching frequencies. In domestic or Industrial applications, the hybrid renewable energy sources provide power continuity, and improve the power quality of the system as of the MLI the decrease in the switches and increase in the level of MLI and maintaining the approx. unity power factor and improved efficiency [11].

## 2 System Description

The proposed grid connected with hybrid wind and solar sources combined with MLI is shown in block form in Fig. 1. Isolated DC-links from the intended five-level Cascaded Hybrid Based MLI are connected to the input energy from the Wind and PV separately via their respective boost converter-based MPPTs. The DC voltages are obtained from the rectified output voltages of a wind turbine and a PV array, respectively [4]. The MPPT algorithm is utilised to the power semiconductor switches so that the boost converter can obtain the most power possible from the PV array and wind turbine independently. The recommended control approach can be used in conjunction with SPWM to keep the dc-link voltages in balance.

### 2.1 PV Array Modelling

The similar solar cell circuit shown in Fig. 2 consists of an ideal current source, a parallel diode, a series, and parallel resistance. The practical solar modules'  $I_{PV}$ - $V_{PV}$  properties are identified. PV terminal voltage and module output current, respectively, are denoted by " $V_{PV}$ " and " $I_{PV}$ ," while " $I_g$ " is the current produced under a specific solar irradiation. The study's PV array, which consists of 'p' solar panels connected

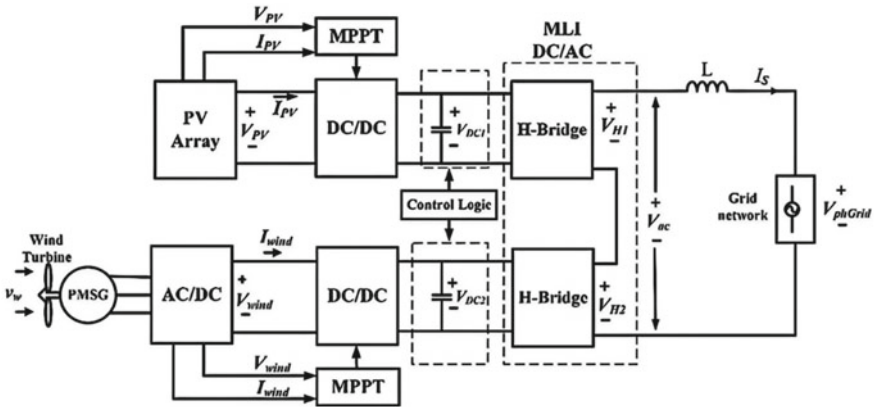


Fig. 1 Grid connected hybrid wind and solar sources

in series to form a PV string and ‘q’ solar panels connected in parallel, will produce the same amount of power if the weather conditions remain the same. However, the changes in temperature and sunlight, so each PV module will generate a different amount of output energy. The different ratings of Pv input like temperature, radiation, the conversion of radiation into voltage and current using different conversion models and finally the power is generated in the pv system [6]. The eight pv arrays are considered and a combination of arrays will produce the output energy with given inputs.

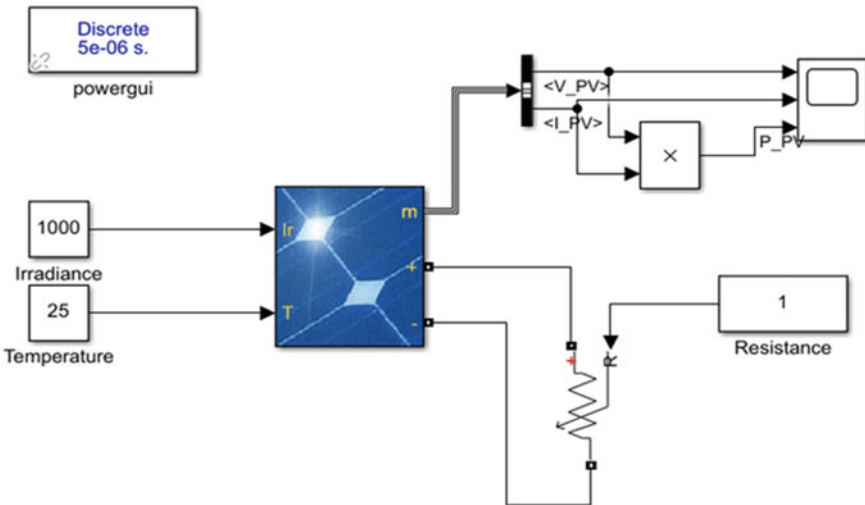


Fig. 2 PV array

## 2.2 Wind Energy Source

The Permanent Magnet Synchronous Generator is used to convert the mechanical energy that the Wind Turbine collects into electrical energy and is part of the wind energy source. The Permanent Magnet Synchronous Generator receives the rated torque it needs to produce three-phase voltage and current from the gearbox, which connects the turbine's shaft to it directly [5]. The output ac voltage is then kept at the desired amplitude and frequency using AC-DC-AC converters. The output power from the permanent magnet synchronous generator is transferred through these converters. The varying wind speed may have an effect on the dc-link voltage. As a result, the amplitude can be altered at the needed grid voltage by maintaining the dc-link voltage constant at its reference value while modifying the wind turbine parameters [7]. By employing the Betz theory to calculate the mechanical power output the wind turbine extracts the kinetic energy of the wind.

## 3 Grid Connected Hybrid Cascaded MLI

The suggested concept, shown in Fig. 1, is made up of two hybrid cell modules connected by two isolated dc links, each of which contains a separate solar and wind system that operates in response to changing solar radiation and wind speed [13]. The anticipated cascaded MLIs that are shown in Fig. 3, uses two hybrid cell modules per phase, resulting in a five-level increase in the converter's output phase voltage on ac side. The device load on the hybrid cell is reduced by higher converter output voltage levels brought on by an increase of hybrid cell modules [9]. Also, the necessity for filters on the AC side may be reduced, perhaps there may be other sources of renewable energy. The recommended maximum power varies according to the varying MPPTs of sources of energy like the sun and wind depending on the available climatic conditions [8]. Because of this, the sources' extractable currents are different, and the isolated dc-link capacitor voltages in the Cascaded MLI are likewise different. Only single-phase mathematical analysis is obtained in this work due to the bidirectional grid connected in three phases of Cascaded MLIs being symmetric. For the investigation of converter functioning, the switching function for each leg of a hybrid cell was built using simple curve fitting [10]. Due to how the power switches are handled, it is never recommended to turn on two switches at once in an HBC leg. If the isolated renewable energy sources connected to the proper hybrid cell dc-link in the planned system are assumed to be identical, the two capacitors of each cell will equally split the available dc voltage [15]. By choosing the right switching function, the desired converter output phase voltage can be achieved. Comparable, isolated dc or renewable energy sources' switching parameters and related voltage levels.

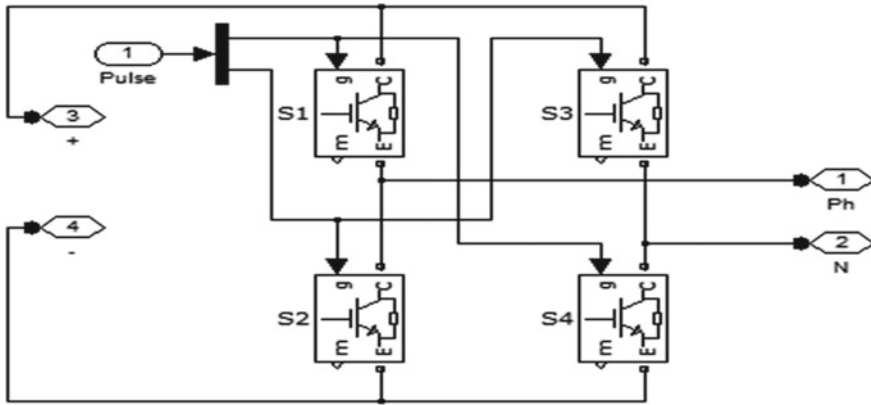


Fig. 3 Multi-level inverter

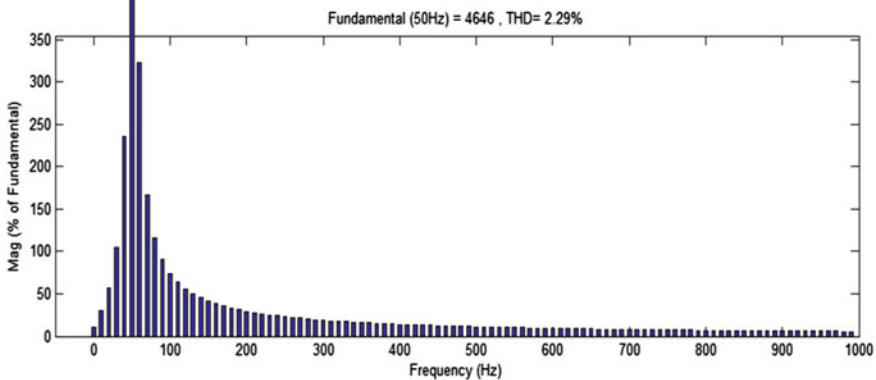
### 4 Control Method and Switching Strategy

While operating and managing hybrid wind and solar-based MLIs, the problem of unbalanced capacitor voltage is resolved using this strategy [12]. Wind and solar energy sources will create different amounts of power in isolated DC cells, which will lead to issues with power quality such as harmonic production and the grid’s introduction of an imbalanced current. In order to assure proper power injection and address concerns with the hybrid renewable energy source, a better control technique using a sinusoidal pulse width modulation scheme is recommended for the cascaded MLIs [14]. The above mentioned are some important strategies we are considering at present, as we are considering two different renewable energy sources which produces unequal power into the MLIs.

### 5 Results and Discussions

The proposed hybrid wind and solar-based grid is to test the effectiveness of the recommended control strategy, the model is simulated and its performance is assessed under various environmental situations. The wind speed and solar irradiation variables are altered. The wind speed and sun irradiation values are taken as per standard ratings respectively and then due to different frequencies the harmonics are generated in the system. The total harmonic distortion of the system is reduced to 2% shown in Fig. 4 so that the system is more efficient and stable, as we use the hybrid model there exists unbalance in the system and due to non-linear loads, the harmonics are developed in the system so from this paper the total harmonics are reduced to 2% which does not affect the system performance and appliances used. So, by the wind and solar energy hybrid model, the multi-input inverter is used in order to produce the

sinusoidal waveforms without any distortion so the harmonics in the system should not exceed 5% so that its performance will not be affected. So, from this paper, we have reduced the harmonics, improved efficiency of the system and maintained the power continuity. The output waveforms of the system are obtained as follows in Fig. 5 the proposed system with multi-input inverter output voltage waveform, where the voltage levels at each level are obtained, in Fig. 6 depicts the output waveform of single level inverter voltage. In Fig. 7 waveforms of the multi-input inverter proposed when the wind and PV array output voltages are both present and obtaining the sinusoidal voltage from the system. Figure 8 depicts the waveforms of the multi-inverter currently in use when the wind turbine and solar panel output voltages are both present. Figure 9 waveform produced when the proposed multi-input inverter is powered by the PV array. The waveforms of the ac output current and the dc bus voltage, Fig. 10 waveforms produced when the PV array is delivering power using the existing multi-input inverter. The waveforms of the ac output current and the dc bus voltage. Figure 11 Waveforms of the proposed multi-input inverter while receiving power from the wind turbine. The waveforms of the ac output current and the dc bus voltage. Figure 12 Current multi-input inverter waveforms during periods of power supply from a wind turbine. Waveforms for the ac output current and dc bus voltage. Figure 13 The proposed multi-inverter's waveforms when the PV array and the wind turbine are both producing power are the ac output current and dc bus voltage waveforms.



**Fig. 4** Total harmonic distortion of proposed system

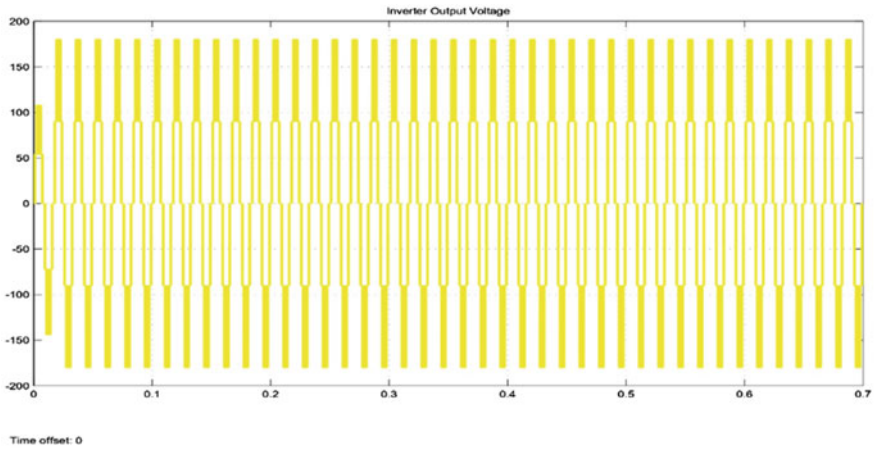


Fig. 5 The multi-input inverter’s proposed voltage waveform

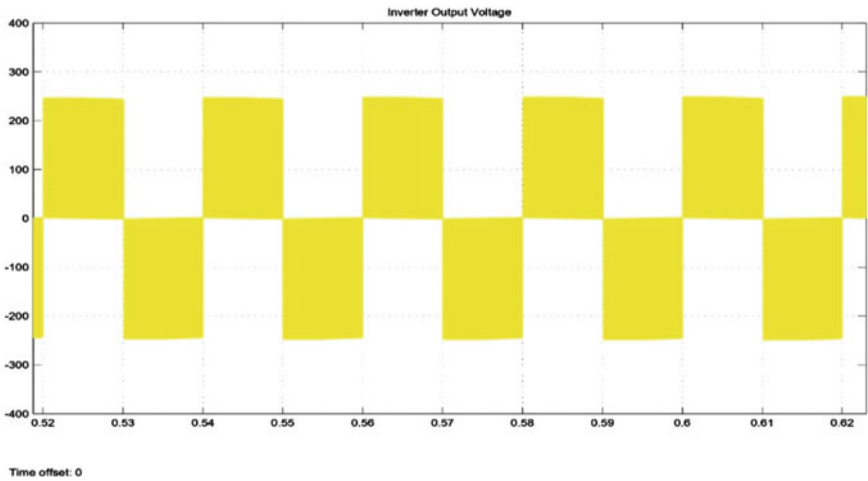
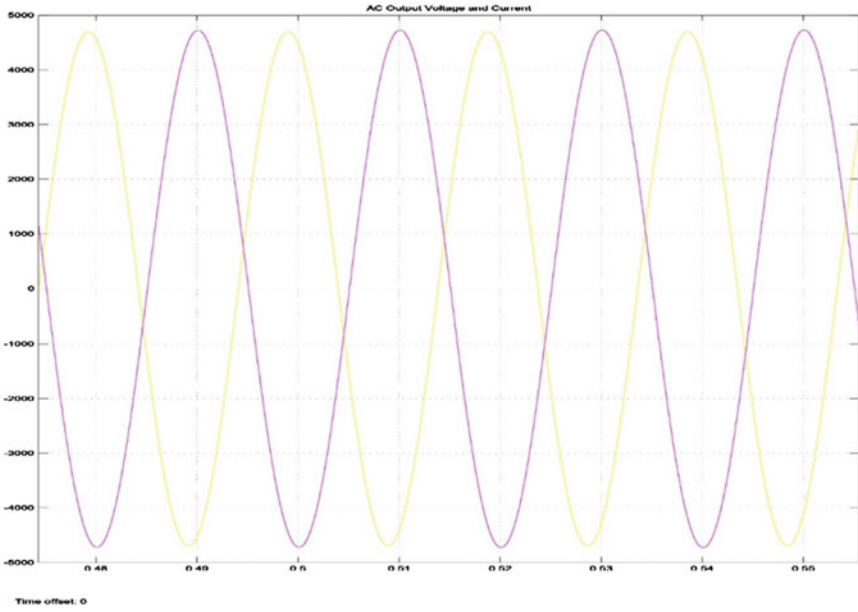
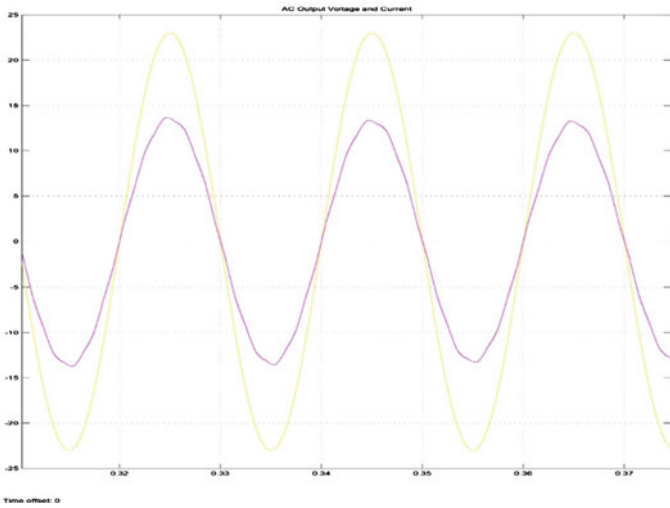


Fig. 6 Output voltage of the system’s existing multi-inverter waveform

From Table 1 we can observe the various pv inputs, the different irradiance and temperature values are provided based on the climatic changes as the climate changes and we do not obtain the temperature constant so there is a change in the values to generate the system with different irradiance and temperatures the pv array is provided with different input values as to obtain the pv voltage and current in different climatic conditions so the pv array will generate the voltage and current from the inputs of temperature and irradiance, we can observe the voltage and current values from the below Table 1 which depicts the various voltages from the pv array.

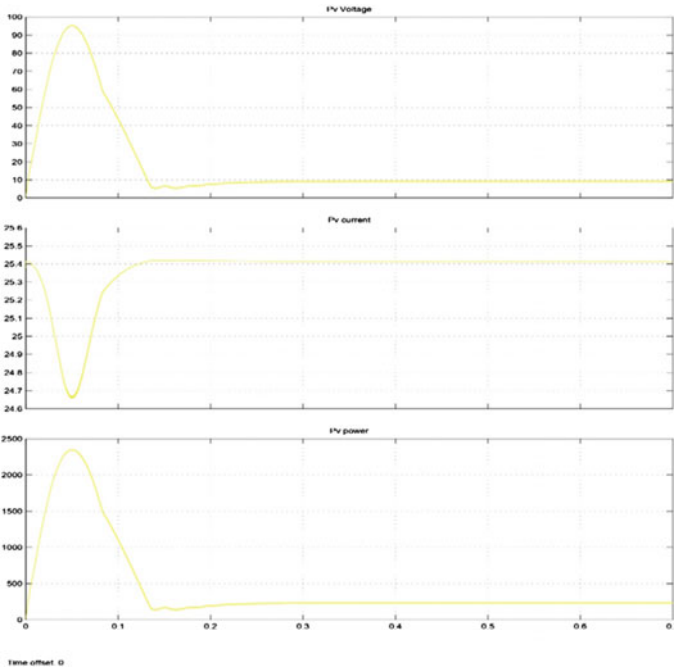


**Fig. 7** Waveforms of the multi-input inverter proposed when the wind and PV array output Voltages are both present



**Fig. 8** Waveforms of the multi-inverter currently in use when the wind turbine and solar panel output voltages are both present

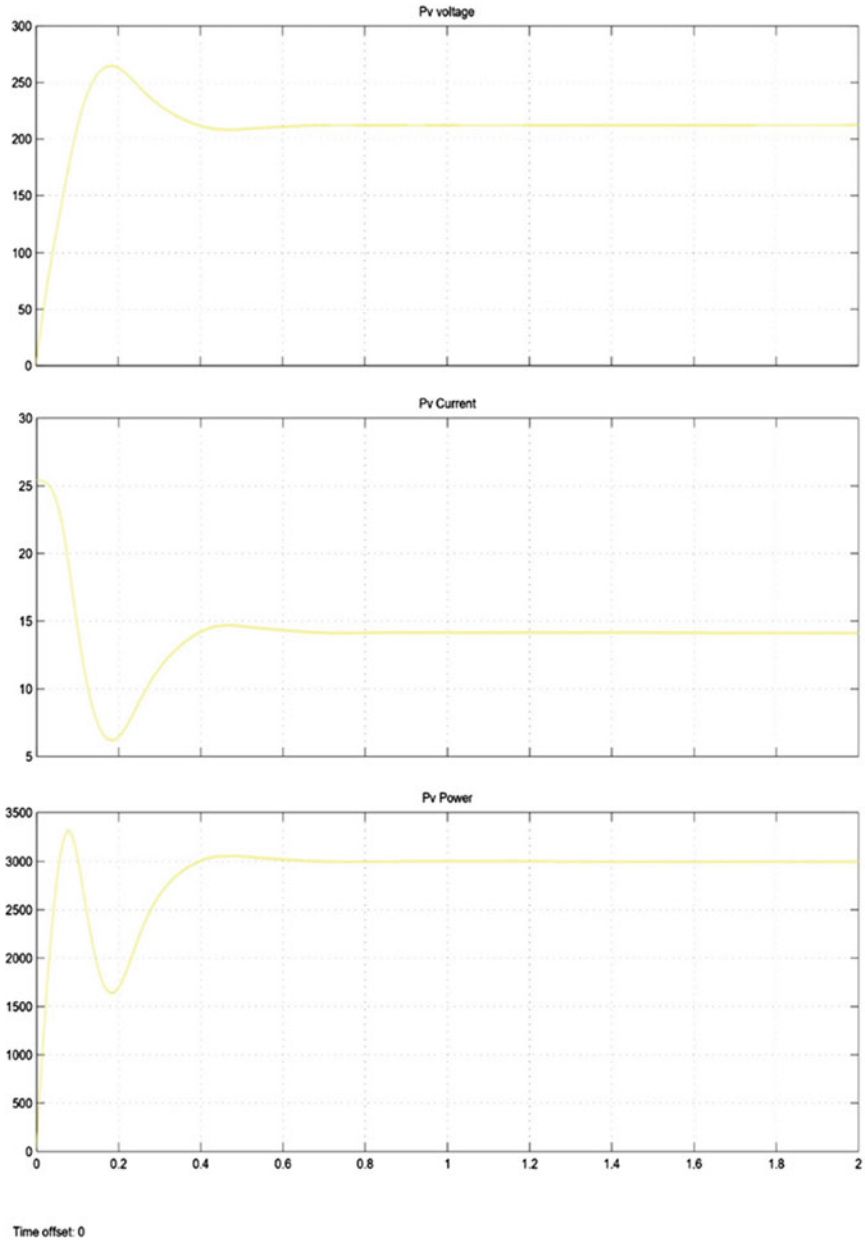




**Fig. 9** The waveforms of the ac output current and the dc bus voltage

From Table 2, we can observe the wind inputs of the system different speeds are provided to the system as the variations in the speed due to climatic conditions to obtain maximum speed there is an adjustable pitch angle in the system with this pitch angle, we can obtain the maximum speed to the system as the wind generates different voltage and current values from the various input speeds, we can observe at which rate the power is generated from the wind input.

From Table 3 we can observe the differences between Comparison Between proposed System and Existing System so we have different aspects into consideration in comparison table so the harmonics level in different systems, the inverter type used in the system different control techniques, operation different sources employed so these are the different aspects that we find the difference in Comparison Between proposed System and Existing System.



**Fig. 10** Waveforms produced when the PV array is delivering power using the existing multi-input inverter. The waveforms of the ac output current and the dc bus voltage  $P_e$

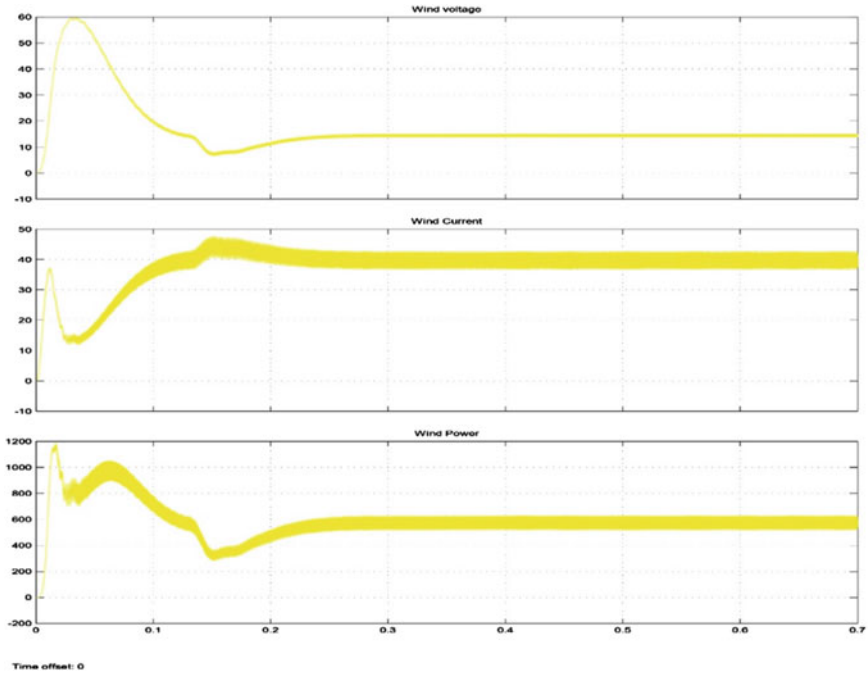


Fig. 11 Waveforms of the proposed multi-input inverter while receiving power from the wind turbine. The waveforms of the ac output current and the dc bus voltage

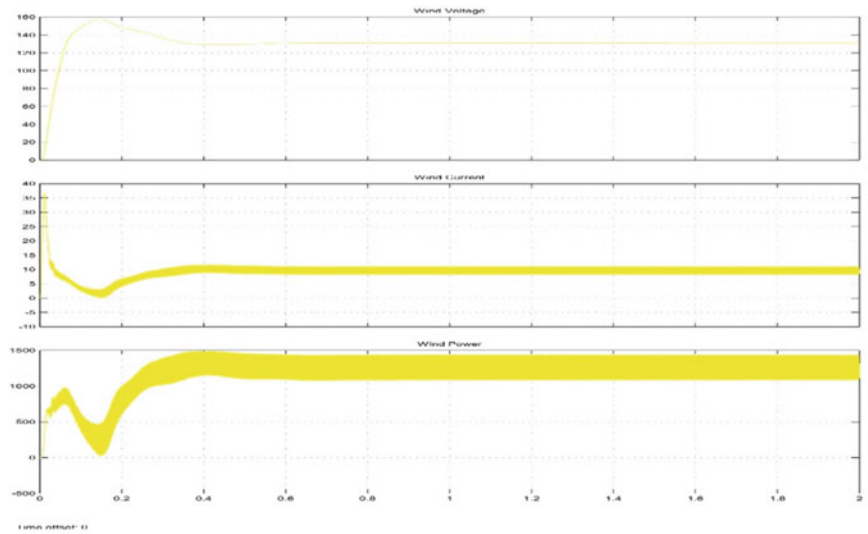
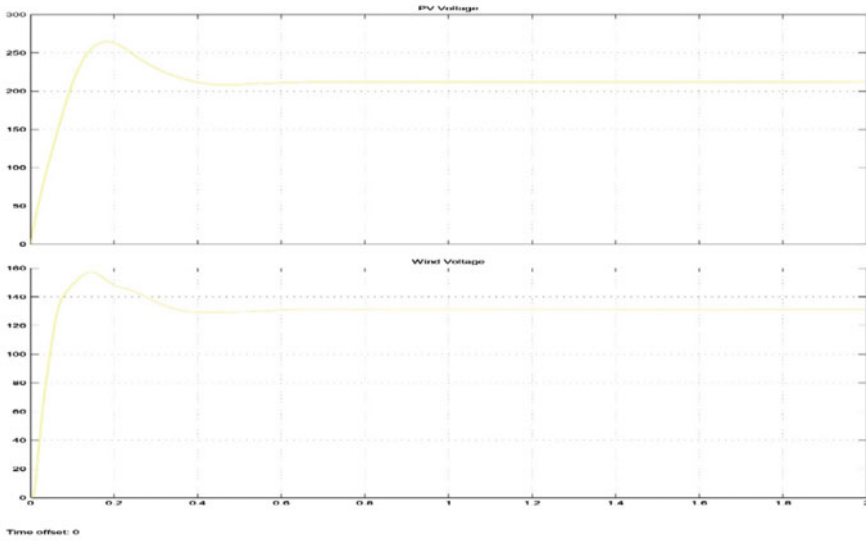


Fig. 12 Current multi-input inverter waveforms during periods of power supply from a wind turbine. Waveforms for the ac output current and dc bus voltage



**Fig. 13** The proposed multi-inverter’s waveforms when the PV array and the wind turbine are both producing power. The ac output current and dc bus voltage waveforms

**Table 1** With different solar irradiance values

Irradiance	Current	Voltage	Temperature
1000	4.537	44.34	25
800	3.721	43.56	20
600	2.765	42.67	30
400	1.765	41.65	40
200	0.987	39.56	50

**Table 2** Wind inputs with different wind speeds

Wind speed (m/sec)	Ac voltage	Dc voltage
1.5	1.9	7.0
1.8	2.3	8.0
2.0	2.5	9.0
2.2	2.9	9.5
2.4	3.0	10
2.5	3.2	12
2.8	3.5	14
3.0	4.2	15

**Table 3** Comparison between proposed system and existing system

S. no	Proposed	Existing
1	Multi-level H-bridge cascaded connection	Single H-bridge connection
2	Separate control over PV and wind sources	Single control
3	Multi-level carrier PWM technique	Sinusoidal PWM technique
4	THD 2%	THD 4%
5	Mainly for industrial applications	Less efficient in industrial applications

## 6 Comparison Between Proposed System and Existing System

## 7 Conclusion

The proposed grid connected five-level MLIs in this work convert the electricity gathered from the Hybrid cascaded MLI into ac power and feed it into the grid system. The coupled wind power sources and PV arrays, which are connected individually to each dc-link, will be used more efficiently using the independent MPPT algorithm. The simulation and experimental studies show that, when combined with the input and output performance parameters, the recommended control strategy and system model extract the maximum amount of power from each renewable energy source. The mathematical modelling of the single-phase grid connected cascaded MLIs has shown the switching function relationships between the dc-link capacitor voltages, the cascaded MLI's output voltage, the dc-link currents, and the grid current. In an integrated wind and solar system with fluctuating DC-link currents, simulations are done to show that DC capacitor balancing is achieved and a sinusoidal-shaped grid current with low THD and UPF is injected into the grid network. It was feasible to obtain good power quality, DC capacitor balancing, and reduced THD by employing the cascaded MLI hybrid model.

## References

1. Wu T.-F, Chang C.-H, Liu Z.-R, Yu T.-H (1998) Single-Stage converters for photovoltaic powered lighting systems with MPPT and charging features. *Proceedings IEEE APEC*:1149–1155
2. Kolhe M, Joshi JC, Kothari DP (2004) Performance analysis of a directly coupled photovoltaic water-pumping system. *IEEE Trans Energy Convers* 19(3):613–618
3. DeBroe AM, Drouilhet S, Gevorgian V (1999) Apeakpowertracker for small wind turbines in battery charging applications. *IEEE Trans Energy Convers* 14(4):1630–1635
4. Solero L, Caricchi F, Crescimbeni F, Honorati O, Mezzetti F (1996) Performance of a 10-kW power electronic interface for combined wind/PV isolated generating systems. In: *Proc IEEE PESC*, pp 1027–1032

5. Wakao S, Ando R, Minami H, Shinomiya F, Suzuki A, Yahagi M, Hirota S, Ohhashi Y, Ishii A (2003) Performance analysis of the PV/wind/wave hybrid power generation system. In: Proc IEEE World Conf Photovolt Energy Conv, pp 2337–2340
6. Borowy BS, Salameh ZM (1996) Methodology for optimally sizing the combination of a battery bank and PV array in a wind/PV hybrid system. *IEEE Trans Energy Conv* 11(2):367–375
7. Kjaer SB, Pedersen JK, Blaabjerg F (2005) A review of single-phase grid-connected inverters For photovoltaic modules. *IEEE Trans Ind Appl* 41(5):1292–1306
8. Chiang SJ, Chang KT, Yen CY (1998) Residential photovoltaic energy storage system. *IEEE Trans Ind Electron* 45(3):385–394
9. Shrestha GB, Goel L (1998) A study on optimal sizing of stand-alone photovoltaic stations. *IEEE Trans Energy Conv* 13(4):373–378
10. Enslin JHR, Snyman DB (1991) Combined low-cost, high-efficient inverter, peak power tracker and regulator for PV applications. *IEEE Trans Power Electron* 6(1):73–82
11. Hussein KH, Muta I, Hoshino T, Osakada M (1995) Maximum photovoltaic power tracking: An algorithm for rapidly changing atmospheric conditions. *Proc Inst Elect Eng* 142(1):59–64
12. Hua C, Lin J, Shen C (1998) Implementation of a DSP-controlled photovoltaic system with peak power tracking. *IEEE Trans Ind Electron*, 45(1):99–107
13. Walker OF (1997) *Wind energy technology*. Wiley, New York
14. Gipe P (1995) *Wind energy comes of age*. Wiley, New York
15. Amei K, Takayasu Y, Ohji T, Sakui M (2002) A maximum power control of wind generator system using a permanent magnet synchronous generator and a boost chopper circuit. *Proc Power Conv* 3:1447–1452

# A Comprehensive Analysis of Autism Spectrum Disorder Using Machine Learning Algorithms: Survey



D. Aarthi  and S. Kannimuthu 

**Abstract** One of the psychological disorders known as autism spectrum disorders (ASD) is a very challenging one to analyze and goes undiagnosed in many people. This condition develops from birth and persists throughout life, and has no cure. It is possible to predict ASD using a variety of indicators, including functional magnetic resonance imaging (fMRI) data, kinematic traits, game-based applications, questionnaires given to parents and guardians, social reciprocity, head motion, motor activities, and eye-tracking. A better prognosis for the patient can be achieved with earlier prediction. This research work provides a thorough overview of the various machine learning and artificial intelligence algorithms utilized for ASD diagnosis and prediction in patients of various ages using clinical methods. This article also emphasizes the datasets that were utilized to predict autism in individuals, their results, limitations, and the hindrances of the methods involved.

**Keywords** Autism spectrum disorder (ASD) · Prediction · Machine learning · Investigation

## 1 Introduction

A pervasive neuro-developmental disease called autism spectrum disorder (ASD) involves social communication and behavioral deficits. The neurological process behind autism is poorly understood [1]. People with autism often throw tantrums to express how uncomfortable they are with the situation or other people. Patients, especially children, display behaviors such as hyperactivity, motor difficulties, mental retardation, and hearing loss [2]. They may also display behaviors like learning disabilities or hyperactivity. Additionally, autistic people have decreased change sensitivity and social-communicative dysfunction [3, 4]. Patients with autism display unpredictable behaviors and events in the early stages of the disease, which could be viewed as a basic difference from those of healthy people. Lying is annoying to

---

D. Aarthi (✉) · S. Kannimuthu  
Karpagam College of Engineering, Coimbatore, Tamil Nadu 641032, India  
e-mail: [aarhideva06@gmail.com](mailto:aarhideva06@gmail.com)

autistic people [5]. Although the majority of researchers agree that this condition is inherited, there are no studies or research to support this. The cause of this illness is essentially unknown [6]. According to a recent poll, 1 in 167 children in Belgium and 1 in 55 children in Japan are thought to have ASD. Autism is becoming ever more prevalent on a global scale. This condition may make it harder for a person to carry out daily tasks and social interactions [7]. Social interaction is now the most effective treatment for autism. Early intervention could increase the likelihood of success. Occasionally, a few illnesses during pregnancy may be harmful to the growing fetus [8].

Patients with lower severity levels of autism can live freely, whereas those with greater severity levels require ongoing care and support [9]. Prior to ASD detection, individuals can benefit from appropriate treatments and medications at an early stage of the illness. The stability of the patient's health can be supported by doctors with early detection of this condition [10]. The majority of experts concur that the complexity of the brain network can be used to moderately indicate this autistic disease [11]. There are no genetic tests available to diagnose ASD. However, the early detection of this disorder may help the patients to enhance their learning capabilities [12]. Recent studies have shown a gradual increase in the study of autism, utilizing diverse experimental approaches and screening technologies. There isn't much research that looks at newborns and toddlers who aren't developing their verbal, motor, or cognitive skills [13]. Autism is also identified by additional facial expressions of people [14, 15]. These findings allowed to track the development of autism in kids and to identify the condition earlier before a diagnosis [16]. Even though a few screening tests can be used to predict ASD in patients, insufficient medical testing can make this illness difficult to diagnose. In order to progress with the condition's diagnosis, doctors follow and evaluate their patients for a variety of behavioral data [17, 53]. The optimum non-invasive method for studying developmental psychopathology is electroencephalography (EEG) [18].

The main contributions of this article are summarized as follows.

This article contributes to the body of understanding regarding autism spectrum disorder and points out potential problems when applying machine learning methods to this disorder's study. The main goal is to thoroughly review ASD prediction and diagnosis by using various techniques. We believe that by describing these methods here, we may help other researchers identify areas in this field where they can be useful.

The structure of this article is organized as follows. The next section presents the related research that were done previously in this domain and is followed by "Investigation of ASD". The fourth section is about the "Discussion" and fifth is "Challenges and Solution". The final section is the "Conclusion and Future Work".



## 2 Related Works

Kazi et al. used five stages to predict ASD, including data gathering from multiple sources, data synthesis, constructing a model to predict autism, evaluating the produced model, and developing a mobile app. They used the Decision Tree-CART method to identify an individual's autistic symptoms. The Random Forest-CART algorithm was used to improve things, and better results were seen. A larger dataset was not sufficient to train the prediction model. Additionally, due to a lack of open-source data, the screening tool does not yield positive results for children younger than three years. For the purpose of calculating performance parameters, AQ-10 datasets were used. According to a comparison of the output from each algorithm [9], the suggested model outperformed the existing Decision Tree-CART algorithm.

Braukmann et al. investigated whether or not low-risk and high-risk infants differed in their anticipatory eye movements. By observing actions made on common items, they used an eye-tracking feature to assess the infant's ten-month eye movements. 36 of the 61 participants in the study were high-risk, whereas 25 were low-risk. In this experiment, participants were instructed to pick up a cup or phone and place it in their mouth or ear. Either the predicted, typical location or a surprising site was the result. Actual target anticipation was deemed to exist if the predicted result and the actual result were identical, while alternative target anticipation was deemed to exist in the opposite situation. This study's limitation was the lack of information on the cohort's analytical results that is currently available [19].

Kimura et al. exposed the impact of social reciprocity, anxiety, and fluency on communicative behaviors in people with ASD and contrasted these with typically developing (TD) adults. In total, 35 people with ASD took part in this study. Social reciprocity was evaluated using the Social Responsiveness Scale (SRS). The higher score suggested a social deficit that was more severe. Verbal generativity was evaluated using the letter fluency task. The count of correct responses was calculated by subtracting the number of incorrect outputs and instances of repeated words [20].

In order to validate the automatic detection of postural control patterns in children with ASD, Yumeng et al. devised a machine learning approach. Twenty-five kids with ASD and twenty-five kids with usual development were told to remain still for 20 s without wearing any shoes. During the allotted period, there were eye-opening and eye-closing motions. The data for the center of pressure (COP) was collected using a force plate. Included in this study were 25 children (ASD and TD). Children with ASD showed a higher COP than those with TD. When compared to settings where the eyes were open, all youngsters showed higher COP when their eyes were closed [21].

By merging the characteristics of functional activities and brain structure, Saran et al. published a work. They represented the brain's structure as a graph and the weight of the graph's nodes according to the fMRI signals. The dataset was taken from the Autism Brain Imaging Data Exchange (ABIDE). According to the topological distance between its nodes, the brain graph was viewed as a collection of regions. For trustworthy and consistent results, a few criteria were taken into account, including

patients who were under the age of 18 and who kept their eyes open during the fMRI collection. They came to the conclusion that the frontal and temporal lobes can be used to diagnose autism based on the findings of their study [22].

Amy and colleagues examined children between the ages of 8 and 14 who were experiencing various spontaneous thought patterns. They also looked into the relationship between automatic viewpoints and resistance to ambiguity. They used a dataset made up of 97 autistic kids and teenagers. The Autism Diagnostic Observation Schedule (ADOS) was used to scale the participants' levels of autism. The Childhood Automatic Thoughts Scale (CATS) data utilized for analyses had a non-normal distribution, and only a small number of participants could support the items within a given subscale or the full measure [24].

A discriminative model for ASD based on phase synchrony was created by Ma and colleagues (PS). Phase Synchronization between different brain regions came next. In order to contrast the outcomes with the PS data, the traditional static FC characteristics were identified. 96 ASD sufferers and 122 healthy people were selected as testing samples after careful consideration. ASD patients may benefit from the PCA-PS model's ability to distinguish between them and healthy people in terms of diagnosis and severity assessments [26].

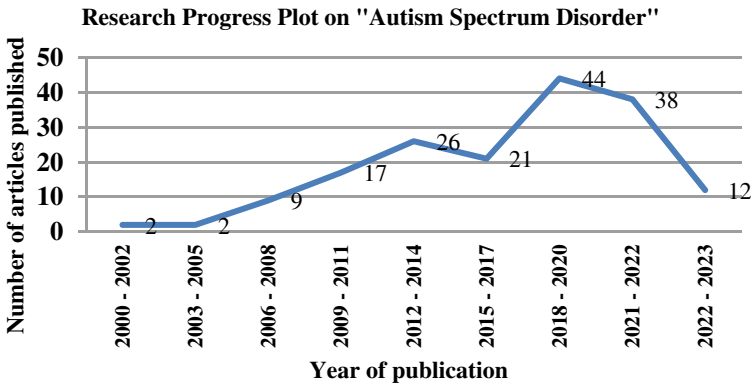
To classify autistic kids, Kang et al. collected characteristics from two modalities such as EEG and eye tracking. Eye-tracking tests were conducted after the recording of resting-state EEG data. 97 kids were given instructions to take individual EEG and eye-tracking tests, followed by power spectrum analysis, eye-tracking data analysis, feature selection, and categorization. By combining EEG and eye-tracking data, the results achieved an accuracy of 85.44% in detecting autism in people with an Area Under Curve (AUC) of 0.93. The research's main drawback is that it did not include kids under the ages of 3 [27].

A culturally sensitive mobile application for diagnosing autism in people was created by Wingfield et al. They used a checklist of symptoms that had been clinically verified to examine and identify autism. They discovered that the RF model performed better than the conventional paper-based technique [28].

Figure 1 shows the progress of research on the Autism Spectrum Disorder from the year 2000 to 2023.

### 3 Investigation of ASD

Complex alterations in brain activity that are seen by fMRI data are associated with ASD [29, 53]. For people of different ages, there are many algorithms that can be used to predict autism. For the purpose of diagnosing autism in patients, researchers draw on a variety of categories, including eye-movement monitoring, fMRI data, motion capture, and questionnaires [25, 52]. An overview of the various techniques, datasets, accuracy metrics, and study limitations for predicting autism is provided in this section. Table 1 summarizes research into the use of artificial intelligence and machine learning techniques to predict ASD in individuals.



**Fig. 1** Research progress plot on “Autism Spectrum Disorder”

## 4 Discussion

This survey reviewed a total of 54 works that applied various machine learning algorithms and predicted ASD in patients of different age groups. The majority of the works involved using Support Vector Machines, Random Forest, and Decision Tree algorithms. The Naive Bayes and Support Vector Machine outperform the decision table in terms of output, which implies that errors are minimized. Unsupervised machine learning techniques also offer useful, clinical classification tools that may be applied in the field to sort or categorize incoming data. The findings presented in this paper demonstrate that there is great value in practical applications for the use of supervised machine learning in ASD research. Although the more complex machine learning models frequently outperform their more straightforward counterparts, there is a trade-off between performance and understanding. It can be challenging to find datasets with enough observations and explanatory variables to train complicated models, yet when given the right amount of data, ML models frequently outperform more straightforward models.

## 5 Challenges and Solutions

A major drawback of machine learning is the complexity of the models. Supervised learning is ineffective for datasets without categorization labels, which is the main challenge faced by the researchers [48]. Without clinical domain expertise, the implementation of machine learning might be problematic and lead to incorrect results [49]. When used in interdisciplinary studies, machine learning is particularly vulnerable to interpretation errors (not unlike other statistical techniques) [50]. An in-depth understanding of both the computational and clinical content domains is necessary

**Table 1** Investigation of various methodologies in predicting ASD

S. no.	Authors	Dataset	Method	Findings	Pitfalls
1	Chaitra et al. [23]	fMRI data from ABIDE dataset with 432 autistic individuals and 556 normally fit individuals	Recursive cluster elimination SVM algorithm	The result showed that the algorithm exhibited an accuracy of 67.3% for predicting ASD and 64.5% for graph measures and 70.1% for combined set	The dataset was a combination of instances from different sites. This results in reduced classification performance
2	Zhong et al. [30]	20 autistic children and 23 TD children	SVM, DT, RF, Linear Discriminant Analysis (LDA) and K-Nearest Neighbor (KNN)	KNN algorithm outperforms well with 88.37% accuracy, 91.3% specificity, 85% sensitivity, AUC of 0.8815	In order to carry out the motor task in smooth manner, children with level 1 of autism were selected
3	Nikita et al. [31]	The dataset consists of 21 including gender, nationality, and ethnicity	Modified Grasshopper Optimization Algorithm (MGOA)	The proposed algorithm with RFC exhibited approximately 99.29% specificity and 100% sensitivity at every phase of life	GOA has less convergence speed. Quantum computing has to be utilized in order to get good computational speed
4	Abbas et al. [32]	Evaluation on a clinical examination of 375 children, 18–72 months old	Multi-modular, machine learning-based assessment	The assessment outperformed with AUC as 0.18 and specificity 0.30 at 90% sensitivity	The clinician module has been applied in a secondary-care setting. In order to get improved accuracy, testing at primary care clinics are mandatory

(continued)

**Table 1** (continued)

S. no.	Authors	Dataset	Method	Findings	Pitfalls
5	Parisot et al. [33]	ABIDE and Alzheimer's Disease Neuroimaging Initiative (ADNI) dataset	Graph Convolutional Networks (GCNs)	A classification accuracy of 70.4% has been achieved for ABIDE dataset and 80.0% for ADNI dataset	The generalization of the developed framework may result in deterioration of performance, if there isn't larger training data for capturing population variability
6	Crasta et al. [34]	EEG data recorded with 18 ASD children between 5 and 12 years and 18 TD children	A modified sensory gating paradigm	ASD children exhibited considerably less gating when compared with TD individuals at P50, N1 and P2 event-related potential components	This research did not use any diagnostic tools other than confirming diagnosis with ASD questionnaire
7	Epalle et al. [35]	ABIDE dataset	A multi-input deep neural network model	78.07% classification accuracy on actual data and 79.13% accuracy using enlarged data	The time taken for training the model is high
8	Dickinson et al. [36]	Spontaneous EEG data of 65 infants with age group between 3 and 9 months	Support Vector Regression (SVR) Analysis	Autism Diagnostic Observation Schedule (ADOS) scores of SVR algorithm of 3 months infant data and 18 months infant data were highly correlated	SVR is not fit to predict the cognitive abilities when 18 months dataset has been considered

(continued)

**Table 1** (continued)

S. no.	Authors	Dataset	Method	Findings	Pitfalls
9	Wei et al. [37]	SALICON, MIT1003, MIT300, and Saliency4ASD datasets	Deep CNN specialized in atypical visual saliency prediction	The proposed algorithm produced better saliency prediction performance than other algorithms that were taken for comparison	The drawback of this paper is that few regions which are considered to be background are stared by ASD individuals, are likely to be ignored
10	Rakhee et al. [38]	Brain MRI and EEG signal, Test exercises guided by authorized personnel, and questionnaire by the parents	NB, AdaBoost, Bagging, DT, RF, and SVM	The model developed helped the physicians to identify the severity level of autism in individuals	Finding learning patterns throughout time to analyze growth variances and predict autism is not the goal of this study
11	Ejlskov et al. [39]	73 candidate disorders spanning mental, cardiometabolic, neurologic, congenital defects, and allergy conditions	Extreme Gradient Boosting (EGB), the traditional generalized linear model (GLM), Elastic Net (EN), Averaging (E-A), and Hill Climbing (E-HC)	Individuals with high risk score had 17% ASD occurrence. F-score was increased by 12% and AUC by 15%	The diagnosis timing was not considered during evaluation
12	Lavanga et al. [40]	EEG data recordings	Linear Discriminant Analysis (LDA)	Multiscale Entropy (MSE), multifractality (MFA) exhibited best discrimination performance with AUC for MFA as 0.74 and MSE as 0.79	The dataset of ASD individuals were limited

(continued)

**Table 1** (continued)

S. no.	Authors	Dataset	Method	Findings	Pitfalls
13	Alivar et al. [41]	Ballistocardiogram (BCG) signals of two male individuals	Artificial Neural Network (ANN) and Support Vector Machine (SVM)	Accuracy of SVM and ANN was 78% and 79% respectively	Undesirably noticeable sleep data need to be extracted for long-term home monitoring system
14	Negin et al. [42]	Expanded Stereotype Behavior Dataset (ESBD)	A non-intrusive vision-assisted method	Histogram of Optical Flow (HOF) descriptor on merging with MLP classifier achieved the finest outcomes	The dataset can be increased with videos that can be used for data demanding deep architectures
15	Vakadkar et al. [43]	The dataset consists of 1054 items with 18 attributes	SVM, RFC, NB, KNN, and Logistic Regression (LR)	LR produced high accuracy of 97.15% and F1 score of 0.98 among all the algorithms for the collected dataset	The dataset is of limited size. Large dataset is necessary for getting accurate model
16	Stevens et al. [44]	A sample of 2400 children with ASD	Gaussian Mixture Model	Higher functioning people improve more quickly throughout therapy, which suggests that they may represent a particular subtype of ASD	The findings in this article are preliminary and need to be confirmed in additional samples of people with ASD. It lacks data from standardized Assessments
17	Shomona Gracia Jacob et al. [45]	ABIDE, UCI-ML, Real-time datasets	CNN, Convolutional Gated Recurrent Neural Network (CGRNN)	It was discovered that the majority of classifier research focused on analyzing and reporting their performance on accuracy, AUC, sensitivity, and specificity	This paper analyzed supervised machine learning methods for finding intriguing information that connects the diversity of ASD

(continued)

**Table 1** (continued)

S. no.	Authors	Dataset	Method	Findings	Pitfalls
18	Zhang et al. [46]	EEG Datasets	Spatial Pattern of the Network (SPN)	Children with varying symptom severity who had ASD and children with TD were compared for potential network differences	The correlation coefficients between the predicted and diagnosed symptom severity reported in both the current and preceding studies were found to be still insufficient, making it challenging to predict the symptom severity of ASD patients with any level of precision
19	Usta et al. [47]	433 children with ASD diagnosis	Naïve Bayes, Generalized Linear Model, Logistic Regression, Decision Tree	Comorbid psychiatric diagnoses are affecting the outcome of ASD symptoms in clinical observation	DT can be subjected to overfitting while using small dataset
20	Deepa et al. [11]	10 behavioral and individual characteristics from UCI Repository	Naïve Bayes, SVM, Decision Table	Compared to Decision Table, Naive Bayes and Support Vector Machine produce best results	Decision Table algorithm has high mean absolute error when compared with NB and SVM

for the use of engineering approaches and the interpretation of the outcomes they produce [51].

In order to achieve higher accuracy for predicting autism spectrum disorder, effective feature selection methods can be devised to choose best features so as to improve the accuracy and avoid overfitting problem. Of late, Deep Ensemble Learning is used which combines several individual models to obtain better generalization performance. Hence, Deep Ensemble Learning algorithms can be utilized to improve the performance. Data imbalance issue can be sorted out by using modern optimization algorithms. For upcoming ASD research projects, the ability of machine learning to extract knowledge from huge datasets will be encouraging.



## 6 Conclusion and Future Work

The best care and treatments can be provided to the ASD individuals with well-timed diagnosis of neurobiological disorders. The level of severity of each autistic individual will vary. Even though there are abundant methods available for predicting autism, its diagnosis is still a challenging task at the earlier stages in children under 2 years. This study has reviewed 50 research articles based on autism spectrum disorder. The most frequently used machine learning algorithm was SVM. Few research show that SVM outperforms in comparison with Decision Table and Naïve Bayes algorithms. In these investigations, machine learning algorithms were used to decide on binary predictions of the disorder and examine the genetic causes of ASD. In the future, a prediction model for autism in people of different ages will be created using deep ensemble learning algorithms, and it will aid in the identification of autistic people with the fewest possible data categories.

## References

1. Kelly E, Escamilla CO, Tsai PT (2020) Cerebellar dysfunction in autism spectrum disorders: deriving mechanistic insights from an internal model framework. *Neuroscience*
2. Pujari SD, Anusha K (2020) A review on prediction of autism using machine learning algorithm. *Int J Adv Sci Technol*
3. Chambo V, Farrer C, Pacherie E, Jacquet PO, Leboyer M, Zalla T (2017) Reduced sensitivity to social priors during action prediction in adults with autism spectrum disorders. *Cognition*
4. Hoogenhout M, Malcolm-Smith S (2014) Theory of mind in autism spectrum disorder: does DSM classification predict development? *Res Autism Spectr Disord*
5. Cantarero K, Byrka K, Krol M (2021) It's not really lying. Autism spectrum disorder relates to lower recognition of other-oriented lies through a decrease in perceived intentionality of the liar. *Res Autism Spectr Disord*
6. Gomot M, Wicker B (2012) A challenging, unpredictable world for people with autism spectrum disorder. *Int J Psychophysiol*
7. Aarathi D, Udhayamoorthi M, Lavanya G (2020) Autism spectrum disorder analysis using artificial intelligence: a survey. *Int J Adv Res Eng Technol (IJARET)* 11(10)
8. Graciarena M (2019) Cytokines and chemokines in novel roles: exploring their potential as predictors of autism spectrum disorder. *Biol Psychiatry*
9. Islam MN, Khan NS, Omar KS (2019) A machine learning approach to predict autism spectrum disorder. In: International conference on electrical, computer and communication engineering (ECCE), Cox'sBazar, Bangladesh
10. Raj S, Masood S (2020) Analysis and detection of autism spectrum disorder using machine learning techniques. In: International conference on computational intelligence and data science (ICCIDS), India
11. Deepa B, Jeen Marseline KS (2019) Exploration of autism spectrum disorder using classification algorithms. In: International conference on recent trends in advanced computing
12. Hanif MK, Ashraf N, Sarwar MU, Adinew DM, Yaqoob R (2022) Employing machine learning-based predictive analytical approaches to classify autism spectrum disorder types. *Hindawi*
13. Johanna JS, Finnemann, Plaisted-Grant K, Moore J, Teufel C, Fletcher PC (2021) Low-level, prediction-based sensory and motor processes are unimpaired in autism. *Neuropsychologia*
14. Brewer R, Bird G, Katie LH. Gray, Cook R (2019) Face perception in autism spectrum disorder: modulation of holistic processing by facial emotion. *Cognition*

15. Shephard E, Milosavljevic B, Mason L, Elsabbagh M, Tye C et al (2020) Neural and behavioural indices of face processing in siblings of children with autism spectrum disorder (ASD): a longitudinal study from infancy to mid-childhood. *ScienceDirect*
16. Geng X, Kang X, Patrick CM Wong (2020) Autism spectrum disorder risk prediction: a systematic review of behavioral and neural investigations. Elsevier
17. Ferrari E, Bosco P, Calderonib S, Oliva P, Palumbo L et al (2020) Dealing with confounders and outliers in classification medical studies: the autism spectrum disorders case study. *Artif Intell Med*
18. Lau-Zhu A, Fritz A, McLoughlin G (2019) Overlaps and distinctions between attention deficit/hyperactivity disorder and autism spectrum disorder in young adulthood: systematic review and guiding framework for EEG-imaging research. *Neurosci Biobehav Rev*
19. Braukmann R, Ward E, Hessels RS, Bekkering H, Jan K. Buitelaar et al (2018) Action prediction in 10-month-old infants at high and low familial risk for autism spectrum disorder. *Res Autism Spectr Disord*, Elsevier
20. Kimura Y, Fujioka T, Jung M, Takashi X. Fujisawa et al (2020) An investigation of the effect of social reciprocity, social anxiety, and letter fluency on communicative behaviors in adults with autism spectrum disorder. *Psychiatry Research*
21. Li Y, Mache MA, Todd TA (2020) Automated identification of postural control for children with autism spectrum disorder using a machine learning approach. *J Biomech*
22. Itani S, Thanou D (2021) Combining anatomical and functional networks for neuropathology identification: a case study on autism spectrum disorder. *Med Image Anal*
23. Chaitra N, Vijaya PA, Deshpande G (2020) Diagnostic prediction of autism spectrum disorder using complex network measures in a machine learning framework. *Biomed Signal Process Control*
24. Keefer A, Kreiser NL, Singh V, Blakeley-Smith A, Reaven J et al (2017) Exploring relationships between negative cognitions and anxiety symptoms in youth with autism spectrum disorder. *Behav Ther*
25. Heinsfeld AS, Franco AR, Craddock RC, Buchweitz A et al (2018) Identification of autism spectrum disorder using deep learning and the ABIDE dataset. *NeuroImage: Clin*
26. Ma X, Wang XH, Li L (2020) Identifying individuals with autism spectrum disorder based on the principal components of whole-brain phase synchrony. *Neurosci Lett*
27. Kang J, Han X, Song J, Niu Z et al (2020) The identification of children with autism spectrum disorder by SVM approach on EEG and eye-tracking data. *Comput Biol Med*
28. Wingfield B, Miller S, Yogarajah P, Kerr D, Gardiner B, Seneviratne S, Samarasinghe P, Coleman S (2020) A predictive model for paediatric autism screening. *Health Inform J*
29. Evelyn MR Lake, Emily S Finn, Stephanie M Noble, Vanderwal T et al (2019) The functional brain organization of an individual allows prediction of measures of social abilities transdiagnostically in autism and attention-deficit/hyperactivity disorder. *Soc Biol Psychiatry*
30. Zhao Z, Zhang X, Li W, Hu X et al (2019) Applying machine learning to identify autism with restricted kinematic features. *IEEE Access*
31. Goel N, Grover B, Anuj, Gupta D, Khanna A et al (2020) Modified grasshopper optimization algorithm for detection of autism spectrum disorder. *Phys Commun*
32. Abbas H, Garberson F, Liu-Mayo S et al (2020) Multi-modular AI approach to streamline autism diagnosis in young children. *Sci Rep natureresearch*
33. Parisot S, Sofia Ira Ktena, Ferrante E, Lee M, Guerrero R et al (2018) Disease prediction using graph convolutional networks: application to autism spectrum disorder and alzheimer's disease. *Med Image Anal*
34. Jewel E. Crasta, William J. Gavin, Patricia L. Davies (2021) Expanding our understanding of sensory gating in children with autism spectrum disorders. *Clin Neurophysiol*
35. Epalle TM, Song Y, Liu Z, Lu H (2021) Multi-atlas classification of autism spectrum disorder with hinge loss trained deep architectures: ABIDE I results. *Appl Soft Comput*
36. Dickinson A, Daniel M, Marin A, Gaonkar B et al (2020) Multivariate neural connectivity patterns in early infancy predict later autism symptoms. *Biol Psychiatry: Cogn Neurosci Neuroimaging*

37. Wei W, Liu Z, Huang L, Nebout A et al (2021) Predicting atypical visual saliency for autism spectrum disorder via scale-adaptive inception module and discriminative region enhancement loss. *Neurocomputing*
38. Kundu R, Das S (2018) Predicting autism spectrum disorder in infants using machine learning. In: *International conference on physics and photonics processes in nano sciences*
39. Ejlskov L, Wulf JN, Kalkbrenne A, Ladd-Acosta C et al (2021) Prediction of autism risk from family medical history data using machine learning: a national cohort study from Denmark. *Biol Psychiatry Glob Open Sci*
40. Lavanga M, Jessie De Ridder, Kotulska K, Moavero R et al (2021) Results of quantitative EEG analysis are associated with autism spectrum disorder and development abnormalities in infants with tuberous sclerosis complex. *Biomed Signal Process Control*
41. Alivar A, Carlson C, Suliman A, Steve et al (2020) Smart bed based daytime behavior prediction in children with autism spectrum disorder—A Pilot Study. *Med Eng Phys*
42. Negin F, Ozyer B, Agahian S, Kacdioglu S et al (2021) Vision-assisted recognition of stereotype behaviors for early diagnosis of autism spectrum disorders. *Neurocomputing*
43. Vakadkar K, Purkayastha D, Krishnan D (2021) Detection of autism spectrum disorder in children using machine learning techniques. *SN Computer Science*
44. Stevens E, Dennis R, Dixon, Marlena N, Novack, Granpeesheh D et al (2019) Identification and analysis of behavioral phenotypes in autism spectrum disorder via unsupervised machine learning. *Int J Med Inform*
45. Jacob MM, Sulaiman MMBA, Bennet B (2022) Algorithmic approaches to classify autism spectrum disorders: a research perspective. In: *The 5th international conference on emerging data and industry 4.0*
46. Zhang Y, Zhang S, Chen B, Lin et al (2022) Predicting the symptom severity in autism spectrum disorder based on EEG metrics. *IEEE Trans Neural Syst Rehabil Eng*
47. Usta MB, Karabekiroglu K, Sahin B, Aydin M et al (2018) Use of machine learning methods in prediction of short-term outcome in autism spectrum disorders. *Psychiatry Clin Psychopharmacol*
48. Kayleigh K. Hyde, Marlena N. Novack, Nicholas LaHaye, Chelsea Parlett-Pelleriti et al (2019) Applications of supervised machine learning in autism spectrum disorder research: a review. *Rev J Autism Dev Disord*
49. Bone D, Matthew S. Goodwin, Matthew P. Black, Chi-Chun Lee et al (2015) Applying machine learning to facilitate autism diagnostics: pitfalls and promises. *J Autism Dev Disord*
50. Kavitha V, Siva R (2023) Classification of toddler, child, adolescent and adult for autism spectrum disorder using machine learning algorithm. In: *2023 9th International conference on advanced computing and communication systems (ICACCS)*
51. Mahedy Hasan SM, Uddin MP, Mamun MA, Sharif MI, Ulhaq A, Krishnamoorthy GA (2023) Machine learning framework for early-stage detection of autism spectrum disorders. *IEEE Access*, 11
52. Khan K, Katarya R (2023) Machine learning techniques for autism spectrum disorder: current trends and future directions. In: *2023 4th International conference on innovative trends in information technology (ICITIIT)*, Kottayam, India
53. Gayatri K, Durga CLS, Bhanu NKS, Neelesh TPS, Tumuluru P, Srithar S (2023) Exploring various aspects in diagnosing autism spectrum disorder (ASD). In: *2023 International conference on computer communication and informatics (ICCCI)*

# Energy-Efficient Cluster Head Election and Data Aggregation Ensemble Machine Learning Algorithm



Kavita Gupta , Shilpi Mittal , and Kirti Walia 

**Abstract** Data transmission and communication in mobile wireless sensor networks are hindered due to the limited energy of the sensor node. This causes various challenges in the communication between sensor nodes having network loss, latency, and in complete transactions. To concern, a clustering-based network model has been developed where the cluster head election is the major issue. Therefore, we proposed an intelligent cluster-based network model with the objective to provide intelligent energy-efficient cluster head election and data aggregation mechanisms using Artificial Intelligence techniques in the mobile sensor network. Also, to overcome the network overhead, a mechanism has been presented to validate data similarity among the nearby sensor nodes. The performance evaluation of the proposed scheme has been conducted using Python with machine learning and the results obtained reflect better performance in terms of cluster head selection and data aggregation.

**Keywords** Wireless sensor networks · Mobile networks · Clustering · Machine learning

## 1 Introduction

In a wireless sensor network, a sensor node is a small component which offers a limited network lifetime due to a limited energy amount of energy level. Their energy level keeps on depleting with the passage of time, and at last the node dies after the loss of some consumption of energy. Nodes in sensor networks perform various functions such as data collection, data processing, transferring, and receiving data packets. As per sensor network architecture, there are various ways of achieving energy efficiency in sensor networks like sensor network topology, data collection schemes, architectural arrangement of nodes, etc. [5] will play an important role

---

K. Gupta (✉) · S. Mittal · K. Walia  
University Institute of Computing, Chandigarh University, Mohali, Punjab, India  
e-mail: [25.kavita@gmail.com](mailto:25.kavita@gmail.com)

K. Walia  
e-mail: [kirti.e8889@cumail.in](mailto:kirti.e8889@cumail.in)

© The Author(s), under exclusive license to Springer Nature Singapore Pte Ltd. 2024  
V. Shrivastava et al. (eds.), *Power Engineering and Intelligent Systems*, Lecture Notes in Electrical Engineering 1097, [https://doi.org/10.1007/978-981-99-7216-6\\_21](https://doi.org/10.1007/978-981-99-7216-6_21)

255

in energy consideration. As per the topological arrangement of sensor nodes in the network, each node consumes a fixed amount of energy in every consecutive round. This topological arrangement is assumed to be energy efficient if it offers a prolonged network lifetime.

Initially, all the sensor nodes have the same amount of energy and consume at a fixed rate. The energy model can be used to predict the life span of the sensor node by computing the residual energy level. With the advancement of technology, machine learning approaches can also be used to offer energy-efficient prolonged networks. Mainly the sensor nodes are used in hostile environments or in far following areas which are not easily accessible. For these applications, nodes must have appropriate battery levels in order to produce a prolonged network lifetime [12]. Protocols and methods can play a role in energy saving. Various routing protocols have been proposed by Younis et al. [18], Chen et al. [6], and Reddy et al. [13] to offer energy-efficient networks. Existing literature advocates that clustering of nodes is the key solution for wireless networks and is further followed by data aggregation. In each cluster, there is one CH (Cluster Head) which collects the data from member nodes and further transmitted it to the sink node.

Selecting the best optimal cluster head scheme for a prolonged network lifetime is very important. After the optimal cluster head election algorithm, the next challenge is to execute data aggregation so as to avoid the aggregation of redundant data. There is a dire need for a mechanism that can avoid redundancy in aggregated data, which further be useful for offering energy-efficient network. Devising an efficient data aggregation approach is also a challenging task. Machine learning can also be considered a good approach for sensor networks. Machine learning and sensor networks can be used in combination to offer energy-efficient networks. Machine learning provides the solution for two major issues of sensor networks, i.e., clustering and data aggregation. Many researchers have proved the use of machine learning algorithms for cluster head selection and data aggregation. This work represents an optimal cluster head selection and aggregation approach for sensor networks using machine learning approaches. The next Sect. 2 represents the work of eminent researchers and Sect. 3 represents the proposed approach following the result and discussions in Sect. 4 and the last section represents the conclusion and future scope of the proposed work.

## 2 Literature Review

This section gives an overview of the feasibility of clustering and data aggregation using machine learning approaches. Ammari and Das [1] raised an essential query regarding the boundaries of power performance of sensor networks—what's the higher sure at the life of a sensor community that collects information from a unique vicinity the use of a positive wide variety of power-restricted nodes. It is very important to find the solution for queries: first, it permits calibration of actual global information-accumulating protocols and know-how of things that save those

protocols from coming near essential limits. Secondly, the dependence of lifetime on elements just like the vicinity of observation, the supply conduct inside that vicinity, base station location, a wide variety of nodes, radio route loss characteristics, performance of node electronics, and the power to be had on a node is exposed. This permits architects of sensor networks to be cognizant of elements that have the finest ability to affect the community's lifetime. By using an aggregate of principle and substantial simulations of built networks, results display that during all information-accumulating eventualities presented in this work. Mhatre et al. [11] proposed a cost-effective method to analyze the performance of nodes in single or multi-hop communication and also analyze the results based on their cluster heads. The researcher advocates a hybrid conversation mode with a mixture of single and multi-hop modes which is cost-effective and powerful also.

Hybrid Energy-Efficient Approach (HEED) proposed by Younis et al. [18] elects the cluster head on a periodic basis using the residual energy of sensor nodes as well as the proximity of node. This protocol offers low communication overhead as well as supports efficient cluster head formation throughout the communication. Results obtained with suitable bounds on node density and inter- and intra-cluster transmission ranges, this protocol can asymptotically nearly honestly assure connectivity of clustered networks. Simulation consequences exhibit that the proposed technique is powerful in prolonging community life and helping scalable statistics aggregation. Chen et al. [6] claim clustering offers a powerful technique for prolonging the life of mobility support sensor networks. Unequal cluster-primarily based totally routing (UCR) protocol distributes the nodes into clusters of unequal sizes. Cluster heads in the direction of the bottom station have smaller cluster sizes than the ones further from the bottom station, accordingly, they are able to keep a few strengths for the inter-cluster records forwarding. A grasping geographic and strength-conscious routing protocol is designed for inter-cluster communication, which considers the tradeoff between the strength fee of relay paths and the residual strength of relay nodes. Simulation consequences display that UCR mitigates the new spot trouble and achieves an apparent development at the network lifetime.

Sensor networks include the number of unattended sensor nodes with limited battery life. Therefore sensor networks require speedy reaction time and record dissemination among supply sensors and sinks, that's an important interest in WSNs and must be performed in a power-green and well-timed manner. This work signifies the alternate-off between power financial savings and supply-to-sink layoff that will expand the operation of sensors and as a result boom the life of the sensor networks. It allows the sink to acquire sensed records in time and offer suitable selections quickly. This proposed dissemination protocol decays the transmission variety of sensors right into a positive range of concentric round bands which is mainly based on the minimum distance among forwarding sensors.

Then, these concentric rounds are based totally on their outdoor radii so as to assist a supply sensor specific its diploma of interest in minimizing metrics, specifically power intake and supply-to-sink put off. Results show that using sensors nodes lies on the shortest distance route among supply and the sink, for identification of proximal forwarders. Quantitative outcomes display that one concentric round minimizes

power intake; the final concentric round minimizes supply-to-sink keep off, and the central concentric round alternates off among the two metrics in propagating the data toward the sink node. Ammari et al. [1] proposed a data protocol that decomposes the transmission range of detectors in a number of concentric bands which covers the minimum distance between successive forwarding detectors.

Anastasi et al. [3] proposed an energy conservation scheme to provide the solution for energy-efficient data attainment. Researchers also highlight the various methods of energy conservation of sensor nodes. Heo et al. [9] proposed the EARQ approach which evaluates the energy consumption cost, delay in transmission, and efficient delivery of data packets to the sink node. This prediction is based on the data received from the neighboring nodes. For data transmission, path with less transmission cost will be chosen for efficient data delivery. Kalman-filter-based energy-efficient network approach proposed by Munari et al. [12] uses the location information of nodes in the network. In this approach, sink node estimates the speed and location of nodes using the Kalman filter which improves the network lifetime.

Watson et al. [17] highlight the role of thinking skills to achieve energy efficiency using energy informatics. The presented literature reveals that environmental sustainability is mandatory to handle. Rault et al. [14] present mapping between extended lifetime and application requirements raised during the designing of the sensor network. The literature presents a systematic view of various energy-efficient schemes to show the link between requirements and optimized objectives. Sheng et al. [16] offered a time stamp-based energy-efficient approach which includes optimal utilization of network resources and computing optimization. The results obtained are assumed to be energy efficient. Guo et al. [8] proposed an approach named SWIPT where energy consumption is computed based on data forwarding. This approach works in two phases: in the first phase received power is split in continuous power streams and in the next phase reset-all algorithm has been proposed to produce optimized and efficient results.

Rehman et al. [15] proposed a cluster head election approach to offer a prolonged network lifetime. The proposed CH election approach elected the cluster head by computing the weight of the node which includes the behavior of sensor nodes to ensure security mechanism, waiting time, and the distance between the nodes. Bayesian estimation approach proposed by Anwar et al. [4] used trust values to protect the sensor network from various attacks. This approach collected the data based on time stamps and estimates the data collection and the results obtained reveal that the approach performs better for malicious node detection which further improves the throughput.

Khan et al. [10] proposed a novel cluster head selection approach that elects the cluster head based on their uniform load distribution. The proposed trust-based approach is compared with existing trust models and performs better for packet delivery ratio and throughput. Amutha et al. [2] highlight the various factors to analyze the performance of sensor networks based on various parameters. The presented work gives a comparative study of cluster-based sensor networks. Gupta et al. [7] proposed an efficient cluster head election approach that selects the cluster head on the basis of a few parameters but incorporating machine learning algorithms will fasten the

cluster head selection mechanism. The next section presents the proposed approach for cluster head selection and data collection and aggregation using machine learning algorithms.

### 3 Proposed Work

#### 3.1 Cluster Formation Using Machine Learning

This section describes a protocol to achieve energy-efficient sensor network using machine learning approaches. Clustering is assumed to offer a promised solution for mobility support sensor networks. Although the sensor nodes are deployed in a hostile environment and communication needs to arrange in the form of clusters. Researchers have proposed various approaches for cluster formation and cluster head (CH) election. Current work promised to provide the solution for two issues, firstly formation of cluster, and secondly CH selection for efficient data delivery. For the first contribution to cluster formation machine learning's coefficient of correlation, approach has been used. In this approach, sensor nodes are arranged in clusters on the basis of a few parameters like temperature, humidity, and other environmental factors.

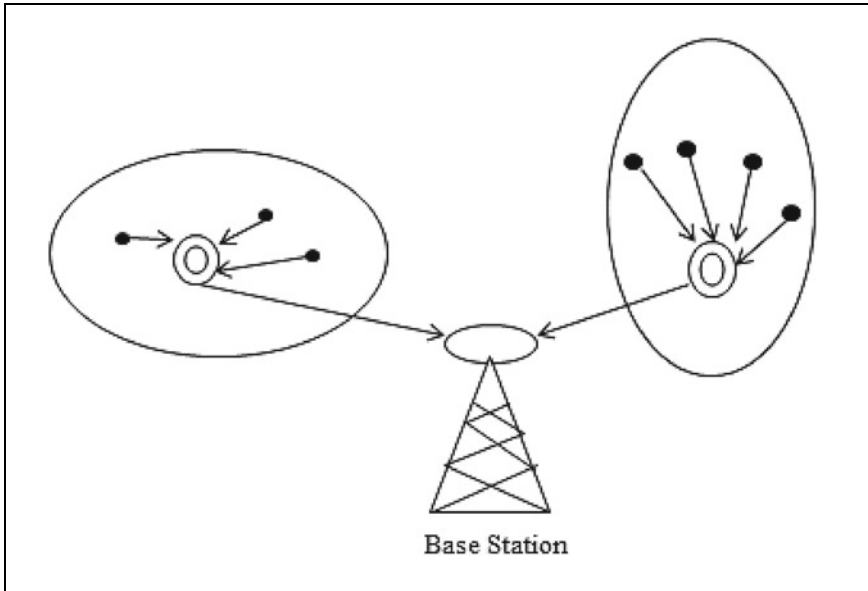
A threshold value will be defined for parameters  $P_1, P_2, \dots, P_n$  to correlate the sensor nodes so as to define clusters as shown in Fig. 1. The selection of Cluster Head (CH) is also a very tedious task because of mobile-natured sensor nodes. For CH selection residual energy level, distance from base station and remaining time of stay of node in network could be considered as few of important parameters. Because of the mobile nature of sensor nodes, the nodes have the tendency of leaving their cluster and tend to join the new cluster. Mobility models can be used to identify the mobility pattern of sensor nodes in the network. Random Way Point Mobility Model is one of the traditional models used to identify the mobility patterns of sensor nodes.

Secondly, for cluster head selection step-by-step approach has been used. In step 1, sensor nodes are taken and all are of equal probability of selecting as cluster heads. In the next step, nodes that are competitive to be cluster head will be taken into consideration based on the values for the above-mentioned parameters, then in the last step sensor node which satisfies the criteria of highest residual energy, highest remaining time of stay, and least distance from the base station will be elected as CH for further communication.

$$Node(x, y) = Max(RTS), Max(RES), Min(dis) \quad (1)$$

where RTS is the remaining time of stay of a node in the sensor network, RES is the residual energy level of the sensor node, and dis denotes the distance of the sensor node from the base station.





**Fig. 1** Sensor network architecture

### ***3.2 Data Aggregation Using Machine Learning***

This work proposes a machine learning-based data aggregation approach for cluster-based networks. In MWSN clusters are formed on the basis correlation coefficient. The cluster head is assumed to have a higher energy level as compared to the other member nodes. CH is responsible to collect from its member nodes and forward it to the base station. During data aggregation, there are chances of sensing the same type of data from nearby nodes. Here, the correlation approach has been used to validate the similarity index among the member nodes. If the similarity index is higher than the specified threshold value then these nodes are considered the part of same cluster and are allowed to send the data to their respective cluster head. At the cluster head level, a machine learning-based higher correlation filter approach has been used for redundant data reduction during data aggregation. In this manner, filtered data will be transmitted to the base station, which reduces the energy consumption rate during the transmission and makes the network more energy efficient. The overall work of the proposed approach is shown in Fig. 2.

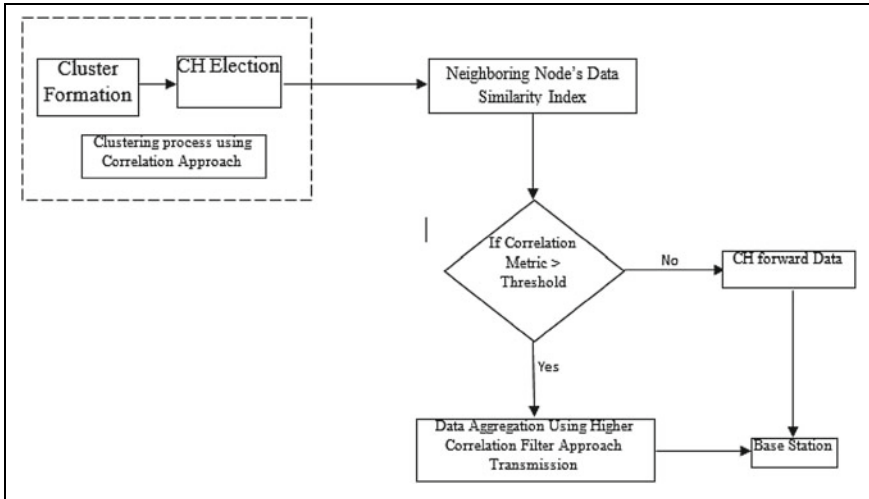


Fig. 2 Join\_R versus data sent to base station

### 3.3 Methods and Tools

In this work, the collected data is analyzed using machine learning algorithms and to find the best suitable approach among linear regression, K-nearest neighbors, Support Vector Machine, and Bayes which are compared based on mean and standard deviation. Table 1 shows the mean value and standard deviation obtained for each of these mentioned approaches and the graphical distribution is depicted in the following graph shown in Fig. 3.

Table 1 Comparison of statistical techniques

Name	Mean(scores)	Std(scores)
lr	0.58333	0.13437
knn	0.96667	0.06667
cart	0.93889	0.08032
svm	0.75	0.09379
Bayes	0.95	0.07638
Voting method	0.96667	0.06667

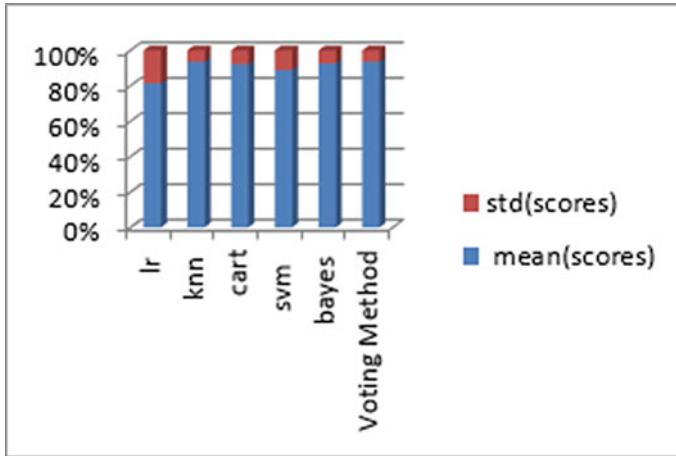


Fig. 3 Dist\_To\_CH versus Data\_R

## 4 Result Analysis

The proposed cluster head election and data aggregation approach has been implemented using Python. Table 1 presents the relationship between the selected CH and the energy level of the sensor node.

---

### Algorithm 1 Cluster Head Election Algorithm

---

- 1: Cluster Formed Using Correlation Approach
  - 2: Data Similarity Index is Computed for the identification of neighboring nodes
  - 3: **if** Correlation Metric Threshold Value **then**
  - 4:   Execute Data Aggregation Process and Send Date to Base Station
  - 5: **else**
  - 6:   Data Send = Base Station
  - 7: **end if**
- 

Figure 4 shows the relationship between two variables who\_CH and the expended energy level of selected CH. Results obtained interpret that the cluster head selection process is executing as the energy level of the existing cluster head reaches a threshold value. X-axis defines the elected cluster head and Y-axis defines the energy level of the selected cluster head. The relationship between the residual energy level and the selected CH is represented by a dot but the figure depicts the high density of dots in the form of a straight line which shows a high degree of correlation between these variables. Nodes are of mobile nature and their energy level changes irrespective of their IDs. In sensor networks energy is playing a very important role, therefore their residual energy computation is very important for sustainable networks. The Radio Energy model can be used to compute the energy level of sensor nodes. The residual

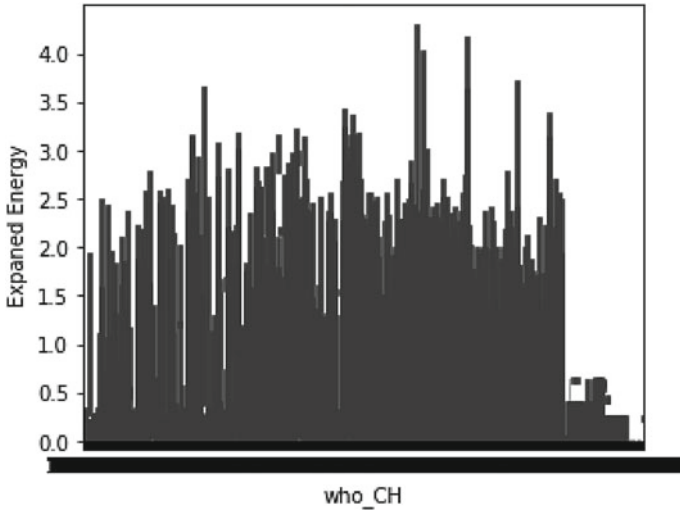


Fig. 4 who\_CH versus energy level

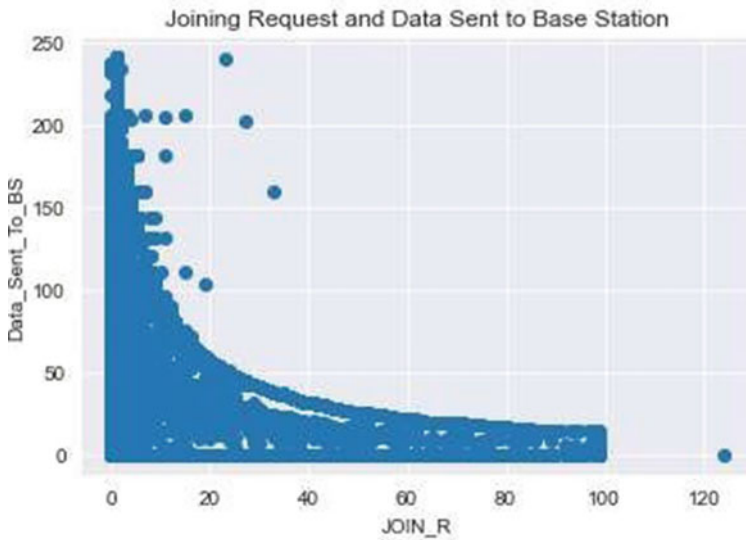
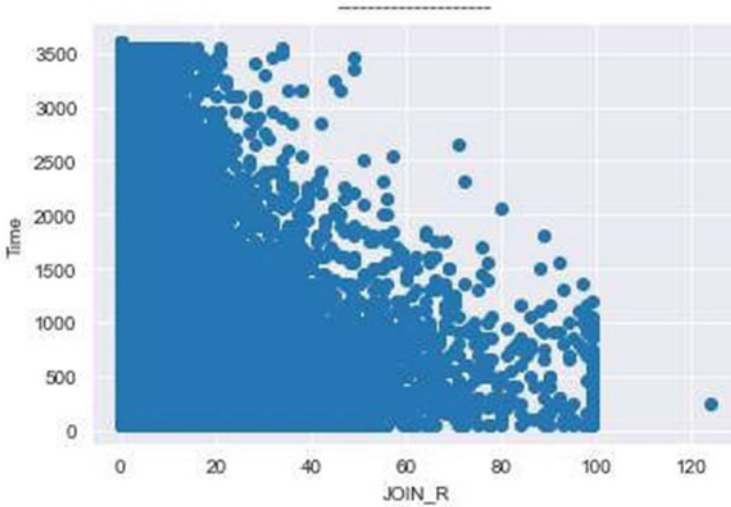


Fig. 5 Join\_R versus time

energy level of the sensor node is playing a very important role in the election of new CH in this work.

Figure 5 shows the relationship between variables Join\_R (Number of join request messages) and the Y-axis represents the number of data packets transmitted to a base station. Results obtained depict that data-sent-rate depends on the number of data



**Fig. 6** Dist\_To\_CH versus Data\_R

packets received from member nodes. Initially, the newly elected CH has a high amount of data packets then more data packets have been transmitted to the base station. The rate of data transmission has a direct relation with the number of data packets received. The rapid fall in the data packet received could be caused due to change of cluster head or the existing CH is no longer in its place due to its mobile nature. Due to CH movements, neighboring nodes may not be aware to send data or in the meantime, any new node may have sent the join request message to be part of its cluster. Therefore, nodes may start joining the new cluster. Figure 6 depicts the relationship between the number of data packets received with respect to the distance of the node from CH. X-axis denotes the distance of the node from the cluster head for the specific simulation round and Y-axis denotes the number of data packets received from member nodes. The node with the shortest distance from CH could send more amount of data packets with less energy consumption rate as compared to the node with a larger distance which will send fewer data packets.

As there will be less energy consumption rate in case of sending the data packets to less distance as compared to data transmission over a long distance. More often data from nearby nodes reach fast but there will be chances of replication of data. The data packet is represented with a dot in this diagram. The high intensity of nodes shows a high degree of correlation among the sensor nodes. During transmission, a node may change its position due to the mobility factor because of a high amount of energy consumption rate during data transmission.

Figure 7 shows the high degree of correlation between variables Join\_R (join request messages) and Time. This figure depicts that as soon as any node advertises the message to join its cluster, the majority of the nearby nodes send the join request

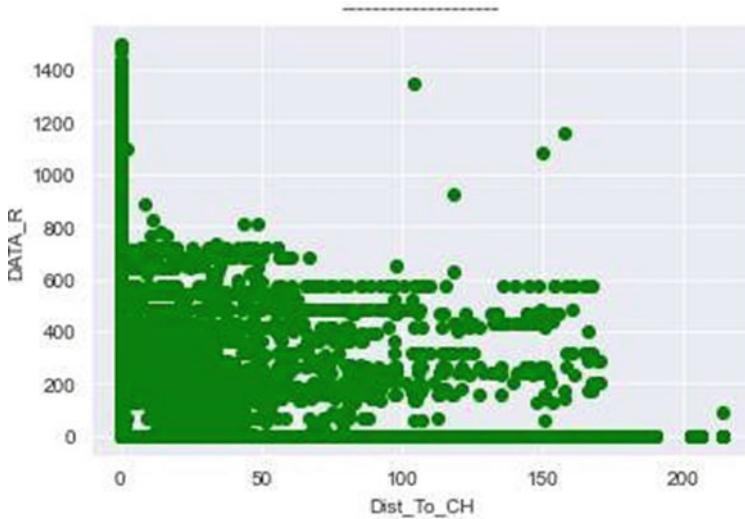


Fig. 7 Join\_R versus time

message to join announces for initially there are more nodes sending the join request message to be part of that cluster. The number of join request messages decreases with time as nodes' energy depleted with time.

## 5 Conclusion

This paper proposed intelligent cluster formation for improving the energy efficiency of sensor nodes while mobility in mobile sensor networks. There is a cluster head election algorithm which has been proposed to select cluster heads intelligently based on the energy level of the sensor node. Also, it has analyzed data duplicity by implementing machine learning algorithms. The proposed work performance determines that the election of a cluster head provides an efficient node with high energy consumption for communication in mobile wireless sensor networks. In the future, the proposed work can be extended to an optimized data aggregation scheme by the filtration process of the duplicate data intelligently.

## References

1. Ammari HM, Das SK (2005) Trade-off between energy savings and source-to-sink delay in data dissemination for wireless sensor networks. In: Proceedings of the 8th ACM international symposium on modeling, analysis and simulation of wireless and mobile systems, pp 126–133
2. Amutha J, Sharma S, Sharma SK (2021) Strategies based on various aspects of clustering in wireless sensor networks using classical, optimization and machine learning techniques: Review, taxonomy, research findings, challenges and future directions. *Compu Sci Rev* 40:100376
3. Anastasi G, Conti M, Di Francesco M, Passarella A (2009) Energy conservation in wireless sensor networks: a survey. *Ad hoc Netw* 7(3):537–568
4. Anwar RW, Zainal A, Outay F, Yasar A, Iqbal S (2019) Btem: belief based trust evaluation mechanism for wireless sensor networks. *Futur Gener Comput Syst* 96:605–616
5. Bhardwaj M, Garnett T, Chandrakasan AP (2001) Upper bounds on the lifetime of sensor networks. In: ICC 2001. In: IEEE international conference on communications. Conference record (Cat. No. 01CH37240), vol 3. IEEE, pp 785–790
6. Chen G, Li C, Ye M, Wu J (2009) An unequal cluster-based routing protocol in wireless sensor networks. *Wirel Netw* 15:193–207
7. Garg A, Gupta K, Singh A (2019) Cluster based energy efficient routing protocol (EERP) for mobile wireless sensor network
8. Guo S, Shi Y, Yang Y, Xiao B (2017) Energy efficiency maximization in mobile wireless energy harvesting sensor networks. *IEEE Trans Mob Comput* 17(7):1524–1537
9. Heo J, Hong J, Cho Y (2009) EARQ: energy aware routing for real-time and reliable communication in wireless industrial sensor networks. *IEEE Trans Ind Inform* 5(1):3–11
10. Khan T, Singh K, Hasan MH, Ahmad K, Reddy GT, Mohan S, Ahmadian A (2021) ETERS: a comprehensive energy aware trust-based efficient routing scheme for adversarial WSNs. *Futur Gener Comput Syst* 125:921–943
11. Mhatre V, Rosenberg C (2004) Design guidelines for wireless sensor networks: communication, clustering and aggregation. *Ad hoc Netw* 2(1):45–63
12. Munari A, Schott W, Krishnan S (2009) Energy-efficient routing in mobile wireless sensor networks using mobility prediction. In: 2009 IEEE 34th conference on local computer networks. IEEE, pp 514–521
13. Rami Reddy M, Ravi Chandra M, Venkatramana P, Dilli R (2023) Energy-efficient cluster head selection in wireless sensor networks using an improved grey wolf optimization algorithm. *Computers* 12(2):35
14. Rault T, Bouabdallah A, Challal Y (2014) Energy efficiency in wireless sensor networks: a top-down survey. *Comput Netw* 67:104–122
15. Rehman E, Sher M, Naqvi SHA, Badar Khan K, Ullah K, et al (2017) Energy efficient secure trust based clustering algorithm for mobile wireless sensor network. *J Comput Netw Commun*
16. Sheng Z, Mahapatra C, Leung VC, Chen M, Sahu PK (2015) Energy efficient cooperative computing in mobile wireless sensor networks. *IEEE Trans Cloud Comput* 6(1):114–126
17. Watson RT, Boudreau MC, Chen AJ (2010) Information systems and environmentally sustainable development: energy informatics and new directions for the is community. In: *MIS quarterly*, pp 23–38
18. Younis O, Fahmy S (2004) HEED: a hybrid, energy-efficient, distributed clustering approach for ad hoc sensor networks. *IEEE Trans Mob Comput* 3(4):366–379

# Multi-sensor Data Fusion for Early Fire Estimation Using ML Techniques



Priyanka Kushwaha, Muskan Sharma, Pragati Kumari, and Richa Yadav

**Abstract** Fire alarms are an essential aspect in providing safety for individuals and structures during a fire emergency. However, traditional fire alarms have several limitations, including false alarms and slow response times. In this study, we describe implementation and comparison of various techniques for machine learning like Naive Bayes, Random Forest, KNN, Logistic Regression, SVM Linear Kernel, and Decision trees to improve fire detection and response using various parameters such as Humidity, Temperature, MQ139, TVOC, and eCO<sub>2</sub>. There are many research papers which use deep learning and artificial intelligence using datasets containing images. However, our model has used a real-time-stamped text dataset and split them into train sets and test sets. Using various machine learning algorithms, different parameters have been calculated such as accuracy, precision, F1score, sensitivity, specificity, kappa, and RMSE values. Our findings suggest that fire alarms play an important role in smart home technology by providing early warning in the event of a fire and helping to protect people and property. Overall, fire alarms are becoming increasingly integrated into smart home technology, providing users with added convenience, safety, and peace of mind.

**Keywords** Fire alarms · Machine learning · Fire detection

## 1 Introduction

To ensure the safety of the people inside and the building, in the event of a fire, fire alarms play a crucial role. They detect the presence of smoke, heat, and other factors and alarm people to leave the place. There are several drawbacks of traditional fire alarms such as [5] alarm triggered by cooking smoke and may have a poor reaction time that may lead to mishappenings. Several new developments have been there in fire alarms as mentioned in [2, 4, 13, 19–21] with the development of machine

---

Supported by organization IGDTUW.

---

P. Kushwaha (✉) · M. Sharma · P. Kumari · R. Yadav  
Indira Gandhi Delhi Technical University for Women, New Delhi, India  
e-mail: [priyankakushwaha533@gmail.com](mailto:priyankakushwaha533@gmail.com)

© The Author(s), under exclusive license to Springer Nature Singapore Pte Ltd. 2024  
V. Shrivastava et al. (eds.), *Power Engineering and Intelligent Systems*, Lecture Notes  
in Electrical Engineering 1097, [https://doi.org/10.1007/978-981-99-7216-6\\_22](https://doi.org/10.1007/978-981-99-7216-6_22)



learning techniques several new opportunities in fire alarm can be seen as mentioned in [14, 15, 18, 20–23, 25]. Machine learning can be used to predict the possibility of fire by analyzing a large amount of data. This will decrease response time, increase accuracy, and decrease the rate of false alarms.

The aim of this study is to use machine learning methods and thus find the drawbacks and advantages in fire alarm detection. So, for accurate fire alarm detection and response, various machine learning methods are used with factors like humidity, temperature, MQ139, TVOC, and eCO<sub>2</sub>.

The volatile compounds present in the atmosphere are measured using the air quality sensor MQ139. As the MQ139 is a metal oxide semiconductor (MOS) device, a metal oxide substance is exploited as its sensing element. When VOCs present in the air come in contact with MQ139 the electrical conductivity of the metal oxide material changes. The bulk of VOCs in the air is measured and used by this change in conductivity of metal oxide material. VOCs are emitted by adhesives, cleaning products, fuels, paints, and many other products in the form of gases. The total amount of volatile organic components in the atmosphere is referred to as Total Volatile Organic Compounds (TVOCs).

TVOC can be measured in micrograms per cubic meter ( $\text{g}/\text{m}^3$ ) or Parts per billion (ppb). The amount of carbon dioxide, i.e., CO<sub>2</sub> present in the atmosphere is referred to as “eCO<sub>2</sub>”, CO<sub>2</sub> is a colorless, odorless gas that can be produced by both human and natural processes. The results from this study will help in understanding the importance of machine learning in fire alarms and fire detection and also will help in creating more accurate fire safety systems. The usage of fire alarms with smart home systems is becoming popular nowadays. For a more accurate and reliable fire safety system fire alarms are made to work with other smart home appliances like smart locks, smart lights, and smart thermostats.

Among the main advantages of fire alarms in smart home technologies are:

- (1) Smart fire alarm system allows you to keep track by smartphone and notifies fire conditions so that necessary actions can be taken. One can immediately get to know about the fire conditions on one's smartphone.
- (2) The other smart devices connected to the fire alarms can automatically respond to the fire conditions like the smart light can turn on and the smart lock can open, etc.
- (3) A more accurate solution can be provided if sensors are connected with other sensors such as smoke and carbon monoxide monitors with other sensors present in the home.
- (4) Smart fire alarms are simple to use and set up as they are generally battery-operated and require no wire. So, they are easy to operate.
- (5) Smart home fire alarms are user-friendly as they can have machine learning algorithms and human-like voices.

## 2 The Approach

### 2.1 *Scaling and Data Preprocessing*

The dataset from [1] is used in this research work, and variables with missing values have been removed. The dataset [1] includes data collected over time from eight controlled fire experiments in a laboratory setting. Half of the experiments utilized an electric fire source, two used paperboard cartons as the source, and the remaining two utilized clothing as the source. Carton\_1, Carton\_2, Clothing\_1, Clothing\_2, Electrical\_1, Electrical\_2, Electrical\_3, and Electrical\_4 are the different datasets as per the fire experiments done in the laboratory. The humidity, temperature, MQ139, TVOC, and eCO2 levels were recorded using sensors at the start of each experiment when the fire was ignited and continued to be recorded until the fire alarm was activated. Any algorithm used to handle data in order to make it simpler and more efficient to apply classification algorithms and, as a result, improve accuracy is referred to as data processing. Techniques used in data processing include Feature scaling, dimensionality reduction, and normalization. In this paper, all of the features are scaled using normalization and feature scaling such that no feature may overpower any other and precise findings can be achieved.

### 2.2 *Algorithms for Machine Learning*

Machine learning algorithms can be unsupervised or supervised. The supervised algorithm initially trains the model using a labeled training dataset, and then the machine predicts the output in accordance with the trained model; supervised approaches can be utilized for classification and regression, while unsupervised machine learning techniques cannot be used for either of these tasks because the model cannot be trained since there is no labeled training dataset. As the early identification of indoor fires utilizing sensor fusion is the main objective of this work, supervised machine learning classification methods will be implemented throughout this paper. Logistic Regression, Random Forest, Support Vector Machine, KNN, SVM-RBF Kernel, SVM Linear Kernel, Decision Tree, and Naive Bayes are the classification techniques implemented. The code for an event's occurrence in logistic regression [7, 8] is 1, whereas the code for an event's absence is 0. The standard notation for a linear model's regression is

$$y = a + bx + e \tag{1}$$

where  $x$  is the independent variable,  $y$  is the dependent variable,  $a$  is the intercept,  $b$  is the regression coefficient, and  $e$  is a system error. SVM [9] is a method of classification that identifies an "optimal" hyperplane as the solution to the learning

problem. The simplest SVM algorithm is known as linear SVM if the hyperplane is in the space of the input data  $x$ . The hypothesis space in this consists of all subsets of hyperplanes with the form  $y = wx + b$ . If the SVM discovers a hyperplane that is distinct from the input data  $x$ , that is, if the hyperplane is caused by the feature space's inner product's kernel  $K$ , also known as the SVM kernel, which defines that space's inner product. The hypothesis space is a collection of "hyperplanes" in feature space that  $K$  induces through the kernel  $K$ . Since no assumptions are made about the dataset when using the  $K$ -Nearest Neighbor approach [6], it is referred to as non-parametric classification. It takes little time to compute and is straightforward and efficient. If the data is continuous, the closest neighbors are determined using the Euclidean distance. When classifying unlabeled data, the value of  $K$  is crucial, and the best value can be discovered by repeatedly running classifiers with different values. As a result, the computing cost is significant, and the algorithm is seen as being lazy. Naive Bayes [10] assigns a given instance the maximum all-likelihood elegance, and the vector of its characteristic is utilized to indicate it. This procedure can be simplified, making it a characteristic vector and a class if we assume that functions are impartially assigned elegance.

$$P(X|C) = P \text{In} P(X|C), \text{ where } X = (x_1 \dots \dots \dots x_n) \quad (2)$$

Nodes in the decision tree are shaped like circles, and they are connected by branches that resemble segments, just like a regular tree. The decision tree's starting node, or root, is referred to as the root node. The decision tree descends from the root node and begins to grow to the right from the left. The chain's final node is known as a leaf node. a set of regression and classification trees, where the predictions are combined and the trees are constructed using a random sample selection to determine the prediction, are used to form the random forest [11, 12].

### 3 Experiments

The Scikit library of Python was used to implement the algorithms [16, 17], The measures of quantitative assessment found where Accuracy, Recall, Precision, RMSE, Sensitivity, F1-score, Kappa, Specificity, and Accuracy can be defined as how close the predictions are to the real values, but to find the perfect model as the data is not balanced, the calculation of other parameters is also done. Actual and anticipated values must be positive for there to be true positive, if actual and predicted values are negative then true negative, if the real value is positive but the predicted one is negative then false negative and if the real value is negative and predicted one is positive then false positive. The number of real positive values from all the positive values is termed precision, while Recall tells the number of predicted positive values out

of real positive values. The number of correct predictions of true positives is given by sensitivity, while the number of correct predictions of true negatives is given by specificity. Root Mean Square Error (RMSE) predicts the quality of the model, a good quality model has a similar RMSE value for test and training sets. Kappa is a better term than accuracy for imbalanced data which gives a comparison between the accuracy observed and some random expected accuracy. The algorithm-wise results and observation are given below.

### 3.1 Logistic Regression

According to Table 1 of logistic regression, Carton\_2 shows the most accurate results, i.e., 1.0 and F1Score as 1.0. The second most accurate prediction is for electrical\_4, i.e., 0.9969, and F1\_score as 0.9969.

**Table 1** Variable calculations by logistic regression

Datasets	Accuracy	Sensitivity	Specificity	Precision	Recall	F1-Score	RMSE	Kappa
Carton_1	0.9633	0.8823	0.9843	0.9633	0.9633	0.9633	0.1915	0.9342
Carton_2	1.0	1.0	1.0	1.0	1.0	1.0	1.0	1.0
Clothing_1	0.9768	0.0	1.0	0.9768	0.9768	0.9768	0.1519	0.9541
Clothing_2	0.9802	1.0	0.9672	0.9802	0.9802	0.9802	0.1405	0.9647
Electrical_1	0.9814	0.2857	1.0	0.9814	0.9814	0.9814	0.1362	0.7335
Electrical_2	0.9725	0.0	1.0	0.9725	0.9725	0.9725	0.1656	0.0
Electrical_3	0.9887	0.9986	0.9487	0.9887	0.9887	0.9887	0.1061	0.9567
Electrical_4	0.9969	1.0	1.0	0.9969	0.9969	0.9969	0.0552	0.9915

### 3.2 K-Nearest Neighbor

According to Table 2 of KNN, Carton\_2 shows the most accurate results, i.e., 1.0 and F1score as 1.0.

**Table 2** Variable calculations by K-nearest neighbor

Datasets	Accuracy	Sensitivity	Specificity	Precision	Recall	F1-Score	RMSE	Kappa
Carton_1	0.9816	1.0	0.9692	0.9816	0.9816	0.9816	0.1354	0.9676
Carton_2	1.0	1.0	1.0	1.0	1.0	1.0	1.0	1.0
Clothing_1	0.9834	0.6666	0.9922	0.9834	0.9834	0.9834	0.1284	0.9676
Clothing_2	0.9986	1.0	1.0	0.9986	0.9986	0.9986	0.0362	0.9976
Electrical_1	0.9973	1.0	1.0	0.9973	0.9973	0.9973	0.0515	0.9667
Electrical_2	0.9756	0.6	0.9937	0.9756	0.9756	0.9756	0.1561	0.4197
Electrical_3	0.9977	1.0	1.0	0.9977	0.9977	0.9977	0.0474	0.9914
Electrical_4	0.9989	1.0	1.0	0.9989	0.9989	0.9989	0.0319	0.9971

### 3.3 SVM

According to Table 3 of SVM, Carton\_2 shows the most accurate results, i.e., 1.0 and F1Score as 1.0.

**Table 3** Variable calculations by support vector machine

Datasets	Accuracy	Sensitivity	Specificity	Precision	Recall	F1-Score	RMSE	Kappa
Carton_1	0.9541	0.8823	0.9841	0.9541	0.9541	0.9541	0.2141	0.9182
Carton_2	1.0	1.0	1.0	1.0	1.0	1.0	1.0	1.0
Clothing_1	0.9768	0.0	1.0	0.9768	0.9768	0.9768	0.1519	0.9541
Clothing_2	0.9815	1.0	0.9731	0.9815	0.9815	0.9815	0.1358	0.9670
Electrical_1	1.0	1.0	1.0	1.0	1.0	1.0	0.0	1.0
Electrical_2	0.9725	0.0	1.0	0.9725	0.9725	0.9725	0.1656	0.0
Electrical_3	0.9943	0.9973	0.9914	0.9943	0.9943	0.9943	0.0750	0.9787
Electrical_4	0.9969	1.0	1.0	0.9969	0.9969	0.9969	0.0552	0.9915

### 3.4 SVM RBF

According to Table 4 of SVM RBF, Carton\_2 shows the most accurate results,i.e., 1.0 and F1Score as 1.0.

**Table 4** Variable calculations by SVM RBF

Datasets	Accuracy	Sensitivity	Specificity	Precision	Recall	F1-Score	RMSE	Kappa
Carton_1	0.9541	0.8823	0.9841	0.9541	0.9541	0.9541	0.2141	0.9182
Carton_2	1.0	1.0	1.0	1.0	1.0	1.0	1.0	1.0
Clothing_1	0.9735	0.0	1.0	0.9735	0.9735	0.9735	0.1624	0.9475
Clothing_2	0.9789	1.0	0.9729	0.9789	0.9789	0.9789	0.1451	0.9623
Electrical_1	0.9787	0.0	1.0	0.9787	0.9787	0.9787	0.1456	0.6588
Electrical_2	0.9725	0.0	1.0	0.9725	0.9725	0.9725	0.1656	0.0
Electrical_3	0.9763	0.9986	0.8547	0.9763	0.9763	0.9763	0.1537	0.9060
Electrical_4	0.9969	1.0	1.0	0.9969	0.9969	0.9969	0.0552	0.9915

### 3.5 Naive Bayes

According to Table 5 of Naive Bayes, Carton\_2 shows the most accurate results, i.e., 0.9933, and F1score as 0.9933.

**Table 5** Variable calculations by Naive Bayes

Datasets	Accuracy	Sensitivity	Specificity	Precision	Recall	F1-Score	RMSE	Kappa
Carton_1	0.9357	1.0	0.9508	0.9357	0.9357	0.9357	0.2534	0.8899
Carton_2	0.9933	0.9705	1.0	0.9933	0.9933	0.9933	0.0813	0.9866
Clothing_1	0.9900	1.0	0.9922	0.9900	0.9900	0.9900	0.0995	0.9807
Clothing_2	0.9920	0.9787	1.0	0.9920	0.9920	0.9920	0.0889	0.9857
Electrical_1	0.9867	1.0	0.9972	0.9867	0.9867	0.9867	0.1151	0.8520
Electrical_2	0.9573	0.8	0.9902	0.9573	0.9573	0.9573	0.2065	0.5196
Electrical_3	0.9673	0.9813	1.0	0.9673	0.9673	0.9673	0.1807	0.8825
Electrical_4	0.9735	1.0	0.988	0.9735	0.9735	0.9735	0.1627	0.9301

### 3.6 Decision Tree

According to Table 6 of the Decision Tree, Carton\_2 shows the most accurate results, i.e., 1.0 and F1Score as 1.0.

**Table 6** Variable calculations by decision tree

Datasets	Accuracy	Sensitivity	Specificity	Precision	Recall	F1-Score	RMSE	Kappa
Carton_1	0.9724	0.9411	0.9692	0.9724	0.9724	0.9724	0.1659	0.9510
Carton_2	1.0	1.0	1.0	1.0	1.0	1.0	0.0	1.0
Clothing_1	0.9933	0.8333	0.9923	0.9933	0.9933	0.9933	0.0812	0.9871
Clothing_2	1.0	1.0	1.0	1.0	1.0	1.0	0.0	1.0
Electrical_1	0.9946	1.0	1.0	0.9946	0.9946	0.9946	0.0728	0.9354
Electrical_2	0.9756	0.6	0.9936	0.9756	0.9756	0.9756	0.1561	0.5907
Electrical_3	0.9977	1.0	0.9913	0.9977	0.9977	0.9977	0.0474	0.9914
Electrical_4	0.9959	1.0	1.0	0.9959	0.9959	0.9959	0.0638	0.9887

### 3.7 Random Forest

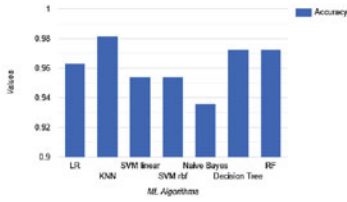
According to Table 7 of Random forest, Carton\_2 shows the most accurate results, i.e., 1.0, and F1score as 1.0.

**Table 7** Variable calculations by random forest

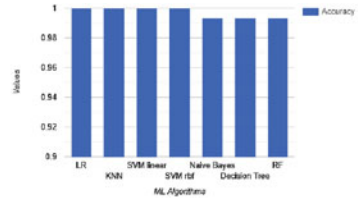
Datasets	Accuracy	Sensitivity	Specificity	Precision	Recall	F1-Score	RMSE	Kappa
Carton_1	0.9724	1.0	0.9538	0.9724	0.9724	0.9724	0.1659	0.9517
Carton_2	1.0	1.0	1.0	1.0	1.0	1.0	0.0	1.0
Clothing_1	0.9933	0.8333	0.9923	0.9933	0.9933	0.9933	0.0812	0.9871
Clothing_2	1.0	1.0	1.0	1.0	1.0	1.0	0.0	1.0
Electrical_1	0.9973	1.0	1.0	0.9973	0.9973	0.9973	0.0515	0.9667
Electrical_2	0.9878	0.8	1.0	0.9878	0.9878	0.9878	0.1104	0.709
Electrical_3	0.9977	1.0	0.9913	0.9977	0.9977	0.9977	0.0474	0.9914
Electrical_4	0.9979	1.0	1.0	0.9979	0.9979	0.9979	0.0451	0.9943

### 3.8 Graphs

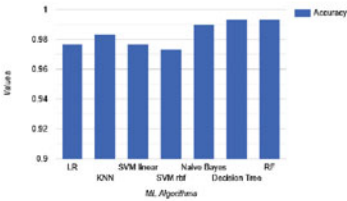
Accuracy comparisons of various ML algorithms according to each dataset are shown in Fig. 1.



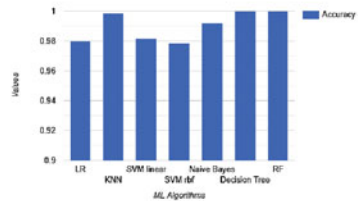
Accuracy of different algorithms for carton\_1



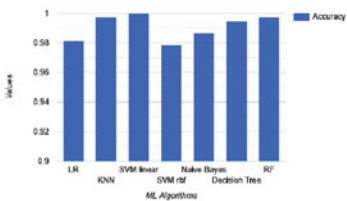
Accuracy of different algorithms for carton\_2



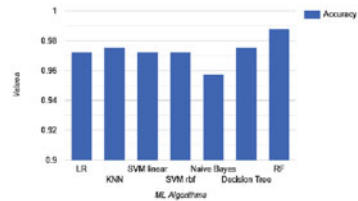
Accuracy of different algorithms for clothing\_1



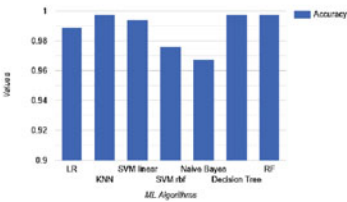
Accuracy of different algorithms for clothing\_2



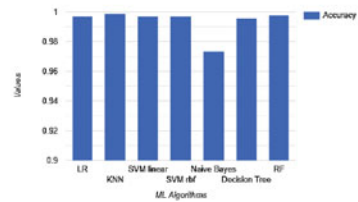
Accuracy of different algorithms for electrical\_1



Accuracy of different algorithms for electrical\_2



Accuracy of different algorithms for electrical\_3



Accuracy of different algorithms for electrical\_4

Fig. 1 Accuracy comparisons of various ML algorithms according to each dataset are show in (a)–(h)

### 4 Observation and Result

Firstly, the comparison of different parameters of all the datasets has been done algorithm-wise. Carton\_2 dataset has shown the most accurate results and F1score value for all ML algorithms. Then graphs were plotted to show the comparison



between various ML algorithms for each and every dataset. KNN, Random Forest, and Decision Tree were found to give the most accurate results for the majority of datasets.

## 5 Sum Up and Future Outlook

The study compared and implemented various machine learning algorithms to improve fire detection and response using different metrics. This study elaborates on the importance of ML techniques for fire alarms and provides insights into the usage of ML to enhance fire safety and response. These results from the study help in the development of fire alarms using machine learning. Future research should explore the potential of other machine learning techniques, for example, deep learning algorithms, for further improvement in the performance shown by fire alarms.

## References

1. Nazir A, Mosleh F, Husam S, Takruri MT et al (2022) Early fire detection: a new indoor laboratory dataset and data distribution analysis. *Fire* 5(11). <https://doi.org/10.3390/fire5010011>
2. Kumar AF, Gaur AS, Singh AT et al (2019) Fire sensing technologies: a review. *IEEE Sens J* 19:3191–3202
3. Maheen JBF, Aneesh RPS (2019) Machine learning algorithm for fire detection using color correlogram. In: 2nd international conference on intelligent computing, instrumentation and control technologies (ICICICT), vol 1. Kannur, India
4. Li, P, F.,Zhao, W,S .: Image fire detection algorithms based on convolutional neural networks. *Case Stud. Therm. Eng.*, 19, 100625. (2020)
5. Chagger RF, Smith DS (2014) *The Causes of False Fire Alarms in Buildings*; Briefing Paper; BRE Global Limited: Watford, UK
6. Taunk K, De S, Verma S, Swetapadma A (2019) A brief review of nearest neighbor algorithms for learning and classification. In: International conference on intelligent computing and control systems (ICCS). <https://doi.org/10.1109/ICCS45141.2019.9065747>
7. Fernandes AA, Figueiredo Filho DB, Rocha EC, Nascimento WD (2020) Read this paper if you want to learn logistic regression. *Revista de Sociologia e Política* 28(1). <https://doi.org/10.1590/1678-987320287406en>
8. Thorat AF (2021) Simply logistic regression
9. Evgeniou F, Pontil T, Massimiliano S (2001) Support vector machines: theory and applications. 2049:249–257. <https://doi.org/10.1007/3-540-44673-712>
10. Sai F, Kamasani M, Mitra S (2021) A study On Naive Bayes classifier. *Naive Bayesat, Chittoor*
11. Ali J, Khan R, Ahmad N, Maqsood I (2012) Random forests and decision trees. *Int J Comput Sci Issues (IJCSI)* 9
12. Farhadi Z, Bevrani H, Feizi-Derakhshi MR (2022) Improving random forest algorithm by selecting appropriate penalized method. *Commun Stat-Simul Comput* 1–16
13. Wang Z, Wang Y, Tian M, Shen J (2023) HearFire: indoor fire detection via inaudible acoustic sensing. In: *Proceedings of the ACM on interactive, mobile, wearable and ubiquitous technologies*, vol 6, pp 1–25. <https://doi.org/10.1145/3569500>
14. Eberbach E, Strzalka F, Dominik S (2021) In search of machine learning theory. [https://doi.org/10.1007/978-3-030-89906-6\\_40](https://doi.org/10.1007/978-3-030-89906-6_40)

15. Yadav R, Tripathi F, Ashutosh S (2021) Machine learning theory and methods. <https://doi.org/10.1201/9781003187059-9>
16. David Paper (2020). Hands-on scikit-learn for machine learning applications: data science fundamentals with python. <https://doi.org/10.1007/978-1-4842-5373-1>
17. Ali A, Amin F, Muhammad S (2019) Hands-on machine learning with scikit-learn
18. Unpingco J (2022) Machine learning. [https://doi.org/10.1007/978-3-031-04648-3\\_4](https://doi.org/10.1007/978-3-031-04648-3_4)
19. Pincott J, Tien F, Paige S, Wei ST et al (2022) Indoor fire detection utilizing computer vision-based strategies. *J Build Eng* 61:105154. <https://doi.org/10.1016/j.jobte.2022.105154>
20. Thanh L, Tho F, Nguyen S (2016) Indoor fire detection using wireless sensor networks. *J Res Dev Inf Commun Technol*. <https://doi.org/10.32913/mic-ict-research.v3.n13.343>
21. EngineersAGuerrazzi@sfpe.org, Society (2022) Fire Scenarios. [https://doi.org/10.1007/978-3-031-17700-2\\_9](https://doi.org/10.1007/978-3-031-17700-2_9)
22. Sarkar D, Bali R, Sharma T (2018) Practical machine learning with python. <https://doi.org/10.1007/978-1-4842-3207-1>
23. Swamynathan M (2017) Mastering machine learning with python in six steps. <https://doi.org/10.1007/978-1-4842-2866-1>
24. Raschka S, Patterson J, Nolet C (2020) Machine learning in python: main developments and technology trends in data science, machine learning, and artificial intelligence. *Information* 11:193. <https://doi.org/10.3390/info11040193>.(2020)
25. Peta S (2022) Python-an appetite for the software industry. *Int J Program Lang Appl* 12:1–14. <https://doi.org/10.5121/ijpla.2022.12401>

# Design and Analysis of Solar Cell Coplanar Antenna for Wireless Applications



**Kathika Jyothi Naga Nivas, Putha Sathish Kumar Reddy, Kappa Ravi Kiran Raju, Chintha Rithvik Kumar Reddy, T. Mary Neebha, and A. Diana Andrushia**

**Abstract** This paper presents the design and simulation of a solar cell coplanar patch antenna for IoT and Wireless sensor Networks. In this proposed work, a single solar cell is used as the radiating element and can be used as a power harvesting device. Initially, coplanar patch antenna is designed and Solar cell is integrated with the patch with a thickness of 0.5 mm. The radiation characteristics of the solar cell-based patch design are compared with a coplanar based same structured antenna without solar cell integration. The proposed antenna is designed at 2.42 GHz frequency without solar cell and with solar cell. The proposed design provides the conversion of light energy to electric energy. The relative study of the design gives the performance measures like return loss, gain, and radiation patterns.

**Keywords** Coplanar · Solar cell · FR-4 substrate · Feed · Patch antenna · Wireless applications

## 1 Introduction

The demand for miniaturized and cost-effective antennas is increasing day to day due to the prosperity of modern communication systems. Patch antennas are a popular choice for wireless applications due to their compact size, ease of integration, and relatively low cost. A patch antenna that integrates solar cells onto its surface is referred to as a solar cell-based patch antenna or a photovoltaic patch antenna. This

---

K. J. N. Nivas (✉) · P. S. K. Reddy · K. R. K. Raju · C. R. K. Reddy · T. M. Neebha · A. D. Andrushia

Department of Electronics and Communication Engineering, Karunya Institute of Technology and Sciences Karunya Nagar, Coimbatore, India

e-mail: [nivaskathika000@gmail.com](mailto:nivaskathika000@gmail.com)

T. M. Neebha

e-mail: [maryneebha@karunya.edu](mailto:maryneebha@karunya.edu)

A. D. Andrushia

e-mail: [diana@karunya.edu](mailto:diana@karunya.edu)

integration's goal is to transform the incoming electromagnetic waves into electrical energy so that the antenna and other devices can be powered. The suggested works include a solar cell antenna with dual functionality that can serve as both a power source for low-power wireless sensor networks and a communication antenna. By simulation and experimentation, the authors show that the design is feasible [1]. The authors developed a dual-function solar cell that can serve as both a power source and an antenna for a wireless sensor network and showed the dual functionality of the design by integrating a microstrip patch antenna with a sun cell [2]. The important part is the design of microstrip antennas, which are common in current communication systems. In [3], microstrip antenna analysis is examined by utilizing several methodologies such as transmission line theory, cavity modelling, and the moment method. A small dual-band solar cell antenna for energy harvesting applications is proposed in [4]. Another energy harvesting antenna is proposed in [5]. The antennas can gather energy from both ambient light and RF transmissions, and the design is suited for the GSM 900 and DCS 1800 frequency bands. A solar cell antenna is proposed in [6] for wireless power transmission applications. The antenna can harvest energy from both ambient light and RF transmissions, and the design is optimized for the 2.45 GHz frequency band. Miniaturization is yet another crucial thing to be considered for such antenna designs. A miniaturized dual-band solar cell antenna for energy harvesting applications is proposed in [7]. The antenna can harvest energy from both ambient light and RF transmissions, and the design is suited for the 2.4 and 5.8 GHz frequency bands. Solar cell-based antennas can be designed using a variety of techniques, including: direct integration of solar cells in antenna [8, 9], hybrid integration which involves integrating solar cells with antenna using a common substrate [10, 11], metamaterial based design [12, 13], multiband designs, thin film designs for flexibility [14]. The above publications contain thorough information on the design, development, and performance evaluation of solar cell-based antennas that incorporate solar cells directly into the antenna surface. Solar cells with a transparent conductive electrode layer or a rough surface that scatters incoming light can lessen optical obstruction [15]. These works show that solar cells can be employed as a reflector in antenna systems to increase the radiation pattern, directivity, and overall performance of the antenna. Solar cell integrated antennas are thus a promising alternative for wireless communication systems and energy harvesting applications. In this work, a solar cell-based microstrip patch coplanar antenna is designed and analyzed. The process of creating a solar cell-based antenna is merging a solar cell and an antenna into a single device. The main concept is to use the solar cell as the antenna substrate and integrate the antenna onto the solar cell's surface. These are some broad guidelines for creating a solar cell-based antenna: The first step in designing a solar cell-based antenna is to select an appropriate solar cell to serve as the antenna's substrate. This will be determined by the antenna's specifications, such as frequency range and power output. The next stage is to decide on the antenna design that will be integrated into the solar cell's surface. This will be determined by the antenna's frequency range and the desired gain. The orientation of the solar cell is critical for best efficiency. The solar cell should be oriented so that the antenna faces the sun, maximizing the amount of power that may be harvested.

After determining the antenna design, it can be integrated into the solar cell's surface. This is achievable through the use of typical printed circuit board (PCB) fabrication procedures. Once the solar cell-based antenna has been constructed, it should be tested to confirm that it matches the specified performance parameters. This is possible using basic antenna testing equipment. Lastly, the design can be adjusted for maximum efficiency by adjusting the antenna design and solar cell orientation. Solar cell and antenna design fundamentals must be understood while creating a solar cell-based antenna. It is advised to contact with professionals in both sectors to verify that the design fits all requirements.

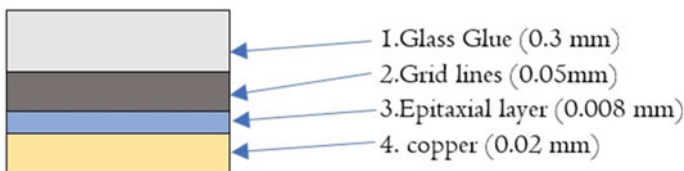
Remarkably, the radiators with solar cell have good antenna characteristics due to the coplanar structure selected for the proposed design. The suggested radiator with solar cell exhibits excellent radiation at the desired frequency range and is beneficial for wireless applications.

The work presented in this paper is sectioned as follows. Section 2 presents the methodology and design of the proposed patch antenna with and without solar cell integration. The analysis part as well as the simulation are listed in Section 3. Finally, conclusion and future scope are presented in Part 4.

## 2 Design Modelling

A solar cell's fundamental structure typically consists of the following layers: The top electrode, also known as the contact layer, is typically formed of a thin layer of metal, such as silver, and serves as the contact for the solar cell's positive side. Anti-reflection coating: This layer is intended to reduce the quantity of light reflected away from the solar cell's surface. A thin covering of silicon dioxide or titanium dioxide is typically used. The absorption layer is the solar cell's heart, where sunlight is absorbed and turned into electrical energy. It is typically made of a semiconductor material such as silicon that has been doped with impurities to form a p-n junction. The structure of the solar cell used in the proposed design is shown in Fig. 1.

The solar cell coplanar patch antenna was designed with HFSS software to analyse the radiation pattern and gain. The planned antenna's dimensions were  $33 \times 23 \times 1.6$  mm in size. The optimized parameters are consistent with the design. The ground plane measurements are  $L = 33$  mm,  $W = 23$  mm, and the substrate is FR-4 with  $H = 1.6$  mm, while the patch dimensions are  $L_p = 16$  mm,  $W_p = 7$  mm. The antenna



**Fig. 1** Solar cell structure

**Fig. 2** Proposed coplanar antenna (CPA) design without solar cell



was built to be coplanar, which implies that all of its components are on the same plane. The FR-4 substrate is utilized because it lowers interference and helps to maintain excellent signal integrity. The substrate was designed first, and then a patch and ground plane was designed over and below it, with the substrate sandwiched between the two layers.

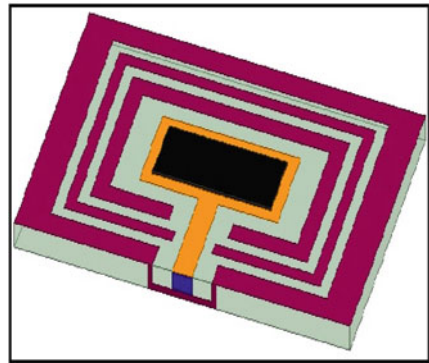
Figure 2 depicts the simulated CPA. The patch was developed in CPA, and a slot was kept in the patch to interface with the solar cell. Figure 3 depicts the planned SC-CPA. The slot in SC-CPA was filled with solar cells, which were then combined with the patch to form a solar cell coplanar patch antenna. The outcomes must vary depending on the design.

The above table depicts the dimensions of the designed antenna. The antenna has ground length ( $L$ ) of 33 mm, ground width ( $W$ ) of 23 mm. The substrate height ( $h$ ) of the antenna is 1.6 mm. The table also describes about the solar dimensions it has solar patch length ( $l$ ) of 10 mm and solar patch width ( $w$ ) of 5 mm. For excitation, we have given the feed for antenna and the feed dimensions are depicted in Table 1. The dimensions of feed are feed width ( $w_f$ ) is 2 mm and feed length ( $L_f$ ) is 8 mm.

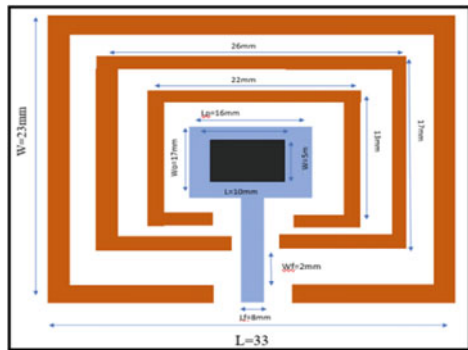
### 3 Results and Analysis

A solar-based antenna is one that is combined with a solar panel or another photovoltaic (PV) device. The equivalent circuit of such an antenna would depend on the antenna's and PV device's individual design and implementation, but in principle, it might be represented by a combination of a radiation element and a PV element. The radiation element, which may be described as a combination of resistance, inductance, and capacitance, would represent the antenna's ability to receive or send electromagnetic waves. The PV element would represent the solar panel or other PV device and might be represented as a current source connected in parallel with a diode. The solar-based antenna's combined equivalent circuit would then be a combination of these two elements in parallel, with the radiation element and PV element sharing a common terminal. The resulting circuit would enable the antenna to receive and transmit electromagnetic waves while also generating solar power.

**Fig. 3** Proposed coplanar antenna design with solar cell (SC-CPA) integration: **a** perspective view **b** top view



(a)



(b)

**Table 1** Detailed specifications of the proposed antenna

	Specifications	Dimension(mm)
Ground length	L	33
Ground width	W	23
Height	h	1.6
Solar patch length	l	10
Solar patch width	w	5
Feed width	w <sub>f</sub>	2
Feed length	L <sub>f</sub>	8

HFSS software was used to develop the solar cell coplanar antenna. Return loss, gain, and radiation pattern were the parameters studied. The simulated findings show a return loss of  $-13.2858$  at a frequency of  $2.42$  GHz. The coplanar solar cell patch antenna has a gain of  $-13.22$  dB. H-Plane and E-Plane radiation patterns were studied. SC-CPA AND CPA had bandwidths of  $20$  MHz and  $23$  MHz, respectively. The obtained Return loss for CPA is  $-12.7326$  and SC-CPA is  $-13.2858$ , as shown

in Fig. 4. Return loss is mostly determined by the antenna’s design, substrate selection, modifying the patch and ground dimensions, and properly positioning silicon material over the patch as a solar cell. The gain obtained for the Coplanar solar cell antenna is  $-13.22$  dB, as shown in Fig. 5. We can see a reduced value of gain due to the silicon characteristics present on the patch. Generally, the gain of a patch antenna is proportional to its size, with larger antennas typically having higher gains. The shape of the patch antenna can also affect its gain, with some shapes (such as circular patches) having higher gains than others. The rise in patch gain is exactly proportional to the increase in antenna design size, but the disadvantage of this statement is the increase in antenna weight. Another effective technique to increase gain is to make the solar cell as transparent as possible, as this will allow it to efficiently emit incoming and outgoing EM waves.

The Radiation pattern displays the results of electric and magnetic field planes at  $90^\circ$  and  $0^\circ$  angles, respectively. It provides the radiation pattern of the Electric field plane at  $90^\circ$ .

The Fig. 5. gives the Gain of the Solar Cell Coplanar Patch Antenna and the value is  $-13.22$  dB.

The orientation of the electric field might change according to the design specifications of the solar cell coplanar patch antenna. The radiation pattern depicts the graphic layout of the antenna’s radiative properties exhibiting the direction of EM waves. Figure 6 depicts the magnetic field plane’s radiation pattern at  $0^\circ$ . The magnetic field plane runs through the centre of the patch and parallel to the surface of the solar cell. The solar cell coplanar patch antenna’s magnetic field of radiation pattern is somewhat directed, providing most radiation perpendicular to the surface of the solar cell coplanar patch antenna. A patch antenna made from solar cells typically has a radiation pattern comparable to that of a normal patch antenna. The radiation pattern of a patch antenna is determined by its dimensions and height

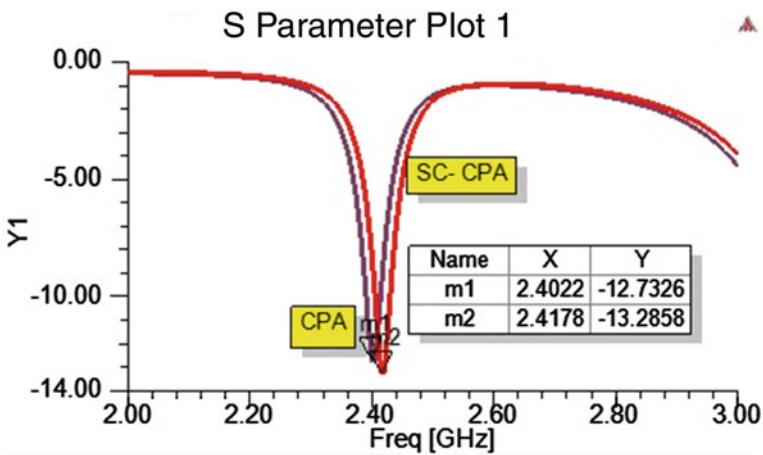
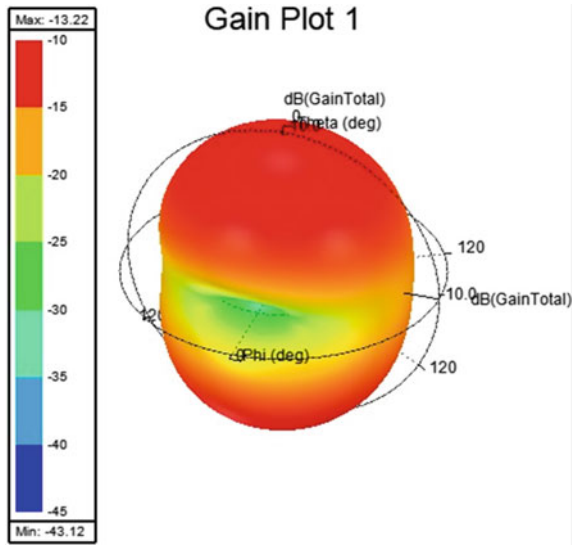


Fig. 4 S11 characteristics of proposed antenna of CPA and SC-CPA antenna



**Fig. 5** Gain plot of proposed SC-CPA antenna



above the ground plane. The patch functions as a resonator, and the radiation pattern is determined by the patch's resonant modes.

A patch antenna typically has a broadside radiation pattern, which means that the highest radiation is perpendicular to the plane of the patch. The pattern is frequently described as having the shape of a doughnut, with a null at the zenith and a maximum towards the horizon. The presence of solar cells may change the radiation pattern of a patch antenna based on solar cells. However, the effect is likely to be small and should not significantly alter the overall radiation pattern of the antenna. The overall performance of the proposed antenna with and without solar cell is summarized in Table 2.

The paper is compared to the other papers with return loss, and Gain. This paper gives the result of return loss around  $-13$  and compared paper gives  $-33.2$ , the gain of this paper is  $-13.22$  dB and the compared paper gives the gain of  $4.19$  dBi. The results vary according to the antenna designs.

The above table compares the return loss, gain and bandwidth between Coplanar Patch Antenna (CPA) and Solar cell Coplanar Patch Antenna (SC-CPA). The return loss for CPA is  $-12.7326$  and the return loss for SC-CPA is  $-13.2858$  which shows that there is a decrease in return loss when placed with Solar cell in CPA. The Gain for two antennas are  $-10.31$  dB and  $-13.22$  dB. The Bandwidth for the two antennas are  $23$  MHz and  $20$  MHz. These are the compared values presented in Table 2.

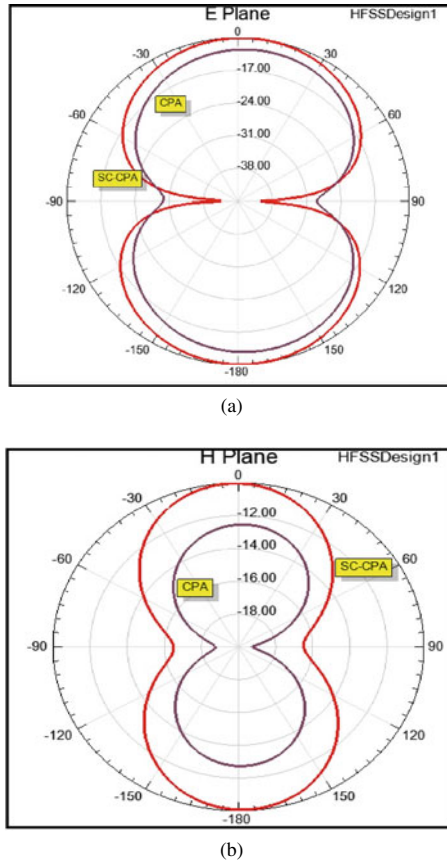


Fig. 6 2D radiation pattern of CPA and SC-CPA: a E plane b H plane

Table 2 Comparison of CPA & SC-CPA

Antenna	Return loss	Gain	Bandwidth
Coplanar Patch Antenna (CPA)	-12.7326	-10.31 dB	23 MHz
Solar cell Coplanar Patch Antenna (SC-CPA)	-13.2858	-13.22 dB	20 MHz

### 4 Conclusion

A novel Coplanar Solar Cell Patch Antenna has been presented. Measurement and simulation show that the antenna provides about -13 return loss. The antenna provides a gain of -13.22 dB. The bandwidth provided by the coplanar solar cell patch antenna was 20 MHz and the result of coplanar antenna without solar cell provides 23 MHz. The light intensity enhances the conductivity of a solar cell in silicon layer. The designed antenna is mainly used in applications like IoT.

## References

1. Chen SH, Liao CY, Wen YH (2014) Design and analysis of a dual-functional solar cell antenna for low-power wireless sensor networks. In: 2014 IEEE international symposium on antennas and propagation & USNC/URSI National radio science meeting. pp 1841–1842
2. Saleem MR, Ziauddin, Schamiloglu E (2018) Dual-function solar cells as power sources for wireless sensor networks. In: 2018 IEEE International conference on communications, control, and computing technologies for smart grids (SmartGridComm). Aalborg, Denmark, pp 1–6
3. Balanis CA (2015) Antenna theory: analysis and design. John Wiley & sons
4. Selvam N, Saranya K Design and analysis of a compact dual-band solar cell antenna for energy harvesting applications. *Wirel Pers Commun* 111(2):893–905
5. Lim CS et al (2017) A dual-band solar cell antenna for RF energy harvesting. *IEEE Trans Antennas Propag* 65(6):2923–2928
6. Chen J et al (2016) Design and optimization of a solar cell antenna for wireless power transfer applications. *IEEE Trans Antennas Propag* 64(10):4378–4387
7. Chen R, Zhang Z, Huang Y, Liu Y (2013) A compact dual-band solar cell antenna for energy harvesting applications. *IEEE Trans Antennas Propag* 61(5):2788–2794
8. Zhu L, Sun Y, Feng Y (2018) A review on direct integration of photovoltaic cells with antennas. *Renew Sustain Energy Rev* 81:305–314
9. Yadav RK, Singh K (2019) Direct integration of a PV cell onto a microstrip patch antenna for efficient wireless energy harvesting. *Microw Opt Technol Lett* 61(10):2518–2523
10. Zhu L, Sun Y, Feng Y (2019) Design and optimization of hybrid solar cell-integrated antennas for wireless sensor networks. *IEEE Trans Antennas Propag* 67(3):1539–1549
11. Samanta SK, Das SS, Sarkar D (2019) Development of a novel hybrid solar cell-integrated patch antenna for energy harvesting applications. *J Electromagn Waves Appl* 33(17):2251–2266
12. Liu J, Zhang Z, Zheng B (2019) Metamaterial-inspired design of a broadband and high-efficiency solar cell antenna. *IEEE Trans Antennas Propag* 67(4):2664–2673
13. Salehi R, Varshney EK (2017) Metamaterial-inspired transparent solar cells integrated with microstrip patch antennas for low-power communication systems. *IEEE Trans Antennas Propag* 65(9):4808–4816
14. Samanta SK, Das SS, Sarkar D (2020) Efficient design and analysis of a solar cell-integrated patch antenna for energy harvesting. *Int J Microw Wirel Technol* 12(1):80–90
15. Kim S, Yun H, Kim KH (2019) Transparent conductive oxide-free solar cells with an embedded metal grid for reduced optical blockage. *Sol Energy Mater Sol Cells* 191:118–125

# Open Permissioned Blockchain Solution for Private Equity Funding Using a Global, Cross-Cloud Network Blockchain Platform



S. Rajarajeswari, K. N. Karthik, K. Divyasri, Anvith, and Riddhi Singhal

**Abstract** The capitalization table, commonly known as a cap table, is a comprehensive record of ownership and equity distribution within a company. It serves as a document, typically in the form of a spreadsheet or database table, that outlines all the securities or shares in a company and presents the equity capitalization of the company. However, cap tables maintained on centralized databases are susceptible to significant attacks. Corda has emerged as a blockchain platform specifically designed for business applications, prioritizing privacy and scalability. Corda operates as a private blockchain, enabling communication exclusively between involved parties in a transaction. Its primary objective is to facilitate secure and efficient value-added transactions and data sharing among businesses. As a solution, a Corda-based platform is proposed to bring together companies and investors for private equity funding. The proposed platform leverages a secure version of the cap table, referred to as a mirror table, to deliver cap table functionalities. By utilizing the blockchain technology provided by Corda, transactions become secure and tamper-proof, significantly reducing the risk of fraudulent activities and enhancing investor confidence. This innovative approach has the potential to revolutionize the crowdfunding industry by establishing a secure and transparent means for businesses to raise capital and for investors to participate in investments.

**Keywords** Blockchain · R3 Corda · Private equity funding · Mirror table · Capitalization table · Smart contracts · Security

## 1 Introduction

Private equity funding is a form of investment in which funds are invested directly into privately held companies. Private equity funding offers several advantages to businesses. It provides access to substantial capital that can be used for various purposes,

---

S. Rajarajeswari (✉) · K. N. Karthik · K. Divyasri · Anvith · R. Singhal  
Ramaiah Institute of Technology, Bangalore, India  
e-mail: [raji@msrit.edu](mailto:raji@msrit.edu)

including business expansion, acquisitions, or strengthening the company's financial position. Additionally, private equity investors often bring industry expertise, strategic guidance, and operational support to help companies achieve their growth objectives. In private equity funding, investors acquire an ownership stake in the company in exchange for their investment. This ownership stake, often represented by equity or shares, gives investors the opportunity to share in the company's profits and value appreciation over time.

Shares are units of ownership in a company that represent a portion of its total equity. When a company issues shares, it is essentially selling a portion of its ownership to investors in exchange for capital. A capitalization table [1], also known as a cap table, is a document that tracks the ownership and equity distribution of a company. It lists all the securities or shares in the company and shows the equity capitalization of a company. It is important because they provide a detailed breakdown of how much of the company each investor owns, and how much they paid for their shares. Cap tables can become complex as a company grows and takes on additional investors. Maintaining an accurate and up-to-date cap table is important for transparency and investor confidence, as errors or omissions can lead to disputes and legal issues. Cap tables stored on a centralized database table [2] can be prone to serious attacks and vulnerabilities [3]. This is where blockchain [4] technology, and specifically the Corda [5] blockchain, can provide enhanced security and transparency by ensuring that transactions are secure and tamper-proof, reducing the risk of fraud and improving investor confidence.

Corda blockchain is suitable for private equity funding [6] platforms due to its design for business use cases, smart contract [7] technology, privacy, and scalability. A private equity funding platform on Corda would enable businesses to raise capital directly from investors, reducing costs, and streamlining the fundraising process. Smart contracts would manage investor agreements, handle dividend payments, and ensure compliance with regulations. Corda's private blockchain ensures privacy and confidentiality for sensitive business and financial information, while its scalability allows for a high volume of transactions to be processed quickly and efficiently.

## 2 Related Work

Corda as a platform is introduced by Brown et al. [8] to reduce the cost of financial services by automating the manual process of synchronization. It emphasizes extensibility, non-functional needs, and engineering for institutional requirements. Corda is designed to record and enforce business agreements between registered financial institutions, and it adopts a novel approach to data distribution and transaction semantics while preserving the benefits of distributed ledgers. Overall, Corda aims to provide a shared ledger fabric for financial service use cases that are implementable in accordance with current legal frameworks and relies on tried-and-true technology. Hern et al. [9] introduced Corda as a decentralized global database and explained

how it works as a platform for decentralized app development. The article highlights Corda's smart contracts, which operates on the JVM, providing access control and schema definitions for decentralized data sharing among multiple nodes with mutual mistrust. The system includes an identity management system and notaries for algorithmic flexibility in distributed consensus systems. Corda does not require mining or chains of blocks and allows users to analyze ledger data with standard SQL queries against established database engines. Lastly, the article outlined future work to improve privacy, security, robustness, and adaptability by integrating other privacy technologies. Valenta et al. [10] compared three DLTs: Hyperledger Fabric, R3 Corda, and Ethereum. It was found that Fabric and Ethereum are both adaptable in different ways, with Ethereum's smart contract engine making it a universal platform and Fabric addressing scalability and privacy challenges with its permission mode and modular architecture. Corda is designed specifically for the financial sector, with legal language added to smart contracts for a regulated environment. Overall, the study highlights the different strengths and weaknesses of each DLT and how they can be applied to different use cases.

Numerous authors have suggested blockchain-based solutions for private equity funding in recent times. Nikhil et al. [11] proposed a blockchain-based method of crowdfunding that creates smart contracts enabling investors to raise and reserve funding for projects while allowing contributors to manage the invested money. The interface was deployed into the Ethereum network, creating a decentralized web app with a user interface for managing projects and requests. This approach is still in its experimental stages, and legal and technical issues need to be addressed. However, the proposed crowdfunding application lays the groundwork for future research and improvements while ensuring the safety of the concepts realized. Dave et al. [12] suggested a decentralized and secure crowdfunding system using blockchain technology that eliminates the need for traditional crowdfunding platforms. This method allows entrepreneurs to collect the entire amount of money raised from investors by removing platform fees and payment handling costs. The proposed system offers a fast and secure way to transfer money from backers to authors. However, the study identified the need for a secure transaction validation mechanism to ensure that only legitimate transactions are stored in the blockchain, protecting business ideas from being replicated after they are published, and creating a proportional compensation system for both miners and backers.

Sahu et al. [13] proposed a blockchain-based method to prevent fraud on crowdfunding platforms using smart contracts. Their primary goal was to create a transparent platform for campaign managers to use the raised funds. The solution was tested on Rinke by Network and implemented using Ethereum and Solidity. The proposed system allowed users to report potential scams and weaknesses in crowdfunding platforms, providing more secure alternatives. The smart contracts interacted with the blockchain network to ensure transparency and prevent fraudulent activities. Campaign designers were restricted from moving invested funds, and investors had to vote for any change in the usage of funds. The approach aimed to increase confidence among investors and promote transparency in the crowdfunding process. Roth et al. [14] proposed the tokenization of equity crowdfunding on a blockchain

as a potential strategy to simplify the process of raising funds for entrepreneurs. They suggested classifying token standards based on UTXOs, layers, and smart contracts and examined the benefits of tokenization, including programmable assets, access to the blockchain ecosystem, improved share division, and the emergence of a viable secondary market. By allowing the ledger of assets to be separated from the crowdfunding platform through tokenization, the cost of secondary market trade and the influence of middlemen are reduced. However, potential disadvantages include knowledge gaps, legal complexities, and high energy consumption in proof-of-work blockchains. Lee and Rahim [15] proposed a decentralized web application called FundDapp that utilizes blockchain technology to protect data in crowdfunding transactions. The application aims to provide a peer-to-peer transfer service and a blockchain website for crowdfunding, which was tested on the Ethereum network. An object-oriented software development model was used to develop the primary functions of the application which included the Python Flask framework and Web3.js library. The study demonstrated that web applications can establish point-to-point communication between two parties using the smart contract mechanism, which could increase the adoption of blockchain technology for enterprise data security. However, the limitations of the application include the need for Metamask installation to use the transaction capability, the lack of a search bar, and no option for users to edit previously submitted comments.

### 3 Proposed Work

The proposed work is to create a Corda blockchain-based equity crowdfunding platform that utilizes decentralized and distributed ledger technology to enable investors to invest in early-stage businesses in exchange for equity ownership. The platform will allow businesses to raise capital by offering equity to a large number of investors, while investors can participate in investment opportunities that were previously only available to venture capitalists and high-net-worth individuals.

In Corda, a state [16] represents a digital representation of an agreement or a fact that needs to be shared between parties in a distributed ledger. States in Corda are immutable, which means that once a state is created, it cannot be modified. Contracts in Corda are the business logic that defines how states can be created, updated, and consumed. A contract can validate that the data in a state is consistent and can enforce specific constraints or conditions that must be met before a state can be considered valid. Flows in Corda are processes that enable parties to agree on and update shared facts, which are represented by states. Flows in Corda are implemented as co-routines, which enable them to suspend and resume execution as needed. Flows can also communicate with each other and exchange information to reach a consensus on the updates to be made to shared states.

Firstly, state objects that represent the shared fact or agreement between parties are defined. Next, the contract code that defines rules for how the state can evolve is written. The flow code that defines the processes of how parties interact with each

other and with the ledger is written. This includes defining the steps for creating, updating, or consuming states. Lastly, the code is tested to ensure that it functions correctly and that all parties can execute transactions according to the defined processes. Figure 1 summarizes the states and flows involved in the funding platform. The description of the states and flows involved is given below.

States:

- EKI state—It represents the details of a share—company name, symbol, total supply, and price for each share.
- Notification state—It represents the information to be broadcasted to all investors from the trustee—company name, symbol, currency, and price for each share.
- Acceptance state—It represents the request made by an investor to the company—investor name, company name, and number of shares requested.
- Mirror state—It represents the various information that will be stored in the mirror table such as investor name, number of shares, and percentage of equity.

Flows:

- CreateAndIssueStock—It is initiated by the company to create a TEST stock.
- IssueMoney—It is initiated by the bank to transfer fiat currency to the investor.
- NotificationFlow—It is initiated by the trustee to broadcast information about available shares to the investor.
- AcceptanceRequest—It is initiated by the investor to create an Acceptance state in order to request the company for the stocks.

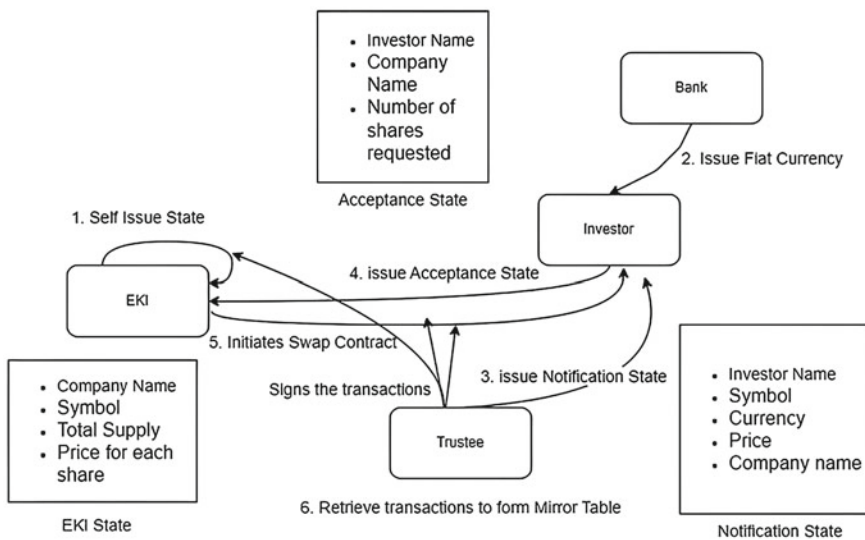


Fig. 1 Architecture diagram depicting the states and flows involved



- AcceptanceValidate—It is initiated by the company to acknowledge the acceptance of the request made by the investor.
- MoveStockInitiator—It is initiated by the company to swap the tokens and USDC between the company and the investor.
- GetTokenBalance—It can be initiated on any node to query token balances.
- Mirror table flow—It is initiated by the company to create a view of the mirror table.

### 4 Methodology

The overview of the process of issuing new shares in a company as fungible tokens, and allowing investors to participate in a crowdfunding campaign to purchase those tokens using USDC stablecoins is shown in Fig. 2. The steps involved are as follows:

Step 1: The company issues new shares as tokens, specifying the name of the company, the symbol of the token, the total supply, and the price of each share. These shares are implemented as fungible tokens, meaning they are interchangeable with one another.

Step 2: The bank issues USDC stablecoins to the shareholder who wishes to participate in the crowdfunding campaign. The bank specifies the amount of USDC to be issued and the party to whom it should be issued.

Step 3: Once the company issues share as tokens, the Trustee broadcasts this information to the investors.

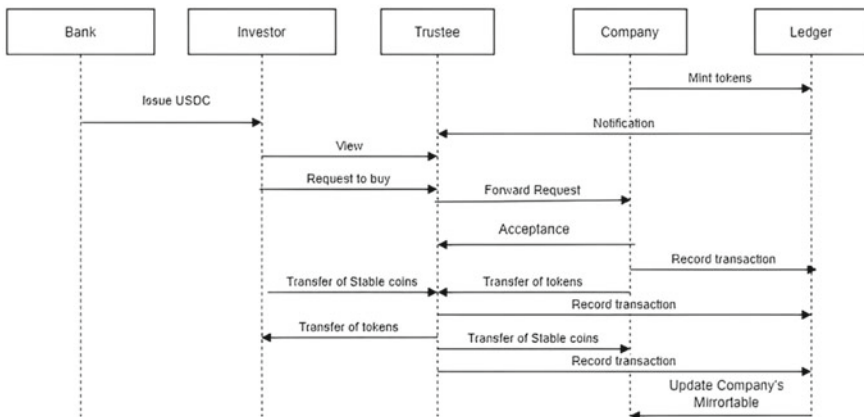


Fig. 2 Sequence diagram depicting the flow of data

Step 4: Investors can then participate in the crowdfunding campaign by sending a request to the company expressing their interest in buying the shares. The Trustee monitors this by adding its signature to the request transaction.

Step 5: The company views the list of requests made and decides to sell shares to one of the interested shareholders. The Trustee monitors this by adding its signature to the swap transactions.

Step 6: Once the company accepts the request, a corresponding number of tokens are transferred from the company's vault to the investor's vault. Its equivalent USDC is transferred from the investor's vault to the company's vault.

Step 7: Finally, the Mirror Table is updated by fetching the details from the transactions logged previously. The mirror table records ownership details for the shares on a blockchain and is updated whenever shares are transferred between investors or between investors and the company.

The implementation of the above process would require the development of smart contracts and the integration of the Mirror table with the blockchain network being used, as well as the integration of the various software components involved in the issuance of tokens and stablecoins.

## 5 Results

The platform provides a user-friendly and effective interface that is developed using React JS and uses restful APIs to communicate with the Corda nodes. The platform guarantees the security and transparency of transactions by employing Corda's blockchain technology, while React JS offers an engaging and responsive user interface for investors and companies. The application provides a streamlined fundraising procedure, which lowers expenses and boosts efficiency for both investors and companies. The platform utilizes a secure version of the capitalization table, called a mirror table, to provide cap table functionalities. The mirror table is stored on the Corda blockchain, ensuring that transactions are secure and tamper-proof, reducing the risk of fraudulent activities, and enhancing investor confidence.

The platform allows businesses to issue shares as tokens on the blockchain and enables investors to participate in crowdfunding campaigns by purchasing these tokens using USDC stablecoins. This tokenization process provides liquidity and flexibility for investors, as they can easily trade and transfer their ownership through the platform. Tokenization also simplifies the process of fractional ownership, enabling investors to purchase smaller portions of shares, which can be beneficial for angel investors seeking to diversify their portfolios. With the platform, investors can participate in crowdfunding campaigns by purchasing company tokens using USDC stablecoins. This simplifies the investment process by leveraging a familiar digital currency and bypassing the complexities of traditional fiat currency transactions. The integration of stablecoins adds stability and reduces the volatility typically associated with cryptocurrency-based investments.

The platform allows businesses to raise capital directly from investors, eliminating the need for intermediaries and reducing administrative costs. This direct peer-to-peer approach cuts out the need for traditional financial institutions, legal intermediaries, and other service providers, resulting in cost savings for both parties involved in the investment process. Moreover, the trustee also provides a layer of trust and security for both investors and companies and provides dispute resolution services. The platform provides investors and companies with easy access to information about the company's stock distribution and individual shareholdings through the mirror table. This transparency allows investors to make informed decisions based on the current ownership structure of the company, facilitating better investment choices.

## 6 Conclusion

The proposed Corda-based platform for private equity crowdfunding is a timely initiative that could provide several benefits to investors and companies. The COVID-19 pandemic has disrupted traditional investment markets, leading to increased interest in alternative investment options like private equity crowdfunding. This platform could democratize access to investment opportunities by making private equity crowdfunding more accessible to a wider range of investors. Additionally, the use of smart contract technology and a secure, decentralized system can improve security, efficiency, and transparency while reducing transaction costs. The off-chain cap table can ensure legal compliance and build trust between investors and the company, while also providing a transparent record of ownership. Furthermore, the platform can help investors take advantage of recent regulatory changes that makes it easier for companies to raise capital through private equity crowdfunding.

In the future, the project could explore further enhancements, such as integrating AI for better decision-making, to improve the platform's usability and effectiveness. The proposed platform could potentially expand its scope to include more features and capabilities to serve its users. It could provide more comprehensive and advanced data analytics tools to investors and companies, enabling them to make better investment decisions and more informed business decisions, respectively. It could also integrate with other blockchain networks or platforms to provide a wider range of investment opportunities and access to a larger pool of investors.

## References

1. Shijaku E (2016) Adding interaction to decision making support tools: what can be learned from the capitalization table (Dissertation)
2. Davenport RA (1978) Distributed or centralized database. *Comput J* 21(1):7–14. <https://doi.org/10.1093/comjnl/21.1.7>
3. Bertino E, Sandhu R (2005) Database security—concepts, approaches, and challenges. *IEEE Trans Dependable Secur Comput* 2(1):2–19. <https://doi.org/10.1109/TDSC.2005.9>

4. Priyadarshini I (2019). Introduction to blockchain technology. *Cyber security in parallel and distributed computing: concepts, techniques, applications and case studies* 91–107
5. Brown RG (2018) *The corda platform: an introduction*. Retrieved, 27, 2018
6. Cendrowski H, Wadecki AA (2012) Introduction to private equity. <https://doi.org/10.1002/9781119203391.ch1>
7. Wang S, Yuan Y, Wang X, Li J, Qin R, Wang FY (2018) An overview of smart contracts: architecture, applications, and future trends. In: *2018 IEEE Intelligent Vehicles Symposium (IV)*. IEEE, pp 108–113
8. Richard B, James C, Grigg I, Mike H (2016) *Corda: an introduction*
9. Hearn M, Richard B (2019) *Corda: a distributed ledger*
10. Martin V, Philipp S (2019) Comparison of ethereum, hyperledger fabric and corda
11. Yadav N, Sarasvathi V (2020). [IEEE 2020 third international conference on smart systems and inventive technology (ICSSIT) - Tirunelveli, India (2020.8.20–2020.8.22)] 2020 third international conference on smart systems and inventive technology (ICSSIT) - venturing crowdfunding using smart contracts in blockchain, pp 192–197. <https://doi.org/10.1109/icssit48917.2020.9214295>
12. Dave M, Garg R, Dua M, Hussien J (eds) (2021) *Proceedings of the international conference on paradigms of computing, communication and data sciences. Algorithms for intelligent systems*. <https://doi.org/10.1007/978-981-15-7533-4>
13. Balas VE, Semwal VB, Khandare A, Patil M (2021). [Lecture notes in networks and systems] *Intelligent computing and networking*, vol 146 (Proceedings of IC-ICN 2020)
14. Wendt K (ed) (2021) *Theories of change. Sustainable finance*. <https://doi.org/10.1007/978-3-030-52275-9>
15. Lee W, Rahim N (2021) Decentralized application for charity organization crowdfunding using smart contract and blockchain. *Appl Inf Technol Comput Sci* 2(2):236–248. Retrieved from <https://publisher.uthm.edu.my/periodicals/index.php/aitcs/article/view/2202>
16. Mohanty D, Mohanty D (2019) *Corda architecture. R3 corda for architects and developers: with case studies in finance, insurance, healthcare, travel, telecom, and agriculture*, pp 49–60

# The Challenge of Recognizing Artificial Intelligence as Legal Inventor: Implications and Analysis of Patent Laws



Kanishka Vaish, Rajesh Bahuguna, Samta Kathuria, Kapil Joshi, Rishika Yadav, and Rajesh Singh

**Abstract** Innovations in AI have altered various industries, changed how we think of plausible solutions for any problem, and allowed us to create products, thoughts, and concepts that were previously unimaginable. As a result, more patent applications for inventions created by AI have been filed, raising several questions about the legal standing of AI as an inventor. In addition to offering a critical study of the worldwide legal system regulating the patenting of AI-generated work, this non-empirical research article explores the consequences and difficulties of acknowledging AI as an inventor. By reviewing the existing legal framework, examining inventorship criteria, analyzing challenges tied to legal inventorship for AI-generated inventions, reviewing relevant case law, and proposing potential solutions, this study sheds light on the complex legal, ethical, and social considerations involved. Furthermore, it suggests future research directions, including the exploration of dedicated patent laws and regulations for AI-generated inventions, as well as investigations into the ethical and social implications and potential consequences of acknowledging AI as a legal inventor.

**Keywords** AI · Machine learning · Robotics · Patent laws · Inventor

---

K. Vaish (✉) · R. Bahuguna · S. Kathuria  
Law College Dehradun, Uttarakhand University, Dehradun 248007, India  
e-mail: [kanishkavaish1999@gmail.com](mailto:kanishkavaish1999@gmail.com)

K. Joshi · R. Singh  
Uttarakhand Institute of Technology, Uttarakhand University, Dehradun 248007, India

R. Yadav  
Department of Computer Science and Engineering, Graphic Era Hill University, Dehradun, India  
e-mail: [ryadav@gehu.ac.in](mailto:ryadav@gehu.ac.in)

# 1 Introduction

As per the Markets report, the business for AI is expected to increase at a CAGR of 36.2% during the projected period, from \$ 86.9 billion in 2022 to \$ 407.0 billion by 2027 [1]. The growth of AI has been facilitated by the development of new techniques and models, faster computer processing, data availability, and other variables. Manufacturing, shopping, medical care, and finance are just a few of the industries that use AI. The development of various technologies and the accessibility of additional data have all enabled the proliferation of AI applications. Consequently, organizations and enterprises may now employ AI for a range of functions, including identifying fraudulent activity and maintenance prediction to customer service and data analysis [2].

Intellectual property law as we know it is challenged by the idea of AI as an inventor. Important issues regarding the ownership and defense of AI-generated inventions are raised by this. It is not yet apparent if AI may be acknowledged as a legal inventor, despite the fact that AI-generated output is growing more and more common. The inventor must be a natural person according to existing patent laws, which further complicates the situation [3]. In the present-day patent system, there is one requirement for inventorship that the creation must be novel in nature. Also, the person who invented it must have made a substantial contribution to the innovation. Since the AI system developed the concept, yet a human may have contributed to the programming of the AI system, it is uncertain who would fit these conditions in the case of inventions produced by AI. Recognizing AI as an inventor raises legal questions that could result in drawn-out legal disputes because the present-day patent system requires inventors to be human [4]. The following are the goals of this essay:

- To give a general introduction to AI and its applications, investigate the requirements for legal inventorship with patent rules, and evaluate relevant case law and global viewpoints.
- To analyze the legal challenges and implications of recognizing AI as a legal inventor under patent laws, propose potential solutions, and provide implications for policy and practice.

The paper begins with an overview of AI, including its definition, types, and applications in Sect. 2. It then examines the criteria for legal inventorship under patent laws and the challenges of assigning inventorship to AI-generated inventions under Sect. 2. Under Sect. 3 case law related to AI-generated inventions and international perspectives on the issue of legal inventorship have been discussed. The implications of recognizing AI as a legal inventor are discussed, including economic, social, ethical, moral, and patent system implications are explored under Sect. 4. Section 5 proposed solutions for recognizing AI as a legal inventor and implications for future legal and technological developments. The study highlights the need for policy and practice to keep up with the rapidly evolving field of AI and the importance of considering the implications of recognizing AI as a legal inventor. Section 6 provides the future of developing new models for determining legal inventorship and analyzing

the potential economic impacts of recognizing AI as a legal inventor. Section 7 concludes by discussing the significant implications.

### ***1.1 Social Significance***

This research holds significant social importance in the context of our rapidly advancing technological landscape. As AI continues to evolve and demonstrate remarkable abilities in generating novel and inventive solutions, it raises critical questions regarding the legal framework surrounding intellectual property rights. This study's social significance lies in its exploration of the implications of recognizing AI as a legal inventor within patent laws. The outcome of this research has the potential to shape the future of innovation, entrepreneurship, and technological progress [5]. By examining the current legal landscape, the paper sheds light on the potential barriers or opportunities that arise when granting AI systems inventorship rights. Addressing this issue has broad social ramifications. Determining whether AI can be recognized as a legal inventor affects various stakeholders, including inventors, researchers, companies, and society at large. The findings of this study can impact the fairness of intellectual property systems, the balance between individual and collective contributions to innovation, and the promotion of responsible AI development. Moreover, this research helps society navigate the ethical and legal complexities associated with AI's increasing autonomy.

### ***1.2 Research Methodology***

The methodology employed for this paper is a non-empirical research approach, which involves the analysis of existing literature, case law, and legal frameworks related to the issue of recognizing AI as a legal inventor under patent laws. An organized search and analysis of pertinent literature, case law, and legal frameworks concerning the recognition of AI as a legitimate inventor under patent laws were part of the non-empirical research approach employed in this paper. The research was carried forward by using several kinds of databases, including LexisNexis, Westlaw, and Google Scholar, as well as additional academic and legal sources. To uncover relevant information, search terms including "AI inventorship," "patent law," "IP," "machine learning," and "AI" were employed. No particular era or region was excluded from the search. Instead, it aimed to provide a comprehensive overview of the legal landscape related to the recognition of AI as a legal inventor. To retrieve relevant sources, the search was conducted by using titles, abstracts, and full-text articles.

## 2 Overview of Artificial Intelligence

The future belongs to AI, not just for Russia but for the entire human race. It brings with it enormous potential as well as unpredictable threats. As per the vision of, Russian President Vladimir Putin [6], whoever seizes control of this arena will likewise seize control of the entire earth. The ability of a modern computer system to perform tasks that often require human intelligence, such as learning, problem-solving, and decision-making, is referred to as AI. The broad field of AI in the fields of engineering and computer science is focused on the creation of intelligent computers that can do jobs that ordinarily need human intellect [7]. Based on its abilities AI can be divided into a number of categories, including:

### (A) Rule-Based or Expert Systems

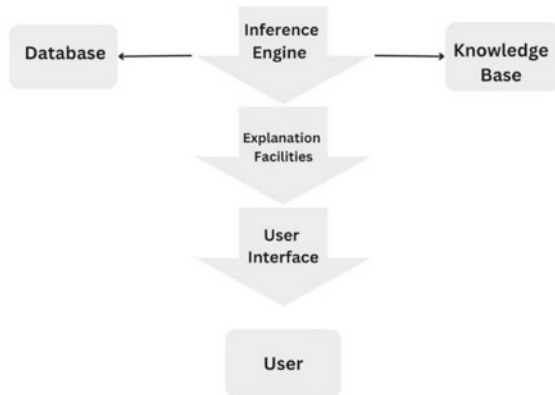
To make decisions based on incoming data, these systems use a set of pre-defined rules or if-then statements. They are frequently employed in industries like banking and medicine. Expert systems come to a conclusion or make a choice based on a combination of data and rules. The rules are frequently expressed in the form of if-then statements, where the system evaluates the input data to a set of requirements before acting in line with the findings [8].

Figure 1 is about the structure of expert systems which are commonly used in fields like medicine and finance, where they can be used to make decisions based on large amounts of data and complex rules

### (B) Machine Learning (ML)

This kind of AI makes use of statistical models and algorithms to give machines the ability to learn about data and get better over time. Applications like speech recognition, picture recognition, and NLP [9] all frequently employ this. Large-scale data is used to train ML algorithms, which can then use the data to find patterns and predict future outcomes. These forecasts depend on statistical models that provide

**Fig. 1** Rule-Based Expert system structure



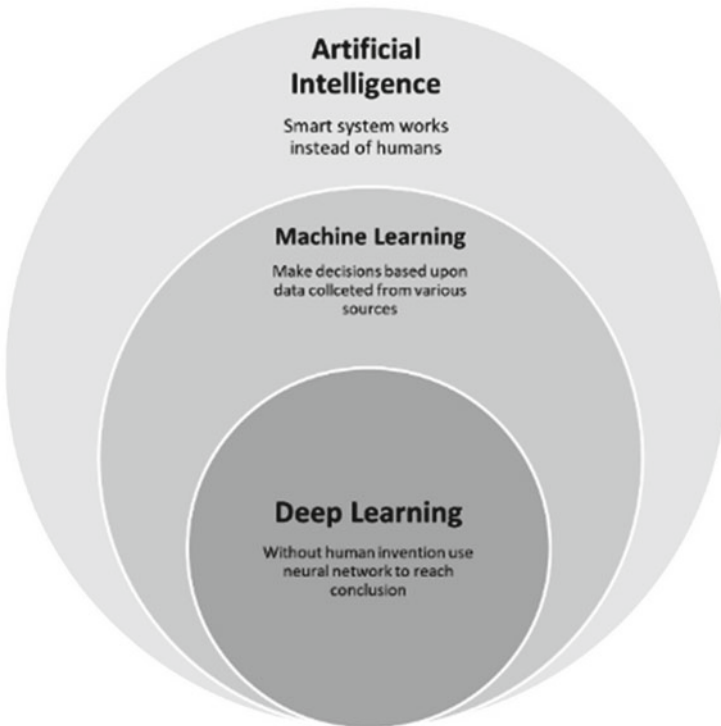


the computer with the ability to identify and classify data into several categories or forecast future events. Natural language processing, speech recognition, image recognition, and recommendation systems are just a few of the many uses for machine learning [10].

**(C) Deep Learning (DL)**

By utilizing artificial neural networks, this kind of ML aims to replicate how the human brain functions. Language translation and NLP are just a few of the applications that tremendously benefit from DL. For example, deep learning algorithms can be trained to recognize and classify objects in images like cars, buildings, and animals [11]. They can be applied to study speech patterns as well as hear spoken words and phrases. NLP uses DL to build models of language that can comprehend the meaning of the text and provide responses that are human-like [12].

Figure 2 While ML focuses on methods that allow computers to learn from data, and DL is a subset of machine learning that uses neural networks with numerous layers, is about the scope of AI includes the vast subject of constructing intelligent systems



**Fig. 2** Ambit of AI, ML, and DL

### (D) Natural Language Processing (NLP)

Computers can understand and translate spoken and written human language thanks to this type of AI. This is used in applications like language translation, virtual assistants, and chatbots. In order for computers to engage with people in a way that feels natural and intuitive, NLP tries to enable them to understand both spoken and written human language. A range of techniques and tools, such as DL, ML, and linguistics, are used by NLP systems to process and analyze human language [13].

### (E) Robotics

This kind of AI employs machines to carry out operations that demand direct physical contact with the environment. Manufacturing, healthcare, and other industries all use robots [14]. The creation of machines that can carry out activities autonomously or with little assistance from humans is the main objective of robotics technology. AI is used in finance to identify fraud, evaluate risks, and analyze investments, assisting financial firms in making better decisions [15]. AI is used in industry to improve operations through process optimization, quality control, and predictive maintenance [16].

## 3 Patent Laws and Legal Inventorship

Patent laws are designed to defend inventors and honor their creative effort. Only the inventor (or inventors) may file an application for a patent for their innovation in the majority of nations [17]. The basis for choosing who should be listed as the inventor of a specific invention is also provided by patent laws [18]. To obtain a patent, the invention must meet certain criteria that vary by jurisdiction but generally include:

1. **Originality:** The invention must be brand-new and unheard-of. This means that prior to the filing date of the patent application, the invention cannot have been publicly used, offered for sale, or discussed in any printed publication.
2. **Inventive step/non-obviousness:** The invention must be obscure to someone with common knowledge of the field [19]. An innovative step must be present in the invention that a person operating in the same field would not recognize [20].
3. **Utility/Industrial applicability:** The invention must have practical use to achieve certain objectives and be capable of being made or used in some kind of industry. The invention must not be purely theoretical or abstract [21].
4. **Enablement/Description:** The patent application must describe the invention in sufficient detail so that a person having ordinary skills in the relevant field can understand how to make and use the invention. The description must enable a person to carry out the invention without undue experimentation [22].
5. **Statutory Subject Matter:** The invention must be eligible for patent protection under the relevant law [23].

**Fig. 3** Criteria for patent eligibility

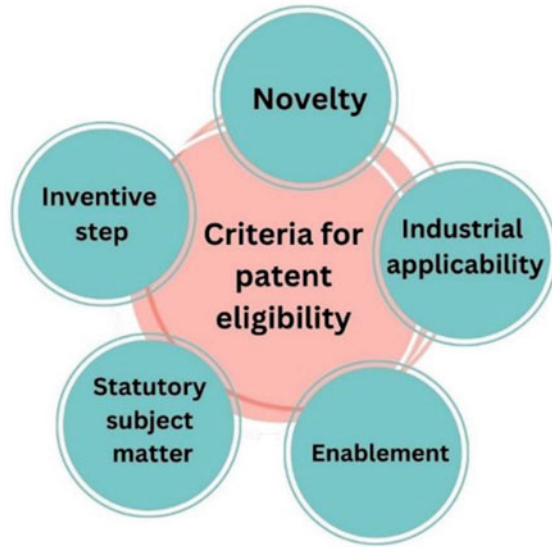


Figure 3 explains the patenting criteria. An innovation needs to be new, not already known, and useful in order to qualify for a patent. Natural laws, abstract concepts, and phenomena are typically not patentable.

## 4 Case Law and International Perspectives

Around the globe, there have been a few well-known instances of AI-generated inventions that have brought to light the difficulties in identifying the inventorship and patenting for such creations. Here are some examples:

### Dabus

In 2019, an AI system called DABUS (Device for the Autonomous Bootstrapping of Unified Sentience) was credited with inventing two new products—a food container and a flashlight—by an inventor Dr. Thaler. Dr. Thaler argued that DABUS should be recognized as the inventor, as it had created the inventions without any human involvement or intervention. He also thought that recognizing AI as creators would foster innovation and the development of revolutionary AI technologies. The United States Patent and Trademark Office (USPTO) rejected the patent applications, despite the fact that only a real person can be identified as an inventor [24].

### **Thaler V Commissioner of Patents**

In 2021, the Federal Court of Australia dismissed an appeal by Dr. Thaler against the Australian Patent Office's decision to refuse his patent applications for two AI-generated inventions. The court ruled that an inventor must be a natural person and that the AI system cannot be named an inventor [25]. Because an inventor must be a natural person and the AI system could not be listed as an inventor, the Australian Patent Office rejected the patent applications. Dr. Thaler had appealed the ruling, claiming that the current patent system was inadequate to address the special capabilities of AI and that recognizing AI as inventors would encourage innovation [26]. Some legal professionals and business organizations have applauded the ruling, arguing that it clarifies and stabilizes Australian patent law [27].

### **The University of Surrey V. Mipsology SA**

In a lawsuit in the UK, the University of Surrey asserted that a patent application for a better technique of encoding video data was the sole creation of an AI system it had created. The patent application was rejected by the UK Intellectual Property Office because it was determined that the AI system did not satisfy the requirements for inventorship [28].

### **Warner-Lambert Company LLC V. Actavis Group PTC EHF**

In this case, the UK High Court considered the patentability of a new drug compound created using AI. The court held that the drug was not patentable because it was obvious to a skilled person in the field, even though it was created using AI [29].

These examples demonstrate the persistent uncertainty and divergence around the obtaining a patent and the inventorship of inventions made possible by artificial intelligence. A human inventor must be identified in the patent application in several nations, notably the US and Australia, where there is a specific legal definition of what constitutes an inventor. The UK and Europe, on the opposite hand, adopt a more permissive stance and permit the naming of entities other than people as innovations in applications for patents [30]. Although it has not yet become a legally binding ruling, the Japan Patent Office recently recognized an AI system as an inventor in a patent application [31]. The issue of legal inventorship for AI-generated inventions is likely to become increasingly important as AI technology continues to advance and becomes more prevalent in various industries [32].

## **5 Implications of Recognizing AI as a Legal Inventor**

A significant change in how we see innovation and intellectual property would result from AI being recognized as a legal inventor. There would be huge, if AI were to be acknowledged as a legitimate inventor. Here are a few instances:

- (a) **Ethical and Moral Implications:** A lot of questions are raised when we are recognizing AI as a legal creator. For instance, it begs the question of what

creativity and innovation are, as well as whether machines can be genuinely referred to as “creative” in the same sense as people [33].

- (b) **The patent system:** If AI is granted as a legal inventor, then the present patent system collapses. Specifically, while determining who owns the rights to an invention and who is entitled to financial compensation for its use is the biggest challenge. It could also raise questions about the role of patent law in incentivizing innovation, particularly if AI-generated inventions are more prevalent in the future [34].
- (c) **Social and economic repercussions:** By altering how invention is rewarded and encouraged, the legalization of AI as an inventor may have a huge effect on the economy [35].

## 6 Potential Solutions for Recognizing AI as a Legal Inventor

Numerous obstacles must be overcome before AI may be considered a legitimate creator, and their legal, ethical, and social ramifications must all be carefully considered [36]. The following are some potential answers and future directions that might be investigated in order to overcome these issues:

- (a) **Co-inventorship:** Recognizing the AI system’s human inventors as co-inventors is still another option. This strategy could help to ensure that human inventors continue to receive credit and compensation for their efforts by acknowledging their role in the development of the AI system [37].
- (b) **Legal framework:** A new legal framework that recognizes AI as a legitimate creator and includes proper rules for assessing the requirements for inventorship, ownership, and reward [38] could be one option. This could include developing specific regulations and laws that address the unique characteristics of AI-generated inventions, such as the fact that they do not have the legal capacity to enter into contracts [39].
- (c) **Industry standards and best practices [37]:** The creation of industry standards and best practices that specify how to manage inventions produced by AI is another potential remedy [40]. These could include recommendations on how to resolve disputes involving AI-generated inventions as well as rules on matters like ownership, responsibility, and infringement [41].
- (d) **Hybrid models:** Using a hybrid model that incorporates aspects of the aforementioned strategies is one option. This might entail giving the AI system specific rights and safeguards while also making sure that human inventors retain ownership of the innovation [42].
- (e) **Licensing agreements:** Utilizing licensing agreements to resolve ownership and control of inventions produced by AI is another option. For instance, a business that generates an idea using AI could obtain a license from the owner of the AI system [43]. This would enable the business to market the invention

while also guaranteeing that the person who created the AI system is paid for their efforts.

- (f) **Decentralized models:** A decentralized paradigm has been proposed as being better suitable for recognizing AI as a legal inventor. In order to do this, a system where numerous stakeholders, including the AI system and its developers, can participate in the invention and benefit from the results must be developed. Such a model would necessitate the establishment of new governing bodies and legislative frameworks [44].
- (g) **Social contracts:** Another potential solution is to use social contracts to govern the ownership and control of AI-generated inventions. This would involve creating informal agreements between the parties involved, based on shared ethical principles and values.

## 7 Results and Discussion

The study presented several notable cases and international perspectives on the patentability and inventorship of AI-generated inventions. These cases shed light on the challenges and uncertainties surrounding the recognition of AI as a legal inventor. The examination of these examples and viewpoints has made clear the necessity of a thorough and modern legal framework that can address the particular properties of inventions produced by AI. The lack of agreement and consistency across various nations on the recognition of AI as a legal creator is one of the study's major results. Countries with strong definitions of inventorship, such as the United States and Australia, call for a natural person to be identified as an inventor. In contrast, nations with more open policies, notably the United Kingdom and Europe, let non-human entities, including AI systems, to be recognized as inventors. Potential solutions were explored to address the challenges of recognizing AI as a legal inventor. One suggested solution is to create a new legal framework that specifically addresses the criteria for inventorship, ownership, and compensation in AI-generated inventions.

## 8 Way Forward

The legal system and regulations will probably need to be changed as AI technology develops to take these advancements into account. To make sure that legal frameworks continue to be applicable and efficient, it is crucial to have constant conversations and involvement between the legal and technological sectors. Although there may be solutions, cooperation and involvement between legal, technological, and social players will be necessary to build a legal framework that addresses the special features of inventions produced by AI. To address the particular issues that AI presents, ethical norms and guidelines must be created. This requires cooperation across stakeholders

in the legal, technological, and societal realms. A culture of ethical innovation should be supported in order to make certain that the development of AI takes into account the wider effects of AI on society. We can ensure that the benefits of AI are achieved while also taking into account important ethical and social challenges by doing these things.

## 9 Conclusion

The complicated issue of whether AI may be acknowledged as a legal inventor poses significant ethical, societal, and legal issues. The special capabilities and constraints of AI systems were not intended to be addressed by the current legal framework for patents and intellectual property. To properly address the issues raised by AI-generated innovations, new legal frameworks and governance structures are therefore required. Although artificial intelligence (AI) is increasingly used to create ideas, the current patent system was created for human inventors and does not explicitly acknowledge AI as a legitimate creator. This presents a range of challenges related to inventorship criteria, ownership, and compensation. Future research directions could include further exploration of the ethical and social implications of recognizing AI as a legal inventor, developing new models for determining legal inventorship, and analyzing the potential economic impacts of recognizing AI as a legal inventor.

## References

1. Artificial Intelligence Market Report: Size, Growth & Analysis. (n.d.). Markets and markets. Retrieved February 18, 2023, from <https://www.marketsandmarkets.com/Market-Reports/artificial-intelligence-market-74851580.html>
2. Andresen SL (2002) John McCarthy: father of AI. *IEEE Intell Syst* 17(5), Article 5
3. Kenneth-Southworth E, Li Y (2023) AI inventors: deference for legal personality without respect for innovation? *J Intellect Prop Law Pract* 18(1), Article 1
4. Kokane S (2021) The intellectual property rights of artificial intelligence-based inventions. *J Sci Res* 65(2)
5. Thaldar D, Naidoo M (2021) AI inventorship: the right decision? *S Afr J Sci* 117(11–12):1–3
6. Putin: Leader in artificial intelligence will rule world. (n.d.). Retrieved February 18, 2023, from <https://www.cnn.com/2017/09/04/putin-leader-in-artificial-intelligence-will-rule-world.html>
7. Chesterman S (2020) Artificial intelligence and the limits of legal personality. *Int Comp Law Q* 69(4), Article 4
8. Kretschmer M, Meletti B, Porangaba LH (2022) Artificial intelligence and intellectual property: copyright and patents—a response by the *CREATE Centre to the UK Intellectual Property Office's open consultation*. *J Intellect Prop Law Pract*
9. Lada M (2022) Artificial intelligence, inventorship and the myth of the inventing machine: can a process be an inventor? *Inf Commun Technol Law* 1–40
10. George A, Walsh T (2022) Can AI invent? *Nat Mach Intell* 1–4
11. Singh N, Bandyopadhyay TK, Sahoo N, Tiwari K (2021) Intellectual property issues in artificial intelligence: specific reference to the service sector. *Int J Technol Learn Innov Dev* 13(1), Article 1

12. Yanisky-Ravid S, Jin R (2021) Summoning a new artificial intelligence patent model: In the age of crisis. *Mich. St. L. Rev* 811
13. Narayanan RR, Durga N, Nagalakshmi S (2022) Impact of artificial intelligence (AI) on drug discovery and product development. *Indian J Pharm Educ Res* 56:S387–S397
14. Dharmapuri Selvakumar M (2022). A Robot in IP-the issues and need for legislation. *J Intellect Prop Rights (JIPR)* 25(6), Article 6
15. Craig CJ (2022) The relational robot: a normative lens for AI legal neutrality—commentary on Ryan Abbott, the reasonable robot. *Jerus Rev Leg Stud* 25(1), Article 1
16. Bennett B, Daly A (2020) Recognising rights for robots: can we? Will we? Should we? *Law Innov Technol* 12(1), Article 1
17. Adde L, Smith J (2021) Patent pending: the law on AI inventorship. *J Intellect Prop Law Pract*
18. Deshpande R, Kamath K (2020) Patentability of inventions created by AI—the DABUS claims from an Indian perspective. *J Intellect Prop Law Pract* 15(11):879–889
19. Heon L (2022) Artificially obvious but genuinely new: how artificial intelligence alters the patent obviousness analysis. *Seton Hall Law Rev* 53(1):8
20. Ebrahim TY (2020) Artificial intelligence inventions & patent disclosure. *Penn St. L Rev* 125:147
21. Lim PH, Li P (2022) Artificial intelligence and inventorship: patently much ado in the computer program. *J Intellect Prop Law Pract* 17(4):376–386
22. Vanherpe J (2021) IP and AI-A tale of two acronyms. *Artif Intell Law*; 2021/05/05–2021/05/05
23. Gibson S, Newman J (2020) What happens when AI invents: is the invention patentable? *AI Mag* 41(4), Article 4
24. Oriakhogba DO (2021) What If DABUS came to Africa? Visiting AI inventorship and ownership of patent from the Nigerian perspective. *Bus Law Rev* 42(2), Article 2
25. Kanna R, Singh P (2021) Thaler v commissioner of patents [2021] FCA 879: DABUS-an ‘Inventor’? *Indian J Artificial Intel L* 2:7
26. Liberman A (2022) One small step for ‘artificial intelligence’ and a giant leap for the Australian patent system? The Federal Court decision in *Thaler v Commissioner of Patents*. *J Intellect Prop Law Pract* 17(2), Article 2
27. Jenkins G (2021) Thaler strikes again, down under: artificial intelligence systems as inventors not ruled out (yet). *J Intellect Prop Law Pract*
28. Who is Mipsology? (n.d.). Mipsology. Retrieved February 18, 2023, from <https://mipsology.com/who-is-mipsology/>
29. Warner-Lambert Company LLC (Appellant) v Generics (UK) Ltd t/a Mylan and another (Respondents). Retrieved February 18, 2023, from <https://www.supremecourt.uk/cases/docs/uksc-2016-0197-judgment.pdf>
30. del Mar Marono Gargallo M (2020) The concept of inventor in patent law and artificial intelligence systems. *Cuad Derecho Transnacional* 12:510
31. Schiemer J, Tawse N, O’Rourke JS (2019) Artificial intelligence and intellectual property: who owns property created by an algorithm or a robot? In: SAGE business cases. The Eugene D. Fanning Center for Business Communication, Mendoza College
32. Coguic L (2021) Forward thinking or right on time? A proposal to recognize authorship and inventorship to artificial intelligence. *Indon J Int’l Comp L* 8:223
33. Gibson J (2021) Artificial intelligence and patents: DABUS and methods for attracting enhanced attention to inventors. *Queen Mary J Intellect Prop* 11(4), Article 4
34. Rudzite L (2022) Certification as a remedy for recognition of the role of AI in the inventive process. *Int Comp Jurisprud* 8(1):112–128
35. Kidd M (2020) Using AI to invent? Australasian Biotechnology therapeutics: should artificial intelligence be recognised for inventive activity 30(1)
36. Fujii H, Managi S (2018) Trends and priority shifts in artificial intelligence technology invention: a global patent analysis. *Econ Anal Policy* 58:60–69
37. Adaka EE, Olubiyi IA (2022) Lessons for Nigeria: determining authorship and inventorship of artificial intelligence generated works. *J Intellect Prop Inf Technol Law (JIPIT)* 2(1):15–48



38. Schwartz DL, Rogers M (2022) Inventorless inventions? The constitutional conundrum of AI-produced inventions. *Harv J Law Technol* 35(2)
39. Naidoo M (2022) AI and legal personhood: an African perspective 906–906
40. Foss-Solbrekk K (2021) Three routes to protecting AI systems and their algorithms under IP law: the good, the bad and the ugly. *J Intellect Prop Law Pract* 16(3), Article 3
41. Saw CL, Chan S (2022) Of inventorship and patent ownership: examining the intersection between *Artificial Intelligence and Patent Law*. *Singap J Leg Stud*, Forthcoming
42. Devarapalli P (2020) Submission in response to the WIPO's 'draft issues paper on intellectual property policy and artificial intelligence' (Ref. No. WIPO/IP/AI/2/GE/20/1). Devarapalli, Pratap, Submission in Response to the *Wipo's* "Draft Issues Paper on Intellectual Property Policy and Artificial Intelligence" (Ref. No. Wipo/Ip/Ai/2/Ge/20/1) (Feb 14, 2020)
43. Patra DSP (2022) Artificial inventors: a shift in traditional policy paradigm. *J Intellect Prop Rights (JIPR)* 26(3):119–126
44. Koopmann T, Stubbemann M, Kapa M, Paris M, Buenstorf G, Hanika T, Hotho A, Jäschke R, Stumme G (2021) Proximity dimensions and the emergence of collaboration: a HypTrails study on German AI research. *Scientometrics* 1–22
45. Chimuka G (2019) Impact of artificial intelligence on patent law. Towards a new analytical framework—[the Multi-Level Model]. *World Patent Information* 59:101926

# Comparative Analysis of Imbalanced Malware Byteplot Image Classification Using Transfer Learning



M. Jayasudha, Ayesha Shaik, Gaurav Pendharkar, Soham Kumar, B. Muhesh Kumar, and Sudharshanan Balaji

**Abstract** Cybersecurity is a major concern due to the increasing reliance on technology and interconnected systems. Malware detectors help mitigate cyber attacks by comparing malware signatures. Machine learning can improve these detectors by automating feature extraction, identifying patterns, and enhancing dynamic analysis. In this paper, the performance of six multiclass classification models is compared on the Malimg dataset, Blended dataset, and Malevis dataset to gain insights into the effect of class imbalance on model performance and convergence. It is observed that the more the class imbalance less the number of epochs required for convergence and a high variance across the performance of different models. Moreover, it is also observed that for malware detectors ResNet50, EfficientNetB0, and DenseNet169 can handle imbalanced and balanced data well. A maximum precision of 97% is obtained for the imbalanced dataset, a maximum precision of 95% is obtained on the intermediate imbalance dataset, and a maximum precision of 95% is obtained for the perfectly balanced dataset.

**Keywords** Byteplot representation · Class imbalance · Multiclass classification · Domain adaptation · Convolution neural networks

---

M. Jayasudha · A. Shaik · G. Pendharkar (✉) · S. Kumar · B. Muhesh Kumar · S. Balaji  
Vellore Institute of Technology, Chennai 600127, Tamil Nadu, India  
e-mail: [gauravsandeep.p2020@vitstudent.ac.in](mailto:gauravsandeep.p2020@vitstudent.ac.in)

M. Jayasudha  
e-mail: [jayasudha.m@vit.ac.in](mailto:jayasudha.m@vit.ac.in)

A. Shaik  
e-mail: [ayesha.sk@vit.ac.in](mailto:ayesha.sk@vit.ac.in)

S. Kumar  
e-mail: [soham.kumar2020@vitstudent.ac.in](mailto:soham.kumar2020@vitstudent.ac.in)

B. Muhesh Kumar  
e-mail: [muheshkumar.b2020@vitstudent.ac.in](mailto:muheshkumar.b2020@vitstudent.ac.in)

S. Balaji  
e-mail: [sudharshanan.pb2020@vitstudent.ac.in](mailto:sudharshanan.pb2020@vitstudent.ac.in)

## 1 Introduction

Cyber threats are still a big issue for people, businesses, and governments all around the world. The growing reliance on technology and networked systems has increased the sophistication and prevalence of cyberattacks, posing a serious danger to data security and privacy [1]. Phishing, ransomware, and distributed denial-of-service (DDoS) attacks are among the most typical forms of cyber attacks. These attacks can cause significant financial and reputational damage, disrupt essential services, and even pose a threat to national security. In response, there has been a growing emphasis on cybersecurity measures, including the adoption of advanced encryption technologies and the implementation of comprehensive cyberdefense strategies.

A malware detector is a software tool designed to identify and remove malicious software, also known as malware, from a computer or network. The detector typically works by scanning files and system components for suspicious behavior or known patterns of malicious code. Malware Analysis typically involves two techniques, static analysis, and dynamic analysis. Static analysis is a method used to examine the behavior and structure of a malware sample without executing it. This type of analysis involves analyzing the binary code of the malware and identifying its various components, such as function calls, system calls, libraries imported, and metadata like file size, timestamps, and digital signatures [2]. Dynamic malware analysis involves running the malware in a controlled environment to observe its behavior, which helps to identify the malicious actions that it performs on a system [2].

Traditional malware detection techniques rely on signature-based detection, which can be limited in its ability to detect new and emerging threats. Machine Learning can help in detecting previously unknown malware by identifying subtle patterns in the malware behavior. It can automate the process of feature extraction by converting malware files into byteplot representations. Furthermore, it can improve dynamic analysis by identifying suspicious behavior patterns in real time and flagging potentially malicious activities and software. Overall, machine learning can make malware detection more efficient, robust, and sophisticated.

The malware byteplot image datasets used for the proposed work are the Maling dataset [3] and the Malevis dataset [4]. A hybrid dataset is created by blending the two open-source datasets. Moreover, a comparative analysis is carried out on the three datasets to acquire insights into the effect of class imbalance on malware byteplot image classification. The state-of-the-art CNNs are used to achieve the multiclass classification of malware and compare their performance.

The comparative analysis will foster the development of machine learning-based malware detectors by helping to choose the right model based on the ability of the model to handle class imbalance.

## 2 Related Work

The multiclass classification of malware byteplot images has been tried in literature by using various data augmentation techniques, sequential modeling, and convolutional neural networks. Agarap et al. 2017 discuss an SVM-based deep learning model to classify the byteplot images in the Maling dataset with various feature extractors like MLP, CNNs, and GRUs. They achieve a predictive accuracy of 84.92% with the Maling dataset and GRU-SVM model. The usage of sequential models to process the byteplot images of varied sizes is commendable but the accuracy is comparatively decent [5]. Kalash et al. (2018) designed a CNN-based framework that is proposed to render better performance than the traditional approaches of shallow learning for malware classification using byteplot images. They tested the model on the Maling dataset and Microsoft dataset resulting in an accuracy score of 98.52 and 99.97% accuracy, respectively. The accuracy of the customized framework is commendable but, on the other hand, only accuracy is used as the primary metric on an imbalanced dataset like the Maling dataset [6].

Lo et al. (2019) discussed an Xception model that performs better than existing models like VGG16 and other traditional models like KNN and SVM. XceptionNet obtains the highest validation accuracy against the other models VGG16, KNN, and SVM. The high accuracy is commendable but the usage of accuracy as the primary metric can be misleading on the actual nature of the model [7]. Singh et al. 2019 prepared a malware dataset using data collection, and deep neural networks are designed to classify the images across 22 families. An accuracy of 98.98 and 99.40% using deep CNN and ResNet-50, respectively, is achieved. The high accuracy is commendable [8].

Go et al. (2020) experimented ResNeXt model for the classification of malware byteplot images. They achieve an accuracy of 98.32 and 98.86% on the Maling dataset and Maling dataset, respectively, after image enhancement. The enhancement of image quality and the resulting high accuracy is commendable but accuracy cannot be a sufficient metric to evaluate the model quality for an imbalanced dataset like the Maling dataset [9]. Ghouti et al. 2020 discussed an approach of extracting image features after a principal component analysis and then using an SVM to perform the classification. They use the Maling, Ember, and BIG 2015 malware datasets to reach accuracy values of 99.8, 91.1, and 99.7%, respectively. Evaluation of the model on different datasets gives a good understanding of the model quality but dimensionality reduction can lead to the loss of information [10]. Mitsuhashi et al. 2020 discussed an approach to solve the data imbalance using the undersampling technique and fine-tuning VGG19 on the Maling dataset. They obtained an accuracy of 99.72%. The high accuracies and data augmentation are commendable but the usage of accuracy as the primary metric can be misleading for an imbalanced dataset like the Maling dataset [11]. Danish Vasan et al. 2020 experimented with transfer learning using the Maling dataset and IoT-android mobile dataset. The performance of this model is compared with existing pre-trained CNNs. The Maling malware dataset shows an accuracy of 98.82%, and the IoT-android mobile dataset shows an accuracy of

about 97.35%. The high accuracies are commendable but the usage of accuracy as the primary metric can be misleading for an imbalanced dataset like the Malimg dataset [12].

Aslan et al. (2021) discussed a hybrid model integrating the performance of two pre-trained models namely AlexNet and ResNet152 in an optimal manner. The model is tested on Malimg, Microsoft BIG 2015, and Malevis datasets. For the Malimg dataset, it gives 97.78% accuracy. The higher accuracy and usage of a hybrid model are commendable but the usage of accuracy as the primary metric can be misleading for an imbalanced dataset like the Malimg dataset [13]. Asam et al. 2021 discussed an approach to the extraction of features from multiple CNNs and fusing their results. Finally, using an SVM to discriminate between them. The architecture achieves an accuracy of 98.61%, an F-score of 0.96, a precision of 0.96, and a recall of 0.96. The performance of the model is good and its evaluation using different classification metrics is commendable [14]. Awan et al. 2021 discussed a spatial attention and convolutional neural network approach for the multiclass classification of malware. They achieve a precision of 97.42%, a recall of 97.95%, a specificity of 97.33%, and an F1-score of 97.32%. The performance of the model is good based on the reported classification metrics.[15]

Mallik et al. (2022) described an approach to resolve data imbalance using data augmentation and the augmented dataset is classified by using two LSTM layers and one VGG Net. The overall results from each are integrated and combined. Treating the malware file bits as a bidirectional dependency is commendable [16]. AlGarni et al. 2022 compared the performance of EfficientNetB3 on Imagenet and Malimg datasets. They obtain an accuracy of 99.93% on the Malimg dataset. The comparison of the performance of the model on two datasets is commendable but accuracy cannot be a sufficient metric to evaluate the model quality for an imbalanced dataset like the Malimg dataset [17]. Adem Tekerek et al. 2022 resolved the classification by data augmentation using CycleGAN and use different CNNs for classification. They achieve an accuracy of 99.86% for the BIG2015 dataset and 99.60% for the Dumpware10 dataset. The high accuracy is commendable [18].

### 3 Proposed Architecture

Figure 1 shows the architecture diagram for the flow of data for the comparison of the imbalanced image classification of three different malware datasets. Two malware image datasets are available, namely, the Malimg dataset and the Malevis dataset. Both datasets are blended into a single dataset of intermediate imbalance. All the images from the respective datasets are subject to an initial Image Preprocessing comprising Image Resizing and Augmentation. At the end of this stage, there are three splits available for each dataset: train, validation, and test. Following this, a set of six models are experimented on each of the datasets and evaluated based on Weighted Precision, Weighted Recall, and Weighted F1-score. The performance metrics for each of the models are taken into account for comparative analysis of the

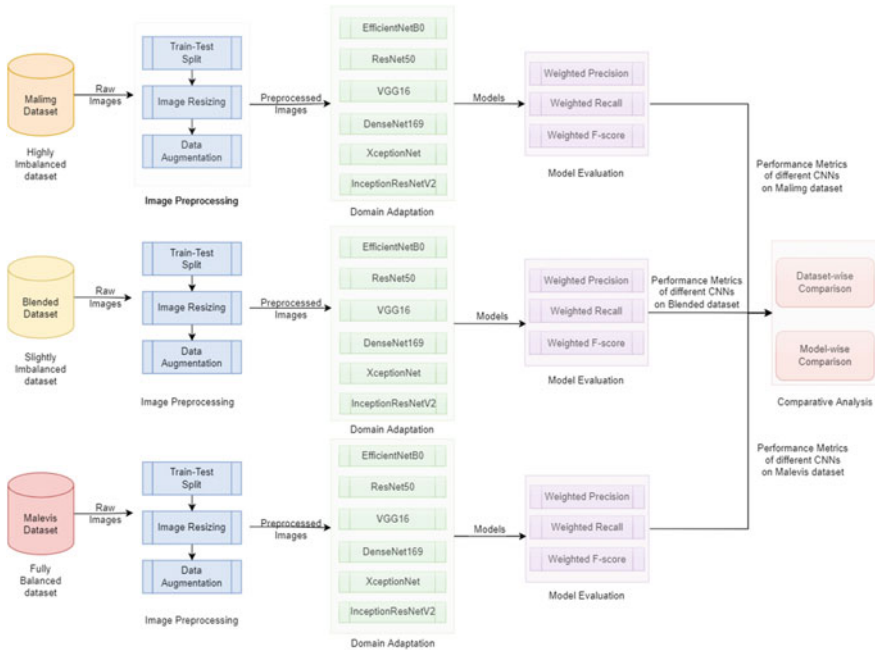


Fig. 1 Architecture diagram

variation of model performance based on malware class imbalance. The models were trained using GPU P100. In the forthcoming sections, each of the steps is discussed in detail.

## 4 Proposed Methodology

### 4.1 Data Blending

The act of merging data from many sources, sometimes with different formats or structures, to produce a single dataset that can be utilized for analysis is known as data blending. A blended dataset is created by blending 5 major classes from the Maling dataset into the 25 malware classes of the Malevis dataset. Finally, three datasets are obtained namely the Maling dataset as a fully imbalanced dataset, the Blended dataset as a dataset of intermediate imbalance, and the Malevis dataset as a perfectly balanced dataset. The class distribution of the datasets is shown in Fig. 2 using the bar charts.

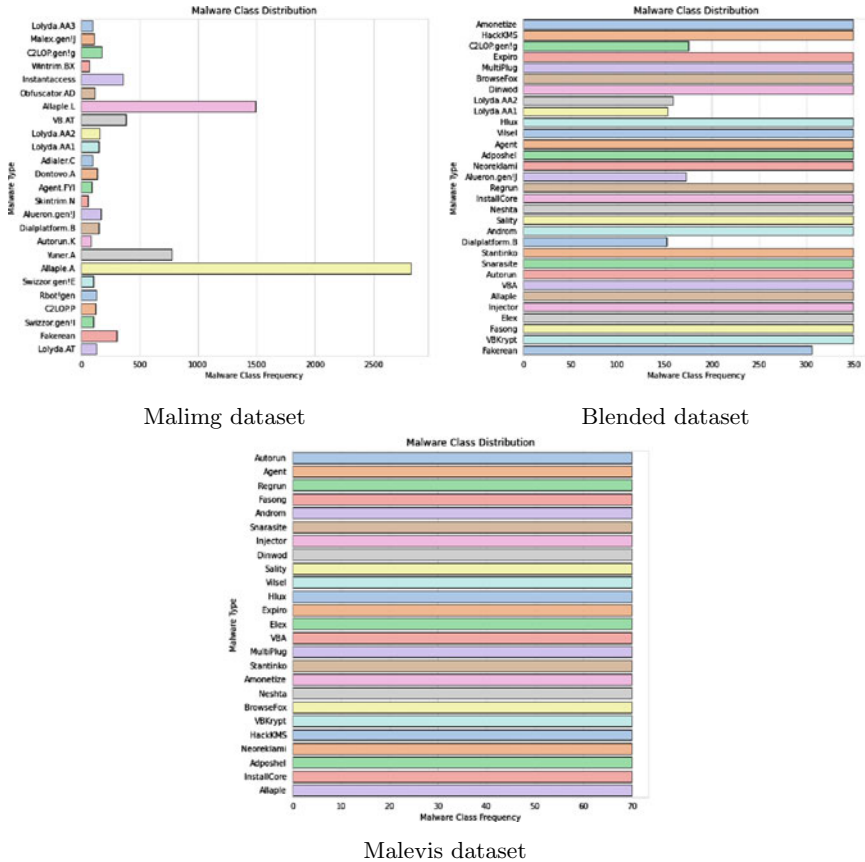


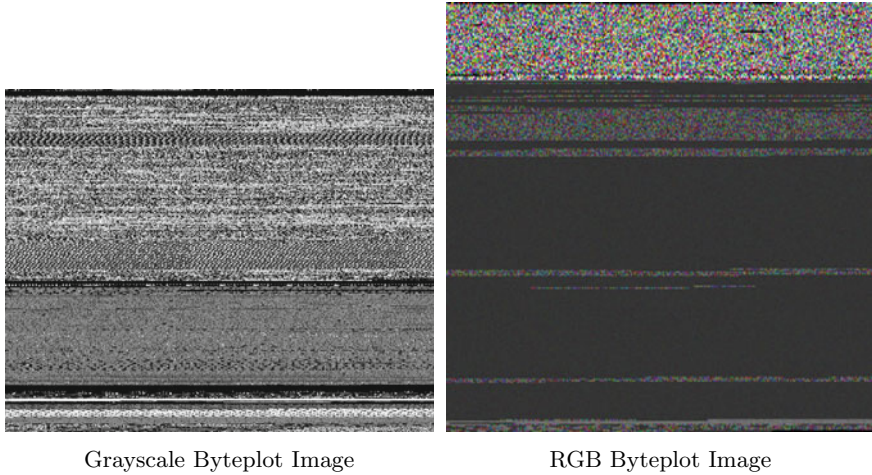
Fig. 2 Class distribution of the three datasets

### 4.2 Image Preprocessing

Image preprocessing is a preliminary step to normalize and augment the image data before feeding it into a neural network for training. Among the datasets, the Maling dataset comprises grayscale images and the Malevis dataset comprises RGB images as shown in Fig. 4. Consequently, the Blended dataset consists of both grayscale and RGB images. Moreover, the Maling dataset has all the images of different sizes which need to be converted to a single image size. After the data is split into a train, test, and validation, all the images are converted RGB and resized to 75 by 75. Following this, the images are augmented by rotating and translating the images which make the model rotation and translation invariant. The whole process for image preprocessing is shown in Fig. 3.



**Fig. 3** Image preprocessing



**Fig. 4** Types of byteplot images

### 4.3 Domain Adaptation

Domain adaptation in transfer learning refers to the process of using knowledge gained from one domain to improve the model performance in a different but related domain. It involves transferring knowledge from a source domain to a target domain, where the data distributions may be different. The data distribution of byteplot images is learned by the model after making the last few feature extraction layers trainable. In addition to it, dropout regularization layers are added to the architecture to mitigate the chance of overfitting for the fully balanced dataset. Moreover, the models are trained with Early Stopping by monitoring the validation loss of each epoch. These additional components to architecture make it less prone to overfitting.

For each of the datasets, six state-of-the-art convolutional neural networks experimented particularly XceptionNet [19], EfficientNetB0 [20], ResNet50 [21], DenseNet169 [22], VGG16 [23], and InceptionResNetV2 [24].



#### 4.4 Evaluation Metrics

A machine learning evaluation metric is a numerical measure that is used to evaluate the effectiveness of a machine learning model. It is used to evaluate how well the model's predictions match the actual outcomes or labels of the data used to train and test the model. For an imbalanced multiclass classification problem, the common accuracy metric is not appropriate since does not take into consideration the support images available across each of the classes. Hence, the most appropriate metrics for the evaluation of each of the six models are weighted precision, weighted recall, and weighted F1-score as depicted in the Eqs. 1, 2, and 3, respectively. In the test data, every class has a specific number of images for evaluation  $w_i$  and the precision  $p_i$ , recall  $r_i$ , and F1-score  $f1_i$  on comparison with the ground truth.

$$\text{Weighted Precision} = \frac{\sum_{i \in C} w_i * p_i}{\sum_{i \in C} w_i} \quad (1)$$

$$\text{Weighted Recall} = \frac{\sum_{i \in C} w_i * r_i}{\sum_{i \in C} w_i} \quad (2)$$

$$\text{Weighted F1 - score} = \frac{\sum_{i \in C} w_i * f1_i}{\sum_{i \in C} w_i} \quad (3)$$

The use of weighted metrics helps in standardizing the performance of models across datasets of different extents of imbalance. In the forthcoming section, the models and performance are compared using these metrics.

## 5 Results and Discussion

In most cases, machine learning-based malware detectors are the multiclass classifiers. In this paper, the focus is on the comparison of multiclass classification of malware byte plot images on three different datasets. Table 1 shows the evaluation metrics for six CNNs across three datasets. From the results, it is evident that the more balanced the dataset is, less is the variance in the performance of models. In the Malimg dataset, there is a high variance across the evaluation metrics of the six models. The best performance is achieved by EfficientB0 with a precision of 97%, recall of 96%, and F1-score of 96%. In the case of the Blended dataset, the best performance is achieved by ResNet50 with precision, recall, and F1-score of 95%. For Malevis dataset, almost all models perform well because of the balance in its class distribution. However, XceptionNet, EfficientB0, and DenseNet169 are performing the best with precision, recall, and F1-score of 95%.

**Table 1** Evaluation metrics for CNNs (in %)

Model	Maling			Malevis			Blended		
	P	R	F1	P	R	F1	P	R	F1
XceptionNet	87	86	85	95	95	95	92	92	92
EfficientNetB0	97	96	96	95	95	95	92	92	92
ResNet50	95	95	95	93	93	93	95	95	95
VGG16	79	80	79	93	92	92	92	92	92
DenseNet169	95	96	95	95	95	95	94	94	94
InceptionResNetV2	91	91	91	94	93	93	93	93	93

## 5.1 Comparison Across Models

Precision is the most important metric for a malware detector because false positives turn out to be more expensive than false negatives. Therefore, alterations of the validation precision are examined over the time of all the epochs as shown in Fig. 5. XceptionNet performs well for each epoch for the Blended dataset and Malevis dataset but is not able to learn well from imbalanced data. ResNet50, EfficientNetB0, and DenseNet169 both perform well with balanced as well as imbalanced data. VGG16 does not learn from imbalanced data but performs well for balanced data. InceptionResNetV2 has decent overall performance but its training history has a lot of spikes in validation loss and evaluation metrics making it unreliable.

## 5.2 Comparison Across Datasets

Previously, the comparison was done by comparing the performance of different models on each of the datasets. Now, a comparison is carried out based on the datasets. The boxplot for model convergence is basically based on the distribution of the number of epochs required by each of the models and the distribution of the F1-score is also examined as shown in Fig. 6. From the convergence boxplot, it's evident that the Maling dataset takes minimum epochs for convergence and the Malevis dataset takes the maximum epochs for convergence. The median epochs and median F1-score are represented by the horizontal line in the box which is perfectly in the center for the perfectly balanced and most deviated for the unbalanced dataset. Moreover, there is a high variance in the performance of the models for the Maling dataset compared to the other datasets. However, the evaluation metrics are one of the aspects but the size of the model and complexity must also be taken into account. Overall, it is evident that the imbalance in the class distribution directly affects the convergence of the model and its performance.

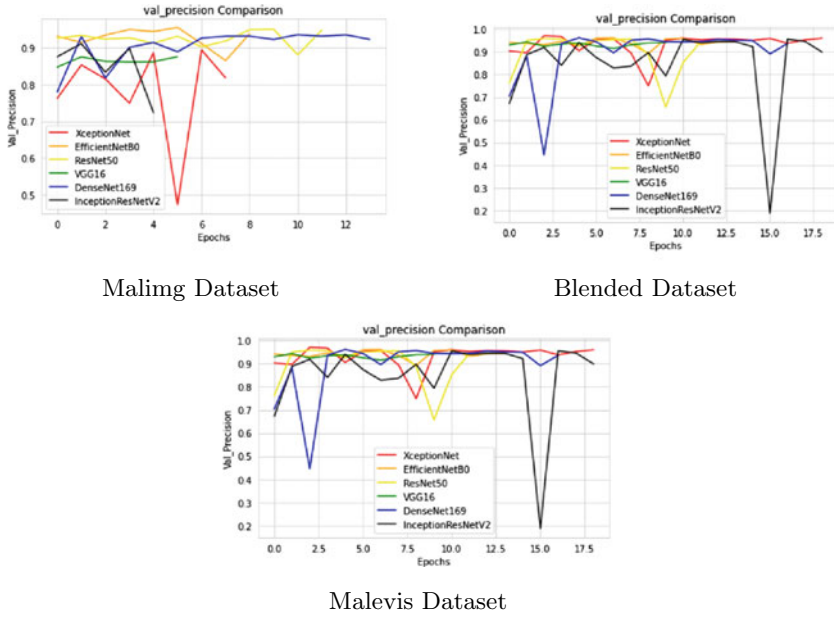


Fig. 5 Model-wise comparison of validation precision metric while training

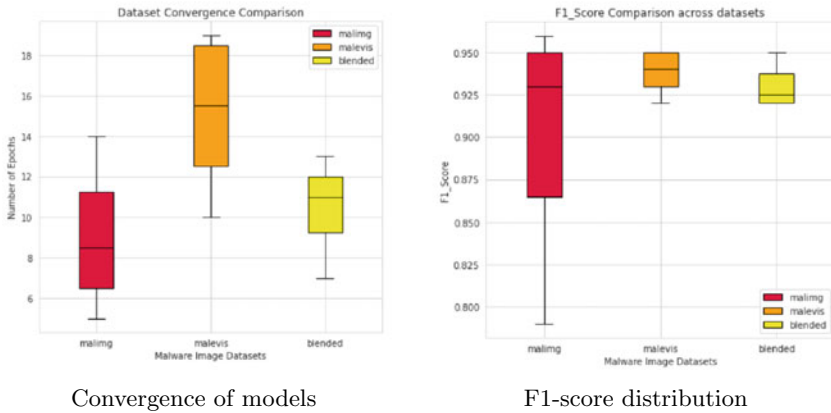


Fig. 6 Dataset-wise comparison

### 5.3 Comparison with Existing Benchmarks

From the literature survey, it is seen that most of the papers consider accuracy as the primary metric for an imbalanced malware dataset like the Maling dataset. Accuracy is not the appropriate metric with reference to imbalanced classification resulting in model evaluation biased to the majority classes. Alternatively, weighted precision

and weighted recall can serve as the primary metric. The F1-score shall be used to condense the precision and recall into a single metric to foster model selection. In the literature, the precision obtained on the Maling dataset is between 97 and 98% which is very close to the performance of EfficientNetB0 on that dataset. However, on Malevis dataset the precision ranges from 96% to 98% which is slightly higher than the maximum precision of 95% obtained on this dataset.

This paper contributes a blended dataset and the results for the same are a new finding. Moreover, a comparison of transfer learning on state-of-the-art CNNs serves as a head start to designing new malware detectors by reducing the experimentation required for model selection. Consequently, it saves the available hardware resources that can be utilized for more intensive tasks.

## 6 Conclusion

A blended dataset is created by the data blending of the Maling dataset and the Malevis dataset. The newly prepared dataset has an intermediate class imbalance compared to the two parent datasets. Finally, a maximum precision of 97% is obtained for the imbalanced dataset, a maximum precision of 95% is obtained for the intermediate imbalance dataset, and the perfectly balanced dataset. From the comparative analysis, it is observed that the more the class imbalance in the dataset more is the variance in the performance of different models and the number of epochs required for convergence. Moreover, it is also observed that for malware detectors ResNet50, EfficientNetB0, and DenseNet169 can handle imbalanced and balanced data well. On the other hand, VGG16 and XceptionNet were sensitive to class imbalance. This comparative analysis can help in choosing the models for experimentation while training any machine learning-based malware detectors.

## References

1. Akhtar MS, Feng T (2022) Malware analysis and detection using machine learning algorithms. *Symmetry* 14(11):2304. <https://doi.org/10.3390/sym14112304>
2. Saxe J, Sanders H (2018) Malware data science: attack detection and attribution. No Starch Press
3. Nataraj L, Karthikeyan S, Jacob G, Manjunath BS (2011) Malware images: visualization and automatic classification. In: Proceedings of the 8th international symposium on visualization for cyber security, pp 1–7
4. Bozkir A, Cankaya A, Aydos M (2019) Utilization and comparison of convolutional neural networks in malware recognition. <https://doi.org/10.1109/SIU.2019.8806511>
5. Awan MJ, Masood OA, Mohammed MA, Yasin A, Zain AM, Damaševičius R, Abdulkareem KH (2021) Image-based malware classification using VGG19 network and spatial convolutional attention. *Electronics* 10:2444. <https://doi.org/10.3390/electronics10192444>

6. Kalash M, Rochan M, Mohammed N, Bruce ND, Wang Y, Iqbal F (2018) Malware classification with deep convolutional neural networks. In: 2018 9th IFIP international conference on new technologies, mobility and security (NTMS). IEEE, pp 1–5
7. Lo WW, Yang X, Wang Y (2019) An xception convolutional neural network for malware classification with transfer learning. In: 2019 10th IFIP international conference on new technologies, mobility and security (NTMS). IEEE, pp 1–5
8. Singh A, Handa A, Kumar N, Shukla SK (2019) Malware classification using image representation. In: Dolev S, Hendlar D, Lodha S, Yung M (eds) *Cyber security cryptography and machine learning*. CSCML 2019. Lecture notes in computer science, vol 11527. Springer, Cham. [https://doi.org/10.1007/978-3-030-20951-3\\_6](https://doi.org/10.1007/978-3-030-20951-3_6)
9. Go JH, Jan T, Mohanty M, Patel OP, Puthal D, Prasad M (2020) Visualization approach for malware classification with ResNeXt. *IEEE Congress on Evolutionary Computation (CEC)*. Glasgow, UK, pp 1–7. <https://doi.org/10.1109/CEC48606.2020.9185490>
10. Ghouti L, Imam M (2020) Malware classification using compact image features and multiclass support vector machines. *IET Inf Secur* 14(4):419–429
11. Mitsuhashi R, Shinagawa T (2020) High-accuracy malware classification with a malware-optimized deep learning model. [arXiv:2004.05258](https://arxiv.org/abs/2004.05258)
12. Vasan D, Alazab M, Wassan S, Naeem H, Safaei B, Zheng Q (2020) IMCFN: Image-based malware classification using fine-tuned convolutional neural network architecture. *Comput Netw* 171:107138
13. Aslan Ö, Yilmaz AA (2021) A new malware classification framework based on deep learning algorithms. *IEEE Access* 9:87936–87951
14. Asam M, Khan SH, Jamal T, Zahoor U, Khan A (2021) Malware classification using deep boosted learning. [arXiv:2107.04008](https://arxiv.org/abs/2107.04008)
15. Awan MJ, Masood OA, Mohammed MA, Yasin A, Zain AM, Damaševičius R, Abdulkareem KH (2021) Image-based malware classification using VGG19 network and spatial convolutional attention. *Electronics* 10:2444. <https://doi.org/10.3390/electronics10192444>
16. Mallik A, Khetarpal A, Kumar S (2022) ConRec: malware classification using convolutional recurrence. *J Comput Virol Hack Tech* 18:297–313. <https://doi.org/10.1007/s11416-022-00416-3>
17. AlGarni MD, AlRoobaea R, Almotiri J, Ullah SS, Hussain S, Umar F (2022) An efficient convolutional neural network with transfer learning for malware classification. *Wirel Commun Mobile Comput* 2022:1–8
18. Tekerek A, Mutlu Yapici M (2022) A novel malware classification and augmentation model based on convolutional neural network. *Comput Secur* 112:102515. ISSN 0167-4048, url-<https://doi.org/10.1016/j.cose.2021.102515>
19. Chollet F (2017) Xception: deep learning with depthwise separable convolutions. In: *Proceedings of the IEEE conference on computer vision and pattern recognition*, pp 1251–1258
20. Tan M, Le Q (2019) Efficientnet: Rethinking model scaling for convolutional neural networks. In: *International conference on machine learning*. PMLR, pp 6105–6114
21. He K, Zhang X, Ren S, Sun J (2016) Deep residual learning for image recognition. In: *Proceedings of the IEEE conference on computer vision and pattern recognition*, pp 770–778
22. Huang G, Liu Z, Van Der Maaten L, Weinberger KQ (2017) Densely connected convolutional networks. In: *Proceedings of the IEEE conference on computer vision and pattern recognition*, pp 4700–4708
23. Simonyan K, Zisserman A (2014) Very deep convolutional networks for large-scale image recognition. [arXiv:1409.1556](https://arxiv.org/abs/1409.1556)
24. Szegedy C, Ioffe S, Vanhoucke V, Alemi A (2017) Inception-v4, inception-resnet and the impact of residual connections on learning. In: *Proceedings of the AAAI conference on artificial intelligence*, vol 31, No 1

# Recommender Systems for Personalized Business Marketing: Employing Artificial Intelligence and Business Intelligence in Machine Learning Techniques



N. Poornima, C. Sridharan, A. Pavithra, R. Narendiran, B. Vijay, and V. S. Neelesh

**Abstract** The prediction of a business plays a major role in market analysis. In order to look for the business potential in the market, we have conducted a study to explore how the combination of artificial intelligence (AI) and business intelligence (BI) techniques can be used for regional market analysis to get the best potential in an area and predict the business. Our research focused on analyzing and interpreting data from various sources, such as demographics, economic indicators, consumer behavior, and social media. Decisions are made in terms of two parameters: insight and forecast. We aimed to generate insights and forecasts that would assist businesses in making informed decisions. To achieve the insight and forecast, we used the OSEMN framework. OSEMN stands for Obtain, Scrub, Explore, Manipulate, and Interpret. This framework is useful in gathering relevant data, cleaning and preparing it for analysis, exploring patterns and trends, manipulating the data as needed, and interpreting the findings. We conducted a regional market analysis case study, by employing machine learning algorithms and data mining techniques within this framework. Our project resulted in providing a piece of valuable information on market trends, customer preferences, and potential investment opportunities. These results demonstrated the potential of AI and BI in enhancing business intelligence and decision-making processes, particularly in the context of regional market analysis. We highlighted the benefits of utilizing AI and BI technologies while acknowledging

---

N. Poornima (✉) · C. Sridharan · A. Pavithra · R. Narendiran · B. Vijay · V. S. Neelesh  
Vellore Institute of Technology, Vellore Campus, India  
e-mail: [poornima.n@vit.ac.in](mailto:poornima.n@vit.ac.in)

A. Pavithra  
e-mail: [pavithra.a2020@vitstudent.ac.in](mailto:pavithra.a2020@vitstudent.ac.in)

R. Narendiran  
e-mail: [narendiran.2020@vitstudent.ac.in](mailto:narendiran.2020@vitstudent.ac.in)

B. Vijay  
e-mail: [vijay.b2020@vitstudent.ac.in](mailto:vijay.b2020@vitstudent.ac.in)

V. S. Neelesh  
e-mail: [neelesh.vs2020@vitstudent.ac.in](mailto:neelesh.vs2020@vitstudent.ac.in)

the boundaries and challenges they may present. We also discussed the implications and limitations of this approach. We have suggested some potential areas for further study in this field, recognizing the need for ongoing research to refine and expand upon these techniques.

**Keywords** Business intelligence · Artificial intelligence · Machine learning algorithms

## 1 Introduction

Artificial Intelligence (AI) and Business Intelligence (BI) techniques have transformed the business landscape. With these techniques, businesses can analyze vast amounts of data and generate actionable insights, unlocking immense value in market analysis and expansion. This research paper explores using AI and BI techniques for regional market analysis and predicting business potential. We will showcase the power of these tools in driving business growth and competitiveness and provide valuable insights for businesses looking to capitalize on their potential. AI and BI techniques are powerful tools for businesses that want to get a competitive advantage. AI techniques include machine learning, natural language, and deep learning [1, 2]. BI techniques, on the other hand, include data mining, data warehousing, and online analytical processing (OLAP). It involves analyzing the local market and identifying potential opportunities and threats. AI and BI techniques can be used to analyze market trends, customer behavior, and competitor strategies, among other factors. Predicting business potential is another area where AI and BI techniques can be used. These techniques can help businesses forecast sales [3], identify new markets, and optimize pricing strategies. AI and BI techniques can also be used to identify potential risks and mitigate them. AI and BI techniques are powerful tools for businesses that want to get a competitive advantage. Businesses can unlock immense value in market analysis and expansion by using these techniques for regional market analysis and predicting business potential. The insights gained from AI and BI techniques can help business people make better decisions, optimize their operations, and increase revenue. The research paper includes several key sections that follow a structured approach. The related research section reviews the existing literature on the topic and lists relevant references. The proposed work and business model are then explained in detail in the proposed work section. The system model section provides research objectives and outcomes, such as reliability, redundancy, and accuracy, and compares the variations in using different Machine Learning Algorithms through tables. The expected and achieved results are then discussed in the result section. The conclusion section of the paper discusses the findings from the case study, highlights the limitations of the proposed model, and suggests potential strategies to overcome these limitations. The paper provides an in-depth analysis of the proposed model, its results, and limitations, indicating a comprehensive study of the subject matter.

## 2 Related Research

With Artificial Intelligence, Business Intelligence, and Machine Learning Techniques, businesses can analyze vast amounts of data using those techniques which is available across several heterogeneous platforms and effectively use it for business intelligence and generate actionable insights, unlocking immense value in market analysis and expansion [4–6]. There are excessive information resources but with insufficient accuracy. Hence the data must be extracted from an unstructured database hence we can use modules such as “database bottom information resource processing” and “Resource Attribute Recognition of Unstructured Database” for feature extraction from multimedia information resources [7, 8]. The AI systems can be trained to be a contributing member of the organization board of C-Level members. With the knowledge gained, AI can assist in problem solving [9]. The AI will help in strategic decision-making of the organization with data [10]. The combination of AI and DBMS technology holds great potential for the future of computing [11, 12]. AI can increase productivity, gain a competitive advantage, and complement human intelligence [13], furthermore, reducing cost of operations. Businesses of all types and sizes are considering artificial intelligence to solve their problems [14]. The scope of AI in business transformation is constantly growing. AI is an important technology supporting daily social life and economic activities [15]. The continuing advancement of DBMS technology as well as next-generation computing depends on AI/DB integration. We get access to large amounts of shared data for knowledge processing. The Application of Intelligent Database for Modern Information Management is a computer database that plays a critical part in information management [16]. Business units at present need more information and technical data to defend against business rivals [17]. The database management system has a major role in solving this problem for businesses. It involves three levels of modeling for abstraction—knowledge model, conceptual model, and the relational model. Business intelligence (BI) solutions emphasize mounting improved visions and crystal understanding of organizational performance built on data insights, A potential role of big data and artificial intelligence in the path toward a collective approach to knowledge management [18]. This is a data-intensive application hence tuning is an essential aspect [19]. DBMS has hundreds of configuration “knobs”. Hence, we can use a combination of supervised and unsupervised machine learning methods to select the most impactful knobs, map unseen database workloads to previous workloads from which we can transfer experience, and recommend knob settings. Nevertheless, data is increasing exponentially requiring more proficiency from the available data storage technologies, data processing, and analysis. Such continuous massive growth of structured and unstructured data is referred to as a “Big data”. NoSQL is a modern database technology that is designed to provide scalability to support voluminous data, so it has become the most practical database option as a result. Organizational decision-making processes are still susceptible to errors and biases. Business analytics (BA) [10] is one of the approaches to support managers in making well-informed/evidence-based business decisions. Businesses implement



business intelligence (BI) to improve performance, but this initiative frequently does not coincide with the business process management (BPM) strategy. Managers need information to make decisions, therefore it appears plausible to create business value with BI by coordinating BI and BPM projects through machine learning algorithms [20] involving several steps. Improving business intelligence through machine learning algorithms requires a comprehensive understanding of the business problem, the data, and the machine learning models [21]. The user does not understand the normal processing data, so we want to visualize it. Hence, integrated management of multisource heterogeneous satellite data [22] based on the spatial database [23] provides a comprehensive and integrated system for managing and utilizing satellite data, which can support scientific research, policy-making, business potential, and operational activities in various fields [24]. In today's dynamic business environment, identifying the right business opportunity in a particular region is critical to success. Artificial Intelligence (AI) and Business Intelligence (BI) are powerful tools that can help businesses make informed decisions by analyzing market trends and customer behavior.

### 3 Proposed Work

The research paper is concentrated to evaluating the business potential in some areas specified [25], by developing a predictive model using the Machine Learning Techniques. For this paper, the analysis was done with an artificially synthesized dataset which has attributes named region, population, area, literacy rate, accessibility, start\_amount\_investment, type of industry, etc. Models of Classification such as logistic Regression, decision trees, random forests, and support vector machines here were implemented and worked and evaluated for accuracy in predicting business potential. There are certain metrics such as accuracy, precision, recall, and F1-score for evaluation that are used to assess the model. To ensure the reliability and generalizability of the model, the dataset have been split (training and testing). To minimize the biases and overfitting, techniques such as cross validation have been enforced and empowered. From all of these steps, the outcoming result would identify the most accurate and efficient algorithm for the prediction of business potential. This study will look into the attributes that contribute to the success factors of the predictions, and the most valuable insights into the key influencing factors for successful business in a specific area. This paper and the outcome would be needful for entrepreneurs, owners of the business, and the policymakers, providing them with a powerful tool to assess the viability of business ventures in specific areas. This would enable the resource allocation for the venture, altering the business strategies and resource risk management. On the whole hand, this paper would give a better understanding of the complex relationship between area-specific factors and business success, facilitating informed decision-making in the dynamic business landscape, Fig. 1. The system model may be divided into many essential steps:

**Fig. 1** Working diagram of the model proposed



**Data Collection**—This is the step where the data is gathered for the entire process from various sources such as customer, sales, social media, and more data. To find the fitting and the pattern, this data is used.

**Data Cleaning and Preprocessing**—After fetching all the required data, we need to perform all the steps of cleaning/scrubbing before it is taken into an analysis state.

**Feature Extraction**—Here, the data is moved to the next stage where the relevant features are extracted from it such as region, population, area, literacy rate, accessibility, start\_amount\_investment, and type of industry from the dataset.

**Machine Learning Models**—Algorithms which could benefit the efficiency of the model have been occupied in this stage.

**Model Training and Validation**—The algorithms and the model trained and tested are validated using accuracy, F2-score, precision, and recall metrics.

**Model Selection**—On evaluating the model based on the metrics, the best model is selected for future process and deployed nearby.

**Business Insights**—After the deploy period of the model, the obtained insights would tell the benefits stated as the result of the research.

Deployment—Selected models are deployed, and insights obtained would better the new business.

## 4 System Model

### 4.1 Research Objective

**Objective 1:** “The objective of this research is to identify the most accurate ML algorithms for predicting business potential in a given region and to increase the overall accuracy of the system through these algorithms.”

**Objective 2:** “The objective of this research is to develop a user-friendly website or code for the system that enables businesses to easily access and find the best solution from the analysis.”

**Objective 3:** “The objective of this research is to assess the reliability and redundancy of the system by testing it on dataset and comparing the results.”

### 4.2 Dataset Description

Table 1 represents the performance of different machine learning algorithms (Naive Bayes, Regression, K-Nearest Neighbors, Decision Tree, and Random Forest) on an artificially synthesized dataset. The dataset consists of 1000 instances, with 700 instances used for testing T1 and the remaining 300 instances used for training. Two hundred instances were used for testing T2, and the remaining 800 instances were used for training. The Naive Bayes algorithm achieved a 60% accuracy rate on both test sets (T1 and T2). The Regression algorithm performed better with an accuracy rate of 80% on test set T1, dropping to 70% on test set T2. The K-Nearest Neighbors algorithm had a lower accuracy rate of 50% on test set T1 and even lower at 16% on test set T2. On the other hand, the Decision Tree algorithm showed a very low accuracy rate of 16.6% on test set T1, indicating poor performance. However, it performed exceptionally well on test set T2, achieving an accuracy rate of 98%. Similarly, the Random Forest algorithm also demonstrated a high accuracy rate of 57% on test set T1 but greatly improved to 98% on test set T2. The table illustrates the varying performance of different machine learning algorithms on the artificially synthesized dataset. It highlights the importance of considering algorithm selection and dataset characteristics for higher accuracy rates.

**Table 1** Performance comparison table of machine learning algorithms on an artificially synthesized dataset

Dataset name	Artificially synthesized dataset				
Size	1000				
	Naive Bayes	Regression	KNN	Decision tree	Random forest
Test [T1]	700	700	700	700	700
Training [T1]	300	300	300	300	300
Accuracy [T1]	60%	80%	50%	16.6%	57%
Test [T2]	200	200	200	200	200
Training [T2]	800	800	800	800	800
Accuracy [T2]	60%	70%	16%	98%	98%

**Table 2** The software description

Coding	Python, R
Libraries	R [e1071, caret, glmnet], Python [scikit-learn, statsmodels, NumPy]
Visualization tools	Power Bi

### 4.3 Software Description

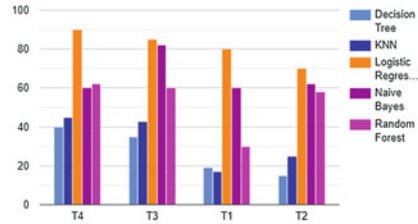
Table 2 describes Python and R are programming languages used in the research paper. Python offers libraries like scikit-learn, statsmodels, and NumPy, which provide tools for scientific computing, data analysis, and machine learning. R, on the other hand, has libraries such as e1071, caret, and glmnet that are well-suited for statistical modeling and data mining. These libraries offer various algorithms and techniques for tasks such as classification, regression, and clustering. Additionally, Power BI is a visualization tool that enables researchers to create interactive dashboards and reports to effectively present their findings. By combining these software and libraries, we have performed data analysis, built predictive models, and communicated results in a comprehensive and visually appealing manner.

## 5 Mapping Research Objectives with Outcomes

### Outcome 1

The above bar chart shows accuracy levels of various machine learning algorithms used for predicting the target variable and their consistencies in terms of accuracy. The x-axis (abscissa) of the graph depicts the algorithms used (Naïve Bayes, Regression, KNN, Decision Tree, and Random Forest), and the y-axis (ordinate) depicts the percentage of accuracy. The superior predictive capability of Regression is evident

**Fig. 2** Algorithm performance on artificially synthesized dataset using bar chart (Comparison of algorithms using accuracy)



from the height of the bar since it has the tallest bar as compared to the rest. The graph also portrays that the Naive Bayes and Random Forest algorithms exhibit moderate levels of accuracy, while KNN and Decision Tree algorithms show least levels of accuracy (Fig. 2).

**Outcome 2**

In the survey conducted on the website’s user-friendliness, people were asked to rate the website on a scale of 0 to 5; as a result, 32 responses were received out of which nine users rated it as 5, fourteen users rated it as 4, six users rated it as 3, three users rated it as 2, and not even a single user rated it as 0. Even though a few users found it to be less user-friendly which resulted in the rating of 2 or 3, most of the users were completely satisfied with the website’s user-friendliness by rating it with 4 or 5 which portrays that the website is mostly user-friendly. But the sample size of 32 respondents or users may not give us a clear idea about all the users.

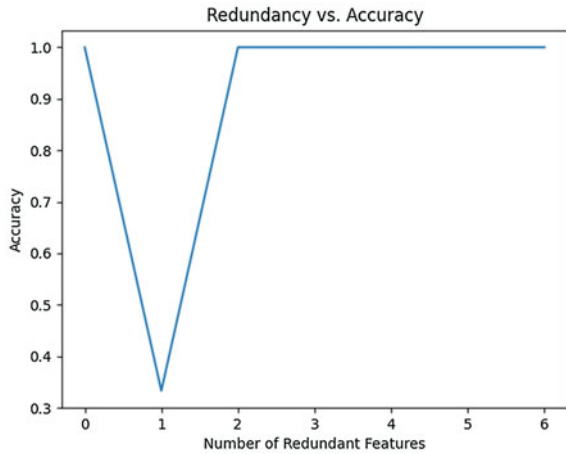
**Outcome 3**

Figure 3 shows that any kind of redundant or unnecessary data can be identified and removed by increasing the accuracy and reliability of the outcomes. With the help of the training and testing sets prepared by dividing the dataset, we can assess the performance of machine learning algorithms on raw and unexplored data; as a result, we can identify whether the model is underfitting or overfitting. The model can be optimized to provide robustness and maximum accuracy by iterating it through different split ratios and by evaluating the resulting model’s performance. Hence, cleaning and refining of the dataset leads to better understanding and decision-making, improved efficiency, and reduction in the risk of errors or bias in analysis.

**6 Result and Future Work**

The result of these outcomes tells that the Regression algorithm is suitable for predicting the target variable using feature datum. The algorithm consistently shows high accuracy in both Test [T1] and Test [T2]. So it will predict the accurate outcome. By utilizing this algorithm, business stater are informed decisions based on the predicted outcomes. Overall, the Regression algorithm provides valuable insights and provides better decisions for business starters. Now our careful consideration

**Fig. 3** Redundancy vs Accuracy



is needed for data sources, quality, machine learning algorithms, model interpretation, scalability, security, and privacy. Improvements in external data sources, real-time analysis, natural language processing, and data presentation can revolutionize decision-making processes. Limitations of implementing a machine learning model for business suggestions include limited and unrepresentative datasets, inappropriate model selection, overfitting, and interpretability. Future research can address these limitations by using larger, more representative datasets, employing additional machine learning algorithms, and considering other factors such as market movements and demographic data.

## References

1. Tamang MD, Shukla KV, Anwar S, Punhani R (2021) Improving business intelligence through machine learning algorithms. In: 2021 2nd international conference on intelligent engineering and management (ICIEM), London, United Kingdom, 2021, pp 63–68. <https://doi.org/10.1109/ICIEM51511.2021.9445344>
2. Tcukanova OA, Yarskaya AA and Torosyan AA (2022) Artificial intelligence as a new stage in the development of business intelligence systems. In: 2022 international conference on quality management, transport and information security, information technologies (IT&QM&IS), Saint Petersburg, Russian Federation, 2022, pp 315–318. <https://doi.org/10.1109/ITQMIS56172.2022.9976832>
3. Razmochaeva NV, Klionskiy DM, Chernokulsky VV (2018) The investigation of machine learning methods in the problem of automation of the sales management business-process. In: IEEE International conference “quality management, transport and information security, information technologies” (IT&QM&IS), St. Petersburg, Russia, pp 376–381. <https://doi.org/10.1109/ITMQIS.2018.8525008>
4. Atul Khedkar S, Shinde SK (2018) Customer review analytics for business intelligence. In: 2018 IEEE international conference on computational intelligence and computing research (ICCIC), Madurai, India, 2018, pp 1–5. <https://doi.org/10.1109/ICCIC.2018.8782305>

5. Ruhela S (2019) Thematic correlation of human cognition and artificial intelligence. In: 2019 Amity international conference on artificial intelligence (AICAI), Dubai, United Arab Emirates, 2019, pp 367–370. <https://doi.org/10.1109/AICAI.2019.8701337>
6. Sharma R, Srinath P (2018) Business intelligence using machine learning and data mining techniques - an analysis. In: 2018 second international conference on electronics, communication and aerospace technology (ICECA), Coimbatore, India, 2018, pp 1473–1478. <https://doi.org/10.1109/ICECA.2018.8474847>
7. Deng J, Li C, Zhou B (2019) Analysis of feature extraction methods of multimedia information resources based on unstructured database. In: 2019 international conference on intelligent transportation, big data & smart city (ICITBS), Changsha, China, 2019, pp 236–240. <https://doi.org/10.1109/ICITBS.2019.00063>
8. Lee Z-J, Lee C-Y, Chou S-T, Ma W-P, Ye F, Chen Z (2019) A distributed intelligent algorithm applied to imbalanced data. In: 2019 IEEE international conference of intelligent applied systems on engineering (ICIASE), Fuzhou, China, 2019, pp 136–138. <https://doi.org/10.1109/ICIASE45644.2019.9074009>
9. Sun W, Gao X (2018) The construction of undergraduate machine learning course in the artificial intelligence era. In: 2018 13th international conference on computer science & education (ICCSE), Colombo, Sri Lanka, 2018, pp 1–5. <https://doi.org/10.1109/ICCSE.2018.8468758>
10. Bhattacharya P (2018) Artificial intelligence in the boardroom: enabling ‘machines’ to ‘learn’ to make strategic business decisions. In: 2018 fifth HCT information technology trends (ITT), Dubai, United Arab Emirates, 2018, pp 170–174. <https://doi.org/10.1109/CTIT.2018.8649550>
11. Mohammed TA, Alhayli S, Albawi S, Deniz Duru A (2018) Intelligent database interface techniques using semantic coordination. In: 2018 1st international scientific conference of engineering sciences - 3rd scientific conference of engineering science (ISCES), Diyala, Iraq, 2018, pp 13–17. <https://doi.org/10.1109/ISCES.2018.8340520>
12. Rosa MF, Alturas B (2020) Business intelligence solution in project monitoring and control. In: 2020 15th Iberian conference on information systems and technologies (CISTI), Seville, Spain, 2020, pp 1–6. <https://doi.org/10.23919/CISTI49556.2020.9140916>
13. Pinheiro L, Oliveira P, Bernardino J, Pedrosa I (2020) Business intelligence applied in buildings energy efficiency. In: 2020 15th Iberian conference on information systems and technologies (CISTI), Seville, Spain, 2020, pp 1–6. <https://doi.org/10.23919/CISTI49556.2020.9141019>
14. Georgieva P (2022) Artificial intelligence for implementation of business model innovation in an industrial company. In: 2022 international conference on communications, information, electronic and energy systems (CIEES), Veliko Tarnovo, Bulgaria, 2022, pp 1–6. <https://doi.org/10.1109/CIEES55704.2022.9990677>
15. Ding S, Huang H, Zhao T, Fu X (2019) Estimating socioeconomic status via temporal-spatial mobility analysis - a case study of smart card data. In: 2019 28th international conference on computer communication and networks (ICCCN), Valencia, Spain, 2019, pp 1–9. <https://doi.org/10.1109/ICCCN.2019.8847051>
16. Wazurkar P, Bhadoria RS, Bajpai D (2017) Predictive analytics in data science for business intelligence solutions. In: 2017 7th international conference on communication systems and network technologies (CSNT), Nagpur, India, 2017, pp 367–370. <https://doi.org/10.1109/CSNT.2017.8418568>

17. Wannalai N, Mekruksavanich S (2019) The application of intelligent database for modern information management. In: 2019 joint international conference on digital arts, media and technology with ECTI Northern section conference on electrical, electronics, computer and telecommunications engineering (ECTI DAMT-NCON), Nan, Thailand, 2019, pp 105–108. <https://doi.org/10.1109/ECTI-NCON.2019.8692242>
18. Bao L, Le Y (2018) A spatial big data framework for maritime traffic data. In: 2018 3rd international conference on computational intelligence and applications (ICCIA), Hong Kong, China, 2018, pp 244–248. <https://doi.org/10.1109/ICCIA.2018.00054>
19. Delen D, Moscato G, Toma IL (2018) The impact of real-time business intelligence and advanced analytics on the behaviour of business decision makers. In: 2018 International conference on information management and processing (ICIMP), London, UK, 2018, pp 49–53. <https://doi.org/10.1109/ICIMP1.2018.8325840>
20. Vyawahare HR, Karde PP, Thakare VM (2018) A hybrid database approach using graph and relational database. In: 2018 international conference on research in intelligent and computing in engineering (RICE), San Salvador, El Salvador, 2018, pp 1–4. <https://doi.org/10.1109/RICE.2018.8509057>
21. Ong Y-S, Gupta A (2019) AIR5: five pillars of artificial intelligence research. *IEEE Trans Emerg Top Comput Intell* 3(5):411–415. <https://doi.org/10.1109/TETCI.2019.2928344>
22. Feng S (2019) Research on demand control of business intelligence. In: 2019 international conference on machine learning, big data and business intelligence (MLBDBI), Taiyuan, China, 2019, pp 292–295. <https://doi.org/10.1109/MLBDBI48998.2019.00065>
23. Shin H, Lee K, Kwon H-Y (2020) Performance evaluation of spatial data management systems using GeoSpark. In: 2020 IEEE international conference on big data and smart computing (BigComp), Busan, Korea (South), 2020, pp 197–200. <https://doi.org/10.1109/BigComp48618.2020.00-75>
24. Joseph RB, Lakshmi MB, Suresh S, Sunder R (2020) Innovative analysis of precision farming techniques with artificial intelligence. In: 2020 2nd international conference on innovative mechanisms for industry applications (ICIMIA), Bangalore, India, 2020, pp 353–358. <https://doi.org/10.1109/ICIMIA48430.2020.9074937>
25. Hashemi M, Karimi HA (2020) Weighted machine learning for spatial-temporal data. *IEEE J Sel Top Appl Earth Obs Remote Sens* 13:3066–3082. <https://doi.org/10.1109/JSTARS.2020.2995834>



# Blockchain Technology for Secure Smart Grid Access Control



Vijendra Kumar Maurya, Rakshit Kothari, Payal Sachdev,  
and Narendra Singh Rathore

**Abstract** The use of smart grid technologies, in the energy sector has brought about upgrade, such as high efficiency, lower operating costs and better energy management. However, it has also established security aspects. Safeguarding the smart grid is of importance due to its role as essential infrastructure. The innovative potential of blockchain holds promise in enhancing the security of the grid. This paper aims to explore how blockchain technology can be utilized for protecting the grid. It delves into the security issues associated with grids and investigates how blockchain can address them. Additionally, it provides an analysis of studies on blockchain and its application, in grid protection while considering the pros and cons of utilizing blockchain based solutions.

**Keywords** Smart grid · Blockchain · Renewable energy · Distributed ledger · Phishing

## 1 Introduction

Blockchain technology is a decentralized database that has industry specific capabilities in different dimensions. It has the capacity to store and control transactions. Due to its immutable, safe and transparent qualities. It can be utilized to any type of multistep layout based program needing security, monitoring and visible. By eliminating the need for a middleman and connecting the buyer and the seller directly, blockchain technology lowers the cost of transactions and fees. An impermeable data record that is accessible to all members of the network can be created using

---

V. K. Maurya

Associate Professor, Department of Computer Science and Engineering, Geetanjali Institute of Technical Studies, Dabok, Udaipur, India

R. Kothari (✉) · P. Sachdev

Assistant Professor, Department of Computer Science and Engineering, Geetanjali Institute of Technical Studies, Dabok, Udaipur, India

e-mail: [rakshit007kothari@gmail.com](mailto:rakshit007kothari@gmail.com)

N. S. Rathore

Campus Director, Geetanjali Institute of Technical Studies, Dabok, Udaipur, India

this technology, resulting in a reliable, strong, and open network [2]. Blockchain technology offers a wide range of applications in the production, delivery, transmission, and usage phases that can help with present difficulties in the power sector. An improved electricity transmission system called the “smart grid” oversees and regulates the supply of electrical energy from thermal power plants to consumers. The smart grid uses advanced sensor, communication, and control technologies to increase the energy system’s dependability, efficiency, and environmental responsibility [7]. The capacity to gather and analyze statistics in actual time is one of the fundamental components of the smart grid, enabling utilities to keep an eye on the grid’s operation and spot possible problems before they become serious ones. Smart meters are an essential part of the smart grid because they give utilities detailed data on energy usage trends and help them better balance supply and demand for energy. Additionally, utilities may remotely manage and monitor the flow of power thanks to the smart grid’s sophisticated communications and control systems [1]. These innovations include sophisticated metering infrastructure, which enables communication in both directions between utility and consumers, and transmission automation systems, which may automatically redirect electricity in the case of an outage. The smart grid’s usage of energy via renewable resources like wind and sunshine is a crucial component. The effective incorporation of renewable energy sources into the electrical power system may be facilitated by the smart grid, which will reduce emissions of greenhouse gases and increase the reliability of the energy industry. A vital component of the grid protection of the energy system is responsible for identifying and correcting flaws in different machines, such as engines, transformers, and cables [9]. Taking into account the electronic layer, the design of power systems mechanization usually uses a centralized stability controller and consolidated system of communication to collect data and send indications for regulation and safety [13].

Figure 1 illustrates some of the numerous ways that blockchain technology is being used in smart grid systems. The smart grid is a substantial improvement in the way power is delivered since it offers a more sustainable, dependable, and effective way of handling and distributing electricity [24]. The Smart grid system is seen in Fig. 2. The integration of cutting-edge security measures is essential to guaranteeing the reliability and safety of the power system, but the smart grid also offers new security concerns. Digital information technology is used by the smart grid, an improved electrical power system, to regulate, manage, transmit, control and monitor energy. It incorporates cutting-edge detecting, communication, and control technology to boost the energy grid’s effectiveness, dependability, and sustainability. The smart grid, however, also creates fresh security difficulties. Distribution and production of protection systems are regarded as critical components of the modern smart grid ecosystem because they may isolate problematic segments and sustain the operation of vital loads. Table 1 compares the traditional electricity system to the smart grid using blockchain technology [13, 21].

## 2 Component of Smart Grids

The smart grid consists of a number of parts that interact to enhance the effectiveness, dependability, and security of the electrical system. Here are a few of the most important elements of the smart grid.

### 2.1 Smart Meters

Smart meters are technological devices that monitor and record real-time energy usage. Smart meters for SSE are shown in Fig. 3. The utility and the client may communicate with each other in two directions thanks to them, which are utilized to

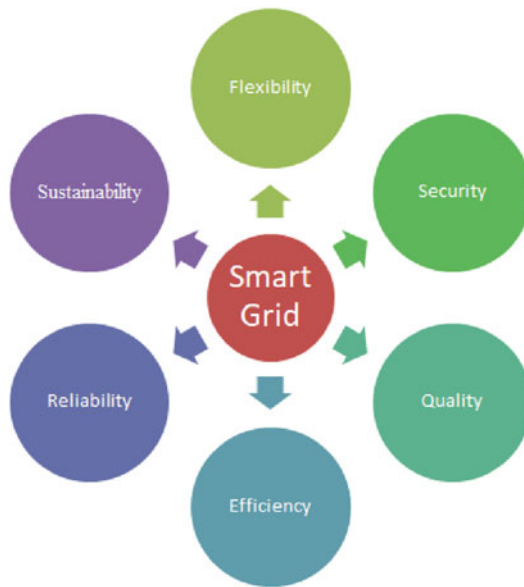


Fig. 1 Smart grid applications in blockchain technology

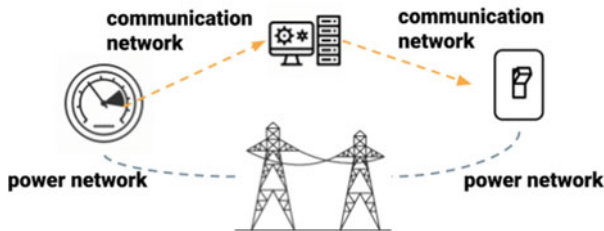


Fig. 2 Smart grid system

replace conventional mechanical meters. Consumers may measure their energy use and modify how they act to save money and lessen their environmental impact, and this enables services to monitor and manage power usage continuously.

### 2.2 Phasor Measurement Units (PMUs)

PMUs are advanced sensors that instantly identify the electrical signals of the power generating network and provide accurate and live information in the system. Grid operators may utilize these data to speed up and effectively identify and resolve the issues like voltage fluctuation and power outages.

**Table 1** Comparing conventional grid and smart grid

S. no.	Features	Conventional grid	Smart grid
1	Energy generation	Centralized	Distributed
2	Energy distribution	Unidirectional	Bidirectional
3	Energy storage	Limited	Advanced
4	Security	Basic	Advanced
5	Communication	Basic	Advanced
6	Customer control	Basic	Advanced
7	Renewable unification	Limited	Advanced
8	Fault detection	Manual	Automated
9	Restoration	Manual	Automated
10	Metering	Manual	Automated

**Fig. 3** SSE—Smart meter.

Source sse.co.uk



### 2.3 Sensors

The smart grid uses sensors to track a variety of electrical system parameters, such as moisture, humidity, temperature, and voltage levels. Grid operators may use these sensors to collect crucial data that will help them spot possible hazards early stage and action taken accordingly.

### 2.4 Information Transfer and Distribution

The smart grid relies on advanced communication and networking technologies to transfer information between various components associated with the grid. It involves fiber optic cables, wireless networks, and electronics communication methods which enable grid operators to keep aware with situation and regulate the grid accordingly [15, 23]. The smart grid is an integrated system of hardware, software and communication technologies that work together to improve the efficiency, reliability and security of the electricity grid. By adopting advanced sensors, communication technologies and control systems, the smart grid has the potential to revolutionize the way we produce, distribute and consume electricity according to demands.

## 3 Security Challenges of the Smart Grids

Smart grid security challenges include data privacy, cyber security and operational security. These challenges arise from complex and interconnected nature of the smart grid which creates vulnerabilities that can be exploited by malicious actors [3]. Data privacy is a critical concern in the smart grid because it involves sensitive customer information, including consumption patterns, billing information, and personal data. There are some issues in smart grids as shown in Fig. 4.

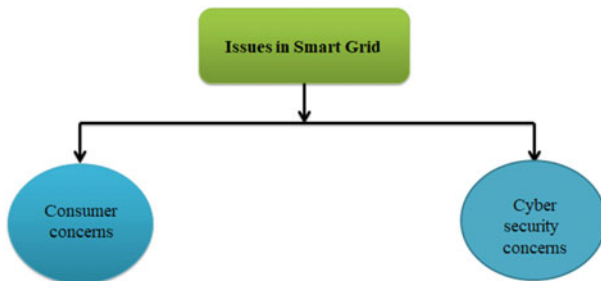


Fig. 4 Types of issues in smart grid

Cyber security is also a crucial concern given the increasing number of cyber-attacks aiming critical infrastructure including the smart grid [19]. Operational security is a challenge because of the complexity of the smart grid which creates numerous opportunities for human error and technical failure. There is some security risk that may occur in smart grid.

### ***3.1 Phishing***

Phishing attacks in smart grids can target various stakeholders including utility employees, related customers and third party vendors. For ex. a hacker can send a phishing message to a consumer that looks to be from an authorized party such as a manager or a vendor, requesting private data or clicking on a link that could be fraud [9, 16]. In the same manner customers may receive phishing emails that seem to be from the hacker asking them to provide personal information or click on a link to pay their bills. In the smart grid, phishing contains a huge security issue. It is a type of attack involving social engineering where an attacker delivers spam emails or text messages in an attempt to trick people into disclosing sensitive information such as login credentials or financial information. Phishing attempts can be harmful for smart grid safety by allowing attackers to obtain access to vital systems or collect crucial information.

In the smart grid, phishing poses a huge security issue. Phishing is a type of attack involving social engineering whereby an attacker delivers bogus emails or text messages in an attempt to trick people into disclosing sensitive information such as login credentials or financial information. Phishing attempts can threaten smart grid safety by allowing attackers to obtain access to vital systems or collect crucial information.

### ***3.2 Malware Spreading***

The integrity, reliability, and security of the smart grid are all at danger due to a large security risk [5, 18]. Spyware is malicious software that infects computers and does harm such as gathering private information or disrupting crucial services. Various attack vectors, including as email attachments, infected USB drives, and software flaws, can propagate malware in the smart grid. Once malware has compromised a smart grid system, it may quickly propagate to other systems and devices. Additionally, malware may seriously harm smart grid components like SCADA systems and smart meters by causing them to malfunction or stop working completely. This might lead to equipment damage, power outages, and other interruptions that could have detrimental effects on the grid and its users [20].

### ***3.3 Denial-of-Service (DoS)***

DoS attacks pose a significant security risk to smart grids. A Distributed Denial of Service (DDoS) attack is a cyber-attack in which hackers attempt to overwhelm or disrupt a system, network, or service by using overloaded or sent traffic. Fraudulent packets. In smart grids, DoS attacks can disrupt the current flow, causing blackouts, equipment damage, and other security issues [14]. DoS attacks can target various components of the smart grid, including SCADA systems, communication networks, and smart meters. For example, an attacker could flood a communication network with traffic, causing it to become overloaded and unable to transmit data. Likewise, an attacker can send a large number of malicious packets to a smart meter, causing it to stop working or become unresponsive [22, 26].

### ***3.4 Man in the Middle***

Man in the Middle attacks are security threat in the smart grids. In a Man in middle attack, an attacker intercepts and modifies communication between two parties without knowing either party communication tampered. In the smart grids, Man in middle attacks can allow an attacker to modify data and commands send between smart devices, control systems and other network elements used in systems. This can result in equipment damage the power breakdown and unauthorized access to sensitive information. One common form of attack in the smart grid is replay attack. In replay attack attacker intercepts a legitimate message then records it and then sends the same message again at a later time. Due to this the system will perform an action such as turning off a critical component of the grid [17]. Another form of this attack in the smart grid is injection attack. In injection attack an attacker insert malicious code or data into a legitimate communication stream. This can allow the attacker to take control of a device or system and steal sensitive information from the device.

## **4 Role of Blockchain Embedded with Smart Grid**

The blockchain provide mechanism to the previously identified hurdles. It offers management of data, a mechanism, and regulation of cost and technology issues, including transaction amount between different networks. It improves openness among stockholder while maintaining data confidentiality, security and safety. It also makes simpler energy demand as well as supply chain having fewer losses. It helps in grid monitoring of operation from several energy sources every time, with coordination between energy owners. In a smarts grid, the blockchain additionally controls voltage and frequency. We can calculate the quantity of energy

produced and utilized using the technology known as block chain. It also handles smart grid's safety, can't be changed, can be transparent, and decentralization are three main benefits of blockchain in smart grid security [10]. Blockchain creates unbreakable and unchangeable record of every single transaction, allowing for secure data tracking and verification [25]. The increased connectivity and interdependence of smart grid components increase the attack surface for malicious actors, making it susceptible to cyber-attack. To address these security challenges there is a need for security solutions which can provide secure and reliable operation of the smart grid. One promising technology that has the potential to improve the security of the smart grid is blockchain. Block chain is a distributed ledger system that allows for safe, translucent and impermeable transactions. Blockchain offers a safe and decentralized framework that can assist address many of the smart grid's safety concerns. The openness of block chain additionally renders it simpler to identify and thwart fraudulent activity, boosting the smart grid's safety as a whole. Finally, the decentralized structure of blockchain removes the demand for a governing body, lowering the danger of one point of breakdown.

## 5 Existing Research on Blockchain and Smart Grid Security and Solution

To decentralize grid functioning, distributed automated drivers are utilized. The data was collected and monitored using the Phasor Management Unit (PMU), Remote Terminal Unit (RTU), Supervisory control and data acquisition (SCADA), and smart meter [4, 6, 11]. It is difficult to manage and operate distributed energy resources. More effort is required to improve cooperation between decentralized and centralized stack holders. The SCADA unit collects data from distant terminals and transmits it in simple text to the primary control center. This centralized data gathering and storing system is extremely vulnerable to cyber assault. As result, security is one of the most significant and hardest concern confronting the present smart grid. Many researches have been conducted to investigate the application of block chain technology in smart grid safety [8, 12]. Other studies have focused on using block chain for secure and reliable communication in the smart grid. Some studies have also explored the use of block chain for secure billing and payment systems in the smart grid. Overall, existing research has demonstrated the potential of block chain in improving the security of the smart grid. To mitigate the risk of phishing attacks in the smart grid, utilities should implement robust security measures, such as user education and awareness programs, two-factor authentication, and email filters. User education and awareness programs can help employees and customers identify phishing emails and avoid falling prey to these attacks. Figure 5 represents the average throughput versus Transactions Per Second (TPS) in Smart Grid System.

Two-factor authentication can add an additional layer of security by requesting users to provide a second form of identification in addition to their login credentials,



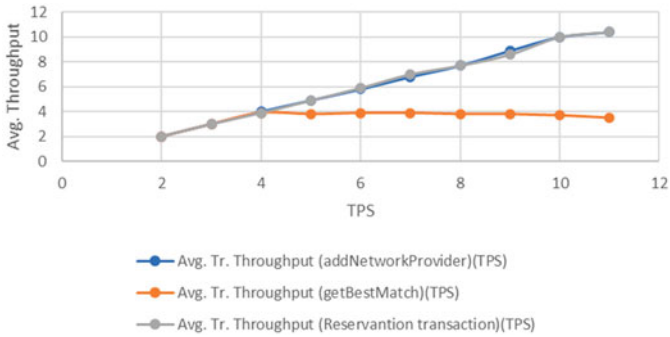


Fig. 5 Average throughput versus TPS in smart grid using blockchain

such as a digital token or an electronic fingerprint scan. Email filtering can also assist detect and prevent emails that are phishing from reaching users to mitigate the risk of eavesdropping and traffic analysis in the smart grid, utilities should implement robust security measures, such as encryption and secure communication protocols. Encryption can help protect sensitive data by scrambling the data so that it is unreadable without the correct decryption key. Secure communication protocols, such as HTTPS or SSL, can also help protect smart grid communications by encrypting data transmissions and authenticating users. Utilities should install comprehensive security measurements, such as segmenting the network, access limits, and systems that detect and prevent intrusions, to reduce the danger of denial of service attacks in the context of the smart grid. Network segmentation can help isolate critical systems from less secure systems reducing the impact of DOS attack. Access controls can limit user access to critical systems and prevent unauthorized user from introducing a DoS attack into grid. Intrusion detection and prevention systems can help detect and block DoS attacks before they can cause significant damage [27]. In addition to these measures, utilities should also prioritize user education and awareness programs. User education and awareness programs can help employees and customers identify DoS attacks and take appropriate action to prevent them. For example, employees can be trained to recognize suspicious network traffic and report it to the appropriate authorities. To prevent MitM attacks in the smart grid, encryption and authentication are critical. Encryption ensures that data is protected from interception and modification, while authentication ensures that only authorized devices and users can access the system. Additionally, the implementation of secure communication protocols such as SSL/TLS can also prevent Man in middle attacks. It is important for organizations in the energy sector to regularly assess their systems’ vulnerability to MitM attacks and implement appropriate security measures to protect against them.

## 6 Purposed Methodology to Avoid Security Risk

Blockchain technology offers several potential methodologies to enhance security and mitigate risks in the smart grid. Here is a proposed methodology leveraging blockchain to address security risks.

**Distributed Ledger:** Implement a distributed ledger using blockchain technology to create a decentralized and tamper-proof record of transactions and data exchanges within the smart grid. This ensures transparency and immutability, reducing the risk of unauthorized modifications or data tampering.

**Identity and Access Management:** Utilize blockchain for identity and access management (IAM) to securely authenticate and authorize devices, users, and service providers within the smart grid. Blockchain-based IAM can enhance security by eliminating single points of failure and reducing the risk of identity theft or unauthorized access.

**Data Integrity and Verification:** Leverage blockchain's cryptographic features to ensure data integrity and verification throughout the smart grid. By storing data hashes on the blockchain, any unauthorized changes to data can be detected, maintaining the integrity of critical information and preventing malicious activities.

**Smart Contracts:** Utilize smart contracts, which are self-executing contracts with predefined rules and conditions, to automate and secure interactions between different entities in the smart grid. Smart contracts enable secure and tamper-proof execution of transactions, ensuring that predefined conditions are met before any actions are taken.

**Energy Trading and Billing:** Implement blockchain-based energy trading platforms that enable peer-to-peer energy transactions, ensuring transparency and trust among participants. Smart contracts can facilitate secure and automated energy trading, eliminating the need for intermediaries and reducing the risk of fraud or billing discrepancies.

**Cyber Threat Detection and Response:** Utilize blockchain's decentralized nature to enhance cyber threat detection and response mechanisms in the smart grid. Analyzing security related data from multiple nodes in the blockchain network, anomalies and potential threats can be identified effectively, enabling timely responses and mitigation measures.

## 7 Conclusion

The smart grids are a critical electrical infrastructure that require high level of security that measures the malicious attacks. The use of blockchain protocol has an opportunity to improve smart grid security by using a tamper-proof and decentralize network. Current research has showcased the potential of block chain in addressing some of the security challenges facing the smart grid. The use of block chain algorithms in smart grid safety is an exciting field of research that has the probability

to enhance the smart grid's reliability, safety, and efficiency along with security. As smart grids infrastructures continue growing leap and bounce, so there is need of innovative security solutions. Future research should focus on more addressing the implacability issues of block chain technology as well as exploring new and latest use cases for block chain in smart grid security systems.

## References

1. Ahmad T, Zhang D, Huang C, Zhang H, Dai N, Song Y, Chen H (2021) Artificial intelligence in sustainable energy industry: status quo, challenges and opportunities. *J Clean Prod* 289:125834
2. Ahmed M, Zheng Y, Amine A, Fathiannasab H, Chen Z (2021) The role of artificial intelligence in the mass adoption of electric vehicles. *Joule* 5(9):2296–2322
3. Boneh D, Boyen X (2004) Efficient selective-id secure identity-based encryption without random oracles. In: 34th annual international conference on the theory and applications of cryptographic techniques (EUROCRYPT), Springer, Switzerland, pp 223–238
4. Bose BK (2017) Artificial intelligence techniques in smart grid and renewable energy systems—some example applications. *Proc IEEE* 105(11):2262–2273
5. Chen C, Chen J, Lim HW, Zhang Z, Feng D, Ling S, Wang H (2013) Fully secure attribute-based systems with short ciphertexts/signatures and threshold access structures. In: *CT-RSA, Lecture notes in computer science*, vol 7779, pp 50–67
6. Cheung L, Newport CC (2007) Provably secure ciphertext policy abe. In: *ACM conference on computer and communications security*, pp 456–465
7. Delerablée C (2007) Identity-based broadcast encryption with constant size ciphertexts and private keys. *Asiacrypt* 4833:200–215
8. Foster I, Kesselman C, Tuecke S (2001) The anatomy of the grid: enabling scalable virtual organizations. *Int J Supercomput Appl* 15(3):200–222
9. Goyal V, Pandey O, Sahai A, Waters B (2006) Attribute-based encryption for fine-grained access control of encrypted data. In: Juels A, Wright RN, di Vimercati SDC (eds) *ACM conference on computer and communication security*. ACM, pp 89–98
10. Guo F, Mu Y, Susilo W, Wong DS, Varadharajan V (2014) CP-ABE with constant-size keys for lightweight devices. *IEEE Trans Inf Forensics Secur* 9(5):763–771
11. Guo F, Mu Y, Chen Z (2007) Identity-based encryption: How to decrypt multiple ciphertexts using a single decryption key. In: *Proceedings pairing*, vol 4575, pp 392–406
12. Guo F, Mu Y, Chen Z, Xu L (2007) Multi-identity single-key decryption without random oracles. In: *Proceedings Inscrypt*, vol 4990, pp 384–398
13. Guo F, Mu Y, Susilo W (2012) Identity-based traitor tracing with short private key and short ciphertext. In: *Proceedings ESORICS*, vol 7459, pp 609–626
14. Guo H, Xu C, Li Z, Yao Y, Mu Y (2013) Efficient and dynamic key management for multiple identities in identity-based systems. *Inf Sci* 221:579–590
15. Khaleel M, Abulifa SA, Abulifa AA (2023) Artificial intelligent techniques for identifying the cause of disturbances in the power grid. *Brill: Res Artif Intell* 3(1):19–31
16. Khan F, Kothari R, Patel M (2022) Advancements in blockchain technology with the use of quantum blockchain and non-fungible tokens. In: *Advancements in quantum blockchain with real-time applications*. IGI Global, pp 199–225
17. Khan F, Kothari R, Patel M, Banoth N (2022) Enhancing non-fungible tokens for the evolution of blockchain technology. In: *2022 international conference on sustainable computing and data communication systems (Icscds)*. IEEE, pp 1148–1153
18. Kim SK, Huh JH (2018) A study on the improvement of smart grid security performance and blockchain smart grid perspective. *Energies* 11(8):1973

19. Kothari R, Choudhary N, Jain K (2021) CP-ABE scheme with decryption keys of constant size using ECC with expressive threshold access structure. In *Emerging trends in data driven computing and communications: proceedings of DDCT 2021*. Springer, Singapore, pp 15–36
20. Lewko AB, Okamoto T, Sahai A, Takashima K, Waters B (2010) Fully secure functional encryption: Attribute-based encryption and (hierarchical) inner product encryption. In: Gilbert H (ed) *Eurocrypt*. Lecture notes in computer science, vol 6110, pp 62–91
21. Lo KL, Zakaria Z (2004) Electricity consumer classification using artificial intelligence. In: *39th International universities power engineering conference*. UPEC, vol 1. IEEE, pp 443–447
22. Musleh AS, Yao G, Muyeen SM (2019) Blockchain applications in smart grid-review and frameworks. *IEEE Access* 7:86746–86757
23. Ostrovsky R, Sahai A, Waters B (2007) Attribute-based encryption with non-monotonic access structures. In: *Proceedings ACM conference on computer and communication security*, pp 195–203
24. Pilkington M (2016) *Blockchain technology: principles and applications*. In: *Research handbook on digital transformations*. Edward Elgar Publishing, pp 225–253
25. Richter L, Lehna M, Marchand S, Scholz C, Dreher A, Klaiber S, Lenk S (2022) Artificial intelligence for electricity supply chain automation. *Renew Sustain Energy Rev* 163:112459
26. Vyas K, Jain G, Maurya VK, Mehra A (2016) Comparative analysis of MCML compressor with and without concept of sleep transistor. In *Proceedings of international conference on ICT for sustainable development: ICT4SD, Vol 1*. Springer, Singapore, pp 251–260
27. Yapa C, de Alwis C, Liyanage M, Ekanayake J (2021) Survey on blockchain for future smart grids: technical aspects, applications, integration challenges and future research. *Energy Rep* 7:6530–6564

# Tie-Line Power Frequency Stability Control of an Interconnected Hybrid Power System Using a Virtual Inertia Controller by the GWO Algorithm



R. Aravinda Raj, P. Malathy, D. Manivasagan, N. Mayilvaganan, and S. Mohamed Basith

**Abstract** Recently, several significant growth in the perception of Renewable Energy Sources (RES) in power systems, has led to a drop in the complete system inertia. The tie-line power movement and frequency stability control are two important aspects of power system operation. In this paper, a virtual inertia controller is proposed for a hybrid interconnected power system to enhance the frequency stability and control the tie-line power flow. The VIC follows the inertia of synchronous generators using power electronics converters. The controller calculates the power imbalance concerning the generation and consumption in the power system and provides a proportional response to maintain the system frequency within the desired range. The Grey Wolf Optimization (GWO) algorithm can be used to enhance the controller parameters, such as the gain and time constant, to minimize the frequency deviation in the power system. The proposed controller is designed to regulate the power output of renewable energy sources and provide a frequency response during a disturbance. The model result demonstrates that the suggested controller enhances the frequency stability and reduces the power fluctuations caused by the RES.

**Keywords** Tie-line · Solar · Wind · Diesel generator · Synchronous generator · Virtual inertia controller · Grey Wolf Optimization (GWO) · Frequency control

## 1 Introduction

This exploration proposes a virtual synchronous generator (VSG) control technique for recurrence strength control in environmentally friendly power frameworks. The VSG is a power converter with a connection to the grid that serves as a synchronous

---

R. A. Raj (✉) · D. Manivasagan · N. Mayilvaganan · S. M. Basith  
Vaigai College of Engineering, Madurai, Tamil Nadu, India  
e-mail: [aravindvceeee@gmail.com](mailto:aravindvceeee@gmail.com)

P. Malathy  
PSNA College of Engineering and Technology, Dindigul, Tamil Nadu, India

generator and gives the system inertia [1]. A virtual dormancy regulator will be utilized to keep up with recurrence dependability in power frameworks with a high entrance of environmentally friendly power sources. The regulator depends on the idea of virtual dormancy and can reproduce the way of behaving of simultaneous generators [2–18]. The VIC-based power flow management plan for hybrid AC/DC microgrids. The regulator is intended to give recurrence dependability and increment the powerful reaction of the microgrid [3]. The system's operating conditions are used by the VIC to adjust the controller gains in real time through a feedback loop. They assess the presentation of the proposed regulator utilizing recreations on a two-region power framework and exhibit that it further develops recurrence soundness contrasted with customary control strategies [1, 19–24].

An interconnected power framework is an organization of force producing units and burdens that are connected together through transmission lines. In such a framework, it is essential to keep up with recurrence strength, which alludes to the capacity of the framework to keep a consistent and steady recurrence notwithstanding changes in load interest or age. Attach line power alludes to the power that is traded between two interconnected power frameworks through a tie-line. Tie-line power is utilized to adjust the power age and burden interest between the two frameworks. On the off chance that the tie-line power isn't as expected controlled, it can prompt recurrence shakiness in the two frameworks. A VIC can be used to improve frequency stability. The essential idea of a virtual idleness regulator is to give extra inactivity to the framework by impersonating the way of behaving of a conventional mechanical generator. This is accomplished by simulating the synchronous generator's rotational inertia with a power electronic converter. In order to maintain a constant frequency, the VIC adjusts the power flow between the hybrid power systems and monitors the power of the tie-lines. During transient conditions, such as sudden shifts in generator output or load demand, the VIC can improve frequency stability by providing the system with additional inertia.

## 2 Related Work

Ahmed et al. proposed a financially savvy control method for a half breed energy framework that consolidates sunlight based photovoltaic and wind turbine innovations. The control procedure empowers the most extreme power point following from the photovoltaic cluster and wind turbine, paying little mind to shifting climatic circumstances, without the requirement for estimating the irradiance or wind speed [25]. Yang et al. presented an ideal booking approach for a breeze sun based capacity age framework. In order to optimize the scheduling of the system components, this strategy takes into account the relationship that exists between load, photovoltaic output, and wind power [26]. Yu et al. directed a concentrate on the construction plan and control arrangement of a 3 KW wind and sun oriented half-and-half power framework for 3G base stations. The mixture framework was executed to save power and guarantee the ceaseless power supply to 3G base stations [27]. Mendez et al.

carried out a half breed breeze sunlight based power age framework to meet the electric energy prerequisites of little power beneficiaries at two research centers. The framework used a 600 W 3-stage long-lasting magnet simultaneous generator (PMSG)- based breeze power age framework and a sun oriented power age framework comprising of three 190W mono precious stone sun powered chargers [28]. Vasant et al. proposed a framework pointed toward diminishing the power interest on regular power age sources by enhancing the usage of normal assets. The system's primary goal is to generate electricity from renewable energy sources [29].

Chen et al. introduced a wave and wind-based multi-energy hybrid power system to enhance the quality and stability of the power supply. The framework joins wave energy and wind energy to lay out a solid and effective power age framework [30]. Habibzadeh et al. planned circuit and framework setups for energy gatherers that use supercapacitors as energy cushions and half-and-half sunlight based and wind power hotspots for power supply. This plan wipes out the requirement for enormous supercapacitor support by utilizing the correlative idea of sunlight based and wind power sources [31]. Sree et al. presented the use of a Distributed Power Flow Controller to implement a solar-wind connected system without the need for custom power devices. The framework's exhibition was approved through reproductions utilizing MATLAB/SIMULINK programming [32]. Kumar and co. carried out a comparison of MPPT controllers for wind power and photovoltaic systems in a hybrid renewable energy system. They looked at the exhibition of regulators fabricated utilizing Bother and Notice (P&O) calculation for PV frameworks and Slope Climbing Search (HCS) calculation for wind power frameworks, as well as regulators executed utilizing Fluffy Rationale Control (FLC) [33]. Zhang et al. fostered a control framework for canny battery charging and releasing cycles in a cross breed sun based and wind power framework. Software and a PIC16F877 signal chip computer were used in the control system, and a hardware design scheme was also provided [34].

## 3 Power System Modeling

### 3.1 Two-Area Power System

It is typically done using differential equations that label the dynamics of the system [35–37]. Here is an example of such a model.

#### 3.1.1 Assumptions

Each area has one synchronous generator related to a load.

- The power system is connected done a tie-line.
- The generators are supposed to be operating in droop control mode.
- The virtual inertia controller is applied at the tie-line.

There are individual loads and a generator connected to a turbine in every area. The turbine is connected to the grid and can generate or consume power based on the load demand. The VIC is added to provide frequency stability control. The VIC works by simulating the effects of inertia on the grid. When there is an unexpected change in load demand or a generator goes offline, the virtual inertia controller responds by injecting or absorbing power to maintain a stable frequency. The amount of power injected or absorbed is based on the VIC constant that can be tuned to attain the frequency stability in the desired level.

The model can be further developed by including additional components such as governors, excitation systems, and transmission lines. However, this basic model captures the essential dynamics and provides a framework for evaluating and controlling frequency stability.

### 3.1.2 Modeling

For each area, we can represent the synchronous generator and the load as a single bus with a phase angle and magnitude voltage.

- The power output of the generator is given by the droop control equation:

$$P = P_{max} - k_p(w - w_0) \quad (1)$$

- where  $P$  indicates output of real power,  $P_{max}$  denotes output of maximum power,  $k_p$  represents droop constant,  $w$  denotes generator frequency, and  $w_0$  is the nominal frequency. The load in each area is represented as a constant power load, i.e., the power consumed is constant irrespective of the frequency.
- The tie-line between the two areas is represented as a transmission line with a resistance and reactance.
- The VIC is presented at the tie-line and provides an additional damping effect to increase the system's stability.
- The VIC's control strategy is based on the frequency deviation across the tie-line. When there is a frequency deviation, the virtual inertia controller injects a power signal into the system to counteract the deviation. The injected power signal is related to the frequency variations and the virtual inertia constant.
- The VIC's mathematical model can be represented as follows:

$$\Delta P = k_{vi}(\Delta w) \quad (2)$$

where,  $\Delta P$  is the injected power,  $k_{vi}$  is the VIC constant, and  $\Delta w$  is the frequency deviation across the tie-line.

With these assumptions and modeling, we can simulate the two-area power system with tie-line power frequency stability control using virtual inertia controller. Each area has a load and a generator connected to a turbine. The turbine is connected to the grid and can generate or consume power based on the load demand. The VIC is added to provide frequency stability control.



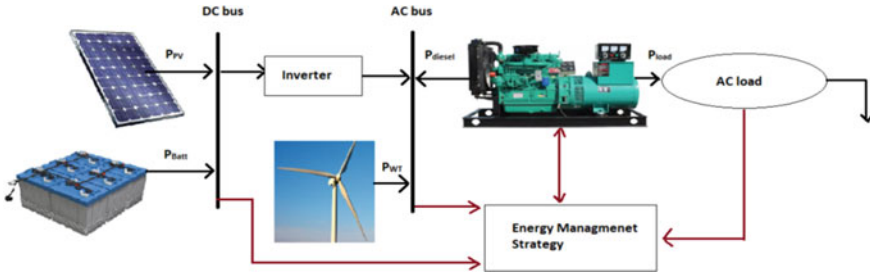


Fig. 1 Hybrid power system

### 3.2 Hybrid System

In Fig. 1. Hybrid interconnected power systems are complicated systems that combine wind turbines, solar panels, conventional power plants (Diesel), and other types of power sources. Attributable to the RES’s irregular nature, cross breed interconnected power frameworks can encounter vacillations in power yield, which can prompt unsteadiness in the framework’s recurrence. The system’s frequency stability can be enhanced and these fluctuations reduced with the help of virtual inertia control.

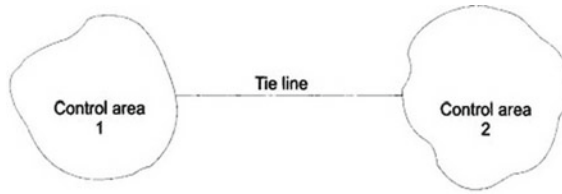
### 3.3 Tie-Line Power Flow

In a power system, a tie-line refers to the transmission line that connects two or more regions or areas of the power grid. Tie-lines are used to transfer power from one area to another to maintain balance and stability. When there is a power generation imbalance and consumption among two areas connected by a tie-line, the power flow on the tie-line changes, which can impact the frequency stability.

To avoid this, tie-line power frequency stability control is implemented to ensure that the frequency remains stable and within acceptable limits. One approach to tie-line power frequency stability control is the use of virtual inertia controllers. These controllers mimic the synchronous generator’s behavior by injecting a synthetic inertia response into the power system. This helps to stabilize the frequency and power in Fig. 2.

Let us consider the following two-area system variables:

- $P_1$  and  $P_2$ : active power generated in regions 1 and 2 respectively
- $Q_1$  and  $Q_2$ : reactive power generated in regions 1 and 2 respectively
- $V_1$  and  $V_2$ : voltage in regions 1 and 2 respectively
- $\delta_1$  and  $\delta_2$ : phase angle in regions 1 and 2 respectively



**Fig. 2** Tie-line control

**Step: 1** Determine the solar and wind power generation:

Obtain the real power output ( $P_{solar}$ ) of the solar generation system in watts.

Obtain the real power output ( $P_{wind}$ ) of the wind generation system in watts.

**Step: 2** Calculate the total renewable power generation:

Add the solar and wind power outputs to obtain the total renewable power generation ( $P_{renewable}$ ) in watts:

$$P_{renewable} = P_{solar} + P_{wind} \tag{3}$$

**Step: 3** Determine the diesel generator power output:

Obtain the real power output ( $P_{diesel}$ ) of the diesel generator in watts.

**Step: 4** Calculate the power flow on the tie-line:

The power flow on the tie-line represents the net power transfer between the renewable sources and the diesel generator.

If  $P_{renewable}$  is greater than  $P_{diesel}$ , the excess power flows from the renewable sources to the diesel generator. Power flow on the tie-line,

$$P_{tie\ line} = P_{renewable} - P_{diesel} \tag{4}$$

If  $P_{renewable}$  is less than  $P_{diesel}$ , the diesel generator compensates for the power deficit.

Power flow on the tie-line,

$$P_{tie\ line} = -(P_{diesel} - P_{renewable}) \tag{5}$$

### 3.4 Frequency Control

The not entirely set in stone by the equilibrium among the stockpile of force from generators and the interest for power from buyers. The frequency can turn to its

nominal value if there is an imbalance in the demand for power, which can result in voltage instability and system collapse. Thus, recurrence control is fundamental to guarantee the steadiness and dependability of the power framework. By adjusting the generators' output in real time to meet the demand for power, frequency control is achieved. This is finished through a blend of programmed control frameworks and human administrators who screen the framework and make manual changes when important. A portion of the vital parts of recurrence control incorporates lead representatives, programmed age control (AGC), and load shedding.

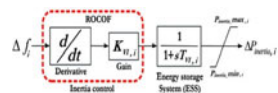
Lead representatives are gadgets that manage the speed of generators by controlling how much fuel or water is provided to the turbines. AGC is a modernized control framework that consistently screens the recurrence and changes the result of the generators as needed. Load shedding is a final hotel measure that includes removing capacity to specific regions of the network to keep up with the general steadiness of the framework.

### 3.5 VIC

Power systems employ a VIC control strategy to match the inertial response of conventional synchronous generators. The ability of synchronous generators in a power system to absorb or supply power in response to changes in the frequency of the system is known as the inertial response. This contributes to the stability of the system. VICs are intended to resolve this issue by giving a VIC that imitates the coordinated generator conduct. This is accomplished by estimating the recurrence varieties in the framework and utilizing this data to compute the expected power reaction. The VIC then, at that point, conveys messages to the RES inverters to change their result power appropriately to give the vital reaction. The renewable energy sources' power output is adjusted by the virtual inertia controller in response to changes in the system frequency. Assuming that the recurrence of the framework begins to drop, the regulator will build the RES yield ability to make up for the drop in dormancy. In the event that the recurrence begins to rise, the regulator will diminish the power result to try not to over-burden the framework.

In Fig. 3. A Virtual Latency Regulator (VIC) includes parts, for example, recurrence estimation, inactivity imitating calculation, power estimation, power balance signal age, coordination with the control framework, correspondence and input circles, and insurance and security instruments. The VIC is able to replicate the stabilizing effects of conventional rotating inertia and improve the stability and response of power systems with a high integration of renewable energy thanks to these components.

Fig. 3 VIC



The idea of VIC can be applied to a consolidated power framework that incorporates both sunlight based, wind and diesel power sources. In this framework, the sun oriented, wind power source can be displayed as a variable power source that is impacted by changes in sun based irradiance and wind speed, while the diesel power source can be demonstrated as a consistent power source. To determine the virtual inactivity regulator, we can begin with the power balance condition for a power framework:

$$P(t) = P_{gen}(t) - P_{load}(t) \quad (6)$$

where,  $P(t)$  is the net power in the system at time  $t$ ,  $P_{gen}(t)$  is the total power generated by all the power sources in the system at time  $t$ , and  $P_{load}(t)$  is the total power consumed by all the loads in the system at time  $t$ .

Assuming that the system has a constant frequency, we can differentiate the power balance equation with respect to time to obtain:

$$\frac{dP(t)}{dt} = \frac{dP_{gen}(t)}{dt} - \frac{dP_{load}(t)}{dt} \quad (7)$$

The left-hand side of the equation denotes the rate of change of net power in the system, which is proportional to the system frequency deviation. Therefore, we can write

$$\frac{df(t)}{dt} = \left( \frac{1}{M_{eff}} \right) * \left( \frac{dP_{gen}(t)}{dt} - \frac{dP_{load}(t)}{dt} \right) \quad (8)$$

where,  $\frac{df(t)}{dt}$  is the rate of change of system frequency deviation,  $M_{eff}$  is the effective inactivity constant, and  $\frac{dP_{gen}(t)}{dt}$  and  $\frac{dP_{load}(t)}{dt}$  are the rates of change in power generation and consumption, respectively.

The VIC can be designed to provide a power response that simulates the behavior of a physical inertia response. This can be achieved by adding a feedback term to the power balance equation, which is proportional to the frequency deviation:

$$P_{ctrl}(t) = P_{ref} + \left( k_p * \frac{df(t)}{dt} \right) \quad (9)$$

where  $P_{ctrl}(t)$  is the power set point for the power sources in the system,  $P_{ref}$  is the reference power set point,  $k_p$  denotes proportional gain, and  $\frac{df(t)}{dt}$  is the frequency deviation.

The VIC can be executed in a half-and-half power framework by setting  $P_{ref}$  to the power result of the diesel power source and utilizing the sun oriented, wind power source to change the power set point as per changes in sun based irradiance.

Determine the power disparity: Decide the contrast between the information power and the resulting power, like the overall strategy. However, the calculation of the power imbalance might need to take into account how VIC affects power flow when it is active. This can be accomplished by including the virtual dormancy commitment given by the VIC in the result power estimation.

$$\begin{aligned} \text{Power Im balance} &= \text{Input Power} \\ &- (\text{Output Power} - \text{Virtual Inertia Contribution}) \end{aligned} \quad (10)$$

The amount of power injected or absorbed by the VIC to mimic the inertia response is known as the virtual inertia contribution. Examine the power disparity: As in the past, break down the determined power lopsidedness to survey the converter's presentation. Be that as it may, when VIC is utilized, it is fundamental to consider the effect of the VIC on power stream and strength. A careful examination ought to be led to guarantee the viability of the VIC in giving virtual latency and keeping up with the power balance.

$$\text{Power Im balance} = \text{Total Power Generation} - \text{Total Power Consumption} \quad (11)$$

If the power imbalance is positive, the system is producing too much power, which can raise frequency and voltage. On the off chance that the power irregularity is negative, it implies there is a lack of force, which can cause recurrence and voltage drop. In rundown, the VIC is a control framework that mimics the actual idleness reaction conduct in a power framework. It very well may be applied to a joined power framework that incorporates the two RES (sunlight based, wind) and diesel power sources to settle the recurrence of the framework in light of unexpected changes in power interest or age.

### **3.6 Synchronous Generator-Based Virtual Inertia Controller (SGVIC)**

The simultaneous generator-based virtual dormancy regulator (SGVIC) is a specific control framework created to acquaint engineered or virtual idleness with power frameworks. A power system's ability to withstand disturbances is facilitated by inertia, which is crucial to its ability to maintain stability. Generally, coordinated generators have been depended upon to give intrinsic idleness because of their turning masses. Nonetheless, as sustainable power sources and power electronic-based gadgets like breeze turbines and sun powered chargers are coordinated into the matrix, the presence of simultaneous generators might decrease. This decrease in simultaneous generators can prompt a decrease in framework latency, presenting difficulties for keeping up with framework soundness.

To handle this issue, the SGVIC offers an answer by recreating or repeating the inactivity reaction of coordinated generators. Normally, this regulator is executed in power electronic-based gadgets, for example, lattice associated inverters used in environmentally friendly power frameworks. The SGVIC continually screens the recurrence of the power framework. At the point when an unsettling influence happens, for example, an unexpected loss of burden or age, the SGVIC quickly answers by infusing or retaining the ability to mirror the idleness reaction. The SGVIC can provide or absorb power as needed by utilizing the energy stored in power electronic devices' DC link capacitors. It absorbs power when the frequency is raised, and it injects power when the frequency is lower. This powerful reaction balances out the framework and upgrades its transient way of behaving. Basically, the SGVIC actually copies the impacts of manufactured latency, like that given by coordinated generators, without depending on physical turning masses.

### 3.7 Energy Storage System

To design an energy storage system (ESS) based virtual inertia controller, the following steps can be followed:

- **System Modeling:** Create a mathematical model of the power system, incorporating the ESS, grid dynamics, and loads. This model should encompass the ESS's characteristics, such as response time, energy capacity, and power conversion efficiency.
- **Inertia Emulation Algorithm:** Develop an algorithm that emulates inertia by analyzing the grid frequency deviations. This algorithm should estimate the necessary virtual inertia contribution from the ESS and compute the appropriate power response to match the desired response characteristics.
- **Control Strategy:** Formulate a control strategy that integrates the inertia emulation algorithm with the ESS control system. Consider factors like frequency droop control, power ramp rate limitations, and communication latency between the ESS and the grid control center.
- **Controller Implementation:** Implement the control strategy in either hardware or software, depending on the ESS architecture. Ensure seamless integration with ESS components such as power converters, energy storage units (batteries, capacitors, etc.), and grid connection points.
- **Power Electronic Converters with Inertia Emulation:** Power electronic converters, such as voltage source converters (VSCs), can be designed to emulate the inertia of synchronous generators. By incorporating additional control algorithms, these converters can respond to changes in system frequency similar to a synchronous generator. The inertia emulation enables the converter to contribute to frequency regulation and stability.

### 3.8 GWO Algorithm

GWO algorithms are one type of optimization algorithm that can be used to optimize the performance of the VIC. It works by simulating the behavior of a swarm of particles, every representing a potential solution to the optimization problem. The particles travel through the solution space, searching for the optimal solution based on the fitness function of the problem [38]. To implement the tie-line power frequency stability control using VIC GWO algorithm in a hybrid interconnected power system, the following footsteps can be taken:

- Design the VIC to match the synchronous generator's behavior. This can be done by modeling the controller to provide the required damping and inertia to the power system.
- Implement the GWO algorithm to optimize the performance of the VIC. The GWO algorithm can be used to novelty the optimal parameters for the controller, such as the gain and time constant.
- Integrate the VIC and GWO algorithm into the control system of the hybrid interconnected power system. This can be done by connecting the controller to the power system through the tie-line, which is the transmission line that associates two or more power systems.
- Test and evaluate the control system under various operating conditions. This can be done by simulating the power system under different scenarios, such as fluctuations in load demand or dissimilarities in the output of the renewable energy sources.

#### 3.8.1 GWO Iteration Flow Methods

Grey Wolf Algorithm iteration: Iterate through a series of generations, where each generation consists of the following steps:

- a. Update the positions of the grey wolves based on their current fitness values. This step simulates the social behavior and hunting dynamics of grey wolves, such as alpha, beta, delta, and omega.
- b. Evaluate the fitness of the updated positions.
- c. Update the alpha, beta, delta, and omega positions based on the updated fitness values.
- d. Repeat steps a-c until the termination condition is met, such as reaching a maximum number of generations or achieving a desired fitness level.

Virtual inertia controllers contribute to power system stability by enhancing the damping of oscillations and maintaining system equilibrium. They provide active power control, responding to disturbances and restoring the balance between generation and demand [39]. By adjusting their power output in real-time, these controller-based algorithms help dampen frequency deviations and prevent instability, which

can lead to blackouts or equipment damage. Overall, the use of virtual inertia controllers and GWO algorithms can help improve the stability and reliability of hybrid interconnected power systems that utilize multiple sources of energy.

## 4 Simulation and Results

Reproduction studies can be directed to assess the viability of various virtual dormancy control procedures in keeping up with tie-line power recurrence steadiness in an interconnected power framework. Modeling the behavior of various power generators, transmission lines, and loads as well as evaluating various control algorithms under various operating conditions can be part of these investigations. The consequences of these reproductions can give bits of knowledge into the VIC's presentation and assist with recognizing regions for plan and power framework activity. The virtual idleness regulator ought to be coordinated into the general control plot, cooperating with other control instruments, for example, programmed age control (AGC), recurrence control, and power stream regulators. Legitimate coordination guarantees ideal control of the tie-line power stream.

The boundaries, for example, the hang consistent R, framework latency steady H, damping coefficient D, virtual idleness control gain ( $K_{vi}$ ), and virtual idleness time steady ( $T_{vi}$ ), add to the general framework conduct and control execution in mixture regions. The solar system time constant ( $T_{pv}$ ) and the wind turbine time constant ( $T_{wt}$ ), both of which may be relevant to particular generation sources, are included in the system as well.

By and large, these reproduction boundaries give a complete depiction of the vital qualities and control settings of the power framework in crossover regions, empowering exact examination (decrease THD values) and evaluation of the framework's dynamic way of behaving and soundness.

The tie-line power changes between a conventional controller at the load side and a VIC in solar farms are driven by different factors. The conventional controller adjusts generation setpoints in response to load variations, while the VIC in solar farms modulates solar generation to emulate the stabilizing effects of inertia.

Figure 4 shows when using a conventional controller at the load side, the tie-line power changes are typically driven by changes in load demand. If the load demand increases, the conventional controller adjusts the setpoints of the generator control variables, such as governor valve position or excitation voltage, to increase the power output of the connected generators. This increase in power output leads to an increase in tie-line power to meet the increased load demand. In the case of a VIC in solar farms, the tie-line power changes are primarily influenced by variations in solar generation. Solar farms with VICs utilize control algorithms and real-time measurements to emulate the inertial response of traditional synchronous generators.



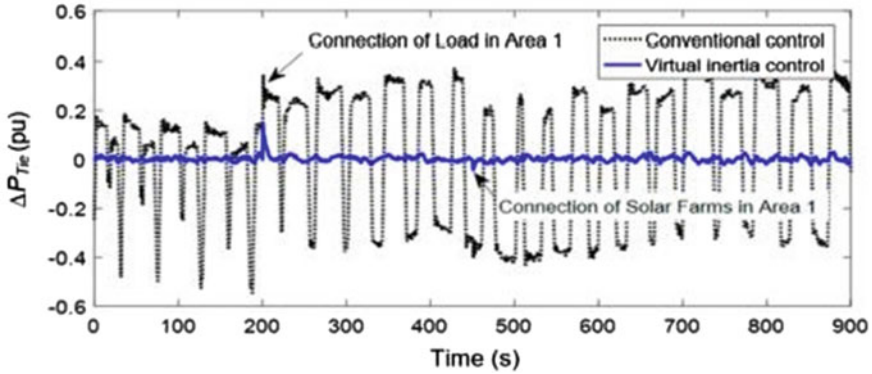


Fig. 4 Tie-line power changes

In a typical MPPT system, the voltage and current waveforms of the solar panels can exhibit variations due to changing environmental conditions and the tracking algorithm of the MPPT controller. The MPPT controller adjusts the operating voltage and current to keep the panels operating at their maximum power point (MPP). As a result, the voltage and current waveforms may undergo adjustments to maintain optimal power output in Fig. 5.

Figure 6 shows the stator current waveform and frequency control are closely related. When the generator is operating under a stable load condition, the frequency control mechanisms maintain a constant rotational speed, which in turn ensures a stable frequency of the electrical output. As a result, the stator current waveform will also remain relatively stable. However, under varying load conditions or if there are sudden changes in the load connected to the generator, the stator current waveform may fluctuate. This is because the current drawn by the load will affect the

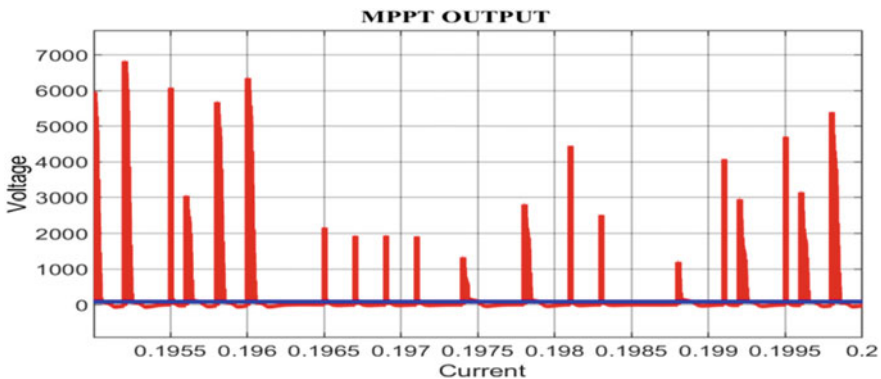
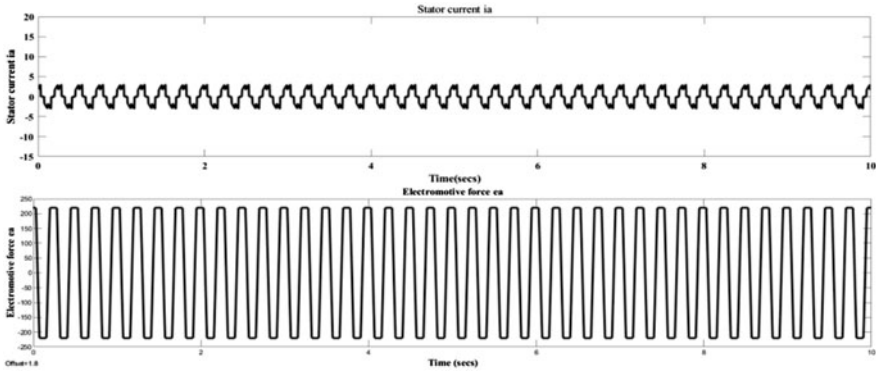


Fig. 5 Solar MPPT controller output



**Fig. 6** Diesel generator output

generator's internal impedance, which can influence the shape of the current waveform. In such cases, the governor system responds by adjusting the fuel supply to maintain the frequency within acceptable limits. The simulation parameters for Area-1 and Area-2 in a power system analysis. These parameters play a crucial role in modeling and simulating the behavior of the power system, enabling the analysis and control of its dynamics. In Area-1, the frequency bias factor ( $B_i$ ), is set to 0.3483 p.u.MW/Hz, indicating the response of the area's frequency to changes in system load. The area control error gain ( $k_i$ ), is 0.3 s, representing the gain applied to the control signal based on the error between the desired and actual values of the controlled variable. The governor time constant ( $T_g$ ), and turbine time constant ( $T_t$ ), are 0.08 s and 0.4 s, respectively, characterizing the response times of the governor and turbine systems. Similarly, in Area-2, the corresponding parameters are defined. The frequency bias factor,  $B_i$ , is 0.3827 p.u. MW/Hz, implying a different response characteristic compared to Area-1. The area control error gain ( $k_i$ ), is 0.2 s, indicating a different control sensitivity. The governor time constant ( $T_g$ ), and turbine time constant ( $T_t$ ), are 0.06 s and 0.44 s, respectively, representing the response dynamics specific to Area-2.

When examining the system with virtual inertia control (represented by the Blue solid line) and comparing it to the system without virtual inertia control (represented by the Black dotted line), several significant improvements are observed. The settling time can vary significantly depending on the characteristics of the power system and the control mechanisms in place. In general, systems with higher levels of inertia (e.g., conventional synchronous generators) tend to have longer settling times compared to systems with lower inertia (e.g., systems with a high penetration of renewable energy sources) in Fig. 7.

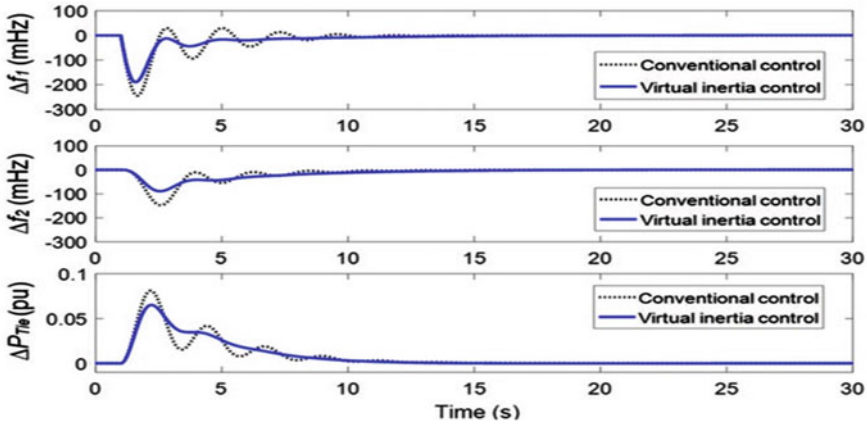


Fig. 7 Frequency stability with and without virtual inertia control

Firstly, the system with virtual inertia control exhibits enhanced frequency performance. This means that it can maintain a more stable and accurate frequency throughout the operation, even in the presence of disturbances or sudden load changes. The virtual inertia control helps in regulating and adjusting the frequency response, mitigating the adverse effects of reduced system inertia. Secondly, the magnitude of system transients is reduced in the presence of virtual inertia control. Transients refer to sudden changes or fluctuations in system variables such as frequency or power. By incorporating virtual inertia control, the system can better dampen these transients, resulting in a smoother response (frequency of oscillation reduced) and avoiding any excessive deviations (settling time reduced) or oscillations.

Furthermore, the implementation of virtual inertia control in the interconnected power system brings noticeable improvements in transient frequency stability. This means that the system can recover more quickly and maintain its stability after experiencing disturbances, such as sudden load changes or the loss of generation units. Additionally, the tie-line power is positively affected by the implementation of virtual inertia control. The tie-line power represents the exchange of electrical power between different areas or regions within the interconnected power system. By utilizing virtual inertia control, the tie-line power can be regulated more effectively, ensuring efficient power flow and balancing between different areas.

The settling time for frequency deviation can vary from a few seconds to several minutes, depending on the system's characteristics, control mechanisms, and the severity of the disturbance. Advanced control techniques, such as virtual inertia control and fast-acting governor systems, can help reduce the settling time by providing rapid and accurate responses to frequency deviations. Additionally, proper coordination among different control devices and control strategies can contribute to faster settling times in Fig. 8.

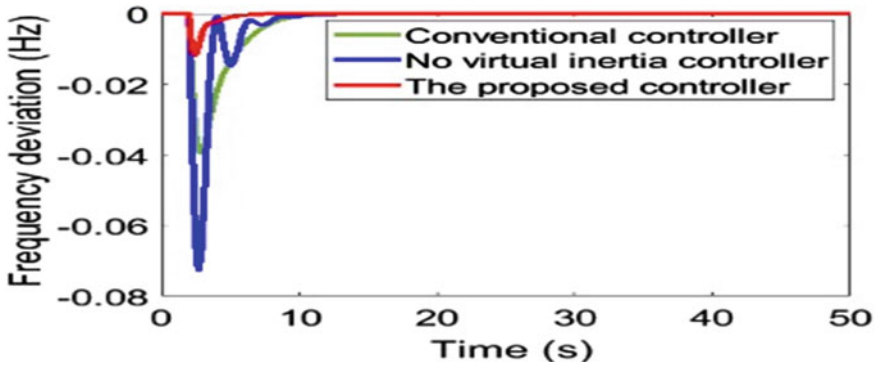


Fig. 8 GWO based frequency stability

It is important to note that settling time is typically defined based on specific criteria, such as the time required for the frequency deviation to reach a certain percentage of its final stable value or to stay within a specific tolerance band around the nominal frequency. The VIC measures the Rate of Change of Frequency (ROCOF) of the grid. Based on the ROCOF measurements, the VIC adjusts the power output of the converter-interfaced generation units. If the frequency is rising (positive ROCOF), the VIC can reduce the power output to absorb excess energy and slow down the frequency increase. Conversely, if the frequency is falling (negative ROCOF), the VIC can increase the power output to inject additional energy and help raise the frequency.

Overall, the introduction of virtual inertia control in the power system demonstrates its effectiveness in enhancing stability, response speed, frequency performance, transient mitigation, transient frequency stability, and tie-line power regulation. These improvements contribute to a more reliable and resilient power system operation, particularly in scenarios with reduced system inertia.

Comparing the response of the system under two conditions, namely normal system inertia and low system inertia (reduced by 50% in each area), the system equipped with virtual inertia control consistently shows superior stability and faster response when compared to traditional control methods.

Table 1 presents the mean absolute frequency deviation (in Hz) under different system inertia conditions and various virtual inertia control methods. The values in Table 2 provide insights into the dynamic response characteristics under different loading conditions, including rise time, settling time, maximum overshoot, and peak time.

**Table 1** Frequency analysis

System inertia in percentage	Frequency deviation (Hz)				
	No VIC	VIC	VIC based fuzzy	VIC based PSO	VIC GWO
High (100%)	0.03752	0.03376	0.0310	0.01070	0.00987
Medium (50%)	0.04103	0.03567	0.0339	0.01081	0.0101
Low (25%)	0.62555	0.08211	0.0812	0.01375	0.01135

**Table 2** Dynamic response analysis

Various loading condition $\Delta P_L$	$T_r$ (s)	$T_s$ (s)	$M_p$	$T_p$ (s)
True	0.1834	22.2908	0.0012	1.0510
50%	0.1673	22.9463	0.0029	1.0502
100%	0.1822	22.9510	0.0028	1.0406

## 5 Conclusion

All in all, the utilization of a VIC has been demonstrated to be a compelling technique for keeping recurrence strength and controlling the tie-line power stream in a hybrid interconnected framework. This method considers the virtual expansion of latency to the framework, which can assist with moderating the effect of abrupt changes in power interest or supply.

In general, this study demonstrates the significance and potential of virtual inertia control as a tool for enhancing power system stability and reliability, but only in the context of hybrid interconnected power systems. The VIC is able to add stability and control to the system by modeling the behavior of conventional synchronous generators. The controller design can be improved and its application to other kinds of power systems can be investigated through additional research.

**Acknowledgements** We would like to express our sincere gratitude to all those who have contributed to the successful completion of this research paper. We extend our thanks to our supervisor Dr. Malathy P, for her guidance, encouragement, and support throughout this research. We would also like to acknowledge the valuable feedback and suggestions provided by our colleagues Mr. Manivasagan D, Mr. Mayilvaganan N and Mohamed Basith S. Furthermore, we extend our appreciation to the anonymous reviewers for their constructive criticism and valuable comments that have helped to improve the quality of this paper.

## References

1. Rahman FS, Kerdphol T, Watanabe M, Mitani Y (2018) A study on the placement of virtual synchronous generator in a two-area system. In: Proceedings of IEEE innovative smart grid technologies Asia, pp 782–786
2. Kerdphol T, Rahman FS, Mitani Y, Hongesombut K, Küfeoğlu S (2017) Virtual inertia control-based model predictive control for microgrid frequency stabilization considering high renewable energy integration. *Sustainability* 9(5):773
3. Fang J, Li H, Tang Y, Blaabjerg F (2018) Distributed power system virtual inertia implemented by grid-connected power converters. *IEEE Trans Power Electron* 33(10):8488–8499
4. Gulzar MM, Iqbal M, Shahzad S, Muqet HA, Shahzad M, Hussain MM (2022) Load frequency control (LFC) strategies in renewable energy-based hybrid power systems: a review. *Energies* 15(10):3488. <https://doi.org/10.3390/en15103488>
5. Gupta A, Manocha AK (2021) Designing of 2-degree of freedom load frequency controller for power system using novel improved pole clustering and genetic method of reduced-order modelling. *Int Trans Electr Energy Syst* 31:e13063
6. Barakat M, Donkol A, Hamed HFA, Salama GM (2021) Harris hawks-based optimization algorithm for automatic LFC of the interconnected power system using PD-PI cascade control. *J Electr Eng Technol* 16(4):1845–1865
7. Guha D, Roy PK, Banerjee S, Purwar S (2022) Model order reduction of power systems and application of internal model control (IMC). In: Guha D, Roy PK, Banerjee S, Purwar S (eds) Application of intelligent control algorithms to study the dynamics of hybrid power system, pp 173–197. Springer, Singapore. [https://doi.org/10.1007/978-981-19-0444-8\\_7](https://doi.org/10.1007/978-981-19-0444-8_7)
8. Gulzar MM, Sibtain D, Ahmad A, Javed I, Murawwat S, Rasool I, Hayat A (2022) An efficient design of adaptive model predictive controller for load frequency control in hybrid power system. *Int Trans Electr Energy Syst* 1–14. <https://doi.org/10.1155/2022/7894264>
9. Padhi JR, Debnath MK, Kar SK (2022) Self-tuning fuzzy-PI controller for load frequency control analysis with the integration of wind energy. *Energy Sources Part A: Recover Util Environ Eff* 44(1):613–631
10. Raja Shekar J, Sangameswara Raju P, Kumudini Devi RP (2019) Virtual inertia and virtual resistance-based power frequency control in a hybrid power system with wind and hydro power sources, electric power components and systems, vol 47, Issue: 5–6, pp 486–498. <https://doi.org/10.1080/15325008.2019.1610475>
11. Kerdphol T, Rahman FS, Mitani Y, Hongesombut K, Küfeoğlu S (2017) Virtual inertia control-based model predictive control for microgrid frequency stabilization considering high renewable energy integration. *Sustainability* 9:773
12. Kerdphol T, Rahman FS, Mitani Y, Watanabe M, Küfeoğlu SR (2018) Virtual inertia control of an islanded microgrid considering high penetration of renewable energy. *IEEE Access* 6:625–636
13. Dechanupaprittha S, Hongesombut K, Watanabe M, Mitani Y, Ngamroo I (2007) Stabilization of tie-line power flow by robust SMES controller for interconnected power system with wind farms. *IEEE Trans Appl Supercond* 17:2365–2368
14. Datta M, Ishikawa H, Naitoh H, Senjyu T (2012) Frequency control improvement in a PV-diesel hybrid power system with a virtual inertia controller. In: Proceedings of the 2012, 7th IEEE conference on industrial electronics and applications (ICIEA 2012), Singapore, pp 1167–1172, 18–20
15. Lee DJ, Wang L (2008) Small-signal stability analysis of an autonomous hybrid renewable energy power generation/energy storage system part I: time-domain simulations. *IEEE Trans Energy Convers* 23:311–320
16. Zhao J, Lyu X, Fu Y, Hu X, Li F (2018) Coordinated microgrid frequency regulation based on DFIG variable coefficient using virtual inertia and primary frequency control. *IEEE Trans Energy Convers* 31:833–884
17. Clerc M, Kennedy J (2002) The particle swarm—explosion, stability, and convergence in a multidimensional complex space. *IEEE Trans Evol Comput*

18. Tasnim MF, Anwar SI, Rakibul Islam SM, Hoque MM, Ali MH (2018) Design of virtual inertia controller for inverter-based microgrid using GWO algorithm. *International J Renew Energy Res* 8(2):922–930
19. Guha D, Roy PK, Banerjee S (2016) Load frequency control of interconnected power system using grey wolf optimization. *Swarm Evol Comput* 27:97–115. <https://doi.org/10.1016/j.swevo.2015.10.004> (2016)
20. Pathak N, Ashu Verma TS, Bhatti IN (2019) Modeling of HVDC tie links and their utilization in AGC/LFC operations of multiarea power systems. *IEEE Trans Industr Electron* 66(3):2185–2197. <https://doi.org/10.1109/TIE.2018.2835387>
21. Kerdphol T, Rahman FS, Mitani Y, Watanabe M, Kufeoglu S (2018) Robust virtual inertia control of an islanded microgrid considering high penetration of renewable energy. *IEEE Access* 6:625–636
22. Yan RF, Saha TK, Modi N, Masood NA, Mosadeghy M (2015) The combined effects of high penetration of wind and PV on power system frequency response. *Appl Energy* 145:320–330
23. Lal DK, Dash BB, Akella A (2011) Optimization of PV/wind/micro-hydro/diesel hybrid power system in homer for the study area. *Int J Electr Eng Inform* 3(3):307–325
24. Elhadidy M, Shaahid S (2000) Parametric study of hybrid (Wind+Solar+Diesel) power generating systems. *Renew Energy* 21(2):129–139
25. Theubou T, Wamkeue R, Kamwa I (2012) Dynamic model of diesel generator set for hybrid wind-diesel small grids applications. In: *Proceedings of the IEEE on Electrical and Computer Engineering*, pp 1–4
26. Ahmed NA, Miyatake M (2020) A stand-alone hybrid generation system combining solar photovoltaic and wind turbine with simple maximum power point tracking control. In: *CES/IEEE 5th international power electronics and motion control conference, Shanghai, China*, pp 1–7
27. Yang G, Zhou M, Lin B, Du W (2020) Optimal scheduling the wind-solar-storage hybrid generation system considering wind-solar correlation. In: *IEEE PES Asia-pacific power and energy engineering conference (APPEEC), Hong Kong, China*, pp 1–6. <https://doi.org/10.1109/APPEEC.2013.6837181>
28. Yu W, Qian X (2019) Design of 3KW wind and solar hybrid independent power supply system for 3G base station. In: *Second international symposium on knowledge acquisition and modeling, Wuhan, China*, pp 289–292
29. Çimen H, Oguz E, Oguz Y, Oguz H (2021) Power flow control of isolated wind-solar power generation system for educational purposes. In: *22nd Australasian universities power engineering conference (AUPEC), Bali, Indonesia*, pp 1–5
30. Vasant LG, Pawar VR (2017) Solar-wind hybrid energy system using MPPT. In: *International conference on intelligent computing and control systems (ICICCS)*. Madurai, India, pp 595–597. <https://doi.org/10.1109/ICCONS.2017.8250531>
31. Chen M, Huang L, Yang J, Lyu Y (2017) Design and simulation of multi-energy hybrid power system based on wave and wind energy. In: *20th international conference on electrical machines and systems (ICEMS), Sydney, NSW, Australia*, pp 1–6. <https://doi.org/10.1109/ICEMS.2017.8056368>
32. Habibzadeh M, Hassanaliheragh M, Soyata T, Sharma G (2017) Solar/wind hybrid energy harvesting for supercapacitor-based embedded systems. In: *IEEE 60th international midwest symposium on circuits and systems (MWSCAS), Boston, MA, USA*, pp 329–332. <https://doi.org/10.1109/MWSCAS.2017.8052927>
33. Sree VS, Reddy GP, Rao CS (2021) Mitigation of power quality issues in hybrid solar-wind energy system using distributed power flow controller. In: *IEEE international women in engineering (WIE) conference on electrical and computer engineering (WIECON-ECE), Dhaka, Bangladesh*, pp 162–166. <https://doi.org/10.1109/WIECON-ECE54711.2021.9829624>
34. Kumar AVP, Parimi AM, Rao KU (2015) Implementation of MPPT control using fuzzy logic in solar-wind hybrid power system. In: *IEEE international conference on signal processing, informatics, communication and energy systems (SPICES), Kozhikode, India*, pp 1–5. <https://doi.org/10.1109/SPICES.2015.7091364>

35. Zhang F, Wang Y, Shang E (2008) Design and realization of controller in wind solar hybrid generating system. In: Joint international conference on power system technology and IEEE power India conference, New Delhi, India, pp 1–6. <https://doi.org/10.1109/ICPST.2008.474537>
36. Kumar NP, Balaraman K, Atla CSR (2016) Optimizing system elements for hybrid wind - solar PV power plant. In: Biennial international conference on power and energy systems: towards sustainable energy (PESTSE), Bengaluru, India, 2016, pp 1–6. <https://doi.org/10.1109/PES TSE.2016.7516421>
37. Sharma B, Dahiya R (2020) Improved modular flying capacitor converter based grid-tied hybrid wind solar energy system. In: IEEE 9th power India international conference (PIICON). Sonapat, India, pp 1–5. <https://doi.org/10.1109/PIICON49524.2020.9113043>
38. Guha D, Roy PK, Banerjee S (2016) Load frequency control of interconnected power system using grey wolf optimization. *Swarm Evol Comput* 27:97–115
39. Sulaiman MH, Mustaffa Z, Mohamed MR, Aliman O (2015) Using the gray wolf optimizer for solving optimal reactive power dispatch problem. *Appl Soft Comput* 32:286–292



# Lithium-Ion Batteries: Prognosis Algorithms, Challenges and Future Scenario



Gaurav Malik and Manish Kumar Saini

**Abstract** This study concentrates on different types of prognosis algorithms for forecasting lithium-ion battery parameters. Various SoC estimation techniques are examined and compared based on their SoC estimation performance indexes. SoC estimation methods are broadly classified as Kalman filter, particle filter, data-driven and hybrid methods. These types of filters are compared based on the complexity of the implementation on hardware as well as their performance parameters such as statistics (errors), driving test schedules, laboratory testing data, type of battery model used and different types of prognosis methods used in the SoC estimation. It helps in the proper selection of the hardware and methods for battery model parameter forecasting which is critical for electrical vehicle (EVs) battery management system coordination and control. This study also focuses on the challenges faced by the different SoC prognosis methods and their modern trends to improve the forecasting of important parameters of the batteries.

**Keywords** SoC · Kalman filter · Particle filters · Neural network

## 1 Introduction

Due to the rapid consumption of non-renewable resources, greenhouse gas emissions are increased which causes global warming. Global warming [1] causes instability in the earth's environmental conditions such as temperature rise, weather change, unseasonal precipitation and rise in sea level. To maintain sustainable development and stop global warming, alternate options of clean energy transport are used. The research conducted by International Renewable Energy Agency (IRENA) indicates that there will be a considerable increase in the number of EVs in the year 2030 [2]. In the year 2030, there will be around 900 million EVs with two wheels or three wheels. This has the potential to bring about significant shifts in a country's transportation economy [3].

---

G. Malik · M. K. Saini (✉)

Deenbandhu Chhotu Ram University Science and Technology, Murthal, Haryana, India  
e-mail: [manishkumar.ee@dcrustm.org](mailto:manishkumar.ee@dcrustm.org)

It is essential to monitor the functioning of lithium-ion batteries because they are being employed in an increasing number of aspects of day-to-day life. If a battery is used in situations that are outside of its normal range of functionality, both its performance and its lifespan will decrease at a very fast rate. The use of a battery management system (BMS) prevents the battery from fault. The controller is the heart of the battery management system [4], which collects important sensor data and processes it for battery parameter information such as SoC and SoH.

## 2 SoC Estimation Methods

The SoC is a function of the open-circuit voltage (OCV) of the battery. As a result, there is a monotonical relationship between the SoC and OCV of the lithium-ion battery. This method is also known as the tabulation method because it requires a large table to establish the relationship between the SoC and OCV of the battery [5]. With this method, SoC estimation can only be conducted offline. AC impedance of the battery is analysed with the impedance analyser at different frequencies of the voltage signal to the battery. A lookup table is formed between the AC impedance variation and frequency at different SoCs of the battery [6].

### 2.1 Coulomb Counting Method

Coulomb counting [7] is always used in association with other filtering and data-driven methods due to its lack of initial charge information present in the battery. The Coulomb counting method is given by the equation:

$$\text{SoC}(t) = \text{SoC}(0) + \frac{\eta_i * \left( \int_0^t I(t) dt \right)}{C_{actual}} \quad (1)$$

$\eta$  = coulombic efficiency which lies between 0.9 and 1.  $I(t)$  is the current flowing through the battery at any instant of time,  $t$ .  $\text{SoC}(0)$  is the initial amount of charge present in the battery,  $C_{actual}$  is the available capacity of the battery and  $\eta_i$  is the charging and discharging efficiency of the battery. The Coulomb counting method is affected by the noisy measurement of the current and slow self-discharging current.

## 2.2 Model-Based Approaches

EM is based on the mass and energy transportation phenomenon [8] inside the battery. It also takes care of the energy flow at the charging and discharging duration of the battery. The electrochemical model takes care of the electrochemical phenomenon by using complex electrochemical equations [9]. Initially, the electrochemical battery modelling was based on the porous electrode theory and considered the concentration of the electrolyte [10], which leads to distributed parameters to the battery. The distributed parameter required a complex computation. Therefore, this distributed model is converted to a single-particle (SP) model [11] which deals with the macroscopic particle level. Battery models of a lithium-ion battery are represented by dynamic parameters such as resistance and capacitance of the battery [12]. Capacitance and resistance of the battery change with the life cycle of the battery.

The EIM is obtained by the complex division of AC voltage and current of the battery over a wide range of frequencies at a specified SoC [13]. At high frequencies, battery impedance can be modelled as pure resistance. At low frequencies, the battery impedance has a constant slope and can be presented by a constant phase element (CPE) known as the Warburg element. A semi-circle is formed at the mid-frequency band which is represented as an electrochemical phenomenon in the battery. It can be modelled as constant resistance connected in parallel with CPE and known as  $Z_{arc}$  element [14]. Battery model accuracy is increased by using the addition of the Warburg element and CPE to represent different aspects of the battery [15]. Creating a decent model is difficult, time-consuming and requires prior knowledge.

## 2.3 Filter Based Approaches

Kalman filter is a linear estimator which can be implemented on the linear system parameter estimation or state estimation of the system. A linear system can be represented in the state-space model in matrix form which can be used for the state estimation of the system. Since a lithium-ion battery is a non-linear system, a linear Kalman filter cannot be utilized to accurately estimate the state of charge of the battery. But the importance of the linear Kalman filter cannot be ignored in terms of state-space modelling [16].

An extended Kalman filter (EKF) is used for the SoC estimation of the battery. The lithium-ion battery non-linear relationship is linearized using the Taylor series first-order approximation in an EKF [17]. The order of approximation of the Taylor series determines the order of the EKF. As the order of the filter is increased, the accuracy of the estimation of the parameters is increased but it increases the hardware requirement [18]. The dual Extended Kalman filter (DEKF) method simultaneously estimates both the parameter and SoC of the battery [19]. In the dual approach [20], parameters are updated on the macro time scale, whereas SoC is updated on the micro time scale. The battery electrical parameters such as resistance and capacitance are

slowly varying parameters compared to SoC and the temperature of the battery. Therefore, a multi time scale dual Kalman filter [21] is used for the parameter as well as the SoC estimation of the battery. As the size of the error innovation matrix increases, it can cause divergence in the Kalman filter. An adaptive filter can modify the primary model and statistics of the noise covariance matrix if dynamics of the target have changed. In [22], error innovation covariance is updated using the error innovation sequence present in the sliding window. The size of sliding window is determined by optimization methods.

In EKF, Jacobian is calculated for the state-space matrix up to first-order approximation which causes error in the estimation. Sigma-point Kalman filtering (SPKF) is an alternate approach which mitigates the burden of Jacobian-matrices computation present in EKF. In this method, a set of sigma points are selected based on the number of state variables present in the state-space equation. If the number of state variables is  $N$  then  $2N + 1$  sigma points must be selected. Sigma-point Kalman filter [23] has been divided into an unscented Kalman filter and a centre-difference Kalman filter.

The central difference Kalman filter employs a polynomial approximation of the non-linear problem based on the sterling interpolation method, hence eliminating the need to compute the derivation. However, the ultimate procedure is essentially comparable to the UKF. Its theoretical precision is also marginally superior to that of UKF. Having a single tuning parameter, the CDKF is simple to implement. When predicting battery SoC, CDKF performs better than EKF. Instead of using the Taylor series, the UKF estimates covariance using available measured data. In [24], SoC is estimated using UKF which is used for state of power estimation of hybrid EVs. The computation cost depends on the selection of sigma points in the UKF [25]. A large number of sigma points can increase the computation burden on the hardware. This problem is addressed by the sigma transformation methods. Square Root Spherical Unscented Kalman filter (SR-UKF) uses the spherical transformation for sigma points which reduces the number of sigma points [26]. For  $N$  variables, there are  $N + 2$  sigma points which are  $2N + 1$  in unscented transformation. In simplex transformation, the  $N + 1$  sigma points are present but it suffers from a convergence problem. In the case of spherical transformation, the convergence of the system is increased by reducing the sigma point's spherical radius.

The cubature rule with Bayesian filter outperforms the UKF and EKF filters [27]. The cubature rule is derivative-free and uses the  $2N$  cubature points for the mean and covariance estimation. The third-degree cubature rule is sufficient for the non-linear system having Gaussian property. In [28], adaptive cubature Kalman filter (ACKF) is proposed which adaptively updates the process covariance matrix as well as the measurement noise covariance matrix using adaptive law. ACKF is more accurate and robust than the CKF and EKF, but it requires more computation time.

Bayesian filter methods are derived from Bayes' rule of conditional probability  $P(A|B)$  is the probability of event  $A$  given that  $B$  has already occurred [29]. The Monte Carlo sampling method can represent a non-Gaussian probability distribution function which avoids Gaussian model error having mean and variance as measurement parameters [30]. A fused multi-battery model [31] with a particle filter is used

for the real-time SoC estimation. Improved sampling methods used in particle filter increase the accuracy and reduce the number of particles [32]. Particle filter accuracy depends on the probability distribution of the particles.

A large amount of data is required for lithium-ion battery training and testing under various operating conditions. These methods are also known as the black-box model which requires data to know the system characteristics [43]. A deep study of system and battery modelling is not required because data-driven methods [44] are based on the available dataset.

## ***2.4 Data-Driven Approaches***

Data-driven methods include training methods for neural networks, machine learning, fuzzy rule-based techniques, and other techniques that are based on the statistics of available experimental data. These methods are also known as the black-box model [43]. A deep study of system and battery modelling is not required because data-driven methods are based on the available dataset [44]. The data-driven method can be categorized into distinct areas such as neural networks, fuzzy rule-based algorithms, regression models for machine learning, probabilistic methods, recurrent neural network techniques and hybrid techniques.

The field of battery research heavily employs feed-forward neural network (FNN) techniques due to their relative ease of construction, increased computational intelligence and enhanced generalization. A feed-forward back-propagation neural network (BPNN) model consists of three layers, an input layer, a hidden layer for weight adjustment and the output layer [33]. A good global approximation performance can be achieved with a feed-forward self-learning technique called a radial basis function neural network (RBFNN) [34]. WNN's data-driven structure is influenced by mathematical concepts and features in terms of neuron minimization and error reduction [35]. Time-delay neural network (TDNN) investigates SoC in time series using both current and historical inputs. In [36], an intelligent SoC estimate model for lithium-ion batteries was developed using TDNN with two hidden layers. A neural network having two or more hidden layers is known as a deep feed-forward neural network (DFNN). In [37], DFNN is proposed for SoC estimation during various driving cycles and different temperatures of the lithium-ion battery.

Using classification and regression approaches, noise and over-fitting may be corrected, resulting in quick and accurate SoC estimation results [38]. In support vector machine (SVM) [39], data classification is defined by the design of hyper-planes in high-dimensional space. Random forest (RF) is done based on trees in forests at random. The boot-strapping method chooses original data at random. Using binary splits, decision trees are obtained from the new dataset. RF [40] does not over-fit as a predictor and handles huge datasets quickly and effectively, resulting in higher performance.

A more complex and non-linear system can be analysed with probabilistic methods [41]. A Gaussian process regression (GPR) can parameterize and maximize the marginal likelihood function of the system which can be done by a probabilistic formulation and interpretation analytically. The GPR [42] can be trained by the dataset used for the training purpose and the initialization of the hyper-parameters. To estimate the parameters of non-linear systems, recurrent-neural networks (RNNs) consider the state of the system at each layer of the network. The learning and computational speed can be increased with the non-linear autoregressive exogenous neural network (NARXNN) algorithm for lithium-ion battery non-linear properties [43]. Awadallah et al. came up with ANFIS [44] based SoC estimate model while taking into account the various Gaussian membership function parameters (MFs) and different temperatures.

Hybrid method combines both data-driven methods and different optimization techniques to improve the accuracy of SoC estimation of lithium-ion batteries. A genetic algorithm (GA) is easy to implement and can be used over different types of battery parameter estimations [45] and particle swarm optimization (PSO) [46].

### 3 Comparison and Challenges with Prognosis Methods

SoC methods can be broadly compared based on four different categories such as non-linear filters, particle filters (likelihood methods), data-driven methods and hybrid methods. The first category includes non-linear filters as shown in Table 1. An EKF filter is best suitable for noisy measurement and non-linear systems with MAE of less than 4%. There are other variants such as DEKF, AIEKF and IAEKF developed which reduce the MAE, but these methods increase computational time of the filters.

The particle filter methods represented in Table 1 also known as Sequential Monte Carlo (SMC), Bayesian filter, particle filter, likelihood methods) which are based on the number of particles used in the SoC estimation. The improved PF reduces the MAE to 0.6%. These filters are better than EKF filters in terms of accuracy at the cost of implementation complexity and computational time. Their stability depends on the number of particles used and the distribution of the particles in the sample space. Particles lose their diversity after a few iterations in the particle filter which requires different sampling methods to maintain its diversity of particles.

In the third category, statics and data-driven methods, such as fuzzy rule-based neural network algorithms (in Table 2,  $V$  = Terminal voltage of the battery,  $I$  = Terminal current of the battery,  $T$  = Operating temperature of the battery), are employed for SoC estimates. The NARXNN method claims the MAE of 0.38% which is better than the previous methods, machine learning methods. The amount of data and variables used in machine learning increases the complicity in the SoC estimation. The number of variables ( $V, I, T$ ) used in the data-driven methods increases the accuracy but at the same time, it increases the computational time.

The fourth category as shown in Table 2 combines optimization approaches with filters and neural network methods. These methods utilize the best functions in two

**Table 1** Comparison of Kalman filters and particle filter

Kalman filter family					
Ref. no.	Filter type	Battery model	Complexity	Error (MAE)	Dataset type used
[47]	DAEKF	1-RC	Very high	± 2% (RE)	DST, FUDS
[48]	Intelligent-AEKF	1-RC	Very high	0.099% (MAE)	NASA
[49]	AIEKF	1-RC	High	0.3% (MAE)	HPPC
[50]	IAEKF	1-RC	High	2.96% (MAE)	FUDS
[51]	ATSDEKF	UT- model	Very high	2.82% (RMSE)	BJDST
[52]	VFFAKF	linear model	Very high	<1.4% (RMSE)	FUDS
<i>Particle filter (based on the selection of the number of particles)</i>					
	Filter type	Battery model	Complexity	Error	No. of particles
[53]	AUKF	2-RC model	High	0.2% (MAE)	2N + 1
[54]	SPKF	1-RC	High	0.0197 (MAE)	2N + 1
[55]	SPKF	ECMwH	Very high	<0.5% (RMSE)	2N + 1
[56]	ACKF	PBM	Very High	0.4% (RMSE)	2N
[30]	PF	Not used	Very High	–	–
[57]	Improved PF	1-RC	Very high	0.6% (MAE)	–

Complexity: Low = <math>O^3</math>, medium =  $O^3$ , high = >  $O^3$ , where  $O$  is the dimension of the state matrix formed. VFFAKF = Variable Forgetting Factor Adaptive Kalman Filter, ATSDEKF = Adaptive Time Scale Dual Extend Kalman Filtering, UOB Lab = University of Oviedo Battery Laboratory, RE = relative error, MAE = Mean average error, RMSE = Root mean squared error, UDDS = Urban dynamometer driving schedule, BJDST = Beijing Dynamic Stress Test, UT = Unsymmetrical Thevenin model, NEDC = New European driving cycle, FUDS = Federal Urban driving schedule, NASA = Data repository of NASA

**Table 2** Comparison table of data-driven methods

Data-driven methods					
Ref. no.	Filter type	Activation function	Input variables	Error	Dataset type used
[44]	ANFIS	–	OCV, T	–	Lab data
[59]	DRNN	Sigmoid	V, I, T	1.6% (MAE)	Lab
[60]	TCN	Sigmoid	V, I, T	0.67% (MAE)	US06
[61]	NARX	–	V, I	1.03% (MAE)	DST, UDDS
<i>Hybrid methods</i>					
	Method-I	Method-II	Input variables	Error	Dataset type used
[62]	CKF	LSTM	V, I, T	2% (MAE)	UDDS, FUDS
[63]	EKF	SVM	V, I, T	<2% (MAE)	Lab-Data
[64]	AEKF	ESG	V, I	0.79% (RMSE)	NEDC, DST
[65]	EKF	PF	V, I, T	0.61% (RMSE)	UDDS

or more methods which improves the overall accuracy. It can also combine the EKF with PF, and machine learning methods [58] to reduce the MAE error by less than 2%. These methods are more complex to implement and require fast computational hardware.

## 4 Selection and Future Scenario

The Kalman filter using the 1-RC model is the more robust and of low computational cost within the optimal accuracy of SoC estimation under the noisy condition of the measurement and imperfection in the state-space models. The development of the Kalman filter variants is more accurate than EKF filter. Particle filter is better than Kalman filter in terms of accuracy but more complex than Kalman filter. Data-driven methods depend on the training data which can vary from cell to cell present in the battery. Therefore, these methods cannot be implemented on the other battery that has different characteristics. Hybrid methods are more accurate than the other methods because of the fusion of two or more techniques, but they are more complex than the filter and data-driven methods. The utility of these methods depends on the compatibility of the application.

SoC is the critical parameter for the battery management system which controls the various functions related to the battery. SoC estimation is selected in such a way that it can optimally utilize the hardware computational power without losing the required accuracy used in the application of the battery management system.

## References

1. IRENA (2023) Renewable capacity statistics 2023. International Renewable Energy Agency, Abu Dhabi
2. Lin Z, Wang P, Ren S, Zhao D (2023) Economic and environmental impacts of EVs promotion under the 2060 carbon neutrality target—A CGE based study in Shaanxi province of China. *Applied Energy* 332:120501
3. Chong D, Wang N, Su S, Li L (2023) Global warming impact assessment of asphalt pavement by integrating temporal aspects: a dynamic life cycle assessment perspective. *Transp Res Part D: Transp Environ* 117:103663
4. Dai H, Zhang X, Wei X, Sun Z, Wang J, Hu F (2013) Cell-BMS validation with a hardware-in-the-loop simulation of lithium-ion battery cells for electric vehicles. *Int J Electric Power Energy Syst* 52:174–184
5. Kim J, Seo G, Chun C, Cho B, Lee S (2012) OCV hysteresis effect-based SOC estimation in extended Kalman filter algorithm for a LiFePO<sub>4</sub>/C cell. In: 2012 IEEE international electric vehicle conference, pp 1–5
6. Rodrigues S, Munichandraiah N, Shukla AJJoSSE (1999) AC impedance and state-of-charge analysis of a sealed lithium-ion rechargeable battery. 3(7–8):397–405
7. Zhang S, Guo X, Dou X, Zhang X (2020) A data-driven coulomb counting method for state of charge calibration and estimation of lithium-ion battery. *Sustain Energy Technol Assess* 40:100752



8. Xiong R, Cao J, Yu Q, He H, Sun F (2018) Critical review on the battery state of charge estimation methods for electric vehicles. *IEEE Access* 6:1832–1843
9. Schmidt AP, Bitzer M, Imre ÁW, Guzzella L (2010) Experiment-driven electrochemical modeling and systematic parameterization for a lithium-ion battery cell. *J Power Sources* 195(15):5071–5080
10. Doyle M, Fuller TF, Newman J (1993) Modeling of galvanostatic charge and discharge of the lithium/polymer/insertion cell. *J Electrochem Soc* 140(6):1526–1533
11. Haran BS, Popov BN, White RE (1998) Determination of the hydrogen diffusion coefficient in metal hydrides by impedance spectroscopy. *J Power Sources* 75(1):56–63
12. Navas SJ, González GMC, Pino FJ, Guerra JJ (2023) Modelling Li-ion batteries using equivalent circuits for renewable energy applications. *Energy Reports* 9:4456–4465
13. Li M (2017) Li-ion dynamics and state of charge estimation. *Renew Energy* 100:44–52
14. Xu J, Mi CC, Cao B, Cao J (2013) A new method to estimate the state of charge of lithium-ion batteries based on the battery impedance model. *J Power Sources* 233:277–284
15. Dai H, Jiang B, Wei XJE (2018) Impedance characterization and modeling of lithium-ion batteries considering the internal temperature gradient 11(1):220
16. Plett GL (2006) Sigma-point Kalman filtering for battery management systems of LiPB-based HEV battery packs: Part 1: Introduction and state estimation. *J Power Sources* 161(2):1356–1368
17. Mastali M, Vazquez-Arenas J, Fraser R, Fowler M, Afshar S, Stevens M (2013) Battery state of the charge estimation using Kalman filtering. *J Power Sources* 239:294–307
18. Wang D, Yang Y, Gu T (2023) A hierarchical adaptive extended Kalman filter algorithm for lithium-ion battery state of charge estimation. *J Energy Storage* 62:106831
19. Xiong R, Sun F, Chen Z, He H (2014) A data-driven multi-scale extended Kalman filtering based parameter and state estimation approach of lithium-ion polymer battery in electric vehicles. *Appl Energy* 113:463–476
20. Wang C, Wang S, Zhou J, Qiao J, Yang X, Xie Y (2023) A novel back propagation neural network-dual extended Kalman filter method for state-of-charge and state-of-health co-estimation of lithium-ion batteries based on limited memory least square algorithm. *J Energy Storage* 59:106563
21. Bai W et al (2022) State of charge estimation for lithium-ion batteries under varying temperature conditions based on adaptive dual extended Kalman filter. *Electric Power Syst Res* 213:108751
22. He H, Xiong R, Guo H (2012) Online estimation of model parameters and state-of-charge of LiFePO<sub>4</sub> batteries in electric vehicles. *Appl Energy* 89(1):413–420
23. Wang L, Wang L, Liao C, Liu J (2009) Sigma-point Kalman filter application on estimating battery SOC. In: 2009 IEEE vehicle power and propulsion conference, pp 1592–1595
24. Wang W, Wang X, Xiang C, Wei C, Zhao Y (2018) Unscented Kalman filter-based battery SOC estimation and peak power prediction method for power distribution of hybrid electric vehicles. *IEEE Access* 6:35957–35965
25. Vedhanayaki S, Indragandhi V (2023) Certain investigation and implementation of Coulomb counting based unscented Kalman filter for state of charge estimation of lithium-ion batteries used in electric vehicle application. *Int J Thermofluids* 18:100335
26. Aung H, Low KS, Goh ST (2015) State-of-charge estimation of lithium-ion battery using square root spherical unscented Kalman Filter (Sqrt-UKFST) in nanosatellite. *IEEE Trans Power Electron* 30(9):4774–4783
27. Arasaratnam I, Haykin S (2009) Cubature Kalman filters. *IEEE Trans Autom Control* 54(6):1254–1269
28. Xia B, Wang H, Tian Y, Wang M, Sun W, Xu Z (2015) State of charge estimation of lithium-ion batteries using an adaptive cubature Kalman Filter. *Energies* 8(6)
29. A Bayesian approach to battery prognostics and health management. In: *Advances in battery manufacturing, service, and management systems: IEEE*, pp 151–174 (2017)
30. Schwunk S, Armbruster N, Straub S, Kehl J, Vetter MJJoPS (2013) Particle filter for state of charge and state of health estimation for lithium–iron phosphate batteries 239:705–710

31. Zhou D, Zhang K, Ravey A, Gao F, Miraoui A (2016) Online estimation of lithium polymer batteries state-of-charge using particle filter-based data fusion with multimodels approach. *IEEE Trans Ind Appl* 52(3):2582–2595
32. Biazi V, Moreira AC, Pinto JL, Nascimento M, Marques (2023) A particle filter-based virtual sensor for estimating the state of charge and internal temperature of lithium-ion batteries: implementation in a simulated study case. *J Energy Storage* 61:106814
33. He W, Williard N, Chen C, Pecht M (2014) State of charge estimation for Li-ion batteries using neural network modeling and unscented Kalman filter-based error cancellation. *Int J Electr Power Energy Syst* 62:783–791
34. Chang W-Y (2013) Estimation of the state of charge for a LFP battery using a hybrid method that combines a RBF neural network, an OLS algorithm and AGA. *Int J Electr Power Energy Syst* 53:603–611
35. Chen H-Y, Liang J-W (2017) Adaptive wavelet neural network controller for active suppression control of a diaphragm-type pneumatic vibration isolator. *Int J Control, Autom Syst* 15(3):1456–1465
36. Chaoui H, Ibe-Ekeocha CC, Gualous H (2017) Aging prediction and state of charge estimation of a LiFePO<sub>4</sub> battery using input time-delayed neural networks. *Electric Power Syst Res* 146:189–197
37. Chemali E, Kollmeyer PJ, Preindl M, Emadi A (2018) State-of-charge estimation of Li-ion batteries using deep neural networks: a machine learning approach. *J Power Sources* 400:242–255
38. Zazoum B (2023) Lithium-ion battery state of charge prediction based on machine learning approach. *Energy Reports* 9:1152–1158
39. Antón JÁ, Nieto PG, de Cos Juez F, Lasheras FS, Vega MG, Gutiérrez MR (2013) Battery state-of-charge estimator using the SVM technique. *Appl Math Modell* 37(9):6244–6253
40. Ibrahim IA, Khatib T (2017) A novel hybrid model for hourly global solar radiation prediction using random forests technique and firefly algorithm. *Energy Convers Manag* 138:413–425
41. Zou R, Duan Y, Wang Y, Pang J, Liu F, Sheikh SR (2023) A novel convolutional informer network for deterministic and probabilistic state-of-charge estimation of lithium-ion batteries. *J Energy Storage* 57:106298
42. Sahinoglu GO, Pajovic M, Sahinoglu Z, Wang Y, Orlik PV, Wada T (2018) Battery state-of-charge estimation based on regular/recurrent gaussian process regression. *IEEE Trans Ind Electron* 65(5):4311–4321
43. Liu K, Shang Y, Ouyang Q, Widanage WD (2021) A data-driven approach with uncertainty quantification for predicting future capacities and remaining useful life of lithium-ion battery. *IEEE Trans Ind Electron* 68(4):3170–3180
44. Awadallah MA, Venkatesh B (2016) Accuracy improvement of SOC estimation in lithium-ion batteries. *J Energy Storage* 6:95–104
45. Ali MZ, Awad NH, Suganthan PN, Shatnawi AM, Reynolds RG (2018) An improved class of real-coded genetic algorithms for numerical optimization. *Neurocomputing* 275:155–166
46. Ye L-H, Chen S-J, Shi Y-F, Peng D-H, Shi A-P (2023) Remaining useful life prediction of lithium-ion battery based on chaotic particle swarm optimization and particle filter. *Int J Electrochem Sci* 18(5):100122
47. Shuzhi Z, Xu G, Xiongwen Z (2021) A novel one-way transmitted co-estimation framework for capacity and state-of-charge of lithium-ion battery based on double adaptive extended Kalman filters. *J Energy Storage* 33:102093
48. Sun D et al (2021) State of charge estimation for lithium-ion battery based on an intelligent adaptive extended Kalman filter with improved noise estimator. *Energy* 214:119025
49. He Z et al (2021) State-of-charge estimation of lithium ion batteries based on adaptive iterative extended Kalman filter. *J Energy Storage* 39:102593
50. Nian P, Shuzhi Z, Xiongwen Z (2021) Co-estimation for capacity and state of charge for lithium-ion batteries using improved adaptive extended Kalman filter. *J Energy Storage* 40:102559
51. Wu M, Qin L, Wu G (2021) State of charge estimation of power lithium-ion battery based on an adaptive time scale dual extended Kalman filtering. *J Energy Storage* 39:102535

52. Wu M, Qin L, Wu G, Huang Y, Shi C (2021) State of charge estimation of power lithium-ion battery based on a variable forgetting factor adaptive Kalman filter. *J Energy Storage* 41:102841
53. Lin X, Tang Y, Ren J, Wei Y (2021) State of charge estimation with the adaptive unscented Kalman filter based on an accurate equivalent circuit model. *J Energy Storage* 41:102840
54. Khan HF, Hanif A, Ali MU, Zafar A (2021) A Lagrange multiplier and sigma point Kalman filter based fused methodology for online state of charge estimation of lithium-ion batteries. *J Energy Storage* 41:102843
55. Sun C, Lin H, Cai H, Gao M, Zhu C, He Z (2021) Improved parameter identification and state-of-charge estimation for lithium-ion battery with fixed memory recursive least squares and sigma-point Kalman filter. *Electrochimica Acta* 387:138501
56. Li X, Huang Z, Tian J, Tian Y (2021) State-of-charge estimation tolerant of battery aging based on a physics-based model and an adaptive cubature Kalman filter. *Energy* 220:119767
57. Bian Z, Ma Y (2021) An Improved Particle Filter Method to Estimate State of Health of Lithium-Ion Battery\*\*This research is supported by the National Nature Science Foundation of China (No. 61520106008, No. U1564207 and No. 61503149), the State Administration for Market Regulation of China (No. S2020MK684). *IFAC-PapersOnLine* 54(10):344–349
58. Liu X, Li K, Wu J, He Y, Liu X (2021) An extended Kalman filter based data-driven method for state of charge estimation of Li-ion batteries. *J Energy Storage* 40:102655
59. Che Y, Liu Y, Cheng Z, Zhang J (2021) SOC and SOH Identification method of Li-Ion battery based on SWPSO-DRNN. *IEEE J Emerg Select Topics Power Electron* 9(4):4050–4061
60. Liu Y, Li J, Zhang G, Hua B, Xiong N (2021) State of charge estimation of lithium-ion batteries based on temporal convolutional network and transfer learning. *IEEE Access* 9:34177–34187
61. Wang Q, Gu H, Ye M, Wei M, Xu X (2021) State of charge estimation for lithium-ion battery based on NARX recurrent neural network and moving window method. *IEEE Access* 9:83364–83375
62. Shu X, Li G, Zhang Y, Shen S, Chen Z, Liu Y (2021) Stage of charge estimation of lithium-ion battery packs based on improved cubature Kalman filter with long short-term memory model. *IEEE Trans Transp Electric* 7(3):1271–1284
63. Sun T, Wu R, Cui Y, Zheng Y (2021) Sequent extended Kalman filter capacity estimation method for lithium-ion batteries based on discrete battery aging model and support vector machine. *J Energy Storage* 39:102594
64. Ye Y, Li Z, Lin J, Wang X (2021) State-of-charge estimation with adaptive extended Kalman filter and extended stochastic gradient algorithm for lithium-ion batteries. *J Energy Storage* 103611
65. Zhengxin J, Qin S, Yujiang W, Hanlin W, Bingzhao G, Lin H (2021) An Immune Genetic Extended Kalman Particle Filter approach on state of charge estimation for lithium-ion battery. *Energy* 230:120805

# Diseased Leaf Identification Using Bag-of-Features and Sigmoidal Spider Monkey Optimization



Rajani Kuamri<sup>ID</sup> and Sandeep Kumar<sup>ID</sup>

**Abstract** Agricultural products decide the economy of a country like India. The agricultural business has the involvement of a large population. The quality and quantity of agricultural products highly depend on environmental conditions and facilities provided to farmers. Timely and efficient detection of diseases in plants and crops is one of the most critical issues that affect crop production. Therefore, it is highly desirable to develop some cheap and easy-to-handle automated plant disease detection systems for the timely treatment of plants. Leaves are considered a primary source of information about the health of plants. In the case of plants, the disease may be easily visualized and identified by observing its effect on leaves. Therefore, this paper introduces a bag-of-features in sigmoidal spider monkey optimization to identify a diseased leaf, separating the diseased leaf from a healthy leaf. The investigational outcomes show the superiority of the anticipated technique in contrast to other meta-heuristic-based systems.

**Keywords** Plant disease identification · Bag-of-Words · Classification · Clustering · Spider monkey optimization · Feature extraction · Optimization

## 1 Introduction

India is an agrarian civilization largely dependent on agricultural production and livestock. The agriculture sector shares almost 18% part of India's GDP and almost 50% workforce directly or indirectly provided by agriculture and related segments. Therefore, the agriculture sector requires new technologies and innovations that can

---

R. Kuamri

ICFAI Business School (IBS) Bangalore, Off-Campus Center of ICFAI Foundation for Higher Education (IFHE) University, Bangalore, India  
e-mail: [rajani.kumari@ibsindia.org](mailto:rajani.kumari@ibsindia.org)

S. Kumar (✉)

Department of Computer Science and Engineering, CHRIST (Deemed to be University), Bangalore, India  
e-mail: [sandeepkumar@christuniversity.in](mailto:sandeepkumar@christuniversity.in)

ease the lives of farmers and other human beings. In India, Krishi Vigyan Kendra transfers helpful information to farmers. However, due to India's large population and geographical diversity, deploying computerized information systems to every farmer is a very tough task. Therefore, it is highly required to identify the role of Information and Communications Technology (ICT) in agriculture. Now, in the era of mobile technologies, it is essential to develop new technologies directly available to farmers at their fingertips within a few moments.

India is a global agricultural motivating force in the present scenario. It is the world's biggest milk producer, spices, and pulses. Regarding livestock, India has the world's most giant cattle herd. In addition, India has the largest cultivation area under rice, wheat, and cotton crops. In producing rice, wheat, sugarcane, cotton, sheep and goat meat, farmed fish, vegetables, fruit, and tea, India has the second position globally. Though agriculture's share in India's financial system has gradually declined at the level of 18% caused by the soaring development of the other sectors like service, industrial, and realty, the agriculture sector has a significant role in India due to three factors. First, almost 75% population is directly or indirectly dependent on agriculture, mainly in rural areas. Second, the population in rural areas is very poor or far from new technologies, and the third important factor is India's food security depends on the production of food grains, cereals, milk, vegetables, and fruits to meet up the demands of a growing population with growing incomes.

Developed countries are enhancing the use of technology-enabled machinery in the agriculture sector to improve the productivity and quality of agricultural products and ultimately increase profit. These new technologies in agriculture using electronic systems are termed e-Agriculture. In e-Agriculture, farmers use new technologies that include computerized machines and satellite systems to get exact information about crops, soil, environmental status, and forecasting about weather conditions. Uses of computers or mobile devices are also useful in better and timely marketing of products. In addition, farmers get up-to-date knowledge of the latest cultivating techniques, new types of machinery, and the availability of seeds and fertilizers. Presently the use of drone cameras, IoT devices, sensors (to measure temperature and moisture levels), and automated irrigation systems is gaining popularity in agriculture. Most technology-based companies are trying to enter the agriculture sector through farm management software, animal and plant data collection and analysis, next-generation farms, precision agriculture and predictive analytics, robotics and drones, sensors, smart irrigation, and many more.

This paper used a recent variant of SMO namely sigmoidal SMO (SSMO) proposed by Sharma et al. [34]. Sharma et al. [34] proposed a new mechanism to decide the perturbation rate ( $pr$ ) using sigmoidal function. SSMO achieved better convergence with modified  $pr$ . Additionally, BoW is used with SSMO for diseased leaf identification. The experimental results of the SSMO technique have been compared with DE, GSA, PSO, and SMO-based diseased leaf identification systems. A detailed description of SSMO is available in Sharma et al. [34].

The rest of the paper is organized as follows. Section 2 summarizes SMO in brief. Section 3 illustrates the proposed clustering method based on SSMO. Experimental

results of SSMO on different benchmarks and leaf dataset along with statistical analyses has been discussed in Sect. 4. Finally, Sect. 5 concludes the paper.

## 2 Literature Review

Agriculture is one of the prime employment of many countries in which various plants are harvested according to the conditions of the environment and availability of soil. However, water shortage, natural disasters, and various plant diseases are some of the common agriculture problems that must be reduced. Technological advancements such as plant disease identification may reduce some of the problems. Automated plant disease identification and soil quality prediction can eliminate the problems of lack of plant disease knowledge as there are very few experts for the same [16, 17, 36, 38]. Furthermore, food productivity may be increased by on-time prevention of diseases. This will also reduce a farmer's time and cost in searching for an expert. Therefore, this paper introduces a novel approach to identifying diseased plants.

Good knowledge and understanding of plants are necessary to identify different types of plants and their health successfully. They can also be learned using leaf characteristics. Conventional plant identification involves extensive knowledge of various aspects of plant biology. It is time-consuming and requires careful examination of plant phenotypes. Due to the complexity of the plants and the similarities between them, the identification process can be very time-consuming. It also requires botanists to identify the exact plants.

The maximum number of plant diseases can be identified through their impact on leaves, such as early and late scorch, Brown and yellow spots, and fungal and bacterial diseases. These diseases can be identified automatically utilizing systematic image processing techniques [14, 21]. Therefore, this paper introduces an automated image processing technique that uses leaf images to identify the diseased plant. It is not a simple task to identify plant disease by image processing as many features are present in the leaves of plants, such as size, color, texture, shape, etc. Numerous image processing techniques have been anticipated to eliminate the problem, and most of them have two steps [14]. First, they extract prominent features from the input images of the leaves and then perform classification of the images into diseased or healthy using a specific classifier. General classifiers used for plant disease identification are support vector machine (SVM) [7], neural network [35], Fisher linear discriminate (FLD) [28], k-nearest neighbor (kNN) [8], and random forest (RF) [15]. The extraction of good features decides the performance of a classifier. Image analysis based on feature extraction techniques is generally classified into two classes handcrafted and automatic features [20]. Handcrafted features generally use texture, shape, and color information. Sakai et al. [30] considered geometrical attributes like area, maximum length, perimeter, and many more to classify the rice grains into four classes. Handcrafted features require the intervention of human experts, which sometimes leads to skipping important features or selecting redundant features. Machine learning-based feature extraction methods are proposed by researchers that do not foist such

constraints to overcome these problems. Subtractive pixel adjacency model (SPAM) [27], Markov features using intra- and inter-block dependencies (CHEN) [3], and convolutional neural network [11] are some of the examples.

Currently, Bag-of-Words (BoW) is the most popular method for classifying images [5], while it was developed for document classification. It builds a histogram of codewords for the considered set of images a classifier uses to classify images. It is an efficient and robust method that recognizes the visual patterns relevant to the image set. Methods that simulate natural phenomena are used for solving complex optimization problems [12, 31], and several swarm-based and evolutionary methods have been developed. Artificial bee colony (ABC) [24], bacterial foraging optimization algorithm (BFO) [6], gravitational search algorithm (GSA) [29], grey wolf optimizer (GWO) [23], particle swarm optimization (PSO) [4], spider monkey optimization (SMO) [2], and whale optimization algorithm (WOA) [22] are some of the nature-inspired methods used for threshold-based clustering.

SMO algorithm is based on the intelligent behavior of spider monkeys [2]. This algorithm is mainly used to solve complex problems [2]. SMO has been deployed to solve problems from various domains since its inception. Recently, Kumar et al. proposed modifications in SMO with improved position update [18], self-adaptation [19], and improved position update [37] with enhanced performance. Some other modifications include applications in image analysis [26], improved convergence [9], PIDA controller [32], local search [10, 33]. Agarwal et al. [1] developed Oscillating SMO and deployed it to classify soil images.

### 3 Proposed Approach

The proposed approach is shown in Fig. 1 that has three major steps:

- the SURF method used to extract useful features from the input leaf images,
- the BoW using SSMO is used to generate a feature histogram after feature extraction, and
- finally, leaf images were classified into diseased and healthy leaves using the SVM classifier.

Each step is discussed in detail in the following subsections.

#### 3.1 Feature Extraction

In image analysis, it is one of the prime steps. The extracted features greatly affect the performance of a classifier. For an efficient image analysis algorithm, extracting relevant and different features is required to differentiate leaf images in the literature number of feature extraction methods available for this purpose. This paper extracts features using the SURF method from leaf images.

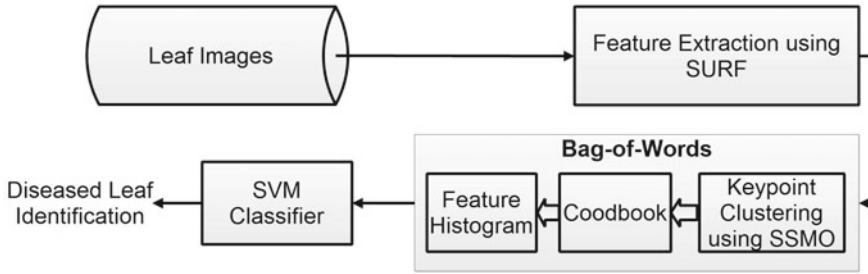


Fig. 1 BoW-based SSMO for leaf image classification

**Speeded-Up Robust Features (SURF)** The SURF is considered one of the best feature extraction approaches compared to other available approaches. Box filters for image convolutions and integral images are the base for the SURF method. Furthermore, the image’s interest points are identified using Hessian matrix approximation. It outperforms other methods of blur, rotation, and change in illumination [13]. These positive sides forced us to use this approach to extract features from the image.

### 3.2 Bag-of-Words (BoW)

The extracted features are deliberated as codewords by BoW. That is representative of several similar patches of the images. This approach transforms the image as a vector of occurrence counts of these codewords. The k-means clustering algorithm is used to engender codeword in basic BoW. Due to its nature, the k-means clustering is inclined mainly toward its initial clusters. Consequently, this anticipated technique uses SSMO-centered clustering, which is more robust than basic K-means.

### 3.3 Classification

Classification of leaf images into different classes performed by SVM classifier after histogram generation of the codewords.

## 4 Experimental Results

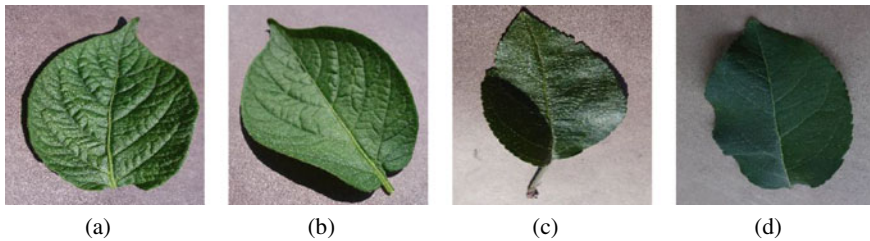
BoW-based SSMO was deployed for classifying leaf images into healthy and diseased categories. These experiments were performed on MATLAB 2022b with an Intel i7 processor with 32 GB RAM and 16 GB GPU. The following section analyzed results for the considered dataset.



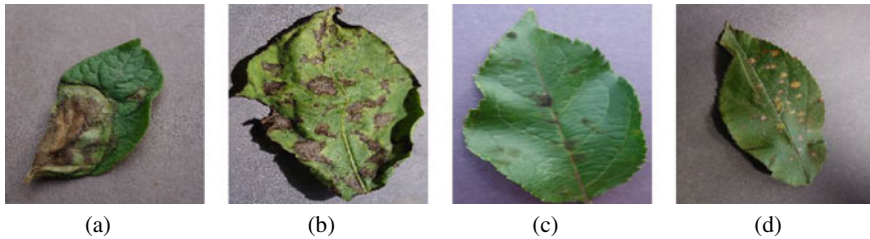
#### 4.1 Result Analysis of Diseased Leaf Identification System

The PlantVillage dataset [25] was selected to check the performance of the proposed diseased leaf identification system, and 1000 images are taken from this dataset. The selected dataset comprises 500 diseased and 500 healthy leaf images. Figures 2 and 3 display four images from healthy and diseased categories, respectively. Furthermore, the dataset is divided into two sets, one for training and another for testing based on random sampling. The multi-class SVM has been used for classification.

The BoW and SSMO-based diseased leaf identification approach has been compared with DE, GSA, k-means, PSO, and SMO-based diseased leaf identification methods. Precision, F-measure, and recall are used to measure the performance and are depicted in Table 1. The best results are shown in bold fonts. The new approach, most of the time, outperforms other considered approaches. The proposed method



**Fig. 2** Sample healthy leaf images of potato (a, b) and apple (c, d) leaves taken from [25]



**Fig. 3** Sample diseased leaf images of potato (a, b) and apple (c, d) leaves taken from [25]

**Table 1** Comparative analysis of different identification methods and the proposed method

S. No.	Algorithm	Accuracy	Classes	Recall	Precision	F1-score
1	Kmeans	81.2	Healthy leaf	73.1	84.5	82.2
			Unhealthy leaf	86.1	70.6	80.1
2	PSO	84.3	Healthy leaf	74.7	87.1	84.7
			Unhealthy leaf	<b>87.1</b>	71.2	83.9
3	GSA	82.3	Healthy Leaf	<b>87.1</b>	79.2	82.7
			Unhealthy leaf	84.9	73.4	81.9
4	DE	81.5	Healthy leaf	73.9	84.7	82.3
			Unhealthy leaf	86.3	<b>70.9</b>	80.7
5	SMO	85.6	Healthy leaf	76.2	89.0	86.1
			Unhealthy leaf	<b>89.2</b>	73.4	85.1
6	SSMO	<b>86.8</b>	Healthy leaf	77.3	89.7	87.2
			Unhealthy leaf	<b>89.9</b>	74.7	86.3

gives 86.8% accuracy, significantly better than other considered methods. Therefore, it can be stated that the new leaf identification method outperforms the existing approaches.

## 5 Conclusion

A new diseased leaf identification system is proposed based on sigmoidal SMO and BoW. A dataset of 1000 images was used from the considered image dataset feature extracted using SURF for training and testing. The SSMO was tested over a set of 12 benchmark, and results are compared with DE, GSA, PSO, and SMO using mean fitness value. The statistical and experimental results show that the novel SSMO method surpasses nature-inspired methods. Furthermore, the proposed approach has been analyzed and compared with DE, GSA, k-means, PSO, and SMO-based methods. Finally, classification is performed using a multi-class SVM classifier. The overall results prove that the SSMO-based BOW method surpasses the currently used approaches with 86.8% accuracy.

## References

1. Agarwal R, Shekhawat NS, Kumar S, Nayyar A, Qureshi B (2021) Improved feature selection method for the identification of soil images using oscillating spider monkey optimization. *IEEE Access* 9:167128–167139
2. Bansal JC, Sharma H, Jadon SS, Clerc M (2014) Spider monkey optimization algorithm for numerical optimization. *Memetic Comput* 6(1):31–47
3. Chen C, Shi YQ (2008) Jpeg image steganalysis utilizing both intrablock and interblock correlations. In: *Proceedings of IEEE international symposium on circuits and systems*, pp 3029–3032
4. Chhikara RR, Sharma P, Singh L (2016) A hybrid feature selection approach based on improved pso and filter approaches for image steganalysis. *Int J Mach Learn Cybern* 7:1195–1206
5. Csurka G, Dance C, Fan L, Willamowski J, Bray C (2004) Visual categorization with bags of keypoints. In: *Workshop on statistical learning in computer vision, ECCV*, vol 1, pp 1–2. Prague
6. Das S, Biswas A, Dasgupta S, Abraham A. Bacterial foraging optimization algorithm: theoretical foundations, analysis, and applications. *Foundations of computational intelligence volume 3: global optimization*, pp 23–55
7. Deepa S (2017) Steganalysis on images using svm with selected hybrid features of gini index feature selection algorithm. *Int J Adv Res Comput Sci* 8
8. Guettari N, Capelle-Laizé AS, Carré P (2016) Blind image steganalysis based on evidential k-nearest neighbors. In: *Proceedings of IEEE international conference on image processing*, pp 2742–2746
9. Gupta K, Deep K (2016) Tournament selection based probability scheme in spider monkey optimization algorithm. In: *Harmony search algorithm*. Springer, pp 239–250
10. Gupta K, Deep K, Bansal JC (2017) Improving the local search ability of spider monkey optimization algorithm using quadratic approximation for unconstrained optimization. *Comput Intell* 33(2):210–240
11. Hanson AM, Joel MG, Joy A, Francis J (2017) Plant leaf disease detection using deep learning and convolutional neural network. *Int J Eng Sci* 5324
12. Hussain K, Mohd Salleh MN, Cheng S, Shi Y (2018) Metaheuristic research: a comprehensive survey. In: *Artificial intelligence review*, pp 1–43
13. Luo J, Oubong G (2009) A comparison of sift, pca-sift and surf. *Int J Image Process (IJIP)* 3(4):143–152
14. Kaur S, Pandey S, Goel S (2018) Plants disease identification and classification through leaf images: a survey. In: *Archives of computational methods in engineering*, pp 1–24
15. Jan K, Jessica F, Vojtěch H (2012) Ensemble classifiers for steganalysis of digital media. *IEEE Trans Inf Forensics Secur* 7:432–444
16. Kumar S, Sharma B, Sharma VK, Poonia RC (2018) Automated soil prediction using bag-of-features and chaotic spider monkey optimization algorithm. In: *Evolutionary Intelligence*, pp 1–12
17. Kumar S, Sharma B, Sharma VK, Sharma H, Bansal JC (2018) Plant leaf disease identification using exponential spider monkey optimization. In: *Sustainable computing: informatics and systems*
18. Kumar S, Sharma VK, Kumari R (2014) Modified position update in spider monkey optimization algorithm. *Int J Emerg Technol Comput Appl Sci* 2:198–204
19. Kumar S, Sharma VK, Kumari R (2014) Self-adaptive spider monkey optimization algorithm for engineering optimization problems. *Int J Inf Commun Comput Technol* 2(2):96–107
20. Lee SH, Chan CS, Mayo SJ, Remagnino P (2017) How deep learning extracts and learns leaf features for plant classification. *Pattern Recognit* 71:1–13
21. Meenakshi, Puja D, Saraswat M, Arya KV (2013) Automatic agricultural leaves recognition system. In: *Proceedings of seventh international conference on bio-inspired computing: theories and applications*, pp 123–131
22. Seyedali M, Andrew L (2016) The whale optimization algorithm. *Adv Eng Softw* 95:51–67

23. Mirjalili S, Mirjalili SM, Lewis A (2014) Grey wolf optimizer. *Adv Eng Softw* 69:46–61
24. Ghareh Mohammadi F, Saniee Abadeh M (2014) Image steganalysis using a bee colony based feature selection algorithm. *Eng Appl Artif Intell* 31:35–43
25. Mohanty SP, Hughes DP, Salathé M (2016) Using deep learning for image-based plant disease detection. *Frontiers Plant Sci* 7:1419
26. Pal SS, Kumar S, Kashyap M, Choudhary Y, Bhattacharya M (2016) Multi-level thresholding segmentation approach based on spider monkey optimization algorithm. In: *Proceedings of the second international conference on computer and communication technologies*. Springer, Berlin, pp 273–287
27. Tomáš P, Patrick B, Jessica F (2010) Steganalysis by subtractive pixel adjacency matrix. *IEEE Trans Inf Forensics Secur* 5:215–224
28. Ramezani M, Ghaemmaghami S (2010) Towards genetic feature selection in image steganalysis. In: *Proceedings of IEEE consumer communications and networking conference*, pp 1–4
29. Esmat R, Hossein N-P, Saeid S (2009) Gsa: a gravitational search algorithm. *Inf Sci* 179(13):2232–2248
30. Sakai N, Yonekawa S, Matsuzaki A, Morishima H (1996) Two-dimensional image analysis of the shape of rice and its application to separating varieties. *J Food Eng* 27(4):397–407
31. Saraswat M, Arya KV, Sharma H (2013) Leukocyte segmentation in tissue images using differential evolution algorithm. *Swarm Evol Comput* 11:46–54
32. Sharma A, Sharma H, Bhargava A, Sharma N, Bansal JC (2016) Optimal power flow analysis using lévy flight spider monkey optimisation algorithm. *Int J Artif Intell Soft Comput* 5(4):320–352
33. Sharma A, Sharma H, Bhargava AA, Sharma N, Bansal JC (2017) Optimal placement and sizing of capacitor using limaçon inspired spider monkey optimization algorithm. *Memetic Comput* 9(4):311–331
34. Sharma B, Sharma VK, Kumar S (2020) Sigmoidal spider monkey optimization algorithm. In: *Soft computing: theories and applications: proceedings of SoCTA 2018*. Springer, Berlin, pp 109–117
35. Sheikhan M, Pezhmanpour M, Shahram Moin M (2012) Improved contourlet-based steganalysis using binary particle swarm optimization and radial basis neural networks. *Neural Comput Appl* 21:1717–1728
36. Vijai S, Misra AK (2017) Detection of plant leaf diseases using image segmentation and soft computing techniques. *Inf Process Agric* 4(1):41–49
37. Swami V, Kumar S, Jain S (2018) An improved spider monkey optimization algorithm. In: *Soft computing: theories and applications*. Springer, Berlin, pp 73–81
38. Zhaobin W, Huale L, Ying Z, TianFang X (2017) Review of plant identification based on image processing. *Arch Comput Methods Eng* 24(3):637–654

# Detection of FDI Attacks on Power Grid Using Graph-Theoretical Methods



Arpita Ghosh and Shubhi Purwar

**Abstract** Smart grid is a reliable and efficient system for electrical power distribution in recent years. One of the drawbacks of this grid is its susceptibility to cyber-attacks. State estimation of the power grid under such an attack is of utmost importance for preventing serious damage to the grid. This paper focuses on the detection of False Data Injection (FDI) attacks that manipulates the Phasor Measurement Unit (PMU) data. An algorithm is presented that can detect the attack zone by analyzing the anomalies in the measurement after the attack. The algorithm is tested on the standard IEEE 118-bus system and the estimation error is used to evaluate the performance of this algorithm. It can successfully detect the attacked buses and estimate the parameters after the attack using graph theoretical methods. The algorithm also differentiates between attacks, load disturbances and single-line faults in the grid.

**Keywords** Cyber-attacks · State estimation · FDI attack · Graph theory

## 1 Introduction

Cyber-attacks are a very serious threat to the power grid. The modern power grid or the smart grid is one of the most developed cyber-physical systems of recent times. The coupling of the computer systems and communication channels with the transmission lines increases the capability and also the complexity of the system. Due to the cyber part in the system, this network is vulnerable to cyber-attacks [1]. The intruder may cause a data attack, or an attack that is both cyber and physical in nature.

---

A. Ghosh (✉) · S. Purwar  
Department of Electrical Engineering, MNNIT Allahabad, Prayagraj, India  
e-mail: [arpita.2021ee04@mnnit.ac.in](mailto:arpita.2021ee04@mnnit.ac.in)

S. Purwar  
e-mail: [shubhi@mnnit.ac.in](mailto:shubhi@mnnit.ac.in)

The attack on the Ukrainian power grid is one of the main events that triggered extensive research on cyber-attacks on the power grid [2]. There has been quite a significant number of cyber-attacks on the power grid following the Ukrainian incident. India, Russia, the US and the Czech Republic are a few of the countries that have faced these major attacks [3]. Most of the major attacks start with small data attacks on the system, which cascade into large-scale attacks and ultimately cause physical damage to the system. Hence, it is very important to detect these attacks in their initial stage.

Data Injection (FDI) attacks are the major data attacks on the power grid. Extensive research has been conducted on the detection of FDI attacks targeting the grid [3–14]. Detection and defense mechanisms using search algorithms are widely studied [4]. These algorithms do not produce satisfactory results in the case of partial observations. In [5], a real-time effective detection algorithm is presented that provides shorter detection time and better accuracy. A graph signal processing-based method is proposed in [6] which can detect attacks on both the phase angles and the magnitudes of the bus voltages. However, this method is implemented on the DC model of the grid. A filtering and learning algorithm using the Kalman filter is presented in [7] that has a 75% higher probability of detecting an attack. Machine learning algorithms [8, 9], data-driven detection [10, 11] and Fourier transform [12] are very popular methods for FDI detection. A comprehensive survey is presented in [13] covering the detection, mitigation and challenges faced in countering FDI attacks.

In this paper, we develop methods to detect small-scale data attacks on the power grid and differentiate these attacks from load disturbances and faults in the transmission lines. The power grid model from [14] is used to study cyber-attacks on the system. The model introduced in [14, 15] is mostly used for the study of cyber-physical attacks on power systems. Unlike these methods, we consider attacks which have no physical component and are only cyber in nature. The modeling in [16, 17] is similar to the works in [15] but the approach is different. This paper presents a method that is an extension of [14] and a data-driven approach for the detection of FDI attacks.

Linear algebra and graph theory are the main tools used for the estimation purpose in this paper. One of the main assumptions for this method (used in [14–17]) is that the grid remains connected after the attack. For this case, since there is no physical attack, the grid topology remains unchanged. Hence, the unchanged admittance matrix of the grid is used for the estimation. In recent works [18], state estimation when the grid is segregated into islands after an attack has also been studied.

For detecting the anomalies in the recorded data, we constantly compare it with the data from the healthy system available to us. If a significant deviation is observed, we apply the algorithms developed to identify the cause. The phase angles at the buses are used for this detection purpose. Phase angles are often used for state estimation and detection of faults [19]. The design and modeling of FDI attacks [20] is discussed in detail in recent works, especially stealthy attacks [21], because these are extremely dangerous for the grid. However, we do not discuss the modeling of FDI attacks in our work; we concentrate on the detection mechanisms. The contributions of this paper are summarized below:

1. We have developed a novel detection algorithm for FDI attacks based on anomalies in the phase angles at the buses by utilizing the network topology properties.
2. This algorithm also successfully recovers the actual phase angles in the attacked zone with negligible error.
3. We also provide detailed case studies to show that this method can differentiate between a FDI attack and the internal disturbances of the grid like load disturbances and line failures.

The following section of this paper describes the modeling of the grid, followed by the attack model and the detailed algorithm developed for detection. The last section consists of the numerical results which shows case studies that prove the efficiency of the algorithm in detecting and differentiating between the different causes of the disturbances/threats to the system.

## 2 Model and Definitions

### 2.1 Power Grid Model

We represent the power grid by a connected undirected graph,  $G = (V, E)$  where the nodes and edges of the graph are denoted by  $V = \{1, 2, 3, \dots, n\}$  and  $E = \{e_1, e_2, \dots, e_m\}$ , respectively. The nodes represent the buses in the network while the edges correspond to the transmission lines of the grid, shown in Fig. 1. We consider the AC power flow model where the transmission lines are characterized by their impedance,  $r_e + ix_e$ , where each edge  $e = \{s, t\}$  connects the buses  $s$  and  $t$  such that  $s, t \in V$ . The status of each node  $x$  is represented by its voltage  $v_x = |v_x|e^{i\theta_x}$ , in which  $|v_x|$  represents the voltage magnitude and  $\theta_x$  represents the phase angle at node  $x$ . The standard AC power flow equations are considered for this paper [22].

The incidence matrix ( $V \times E$ ) of  $G$  is denoted by  $D \in \{-1, 0, 1\}^{|V| \times |E|}$  and defined as follows:

$$d_{zx} = \begin{cases} 1, & \text{if } e_z \text{ is going towards node } x \\ -1, & \text{if } e_z \text{ is moving out from node } x \\ 0, & \text{if } e_z \text{ is not incident to node } x \end{cases}$$

The admittance matrix for AC power flow is defined as  $A = DYD^T \in \mathbb{R}^{|V| \times |V|}$ , where  $Y$  is defined as  $Y = \text{diag}\left(\left[\frac{1}{x_{e_1}}, \frac{1}{x_{e_2}}, \dots, \frac{1}{x_{e_m}}\right]\right)$ , a diagonal matrix with entries equal to the inverse of the reactance values.

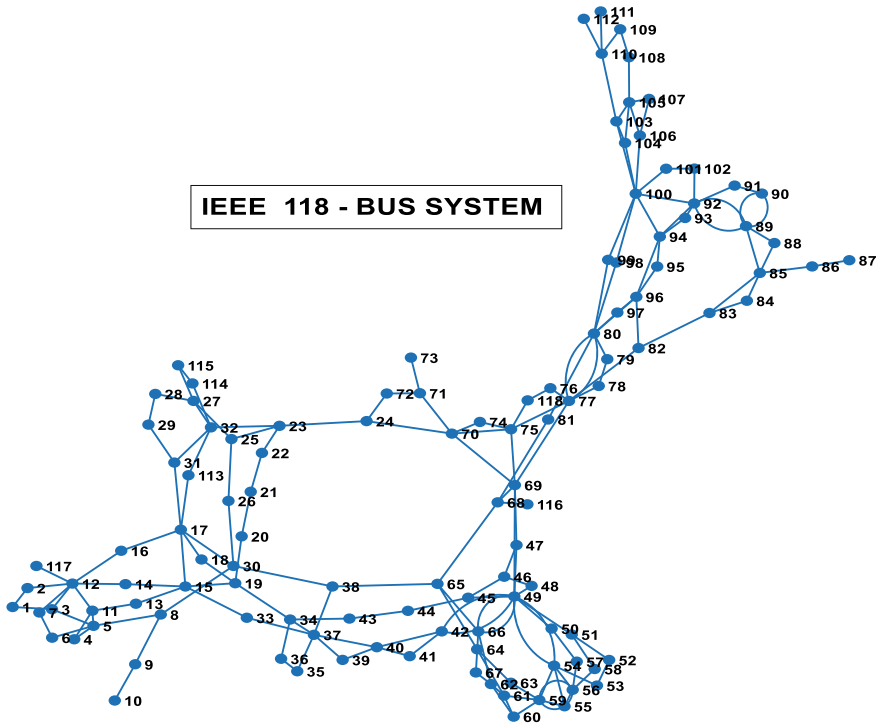


Fig. 1 IEEE 118-bus system in a form of a graph network generated in MATLAB

## 2.2 Basic Graph Theoretical Terms

The graph theoretical terms used in this paper are mostly borrowed from [23, 24]. A few of them are defined below.

*Subgraphs:* Let graph  $G$  have a subset of the nodes  $M$ , then  $G[M]$  denotes the subgraph of  $G$  induced by  $M$ .

*Acyclic Graph:* A graph is acyclic if its vertices cannot be arranged into a cyclic sequence. An acyclic graph must have a vertex of degree less than two.

*Matching:* A matching in a graph is a set of edges, no two of which have a vertex in common. If a subgraph  $M$  of  $G$  is a matching, then each vertex of  $G$  is incident with at most one edge in  $M$ .

**Notations:** If  $X$  is a subgraph of  $G$ , the complement of  $X$  is denoted by  $\overline{X} = G \setminus X$ . If  $X, Y$  are subgraphs of  $G$ , then the submatrix of  $A$  is denoted by  $A_{X|Y}$  such that its rows are from  $V_X$  and columns are from  $V_Y$ . The symbol  $(\prime)$  denotes actual values after an attack and  $(^*)$  denotes observed values after an attack.



### 2.3 Attack Model

We assume that a False Data Injection (FDI) attack takes place on the power grid. The intruder attacks the grid by manipulating the Phasor Measurement Units (PMU) data. We consider the data attacks on the phase angle measurement at the buses. The nodes where the data is manipulated form the attack zone  $H$ . The attack can be modeled as

$$\vec{\theta}_H^* = \vec{\theta}'_H + \vec{z} \tag{1}$$

where  $\vec{\theta}_H^*$  is the observed/manipulated phase angles in the attack zone after the attack,  $\vec{\theta}'_H$  is the actual phase angles after the attack and  $\vec{z}$  is a random vector with arbitrary distribution that distorts the actual data. Since the attack is on a healthy system, the actual value of the phase angles should remain the same before and after the attack. In case of internal disturbances, the value would change after the attack. We have considered attacks on single zones as well as multiple zones in the system.

### 3 State Estimation

The algorithm that is developed for state estimation is discussed in detail in this section. The central idea is to monitor the phase angles. When we observe a change in the phase angles  $\vec{\theta}$ , we calculate the deviation of the measured data from the healthy data. The nodes which have a significant amount of deviation in the phase angles are considered as the attack zone  $H$ . We now use  $\vec{\theta}$ ,  $A$  and observed phase angles outside zone  $H$  after an attack  $\vec{\theta}_{\bar{H}}^*$ , to estimate the phase angles inside the zone  $H$ . If the estimated data is almost equal to the healthy data and significantly different from the observed one, then we conclude that there is some distortion in the data in the form of an FDI attack. The phase angles estimation described in detail in [15] is given by

$$A_{\bar{H}|G}(\vec{\theta} - \vec{\theta}') = 0 \tag{2}$$

This Eq. (2) can be modified into

$$A_{\bar{H}|H}(\vec{\theta}_H - \vec{\theta}'_H) + A_{\bar{H}|\bar{H}}(\vec{\theta}_{\bar{H}} - \vec{\theta}'_{\bar{H}}) = 0 \tag{3}$$

where all the variables are known except  $\vec{\theta}'_H$ , which is the actual phase angles to be estimated. Since only the phase angles inside  $H$  are manipulated, it can be assumed that  $\vec{\theta}_{\bar{H}}^* = \vec{\theta}'_{\bar{H}}$ , for the zone outside  $H$ . Equation (3) holds true for the DC power flow model. Also, there are a few constraints on the attack zone. The attack zone must

be acyclic in nature and there should be a matching between the nodes of  $H$  and  $\overline{H}$  [15]. To extend this estimation problem to the AC power flow model, we relax the constraints to form the optimization problem

$$\|A_{\overline{H}|H}(\vec{\theta}_H - \vec{\theta}'_H) + A_{\overline{H}|\overline{H}}(\vec{\theta}_{\overline{H}} - \vec{\theta}'_{\overline{H}})\|_2 < \epsilon \quad (4)$$

We solve this optimization problem to estimate the actual values of the phase angles. The detailed algorithm, its implementation and performance analysis are discussed hereafter.

---

Algorithm 1: Detection of FDI attacks

---

Input: A connected graph  $G$ , healthy phase angles  $\vec{\theta}$  and  $\vec{\theta}^*$ , phase angles after attack/disturbance

1. Compute the error between the healthy data and new data at each node  $i$
  2. If the  $error(V_i) > \delta$ , then node  $V_i$  is affected
  3. Form the attack zone  $H$  with the affected nodes  $n(V_i)$
  4. Compute the solution to Eq. (4) by convex optimization
  5. Compute the error  $\epsilon$  between the estimated data and the healthy data
  6. Analyzing  $\epsilon$  with  $\epsilon_{thres}$  and number of affected nodes ( $n$ ) with  $n_{thres}$ , we detect if it is a load disturbance, line failure or FDI attack
  7. The estimation error  $\epsilon_{est}$  is used to evaluate the accuracy of the solution.
- 

## 4 Numerical Results

Healthy system data and the observed phase angles are fed to the algorithm as input, at regular intervals. The program checks the anomaly in  $\vec{\theta}$  to identify the attacked nodes. If the deviation is negligible ( $< \delta$ ) at all the nodes, then the system is identified to be in healthy condition and the program doesn't execute Steps 4–7. It waits for the next set of observations and repeats itself. Unless a disturbance zone is identified, the algorithm executes Steps 1–3, identifies the system state and waits for new data. Once a disturbance zone is detected, we use state estimation and comparative data analysis to identify the cause of the disturbance.

The IEEE 118-bus benchmark system [25] is used to evaluate the performance of this algorithm. The CVX toolbox [26] in MATLAB is used for solving the optimization problem, while MATPOWER [27] is used for calculation of the phase angles under the AC power flow model. The value of  $\delta$  is taken as 2% that is used to form the zone  $H$  and value of  $\epsilon$  is 0.01. The threshold value  $\epsilon_{thres}$  is taken as 2, and the threshold value for number of nodes affected,  $n_{thres}$ , is taken as 10.

**Case 1: Load Disturbance**

Load disturbance ( $<\pm 5\%$ ) at each node of the 118-bus system is simulated for this problem. For most of the nodes (85% of cases), the change in phase angles is negligible, i.e., less than  $\delta$ . For the remaining nodes, the phase angles are estimated and compared with  $\epsilon_{thres}$  and  $n_{thres}$ . For 83% of cases, the error is less than 2% and the number of nodes affected is less than 10. Only 3 out of 118 cases don't hold true for this classification.

**Case 2: Line Failure**

For line failures (or single-line faults), the change in phase angles is usually much higher than that of the load disturbance. All single-line failures are considered for the IEEE 118-bus systems. There are 9 cases where the load flow doesn't converge. So, we exclude these from the analysis. For 91% of cases, the change in phase angles is significant ( $>2\%$ ). The angles are estimated as in the case of load disturbance, and the deviation from the healthy data along with the number of nodes affected are analyzed.

For 70% of cases, the number of nodes affected is greater than 10, while the error with respect to the healthy data is more than 2% in 36% of cases. Only 8% of cases in case of single-line faults do not follow this classification. From the analysis of this data, we can conclude that if any of the two conditions  $n > n_{thres}$  or  $\epsilon > \epsilon_{thres}$  holds true, then we can conclude that we have a line failure in the system.

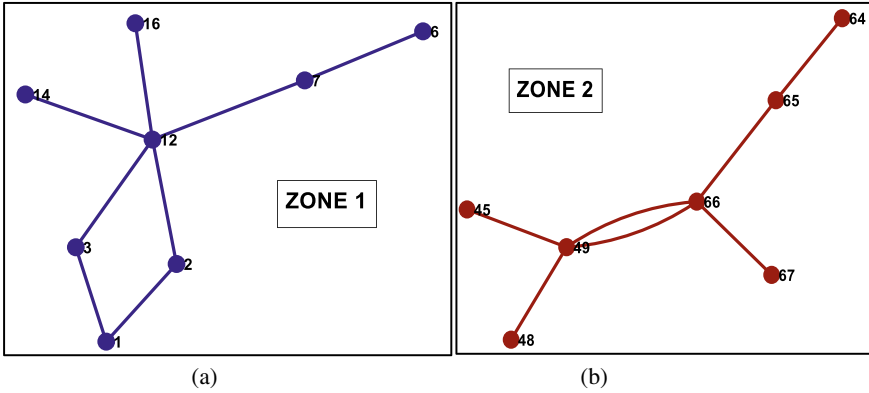
**Case 3: FDI Attack**

For the FDI attack, the change in phase angles depends on the distortion factor  $\vec{z}$ . The threshold value is used for differentiating the healthy zone from the attack zone. We consider multiple case studies in this scenario with single and multiple attack zones.

*Single attack zone:* Two cases with single attack zones are shown in Fig. 2. When the phase angles at these nodes are estimated, then the error between the estimated angles and the healthy data is almost zero in both the cases. The data for both these cases are shown in Tables 1 and 2.

*Multiple attack zone:* If the attack takes place on multiple zones with the grid simultaneously, this algorithm can detect the zone and estimate the phase angles correctly. One such case study is shown in Fig. 3. The attack zones within the grid are marked in the figure. This algorithm is able to exactly recover the phase angles in this case, and the error between the estimated angles and the healthy data is almost zero as the previous cases. The data for multiple attack zone is shown in Table 3.

From this detailed analysis of the various cases, we can conclude that if  $\epsilon$  is close to zero, then we can identify this as a False Data Injection attack, irrespective of the number of nodes affected. If  $\epsilon$  is more than zero but less than  $\epsilon_{thres}$  and number of nodes affected is less than  $n_{thres}$ , we can conclude a load disturbance on the system. If either of  $\epsilon$  or  $n$  crosses the threshold failures, we identify it to be a single-line fault.



**Fig. 2** (a) The first attack zone (Zone 1) and (b) the second attack zone (Zone 2)

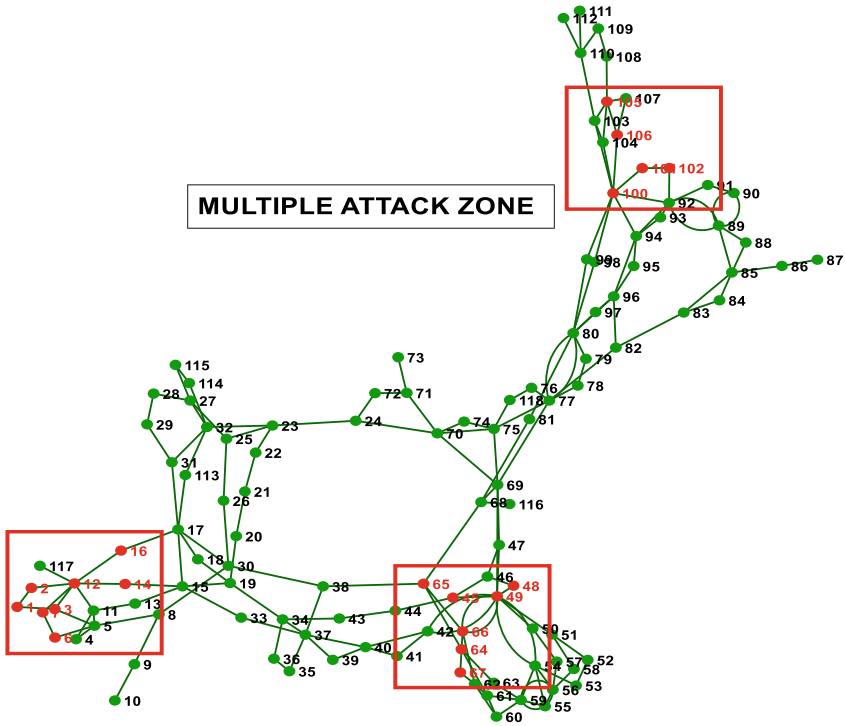
**Table 1** Measured, actual and estimated data for Zone 1

Node No.	$\theta_{\text{observed}}$	$\theta_{\text{actual}}$	$\theta_{\text{estimated}}$
1	11.30192	10.97274	10.9727
2	11.85792	11.51255	11.5125
3	12.21188	11.85619	11.8562
6	13.69063	13.29187	13.2919
7	13.23276	12.84734	12.8473
12	12.86358	12.48891	12.4889
14	12.1246	11.77146	11.7715
16	12.55296	12.18734	12.1873

**Table 2** Measured, actual and estimated data for Zone 2

Node No.	$\theta_{\text{observed}}$	$\theta_{\text{actual}}$	$\theta_{\text{estimated}}$
45	16.24576	15.77258	15.77258
48	20.61906	20.0185	20.0185
49	21.65226	21.02161	21.02161
64	25.33116	24.59336	24.59336
65	28.55068	27.7191	27.7191
66	28.38544	27.55868	27.55868
67	25.66654	24.91897	24.91897

For the FDI attacks, the estimation error  $\epsilon_{est}$  is used to measure the accuracy of the detection algorithm. It is computed as  $\|\theta_{est} - \theta_{actual}\|_2 / \|\theta_{actual}\|_2 * 100$  in percentage. The value of  $\epsilon_{est}$  is  $5.0499 \times 10^{-9}\%$  for single attack zone 1 (Table 1),  $3.5555 \times 10^{-10}\%$  for single attack zone 2 (Table 2) and  $1.3600 \times 10^{-8}\%$  for multiple



**Fig. 3** Multiple attack zones in 118 bus system generated in MATLAB. The blue nodes are the healthy ones, whereas the red ones show the attacked nodes

attack zones (Table 3). These values affirm that the algorithm correctly estimates the system states in case of an FDI attack.

All the figures used in this paper are generated by MATLAB using the graph and network algorithms used in network analysis.

**Table 3** Measured, actual and estimated data for multiple attack zones

Node No.	$\theta_{\text{observed}}$	$\theta_{\text{actual}}$	$\theta_{\text{estimated}}$
1	11.30192	10.97274	10.97274
2	11.85792	11.51255	11.51255
3	12.21188	11.85619	11.85619
6	13.69063	13.29187	13.29187
7	13.23276	12.84734	12.84734
12	12.86358	12.48891	12.48891
14	12.1246	11.77146	11.77146
16	12.55296	12.18734	12.18734
45	16.24576	15.77258	15.77258
48	20.61906	20.0185	20.0185
49	21.65226	21.02161	21.02161
64	25.33116	24.59336	24.59336
65	28.55068	27.7191	27.7191
66	28.38544	27.55868	27.55868
67	25.66654	24.91897	24.91897
100	28.90061	28.05884	28.05884
101	30.53629	29.64688	29.64688
102	33.33594	32.36499	32.36499
105	21.26287	20.64357	20.64357
106	20.99491	20.3834	20.3834

## 5 Conclusion

This algorithm performs satisfactorily with the IEEE 118-bus system. One of the drawbacks of this method is that it doesn't hold true for all the cases of line failures and load disturbances. However, it can correctly identify load disturbance and line failures for 91% and 92% of cases, respectively. For FDI attacks, it detects the attack area and estimates the system parameters correctly for 100% of the cases. The estimation error for the FDI attack is  $\varepsilon_{est} \approx 0$ , affirming the reliability of the method. This algorithm performs significantly well when the attack area is small. Unlike previous detection methods, this algorithm is independent of the size of the grid. Hence, it is very effective in detecting small undetectable attacks in large grids. Its performance in terms of differentiating between load disturbances and line failures can be improved further. If the intruder physically attacks the grid along with the FDI attack, this algorithm will not work. This is the future scope of this work.

The control center for the power grid can usually handle small disturbances and attacks in the system. Small-scale attacks usually do not cause much damage, but it is very important to detect them. If left undetected, it may cascade into bigger problems. When the attack area increases, it will cause significant changes in the

load. If the attacker is able to change the breaker status of the lines, it will lead to line failures in the grid causing serious blackout situations.

## References

1. Yu X, Xue Y (2016) Smart grids: a cyber-physical systems perspective. *Proc IEEE* 104(5):1058–1070
2. Fairley P (2016) Cybersecurity at U.S. utilities due for an upgrade: tech to detect intrusions into industrial control systems will be mandatory [news]. *IEEE Spectrum* 53(5):11–13
3. Duo RW, Zhou M, Abusorrah A (2022) A survey of cyber attacks on cyber physical systems: recent advances and challenges. *IEEE/CAA Journal of Automatica Sinica* 9(5):784–800
4. Hao J, Piechocki RJ, Kaleshi D, Chin WH, Fan Z (2015) Sparse malicious false data injection attacks and defense mechanisms in smart grids. *IEEE Trans Ind Inf* 11(5):1–12
5. Huang Y, Tang J, Cheng Y, Li H, Campbell KA, Han Z (2016) Real-time detection of false data injection in smart grid networks: an adaptive CUSUM method and analysis. *IEEE Syst J* 10(2):532–543
6. Drayer E, Routtenberg T (2020) Detection of false data injection attacks in smart grids based on graph signal processing. *IEEE Syst J* 14(2):1886–1896
7. Chattopadhyay A, Mitra U (2020) Security against false data-injection attack in cyber-physical systems. *IEEE Trans Control Netw Syst* 7(2):1015–1027
8. Li Y, Wei X, Li Y, Dong Z, Shahidehpour M (2022) Detection of false data injection attacks in smart grid: a secure federated deep learning approach. *IEEE Trans Smart Grid* 13(6):4862–4872
9. Lei W, Pang Z, Wen H, Hou W, Han W (2022) FDI attack detection at the edge of smart grids based on classification of predicted residuals. *IEEE Trans Ind Inf* 18(12):9302–9311
10. Shi J, Liu S, Chen B, Yu L (2021) Distributed data-driven intrusion detection for sparse stealthy FDI attacks in smart grids. *IEEE Trans Circuits Syst II Express Briefs* 68(3):993–997
11. Lakshminarayana S, Kammoun A, Debbah M, Poor HV (2021) Data-driven false data injection attacks against power grids: a random matrix approach. *IEEE Trans Smart Grid* 12(1):635–646
12. Dehghani M, Niknam T, Ghiyasi M, Siano P, Haes Alhelou H, Al-Hinai A (2021) Fourier singular values-based false data injection attack detection in AC smart-grids. *Appl Sci* 11(12):5706
13. Musleh AS, Chen G, Dong ZY (2020) A survey on the detection algorithms for false data injection attacks in smart grids. *IEEE Trans Smart Grid* 11(3):2218–2234
14. Soltan S, Zussman G (2017) Power grid state estimation after a cyber-physical attack under the AC power flow model. In: 2017 IEEE power and energy society general meeting, Chicago, IL, USA
15. Soltan S, Yannakakis M, Zussman G (2018) Power grid state estimation following a joint cyber and physical attack. *IEEE Trans Control Netw Syst* 5(1):499–512
16. Soltan S, Zussman G (2019) EXPOSE the line failures following a cyber-physical attack on the power grid. *IEEE Trans Control Netw Syst* 6(1):451–461
17. Soltan S, Yannakakis M, Zussman G (2019) REACT to cyber attacks on power grids. *IEEE Trans Netw Sci Eng* 6(3):459–473
18. Huang Y, He T, Chaudhuri NR, La Porta TF (2022) Link state estimation under cyber-physical attacks: theory and algorithms. *IEEE Trans Smart Grid* 13(5):3760–3773
19. Tate JE, Overbye TJ (2008) Line outage detection using phasor angle measurements. *IEEE Trans Power Syst* 23(4):1644–1652
20. Padhan S, Turuk A (2022) Design of false data injection attacks in cyber-physical systems. *Inf Sci* 608:825–843
21. Bienstock D, Escobar M (2017) Computing undetectable attacks on power grids. *SIGMETRICS Perform Eval Rev* 45(2):115–118
22. Bergen R, Vittal V (1999) Power systems analysis. Prentice-Hall, Upper Saddle River, NJ

23. Bondy JA, Murty U (2017) Graph theory, graduate texts in mathematics, vol 244200. Springer, Heidelberg
24. Bapat R (2010) Graphs and matrices. Springer, New York
25. IEEE benchmark systems. <http://www.ee.washington.edu/research/pstca/>. Last Accessed 05 Feb 2023
26. Grant M, Boyd S. CVX: Matlab software for disciplined convex programming, version 2.1. <http://cvxr.com/cvx>. Last Accessed 03 Jan 2023
27. Zimmerman RD, Murillo-Sánchez CE, Thomas RJ (2011) MATPOWER: steady-state operations, planning, and analysis tools for power systems research and education. IEEE Trans Power Syst 26(1):12–19



# Author Index

## A

Aarathi, D., 241  
Abhijit, 217  
Abhinav, 89  
Abubeker, K. M., 217  
Aditi Ghosh, 205  
Akhil, S., 217  
Akshat Kumar, V. K., 217  
Aniruddha Prabhu, B. P., 39  
Anurag Paliwal, 67  
Anusha Danday, 155  
Anvith, 289  
Arabindo Chandra, 27  
Aravinda Raj, R., 349  
Arpita Ghosh, 391  
Asif Mushtaq Bhat, 79  
Ashutosh Tripathi, 89  
Ayesha Shaik, 313  
Ayushi Gill, 67

## B

Ben K. Jose, 217

## C

Chandradeep Bhatt, 39  
Chintha Rithvik Kumar Reddy, 279

## D

Dharminder Chaudhary, 105  
Diana Andrushia, A., 279  
Divyasri, K., 289  
Dushyant Kumar Yadav, 105  
Felista Sugirtha Lizy, R., 53

## G

Gaikwad Anshul J., 117  
Gaurav Malik, 369  
Gaurav Pendharkar, 313  
Gaurav Shrivastava, 167  
Gopi Krishna Rao, P. V., 1

## H

Hanuma Naik, R., 1  
Hemlal Sahu, 105

## I

Ila Pant Bisht, 193

## J

Jayasudha, M., 313  
Jijo Francis, 145  
Jojo James, 145

## K

Kalaiselvi, T., 179  
Kanishka Vaish, 299  
Kannimuthu, S., 241  
Kapil Joshi, 299  
Kappa Ravi Kiran Raju, 279  
Kathika Jyothi Naga Nivas, 279  
Karthik, K. N., 289  
Kavita Gupta, 255  
Khairul Hafezad Abdullah, 39  
Kirti Walia, 255

**L**

Lakshmanan Palani, 133  
Lakshmi Kaliappan, 133

**M**

Malathy, P., 349  
Manasa, S., 89  
Manish Kumar Saini, 369  
Manivasagan, D., 349  
Mary Neebha, T., 279  
Mayilvaganan, N., 349  
Milan Basu, 27  
Mohamed Basith, S., 349  
Mohammad Abid Bazaz, 79  
Muhesh Kumar, B., 313  
Murugesan Manivel, 133  
Muskan Sharma, 267

**N**

Narendiran, R., 325  
Narendra Singh Rathore, 337  
Neelesh, V. S., 325  
Nikhil S. Damle, 117

**O**

Otturu Madhu Murali, 105

**P**

Parthajit Roy, 205  
Pavithra, A., 325  
Payal Sachdev, 337  
Poornima, N., 325  
Pragati Kumari, 267  
Pratik P. Shastrakar, 117  
Priyanka Kushwaha, 267  
Putha Sathish Kumar Reddy, 279

**Q**

Quang-Vinh Dang, 15

**R**

Rahul Chauhan, 39  
Rajani Kuamri, 381  
Rajarajeswari, S., 289  
Rajasekhar, M. V., 1  
Rajesh Bahuguna, 299

Rajesh Singh, 299  
Raj Kishor Bisht, 193  
Rakesh Dani, 39  
Rakesh Kumar, G., 227  
Rakshit Kothari, 67, 337  
Rama Devi, 89  
Richa Yadav, 267  
Riddhi Singhal, 289  
Rishika Yadav, 299

**S**

Sabeen Govind, 145  
Saisamudra, K., 227  
Samta Kathuria, 299  
Sandeep Kumar, 381  
Sanjay Jasola, 193  
Sardey Bhagyashri R., 117  
Satyanarayana Murthy, T., 155  
Saurabh Rana, 105  
Shilpi Mittal, 255  
Shiva Kumar, K., 227  
Shubhi Purwar, 391  
Siva Gayatri Venkata Naga Datta Sai  
Ammanamanchi, 105  
Sivaranjani Subramani, 133  
Soham Kumar, 313  
Soumyajit Datta, 27  
Sowmya, G., 1  
Sreenivasa Rao, N., 1  
Sridharan, C., 325  
Srinivas, G., 227  
Sriramakrishnan, P., 179  
Subhash Chandra, 167  
Sudharshanan Balaji, 313  
Sumana Chowdhuri, 27  
Syedsafi, S., 179

**T**

Tejaswaroop, K., 227  
Tushar Sharma, 39

**V**

Vijay, B., 325  
Vijendra Kumar Maurya, 67, 337

**Y**

Yogendra Kumar Upadhyaya, 89  
Yogesh Lohumi, 193